SMALL RNAS AS A DIVERSE TOOLKIT OF BACTERIA

EDITED BY: Olga N. Ozoline and Klaus Neuhaus
PUBLISHED IN: Frontiers in Molecular Biosciences

frontiers Research Topics

frontiers

ISSN 1664-8714
ISBN 978-2-88971-963-1
DOI 10.3389/978-2-88971-963-1

About Frontiers

Frontiers is more than just an open-access publisher of scholarly articles: it is a pioneering approach to the world of academia, radically improving the way scholarly research is managed. The grand vision of Frontiers is a world where all people have an equal opportunity to seek, share and generate knowledge. Frontiers provides immediate and permanent online open access to all its publications, but this alone is not enough to realize our grand goals.

Frontiers Journal Series

The Frontiers Journal Series is a multi-tier and interdisciplinary set of open-access, online journals, promising a paradigm shift from the current review, selection and dissemination processes in academic publishing. All Frontiers journals are driven by researchers for researchers; therefore, they constitute a service to the scholarly community. At the same time, the Frontiers Journal Series operates on a revolutionary invention, the tiered publishing system, initially addressing specific communities of scholars, and gradually climbing up to broader public understanding, thus serving the interests of the lay society, too.

Dedication to Quality

Each Frontiers article is a landmark of the highest quality, thanks to genuinely collaborative interactions between authors and review editors, who include some of the world's best academicians. Research must be certified by peers before entering a stream of knowledge that may eventually reach the public - and shape society; therefore, Frontiers only applies the most rigorous and unbiased reviews.
Frontiers revolutionizes research publishing by freely delivering the most outstanding research, evaluated with no bias from both the academic and social point of view. By applying the most advanced information technologies, Frontiers is catapulting scholarly publishing into a new generation.

What are Frontiers Research Topics?

Frontiers Research Topics are very popular trademarks of the Frontiers Journals Series: they are collections of at least ten articles, all centered on a particular subject. With their unique mix of varied contributions from Original Research to Review Articles, Frontiers Research Topics unify the most influential researchers, the latest key findings and historical advances in a hot research area! Find out more on how to host your own Frontiers Research Topic or contribute to one as an author by contacting the Frontiers Editorial Office: frontiersin.org/about/contact

SMALL RNAS AS A DIVERSE TOOLKIT OF BACTERIA

Topic Editors:
Olga N. Ozoline, Institute of Cell Biophysics (RAS), Russia
Klaus Neuhaus, Technical University of Munich, Germany

Citation: Ozoline, O. N., Neuhaus, K., eds. (2021). Small RNAs as a Diverse Toolkit of Bacteria. Lausanne: Frontiers Media SA. doi: 10.3389/978-2-88971-963-1

Table of Contents

frontiers in Molecular Biosciences

EDITORIAL
published: 10 November 2021
doi: 10.3389/fmolb.2021.791021

Editorial: Small RNAs as a Diverse Toolkit for Bacteria

Olga Ozoline and Konstantin Shavkunov*

Pushchino Scientific Center for Biological Research of the Russian Academy of Sciences, Laboratory of Functional Genomics and Cellular Stress, Institute of Cell Biophysics of the Russian Academy of Sciences, Pushchino, Russia

Keywords: bacterial sRNAs, sRNA processing and function, sRNA-mediated intracellular regulatory pathways, sRNAs for intercellular communication, coding sRNAs

Editorial on the Research Topic

Small RNAs as a Diverse Toolkit for Bacteria

INTRODUCTION

Bacteria use diverse regulatory RNAs to coordinate their physiological processes. Although their spectrum differs from that of higher organisms, the basic principles of action are similar, and many types of non-coding RNAs are present in both kingdoms. Being multifunctional in their ability to interact with various proteins and nucleic acids, small RNAs (sRNAs) encoded by their own genes, as well as fragments of tRNAs, rRNAs, 3′-UTRs, and antisense RNAs, have recently gained increasing attention due to their potential ability to act as signaling molecules establishing interkingdom communications between hosts and microbes. Thus, the goal of the Research Topic was to collect cutting-edge studies exploring biogenesis and RNA-mediated regulatory pathways operating inside bacterial cells and beyond their boundaries.

OPEN ACCESS

Edited and reviewed by:
André P. Gerber,
University of Surrey, United Kingdom

****Correspondence:***
Olga Ozoline
ozoline@rambler.ru

Specialty section:
This article was submitted to Protein and RNA Networks, a section of the journal Frontiers in Molecular Biosciences

Received: *07 October 2021*
Accepted: *19 October 2021*
Published: *10 November 2021*

Citation:
Ozoline O and Shavkunov K (2021) Editorial: Small RNAs as a Diverse Toolkit for Bacteria. Front. Mol. Biosci. 8:791021. doi: 10.3389/fmolb.2021.791021

Diverse Functions Performed by sRNAs Inside Bacterial Cells

The regulatory potential of sRNAs was addressed in five papers. Focusing on the most recent host-pathogen interaction studies, J. J. González Plaza reviewed sRNA-mediated mechanisms providing "the perspective for pathogens" to survive upon entering a host and withstanding such stresses as temperature and pH shifts, oxidative bursts, and iron and nutrient starvation. In addition to direct interactions of several model sRNAs with target mRNAs, the author also discussed their involvement in the regulation of protein regulators and an ability of RNA chaperones to modulate sRNA activity. Many bacterial pathogens causing infections in metazoans, animals, and plants are discussed in this highly informative review with the conclusion that sRNAs as a therapeutic target provide a great opportunity to tackle antibiotic resistance through gene-based treatment.

The ability of sRNAs to modulate the intracellular concentration of regulatory proteins was evaluated by P. M. Sobrero and Valverde. Focusing primarily on the phylogenetic analysis of CsrA family RNA binding proteins, able to affect transcription termination, translation, and stability for hundreds of target RNAs, the authors also discussed mimic Csr/Rsm family sRNAs that expose multiple short hairpins with an unpaired GGA triplet targeted by CsrA, so that CsrA dimers become sequestered in large nucleoprotein complexes. In *Pseudomonas* pangenome the authors revealed five new subfamilies of Rsm genes and discussed the possibility that multiple paralogues may have evolved for regulation of different subsets of target mRNAs.

London et al. studied participation of sRNAs in the envelope stress response in *E. coli* mediated by σ^E. The central role in this signal transduction system belongs to the anti-sigma factor RseA, which

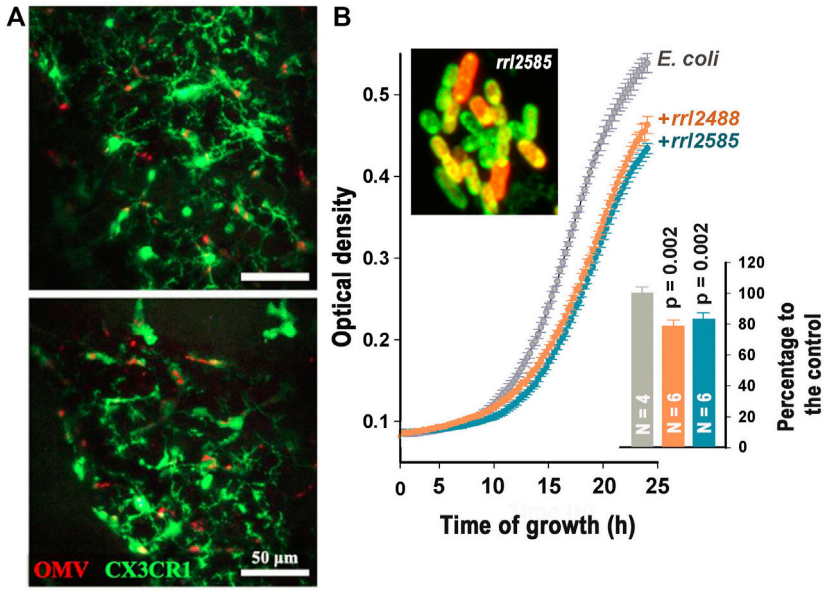

FIGURE 1 | (A): Merged intravital images of murine cortex captured 24 h after injection of *Aggregatibacter actinomycetemcomitans* EVs (OMV) through the tail vein showing colocalization of GFP-stained microglial cells and EVs (red fluorescence). (Ha et al.) **(B)**: Merged image of rrl_2585-Cy 5 (red fluorescence) penetrated into *E. coli* cells and suppression of *E. coli* growth dynamic by two RNA fragments from the secretome of *R. rubrum* (Markelova et al.).

spans the inner membrane and utilizes its cytoplasmic domain for sequestering σ^E. By screening a plasmid library with 30 mostly characterized sRNAs, the authors identified RyhB and FnrS as positive regulators of rseA expression at the posttranscriptional level and evidenced a direct interaction between RyhB and RseA-mRNA 5′-UTR.

In their mini review, Quendera et al. observed the main mechanisms employed by sRNAs for regulatory interaction and conducted a comprehensive analysis of information available on the structure of major ribonucleases and RNA-binding proteins (RBPs) that globally mediate sRNA functioning in prokaryotes. Bringing to attention recent evidence for a wide range of functions of these proteins, the authors cover their involvement in sRNA folding, promotion of sRNA/mRNA basepairing *in cis* and *in trans*, and control of sRNA stability. A special focus was placed on the absence of ProQ and/or Hfq homologs in some organisms, indicating that there are more protein partners for sRNAs to be discovered.

Probably the least studied functionality of potentially regulatory RNAs is described in the paper by Ardern et al. The authors investigated short open reading frames identified in RNAs transcribed from the opposite strand of protein coding genes and gave strong evidence for the functional significance of proteins resulting from abundant antisense translation events registered in model bacteria. A demand for the addition of such embedded antisense protein-coding genes to genome annotations and standardization of methods for their prediction is substantiated and novel strategies for research are proposed.

Expression of sRNA-coding genes was addressed in the paper by Kiselev et al. Using a number of available *E. coli* RNA-seq data sets enriched with *in silico* promoter prediction data, the authors analyzed the pattern of transcripts synthesized from divergently transcribed non-coding RNAs. Being subjected to double regulatory pressure and depending on local dynamics of intensively transcribed DNA, those genes often demonstrate substantial heterogeneity in location of apparent transcription start sites. This means that the same locus can produce transcripts differing in length and hence have different folds and stability. Functionality of such isoforms deserves special attention.

Short RNAs as Signal Molecules in Interkingdom and Interspecies Communications

The paper by Joshi et al. provides the first study characterizing small RNAs released in extracellular vesicles (EV) of an opportunistic pathogen *Staphylococcus aureus*. The authors used iron-depleted medium supplemented with vancomycin, i.e. conditions that mimic an infection treated with antibiotics. As expected, the RNA cargo was enriched with fragments derived from different types of RNAs, but particular attention was paid to the presence of SsrA, RsaC, and RNAIII confirmed by PCR.

Based on the previous observation that EVs of periodontopathogen *Aggregatibacter actinomycetemcomitans* can cross the blood–brain barrier and that their RNA cargo can promote the secretion of proinflammatory cytokines, Ha et al. tested whether the murine brain immune cells can take up bacterial EVs injected through tail veins and convert this to the immune response. Using intravital imaging of the cortex, the authors for the first time captured injected vesicles in meningeal macrophages and microglial cells (**Figure 1A**) and confirmed their ability to promote the secretion of proinflammatory cytokines using a murine microglia cell line BV2. Since only RNAse treatment of EVs lysate prevented elevated secretion of

IL-6, the authors concluded that RNA rather than DNA cargo is the pivotal factor for immune response.

The effect of EV-RNAs on bladder cells turned out to be different (Dauros-Singorenko et al.). The authors compared the iron-responsive effect of RNA cargo from vesicles released by pathogenic (UPEC 536) and probiotic (Nissle 1917) strains of *Escherichia coli* and found 10-fold more lipopolysaccharides associated with purified RNAs from the pathogenic strain. UPEC EV-RNAs delivered to cultured bladder cells in artificial liposomes changed their transcriptome, while EV-RNAs of a non-pathogenic strain did not. However, the effect of lipopolysaccharides, co-purified with RNA samples, on cytokine secretion and gene expression was almost the same as the effect of UPEC EV-RNAs. Thus, it became clear that the presence of lipopolysaccharides should be taken into account upon analysis of interkingdom communications.

To study interspecies communications, the authors (Markelova et al.) analyzed bacterial RNAs secreted by *Escherichia coli* alone and together with *Prevotella copri* or *Rhodospirillum rubrum*. Differential profiling of reads obtained with RNA-seq revealed the dependence of *E. coli* RNA secretome on the presence of competing bacteria and selecting alien oligonucleotides potentially involved in interspecies communication. An ability of two oligonucleotides to penetrate into *E. coli* cells was tested and confirmed using confocal microscopy. Fragments rrl_2488 and rrl_2585 belonging to *R. rubrum* significantly reduced the growth dynamic of *E. coli* (**Figure 1B**), while the inhibitory effect of two *P. copri* RNA fragments was observed only in the presence of their complementary oligonucleotides. To our knowledge, this is the first experimental evidence indicating an ability of bacterial RNAs to suppress the growth of other bacteria.

AUTHOR CONTRIBUTIONS

All authors listed have made a substantial, direct, and intellectual contribution to the work and approved it for publication.

FUNDING

The research of the authors was supported by a grant from the Russian Science Foundation (No 18-14-00348-P).

ACKNOWLEDGMENTS

We thank all the authors who contributed to this Research Topic and the reviewers for their helpful and insightful comments.

Conflict of Interest: The authors declare that the research was conducted in the absence of any commercial or financial relationships that could be construed as a potential conflict of interest.

Publisher's Note: All claims expressed in this article are solely those of the authors and do not necessarily represent those of their affiliated organizations, or those of the publisher, the editors and the reviewers. Any product that may be evaluated in this article, or claim that may be made by its manufacturer, is not guaranteed or endorsed by the publisher.

frontiers in Molecular Biosciences

MINI REVIEW
published: 13 May 2020
doi: 10.3389/fmolb.2020.00078

RNA-Binding Proteins Driving the Regulatory Activity of Small Non-coding RNAs in Bacteria

*Ana P. Quendera, André F. Seixas, Ricardo F. dos Santos, Inês Santos, João P. N. Silva, Cecília M. Arraiano and José M. Andrade**

Instituto de Tecnologia Química e Biológica António Xavier, Universidade Nova de Lisboa, Oeiras, Portugal

Small non-coding RNAs (sRNAs) are critical post-transcriptional regulators of gene expression. Distinct RNA-binding proteins (RBPs) influence the processing, stability and activity of bacterial small RNAs. The vast majority of bacterial sRNAs interact with mRNA targets, affecting mRNA stability and/or its translation rate. The assistance of RNA-binding proteins facilitates and brings accuracy to sRNA-mRNA basepairing and the RNA chaperones Hfq and ProQ are now recognized as the most prominent RNA matchmakers in bacteria. These RBPs exhibit distinct high affinity RNA-binding surfaces, promoting RNA strand interaction between a *trans*-encoding sRNA and its mRNA target. Nevertheless, some organisms lack ProQ and/or Hfq homologs, suggesting the existence of other RBPs involved in sRNA function. Along this line of thought, the global regulator CsrA was recently shown to facilitate the access of an sRNA to its target mRNA and may represent an additional factor involved in sRNA function. Ribonucleases (RNases) can be considered a class of RNA-binding proteins with nucleolytic activity that are responsible for RNA maturation and/or degradation. Presently RNase E, RNase III, and PNPase appear to be the main players not only in sRNA turnover but also in sRNA processing. Here we review the current knowledge on the most important bacterial RNA-binding proteins affecting sRNA activity and sRNA-mediated networks.

Keywords: RNA-binding proteins, RNA chaperone, ribonucleases, small non-coding RNAs, CsrA, Hfq, ProQ

OPEN ACCESS

Edited by:
Olga N. Ozoline, Institute of Cell Biophysics (RAS), Russia

Reviewed by:
Irina Masulis, Institute of Cell Biophysics (RAS), Russia
Claudio Valverde, National University of Quilmes, Argentina

***Correspondence:**
José M. Andrade
andrade@itqb.unl.pt

Specialty section:
This article was submitted to Protein and RNA Networks, a section of the journal Frontiers in Molecular Biosciences

Received: *20 January 2020*
Accepted: *06 April 2020*
Published: *13 May 2020*

Citation:
Quendera AP, Seixas AF, dos Santos RF, Santos I, Silva JPN, Arraiano CM and Andrade JM (2020) RNA-Binding Proteins Driving the Regulatory Activity of Small Non-coding RNAs in Bacteria. Front. Mol. Biosci. 7:78. doi: 10.3389/fmolb.2020.00078

INTRODUCTION

The majority of small non-coding RNAs (sRNAs) interact with a complementary mRNA through an antisense mechanism, leading to the formation of a duplex sRNA-mRNA region. Consequently, expression from the target mRNA is affected and frequently repressed (Storz et al., 2011). sRNA-mediated networks are cost efficient and often more rapid in the reprogramming of gene expression than pathways that rely exclusively on regulatory proteins (Shimoni et al., 2007). However, the interaction between sRNAs and RNA-binding proteins (RBPs) is often critical for the regulatory activity of sRNAs. RNA-binding proteins are a diverse class of proteins ubiquitously found in all living organisms and that control all steps of the life of an RNA (Smirnov et al., 2017a). The capacity of these proteins to recognize and bind RNA molecules arises from the presence of well-defined RNA-binding domains, such as the canonical S1 domain, cold shock

domain (CSD), K homology (KH) domain, amongst others (Holmqvist and Vogel, 2018). Additional regions may also contribute to RNA-protein interactions, like the disordered regions that confer flexibility to proteins. The overall fold of the protein and the recognition of different RNA-binding motifs determines the interaction with RNA in a sequence- and/or structure-specific dependent manner. RBPs and sRNAs networks have been extensively studied in Eukarya and Bacteria, with a current lack of information about this regulation in Archaea (Gelsinger and DiRuggiero, 2018). Though many RBPs can be found in bacteria only few have been shown to associate with sRNAs. However, these participate in a variety of reactions that affect the catalytic and molecular recognition properties of sRNAs.

RNA chaperones constitute a specific group of RBPs that transiently bind and induce structural changes in RNA substrates by melting RNA secondary structures (Woodson et al., 2018). Such structural rearrangements influence not only the stability of sRNA and mRNA molecules but also facilitate the basepairing of sRNAs and mRNAs. Moreover, RNA chaperones that bind simultaneously the sRNA and the target mRNA, bring them closely together in a complex, promoting the annealing and formation of stable RNA-RNA interactions. Though sRNA-mRNA basepairing can occur in the absence of RNA chaperones, their presence greatly accelerates this process (Rajkowitsch and Schroeder, 2007; Panja et al., 2013). Three major RNA chaperones that assist sRNA function in bacteria are currently known: the Sm family member Hfq (Santiago-Frangos and Woodson, 2018), the FinO family member ProQ (Smirnov et al., 2016) and the prototype of its family CsrA (Müller et al., 2019). Despite being widespread, these RBPs are not evenly present in bacteria and the interactome studies of these RNA chaperones indicate they preferably bind different sRNAs (**Figure 1**), suggesting more specialized roles for each of them (Holmqvist et al., 2016, 2018; Smirnov et al., 2016; Melamed et al., 2019).

Ribonucleases (RNases) are another group of specific RBPs that interact with sRNAs. These enzymes are responsible for the catalytic cleavage of all classes of RNA (Arraiano et al., 2010). The stability of sRNAs results from the interplay between RNA chaperones and RNases with the sRNAs, as RNA chaperones may protect or expose the sRNAs to the nucleolytic action of RNases (Holmqvist and Vogel, 2018). The main RNases implicated in sRNA turnover are the endonucleases RNase E and RNase III and the exonuclease PNPase (Saramago et al., 2014). In this mini review, we summarize the current information on the major RNA chaperones and RNases governing the activity of bacterial sRNAs.

RNA CHAPERONES

Hfq

Hfq is widely recognized as a global regulator and key element of sRNA-based networks. Hundreds of sRNA molecules have been reported in *Escherichia coli*, and ∼30% rely on Hfq to carry on their functions (Vogel and Luisi, 2011). Hfq is particularly important for the action of *trans*-encoded sRNAs (which are expressed from a different genomic region than their mRNA targets), stabilizing the imperfect basepairing between sRNA/mRNA pairs. At least in Gram-negative bacteria, Hfq primary role is to promote the annealing of sRNA-mRNA duplexes, acting as a molecular "matchmaker," but its role in Gram-positive bacteria is more controversial (Woodson et al., 2018; Dos Santos et al., 2019). Interestingly, Hfq can bind other substrates including rRNA (Andrade et al., 2018), tRNA (Lee and Feig, 2008), and even DNA molecules (Cech et al., 2016). The wide substrate selection of Hfq suggests additional functions for this protein in the cell, such as its involvement in ribosome biogenesis and translation fidelity (Andrade et al., 2018), and DNA compaction (Jiang et al., 2015; Malabirade et al., 2017). Hfq is also involved in many protein-protein interactions (Caillet et al., 2019), namely with proteins involved in RNA degradation, such as RNase E (Morita et al., 2005), PNPase (Mohanty et al., 2004), and Poly(A) Polymerase (Le Derout et al., 2003). These Hfq-based complexes hint a close relationship between Hfq and the RNA degradation machinery.

Interactome studies identified thousands of Hfq-bound RNA pairs, dominated by mRNA-sRNA pairs exhibiting sequence complementarity (Holmqvist et al., 2016; Melamed et al., 2016; Mihailovic et al., 2018). Hfq binds single-stranded RNA showing a preference for $(ARN)_n$ motifs frequently found on mRNA (Link et al., 2009) and short poly(U) tails present at the 3′-end of sRNAs (Sauer and Weichenrieder, 2011; Sauer et al., 2012). Hfq binds transiently to sRNA and mRNA, dissociating from the RNA duplex soon after basepairing occurs (Fender et al., 2010; Hwang et al., 2011). This widely conserved protein is composed by two N-terminal structural motifs (Sm1 and Sm2) and a variable intrinsically disordered C-terminal tail. The Hfq Sm motifs are characteristic of the Sm/Lsm family of RNA-binding proteins (Møller et al., 2002). Members of this family typically adopt a multimer ring-like architecture, with Hfq assembling into an homohexamer. Multiple RNA-binding surfaces are consequently present in the Hfq ring: the proximal face, the distal face, the lateral rim and the C-terminal tail. The RNA is wrapped around the ring, causing reshaping of the RNA's secondary structure and/or bringing two different strands of RNA into close proximity (Woodson et al., 2018).

sRNAs have been classified in two major classes according to their dependence on Hfq contact surfaces. The vast majority of bacterial sRNAs belong to class I. Hfq contacts these transcripts through binding of its proximal face to the unstructured U-rich stretches present at the 3′-end of sRNAs. On the other hand, the distal face of the Hfq ring preferentially interacts with ARN motifs in mRNAs. The basic patched rim surface may then interact with UA-rich sites present in both RNAs, coordinating the successful annealing between the sRNA-mRNA pair (Panja et al., 2013; Zhang et al., 2013; Schu et al., 2015). As an example, the iron-responsive class I sRNA RyhB relies on Hfq for successful interaction with its targets (Massé et al., 2003). The less abundant class II sRNAs bind Hfq more tightly, as the interaction is done via the proximal and distal faces of the ring (Panja et al., 2013). Class II sRNAs also use Hfq as a hub for promoting duplex formation to their target mRNAs. This is the case for

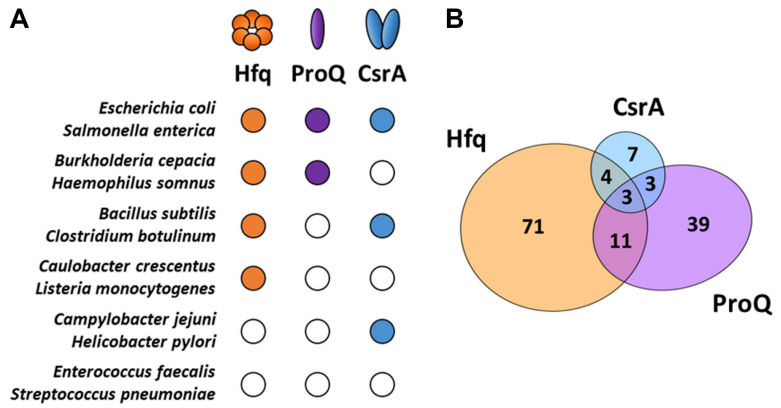

FIGURE 1 | Major RNA chaperones in bacteria. **(A)** RNA chaperone distribution among representative bacteria. The *Escherichia coli* RNA chaperones Hfq, ProQ, and CsrA sequences were used as reference for comparison with other species using the co-occurrence analysis of the STRING database (Szklarczyk et al., 2017). Representative organisms were selected to illustrate the multiple combinations of RNA chaperones expression among bacteria. Close/open circles indicate presence/absence, respectively. **(B)** Venn diagram showing the intersection of sRNA substrates for each one of the RNA chaperones (Hfq, ProQ, and CsrA) in *Salmonella enterica*. Information retrieved from CLIP-seq datasets from Holmqvist et al. (2016, 2018).

the MgrR sRNA regulation of the *eptB* and *ygdQ* transcripts (Kwiatkowska et al., 2018). In both sRNA classes, the C-terminal acidic region of Hfq is suggested to help displace unmatched sRNA-mRNA by transiently competing with the core binding surfaces (Woodson et al., 2018). This competition not only allows for a rapid cycling through the pool of cellular RNAs, but also seems to drive substrate RNA specificity in different bacteria (Santiago-Frangos et al., 2017, 2019).

Hfq remodels RNA conformation by disrupting secondary structures, without the need to hydrolyze ATP. This intrinsic RNA chaperone capability is important to unfold structured RNAs, exposing unpaired RNA stretches for basepairing between complementary strands. One of the best characterized Hfq-dependent sRNAs is MicA, which was found to target the *ompA* mRNA (Udekwu et al., 2005). The RNA chaperone activity of Hfq is also important for remodeling MicA structural elements, altering its stability and binding specificities. Hfq binding rearranges MicA fold to allow exposure of the *ompA*-binding site for pairing that leads to translation repression (Andrade et al., 2013; Henderson et al., 2013). Interestingly, target downregulation may require both Hfq and sRNA independently of an sRNA/Hfq complex formation. The two-step regulation of the *dgcM* mRNA was firstly shown to require Hfq to unfold a 5′-end secondary structure that otherwise occludes the binding sites for the OmrA and OmrB sRNAs. Successful binding of OmrA/B to the early coding sequence of *dgcM* results in translation inhibition of the target mRNA (Hoekzema et al., 2019).

ProQ

ProQ is a recently identified RNA chaperone of the FinO family of RNA-binding proteins commonly found in Proteobacteria (Olejniczak and Storz, 2017). Most of the work on ProQ RNA substrates came from studies performed in *E. coli*, *Salmonella enterica,* and *Legionella pneumophila*, which identified a hundred mRNA transcripts and more than fifty sRNAs as ProQ ligands (Attaiech et al., 2016; Smirnov et al., 2016; Holmqvist et al., 2018; Westermann et al., 2019). ProQ is a monomeric protein with 25 kDa, composed of a α-helical N-terminal domain similar to the RNA-binding domain FinO and a β-sheet C-terminal region partially resembling the eukaryotic Tudor domain. Both regions are connected by a highly flexible and extended linker that is thought to allow the binding and protection of a class of sRNAs that form extended duplexes (Attaiech et al., 2017; Gonzalez et al., 2017; Olejniczak and Storz, 2017). Although both domains contribute to the pairing of complementary RNA molecules, the C-terminal is critical for the RNA strand exchange activity (Chaulk et al., 2011). Unlike Hfq, ProQ binding to RNA is sequence-independent but shows structure preference. ProQ binds double-stranded RNA and prefers highly structured RNAs (Smirnov et al., 2017b; Melamed et al., 2019). The FinO-like domain of ProQ is responsible for this substrate preference (Holmqvist et al., 2018).

Most sRNAs that bind ProQ have unknown functions so far. In contrast to Hfq, the majority of known ProQ-associated sRNAs act *in cis* promoting extensive perfect basepairing with the target mRNA encoded on the opposite strand (Smirnov et al., 2017b). However, ProQ was also found to regulate *trans*-acting sRNAs, assisting the imperfect basepairing with their target mRNAs. Two well characterized examples in *Salmonella* are known: the RaiZ sRNA-*hupA* mRNA and STnc540 sRNA-*mgtB* mRNA (Smirnov et al., 2017b; Westermann et al., 2019). ProQ binds RaiZ through its 3′-terminal stem-loops and promotes interaction of a linear region of this sRNA with the *hupA* mRNA. This three-partner ProQ/RaiZ/*hupA* mRNA complex results in impairment of *hupA* mRNA translation by preventing loading of the 30S ribosome subunit (Smirnov et al., 2017b). STnc540 sRNA also represses the expression of its target mRNA in a ProQ-dependent manner (Westermann et al., 2019). In both examples, ProQ is absolutely required for stability of the sRNAs, affecting their abundance.

Recent work in *E. coli* explores the RNA-RNA interactomes of Hfq and ProQ chaperones using RIL-seq (Melamed et al., 2019). Even though the interactome of ProQ was smaller than the one of Hfq, about a third of the RNA-RNA interactions were common between the two RNA chaperones, with examples like RybB and MalM sRNAs. This suggests complementary or competitive roles for these RBPs. An additional example is found in *Salmonella*, in the regulation mediated by the SraL sRNA. This sRNA binds to the 5′-UTR of the *rho* mRNA, an interaction that can be mediated by ProQ and/or Hfq (Silva et al., 2019). However, the RNAs bound by ProQ generally differ from those bound by Hfq. RIL-seq data revealed that while Hfq-bound RNAs were enriched in both sRNAs and mRNAs, ProQ-bound RNAs were mainly enriched for coding sequences (Melamed et al., 2019). This suggests that the RNA-RNA matchmaking activity of ProQ may not be generalized, unlike observed with Hfq that is primarily involved in sRNA-mediated regulation of mRNA translation. Additional roles for ProQ may include RNA protection from RNase attack or a participation in RNA modification.

CsrA

The CsrA protein was first discovered in *E. coli* and its function attributed to carbon storage and glycogen production, acting as a translational repressor of the *glgC* mRNA (Romeo et al., 1993; Romeo and Babitzke, 2018). In *Pseudomonas aeruginosa* the homolog protein is termed RsmA (for regulator of secondary metabolism) with paralogs (RsmF/N, RsmE, and RsmI) found in different *Pseudomonas* species (Reimmann et al., 2005; Marden et al., 2013; Morris et al., 2013). Members of the CsrA/RsmA family are conserved among Gammaproteobacteria and have been described as global bacterial regulators (Vakulskas et al., 2015). Here we will focus on the information available on the enterobacterial CsrA.

The *E. coli* CsrA is a ∼7 kDa RNA-binding protein and consists of a homodimer, each subunit with five β-strands, one α-helix and an unstructured C-terminal (Gutiérrez et al., 2005; Duss et al., 2014a). The recognition motif is the AUGGA sequence typically localized in the loop of a stem-loop, as determined by SELEX and confirmed through CLIP-seq (Dubey et al., 2005; Duss et al., 2014a; Holmqvist et al., 2016). The most well characterized activity of CsrA is the binding of mRNA, resulting in repression or activation of translation. Typically, CsrA binding occurs in the RBS sequence or overlaps with the initiation codon, leading to a direct inhibition of translation. CsrA can also regulate transcript stability, either by promoting or blocking the access of the mRNA to ribonucleases (Dubey et al., 2005; Schubert et al., 2007; Yakhnin et al., 2013). CsrA also protects sRNAs from RNase E-mediated degradation, as it was shown for the small RNAs CsrB and CsrC (Weilbacher et al., 2003; Vakulskas et al., 2016). Interestingly, CsrA activity on target mRNAs is mostly regulated by the action of the CsrB and CsrC sRNAs (RsmY and RsmZ in Pseudomonads). These highly structured sRNAs are composed of repetitive sequence elements of the recognition motif GGA (22 per molecule in CsrB and 13 in CsrC) with high affinity for the CsrA binding site (Liu et al., 1997; Weilbacher et al., 2003; Duss et al., 2014b). Consequently, CsrB and CsrC act as "sponges" that sequester CsrA protein and prevent its activity (Romeo et al., 2013). The sRNA McaS is also able to modulate CsrA activity though it contains only two recognition sites (Jørgensen et al., 2013). Transcriptomic studies performed in *E. coli* showed that CsrA affects the abundance of 11 sRNAs, including CsrB and CsrC. Additionally, CLIP-seq analysis followed by *in vitro* studies confirmed CsrA binds other sRNAs with high affinity (Potts et al., 2017). In particular, the interaction of CsrA with the sRNAs GadY, Spot 42, and GcvB was shown to significantly overlap with known basepairing regions for these sRNA–mRNA pairs, suggesting that CsrA binding inhibits formation of these RNA duplexes.

CsrA was recently described to act as an RNA chaperone that indirectly promotes the basepairing between the *trans*-acting SR1 sRNA and its primary target the *ahrC* mRNA, which encodes the transcription activator of the arginine catabolic operons in *Bacillus subtilis* (Müller et al., 2019). *In vitro* binding studies demonstrated that CsrA binds these RNAs with high affinity, in the nanomolar range, even in the presence of an mRNA competitor. Further mutational analysis of the SR1 sRNA and the *ahrC* mRNA confirmed binding of CsrA to both transcripts. CsrA facilitates the binding of the SR1 sRNA downstream the start codon of the *ahrC* mRNA and induces conformational changes in the RBS preventing its translation (Müller et al., 2019). Importantly, Hfq was not found to catalyze this interaction and ProQ is not expressed in *B. subtilis*. Interestingly, this suggests that CsrA may act as an alternative RNA chaperone to Hfq and ProQ in assisting sRNA-mRNA basepairing.

RNA- and DNA-Binding Multifunctional Proteins as RNA Chaperones

While Hfq, ProQ, and CsrA may be considered the major RNA chaperones interacting with sRNAs, additional RBPs are known to assist RNA folding and bind sRNAs. Two of such examples include the cold shock proteins (CSPs) and the StpA protein. CSPs are a group of small proteins that display the RNA-binding cold shock domain (CSD) (Phadtare and Severinov, 2010) and can passively remodel RNA structures (Woodson et al., 2018). The major cold shock protein of *E. coli* is CspA that binds RNA with low sequence specificity and in a cooperative fashion (Jiang et al., 1997). CspA activity results in the melting of RNA secondary structures, which favors the unfolded state of transcripts enabling their translation (Rennella et al., 2017). In *Staphylococcus aureus*, a RIP-chip assay identified the RNA targets of CspA, which included several sRNAs (Caballero et al., 2018). Accordingly, it is likely that CspA assists sRNA-mediated regulation. Though not all members of the CSP family are induced by cold, they may be relevant for adaptation to other stresses (Yamanaka et al., 1998). For example, CspC and CspE stimulate translation of *rpoS* (encoding the stress sigma factor S) possibly by altering the secondary structure of the *rpoS* mRNA in *E. coli* (Phadtare and Inouye, 2001; Phadtare et al., 2006) and affect virulence in *Salmonella* (Michaux et al., 2017). *E. coli* StpA is another example of an RNA chaperone that remodels RNA structures without hydrolyzing ATP. StpA has RNA annealing and RNA strand displacement activities (Zhang et al., 1995,

1996). It binds weakly to RNA with preference for unstructured molecules, promoting RNA conformational changes by loosening RNA secondary structures (Mayer et al., 2007). Importantly, the RNA chaperone StpA was found to interact with the small RNA MicF. StpA regulates the stability of MicF sRNA and accelerates its base pairing with the target *ompF* mRNA, acting as a major regulator of the OmpF porin expression (Deighan et al., 2000).

RNASES

RNase E

Homologs of *E. coli* RNase E have been identified in the majority of Proteobacteria classes (Aït-Bara and Carpousis, 2015). This endoribonuclease is composed by a conserved N-terminal catalytic region with an embedded RNA-binding S1 domain, and the unstructured C-terminal non-catalytic region (Bandyra and Luisi, 2018). RNase E cleaves single-stranded RNA, preferably enriched in A/U nucleotides with a stem-loop upstream (Del Campo et al., 2015). Although it prefers substrates with 5′-end monophosphorylated, *in vivo* it is also functional in a 5′-monophosphate-independent pathway (Clarke et al., 2014). Upon Hfq dissociation from the sRNA-mRNA pairs, RNase E can reach and cleave the target mRNA in a linear stretch at the 3′-end of the duplex region (Waters et al., 2017). The sRNAs RyhB and GcvB are typical examples in which sRNA pairing with the coding region promotes mRNA decay via the recruitment of RNase E (Massé et al., 2003; Morita et al., 2005; Lalaouna et al., 2019). Often the base paired sRNA is also degraded with the mRNA. McaS sRNA bound to Hfq interacts with both RNase E and its substrate *csgD* mRNA, leading to the cleavage of both RNAs (Andreassen et al., 2018). RNase E is also critical for the processing of sRNAs from the 3′ UTR of mRNAs, including the release of the CpxQ sRNA from the 3′-end of the *cpxP* mRNA (Chao and Vogel, 2016) and the processing of the precursor RNA to originate the functional ArcZ (Chao et al., 2017). A paralog named RNase G that contains only the catalytic domain of RNase E is also present in *E. coli* and other bacteria (Aït-Bara and Carpousis, 2015). Although this non-essential enzyme shares common activities with RNase E, including rRNA processing and mRNA turnover, no role has been ascribed for RNase G in sRNA processing (Mackie, 2013). Interestingly, RNase E activity on sRNAs can be modulated by other RNA-binding proteins. This is the case of RapZ, an RBP that functions as an adaptor protein in *E. coli*. RapZ binds to the central stem loop of the sRNA GlmZ and RNase E is then recruited for the processing of this sRNA (Göpel et al., 2013), which regulates the *glmS* mRNA encoding the glucosamine-6-phosphate (GlcN6P) synthase. RapZ was recently found to be the receptor for GlcN6P (Khan et al., 2020).

RNase III

RNase III is a widely distributed endoribonuclease involved in the processing of double-stranded RNAs (dsRNAs). *E. coli* RNase III acts as a 52 kDa homodimer, with the catalytic N-terminal domain connected by a short linker to the C-terminal dsRNA-binding domain (Li and Nicholson, 1996). RNase III can cleave the duplex RNA formed between complementary regions of sRNA and its target mRNA (Lybecker et al., 2014; Altuvia et al., 2018). The target-coupled pathway for RNase III degradation mediated via sRNAs is commonly observed in bacteria. In *Salmonella*, RNase III is responsible for the degradation of the dsRNA formed between MicA and its target *ompA* mRNA upon basepairing (Viegas et al., 2011). In *B. subtilis*, the 3′-end of the

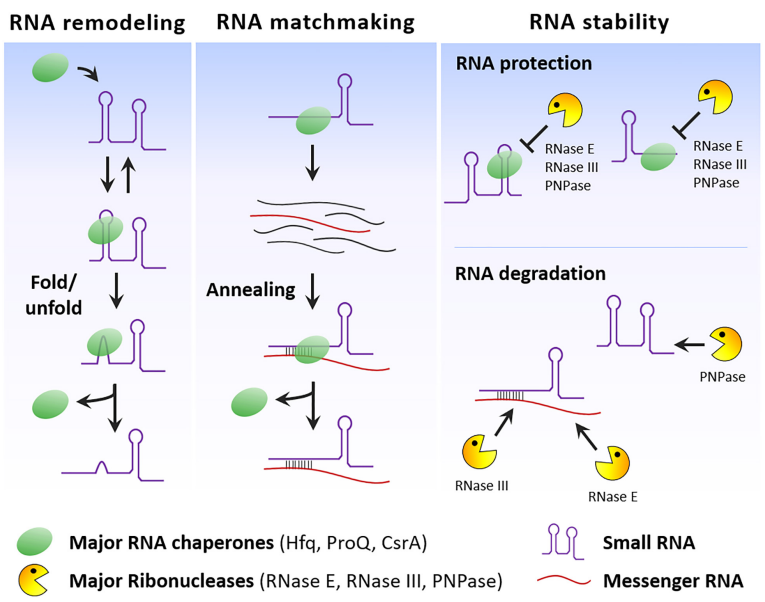

FIGURE 2 | RNA chaperone and RNase activities on sRNAs. Simplified scheme that illustrates the effect of these RNA-binding proteins in different aspects of the sRNA lifetime, namely on the folding of sRNA secondary structures, promotion of sRNA/mRNA basepairing and control of sRNA stability.

antitoxin RatA sRNA forms a large duplex with the *txpA* mRNA that is cleaved by RNase III and prevents the translation of TxpA toxin (Durand et al., 2012). In *Streptococcus pyogenes*, the type II CRISPR-Cas system depends on the maturation of CRISPR RNA by RNase III (Deltcheva et al., 2011).

PNPase

Polynucleotide phosphorylase (PNPase) is a highly conserved 3′–5′ exoribonuclease that processively degrades RNA (Saramago et al., 2014; Dos Santos et al., 2018). PNPase adopts a homotrimeric organization with a ring-like structure, each monomer having a molecular weight of 78 kDa and holding two RNA-binding domains, KH and S1, on the C-terminal (Shi et al., 2008). In *E. coli*, PNPase is the main enzyme involved in the degradation of sRNAs that are not bound to Hfq, as shown for the regulation of different Hfq-dependent sRNAs, such as MicA, GlmY, RyhB, and SgrS levels (Andrade et al., 2012, 2013). This effect is growth-phase regulated and agrees with previous work in which PNPase was found to degrade sRNAs in the absence of their primary target mRNAs (Andrade and Arraiano, 2008). Additionally, PNPase has an unexpected role in *Listeria monocytogenes*, being responsible for the correct processing of an orphan CRISPR RNA (Sesto et al., 2014).

Although to a lesser extent, additional RNases are involved in the regulation of sRNAs. The degradative enzymes YbeY and RNase R are illustrative examples. YbeY is a highly conserved endoribonuclease commonly associated with rRNA processing (Davies et al., 2010). However, YbeY was shown to bind sRNAs and regulate the levels of sRNAs and mRNAs (Pandey et al., 2011). In *Sinorhizobium meliloti* it was shown that YbeY could cleave sRNA-mRNA pairs (Saramago et al., 2017). Inactivation of YbeY in *E. coli* cells exposed to hydroxyurea resulted in the upregulation of many sRNAs involved in the adaptation to oxidative stress (Pandey et al., 2014). Additionally, *Vibrio cholerae* YbeY was found to regulate the abundance of the sRNAs Qrr1-4 (Vercruysse et al., 2014), which are involved in quorum-sensing and virulence (Tu and Bassler, 2007). RNase R is a unique 3′–5′ exoribonuclease able to degrade highly structured RNAs (Dos Santos et al., 2018). There are few described examples of RNase R involved in the regulation of sRNAs. During cold shock in *E. coli*, RNase R is required for the correct processing of the sRNA SsrA/tmRNA (transfer-messenger RNA), involved in protein quality control and ribosome recycling (Cairrão et al., 2003). RNase R was also described to control sRNA stability of the sRNA SR4 and its target *bsrG* mRNA that together constitute a temperature-dependent type I toxin/antitoxin system in *Bacillus subtilis* (Jahn et al., 2012).

CONCLUSION

RNA chaperones can modify sRNA structure, facilitate the basepairing of sRNAs to their target mRNAs and together with RNases control sRNA stability (**Figure 2**). However, some RNA chaperones seem to be specific of some species and the activities performed by these regulators may be compensated by other still unidentified RNA-binding proteins. Several RBPs with unorthodox RNA-binding domains have been identified in humans, expanding the number of proteins that can associate with RNA (Castello et al., 2016). Therefore, it is also possible that additional and probably unconventional RBPs interacting with sRNA are going to be discovered in bacteria. The RNA chaperone ProQ offers us a good example of this potential. A new RNA-seq methodology associated to sample fractionation (Grad-seq) contributed to the identification of ProQ as a novel RBP interacting with sRNAs (Smirnov et al., 2016). Application of this and similar methods may contribute to expand the number of sRNA-protein partners and helps to shed light on the many still unknown functions and physiological roles of sRNAs.

AUTHOR CONTRIBUTIONS

JA outlined the manuscript. AQ, AS, and RS prepared the figures. CA and JA supervised the work. All authors wrote and participated in preparation of the final manuscript.

FUNDING

This work was supported by Project LISBOA-01-0145-FEDER-007660 (Microbiologia Molecular, Estrutural e Celular) funded by FEDER through COMPETE2020 - Programa Operacional Competitividade e Internacionalização (POCI) and by FCT—Fundação para a Ciência e a Tecnologia (Portugal), including Program IF (IF/00961/2014) and Grants PTDC/IMI-MIC/4463/2014 and PTDC/BIA-MIC/32525/2017 to JA, Grant PTDC/BIA-MIC/1399/2014 to CA, the Doctoral fellowships PD/BD/135487/2018 to AQ, and PD/BD/146136/2019 to AS.

REFERENCES

Aït-Bara, S., and Carpousis, A. J. (2015). RNA degradosomes in bacteria and chloroplasts: classification, distribution and evolution of RNase E homologs. *Mol. Microbiol.* 97, 1021–1135 doi: 10.1111/mmi.13095

Altuvia, Y., Bar, A., Reiss, N., Karavani, E., Argaman, L., and Margalit, H. (2018). In vivo cleavage rules and target repertoire of RNase III in *Escherichia coli*. *Nucleic Acids Res.* 46, 10380–10394. doi: 10.1093/nar/gky684

Andrade, J. M., and Arraiano, C. M. (2008). PNPase is a key player in the regulation of small RNAs that control the expression of outer membrane proteins. *RNA* 14, 543–551. doi: 10.1261/rna.683308

Andrade, J. M., Dos Santos, R. F., Chelysheva, I., Ignatova, Z., and Arraiano, C. M. (2018). The RNA-binding protein Hfq is important for ribosome biogenesis and affects translation fidelity. *EMBO J.* 37:e97631. doi: 10.15252/embj.201797631

Andrade, J. M., Pobre, V., and Arraiano, C. M. (2013). Small RNA modules confer different stabilities and interact differently with multiple targets. *PLoS One* 8:e52866. doi: 10.1371/journal.pone.0052866

Andrade, J. M., Pobre, V., Matos, A. M., and Arraiano, C. M. (2012). The crucial role of PNPase in the degradation of small RNAs that are not associated with Hfq. *RNA* 18, 844–855. doi: 10.1261/rna.029413.111

Andreassen, P. R., Pettersen, J. S., Szczerba, M., Valentin-Hansen, P., Møller-Jensen, J., and Jørgensen, M. G. (2018). sRNA-dependent control of curli

biosynthesis in *Escherichia coli*: McaS directs endonucleolytic cleavage of *csg*D mRNA. *Nucleic Acids Res.* 46, 6746–6760. doi: 10.1093/nar/gky479

Arraiano, C. M., Andrade, J. M., Domingues, S., Guinote, I. B., Malecki, M., Matos, R. G., et al. (2010). The critical role of RNA processing and degradation in the control of gene expression. *FEMS Microbiol. Rev.* 34, 883–923. doi: 10.1111/j.1574-6976.2010.00242.x

Attaiech, L., Boughammoura, A., Brochier-Armanet, C., Allatif, O., Peillard-Fiorente, F., Edwards, R. A., et al. (2016). Silencing of natural transformation by an RNA chaperone and a multitarget small RNA. *Proc. Natl. Acad. Sci. U.S.A.* 113, 8813–8818. doi: 10.1073/pnas.1601626113

Attaiech, L., Glover, J. N. M., and Charpentier, X. (2017). RNA chaperones step out of Hfq's shadow. *Trends Microbiol.* 25, 247–249. doi: 10.1016/j.tim.2017.01.006

Bandyra, K. J., and Luisi, B. F. (2018). RNase E and the high-fidelity orchestration of RNA metabolism. *Microbiol. Spectr.* 6:RWR-0008-2017. doi: 10.1128/microbiolspec.RWR-0008-2017

Caballero, C. J., Menendez-Gil, P., Catalan-Moreno, A., Vergara-Irigaray, M., García, B., Segura, V., et al. (2018). The regulon of the RNA chaperone CspA and its auto-regulation in Staphylococcus aureus. *Nucleic Acids Res.* 46, 1345–1361. doi: 10.1093/nar/gkx1284

Caillet, J., Baron, B., Boni, I. V., Caillet-Saguy, C., and Hajnsdorf, E. (2019). Identification of protein-protein and ribonucleoprotein complexes containing Hfq. *Sci. Rep.* 9:14054. doi: 10.1038/s41598-019-50562-w

Cairrão, F., Cruz, A., Mori, H., and Arraiano, C. M. (2003). Cold shock induction of RNase R and its role in the maturation of the quality control mediator SsrA/tmRNA. *Mol. Microbiol.* 50, 1349–1360. doi: 10.1046/j.1365-2958.2003.03766.x

Castello, A., Fischer, B., Frese, C. K., Horos, R., Alleaume, A.-M., Foehr, S., et al. (2016). Comprehensive identification of RNA-binding domains in human cells. *Mol. Cell* 63, 696–710. doi: 10.1016/j.molcel.2016.06.029

Cech, G. M., Szalewska-Pałasz, A., Kubiak, K., Malabirade, A., Grange, W., Arluison, V., et al. (2016). The *Escherichia coli* Hfq protein: an unattended DNA-transactions regulator. *Front. Mol. Biosci.* 3:36. doi: 10.3389/fmolb.2016.00036

Chao, Y., Li, L., Girodat, D., Förstner, K. U., Said, N., Corcoran, C., et al. (2017). *In vivo* cleavage map illuminates the central role of RNase E in coding and non-coding RNA pathways. *Mol. Cell* 65, 39–51. doi: 10.1016/j.molcel.2016.11.002

Chao, Y., and Vogel, J. (2016). A 3' UTR-derived small RNA provides the regulatory noncoding arm of the inner membrane stress response. *Mol. Cell* 61, 352–363. doi: 10.1016/j.molcel.2015.12.023

Chaulk, S. G., Smith Frieday, M. N., Arthur, D. C., Culham, D. E., Edwards, R. A., Soo, P., et al. (2011). ProQ is an RNA chaperone that controls ProP levels in *Escherichia coli*. *Biochemistry* 50, 3095–3106. doi: 10.1021/bi101683a

Clarke, J. E., Kime, L., Romero, A. D., and McDowall, K. J. (2014). Direct entry by RNase E is a major pathway for the degradation and processing of RNA in *Escherichia coli*. *Nucleic Acids Res.* 42, 11733–11751. doi: 10.1093/nar/gku808

Davies, B. W., Köhrer, C., Jacob, A. I., Simmons, L. A., Zhu, J., Aleman, L. M., et al. (2010). Role of *Escherichia coli* YbeY, a highly conserved protein, in rRNA processing. *Mol. Microbiol.* 78, 506–518. doi: 10.1111/j.1365-2958.2010.07351.x

Deighan, P., Free, A., and Dorman, C. J. (2000). A role for the *Escherichia coli* H-NS-like protein StpA in OmpF porin expression through modulation of micF RNA stability. *Mol. Microbiol.* 38, 126–139. doi: 10.1046/j.1365-2958.2000.02120.x

Del Campo, C., Bartholomäus, A., Fedyunin, I., and Ignatova, Z. (2015). Secondary structure across the bacterial transcriptome reveals versatile roles in mRNA regulation and function. *PLoS Genet.* 11:e1005613. doi: 10.1371/journal.pgen.1005613

Deltcheva, E., Chylinski, K., Sharma, C. M., Gonzales, K., Chao, Y., Pirzada, Z. A., et al. (2011). CRISPR RNA maturation by trans-encoded small RNA and host factor RNase III. *Nature* 471, 602–607. doi: 10.1038/nature09886

Dos Santos, R. F., Arraiano, C. M., and Andrade, J. M. (2019). New molecular interactions broaden the functions of the RNA chaperone Hfq. *Curr. Genet.* 65, 1313–1319. doi: 10.1007/s00294-019-00990-y

Dos Santos, R. F., Quendera, A. P., Boavida, S., Seixas, A. F., Arraiano, C. M., and Andrade, J. M. (2018). Major 3'-5' exoribonucleases in the metabolism of coding and non-coding RNA. *Prog. Mol. Biol. Transl. Sci.* 159, 101–155. doi: 10.1016/bs.pmbts.2018.07.005

Dubey, A. K., Baker, C. S., Romeo, T., and Babitzke, P. (2005). RNA sequence and secondary structure participate in high-affinity CsrA-RNA interaction. *RNA* 11, 1579–1587. doi: 10.1261/rna.2990205

Durand, S., Gilet, L., Bessières, P., Nicolas, P., and Condon, C. (2012). Three essential ribonucleases-RNase Y, J1, and III-control the abundance of a majority of *Bacillus subtilis* mRNAs. *PLoS Genet.* 8:e1002520. doi: 10.1371/journal.pgen.1002520

Duss, O., Michel, E., Dit Konté, N. D., Schubert, M., and Allain, F. H. T. (2014a). Molecular basis for the wide range of affinity found in Csr/Rsm protein-RNA recognition. *Nucleic Acids Res.* 42, 5332–5346. doi: 10.1093/nar/gku141

Duss, O., Michel, E., Yulikov, M., Schubert, M., Jeschke, G., and Allain, F. H.-T. (2014b). Structural basis of the non-coding RNA RsmZ acting as a protein sponge. *Nature* 509, 588–592. doi: 10.1038/nature13271

Fender, A., Elf, J., Hampel, K., Zimmermann, B., and Wagner, E. G. H. (2010). RNAs actively cycle on the Sm-like protein Hfq. *Genes Dev.* 24, 2621–2626. doi: 10.1101/gad.591310

Gelsinger, D. R., and DiRuggiero, J. (2018). The non-coding regulatory RNA revolution in archaea. *Genes (Basel)* 9:141. doi: 10.3390/genes9030141

Gonzalez, G. M., Hardwick, S. W., Maslen, S. L., Skehel, J. M., Holmqvist, E., Vogel, J., et al. (2017). Structure of the *Escherichia coli* ProQ RNA-binding protein. *RNA* 23, 696–711. doi: 10.1261/rna.060343.116

Göpel, Y., Papenfort, K., Reichenbach, B., Vogel, J., and Görke, B. (2013). Targeted decay of a regulatory small RNA by an adaptor protein for RNase E and counteraction by an anti-adaptor RNA. *Genes Dev.* 27, 552–564. doi: 10.1101/gad.210112.112

Gutiérrez, P., Li, Y., Osborne, M. J., Pomerantseva, E., Liu, Q., and Gehring, K. (2005). Solution structure of the carbon storage regulator protein CsrA from *Escherichia coli*. *J. Bacteriol.* 187, 3496–3501. doi: 10.1128/JB.187.10.3496-3501.2005

Henderson, C. A., Vincent, H. A., Stone, C. M., Phillips, J. O., Cary, P. D., Gowers, D. M., et al. (2013). Characterization of MicA interactions suggests a potential novel means of gene regulation by small non-coding RNAs. *Nucleic Acids Res.* 41, 3386–3397. doi: 10.1093/nar/gkt008

Hoekzema, M., Romilly, C., Holmqvist, E., and Wagner, E. G. H. (2019). Hfq−dependent mRNA unfolding promotes sRNA −based inhibition of translation. *EMBO J.* 38:e101199. doi: 10.15252/embj.2018101199

Holmqvist, E., Li, L., Bischler, T., Barquist, L., and Vogel, J. (2018). Global maps of ProQ binding In Vivo reveal target recognition via RNA structure and stability control at mRNA 3' ends. *Mol. Cell* 70, 971–982.e6. doi: 10.1016/j.molcel.2018.04.017

Holmqvist, E., and Vogel, J. (2018). RNA-binding proteins in bacteria. *Nat. Rev. Microbiol.* 16, 601–615. doi: 10.1038/s41579-018-0049-5

Holmqvist, E., Wright, P. R., Li, L., Bischler, T., Barquist, L., Reinhardt, R., et al. (2016). Global RNA recognition patterns of post-transcriptional regulators Hfq and CsrA revealed by UV crosslinking *in vivo*. *EMBO J.* 35, 991–1011. doi: 10.15252/embj.201593360

Hwang, W., Arluison, V., and Hohng, S. (2011). Dynamic competition of DsrA and rpoS fragments for the proximal binding site of Hfq as a means for efficient annealing. *Nucleic Acids Res.* 39, 5131–5139. doi: 10.1093/nar/gkr075

Jahn, N., Preis, H., Wiedemann, C., and Brantl, S. (2012). BsrG/SR4 from *Bacillus subtilis* - the first temperature-dependent type I toxin-antitoxin system. *Mol. Microbiol.* 83, 579–598. doi: 10.1111/j.1365-2958.2011.07952.x

Jiang, K., Zhang, C., Guttula, D., Liu, F., Van Kan, J. A., Lavelle, C., et al. (2015). Effects of Hfq on the conformation and compaction of DNA. *Nucleic Acids Res.* 43, 4332–4341. doi: 10.1093/nar/gkv268

Jiang, W., Hou, Y., and Inouye, M. (1997). CspA, the major cold-shock protein of *Escherichia coli*, is an RNA chaperone. *J. Biol. Chem.* 272, 196–202. doi: 10.1074/jbc.272.1.196

Jørgensen, M. G., Thomason, M. K., Havelund, J., Valentin-Hansen, P., and Storz, G. (2013). Dual function of the McaS small RNA in controlling biofilm formation. *Genes Dev.* 27, 1132–1145. doi: 10.1101/gad.214734.113

Khan, M. A., Durica-Mitic, S., Göpel, Y., Heermann, R., and Görke, B. (2020). Small RNA-binding protein RapZ mediates cell envelope precursor sensing and signaling in *Escherichia coli*. *EMBO J.* 39:e103848. doi: 10.15252/embj.2019103848

Kwiatkowska, J., Wroblewska, Z., Johnson, K. A., and Olejniczak, M. (2018). The binding of Class II sRNA MgrR to two different sites on matchmaker protein

Hfq enables efficient competition for Hfq and annealing to regulated mRNAs. *RNA* 24, 1761–1784. doi: 10.1261/rna.067777.118

Lalaouna, D., Eyraud, A., Devinck, A., Prévost, K., and Massé, E. (2019). GcvB small RNA uses two distinct seed regions to regulate an extensive targetome. *Mol. Microbiol.* 111, 473–486. doi: 10.1111/mmi.14168

Le Derout, J., Folichon, M., Briani, F., Dehò, G., Régnier, P., and Hajnsdorf, E. (2003). Hfq affects the length and the frequency of short oligo(A) tails at the 3' end of *Escherichia coli rps*O mRNAs. *Nucleic Acids Res.* 31, 4017–4023. doi: 10.1093/nar/gkg456

Lee, T., and Feig, A. L. (2008). The RNA binding protein Hfq interacts specifically with tRNAs. *RNA* 14, 514–523. doi: 10.1261/rna.531408

Li, H., and Nicholson, A. W. (1996). Defining the enzyme binding domain of a ribonuclease III processing signal. Ethylation interference and hydroxyl radical footprinting using catalytically inactive RNase III mutants. *EMBO J.* 15, 1421–1433. doi: 10.1002/j.1460-2075.1996.tb00484.x

Link, T. M., Valentin-Hansen, P., and Brennan, R. G. (2009). Structure of *Escherichia coli* Hfq bound to polyriboadenylate RNA. *Proc. Natl. Acad. Sci. U.S.A.* 106, 19292–19297. doi: 10.1073/pnas.0908744106

Liu, M. Y., Gui, G., Wei, B., Preston, J. F., Oakford, L., Yüksel, U., et al. (1997). The RNA molecule CsrB binds to the global regulatory protein CsrA and antagonizes its activity in *Escherichia coli*. *J. Biol. Chem.* 272, 17502–17510. doi: 10.1074/jbc.272.28.17502

Lybecker, M., Zimmermann, B., Bilusic, I., Tukhtubaeva, N., and Schroeder, R. (2014). The double-stranded transcriptome of *Escherichia coli*. *Proc. Natl. Acad. Sci. U.S.A.* 111, 3134–3139. doi: 10.1073/pnas.1315974111

Mackie, G. A. (2013). RNase E: at the interface of bacterial RNA processing and decay. *Nat. Rev. Microbiol.* 11, 45–57. doi: 10.1038/nrmicro2930

Malabirade, A., Jiang, K., Kubiak, K., Diaz-Mendoza, A., Liu, F., van Kan, J. A., et al. (2017). Compaction and condensation of DNA mediated by the C-terminal domain of Hfq. *Nucleic Acids Res.* 45, 7299–7308. doi: 10.1093/nar/gkx431

Marden, J. N., Diaz, M. R., Walton, W. G., Gode, C. J., Betts, L., Urbanowski, M. L., et al. (2013). An unusual CsrA family member operates in series with RsmA to amplify posttranscriptional responses in *Pseudomonas aeruginosa*. *Proc. Natl. Acad. Sci. U.S.A.* 110, 15055–15060. doi: 10.1073/pnas.1307217110

Massé, E., Escorcia, F. E., and Gottesman, S. (2003). Coupled degradation of a small regulatory RNA and its mRNA targets in *Escherichia coli*. *Genes Dev.* 17, 2374–2383. doi: 10.1101/gad.1127103

Mayer, O., Rajkowitsch, L., Lorenz, C., Konrat, R., and Schroeder, R. (2007). RNA chaperone activity and RNA-binding properties of the *E. coli* protein StpA. *Nucleic Acids Res.* 35, 1257–1269. doi: 10.1093/nar/gkl1143

Melamed, S., Adams, P. P., Zhang, A., Zhang, H., and Storz, G. (2019). RNA-RNA Interactomes of ProQ and Hfq reveal overlapping and competing roles. *Mol. Cell* 77, 411–425.e7. doi: 10.1016/j.molcel.2019.10.022

Melamed, S., Peer, A., Faigenbaum-Romm, R., Gatt, Y. E., Reiss, N., Bar, A., et al. (2016). Global mapping of small RNA-target interactions in bacteria. *Mol. Cell* 63, 884–897. doi: 10.1016/j.molcel.2016.07.026

Michaux, C., Holmqvist, E., Vasicek, E., Sharan, M., Barquist, L., Westermann, A. J., et al. (2017). RNA target profiles direct the discovery of virulence functions for the cold-shock proteins CspC and CspE. *Proc. Natl. Acad. Sci. U.S.A.* 114, 6824–6829. doi: 10.1073/pnas.1620772114

Mihailovic, M. K., Vazquez-Anderson, J., Li, Y., Fry, V., Vimalathas, P., Herrera, D., et al. (2018). High-throughput *in vivo* mapping of RNA accessible interfaces to identify functional sRNA binding sites. *Nat. Commun.* 9:4084. doi: 10.1038/s41467-018-06207-z

Mohanty, B. K., Maples, V. F., and Kushner, S. R. (2004). The Sm-like protein Hfq regulates polyadenylation dependent mRNA decay in *Escherichia coli*. *Mol. Microbiol.* 54, 905–920. doi: 10.1111/j.1365-2958.2004.04337.x

Møller, T., Franch, T., Højrup, P., Keene, D. R., Bächinger, H. P., Brennan, R. G., et al. (2002). Hfq: a bacterial Sm-like protein that mediates RNA-RNA interaction. *Mol. Cell* 9, 23–30. doi: 10.1016/s1097-2765(01)00436-1

Morita, T., Maki, K., and Aiba, H. (2005). RNase E-based ribonucleoprotein complexes: mechanical basis of mRNA destabilization mediated by bacterial noncoding RNAs. *Genes Dev.* 19, 2176–2186. doi: 10.1101/gad.1330405

Morris, E. R., Hall, G., Li, C., Heeb, S., Kulkarni, R. V., Lovelock, L., et al. (2013). Structural rearrangement in an RsmA/CsrA Ortholog of *Pseudomonas aeruginosa* creates a dimeric RNA-binding protein, RsmN. *Structure* 21, 1659–1671. doi: 10.1016/j.str.2013.07.007

Müller, P., Gimpel, M., Wildenhain, T., and Brantl, S. (2019). A new role for CsrA: promotion of complex formation between an sRNA and its mRNA target in *Bacillus subtilis*. *RNA Biol.* 16, 972–987. doi: 10.1080/15476286.2019.1605811

Olejniczak, M., and Storz, G. (2017). ProQ/FinO-domain proteins: another ubiquitous family of RNA matchmakers? *Mol. Microbiol.* 104, 905–915. doi: 10.1111/mmi.13679

Pandey, S. P., Minesinger, B. K., Kumar, J., and Walker, G. C. (2011). A highly conserved protein of unknown function in *Sinorhizobium meliloti* affects sRNA regulation similar to Hfq. *Nucleic Acids Res.* 39, 4691–4708. doi: 10.1093/nar/gkr060

Pandey, S. P., Winkler, J. A., Li, H., Camacho, D. M., Collins, J. J., and Walker, G. C. (2014). Central role for RNase YbeY in Hfq-dependent and Hfq-independent small-RNA regulation in bacteria. *BMC Genomics* 15:121. doi: 10.1186/1471-2164-15-121

Panja, S., Schu, D. J., and Woodson, S. A. (2013). Conserved arginines on the rim of Hfq catalyze base pair formation and exchange. *Nucleic Acids Res.* 41, 7536–7546. doi: 10.1093/nar/gkt521

Phadtare, S., and Inouye, M. (2001). Role of CspC and CspE in regulation of expression of RpoS and UspA, the stress response proteins in *Escherichia coli*. *J. Bacteriol.* 183, 1205–1214. doi: 10.1128/JB.183.4.1205-1214.2001

Phadtare, S., and Severinov, K. (2010). RNA remodeling and gene regulation by cold shock proteins. *RNA Biol.* 7, 788–795. doi: 10.4161/rna.7.6.13482

Phadtare, S., Tadigotla, V., Shin, W. H., Sengupta, A., and Severinov, K. (2006). Analysis of *Escherichia coli* global gene expression profiles in response to overexpression and deletion of CspC and CspE. *J. Bacteriol.* 188, 2521–2527. doi: 10.1128/JB.188.7.2521-2527.2006

Potts, A. H., Vakulskas, C. A., Pannuri, A., Yakhnin, H., Babitzke, P., and Romeo, T. (2017). Global role of the bacterial post-transcriptional regulator CsrA revealed by integrated transcriptomics. *Nat. Commun.* 8:1596. doi: 10.1038/s41467-017-01613-1

Rajkowitsch, L., and Schroeder, R. (2007). Dissecting RNA chaperone activity. *RNA* 13, 2053–2060. doi: 10.1261/rna.671807

Reimmann, C., Valverde, C., Kay, E., and Haas, D. (2005). Posttranscriptional repression of GacS/GacA-controlled genes by the RNA-binding protein RsmE acting together with RsmA in the biocontrol strain *Pseudomonas fluorescens* CHA0. *J. Bacteriol.* 187, 276–285. doi: 10.1128/JB.187.1.276-285.2005

Rennella, E., Sára, T., Juen, M., Wunderlich, C., Imbert, L., Solyom, Z., et al. (2017). RNA binding and chaperone activity of the *E. coli* cold-shock protein CspA. *Nucleic Acids Res.* 45, 4255–4268. doi: 10.1093/nar/gkx044

Romeo, T., and Babitzke, P. (2018). Global Regulation by CsrA and Its RNA Antagonists. *Microbiol. Spectr.* 6:RWR–0009–2017. doi: 10.1128/microbiolspec.rwr-0009-2017

Romeo, T., Gong, M., Liu, M. Y., and Brun-Zinkernagel, A. M. (1993). Identification and molecular characterization of *csrA*, a pleiotropic gene from *Escherichia coli* that affects glycogen biosynthesis, gluconeogenesis, cell size, and surface properties. *J. Bacteriol.* 175, 4744–4755. doi: 10.1128/jb.175.15.4744-4755.1993

Romeo, T., Vakulskas, C. A., and Babitzke, P. (2013). Post-transcriptional regulation on a global scale: form and function of Csr/Rsm systems. *Environ. Microbiol.* 15, 313–324. doi: 10.1111/j.1462-2920.2012.02794.x

Santiago-Frangos, A., Fröhlich, K. S., Jeliazkov, J. R., Małecka, E. M., Marino, G., Gray, J. J., et al. (2019). Caulobacter crescentus Hfq structure reveals a conserved mechanism of RNA annealing regulation. *Proc. Natl. Acad. Sci. U.S.A.* 166, 10978–10987. doi: 10.1073/pnas.1814428116

Santiago-Frangos, A., Jeliazkov, J. R., Gray, J. J., and Woodson, S. A. (2017). Acidic C-terminal domains autoregulate the RNA chaperone Hfq. *eLife* 6:e27049. doi: 10.7554/eLife.27049

Santiago-Frangos, A., and Woodson, S. A. (2018). Hfq chaperone brings speed dating to bacterial sRNA. *Wiley Interdiscip. Rev. RNA* 9:e1475. doi: 10.1002/wrna.1475

Saramago, M., Bárria, C., Dos Santos, R. F., Silva, I. J., Pobre, V., Domingues, S., et al. (2014). The role of RNases in the regulation of small RNAs. *Curr. Opin. Microbiol.* 18, 105–115. doi: 10.1016/j.mib.2014.02.009

Saramago, M., Peregrina, A., Robledo, M., Matos, R. G., Hilker, R., Serrania, J., et al. (2017). *Sinorhizobium meliloti* YbeY is an endoribonuclease with unprecedented catalytic features, acting as silencing enzyme in riboregulation. *Nucleic Acids Res.* 45, 1371–1391. doi: 10.1093/nar/gkw1234

Sauer, E., Schmidt, S., and Weichenrieder, O. (2012). Small RNA binding to the lateral surface of Hfq hexamers and structural rearrangements upon mRNA

target recognition. *Proc. Natl. Acad. Sci. U.S.A.* 109, 9396–9401. doi: 10.1073/pnas.1202521109

Sauer, E., and Weichenrieder, O. (2011). Structural basis for RNA 3'-end recognition by Hfq. *Proc. Natl. Acad. Sci. U.S.A.* 108, 13065–13070. doi: 10.1073/pnas.1103420108

Schu, D. J., Zhang, A., Gottesman, S., and Storz, G. (2015). Alternative Hfq-sRNA interaction modes dictate alternative mRNA recognition. *EMBO J.* 34, 2557–2573. doi: 10.15252/embj.201591569

Schubert, M., Lapouge, K., Duss, O., Oberstrass, F. C., Jelesarov, I., Haas, D., et al. (2007). Molecular basis of messenger RNA recognition by the specific bacterial repressing clamp RsmA/CsrA. *Nat. Struct. Mol. Biol.* 14, 807–813. doi: 10.1038/nsmb1285

Sesto, N., Touchon, M., Andrade, J. M., Kondo, J., Rocha, E. P. C., Arraiano, C. M., et al. (2014). A PNPase dependent CRISPR System in Listeria. *PLoS Genet.* 10:e1004065. doi: 10.1371/journal.pgen.1004065

Shi, Z., Yang, W.-Z., Lin-Chao, S., Chak, K.-F., and Yuan, H. S. (2008). Crystal structure of *Escherichia coli* PNPase: central channel residues are involved in processive RNA degradation. *RNA* 14, 2361–2371. doi: 10.1261/rna.1244308

Shimoni, Y., Friedlander, G., Hetzroni, G., Niv, G., Altuvia, S., Biham, O., et al. (2007). Regulation of gene expression by small non-coding RNAs: a quantitative view. *Mol. Syst. Biol.* 3:138. doi: 10.1038/msb4100181

Silva, I. J., Barahona, S., Eyraud, A., Lalaouna, D., Figueroa-Bossi, N., Massé, E., et al. (2019). SraL sRNA interaction regulates the terminator by preventing premature transcription termination of *rho* mRNA. *Proc. Natl. Acad. Sci. U.S.A.* 116, 3042–3051. doi: 10.1073/pnas.1811589116

Smirnov, A., Förstner, K. U., Holmqvist, E., Otto, A., Günster, R., Becher, D., et al. (2016). Grad-seq guides the discovery of ProQ as a major small RNA-binding protein. *Proc. Natl. Acad. Sci. U.S.A.* 113, 11591–11596. doi: 10.1073/pnas.1609981113

Smirnov, A., Schneider, C., Hör, J., and Vogel, J. (2017a). Discovery of new RNA classes and global RNA-binding proteins. *Curr. Opin. Microbiol.* 39, 152–160. doi: 10.1016/j.mib.2017.11.016

Smirnov, A., Wang, C., Drewry, L. L., and Vogel, J. (2017b). Molecular mechanism of mRNA repression *in trans* by a ProQ-dependent small RNA. *EMBO J.* 36, 1029–1045. doi: 10.15252/embj.201696127

Storz, G., Vogel, J., and Wassarman, K. M. (2011). Regulation by small RNAs in bacteria: expanding frontiers. *Mol. Cell* 43, 880–891. doi: 10.1016/j.molcel.2011.08.022

Szklarczyk, D., Morris, J. H., Cook, H., Kuhn, M., Wyder, S., Simonovic, M., et al. (2017). The STRING database in 2017: quality-controlled protein-protein association networks, made broadly accessible. *Nucleic Acids Res.* 45, D362–D368. doi: 10.1093/nar/gkw937

Tu, K. C., and Bassler, B. L. (2007). Multiple small RNAs act additively to integrate sensory information and control quorum sensing in *Vibrio harveyi*. *Genes Dev.* 21, 221–233. doi: 10.1101/gad.1502407

Udekwu, K. I., Darfeuille, F., Vogel, J., Reimegård, J., Holmqvist, E., and Wagner, E. G. H. (2005). Hfq-dependent regulation of OmpA synthesis is mediated by an antisense RNA. *Genes Dev.* 19, 2355–2366. doi: 10.1101/gad.354405

Vakulskas, C. A., Leng, Y., Abe, H., Amaki, T., Okayama, A., Babitzke, P., et al. (2016). Antagonistic control of the turnover pathway for the global regulatory sRNA CsrB by the CsrA and CsrD proteins. *Nucleic Acids Res.* 44, 7896–7910. doi: 10.1093/nar/gkw484

Vakulskas, C. A., Potts, A. H., Babitzke, P., Ahmer, B. M. M., and Romeo, T. (2015). Regulation of Bacterial Virulence by Csr (Rsm) Systems. *Microbiol. Mol. Biol. Rev.* 79, 193–224. doi: 10.1128/mmbr.00052-14

Vercruysse, M., Köhrer, C., Davies, B. W., Arnold, M. F. F., Mekalanos, J. J., RajBhandary, U. L., et al. (2014). The highly conserved bacterial RNase YbeY is essential in *Vibrio cholerae*, playing a critical role in virulence, stress regulation, and RNA processing. *PLoS Pathog.* 10:e1004175. doi: 10.1371/journal.ppat.1004175

Viegas, S. C., Silva, I. J., Saramago, M., Domingues, S., and Arraiano, C. M. (2011). Regulation of the small regulatory RNA MicA by ribonuclease III: a target-dependent pathway. *Nucleic Acids Res.* 39, 2918–2930. doi: 10.1093/nar/gkq1239

Vogel, J., and Luisi, B. F. (2011). Hfq and its constellation of RNA. *Nat. Rev. Microbiol.* 9, 578–589. doi: 10.1038/nrmicro2615

Waters, S. A., McAteer, S. P., Kudla, G., Pang, I., Deshpande, N. P., Amos, T. G., et al. (2017). Small RNA interactome of pathogenic *E. coli* revealed through crosslinking of RNase E. *EMBO J.* 36, 374–387. doi: 10.15252/embj.201694639

Weilbacher, T., Suzuki, K., Dubey, A. K., Wang, X., Gudapaty, S., Morozov, I., et al. (2003). A novel sRNA component of the carbon storage regulatory system of *Escherichia coli*. *Mol. Microbiol.* 48, 657–670. doi: 10.1046/j.1365-2958.2003.03459.x

Westermann, A. J., Venturini, E., Sellin, M. E., Förstner, K. U., Hardt, W.-D., and Vogel, J. (2019). The Major RNA-Binding Protein ProQ Impacts Virulence Gene Expression in *Salmonella enterica* Serovar Typhimurium. *mBio* 10:e02504-18. doi: 10.1128/mBio.02504-18

Woodson, S. A., Panja, S., and Santiago-Frangos, A. (2018). Proteins That Chaperone RNA Regulation. *Microbiol. Spectr.* 6, 385–397. doi: 10.1128/microbiolspec.RWR-0026-2018

Yakhnin, A. V., Baker, C. S., Vakulskas, C. A., Yakhnin, H., Berezin, I., Romeo, T., et al. (2013). CsrA activates *flhDC* expression by protecting flhDC mRNA from RNase E-mediated cleavage. *Mol. Microbiol.* 87, 851–866. doi: 10.1111/mmi.12136

Yamanaka, K., Fang, L., and Inouye, M. (1998). The CspA family in *Escherichia coli*: multiple gene duplication for stress adaptation. *Mol. Microbiol.* 27, 247–255. doi: 10.1046/j.1365-2958.1998.00683.x

Zhang, A., Derbyshire, V., Galloway Salvo, J. L., and Belfort, M. (1995). *Escherichia coli* protein StpA stimulates self-splicing by promoting RNA assembly in vitro. *RNA* 1, 783–793.

Zhang, A., Rimsky, S., Reaban, M. E., Buc, H., and Belfort, M. (1996). *Escherichia coli* protein analogs StpA and H-NS: regulatory loops, similar and disparate effects on nucleic acid dynamics. *EMBO J.* 15, 1340–1349. doi: 10.1002/j.1460-2075.1996.tb00476.x

Zhang, A., Schu, D. J., Tjaden, B. C., Storz, G., and Gottesman, S. (2013). Mutations in interaction surfaces differentially impact *E. coli* Hfq association with small RNAs and their mRNA targets. *J. Mol. Biol.* 425, 3678–3697. doi: 10.1016/j.jmb.2013.01.006

Conflict of Interest: The authors declare that the research was conducted in the absence of any commercial or financial relationships that could be construed as a potential conflict of interest.

frontiers in Molecular Biosciences

REVIEW
published: 16 June 2020
doi: 10.3389/fmolb.2020.00101

Small RNAs as Fundamental Players in the Transference of Information During Bacterial Infectious Diseases

*Juan José González Plaza**

Faculty of Forestry and Wood Sciences, Czech University of Life Sciences Prague, Prague, Czechia

Communication shapes life on Earth. Transference of information has played a paramount role on the evolution of all living or extinct organisms since the appearance of life. Success or failure in this process will determine the prevalence or disappearance of a certain set of genes, the basis of Darwinian paradigm. Among different molecules used for transmission or reception of information, RNA plays a key role. For instance, the early precursors of life were information molecules based in primitive RNA forms. A growing field of research has focused on the contribution of small non-coding RNA forms due to its role on infectious diseases. These are short RNA species that carry out regulatory tasks in *cis* or *trans*. Small RNAs have shown their relevance in fine tuning the expression and activity of important regulators of essential genes for bacteria. Regulation of targets occurs through a plethora of mechanisms, including mRNA stabilization/destabilization, driving target mRNAs to degradation, or direct binding to regulatory proteins. Different studies have been conducted during the interplay of pathogenic bacteria with several hosts, including humans, animals, or plants. The sRNAs help the invader to quickly adapt to the change in environmental conditions when it enters in the host, or passes to a free state. The adaptation is achieved by direct targeting of the pathogen genes, or subversion of the host immune system. Pathogens trigger also an immune response in the host, which has been shown as well to be regulated by a wide range of sRNAs. This review focuses on the most recent host-pathogen interaction studies during bacterial infectious diseases, providing the perspective of the pathogen.

Keywords: small RNA, bacteria, infectious disease, information transfer, host-pathogen interaction

OPEN ACCESS

Edited by:
Olga N. Ozoline, Institute of Cell Biophysics (RAS), Russia

Reviewed by:
Claudio Valverde, National University of Quilmes, Argentina
Alfredo Berzal-Herranz, Instituto de Parasitología y Biomedicina López-Neyra, Spain

***Correspondence:**
Juan José González Plaza
gonzalez_plaza@fld.czu.cz; gonzalezplazajuanjose@gmail.com

Specialty section:
This article was submitted to Protein and RNA Networks, a section of the journal Frontiers in Molecular Biosciences

Received: *01 January 2020*
Accepted: *04 May 2020*
Published: *16 June 2020*

Citation:
González Plaza JJ (2020) Small RNAs as Fundamental Players in the Transference of Information During Bacterial Infectious Diseases. Front. Mol. Biosci. 7:101. doi: 10.3389/fmolb.2020.00101

INTRODUCTION

> "*Dizese calétura epidemia porque es común a muchos: perniciosa, porque mata a muchos quanto es de su parte, por tener mucha actividad de calor proveniente (como despues diremos) de vn podrecimiento extremo.*"
>
> "*It is called an epidemic fever because it is common to many: pernicious, because it kills many on its part, due to a lot of heat activity originating (as we will say later) from extreme rotting.* de Viana (1637); plague that heavily struck the port city of Málaga."

A continuous flow of myriads of energy and matter from atomic to beyond gravitational level shapes life on Earth. Information, its structure and movement across hierarchies, has played a paramount role on the evolution of all living or extinct organisms since the appearance of life. For instance, the early precursors of life were information molecules based in primitive RNA forms

(Higgs and Lehman, 2015; Taylor, 2016). The fact that all biological species live in networks, force them to interact with other living beings and the environment (Bermúdez-Barrientos et al., 2020). Interactions, different forms of sociality, transference or reception of information, determine how species perform through evolutionary history. Communication in biology or biocommunication reaches far beyond the human concept of language (Witzany, 2010), and includes a wide variety of forms: sexual deception (color display in orchids to attract pollinators) (Streinzer et al., 2009), vibroacoustic or chemical alarm signaling (alarm pheromones in termites) (Cristaldo et al., 2016), or camouflage (How et al., 2017). Additionally, it encompass hostile communication forms, such as signals to attack among the microbiome (antibiotic production for elimination of competitive bacteria) (Fischbach, 2009; Romero et al., 2011), or counterfeit the defenses of others (fungal RNAs suppressing plant defenses) (Weiberg et al., 2013). Success or failure in the transmission of these signals dramatically affects the prevalence or disappearance of a given set of genes, the basis of Darwinian paradigm (Langdon, 2016).

Infectious diseases are biological examples of competition between species for the same metabolic resources (Herrera and Nunn, 2019), relationships that have been shaped through evolution. In essence, those are evolutionary arms races between hosts and their infectious agents (Ingle et al., 2006; Kuijl and Neefjes, 2009). An infectious disease is a malady caused by a pathogenic organism, including bacteria, fungi, parasites, or viruses (Krämer et al., 2009). The process of infection comprises the change from an outer environment, to another one inside of the host, where the conditions are hostile due to the presence of immune systems. In some animal hosts, the recognition of the pathogen could unchain a series of events leading to an inflammatory response, which represent a plethora of environmental stresses for the bacteria.

Hosts have developed sophisticated mechanisms to sense invaders, and to react against them. Diving at a very deep molecular level one of the first barriers of defense to trigger innate immune responses, is the recognition of pathogen-associated molecular patterns (PAMPs) that will further activate toll-like receptors (TLRs) pathways (Ausubel, 2005; Moresco et al., 2011). Bacteria and archaea have developed during evolution primitive adaptive mechanisms to identify "pathogens" by identification and restriction of foreign genetic material through CRISPR-CAS systems (Hille et al., 2018; Ratner et al., 2019).

The key for the infection success is a quick response and efficient adaptation to a changing hostile environment within the host (Sauder and Kendall, 2018), the translation of cues from the extracellular domain into triggering a set of instructions aimed for the survival of the pathogen. Different molecules play a role in the transference of information, for example during the formation of biofilms, sub-inhibitory concentrations of antibiotics have been proposed to serve as carriers of information between bacteria (Romero et al., 2011). Among different molecules, RNA has achieved a very important role as an information mediator, because it is the molecular link between genome (DNA) and phenotype (proteins or metabolites). It can be quickly recruited during biotic or abiotic stresses. The average life of RNA molecules is short, because the response has been *tuned* to serve for the synthesis of proteins and to be degraded once they are not needed anymore (Gilbertson et al., 2018).

Small regulatory RNAs (sRNAs) are a subset of RNA molecules that are involved in several mechanisms that aid the pathogen in adaptation, counterfeiting, or suppressing the host immune system (González Plaza, 2018), side to side to other molecules participating in this complex process. The sRNAs are transcribed from the genome, but do not follow the canonical path toward protein translation (Waters and Storz, 2009).

One reason for the involvement sRNAs at infection processes, is the flexibility to target a number of genes or transcription factors, leading to continuous ranges of expression and responses to fluctuating environmental stresses, instead of an abrupt triggering or shutting down of the expression. In that regard, Silva and collaborators have shown that SraL sRNA is responsible for regulating the expression of the transcription termination protein Rho (Silva et al., 2019). This protein is essential for the transcription balance in *Bacillus subtilis*, and its impairment affects negatively cell motility, biofilm formation, and sporulation (Bidnenko et al., 2017). Thus, the case of SraL and Rho illustrates a complex system of "regulation of regulators." However, it could be argued that many proteins can carry out similar regulatory roles. Among other reasons, it is probably the faster response of RNAs what has given them a key role during infection, because they do not require translation and it represents a lower energy consumption for the cell. Modulation of the transcriptomic levels allows for a faster response to environmental changes (Sheehan and Caswell, 2018), because it can help to correct or modulate the mRNA levels of many genes before the protein is translated, and ultimately modulate the phenotype according to external fluctuations.

The current review article presents the advances in the field regarding the involvement of sRNAs during bacterial infections, highlighting the latest contributions in the 2 years since my previous review (González Plaza, 2018). The field has expanded broadly, and the number of contributions points toward a future increase in the number of research efforts. The current review aims as well to broaden the scope from diseases affecting humans to other species. It will first cover the type of existing sRNAs and their mode of action, the molecular behavior of sRNAs from the pathogen perspective, and modulation of molecular processes when facing host immune systems. Lastly, different type of sRNAs during several infection processes in a number of species, ranging from plants to animals.

TYPES OF sRNAs

The subset of small regulatory RNAs, termed in literature as sRNAs, are a group of primarily non-coding RNA forms (Waters and Storz, 2009) often ranging from 20 to 200 nucleotides (nt) in length, even reaching up to 500 nt (Carrier et al., 2018a). They carry key roles regulating expression levels in a wide range of prokaryotic or eukaryotic genes (Waters and Storz, 2009; Brant and Budak, 2018; Carrier et al., 2018b). Their targets include important genes that are relevant either for the infection

process or for the defense of the host organism (Guo et al., 2019). A notable feature is their reported participation in *trans*-kingdom communication (Benbow et al., 2018; Zeng et al., 2019; Bermúdez-Barrientos et al., 2020). Attending to their origin, they can be divided in prokaryotic and eukaryotic sRNAs.

Prokaryotic sRNAs

Prokaryotic regulatory RNAs can be classified in three main groups: (i) elements present in the 5′ untranslated regions (UTR), (ii) those acting in *cis* and termed anti-sense RNAs (Lejars et al., 2019), and (iii) those acting in *trans* that are expressed from other genomic regions than their targets (Chakravarty and Massé, 2019). The third type can be originated at intergenic regions, but also at 5′ or 3′ UTR regions, and are usually termed as sRNAs (Carrier et al., 2018a; Chakravarty and Massé, 2019). The *trans*-acting sRNAs are the main focus of the current article. The regulation occurs according to several mechanisms, which have been thoroughly reviewed by Carrier, Lalaouna, and Massé (Carrier et al., 2018a). Briefly:

(i) Binding to a regulatory protein. For example binding of sRNAs to the regulatory CsrA protein, that cannot occlude the Shine Dalgarno (SD) sequence of its target (Romeo and Babitzke, 2018; **Figure 1A**).

(ii) Direct sRNA-mRNA interaction (**Figure 1B**). Trans acting sRNAs bind to their targets with partial complementarity (Caldelari et al., 2013). There are different types of interaction, for instance the destabilization of the mRNA by pairing to upstream locations from RBS (Ross et al., 2019) or by interference with the 5′ UTR (Rübsam et al., 2018). Binding of the sRNA can also mask the ribosomal binding site (RBS), consequently the ribosome cannot bind and the translation of the gene is attenuated (Kiekens et al., 2018). The complex mRNA-sRNA can be subject of degradation by RNaseE (Lalaouna et al., 2013).

(iii) Protein mediation (**Figure 1C**). RNA-binding proteins (RBP) can mediate the regulatory activities of sRNAs, such as Hfq (Beisel and Storz, 2010) or ProQ (Smirnov et al., 2016). The Hfq chaperone mediates interactions between sRNAs and their targets helping to improve base-pair recognition (Massé et al., 2003; Lenz et al., 2004; Holmqvist and Vogel, 2018; Santiago-Frangos et al., 2019). This protein binds to the regulatory RNAs, helps to stabilize them, and leads the base pairing with the targets (Hu et al., 2018; Han et al., 2019). Hoekzema et al. (2019) have suggested an additional mechanism, where the action of Hfq will unfold a hairpin in the targeted mRNA. This activity would create a temporary local structure that facilitates the access of the sRNA. There are other microorganisms where Hfq protein is lacking and FinO, ProQ or RocC carry out its broad regulatory roles: sRNA protection from degradation, alteration of RNA structures to facilitate annealing, stabilization of the sRNA-mRNA complex, or modulation of ribosome binding after the complex is formed, and regulation of RNA degradation (Olejniczak and Storz, 2017).

Eukaryotic sRNAs

In eukaryotes the description of the first types of sRNAs dates back to 1990 with studies reporting silencing of gene expression in petunia plants (Napoli et al., 1990; van der Krol et al., 1990), and later in 1993 in the nematode *Caenorhabditis elegans* (Lee et al., 1993; Wightman et al., 1993).

The main types of described sRNAs range from 20 to 30 nt, and carry out silencing functions by mediation of Argonaute family proteins (Kim et al., 2009). These sRNAs were firstly divided in three classes: microRNAs (miRNAs), small interfering RNAs (siRNAs), and PIWI-interacting RNAs (piRNAs) (Grimson et al., 2008; Okamura and Lai, 2008; Islam et al., 2018). Long-non-coding RNAs (lncRNAs) are a new group of described regulatory molecules over 200 nt (Agliano et al., 2019).

In the case of miRNAs it has been reported that they can control up to 60% of the human transcriptome, therefore, their involvement in the response to infectious diseases is not surprising (Aguilar et al., 2019).

sRNAs REGULATE KEY PROCESSES FOR THE ESTABLISHMENT OF INFECTION

Establishment of infection requires a prompt adaptation effort from a pathogenic perspective, in order to proliferate within the host. There are different type of environmental challenges faced by bacteria when entering the host, including different immune barriers to infection (Chakravarty and Massé, 2019). Regulation of transcription aids to adapt quickly to the newly encountered hostile conditions: changes in nutrient availability, pH, temperature, or presence of antimicrobials among other variables. Together, those force bacteria to behave differently during the infective process in comparison with the free form state. It is during these conditions when the diverse toolkit of RNA regulatory activities greatly help for survival. An overview of the different stresses that bacteria must adapt to when entering a host, and the role of sRNAs, have been summarized in **Table 1**.

The range of adaptations mediated by sRNAs have been grouped in two main related categories: (i) regulation of key bacterial processes for the success of infection, and (ii) regulation of responses against host barriers to infection. Most of them have been described in bacteria causing diseases concerning animals, especially in mammals and mostly humans.

Regulation of Biological Processes

Key biological processes set the basis for the adaptation to the host molecular environment, including important responses such as: temperature sensing, stringent microbial response, biofilm formation and Quorum Sensing (QS), or regulation of virulence.

Temperature Response

One of the first cues helping the pathogen to perceive when it has entered the host is the change in temperature. Besides, it cannot be overlooked that a characteristic of infectious diseases is the hyperthermia response, which elevate the body temperature during inflammation (Kluger et al., 1998; Casadevall, 2016).

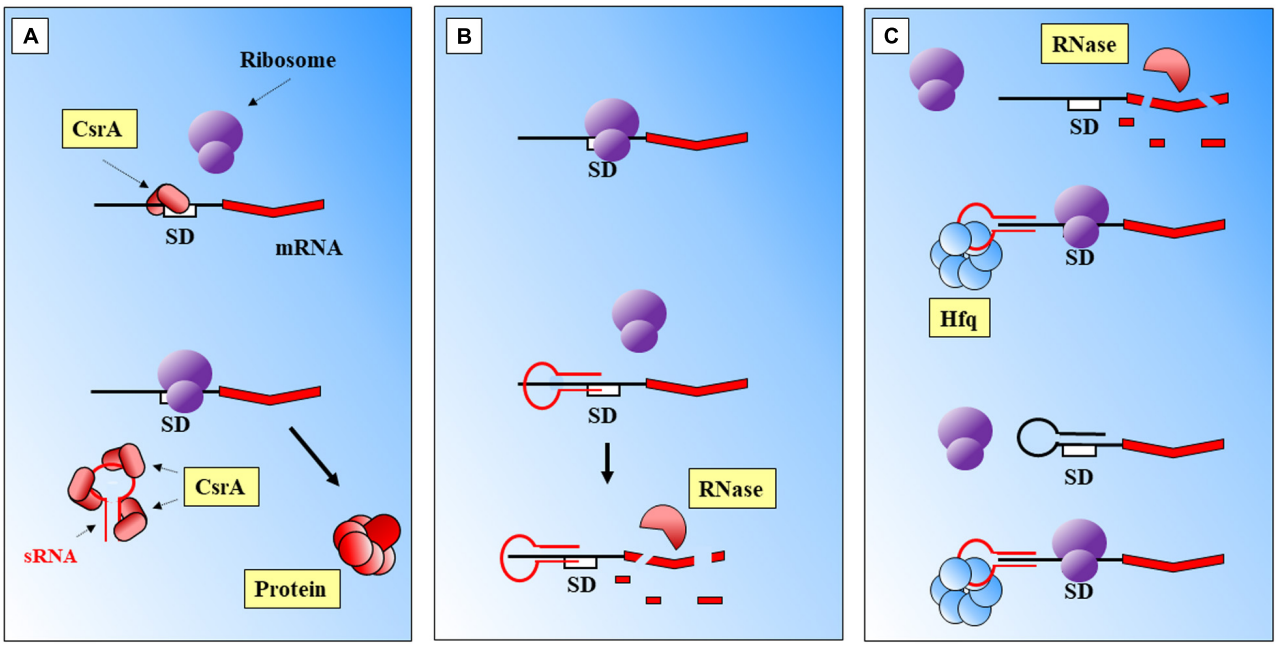

FIGURE 1 | Main modes of action of prokaryotic sRNAs. **(A)** sRNA binding to a CsrA regulatory protein frees the SD region. **(B)** Direct sRNA-mRNA binding. The shown sRNA competes with the ribosome, which cannot bind to the SD site. The mRNA is further degraded. **(C)** Protein mediation. Hfq-sRNA bind to the mRNA and stabilize it, and degradation is prevented. The complex protein-sRNA can unfold secondary structures in the 5′ UTR which will prevent ribosome binding. SD, Shine-Dalgarno. Black thick arrows indicate flow of a biological process, e.g., protein translation. References: Massé et al., 2003; Waters and Storz, 2009; Faucher and Shuman, 2011; Chakravarty and Massé, 2019.

While it is difficult to ascertain, it has been appointed that fever has beneficial effects for the protection against pathogens (Mackowiak, 1981; Casadevall, 2016), since such a high metabolic cost in higher vertebrates would have been lost during evolution if it did not present an advantage (Ostberg et al., 2000).

From a pathogen perspective, RNA presents advantages, as it has been shown to be a relevant molecular thermometer capable of controlling expression of heat shock and virulence genes (Narberhaus, 2010; Loh et al., 2018), when increasing temperatures melt secondary structures and allow access to the ribosome binding site (RBS) (Narberhaus et al., 2006). Through temperature monitorization pathogens can differentiate between free state, insect vector (if present), or hosts with regulated body temperature (González Plaza et al., 2016; Álvarez-Estrada et al., 2018), which could lead as well to develop a specific program to respond to fever (in hosts where this mechanism is present).

A recent study has evaluated the transcriptomic response of the psychrotrophic bacterium *Pseudoalteromonas fuliginea* BSW20308, which is adapted to Arctic environmental conditions (Liao et al., 2019). The aim was to evaluate the impact of global warming over the ecologically dominant genus, where temperature increases may trigger regulation mediated by sRNA. Authors described the whole sRNome (repertoire of sRNAs) when this microorganism grew at different temperatures, from very low ones resembling its natural environmental conditions, to higher temperatures of a global warming scenario. Results, according to authors, indicated an intense involvement of sRNAs in temperature adaptation. A 316 nt novel sRNA, termed Pf1, showed to be correlated with the expression to a wide group of 644 genes mostly annotated in the categories of catabolism, energy, translation, and intracellular transport. As previously mentioned, sRNAs have an ample range of effects over the transcriptome, helping bacteria to regulate their physiology upon environmental perturbations. Besides, since sRNAs are genetic carriers of information not translated into proteins, they can perform their regulatory roles in a faster fashion than other important regulators as heat-shock proteins. Although this characterization relies on an RNA-seq approach and further *in silico* data analyses, it is not surprising such a broad regulatory network as suggested in the article. Either by conservation or convergent evolution as appointed by Narberhaus (2010), this regulatory response is present in many pathogens for adaptation to the host conditions, and may be an important variable to consider during pyrexia (Mackowiak, 1981; Kluger et al., 1998; Ostberg et al., 2000; Casadevall, 2016; González Plaza et al., 2016).

In their analysis of the differential expression between infective and environmental temperatures in *Borrelia burgdorferi*, Popitsch et al. (2017) report a large set of sRNAs with differential expression between both conditions, and also reveal a variety of transcription origins. A brilliant conclusion of this study is that in overall, the mode of action of sRNAs could deeply impact the way we perform genetic studies. Deletion of a gene could erase as well an important regulator for a number of downstream targets. This can undoubtedly represent a confounding factor for the interpretation of results on loss-of-function phenotypes due to the interference of sRNA regulation.

What becomes clear is that monitorization of temperature changes is a central event in the life cycle of bacterial pathogens (Papenfort and Vogel, 2010), and that regulation follows an intricate pathway with several levels. In a fascinating example of interaction between kingdoms and pathogen manipulation, the spirochaetal outer surface (lipo)protein (Osp) C (OspC) from *Borrelia burgdorferi* binds to the SALP15 salivary protein belonging to the tick vector *Ixodes scapularis*. The pathogen uses the insect protein to succeed in the transmission to the mammalian host and its infection (Ramamoorthi et al., 2005). The expression of *ospC* is influenced by RpoS (Hübner et al., 2001), which back was suggested by Lybecker and Samuels (2007) to be regulated by a sRNA in response to temperature (**Figure 2**). RpoS is a key global regulator controlling virulence or response to general stresses in several pathogens (Fang et al., 1992; Suh et al., 1999; Dong and Schellhorn, 2010; Battesti et al., 2011). The regulation of temperature responses mediated by RpoS, is modulated by the sRNA $DsrA_{Bb}$ in *B. burgdorferi*, which is expressed upon increase in temperature (Lybecker and Samuels, 2007). Few years later, it was experimentally confirmed to occur through Hfq mediation (Lybecker et al., 2010; **Figure 2**).

Stringent Response

Stringent response can be defined as the set of bacterial conserved mechanisms activated during nutritional environmental stresses (Poole, 2012; Drecktrah et al., 2018). It produces a general decrease on the expression of genes related with growth, involving synthesis of proteins or nucleic acids, and enhanced transcriptional levels of genes for survival (Chatterji and Ojha, 2001; Poole, 2012; Irving and Corrigan, 2018). When the bacterial stringent response is unleashed, mediation of enzymes such as RelA or SpoT lead to global transcriptomic changes (Atkinson et al., 2011; Shyp et al., 2012). A different version of RelA in *Borrelia burgdorferi*, Rel_{Bbu}, has regulatory capabilities on a third of the sRNAs identified in this bacteria to date (Drecktrah et al., 2018). This pathogen has a life cycle that includes a vertebrate and an invertebrate host, thus, adaptation to different environments in order to regulate the behavior in such disparate conditions represent a challenge for survival. Not surprisingly Drecktrah et al. (2018) found that most of the targets of the regulated sRNAs are involved in two biological processes required during conditions of infection, virulence and metabolism. Interestingly, the sRNAs targets of Rel_{Bbu} are not exclusively found within the chromosome, but could be found as well in plasmids.

Biofilm Formation and Quorum Sensing

Biofilms are bacterial community structures that provide additional protection against the host immune system, e.g., the effect of cytokines (Leid et al., 2005). Biofilm formation requires coordination of QS mechanisms of communication, which are mediated mainly by N-acyl homoserine lactones (AHLs) among other molecules and mainly controlled by the *rhlR-rhlI* and *lasR-lasI* signaling systems (Davies et al., 1998; Lee and Zhang, 2015; **Figure 3**). The AHL N-butanoyl-homoserine lactone (C_4-HSL) is an important molecule in the QS response of *Pseudomonas aeruginosa*. This molecule binds to RhlR and the activated complex regulates positively the expression of *rhlI*, and its translation to RhlI that synthesizes C_4-HSL. The synthesis of RhlR has been positively related with a 74-nucleotide sRNA, PhrD (Malgaonkar and Nair, 2019; **Figure 3**). The interaction between the regulator molecule and the mRNA target was predicted *in silico* and further demonstrated in experimental conditions (which mimicked the host during pathogenesis). While this system seems to act independently of any *P. aeruginosa* proteins (authors expressed it heterologously in *E. coli*), the system achieves better expression levels in the *P. aeruginosa* background, probably assisted by native proteins.

The involvement of sRNAs in the QS response of *P. aeruginosa* was investigated with mutants of AHL synthesis by Thomason et al. (2019), (**Figure 3**). Authors found a group of sRNAs responsive to AHLs treatment, where RhlS (previously SPA0104) (Ferrara et al., 2012) showed the highest accumulation at inductive conditions. This regulator acts positively over the translation of *rhlI*, leading ultimately to the production of C_4-HSL. P27 is another sRNA that regulates negatively the translation of *rhlI* bindings to the 5′ UTR aided by Hfq (Chen et al., 2019; **Figure 3**).

The environmental bacteria *Burkholderia cenocepacia* belongs to the *Burkholderia cepacia* complex (Bcc) and can become an opportunistic pathogen in plants (Mahenthiralingam et al., 2005), but also in patients affected by cystic fibrosis (Drevinek and Mahenthiralingam, 2010). The sRNA ncS35 is involved in growth regulation by predicted binding to mRNA targets, probably facilitating the degradation of the transcript (Kiekens et al., 2018). Authors used a deletion mutant (Δ*ncS35*) in comparison with the wild type (WT) strain, and a complemented Δ*ncS35* overexpressing the sRNA under inductive conditions. The mutant phenotype displayed biofilms with larger aggregates, increased optical density or metabolic activity in comparison with the WT or the complemented mutant. Differential gene expression between the mutant and the WT showed upregulation of genes involved in metabolism both in exponential and stationary growth phases. This indicates a negative regulatory role of ncS35 over bacterial growth. Additionally, authors observed higher expression values for ncS35 when bacteria form biofilms than in free planktonic culture. Additional increases in transcription occurred during nutrient limitation after cultivation in M9 minimal media or in the presence SDS, a known membrane stressor (Flahaut et al., 1996). In overall, the effect of this sRNA is to slow-down growth. The higher expression during presence of stressors, may indicate its involvement in protection of the bacteria by restricting division when environmental conditions are detrimental for the pathogen.

Virulence

Bacterial virulence can be defined as the "relative capacity to overcome available defenses" (Sparling, 1983), or "the relative capacity of a microorganism to cause damage in a host" (Casadevall and Pirofski, 2003). This capability is mediated by virulence genes, which have to fulfill three requirements: (i) active in the interaction between pathogen and host, (ii) direct determinants of the pathogen damage, and (iii) the lack of

TABLE 1 | Adaptation to environmental stresses mediated by sRNAs.

Category	Biological Process or Host Barrier	Type of stimulation	Organism	Infectious disease	sRNA	Mechanism of sRNA action	Physiological effect	Potential value if present in a pathogen	References
Regulation of biological processes	Temperature response	Extreme heat stress	*Pseudo-alteromonas fuliginea* BSW20308	N/A	4 known sRNAs 15 novel sRNAs	Not described	Regulation of genes for adaptation to challenge, e.g., scavenging ROS, oxidation of toxic aldehydes, or antioxidant enzymes.	Adaptation to pyrexia (organisms presenting it), sensing of host temperature	Liao et al., 2019
Regulation of biological processes	Temperature response	Temperature	*Borrellia burgdorferi*	Lyme disease	>1,000	Not described	Regulation of genes involved in metabolism, cell cycle, or infection (among others)	Identification of the molecular program to trigger according to environment	Popitsch et al., 2017
Regulation of biological processes	Stringent response	Stringent response	*Borrellia burgdorferi*	Lyme disease	1/3 of sRNome regulated	Rel_{Bbu} combines enzymatic functions of RelA and SpoT.	Regulation of virulence and metabolism upon stringent response	Adaptation to host/vector/free state	Drecktrah et al., 2018
Regulation of biological processes	QS and Biofilm	Quorum-sensing response	*Pseudomonas aeruginosa*	Opportunistic infection	RhlS (+)	Binds to the 5′ UTR *rhlI* mRNA and stabilizes it, Hfq dependent	Leading to production of C4-HSL	Activation of biofilm genes according to the state of infection	Thomason et al., 2019
Regulation of biological processes	QS and Biofilm	N/A	*Pseudomonas aeruginosa*	Opportunistic infection	P27 (–)	P27 binds to the 5′ UTR *rhlI*, inhibits translation. Hfq dependent	Leading to repression of C4-HSL	Deactivation of biofilm genes according to the state of infection	Chen et al., 2019
Regulation of biological processes	QS and Biofilm	N/A	*Pseudomonas aeruginosa*	Opportunistic infection	RsmV (–)	Targets and binds RsmA and RsmF, also has redundancy of targets with known regulators	Repression of regulators involved in activating/deactivating acute/chronic infection related genes	Switching between infective lifestyles	Janssen et al., 2018b
Regulation of biological processes	QS and Biofilm	High-cell density (biofilm) Presence of membrane stressors	*Burkholderia cenopacia*	Opportunistic infection	ncS35 (–)	Potential binding to the mRNA inhibiting translation	Slows-down growth, restricts division	Triggering of infection related genes when pathogen finds the right environment	Kiekens et al., 2018
Regulation of biological processes	QS and Biofilm	N/A	*Pseudomonas aeruginosa*	Opportunistic infection	PhrD (+)	Positive regulator of RhlR by messenger stabilization (Hfq mediated)	Stabilization of *rhlR* messenger	Regulation of biofilm formation by modulation of a key regulator	Malgaonkar and Nair, 2019
Regulation of biological processes	Virulence	Environmental stress	*Pseudomonas aeruginosa*	Opportunistic infection	ReaL (–)	RpoS controls virulence factors, regulated (–) by ReaL (Hfq dependent base-pairing mechanism)	Wide downstream effects, since it regulates *rpoS* mRNA	Fine tuning of virulence factors	Thi Bach Nguyen et al., 2018

(Continued)

TABLE 1 | Continued

Category	Biological Process or Host Barrier	Type of stimulation	Organism	Infectious disease	sRNA	Mechanism of sRNA action	Physiological effect	Potential value if present in a pathogen	References
Host barriers to infectious diseases	Acid pH	pH, antimicrobials	*Escherichia coli*	Opportunistic / Enterohemorrhagic (if *Escherichia coli* O157:H7) infection	RydC (+) ArrS (+) CpxQ (–)	CpxQ-HfQ bind to mRNA, facilitate access to RNase cleavage site. RydC-HfQ and ArrS opposite effect	Modification of cell membrane versus several stresses. The enzyme transcripts (cyclopropane fatty acid synthase) stabilized and protected from RNAse E	Overcoming one of the first barriers to infection, in order to access the lower gastrointestinal tract	Bianco et al., 2019
Host barriers to infectious diseases	Inflammation	Oxidative burst	*Staphylococcus aureus*	Opportunistic infection. Severe respiratory disorders	RsaC (–)	Binding to the RBS of the gene *sodA* (protection against ROS species).	Targeted gene repression allows transcription of SodM (protection vs. ROS, uses iron as cofactor).	Maintenance of ROS protection when a cofactor is depleted by using different metallic ion.	Lalaouna et al., 2019
Host barriers to infectious diseases	Nutritional immunity	Iron starvation	*Pseudomonas aeruginosa*	Opportunistic infection.	PrrF1 (–) PrrF2 (–)	Inhibition of *antR* translation via Hfq and binding to the SD	Transcribed upon iron starvation, modulate synthesis of proteins containing limiting elements. Modulation of biofilm and virulence via targeting anthranilate degradation pathway.	Avoids synthesis of unnecessary iron-containing proteins when this compound is limited.	Djapgne et al., 2018
Host barriers to infectious diseases	Nutritional immunity	Environmental stresses related with iron withholding and nutrient starvation	*Escherichia coli* W3100	Opportunistic / Enterohemorrhagic (if *Escherichia coli* O157:H7) infection	RyhB (–)	Binds target mRNA via Hfq, allows recognition by degradasome.	Transcribed upon iron starvation, modulate synthesis of proteins containing limiting elements.	Described (previously) to avoid synthesis of iron containing proteins under iron limitation; redirection of metabolic fluxes	Lyu Y et al., 2019
Host barriers to infectious diseases	Nutritional immunity	Nutrient starvation	*Salmonella enterica* serovar Typhimurium	Diarrheal disease / Typhoid fever	STnc1740 (–) RssR (+)	RssR was suggested to bind to the 5′ UTR of *reiD*	Utilization of myo-inositol as carbon source	Redirection of metabolism, growth regardless of host nutritional starvation response	Kröger et al., 2018
Host barriers to infectious diseases	Nutritional immunity	N/A	*Vibrio cholerae*	Cholera disease	MtlS (–)	*Cis*-antisense complementation	Regulation not directly caused by the environmental cue, but target mRNA levels	Regulation of metabolic resources during host nutritional starvation response	Zhang and Liu, 2019

This table contains a list of different adaptations to environmental stresses, either described in environmental bacteria, in characterization studies of pathogen models in the laboratory, or in studies assessing the host-pathogen interaction. Many of these stresses can be encountered by bacteria during infection. The type of small non-coding regulatory RNAs involved. +, positive regulation; –, negative regulation; C4-HSL, N-butanoyl-homoserine lactone; QS, Quorum Sensing; ROS, reactive oxygen species; UTR, untranslated region.

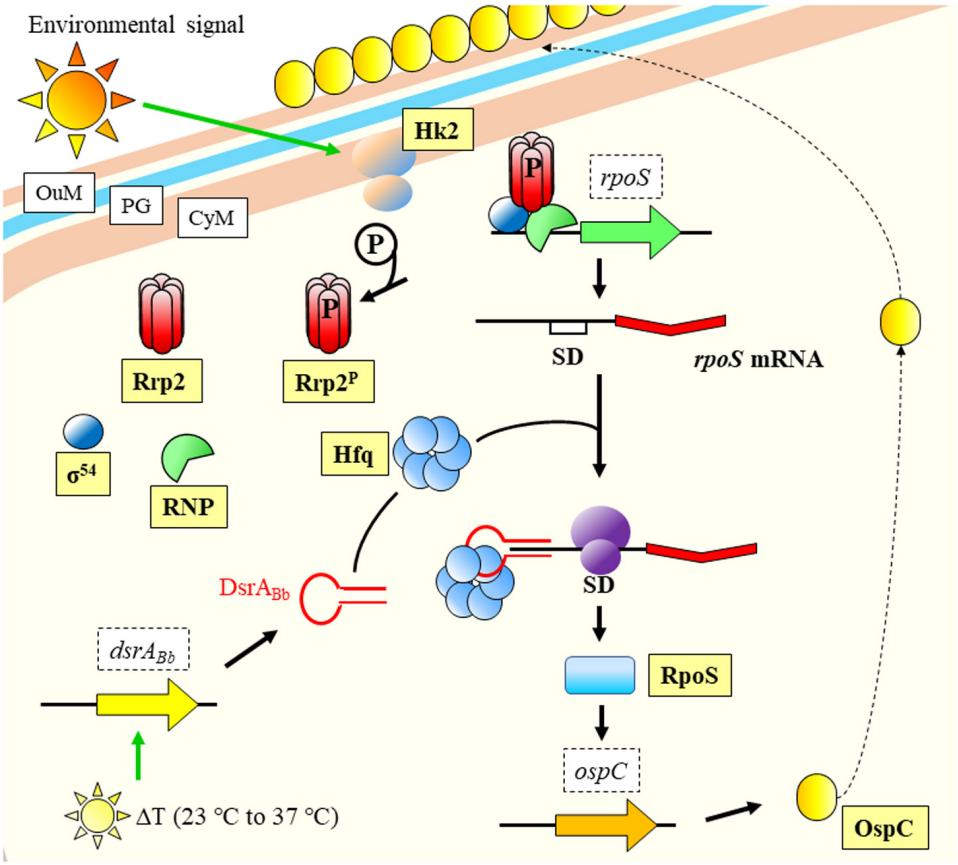

FIGURE 2 | Temperature response model of *Borrelia burgdorferi*. An environmental signal activates Hk2 membrane protein that phosphorylates and activates Rrp2. Together with RNP and σ^{54}, they facilitate transcription of *rpoS*. The mRNA is stabilized by the joint action of $DsrA_{Bb}$ (expressed upon temperature increase to host conditions) and Hfq, and the messenger is translated into protein. RpoS regulates the transcription of *ospC*, which product is displayed on the OuM. CyM, Cytoplasmic membrane; OuM, Outer membrane; PG, peptidoglycan; RNP, RNA Polymerase; SD, Shine-Dalgarno. Black thick arrows indicate flow of a biological process, e.g., protein translation. Green thick arrows indicate activation. References: Burtnick et al., 2007; Lybecker and Samuels, 2007; Lybecker et al., 2010; Radolf et al., 2012; Steere et al., 2016.

those virulence genes in non-pathogenic strains (Wassenaar and Gaastra, 2001). Some authors also use the term "virulence factor" instead of "virulence gene" (Diard and Hardt, 2017).

The role of sRNAs over virulence has been well-characterized in *Pseudomonas aeruginosa*. In this organism, an important system for regulation of virulence is the carbon store regulator (Csr) or repressor of stationary-phase metabolites (Rsm), being the main regulatory protein CsrA (or RsmA) (**Figure 4**). This system can also control other important features of the interaction with the host, such as biofilm formation, carbon metabolism, or stress responses (Romeo and Babitzke, 2018). Central to this system is the Gac/Rsm pathway, where the GacS/GacA two component system has a fundamental role (Coggan and Wolfgang, 2012; **Figure 4**). GacA induces the expression of the sRNAs *rsmY* and *rsmZ*, which can bind to the central regulatory protein RsmA (CsrA) to block its regulatory functions (Kay et al., 2006; **Figure 4**). RsmW is another sRNA that can bind to the regulatory protein (Miller et al., 2016; Valentini et al., 2018). This sRNA mediation can allow cells to respond precisely to environmental challenges, and aid transition from different infective phenotypes in *P. aeruginosa*. Additionally, RsmF/RsmN (a CsrA family protein), have overlapping functions to RsmA (Marden et al., 2013; Romero et al., 2018). Janssen et al. (2018a) have identified RsmV, a new 192-nt small non-coding RNA that has binding activity to RsmA and RsmF. *In vitro* electrophoretic assays confirmed that both proteins bind RsmV probe with high affinity. This interaction was supported by complementation studies using a two-plasmid reporter system in a mutant with high levels of RsmA/RsmF (lacking *rsmV*, *rsmY*, and *rsmZ*). Complementation with a plasmid expressing RsmV antagonized the activity of RsmA/RsmF (**Figure 4**). The displayed redundancy of targets with previously known sRNAs illustrates the fine-tuned coordination of sRNA regulation.

The sigma factor RpoS controls as well a wide number of virulence related genes in *Pseudomonas aeruginosa* under environmental stresses. RpoS translation has been shown to be negatively regulated by the sRNA ReaL, through a Hfq dependent base pairing mechanism (Thi Bach Nguyen et al., 2018; **Figure 3**). As authors point out, this was the first case of a negative sRNA transcriptional regulator of *rpoS*.

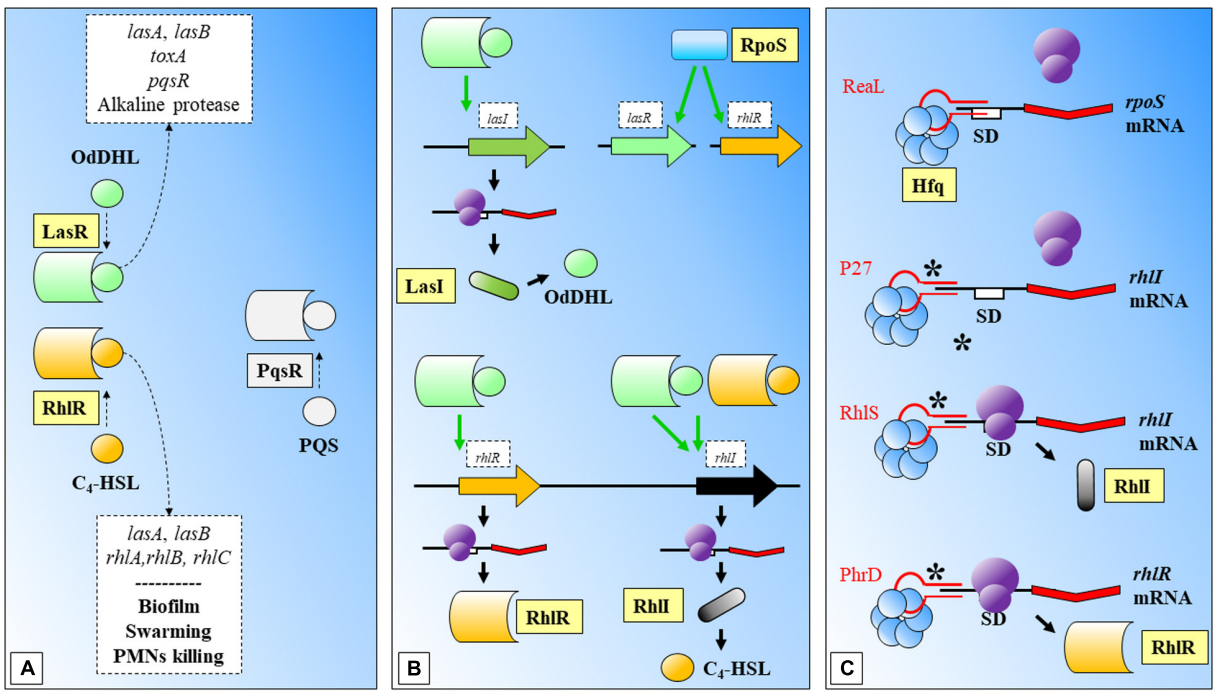

FIGURE 3 | Biofilm formation and Quorum Sensing in *Pseudomonas aeruginosa*. **(A)** LasR and RhlR are two key regulatory molecules that need OdDHL and C_4-HSL participation. LasR-OdDHL regulate the genes included in the upper box. RhlR-(C_4-HSL) regulate genes or affect processes indicated in the lower box. PqrS is another important regulator, it has been shaded as it does not participate in the shown processes. **(B)** LasR and RhlR expression is dependent on RpoS. LasR-OdDHL regulates positively: the expression of *lasI*, and ultimately the synthesis of OdDHL; the expression of *rhlR*; and *rhlI*. RhlR-(C_4-HSL) regulates positively the expression of *rhlI*. **(C)** Mechanisms of action of several sRNAs involved in regulation of the synthesis of regulatory proteins within these signaling systems: ReaL affects negatively the expression of *rpoS*; P27 is another negative regulator, in this case of *rhlI*; RhlS regulates positively *rhlI*; PhrD is a positive regulator of *rhlR*. C_4-HSL: N-butanoyl-homoserine lactone; OdDHL: N-(3-oxododecanoyl)-L-homoserine lactone; PQS: Pseudomonas quinolone signal; SD: Shine-Dalgarno. Black thick arrows indicate flow of a biological process, e.g., protein translation. Green thick arrows indicate activation. Dashed-line text boxes: indicate downstream effects of the two signaling systems, phenotypes are indicated in bold (e.g., swarming). *: indicates that this mechanism of sRNA regulation has been proposed. References: Schuster et al., 2004; Nadal Jimenez et al., 2012; Brouwer et al., 2014; Pita et al., 2018; Thi Bach Nguyen et al., 2018; Chen et al., 2019; Malgaonkar and Nair, 2019.

Host Barriers to Infectious Diseases: sRNA-Mediated Bacterial Adaptation to a Hostile Environment

The second category groups those responses from the pathogen to known barriers of infection, such as acidic pH, inflammation, or nutritional immunity.

Acidic pH: One of the First Barriers to Infection

The acidic pH of the stomach represents one of the first barriers to infection set by the host. Microbial parasites can overcome it through different mechanisms, including the degradation of urea into CO_2 and NH_3 (Burne and Chen, 2000). This strategy increases the survival chances of enteropathogenic organisms, such as *Yersinia pseudotuberculosis*, a Gram-negative food-borne bacterial pathogen (Hu et al., 2010). Another mechanism involves modifying the composition of the cell membrane to withstand sudden exposure to acid pH, by incorporation of different membrane proteins, or the enzymatic modification of the pre-existing fatty acids already in the membrane (Bianco et al., 2019). Cell membrane composition changes have key roles during infective processes, as it determines the fluidity of toxic compounds or antimicrobials. The enzyme cyclopropane fatty acid synthase mediates the incorporation of a methylene group into unsaturated fatty acids. The enzyme transcripts were shown to be stabilized and protected from the degradative activity of RNAse E in *Escherichia coli*, by two sRNAs, RydC, and ArrS; while a third one, CpxQ, had a repressive role (Bianco et al., 2019). While RydC and ArrS mask the mRNA cleavage site that is not available to RNase E, CpxQ increases the accessibility to the same site.

Inflammation: Oxidative Stresses

When the host detect the presence of a pathogen, one of the characteristic responses is inflammation and the subsequent presence of oxidative stresses for the bacteria (Carlos et al., 2018). These stresses are common for extremophiles, such as the haloarchaeon *Haloferax volcanii*. A recent study reports the presence of hundreds of sRNAs in response to oxidative stress caused by hydrogen peroxide in this species (Gelsinger and DiRuggiero, 2018). Despite the potential evolutionary lineage distance between archaea and bacteria, this study shows as well how small regulatory RNAs can play a key role for regulation of biological processes in extreme conditions. In the case of

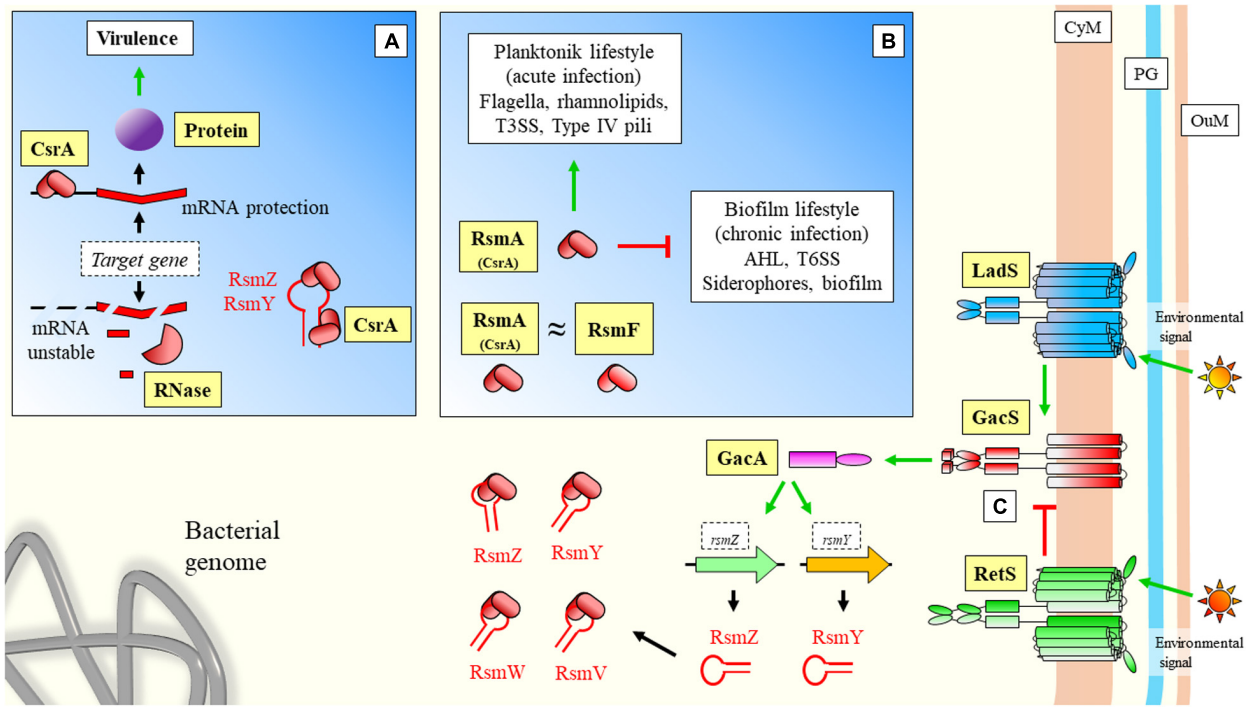

FIGURE 4 | Virulence sRNA mediated regulation in *Pseudomonas aeruginosa*: Role of CsrA regulatory protein and sequestration by sRNAs. **(A)** CsrA has been described to have also a positive effect on target mRNAs by protecting transcripts from degradation. **(B)** Regulatory effects of CsrA. In the case of positive CsrA regulation of targets, when sRNAs bind and sequester this protein, they force the instability and degradation of the messenger **(A)**. In the case of CsrA negative regulation of targets (**Figure 1A**), sRNAs can prevent binding of the regulatory protein to the mRNA allowing translation (where sRNAs have a positive effect over mRNA targets). **(C)** GacS/GacA two component system is either activated by LadS, or inhibited by RetS. These two transmembrane proteins mediate between GacS and environmental stimulation. Upon activaction, Gac promotes the transcription of sRNAs, which can further bind CsrA/RsmA and modify expression of downstream genes. CyM, Cytoplasmic membrane; PG, peptidoglycan; OuM, Outer membrane. Black thick arrows indicate flow of a biological process, e.g., protein translation. Green thick arrows indicate activation. Red thick arrows with flat cap indicate inhibition. Text boxes: indicate downstream effects of RsmA. References: Wei et al., 2001; Records and Gross, 2010; Sonnleitner et al., 2011; Coggan and Wolfgang, 2012; Nadal Jimenez et al., 2012; Marden et al., 2013; Yakhnin et al., 2013; Chambonnier et al., 2016; Janssen et al., 2018a; Romeo and Babitzke, 2018; Valentini et al., 2018.

infectious diseases, the extreme transient conditions relate to the stress caused by the host during oxidative burst, which induce heavily the expression of RsaC sRNA in *Staphylococcus aureus* (Lalaouna et al., 2019). The sRNA binds to the start codon region of the *sodA* mRNA, involved in protection against reactive oxygen species (ROS). The repression of the targeted gene allows the transcription of a second enzyme, SodM, involved in ROS protection but using iron as cofactor, instead of manganese (limited due to the nutritional immunity).

Nutritional Immunity

Besides oxidative stress (although related), pathogen recognition triggers other quick immune responses from the host, aimed to clear the bacteria by restriction of the available metabolic resources. The term "nutritional immunity" (Damo et al., 2013) refers to the limitation by the host of essential elements for the development of the pathogen. This strategy includes targeting of iron, manganese, or glucose (Carlos et al., 2018). Undoubtedly, the decrease in nutrients cellular levels has a direct relationship with the triggering of stringent mechanisms in bacteria. Regarding glucose metabolism, a characteristic behavior of human patients during infective diseases are patterns of transient anorexia that lead to a lower energetic intake, thus, limiting the availability of nutrients. This is a probable evolutionary response from the host, in order to create a metabolically stressful environment for the pathogen. Given that these host-pathogen relationships have developed through evolution, additional layers of regulation must have appeared in key microbial processes, in order to ensure survival of the bacterial strains, where sRNAs play a fundamental role.

In the case of manganese, the host immune system can limit its extracellular levels (Diaz-Ochoa et al., 2014), causing an impairment in the oxidative stress protection machinery from the pathogen, while increasing the oxidative burst. In that regard, the previous example of RsaC, can help *S. aureus* to avoid the synthesis of a non-functional enzyme (SodA) that requires manganese, and synthesize the second enzyme (SodM) that uses available iron as cofactor restoring the oxidative protection.

Besides targeting manganese, iron starvation is another innate immunity strategy of vertebrates, when detrimental bacteria are identified: the so-called "iron withholding strategy" (Ong et al., 2006). From a broader perspective, mechanisms to deal with iron deprivation have been described in environmental bacteria. For instance, the sRNA iron-stress activated RNA 1 (IsaR1) mediates

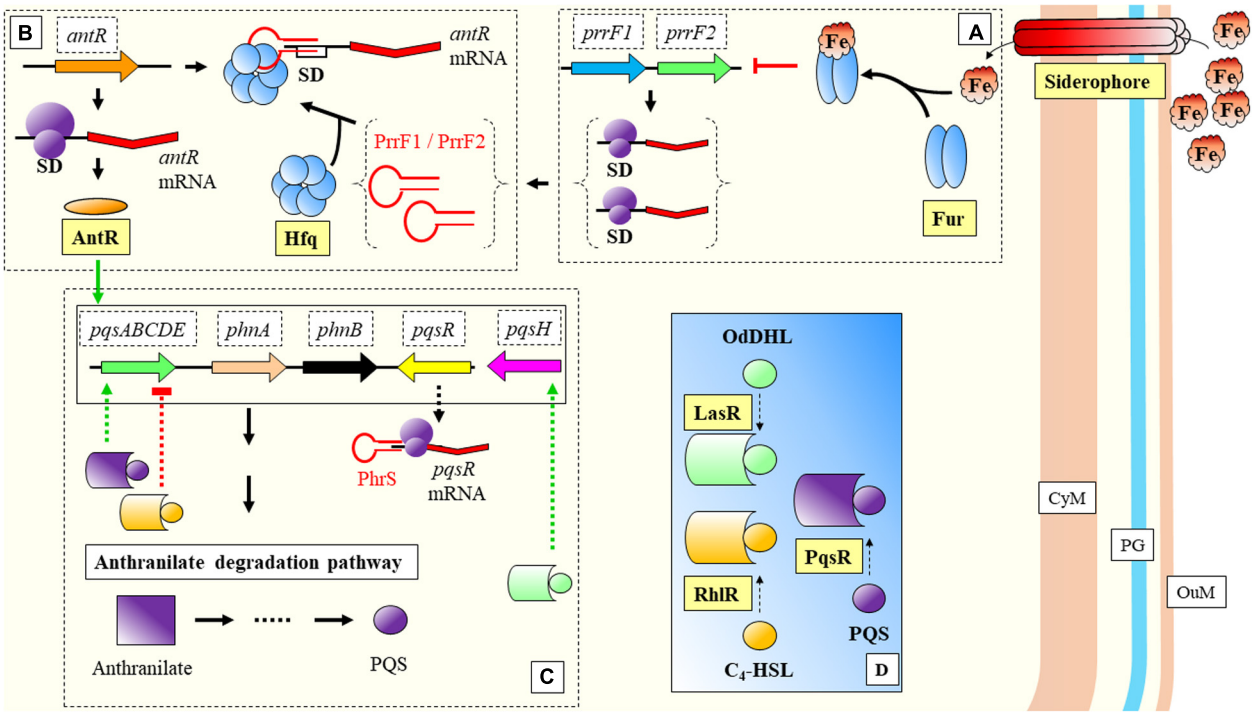

FIGURE 5 | Nutritional immunity response in *Pseudomonas aeruginosa*. **(A)** Excess of extracellular iron is bound to Fur protein that inhibits transcription of PrrF1 and PrrF2. **(B)** PrrF1 and PrfF2 bind to the SD site by mediation of Hfq and block the translation of antR. **(C)** AntR has a positive effect over anthranilate degradation genes. Another sRNA, PhrS, allows the transcription of *pqsR*. **(D)** PqsR is an important regulator, which together with RhlR and LasR have key regulatory effects over genes belonging to the anthranilate degradation pathway (shown in panel **C**). CyM, Cytoplasmic membrane, OuM, Outer membrane; PG, peptidoglycan. Black thick arrows indicate flow of a biological process, e.g., protein translation. Green thick arrows indicate activation (equal for green thick dashed lines). Red thick arrows with flat cap indicate inhibition (equal for red thick dashed lines). References: Dubern and Diggle, 2008; Brouwer et al., 2014; Baker et al., 2017; Djapgne et al., 2018.

the acclimation to conditions of iron starvation and high salinity in cyanobacteria (Rübsam et al., 2018). Even an additional role has been reported in the regulation of osmotic response. IsaR1 down-regulates the expression of the gene *ggpS*, encoding for the enzyme GG-phosphate synthase which is involved in the accumulation of heteroside glucosylglycerol (GG), and the adaptation to high saline concentrations. IsaR1 interferes with the 5′UTR of its target gene, *ggpS*. As it is becoming clear in the sRNAs research field, the *ggpS* regulation strategy does not follow an abrupt "all or nothing" scheme. It rather serves to integrate a wide range of environmental fluctuations in a continuous manner.

The previous model of cyanobacterial regulation in response to low iron, is relevant as well during infection of *P. aeruginosa*. This bacterium is able to detect environmental iron fluctuations, which drive to the expression of virulence genes in response to the host primary line of defense. Two of its sRNAs, PrrF1, and PrrF2, react to iron (Fur mediated) and have been shown to repress anthranilate metabolism (Djapgne et al., 2018; **Figure 5**). These two sRNAs have been described as functional homologs of the RyhB in *E. coli* (Wilderman et al., 2004). The regulatory effect is indirect, as they inhibit the translation of a transcriptional activator, *antR*, with downstream effects over genes for degradation of anthranilate. The metabolic pathway from anthranilate degradation ends with the synthesis of *Pseudomonas* quinolone signal (PQS), relevant for Quorum Sensing (QS) (Brouwer et al., 2014; **Figure 5**). RyhB, was previously described as a negative regulator of genes involved in the control of iron levels within the cell (Massé and Gottesman, 2002). Besides the regulatory activities toward genes related with iron homeostasis, Massé and Gottesman reported the RyhB mediated regulation of three enzymes of the tricarboxylic-acid (TCA) cycle (succinate dehydrogenase, aconitase, and fumarase) (**Figure 6**).

Recently, the contribution of RyhB over the carbon metabolism was quantified (Lyu Y et al., 2019). A mutant was generated by recombination-mediated deletion of RyhB, in comparison with the WT and an inducible mutant. Authors report a redirection of the metabolic flux toward the pentose phosphate pathway. These results support the role of sRNAs in modification of central catabolism in order to adapt to changing environments and allow survival. According to authors, it may be due to the fact that key cellular catabolism enzymes have iron as component of their structure. Several of the enzymes involved in the TCA cycle require iron on their structure (Cornelis et al., 2011). The relationship between carbon and iron levels has been previously addressed in environmental bacteria (Kirchman et al., 2000), and similar mechanisms occur with pathogenic regimes (Andrews et al., 2003). Central carbon metabolism sRNA regulation has been also reported for *Escherichia coli*, according

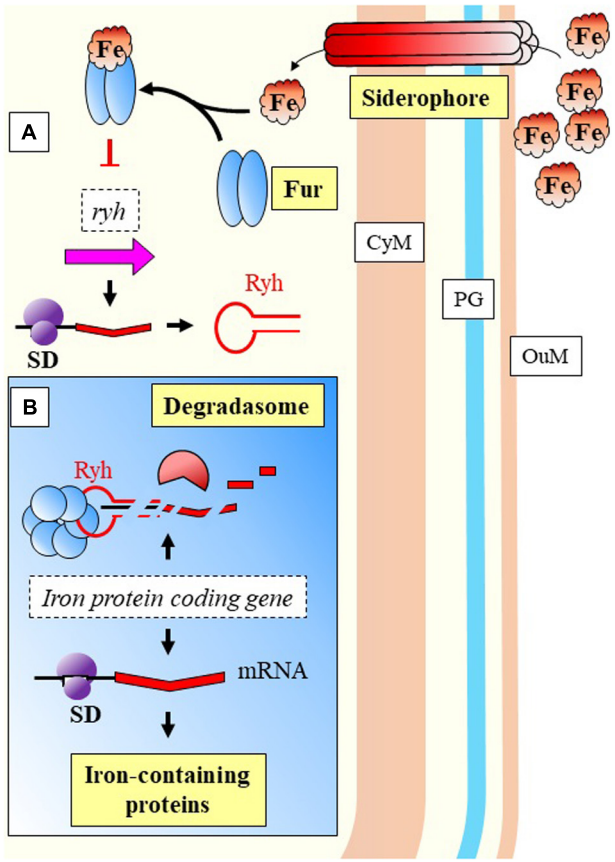

FIGURE 6 | Nutritional immunity response in *E. coli*. **(A)** Excess of extracellular iron is bound to Fur protein that inhibits transcription of Ryh. **(B)** Ryh can inhibit the synthesis of proteins containing iron when this element is limited due to nutritional starvation exerted by the host. Ryh negative regulation is mediated by Hfq, binding to the target mRNAs directing the activity of the degradasome. CyM, Cytoplasmic membrane, OuM, Outer membrane; PG, peptidoglycan. Black thick arrows indicate flow of a biological process, e.g., protein translation. Red thick arrows with flat cap indicate inhibition (equal for red thick dashed lines).

to environmental conditions (Shimizu, 2013; Lyu Y et al., 2019). That is of especial relevance during nutrient starvation, where alternative metabolic resources must be sought.

Another example of adaptation during nutrient limitation can be found in the Gram-negative bacteria *Vibrio cholerae*, responsible for cholera disease. A set of sRNAs (CsrB, CsrC, and CsrD) (functional homologs of RsmA protein and RsmB/C/D sRNAs in *P. aeruginosa*) bind to this protein through a region that resembles the SD of the CsrA mRNA targets (Butz et al., 2019; **Figure 7**). This bacterium adapts to the clear differences and limitations in nutrient content between the human host and the external environment. The mannitol operon is related to the adaptation to aquatic environment and to biofilm formation, and is regulated by the non-coding 120 nt RNA MtlS (Mustachio et al., 2012; Zhang and Liu, 2019). Zhang and Liu (2019) have shown what are the causes determining MtlS regulation. Very interestingly, it is not directly the environmental cue that triggers alterations in the expression level of the sRNA, but the mRNA levels of the target gene, *mtlA*. Another sRNA recently described, CoaR, binds to the mRNA of *tcpI* to block its translation (Xi et al., 2020; **Figure 7**). TcpI is a negative regulator of *tcpA*, a gene encoding the structural major pilin subunit of TCP (Harkey et al., 1994).

INFECTIOUS DISEASES IN PLANTS

Most of the studies involving plants have been conducted in relevant crop species. Understanding the role of sRNAs has interest for breeders and companies, because advances in regulation of the disease could allow to control bacterial pathogens and prevent economic losses. In a world with continuous population growth, the improvement in agriculture efficiency among other measures could help to avoid shortages in food supply and help to mitigate the carbon footprint of agricultural practices (Beebe et al., 2013). Additionally, higher efficiency means that less agricultural land is required, and bigger efforts and extensions could be directed toward maintaining biodiversity (Trewavas, 2001). One of the most interesting aspects of the war between plants and bacteria, is the sessile nature of plants while bacteria have the advantage of being mobile. This fact has forced the evolutionary development in plants of sophisticated mechanisms of defense (Dangl and Jones, 2001). However, the immune response both from plants and animals, can cause a fitness disadvantage if it is held through time and not regulated. The eukaryotic sRNAs aid in the modulation of that response. But in the case of prokaryotes, sRNAs are relevant to fight back, involved in the regulation of different important pathogenic features during infection, such as secretion systems or mobility.

In this never-ending war biofilms help bacteria to endure different stresses, but plant immune systems have "learned" to target key molecules for its formation. Thus, mechanisms to evade the host recognition are necessary for the survival of the pathogen and establishment of a successful infection. In that regard, Nakatsu et al. (2019) have shown that not all isolates of *Pseudomonas syringae* produce AHLs. Many of the reported isolates carry mutations in two key genes: the AHL synthase *psyI*, or the AHL transcription factor *psyR*. Most probably the production of AHLs could have represented a biological burden for the infective processs. Strikingly, these strains still show responses of two sRNAs that should be related with AHLs, RsmY, and RsmX. Furthermore, their expression is enhanced at high cell densities, suggesting the existence of alternative routes for QS signaling. Although further research is needed, the loss of AHLs and the increased levels of these two sRNAs during situations with high number of cells, may reflect the involvement of these regulatory RNAs in mediating the coordination of a QS response.

In another brilliant event of the antagonism, plants have developed the capability to synthesize compounds that interfere with QS signalization. Rosmarinic acid (RA) was reported to bind with RhlR (instead of C_4-HSL), inducing abnormal premature behaviors related with biofilm formation and virulence. When cultures of *Pseudomonas aeruginosa* PAO1 were challenged

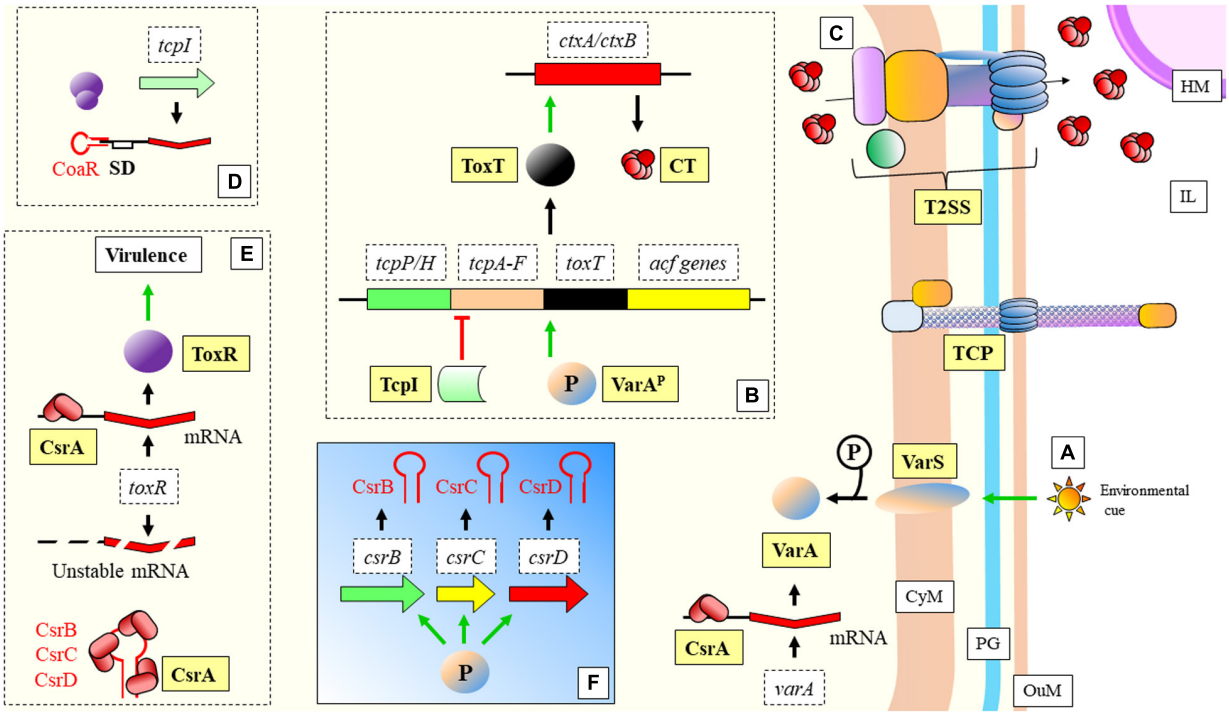

FIGURE 7 | *Vibrio cholerae*: mechanisms of virulence and regulation. **(A)** Environmental cues trigger the signalization in the two-component system VarS/VarA (functional homologs to the GacS/GacA two-component system of *P. aeruginosa*). Phosporilation of VarA activates this protein. Transcription of *varA* is facilitaded by CsrA. **(B)** VarA^P (activated) acts as a transcriptional activator of *toxT*. ToxT activates as well *ctxA/ctxB* encoding the two subunits of the CT protein, which is extruded to the IL through a T2SS **(C)**. The *tcpA* gene, required for the assembly of the TCP, is located in the same operon as *toxT*. TcpI is a transcriptional inhibitor of *tcpA*. TCP structure is necessary for the progression of the disease (bacterial aggregation and microcolony formation). **(D)** CoaR sRNA blocks binding of the ribosome to the *tcpI* mRNA. **(E)** CsrA stabilizes *toxR* mRNA, which is necessary for positive regulation of virulence genes. **(F)** VarA^P activates transcription of CsrB, CsrC, and CsrC sRNAs, which sequester CsrA, yielding an unstable *toxR* transcript. CT, Cholera toxin; CyM, Cytoplasmic membrane; HM, Host cell membrane; IL, Gastrointestinal lumen; OuM, Outer membrane; PG, peptidoglycan; T2SS, Type II secretion system; TCP, Toxin coregulated pilus. Black thick arrows indicate flow of a biological process, e.g., protein translation. Green thick arrows indicate activation. Red thick arrows with flat cap indicate inhibition. References: Hammer and Bassler, 2007; Jang et al., 2011; Cobaxin et al., 2014; Mey et al., 2015; Ng et al., 2016; Dorman and Dorman, 2018; Jemielita et al., 2018; Butz et al., 2019; Xi et al., 2020.

with RA, a group of sRNAs showed differential expression in response to the presence of RA, including the induction of RsmY (Fernández et al., 2018). This study highlights the relevance of sRNAs in the communication process between host and pathogen. If the host detects the presence of the bacteria, it can produce certain defensive compounds that will impair the virulence response of the pathogen through modification of important regulators and alteration of sRNA levels.

Plant-pathogen interaction it is not limited to detection and secretion, but it can reach up to a complex alteration of behaviors through genetic manipulation. Hijacking of the host metabolic machinery is not exclusive of viruses, it is a fine strategy of the gram-negative soil phytopathogen *Agrobacterium tumefaciens* (Gelvin, 2003; Hwang et al., 2017). The evolutionary counter-attack from plants has been the development of mechanisms to disrupt communication among pathogen cells, through the production of γ-aminobutyric acid (GABA) (Sheehan and Caswell, 2018). *Agrobacterium tumefaciens* and other Rhizobiales have an additional offensive strategy consisting in the production of AbcR1, a sRNA that regulates the plant transporter responsible for importing GABA molecules into the cell and its deleterious effects (Wilms et al., 2011). AbcR1 binds to the SD sequence and decreases the stability of the target mRNA.

A different sRNA, the highly conserved PmaR, can be found in *Agrobacterium* species and a specific strain of *Rhizobium* sp. It has been reported to be related to positive regulation of genes involved with peptidoglycan biosynthesis, motility, and virulence according to the study by Borgmann et al. (2018). Additionally, PmaR has a very important role in mediating ampicillin resistance, as observed after studying deletion mutants with impaired survival capabilities in growing concentrations of this antibiotic. The control of the antibiotic resistance gene was proposed by the authors as a means to obtain a biological advantage in the highly competitive rhizosphere environment. PmaR is a positive regulator binding to the 5′UTR, leading to the stabilization of the Shine-Dalgarno region, which would be otherwise prone to form structures preventing ribosome binding or even mRNAs destabilization.

Flowers are sensitive structures of plants, which can be used as an entry point by pathogens. Such an example is *Erwinia amylovora*, a Gram-negative bacteria responsible for fire blight disease in apple or pear trees belonging to Rosaceae (Oh and

Beer, 2005). Once the bacterium enters the host, it spreads using flagella through the vascular system to continue infection. Three sRNAs dependent on Hfq (ArcZ, OmrAB, and RmaA) have been linked to the maintenance of the swimming and motility levels of this bacterium (Zeng and Sundin, 2014). However, the specific molecular regulation mechanisms were not understood. Given that motility is related with flagella, a potential target of regulation mediated by sRNAs is the dual system composed by the proteins FlhD and FlhC regulating the expression of the rest of the genes in the flagellar regulon (Liu and Matsumura, 1994; Frye et al., 2006). Schachterle et al. (2019) researched the involvement of ArcZ, OmrAB, and RmaA in flagellar regulation. First, they found reduced expression levels for regulatory and flagellar structural genes in lack-of-function mutants (Δ*arcZ*, Δ*hfq*, Δ*omrAB,* and Δ*rmaA*) in comparison with the WT. Besides, they observed similar *flhD* mRNA levels in double and triple deletion mutants compared to the single deletion mutants. While ArcZ and RmaA regulate the transcription of *flhD*, the same ArcZ and OmrAB affect post-transcriptionally *flhD* master regulator mRNA.

The broad host range plant pathogen *Pantoea ananatis* is responsible for yield losses in many important crops. The roles and targets of Hfq were unknown, and a recent study measured the molecular and phenotypical differences between a WT strain versus the Δ*hfq* deletion and the *hfq* complementing mutant (Shin et al., 2019). The phenotype of Δ*hfq* strains showed a range of phenotypical impairments such as slower growth rate, or loss of virulence when infecting onion. Within virulence traits, the mutants were affected in swimming motility, had a reduced AHL production, and a decreased ability to form biofilms. The complementing mutant resembled the WT strain phenotype. Authors identified the affected sRNAs by comparison of loss-of-function mutant with WT, both in low-density and high-density conditions. After data analysis, expression levels for 9 sRNAs were assayed through RT-qPCRs (*arcZ*, *fnr*S, *glmZ*, *rpr*A, *rye*B, *ryh*B2, *pPAR*237, *pPAR*238, and *pPAR*395), with reduced transcript levels for all them in the mutant. That was not the case for *glmZ* and *ryhB2*, and authors conclude that it is due to a negative regulation of those two targets by Hfq in WT strains of *P. ananatis*.

The study of Yuan et al. (2019) used *Dickeya dadantii* as a model bacterial pathogen, which depend on swimming motility for migration to the entry structures of the plant. RsmA (CsrA) and RsmB (CsrB) comprise a protein-sRNA system of regulators of the Type III Secretion System (T3SS) and other virulence phenotypes. While RsmA controls negatively *hrpL*, the master regulator of the T3SS, RsmB can sequester the protein. Besides RsmB, AcrZ (Hfq mediation) is as well involved in the regulation of motility and virulence in *D. dadantii*.

INFECTIOUS DISEASES IN ANIMALS

As previously stated, infection represents a competition relationship between pathogenic bacteria and a variety of hosts (ranging from plants to animals) for the same metabolic resources (Rohmer et al., 2011). The development of the field is much broader in humans due to the relevance of infectious diseases from an anthropogenic perspective. For other species, the research interest has been driven by economic interest in farming, because the studied species can potentially act as reservoirs for zoonoses (Slingenbergh et al., 2004), or their potential as model organisms.

Non-vertebrates

Several non-vertebrate metazoans have attracted attention of the research community for different reasons, among them their similarity at innate immune responses with mammals (Tanji and Ip, 2005), because they constitute a vector for infectious diseases (Slingenbergh et al., 2004), or their importance as crop pests (Li et al., 2019).

The model organism *Caenorhabditis elegans* grazes on bacteria in the soil environment. Both bacteria and host establish a relationship which constitutes one of the most clear examples of interkingdom communication (Legüe and Calixto, 2019). It has been reported that *E. coli* sRNAs (OxyS and DsrA) can impact the expression of genes in the host (Liu et al., 2012). The uptake of non-self RNA molecules can happen via RNA transporters that have as well homologs in humans (Legüe and Calixto, 2019), or through membrane vesicle transport (Dauros-Singorenko et al., 2018).

Mutualistic endosymbionts are subjected to genome erosion, e.g., *Buchnera* in aphids (Wernegreen, 2002; Bennett and Moran, 2015). This reduction leads to losses in genes encoding for transcription factors, and highlights the importance of sRNAs as alternative regulatory elements. An early study by Hansen and Degnan (2014) found an interesting lack of mRNA expression in different life stages of *Buchnera*, while it was clear that proteins were differentially expressed. They predicted the involvement of a group of more than 600 sRNAs in protein regulation. Thairu et al. (2018) studied if these sRNAs were to be involved in post-transcriptional regulation events, by evaluation of two life stages of the endosymbiont, the extracellular proliferating stage in aphid embryos of *Acyrthosiphon pisum*, and the intracellular non-proliferating state in bacteriocytes of the same host. After RNA isolation (size $\leq$ 200 nt) and library preparation, authors performed sequencing, where data analysis provided a first indication of a group of 90 differentially expressed putative sRNAs. Authors evaluated *in vitro* the regulatory properties of one of these sRNAs, which putative target is *carB*, by cloning the regulatory element and its predicted coding sequence (CDS) target into two separate plasmids. The CDS was fused with the green fluorescent protein CDS (GFP), and indication in stabilization of mRNA would be suggested by enhanced fluorescence in the dual-plasmid system, in comparison with the control (where the vector that should contain the sRNA was empty). Results indicated that *carB* sRNA stabilizes the messenger of the target, and would compensate for the evolutionary loss of regulatory genes. But also, the changes in the insect diet can exert an effect over the endosymbiont. Thairu and Hansen (2019) measured through transcriptomic approaches if changes in the host diet would affect the sRNA regulatory pathways. Authors found that most of the potential targets among two conditions, when the aphid fed on two plants with notable differences in secondary metabolites, were related with

amino-acid biosynthesis. The results are probably explained by the intimate relationship between the host insect and the endosymbiont, where changing in the host will drive a different transcriptional program to the cohabiting bacterium.

Wolbachia pipientis is an endosymbiont of insects that can affect the host behavior for ensuring its own vertical transmission (Werren et al., 2008). In experiments of infection of *Drosophila melanogaster* specimens or *Aedes albopictus* C6/36 cell lines with *W. pipientis*, Woolfit et al. (2015) examined the transcriptome response of both host and microorganism. Their results yielded a set of reads corresponding to intergenic regions of the bacteria that together with *in silico* candidates, allowed authors to identify two putative sRNAs. While further research is required for a better characterization of *Wolbachia* small regulatory RNAs, authors hypothesize that there could be an involvement in host manipulation.

Vertebrates

High-throughput approaches evaluating the transcriptomic profile of both host and pathogen have become very important for the discovery of new sRNAs and their effect during the infection process (Saliba et al., 2017). The molecular behavior of pathogens is different when cultivated at *in vitro* conditions than when they are interacting with the host (Westermann et al., 2012). This method is known as "dual RNA-seq" (reviewed in Saliba et al., 2017; Westermann et al., 2017) and was used in bacterial infections models first by Westermann et al. (2016), studying the interaction between *Salmonella enterica* serovar Typhimurium and HeLa cells. Authors identified a highly expressed sRNA, PinT, which interacts with mRNAs by Hfq mediation. Not only this approach allows to characterize the bacterial sRNA profile, but also the study revealed a correlation of this sRNA with effects over the host immune pathways.

Non-human Models

A great fraction of the development on the field has been driven by economic interest, in order to understand the life cycle of causative agents for bacterial diseases in aquaculture farming industry. These settings concentrate in a short spatial range a significant number of specimens that could become up to 1,000 times higher than natural populations (Sundberg et al., 2016). Intensive fish farming has led to use of antibiotics, which together with the abnormal number of individuals, turn these exploitations into a hot-spot for the selection and spread of antibiotic resistance in the environment (McPhearson et al., 1991). Furthermore, the selection pressure within the microbiome due to interference and competition, directs toward quick changes in pathogen virulence that could be fixed in the genome (Sundberg et al., 2016). A necessary first step for an accurate understanding of the role of sRNAs at infection processes, is to survey the core repertoire of non-coding RNAs, as reported in a recent study (Segovia et al., 2018). Authors analyzed eleven *P. salmonis* genomes, having described more than 2,000 sRNAs (referred as non-coding RNAs, ncRNAs), from which more than 1,300 formed the ncRNA core group. Analyses of these RNAs have shown that many of the targeted genes in the bacterial genome show similarities to those described in section "sRNAs Regulate Key Processes for the Establishment of Infection." of the current review. Among these similarities: manganese sensing response, membrane transport, components of the Type I and II Secretion Systems, expression of enzymes necessary for tissue colonization and acid resistance, or regulation of carbon flux.

Besides aquaculture, research in other vertebrates has been driven by biomedical interest in species that could serve as an alternative experimental model for human infectious diseases. In comparison with insect species, murine models show additional advantages, such as the presence of adaptive immunity or a wide range of available genetic resources. A murine macrophage line has been used to evaluate the interaction with *Brucella abortus*, a pathogen causing infectious diseases in cattle but also in humans (Golding et al., 2001; Budnick et al., 2018). Several sRNAs have been identified in *Brucella* spp., some of which have been associated with the pathogen virulence (Dong et al., 2018). When the sRNA BASI74 was overexpressed, the virulence of *Brucella* was negatively affected, while deletion had no effect. This is potentially explained by the presence of different copies of the sRNA in the bacterial genome, due to an important regulatory role. It means that while overexpression produces an excessive regulatory response, loss of an sRNA is compensated by different versions or alternative sRNAs. From an evolutionary perspective, it will help the pathogen to maintain regulation of important genes even when some sRNAs are lost from the genome.

Human as a Host

Recognition of bacterial infective agents relies on the innate immunity and a series of germline-encoded pattern-recognition receptors (PRRs) (Sellge and Kufer, 2015; González Plaza, 2018). Among others, TLRs strongly trigger systemic inflammation via macrophages and neutrophils (Moresco et al., 2011). These receptors can sense as well RNA molecules (Kawai and Akira, 2009), especially through TLR3, TLR7, and TLR8 (Hornung et al., 2008; Moresco et al., 2011). These receptors recognize molecules that are essential for the proper biological function of the bacteria, and thus, will be subjected to less evolutionary modifications than others (Akira et al., 2006).

But not in all cases bacterial RNA unleash an inflammatory response. Milillo et al. (2019) have reported down-modulation of MHC-II surface proteins in human monocytes/macrophages in the presence of *Brucella abortus* RNA. Because RNA is a molecule with a short lifespan and is subject to rapid degradation, it is present in alive bacteria rather than in dead cells. Authors argue that their findings suggest how *B. abortus* may thrive undetected within macrophages, due to the impairment of the MHC-II antigen presentation by inhibition of the gene expression. Nevertheless, the effect was also observed with partially degraded RNA. This molecular evasion could happen as well for many other pathogens, that could multiply and cause a serious disease requiring clinical treatment with antimicrobials. However, due to the current antibiotic crisis, the treatment of bacterial infections is becoming increasingly difficult due to the appearance of resistance (Bogaert et al., 2004). Given the role of sRNAs as regulatory molecules, it is clear that understanding their role during infection could lead to improved therapies to control the expression of resistance genes (Dersch et al., 2017). Focusing

on sRNAs as therapeutic targets could be done in two main ways, targeting the mechanisms that regulate the virulence and infection related biological processes in the pathogen, or targeting the expression and regulation of antibiotic resistance genes. The latter group of genes are commonly shared among clinical pathogens in matter of years or months (O'Neill, 2014). Understanding interaction of one gene with its sRNA or set of sRNAs would likely be a universal therapy for different bacteria harboring the same resistance factor and become a promising research area for new treatments where bacteria will not presumably develop resistance (Ghaly and Gillings, 2018).

Respiratory diseases

One of the biggest issues during the onset of viral respiratory tract infections, is the frequent co-occurrence of bacterial infections that can dramatically aggravate the symptoms and the number of deaths (Mallia and Johnston, 2007). One of the explanations is that viral infections weaken host defense mechanisms, such as the clearance of bacteria by ciliated epithelial cells. Viral induced impairment of these processes create a favorable environment for the development of side bacterial infections by opportunistic pathogens (Hendaus et al., 2015).

Among those, *Staphylococcus aureus* can colonize different body surfaces and cause serious respiratory disorders (Lowy, 1998). The pool of more than 600 regulatory sRNAs present in this bacterium remains largely uncharacterized (Tomasini et al., 2014; Sassi et al., 2015; Carroll et al., 2016), but also provides an idea of the potential for adaptation to changing environments and success in the establishment of infection (Bayer et al., 1996). The global regulator *sarA* locus encodes a protein that regulate directly and indirectly genes involved in virulence (Dunman et al., 2001). This locus has three promoters (P2, P3, and P1 according to their genomic order) in a region of 850 bp upstream of the *sarA* coding sequence, and a 196 nucleotide sRNA (teg49) located within two of the promoters (Kim et al., 2014). Three overlapping transcripts including *sarA* ORF are produced. Mutagenesis assays in several regulatory sRNAs and the three promoters, indicated that teg49 is probably generated at the promoter P3 mRNA, likely through cleavage (Manna et al., 2018). Deletion of the P3 promoter resulted in the disappearance of both *sarA* P3 mRNA and teg49, besides lower SarA protein levels. Additional transcriptomics assays in the teg49 mutant, disclosed a group of genes which were up- and down-regulated in the absence of this sRNA. Those genes were involved in regulation, metabolism, and virulence. Teg41 is another sRNA involved in virulence regulation in *S. aureus*. It has been further characterized by Zapf et al. (2019; **Table 2**). This sRNA of approximately 200 nucleotides is located downstream of the transcript region of the potent phenol soluble modulin (PSMs) toxin type α. Authors propose that this sRNA positively regulates the toxin production by mRNA stabilization. Among different assays, they showed how the deletion of the 3′ sRNA region induced decreased levels of the αPSM transcripts, while higher levels of the toxin transcript were reported when Teg41 was overexpressed. The metabolic adaptation to nutritional starvation is also present in this pathogen, with the participation of sRNAs for the regulation of metabolism, as shown for RsaE (Bohn et al., 2010). A recent study on this regulator compared the transcriptomic response of two RsaE mutants, one by deletion, and the other by addition of an inducible promoter, with a wild type strain (Rochat et al., 2018). This sRNA has an effect over genes encoding enzymes of the TCA cycle, but also in the regulation of arginine catabolism, which was newly reported in this study.

Streptococcus pneumoniae is a Gram-positive bacterium that causes a wide range of complications, including sepsis, meningitis, or pneumonia. It has been suggested that it was a magnifying cause of the high death rates during the 1918 influenza pandemic (Mallia and Johnston, 2007). Sinha et al. (2018) studied through a massive RNA sequencing *S. pneumoniae* strain D39W grown in laboratory conditions (**Table 2**). The first list yielded a total of 57 sRNAs, and authors raised the question if those were primarily expressed, or further cleaved by RNase to get to its final form. In that regard, differential RNAseq was carried out, and authors report a group of 44 novel sRNA candidates. These regulatory RNAs fall in three categories: antisense RNAs, short-antisense RNAs, or long-antisense RNAs. Some of these regulatory molecules have been proposed to regulate metabolic responses of the pathogen.

Tuberculosis is one of the most studied infectious diseases due to its incidence. It is estimated to affect 23% of the world population in its latent stage (Lyu L et al., 2019). Although previously the disease was projected to be eradicated by 2010, it has been continuously re-emerging due to a complex combination of factors (Cohen, 2000). The role of sRNAs has been long established, and there is a growing body of knowledge on the topic. However, as reported by Mai et al. (2019), there are considerable gaps of knowledge regarding small regulatory RNAs. The field has discovered until now a wide set of these molecules, but bigger efforts to elucidate their molecular mechanisms of action are needed. The sRNA 6C (six cytosine residues) was hypothesized, by the authors of this study, to play an important role in regulation of cell division of *Mycobacterium tuberculosis (M. tb)* (Mai et al., 2019). In their experiments, the authors used a vector to overexpress 6C sRNA of *M. tb*, and transformed *Mycobacterium smegmatis*. Analyses of expression through RNAseq indicate that the potential targets of 6C could be under negative regulation, through base pairing to the mRNA targets at the C-rich loops. While in Gram-negative bacteria the interaction must be mediated by Hfq, in high GC Gram-positive bacteria has been hypothesized the presence of putative chaperones, or as in this study by direct binding mechanisms independent of chaperones (Mai et al., 2019; **Table 2**).

Additional regulation of *Mycobacterium tuberculosis* by sRNAs was provided in the study of Gerrick et al. (2018), who tested the landscape of small regulatory RNAs in the presence of five stresses relevant for the pathogen, having found 189 sRNAs (**Table 2**). The direct interaction of one of those sRNAs, MrsI, with the target mRNA is potentially mediated by non-canonical chaperones, given that there are no described HfQ or ProQ homologs in mycobacteria. MrsI is expressed in conditions of iron starvation and membrane stress, when the host immune system triggers an inflammatory response including an iron withholding

TABLE 2 | Relevant sRNAs of several infectious diseases having humans as a host.

Pathogen	Infection	sRNA	Mechanism of action	Effect on bacterial physiology	References
Escherichia coli O157:H7	Enterohemorrhagic	DicF	Hfq mediated. Liberates a secondary structure blocking the SD site of *pchA* mRNA.	Promotion of virulence: indirect enhancement of the expression of the LEE pathogenicity island during low oxygen conditions.	Melson and Kendall, 2019
Escherichia coli O157:H7	Enterohemorrhagic	Esr41	Hfq mediated. Forms a ternary complex with *ler* mRNA to repress *ler* expression.	Regulation of *ler* decreases adhesion ability of the pathogen, activation of *fliA* transcription has a positive regulatory effect over flagellum genes, and ultimately mobility.	Sudo et al., 2018
Listeria monocytogenes	Listeriosis	LhrC	Binding upstream from RBS, decrease mRNA stability.	Regulation of heme use and detoxification.	Ross et al., 2019
Listeria monocytogenes	Listeriosis	Ril47	Binding to SD, decrease mRNA stability.	Regulation of *ilvA* expression prevents isoleucine synthesis.	Marinho et al., 2019
Mycobacterium tuberculosis	Tuberculosis	6C	Negative regulation of targets by chaperone-independent binding to mRNAs.	Some targets include DNA replication or protein secretion.	Mai et al., 2019
Mycobacterium tuberculosis	Tuberculosis	189 sRNAs; MrsI	Target binding by non-canonical chaperones.	The studied sRNA is expressed during iron starvation and membrane stress.	Gerrick et al., 2018
Mycobacterium tuberculosis	Tuberculosis	ASdes	N/A	sRNA detected in plasma of patients, diagnostic biomarker potential.	Fu et al., 2018
Salmonella enterica serovar Typhimurium	Typhoid fever	STnc540	Hfq independent, mediation by ProQ.	Represses the expression of a magnesium-translocating P-type ATPase.	Westermann et al., 2019
Staphylococcus aureus	Opportunistic	Teg41	Suggested stabilization of the mRNA.	Positive regulation of PSM toxins.	Zapf et al., 2019
Staphylococcus aureus	Opportunistic	Teg49	Undetermined.	Teg49 potentially regulates regulatory factors, virulence, and metabolism. Together they affect virulence at infected tissues.	Manna et al., 2018
Streptococcus pneumoniae	Sepsis, meningitis, pneumonia	112 sRNAs	N/A	Regulation of different targets, some related to pathogen metabolism.	Sinha et al., 2018

LEE, locus of enterocyte effacement; RBS, ribosome binding site; PSM, phenol soluble modulin.

strategy, especially when entering macrophages. This response seems to be activated when the bacteria starts to suffer membrane and oxidative stresses, as the previous state of iron deprivation. This anticipatory response is not exclusive for *M. tuberculosis*, but according to authors has been observed in different prokaryotic organisms and it may have been developed as an evolutionary response to the inflammatory response by the host.

There is interest in developing sRNAs as stable markers for early diagnosis of the disease (Fu et al., 2018). Bacterial cell cultures of tuberculosis were studied by Fu and collaborators (Fu et al., 2018), who report four types of sRNAs (ASdes, ASpks, AS1726, and AS1890) (**Table 2**). On a first phase of this study, the authors tested whether these sRNAs would be detectable in the supernatant of cultures of *Mycobacterium bovis* BCG. Cultures of BCG were selected because the regulatory RNAs display 100% identity *in silico* between both strains. Once it was clear that the methodology was robust for identification of sRNAs from supernatant, authors tested the plasma of infected patients (*Mycobacterium tuberculosis*) in comparison with healthy controls. Among the four above mentioned regulatory RNAs, only ASdes was traced to the plasma of most tuberculosis patients, with statistical significance. These results are promising for the development of quick diagnostic assays based on the detection in blood or saliva of sRNAs derived from pathogens.

Gastrointestinal pathogenic diseases

When enterohemorrhagic *Escherichia coli* O157:H7 (EHEC), a food-borne pathogen, enters the digestive tract, it must adapt from oxygen rich environments to an increasingly oxygen-limiting environment toward the colon, where pathogens sense the differential gas concentrations and start to express their virulence factors (Melson and Kendall, 2019). As mentioned above, this is a key behavior of bacterial strains in order to set the basis of the infection onset, which seems to have evolved to start from a very low number of input cells (Van Elsas et al., 2011). DicF is a sRNA dependent on Hfq directly targeting the SD sequence of the transcriptional activator *pchA*, to promote its expression under low oxygen conditions (Melson and Kendall, 2019; **Table 2**). Ultimately, DicF has an effect over virulence by indirect increase of the expression of the locus of enterocyte effacement (LEE) pathogenicity island, but only when Hfq is present and oxygen concentration is very low (**Figure 8**). This means that during the disease establishment and progression, the pathogen has a mechanism to sense when it has reached the colon so that the virulence factors should be expressed at the right time. One of the most relevant and novel aspects of the previous study, is the reporting on a sRNA that has a positive expression effect by liberating a transcriptional activator virulence gene from its own mRNA repressive activities (**Figure 8**). Another sRNA was recently shown to be involved in regulation of LEE and flagellar genes (Sudo et al., 2018). Esr41 requires Hfq mediation, and

has regulatory functions over cell motility (Sudo et al., 2014) by induced activation of *fliA*, which encodes the transcription factor σ^{28} that regulates the expression of the class 3 flagellin subunit genes (Aldridge et al., 2006). Esr41 forms a ternary complex with the *ler* mRNA and Hfq for repression of the gene (**Figure 9**), leading to consequent repression of the LEE and a decrease in the adhesion ability of the pathogen (Sudo et al., 2018).

Listeria monocytogenes is the causative agent of listeriosis (Ágoston et al., 2009), characterized by different episodes of fever, diarrhea, or meningoencephalitis among other symptoms (Swaminathan and Gerner-Smidt, 2007). There are mainly two forms of this disease, the non-invasive gastrointestinal febrile manifestation, and the invasive life-threatening form causing for instance meningoencephalitis (Allerberger and Wagner, 2010). In this organism, the seven sRNAs comprising the LhrC family act by regulating the target *tcsA* that encodes a virulence protein, $CD4^{+}$ T cell-stimulating antigen (Sanderson et al., 1995). The regulatory mechanism of LhrCs was recently elucidated, and follow a non-canonical pathway, where sRNAs bind far upstream of the RBS, impairing the stability of the mRNA through the participation of an unknown RNase decreasing the messenger half-life (Ross et al., 2019; **Table 2**). During the nutritional starvation confronted by the pathogen in the host, the bacteria can make use of the available iron at the host iron-containing proteins, as the heme group in hemoglobin (Cassat and Skaar, 2013). LhrC1-5, belonging to the LhrC family of sRNAs, has been related to the regulation of heme usage in this pathogen. dos Santos et al. (2018) have shown the involvement of these five sRNAs in the regulation of three genes that control heme toxicity (*tcsA*, *oppA*, and *lapB*). Besides, authors found indications of regulation through these sRNAs of three genes related with the uptake and use of heme. Host induced starvation of amino acids is one of the strategies of nutritional immunity used by mammalian hosts to limit the infection (Zhang and Rubin, 2013). In *L. monocytogenes* Ril47 is an sRNA under control of the stress activated sigma factor sigma B (σ^{B}), which is involved in a plethora of environmental stresses affecting the pathogen (Dorey et al., 2019). Ril47 binds to the SD sequence of the *ilvA* mRNA decreasing its stability, as suggested by a recent study (Marinho et al., 2019). The consequence is a negative regulation of isoleucine biosynthesis by prevention of threonine deaminase synthesis (which is encoded by *ilvA*).

Bacteria belonging to the genus *Salmonella* cause mainly two affections: diarrheal disease and typhoid fever. The latter has a mortality rate of 10−20% if it is not treated with antibiotics, being its causative agent is *Salmonella enterica* serovar Typhimurium (Fàbrega and Vila, 2013). An example of influence of sRNAs over the nutritional adaptation of this pathogen was provided in the study of Kröger et al. (2018), where they report two novel sRNAs involved in positive (STnc1740) and negative (RssR) modulation of the growth of *S. enterica* serovar Typhimurium, through utilization of myo-inositol as carbon source. While the role of Hfq has been widely studied in this pathogen, Westermann et al. (2019) evaluated the contribution of ProQ as alternative RBP. Authors followed a previous study where ProQ was reported to display novel posttranscriptional regulatory activities (Smirnov et al., 2016). The study from Westermann sought to shed light over the role of ProQ in virulence by altering the phenotype (deletion of the RBP) and used a dual RNA-seq approach. The invasion capabilities of the single mutant were decreased (2-fold vs. WT), but no dramatic differences were found when the RBP was overexpressed. While these phenotypes were observed when infecting HeLa cells, very mild virulence was reported during infection of human phagocytic cells. Further evaluation of the dual RNA-seq results (HeLa cells as host) revealed alteration in metabolism of the host and immune signaling pathways. The mutant pathogen had a range of transcriptomic alterations over genes involved in chemotaxis and motility (downregulation), or in ribosomal and invasion genes (upregulation). In their analysis authors identified STnc540 as an sRNA independent of Hfq and regulated by ProQ. The interplay between sRNA and RBP was further shown to affect the expression of a magnesium-translocating P-type ATPase.

Antibiotic resistance

Antibiotic resistance is a serious concern for society that threatens health systems worldwide (O'Neill, 2014). One the biggest problems is the continuous appearance of novel mechanisms of resistance often fuelled by the natural presence of those mechanisms in the environment, quick global spread of antibiotic resistance genes (ARGs), uptake by pathogenic bacteria that can become resistant to several antibiotics, and lastly the lack of alternatives for treatment of infections caused by multidrug resistant bacteria (MDR) (O'Neill, 2014). The emergence of novel antibiotic resistance genes has dramatic consequences when they reach the clinical practice as they will be irreversibly fixed (Böhm et al., 2020). This brings to memory ideas of bacterial caused plagues in the pre-antibiotic era, when there were no means of controlling pathogens. Resistance to antimicrobials is additionally shaped by environmental stresses (in many cases of anthropogenic origin) faced by bacteria (Poole, 2012), but also interestingly coincide with those highlighted in section "sRNAs Regulate Key Processes for the Establishment of Infection."

Genes conferring resistance to antibiotics are essentially subjected to genetic regulation, and thus, their expression can be as well tuned by sRNAs (Lalaouna et al., 2014). This fact makes sRNAs a potentially invaluable tool to treat emerging infections mediated by antibiotic resistant bacteria (ARBs). An increasing number of studies point toward that direction, and have been excellently reviewed by Lalaouna et al. (2014), Dersch et al. (2017), Felden and Cattoira (2018). The antibiotic susceptibility of multidrug-resistant (MDR) *Pseudomonas aeruginosa* was dramatically altered when AS1974 sRNA was overexpressed (Law et al., 2019). Authors of the study carried out a first screening on the sRNAs repertoire on three MDR clinical isolates, having found three small-regulatory RNAs that were significantly downregulated. Targets of AS1974 are involved mostly in pathways related with drug-resistance, but also regulation over oxidative stress, pilus biogenesis, and iron acquisition.

Escherichia coli can activate a stress-response mechanism mediated by RpoS (Poole, 2012). However, this mechanism is under regulation of a non-coding RNA, rprA, which induced

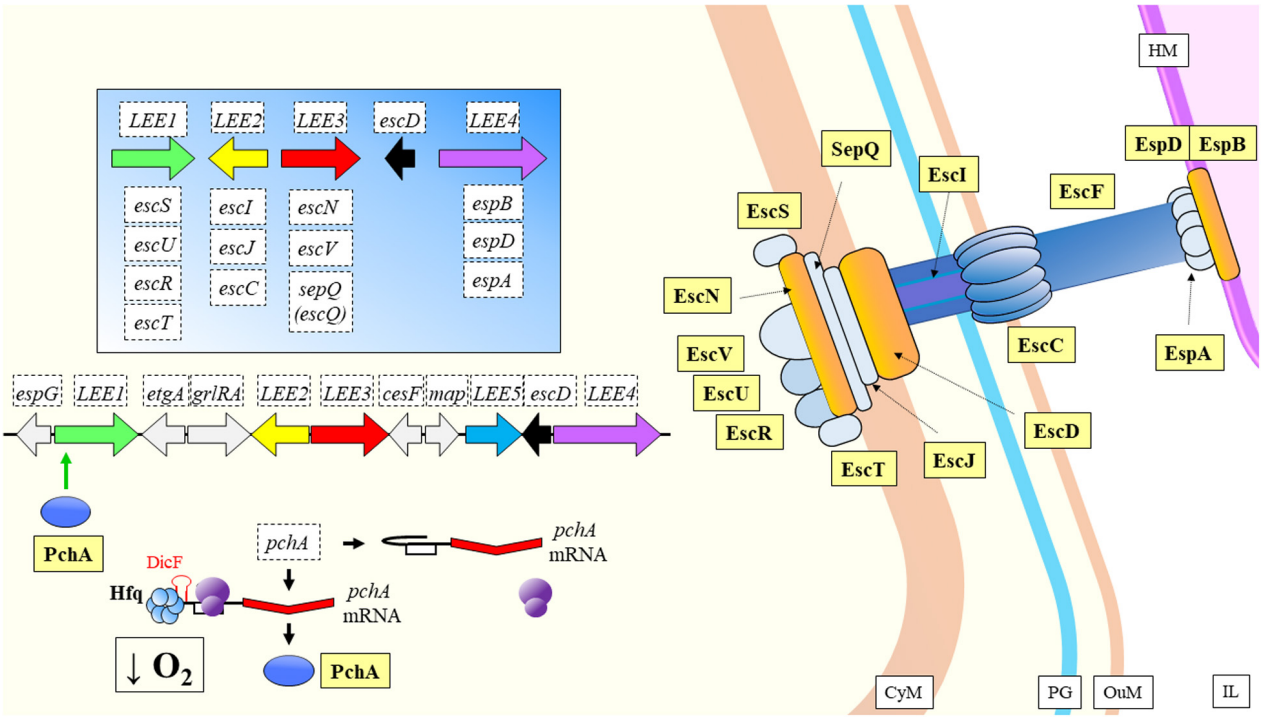

FIGURE 8 | Type III secretion system in EHEC. The *pchA* transcript has autoinhibitory activity, as it forms a secondary structure covering the SD site. When concentration of oxygen is low, DicF by mediation of Hfq frees the SD of pchA, allowing translation. PchA activates transcription of LEE genes involved in the synthesis of components of the T3SS. CyM, Cytoplasmic membrane; HM, Host cell membrane; IL, Gastrointestinal lumen; OuM, Outer membrane; PG, peptidoglycan; T3SS, Type III secretion system. Black thick arrows indicate flow of a biological process, e.g., protein translation. Green thick arrows indicate activation. References: Deng et al., 2004; Pallen et al., 2005; Izoré et al., 2011; Ruano-Gallego et al., 2015; Furniss and Clements, 2018; Pena et al., 2019.

ampicillin resistance when overexpressed (Sahni et al., 2019). The mRNA levels of this sRNA had been previously shown to increase in cells when treated with sub-inhibitory concentrations of ampicillin (Gutierrez et al., 2013).

Shigella strains are gaining attention due to the accumulation of resistances toward antibiotics (Puzari et al., 2018), for instance using efflux pumps to extrude fluoroquinolones from their intracellular space (Roy et al., 2020). Gan and Tan (2019) evaluated whether the sRNA SdsR, a transcriptomic regulator of the efflux pump *tolC* in *E. coli* and *Salmonella* (Choi et al., 2018), plays as well a regulatory role in *Shigella sonnei* or not. Although in previous reports SdsR lowers the levels of TolC mRNA and increases its sensitivity to fluoroquinolones, in their study the authors found that at decreasing levels of TolC mRNA the strain was less sensitive to antibiotics, such as norfloxacin.

DISCUSSION

This review focuses on the latest advances on small non-coding regulatory RNAs involved in bacterial infections, a field that has grown substantially in the last 2 years since the appearance of a previous review article (González Plaza, 2018). The importance of studying infectious diseases lies within the fact that global warming can lead to changing patterns in the distribution of bacteria causing diseases, or in the vectors harboring those microorganisms (Cohen, 2000; Epstein, 2001; Rodó et al., 2002; Khasnis and Nettleman, 2005). But not only from an anthropogenic perspective, these changing patterns in the distribution of infectious diseases can even cause the extinction of whole species (Harvell et al., 2002; Pounds et al., 2006).

Transference of information is a key process for quick adaptation to dynamic environments or species interactions, being one clear example the host-pathogen relationship. Infectious diseases have been shaped by co-evolution between pathogen and animal or plant hosts, both competing for the same metabolic resources. Due to the nature of RNA as a molecule with a short life-span, its role for modulation of environmental signals is of paramount importance for success of infection. This process represents a challenge for the survival of the bacteria, because the host sets a wide range of measures to limit the growth of the microbial strains, eliminate them, and recover homeostasis. The overall role of sRNAs is to fine-tune the bacterial response to different stresses, with an impressive amount of mechanisms of induction/repression of transcription. Not only they affect specific genes involved at synthesis/degradation pathways, but in many cases, they regulate the activity of transcription factors and regulators. Out of several studies it is clear that sRNAs can have multiple targets, and even achieve regulatory redundancy with other non-coding regulatory RNAs.

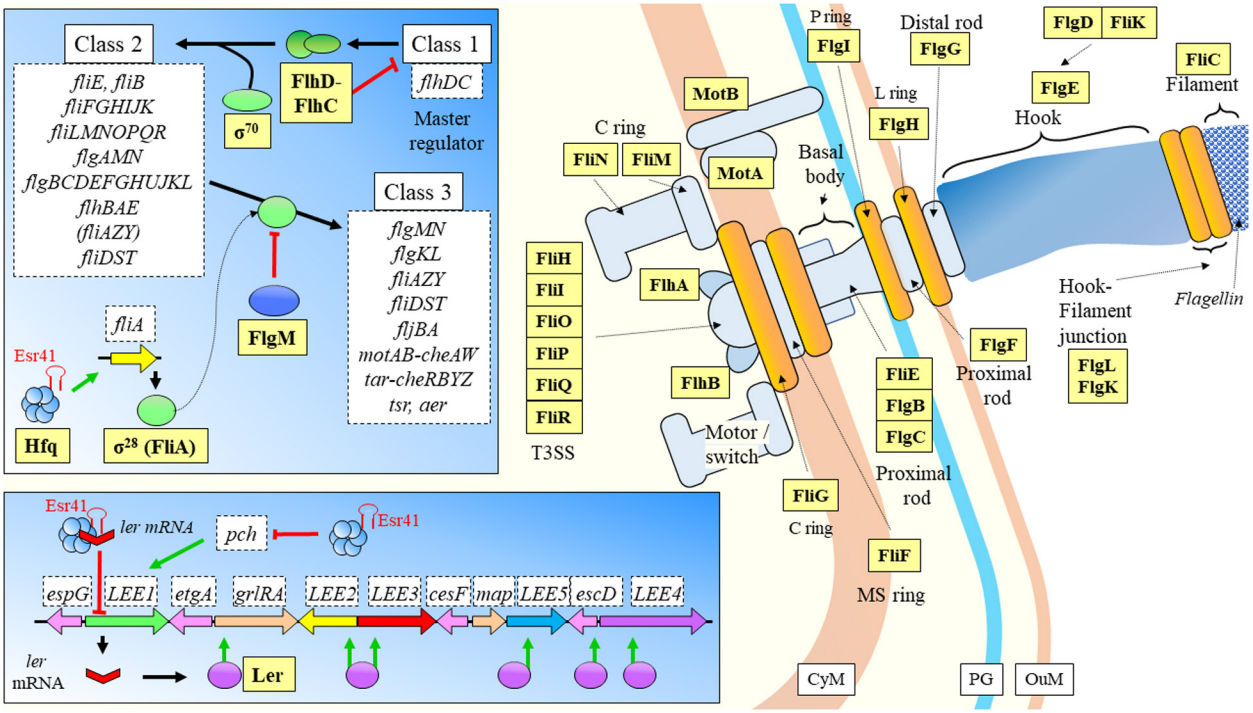

FIGURE 9 | EHEC flagellar system. The *fliA* encodes for a transcription factor controlling expression of class 3 genes. The sRNA Esr41 regulates positively via Hfq mediation *fliA*. The flagellar system is regulated by sRNAs at a key point. Esr41 has as well repressing activities over LEE1 operon, when it forms a ternary complex with Hfq and *ler* mRNA. This inhibition compromises coding of Ler protein, which is a transcriptional activator of different genes at the LEE. Esr41 has as well inhibitory activities over *pch* that facilitate LEE1 gene expression through promoter binding. CyM, Cytoplasmic membrane; HM, Host cell membrane; IL, Gastrointestinal lumen; OuM, Outer membrane; PG, peptidoglycan; T3SS, Type III secretion system. Black thick arrows indicate flow of a biological process, e.g., protein translation. Green thick arrows indicate activation. Red thick arrows with flat cap indicate inhibition. References: Kalir et al., 2001; Chevance et al., 2006; Frye et al., 2006; Liu and Ochman, 2007; Chevance and Hughes, 2008; Sudo et al., 2014, 2018; Bhatt et al., 2016 and KEGG (https://www.genome.jp/kegg/pathway/eco/eco02040.html).

Innate immune system response can limit nutrient (e.g. iron and manganese) availability to induce death of the pathogen, and a series of sRNAs help bacteria to quickly adapt to immune system challenges, such as the iron or nutrient withholding strategy, where the host limits the available resources in order to limit the survival chances of the invading bacteria. Bacteria encounter some other challenges in the host, for instance acid pH in the stomach of animals, or inflammation leading to oxidative stress. Many of these microbial responsive strategies seem to be conserved from environmental bacteria to pathogens (e.g., involvement of sRNAs in oxidative stress response due to salinity or inflammation), although it could have appeared owing to convergent evolution since sRNAs are very flexible molecules in their activities.

As presented in this review, a very useful approach, is to study both mRNA and sRNAs in the same samples, because it can lead to elucidate regulatory networks.

A number of the studies reviewed here are focused on surveying the sRNome repertoire, or also on the regulation of targets. There is a need to carry on with these studies, since this basic research is fundamental for being able to understand e.g., which genes could be directly modulated by the pathogen. This brings to memory the Spanish Presidential Elections in 2019, where as always, political parties kept promising the rise in research funds to 2% of GDP. Although every Spanish Scientist understands the magnitude of this false assertion, it was concerning how politicians have made theirs the mantra of "Applied Science" as the sole generator of progress and development. For instance, Pfizer was reported to have abandoned recently their program of applied research in neurodegenerative diseases (Trullàs, 2019), which should be an example of "*how could we apply what we do not fully understand*?". This seems to be a trend in every scientific system around the world (Lindsley, 2016), where the *application paragraph* is requested at every grant proposal, and does not seem possible to carry out a research project where the main aim is to obtain a "*general understanding of nature and its laws*" (Bush, 1945). It becomes clear why these type of basic studies are needed, because control of infections through drugs that can target pathogen sRNA regulation are not possible without a deep understanding of their structure, modes of regulation, behavior patterns during infection, or what genes alter their expression during infection. Small non-coding regulatory RNAs are a promising therapeutic target in the fight against multidrug-resistant bacteria, and since these molecules are less prone to

changes, we may have a great opportunity to tackle antibiotic resistance through gene-based therapies.

Having said that, what is still largely missing in the field are more studies focusing on the inter-kingdom exchange of sRNAs, either as counterfeit to impair the activity of the bacteria, or as a pathogenic mechanism to hijack the metabolic machinery of the host. Many protein effectors, such as those translocated by the T3SS can modify the response from the host. In the case of sRNAs, membrane vesicles (MVs) can carry the genetic material to their targets protecting it from degradation (Toyofuku et al., 2019), and ultimately subvert the molecular behavior of the host (Ghosal, 2017; González Plaza, 2018).

Lastly, the wide regulatory effects of sRNAs over the transcriptome must be taken in account due to their potential to impact genetic studies where a loss-of-function phenotype is considered as suggested by Popitsch et al. (2017). Deletion may affect expression of unannotated sRNAs and have undesired effects over the phenotype because regulation of a number of targets could be lost. It could as well potentially affect the expression of targets if some coding genetic regions carrying sRNAs are overexpressed. These possibilities invite to consider carefully the presence of small regulatory RNAs in genetic studies, and maybe even revisit some of the studies to date.

AUTHOR CONTRIBUTIONS

JG reviewed the literature, constructed all tables and figures according to published literature, and wrote the manuscript.

FUNDING

The author has been funded by projects IGA No. B_19_04 from the Faculty of Forestry and Wood Sciences (Czech University of Life Sciences, Prague); and "Advanced research supporting the forestry and wood-processing sector's adaptation to global change and the 4th industrial revolution," OP RDE, Ministry of Education Youth and Sports of Czechia, Grant No. CZ.02.1.01/0.0/0.0/16_019/0000803.

ACKNOWLEDGMENTS

I want to thank Assoc. Prof. J. Šobotník, for comments regarding the introduction and Ph.D. candidate P. Stiblík for technical support. I want to acknowledge the constructive comments of the reviewers.

REFERENCES

Agliano, F., Rathinam, V. A., Medvedev, A. E., Vanaja, S. K., and Vella, A. T. (2019). Long noncoding RNAs in host-pathogen interactions. *Trends Immunol.* 40, 492–510. doi: 10.1016/j.it.2019.04.001

Ágoston, R., Soni, K., Jesudhasan, P. R., Russell, W. K., Mohácsi-Farkas, C., and Pillai, S. D. (2009). Differential expression of proteins in *Listeria monocytogenes* under thermotolerance-inducing, heat shock, and prolonged heat shock conditions. *Foodborne Pathog. Dis.* 6, 1133–1140. doi: 10.1089/fpd.2009.0286

Aguilar, C., Mano, M., and Eulalio, A. (2019). MicroRNAs at the host-bacteria interface: host defense or bacterial offense. *Trends Microbiol.* 27, 206–218. doi: 10.1016/j.tim.2018.10.011

Akira, S., Uematsu, S., and Takeuchi, O. (2006). Pathogen recognition and innate immunity. *Cell* 124, 783–801. doi: 10.1016/j.cell.2006.02.015

Aldridge, P. D., Karlinsey, J. E., Aldridge, C., Birchall, C., Thompson, D., Yagasaki, J., et al. (2006). The flagellar-specific transcription factor, σ28, is the type III secretion chaperone for the flagellar-specific anti- σ28 factor FlgM. *Genes Dev.* 20, 2315–2326. doi: 10.1101/gad.380406

Allerberger, F., and Wagner, M. (2010). Listeriosis: a resurgent foodborne infection. *Clin. Microbiol. Infect.* 16, 16–23. doi: 10.1111/j.1469-0691.2009.03109.x

Álvarez-Estrada, Á, Gutiérrez-Martín, C. B., Rodríguez-Ferri, E. F., and Martínez-Martínez, S. (2018). Transcriptomics of *Haemophilus* (Glässerella) *Parasuis serovar* 5 subjected to culture conditions partially mimetic to natural infection for the search of new vaccine antigens. *BMC Vet. Res.* 14:326. doi: 10.1186/s12917-018-1647-1641

Andrews, S. C., Robinson, A. K., and Rodríguez-Quiñones, F. (2003). Bacterial iron homeostasis. *FEMS Microbiol. Rev.* 27, 215–237. doi: 10.1016/S0168-6445(03)00055-X

Atkinson, G. C., Tenson, T., and Hauryliuk, V. (2011). The RelA/SpoT homolog (RSH) superfamily: distribution and functional evolution of ppGpp synthetases and hydrolases across the tree of life. *PLoS One* 6:e23479. doi: 10.1371/journal.pone.0023479

Ausubel, F. F. M. (2005). Are innate immune signaling pathways in plants and animals conserved? *Nat. Immunol.* 6, 973–979. doi: 10.1038/ni1253

Baker, Y. R., Hodgkinson, J. T., Florea, B. I., Alza, E., Galloway, W. R. J. D., Grimm, L., et al. (2017). Identification of new quorum sensing autoinducer binding partners in: *Pseudomonas aeruginosa* using photoaffinity probes. *Chem. Sci.* 8, 7403–7411. doi: 10.1039/c7sc01270e

Battesti, A., Majdalani, N., and Gottesman, S. (2011). The RpoS-Mediated General Stress Response in *Escherichia coli*. *Annu. Rev. Microbiol.* 65, 189–213. doi: 10.1146/annurev-micro-090110-102946

Bayer, M. G., Heinrichs, J. H., and Cheung, A. L. (1996). The molecular architecture of the sar locus in *Staphylococcus aureus*. *J. Bacteriol.* 178, 4563–4570. doi: 10.1128/jb.178.15.4563-4570.1996

Beebe, S., Rao, I., Mukankusi, C., and Buruchara, R. (2013). *Improving Resource Use Efficiency And Reducing Risk Of Common Bean Production In Africa, Latin America, And The Caribbean, In Eco-Efficiency: From Vision To Reality, 117-134*. Available online at: http://ciat.cgiar.org/wp-content/uploads/2013/04/eco-efficiency_book.pdf (accessed December 17, 2019).

Beisel, C. L., and Storz, G. (2010). Base pairing small RNAs and their roles in global regulatory networks. *FEMS Microbiol. Rev.* 34, 866–882. doi: 10.1111/j.1574-6976.2010.00241.x

Benbow, M. E., Pechal, J. L., Tomberlin, J. K., and Jordan, H. R. (2018). "Interkingdom community interactions in disease ecology," in *The Connections Between Ecology and Infectious Disease. Advances in Environmental Microbiology*, Vol. 5, ed. C. Hurst, (Cham: Springer).

Bennett, G. M., and Moran, N. A. (2015). Heritable symbiosis: the advantages and perils of an evolutionary rabbit hole. *Proc. Natl. Acad. Sci. U.S.A.* 112, 10169–10176. doi: 10.1073/pnas.1421388112

Bermúdez-Barrientos, J. R., Ramírez-Sánchez, O., Chow, F. W.-N., Buck, A. H., and Abreu-Goodger, C. (2020). Disentangling sRNA-Seq data to study RNA communication between species. *Nucleic Acids Res.* 48:e21. doi: 10.1093/nar/gkz1198

Bhatt, S., Egan, M., Jenkins, V., Muche, S., and El-Fenej, J. (2016). The tip of the iceberg: on the roles of regulatory small RNAs in the virulence of enterohemorrhagic and enteropathogenic *Escherichia coli*. *Front. Cell. Infect. Microbiol.* 6:105. doi: 10.3389/fcimb.2016.00105

Bianco, C. M., Fröhlich, K. S., and Vanderpool, C. K. (2019). Bacterial cyclopropane fatty acid synthase mRNA is targeted by activating and repressing small RNAs. *bioRxiv* [Preprint], doi: 10.1128/jb.00461-419

Bidnenko, V., Nicolas, P., Grylak-Mielnicka, A., Delumeau, O., Auger, S., Aucouturier, A., et al. (2017). Termination factor Rho: from the control of pervasive transcription to cell fate determination in *Bacillus subtilis*. *PLoS Genet.* 13:e1006909. doi: 10.1371/journal.pgen.1006909

Bogaert, D., De Groot, R., and Hermans, P. W. M. (2004). *Streptococcus pneumoniae* colonisation: the key to pneumococcal disease. *Lancet Infect. Dis.* 4, 144–154. doi: 10.1016/S1473-3099(04)00938-937

Böhm, M.-E., Razavi, M., Marathe, N. P., Flach, C.-F., and Larsson, D. G. J. (2020). Discovery of a novel integron-borne aminoglycoside resistance gene present in clinical pathogens by screening environmental bacterial communities. *Microbiome* 8:41. doi: 10.1186/s40168-020-00814-z

Bohn, C., Rigoulay, C., Chabelskaya, S., Sharma, C. M., Marchais, A., Skorski, P., et al. (2010). Experimental discovery of small RNAs in *Staphylococcus aureus* reveals a riboregulator of central metabolism. *Nucleic Acids Res.* 38, 6620–6636. doi: 10.1093/nar/gkq462

Borgmann, J., Schäkermann, S., Bandow, J. E., and Narberhaus, F. (2018). A small regulatory RNA controls cell wall biosynthesis and antibiotic resistance. *mBio* 9:e002100-18. doi: 10.1128/mBio.02100-2118

Brant, E. J., and Budak, H. (2018). Plant small non-coding RNAs and their roles in biotic stresses. *Front. Plant Sci.* 9:1038. doi: 10.3389/fpls.2018.01038

Brouwer, S., Pustelny, C., Ritter, C., Klinkert, B., Narberhaus, F., and Häussler, S. (2014). The PqsR and RhlR transcriptional regulators determine the level of *Pseudomonas* quinolone signal synthesis in *Pseudomonas aeruginosa* by producing two different pqsABCDE mRNA Isoforms. *J. Bacteriol.* 196, 4163–4171. doi: 10.1128/JB.02000-2014

Budnick, J. A., Sheehan, L. M., Kang, L., Michalak, P., and Caswell, C. C. (2018). Characterization of three small proteins in Brucella abortus linked to fucose utilization. *J. Bacteriol.* 200:e00127-18. doi: 10.1128/JB.00127-118

Burne, R. A., and Chen, Y. Y. M. (2000). *Bacterial ureases* in infectious diseases. *Microbes Infect.* 2, 533–542. doi: 10.1016/S1286-4579(00)00312-319

Burtnick, M. N., Downey, J. S., Brett, P. J., Boylan, J. A., Frye, J. G., Hoover, T. R., et al. (2007). Insights into the complex regulation of rpoS in *Borrelia burgdorferi*. *Mol. Microbiol.* 65, 277–293. doi: 10.1111/j.1365-2958.2007.05813.x

Bush, V. (1945). *Science - The Endless Frontier*. Washington: Scientific Research and Development.

Butz, H. A., Mey, A. R., Ciosek, A. L., and Payne, S. M. (2019). *Vibrio cholerae* CsrA directly regulates varA to increase expression of the three nonredundant Csr small RNAs. *mBio* 10:e001042-19. doi: 10.1128/mBio.01042-1019

Caldelari, I., Chao, Y., Romby, P., and Vogel, J. (2013). RNA-mediated regulation in pathogenic bacteria. *Cold Spring Harb. Perspect. Med.* 3:10298. doi: 10.1101/cshperspect.a010298

Carlos, A. R., Weis, S., and Soares, M. P. (2018). Cross-talk between iron and glucose metabolism in the establishment of disease tolerance. *Front. Immunol.* 9:2498. doi: 10.3389/fimmu.2018.02498

Carrier, M.-C., Lalaouna, D., and Massé, E. (2018a). Broadening the definition of bacterial small RNAs: characteristics and mechanisms of action. *Annu. Rev. Microbiol.* 72, 141–161. doi: 10.1146/annurev-micro-090817-62607

Carrier, M. C., Laliberté, G., and Massé, E. (2018b). Identification of new bacterial small RNA targets using MS2 affinity purification coupled to RNA sequencing. *Methods Mol. Biol.* 1737, 77–88. doi: 10.1007/978-1-4939-7634-8_5

Carroll, R. K., Weiss, A., Broach, W. H., Wiemels, R. E., Mogen, A. B., Rice, K. C., et al. (2016). Genome-wide annotation, identification, and global transcriptomic analysis of regulatory or small RNA gene expression in *Staphylococcus aureus*. *mBio* 7:1990. doi: 10.1128/mBio.01990-1915

Casadevall, A. (2016). thermal restriction as an antimicrobial function of fever. *PLoS Pathog.* 12:5577. doi: 10.1371/journal.ppat.1005577

Casadevall, A., and Pirofski, L. (2003). The damage-response framework of microbial pathogenesis. *Nat. Rev. Microbiol.* 1, 17–24. doi: 10.1038/nrmicro732

Cassat, J. E., and Skaar, E. P. (2013). Iron in infection and immunity. *Cell Host Microbe* 13, 509–519. doi: 10.1016/j.chom.2013.04.010

Chakravarty, S., and Massé, E. (2019). RNA-dependent regulation of virulence in pathogenic bacteria. *Front. Cell. Infect. Microbiol.* 9:337. doi: 10.3389/fcimb.2019.00337

Chambonnier, G., Roux, L., Redelberger, D., Fadel, F., Filloux, A., Sivaneson, M., et al. (2016). The hybrid histidine kinase LadS forms a multicomponent signal transduction system with the GacS/GacA two-component system in *Pseudomonas aeruginosa*. *PLoS Genet.* 12:e1006032. doi: 10.1371/journal.pgen.1006032

Chatterji, D., and Ojha, A. K. (2001). Revisiting the stringent response, ppGpp and starvation signaling. *Curr. Opin. Microbiol.* 4, 160–165. doi: 10.1016/S1369-5274(00)00182-X

Chen, R., Wei, X., Li, Z., Weng, Y., Xia, Y., Ren, W. R., et al. (2019). Identification of a small RNA that directly controls the translation of the quorum sensing signal synthase gene rhlI in *Pseudomonas aeruginosa*. *Environ. Microbiol.* 21, 2933–2947. doi: 10.1111/1462-2920.14686

Chevance, F. F. V., and Hughes, K. T. (2008). Coordinating assembly of a bacterial macromolecular machine. *Nat. Rev. Microbiol.* 6, 455–465. doi: 10.1038/nrmicro1887

Chevance, F. F. V., Karlinsey, J. E., Wozniak, C. E., and Hughes, K. T. (2006). A little gene with big effects: a serT mutant is defective in flgM gene translation. *J. Bacteriol.* 188, 297–304. doi: 10.1128/JB.188.1.297-304.2006

Choi, J. S., Kim, W., Suk, S., Park, H., Bak, G., Yoon, J., et al. (2018). The small RNA, SdsR, acts as a novel type of toxin in *Escherichia coli*. *RNA Biol.* 15, 1319–1335. doi: 10.1080/15476286.2018.1532252

Cobaxin, M., Martínez, H., Ayala, G., Holmgren, J., Sjoling, A., and Sánchez, J. (2014). Cholera toxin expression by El Tor *Vibrio cholerae* in shallow culture growth conditions. *Microb. Pathog.* 66, 5–13. doi: 10.1016/j.micpath.2013.11.002

Coggan, K. A., and Wolfgang, M. C. (2012). Global regulatory pathways and cross-talk control *Pseudomonas aeruginosa* environmental lifestyle and virulence phenotype. *Curr. Issues Mol. Biol.* 14, 47–70. doi: 10.21775/cimb.014.047

Cohen, M. L. (2000). Changing patterns of infectious disease. *Nature* 406, 762–767. doi: 10.1038/35021206

Cornelis, P., Wei, Q., Andrews, S. C., and Vinckx, T. (2011). Iron homeostasis and management of oxidative stress response in bacteria. *Metallomics* 3, 540–549. doi: 10.1039/c1mt00022e

Cristaldo, P. F., Jandák, V., Kutalová, K., Rodrigues, V. B., Brothánek, M., Jiøíèek, O., et al. (2016). The nature of alarm communication in *Constrictotermes cyphergaster* (Blattodea: Termitoidea: Termitidae): the integration of chemical and vibroacoustic signals. *Biol. Open* 4, 1649–1659. doi: 10.1242/bio.014084

Damo, S. M., Kehl-Fie, T. E., Sugitani, N., Holt, M. E., Rathi, S., Murphy, W. J., et al. (2013). Molecular basis for manganese sequestration by calprotectin and roles in the innate immune response to invading bacterial pathogens. *Proc. Natl. Acad. Sci. U.S.A.* 110, 3841–3846. doi: 10.1073/pnas.1220341110

Dangl, J. L., and Jones, J. D. G. (2001). Plant pathogens and integrated defence responses to infection. *Nature* 411, 826–833. doi: 10.1038/35081161

Dauros-Singorenko, P., Blenkiron, C., Phillips, A., and Swift, S. (2018). The functional RNA cargo of bacterial membrane vesicles. *FEMS Microbiol. Lett.* 365:fny02. doi: 10.1093/femsle/fny023

Davies, D. G., Parsek, M. R., Pearson, J. P., Iglewski, B. H., Costerton, J. W., and Greenberg, E. (1998). The involvement of cell-to-cell signals in the development of a bacterial biofilm. *Science* 280, 295–298. doi: 10.1126/science.280.5361.295

de Viana, J. (1637). *Tratado de Peste, sus Causas y curacion, y el Modo Que se ha tenido de curar las Secas y Carbuncos Pestilentes que Han Oprimido A Esta Ciudad de Málaga este año de 1637., ed. J. Serrano de Vargas y Ureña Málaga*. Available online at: http://bdh.bne.es/bnesearch/biblioteca/Tratado de peste, sus causas y curacion, y el modo que se ha tenido de curar las secas y carbuncos pestilentes que han oprimido a esta ciudad de Malaga este año de 1637. /qls/Viana, Juan de/qls/bdh0000089890;jses (accessed April 5, 2020).

Deng, W., Puente, J. L., Gruenheid, S., Li, Y., Vallance, B. A., Vázquez, A., et al. (2004). Dissecting virulence: systematic and functional analyses of a pathogenicity island. *Proc. Natl. Acad. Sci. U.S.A.* 101, 3597–3602. doi: 10.1073/pnas.0400326101

Dersch, P., Khan, M. A., Mühlen, S., and Görke, B. (2017). Roles of regulatory RNAs for antibiotic resistance in bacteria and their potential value as novel drug targets. *Front. Microbiol.* 8:803. doi: 10.3389/fmicb.2017.00803

Diard, M., and Hardt, W.-D. (2017). Evolution of bacterial virulence. *FEMS Microbiol. Rev.* 41, 679–697. doi: 10.1093/femsre/fux023

Diaz-Ochoa, V. E., Jellbauer, S., Klaus, S., and Raffatellu, M. (2014). Transition metal ions at the crossroads of mucosal immunity and microbial pathogenesis. *Front. Cell. Infect. Microbiol.* 4:2. doi: 10.3389/fcimb.2014.00002

Djapgne, L., Panja, S., Brewer, L. K., Gans, J. H., Kane, M. A., Woodson, S. A., et al. (2018). The *Pseudomonas aeruginosa* PrrF1 and PrrF2 small regulatory RNAs promote 2-alkyl-4- quinolone production through redundant regulation of the antR mRNA. *J. Bacteriol.* 200:e0704-17. doi: 10.1128/JB.00704-717

Dong, H., Peng, X., Liu, Y., Wu, T., Wang, X., De, Y., et al. (2018). BASI74, a virulence-related sRNA in *Brucella abortus*. *Front. Microbiol.* 9:2173. doi: 10.3389/fmicb.2018.02173

Dong, T., and Schellhorn, H. E. (2010). Role of RpoS in virulence of pathogens. *Infect. Immun.* 78, 887–897. doi: 10.1128/IAI.00882-889

Dorey, A., Marinho, C., Piveteau, P., and O'Byrne, C. (2019). Role and regulation of the stress activated sigma factor sigma B (σ B) in the saprophytic and host-associated life stages of *Listeria monocytogenes*. *Adv. Appl. Microbiol.* 106, 1–48. doi: 10.1016/bs.aambs.2018.11.001

Dorman, M. J., and Dorman, C. J. (2018). Regulatory hierarchies controlling virulence gene expression in *Shigella flexneri* and *Vibrio cholerae*. *Front. Microbiol.* 9:2686. doi: 10.3389/fmicb.2018.02686

dos Santos, P. T., Menendez-Gil, P., Sabharwal, D., Christensen, J.-H., Brunhede, M. Z., Lillebæk, E. M. S., et al. (2018). The small regulatory RNAs LhrC1-5 contribute to the response of *Listeria monocytogenes* to heme toxicity. *Front. Microbiol.* 9:599. doi: 10.3389/fmicb.2018.00599

Drecktrah, D., Hall, L. S., Rescheneder, P., Lybecker, M., and Scott Samuels, D. (2018). The stringent response-regulated sRNA transcriptome of *Borrelia burgdorferi*. *Front. Cell. Infect. Microbiol.* 8:231. doi: 10.3389/fcimb.2018.00231

Drevinek, P., and Mahenthiralingam, E. (2010). *Burkholderia cenocepacia* in cystic fibrosis: epidemiology and molecular mechanisms of virulence. *Clin. Microbiol. Infect.* 16, 821–830. doi: 10.1111/j.1469-0691.2010.03237.x

Dubern, J. F., and Diggle, S. P. (2008). Quorum sensing by 2-alkyl-4-quinolones in *Pseudomonas aeruginosa* and other bacterial species. *Mol. Biosyst.* 4, 882–888. doi: 10.1039/b803796p

Dunman, P. M., Murphy, E., Haney, S., Palacios, D., Tucker-Kellogg, G., Wu, S., et al. (2001). Transcription profiling-based identification of *Staphylococcus aureus* genes regulated by the agr and/or sarA loci. *J. Bacteriol.* 183, 7341–7353. doi: 10.1128/JB.183.24.7341-7353.2001

Epstein, P. R. (2001). Climate change and emerging infectious diseases. *Microb. Infect.* 3, 747–754. doi: 10.1016/S1286-4579(01)01429-1420

Fàbrega, A., and Vila, J. (2013). *Salmonella enterica* serovar *Typhimurium* skills to succeed in the host: virulence and regulation. *Clin. Microbiol. Rev.* 26, 308–341. doi: 10.1128/CMR.00066-12

Fang, F. C., Libby, S. J., Buchmeier, N. A., Loewen, P. C., Switala, J., Harwood, J., et al. (1992). The alternative σ factor KatF (RpoS) regulates *Salmonella* virulence. *Proc. Natl. Acad. Sci. U.S.A.* 89, 11978–11982. doi: 10.1073/pnas.89.24.11978

Faucher, S. P., and Shuman, H. A. (2011). Small regulatory RNA and *Legionella pneumophila*. *Front. Microbiol.* 2:98. doi: 10.3389/fmicb.2011.00098

Felden, B., and Cattoira, V. (2018). Bacterial adaptation to antibiotics through regulatory RNAs. *Antimicrob. Agents Chemother.* 62:e002503-17. doi: 10.1128/AAC.02503-2517

Fernández, M., Corral-Lugo, A., and Krell, T. (2018). The plant compound rosmarinic acid induces a broad quorum sensing response in *Pseudomonas aeruginosa* PAO1. *Environ. Microbiol.* 20, 4230–4244. doi: 10.1111/1462-2920.14301

Ferrara, S., Brugnoli, M., de Bonis, A., Righetti, F., Delvillani, F., Dehò, G., et al. (2012). Comparative profiling of *Pseudomonas aeruginosa* strains reveals differential expression of novel unique and conserved small RNAs. *PLoS One* 7:36553. doi: 10.1371/journal.pone.0036553

Fischbach, M. A. (2009). Antibiotics from microbes: converging to kill. *Curr. Opin. Microbiol.* 12, 520–527. doi: 10.1016/j.mib.2009.07.002

Flahaut, S., Frere, J., Boutibonnes, P., and Auffray, Y. (1996). Comparison of the bile salts and sodium dodecyl sulfate stress responses in *Enterococcus faecalis*. *Appl. Environ. Microbiol.* 62, 2416–2420. doi: 10.1128/aem.62.7.2416-2420.1996

Frye, J., Karlinsey, J. E., Felise, H. R., Marzolf, B., Dowidar, N., McClelland, M., et al. (2006). Identification of new flagellar genes of *Salmonella enterica* serovar *typhimurium*. *J. Bacteriol.* 188, 2233–2243. doi: 10.1128/JB.188.6.2233-2243.2006

Fu, Y., Li, W., Wu, Z., Tao, Y., Wang, X., Wei, J., et al. (2018). Detection of mycobacterial small RNA in the bacterial culture supernatant and plasma of patients with active tuberculosis. *Biochem. Biophys. Res. Commun.* 503, 490–494. doi: 10.1016/j.bbrc.2018.04.165

Furniss, R. C. D., and Clements, A. (2018). Regulation of the locus of enterocyte effacement in attaching and effacing pathogens. *J. Bacteriol.* 200:e00336-17. doi: 10.1128/JB.00336-317

Gan, I.-N., and Tan, H. S. (2019). A small RNA decreases the sensitivity of *Shigella sonnei* to norfloxacin. *BMC Res. Notes* 12:97. doi: 10.1186/s13104-019-4124-4124

Gelsinger, D. R., and DiRuggiero, J. (2018). Transcriptional landscape and regulatory roles of small noncoding RNAs in the oxidative stress response of the haloarchaeon *Haloferax volcanii*. *J. Bacteriol.* 200:e00779-17. doi: 10.1128/JB.00779-717

Gelvin, S. B. (2003). Agrobacterium-mediated plant transformation: the biology behind the "gene-jockeying". *Tool. Microbiol. Mol. Biol. Rev.* 67, 16–37. doi: 10.1128/mmbr.67.1.16-37.2003

Gerrick, E. R., Barbier, T., Chase, M. R., Xu, R., François, J., Lin, V. H., et al. (2018). Small RNA profiling in *Mycobacterium tuberculosis* identifies MrsI as necessary for an anticipatory iron sparing response. *Proc. Natl. Acad. Sci. U.S.A.* 115, 6464–6469. doi: 10.1073/pnas.1718003115

Ghaly, T. M., and Gillings, M. R. (2018). Mobile DNAs as ecologically and evolutionarily independent units of life. *Trends Microbiol.* 26, 904–912. doi: 10.1016/j.tim.2018.05.008

Ghosal, A. (2017). Importance of secreted bacterial RNA in bacterial-host interactions in the gut. *Microb. Pathog.* 104, 161–163. doi: 10.1016/j.micpath.2017.01.032

Gilbertson, S., Federspiel, J. D., Hartenian, E., Cristea, I. M., and Glaunsinger, B. (2018). Changes in mRNA abundance drive shuttling of RNA binding proteins, linking cytoplasmic RNA degradation to transcription. *eLife* 7:37663. doi: 10.7554/eLife.37663

Golding, B., Scott, D. E., Scharf, O., Huang, L. Y., Zaitseva, M., Lapham, C., et al. (2001). Immunity and protection against *Brucella abortus*. *Microb. Infect.* 3, 43–48. doi: 10.1016/S1286-4579(00)01350-1352

González Plaza, J. J. (2018). Small RNAs in cell-to-cell communications during bacterial infection. *FEMS Microbiol. Lett.* 365:fny024. doi: 10.1093/femsle/fny024

González Plaza, J. J., Hulak, N., Zhumadilov, Z., Akilzhanova, A., Plaza, J. J. G., Jj, G. P., et al. (2016). Fever as an important resource for infectious diseases research. *Intractable Rare Dis. Res.* 5, 97–102. doi: 10.5582/irdr.2016.01009

Grimson, A., Srivastava, M., Fahey, B., Woodcroft, B. J., Chiang, H. R., King, N., et al. (2008). Early origins and evolution of microRNAs and Piwi-interacting RNAs in animals. *Nature* 455, 1193–1198.

Guo, Z., Li, Y., and Ding, S.-W. (2019). Small RNA-based antimicrobial immunity. *Nat. Rev. Immunol.* 19, 31–44. doi: 10.1038/s41577-018-0071-x

Gutierrez, A., Laureti, L., Crussard, S., Abida, H., Rodríguez-Rojas, A., Blázquez, J., et al. (2013). β-lactam antibiotics promote bacterial mutagenesis via an RpoS-mediated reduction in replication fidelity. *Nat. Commun.* 4:2607. doi: 10.1038/ncomms2607

Hammer, B. K., and Bassler, B. L. (2007). Regulatory small RNAs circumvent the conventional quorum sensing pathway in pandemic *Vibrio cholerae*. *Proc. Natl. Acad. Sci. U.S.A.* 104, 11145–11149. doi: 10.1073/pnas.0703860104

Han, Y., Chen, D., Yan, Y., Gao, X., Liu, Z., Xue, Y., et al. (2019). Hfq globally binds and destabilizes sRNAs and mRNAs in *Yersinia pestis*. *mSystems* 4:245. doi: 10.1128/msystems.00245-219

Hansen, A. K., and Degnan, P. H. (2014). Widespread expression of conserved small RNAs in small symbiont genomes. *ISME J.* 8, 2490–2502. doi: 10.1038/ismej.2014.121

Harkey, C. W., Everiss, K. D., and Peterson, K. M. (1994). The *Vibrio cholerae* toxin-coregulated-pilus gene tcpI encodes a homolog of methyl-accepting chemotaxis proteins. *Infect. Immun.* 62, 2669–2678. doi: 10.1128/IAI.62.7.2669-2678.1994

Harvell, C. D., Mitchell, C. E., Ward, J. R., Altizer, S., Dobson, A. P., Ostfeld, R. S., et al. (2002). Climate warming and disease risks for terrestrial and marine biota. *Science* 296, 2158–2162. doi: 10.1126/science.1063699

Hendaus, M. A., Jomha, F. A., and Alhammadi, A. H. (2015). Virus-induced secondary bacterial infection: a concise review. *Ther. Clin. Risk Manag.* 11, 1265–1271. doi: 10.2147/TCRM.S87789

Herrera, J., and Nunn, C. L. (2019). Behavioural ecology and infectious disease: implications for conservation of biodiversity. *Philos. Trans. R. Soc. B Biol. Sci.* 374:54. doi: 10.1098/rstb.2018.0054

Higgs, P. G., and Lehman, N. (2015). The RNA world: molecular cooperation at the origins of life. *Nat. Rev. Genet.* 16, 7–17. doi: 10.1038/nrg3841

Hille, F., Richter, H., Wong, S. P., Bratovič, M., Ressel, S., and Charpentier, E. (2018). The biology of CRISPR-Cas: backward and forward. *Cell* 172, 1239–1259. doi: 10.1016/j.cell.2017.11.032

Hoekzema, M., Romilly, C., Holmqvist, E., and Wagner, E. G. H. (2019). Hfq-dependent mRNA unfolding promotes sRNA -based inhibition of translation. *EMBO J.* 38:e101199. doi: 10.15252/embj.2018101199

Holmqvist, E., and Vogel, J. (2018). RNA-binding proteins in bacteria. *Nat. Rev. Microbiol.* 16, 601–615. doi: 10.1038/s41579-018-0049-45

Hornung, V., Barchet, W., Schlee, M., and Hartmann, G. (2008). "RNA Recognition via TLR7 and TLR8," in *Toll-Like Receptors (TLRs) and Innate Immunity. Handbook of Experimental Pharmacology*, Vol. 183, eds S. Bauer, and G. Hartmann, (Berlin: Springer), 71–86. doi: 10.1007/978-3-540-72167-3_4

How, M. J., Norman, M. D., Finn, J., Chung, W. S., and Marshall, N. J. (2017). Dynamic skin patterns in cephalopods. *Front. Physiol.* 8:393. doi: 10.3389/fphys.2017.00393

Hu, Y., Lu, P., Zhang, Y., Li, L., and Chen, S. (2010). Characterization of an aspartate-dependent acid survival system in *Yersinia pseudotuberculosis*. *FEBS Lett.* 584, 2311–2314. doi: 10.1016/j.febslet.2010.03.045

Hu, Y., Zhang, L., Wang, X., Sun, F., Kong, X., Dong, H., et al. (2018). Two virulent sRNAs identified by genomic sequencing target the type III secretion system in rice bacterial blight pathogen. *BMC Plant Biol.* 18:1477. doi: 10.1186/s12870-018-1470-1477

Hübner, A., Yang, X., Nolen, D. M., Popova, T. G., Cabello, F. C., and Norgard, M. V. (2001). Expression of *Borrelia burgdorferi* OspC and DbpA is controlled by a RpoN-RpoS regulatory pathway. *Proc. Natl. Acad. Sci. U.S.A.* 98, 12724–12729. doi: 10.1073/pnas.231442498

Hwang, H.-H., Yu, M., and Lai, E.-M. (2017). Agrobacterium -mediated plant transformation: biology and applications. *Arab. B* 15:e0186. doi: 10.1199/tab.0186

Ingle, R. A., Carstens, M., and Denby, K. J. (2006). PAMP recognition and the plant-pathogen arms race. *Bioessays* 28, 880–889. doi: 10.1002/bies.20457

Irving, S. E., and Corrigan, R. M. (2018). Triggering the stringent response: signals responsible for activating (p)ppGpp synthesis in bacteria. *Microbiology* 164, 268–276. doi: 10.1099/mic.0.000621

Islam, W., Noman, A., Qasim, M., and Wang, L. (2018). Plant responses to pathogen attack: small rnas in focus. *Int. J. Mol. Sci.* 19:515. doi: 10.3390/ijms19020515

Izoré, T., Job, V., and Dessen, A. (2011). Biogenesis, regulation, and targeting of the type III secretion system. *Structure* 19, 603–612. doi: 10.1016/j.str.2011.03.015

Jang, J., Jung, K. T., Park, J., Yoo, C. K., and Rhie, G. E. (2011). The *Vibrio cholerae* VarS/VarA two-component system controls the expression of virulence proteins through ToxT regulation. *Microbiology* 157, 1466–1473. doi: 10.1099/mic.0.043737-43730

Janssen, K. H., Diaz, M. R., Gode, C. J., Wolfgang, M. C., and Yahr, T. L. (2018a). RsmV, a small noncoding regulatory RNA in *Pseudomonas aeruginosa* that sequesters RsmA and RsmF from target mRNAs. *J. Bacteriol.* 200:e00277-18. doi: 10.1128/JB.00277-218

Janssen, K. H., Diaz, M. R., Golden, M., Graham, J. W., Sanders, W., Wolfgang, M. C., et al. (2018b). Functional analyses of the RsmY and RsmZ small noncoding regulatory RNAs in *Pseudomonas aeruginosa*. *J. Bacteriol.* 200:e0736-17. doi: 10.1128/JB.00736-17

Jemielita, M., Wingreen, N. S., and Bassler, B. L. (2018). Quorum sensing controls *Vibrio cholerae* multicellular aggregate formation. *eLife* 7:42057. doi: 10.7554/eLife.42057

Kalir, S., McClure, J., Pabbaraju, K., Southward, C., Ronen, M., Leibler, S., et al. (2001). Ordering genes in a flagella pathway by analysis of expression kinetics from living bacteria. *Science* 292, 2080–2083. doi: 10.1126/science.1058758

Kawai, T., and Akira, S. (2009). The roles of TLRs, RLRs and NLRs in pathogen recognition. *Int. Immunol.* 21, 317–337. doi: 10.1093/intimm/dxp017

Kay, E., Humair, B., Dénervaud, V., Riedel, K., Spahr, S., Eberl, L., et al. (2006). Two GacA-dependent small RNAs modulate the quorum-sensing response in *Pseudomonas aeruginosa*. *J. Bacteriol.* 188, 6026–6033. doi: 10.1128/JB.00409-406

Khasnis, A. A., and Nettleman, M. D. (2005). Global warming and infectious disease. *Arch. Med. Res.* 36, 689–696. doi: 10.1016/j.arcmed.2005.03.041

Kiekens, S., Sass, A., Van Nieuwerburgh, F., Deforce, D., and Coenye, T. (2018). The Small RNA ncS35 regulates growth in *Burkholderia cenocepacia* J2315. *mSphere* 3:e0579-17. doi: 10.1128/msphere.00579-517

Kim, S., Reyes, D., Beaume, M., Francois, P., and Cheung, A. (2014). Contribution of teg49 Small RNA in the 5′ upstream transcriptional region of sarA to virulence in *Staphylococcus aureus*. *Infect. Immun.* 82, 4369–4379. doi: 10.1128/IAI.02002-2014

Kim, V. N., Han, J., and Siomi, M. C. (2009). Biogenesis of small RNAs in animals. *Nat. Rev. Mol. Cell Biol.* 10, 127–139.

Kirchman, D. L., Meon, B., Cottrell, M. T., Hutchins, D. A., Weeks, D., and Bruland, K. W. (2000). Carbon versus iron limitation of bacterial growth in the California upwelling regime. *Limnol. Oceanogr.* 45, 1681–1688. doi: 10.4319/lo.2000.45.8.1681

Kluger, M. J., Kozak, W., Conn, C. A., Leon, L. R., and Soszynski, D. (1998). Role of fever in disease. *Ann. N. Y. Acad. Sci.* 856, 224–233. doi: 10.1111/j.1749-6632.1998.tb08329.x

Krämer, A., Akmatov, M., and Kretzschmar, M. (2009). "Principles of infectious disease epidemiology," in *Modern Infectious Disease Epidemiology. Statistics for Biology and Health*, eds A. Krämer, M. Kretzschmar, and K. Krickeberg, (New York, NY: Springer), 85–99. doi: 10.1007/978-0-387-93835-6_5

Kröger, C., Rothhardt, J. E., Brokatzky, D., Felsl, A., Kary, S. C., Heermann, R., et al. (2018). The small RNA RssR regulates myo-inositol degradation by *Salmonella enterica*. *Sci. Rep.* 8:17739. doi: 10.1038/s41598-018-35784-35788

Kuijl, C., and Neefjes, J. (2009). New insight into the everlasting host-pathogen arms race. *Nat. Immunol.* 10, 808–809. doi: 10.1038/ni0809-808

Lalaouna, D., Baude, J., Wu, Z., Tomasini, A., Chicher, J., Marzi, S., et al. (2019). RsaC sRNA modulates the oxidative stress response of *Staphylococcus aureus* during manganese starvation. *Nucleic Acids Res.* 47, 9871–9887. doi: 10.1093/nar/gkz728

Lalaouna, D., Eyraud, A., Chabelskaya, S., Felden, B., and Massé, E. (2014). Regulatory RNAs involved in bacterial antibiotic resistance. *PLoS Pathog.* 10:e04299. doi: 10.1371/journal.ppat.1004299

Lalaouna, D., Simoneau-Roy, M., Lafontaine, D., and Massé, E. (2013). Regulatory RNAs and target mRNA decay in prokaryotes. *Biochim. Biophys. Acta Gene Regul. Mech.* 1829, 742–747. doi: 10.1016/j.bbagrm.2013.02.013

Langdon, J. H (2016). "Case Study 1. The darwinian paradigm: an evolving world view," in *The Science of Human Evolution*, (Cham: Springer), 1–8. doi: 10.1007/978-3-319-41585-7

Law, C. O. K., Huang, C., Pan, Q., Lee, J., Hao, Q., Chan, T. F., et al. (2019). A small RNA transforms the multidrug resistance of *Pseudomonas aeruginosa* to drug susceptibility. *Mol. Ther. Nucleic Acids* 16, 218–228. doi: 10.1016/j.omtn.2019.02.011

Lee, J., and Zhang, L. (2015). The hierarchy quorum sensing network in *Pseudomonas aeruginosa*. *Protein Cell* 6, 26–41. doi: 10.1007/s13238-014-0100-x

Lee, R. C., Feinbaum, R. L., and Ambros, V. (1993). The *C. elegans* heterochronic gene lin-4 encodes small RNAs with antisense complementarity to lin-14. *Cell* 75, 843–854. doi: 10.1016/0092-8674(93)90529-y

Legüe, M., and Calixto, A. (2019). RNA language in *Caenorhabditis elegans* and bacteria interspecies communication and memory. *Curr. Opin. Syst. Biol.* 13, 16–22. doi: 10.1016/j.coisb.2018.08.005

Leid, J. G., Willson, C. J., Shirtliff, M. E., Hassett, D. J., Parsek, M. R., and Jeffers, A. K. (2005). The exopolysaccharide alginate protects *Pseudomonas aeruginosa* biofilm bacteria from IFN-γ-mediated macrophage killing. *J. Immunol.* 175, 7512–7518. doi: 10.4049/jimmunol.175.11.7512

Lejars, M., Kobayashi, A., and Hajnsdorf, E. (2019). Physiological roles of antisense RNAs in prokaryotes. *Biochimie* 164, 3–16. doi: 10.1016/j.biochi.2019.04.015

Lenz, D. H., Mok, K. C., Lilley, B. N., Kulkarni, R. V., Wingreen, N. S., and Bassler, B. L. (2004). The small RNA chaperone Hfq and multiple small RNAs control quorum sensing in *Vibrio harveyi* and *Vibrio cholerae*. *Cell* 118, 69–82. doi: 10.1016/j.cell.2004.06.009

Li, S., Xu, X., Zheng, Z., Zheng, J., Shakeel, M., and Jin, F. (2019). MicroRNA expression profiling of *Plutella xylostella* after challenge with *B. thuringiensis*. *Dev. Comp. Immunol.* 93, 115–124. doi: 10.1016/j.dci.2018.12.008

Liao, L., Liu, C., Zeng, Y., Zhao, B., Zhang, J., and Chen, B. (2019). Multipartite genomes and the sRNome in response to temperature stress of an Arctic *Pseudoalteromonas fuliginea* BSW20308. *Environ. Microbiol.* 21, 272–285. doi: 10.1111/1462-2920.14455

Lindsley, C. W. (2016). Lost in translation: the death of basic science. *ACS Chem. Neurosci.* 7, 1024–1024. doi: 10.1021/acschemneuro.6b00206

Liu, H., Wang, X., Wang, H. D., Wu, J., Ren, J., Meng, L., et al. (2012). *Escherichia coli* noncoding RNAs can affect gene expression and physiology of *Caenorhabditis elegans*. *Nat. Commun.* 3, 1–11. doi: 10.1038/ncomms2071

Liu, R., and Ochman, H. (2007). Stepwise formation of the bacterial flagellar system. *Proc. Natl. Acad. Sci. U.S.A.* 104, 7116–7121. doi: 10.1073/pnas.0700266104

Liu, X., and Matsumura, P. (1994). The FlhD/FlhC complex, a transcriptional activator of the *Escherichia coli* flagellar class II operons. *J. Bacteriol.* 176, 7345–7351. doi: 10.1128/jb.176.23.7345-7351.1994

Loh, E., Righetti, F., Eichner, H., Twittenhoff, C., and Narberhaus, F. (2018). RNA thermometers in bacterial pathogens. *Microbiol. Spectr.* 6:RWR-0012-2017. doi: 10.1128/microbiolspec.RWR-0012-2017

Lowy, F. D. (1998). Medical progress: *Staphylococcus aureus* infections. *N. Engl. J. Med.* 339, 520–532. doi: 10.1056/NEJM199808203390806

Lybecker, M. C., Abel, C. A., Feig, A. L., and Samuels, D. S. (2010). Identification and function of the RNA chaperone Hfq in the Lyme disease spirochete *Borrelia burgdorferi*. *Mol. Microbiol.* 78, 622–635. doi: 10.1111/j.1365-2958.2010.07374.x

Lybecker, M. C., and Samuels, D. S. (2007). Temperature-induced regulation of RpoS by a small RNA in *Borrelia burgdorferi*. *Mol. Microbiol.* 64, 1075–1089. doi: 10.1111/j.1365-2958.2007.05716.x

Lyu, L., Zhang, X., Li, C., Yang, T., Wang, J., Pan, L., et al. (2019). Small RNA profiles of serum exosomes derived from individuals with latent and active tuberculosis. *Front. Microbiol.* 10:1174. doi: 10.3389/fmicb.2019.01174

Lyu, Y., Wu, J., and Shi, Y. (2019). Metabolic and physiological perturbations of *Escherichia coli* W3100 by bacterial small RNA RyhB. *Biochimie* 162, 144–155. doi: 10.1016/j.biochi.2019.04.016

Mackowiak, P. A. (1981). Direct effects of hyperthermia on pathogenic microorganisms: teleologic implications with regard to fever. *Rev. Infect. Dis.* 3, 508–520. doi: 10.1093/CLINIDS/3.3.508

Mahenthiralingam, E., Urban, T. A., and Goldberg, J. B. (2005). The multifarious, multireplicon Burkholderia cepacia complex. *Nat. Rev. Microbiol.* 3, 144–156. doi: 10.1038/nrmicro1085

Mai, J., Rao, C., Watt, J., Sun, X., Lin, C., Zhang, L., et al. (2019). Mycobacterium tuberculosis 6C sRNA binds multiple mRNA targets via C-rich loops independent of RNA chaperones. *Nucleic Acids Res.* 47, 4292–4307. doi: 10.1093/nar/gkz149

Malgaonkar, A., and Nair, M. (2019). Quorum sensing in *Pseudomonas aeruginosa* mediated by RhlR is regulated by a small RNA PhrD. *Sci. Rep.* 9:89. doi: 10.1038/s41598-018-36488-36489

Mallia, P., and Johnston, S. L. (2007). Influenza infection and COPD. *Int. J. COPD* 2, 55–64. doi: 10.2147/copd.2007.2.1.55

Manna, A. C., Kim, S., Cengher, L., Corvaglia, A., Leo, S., Francois, P., et al. (2018). Small RNA teg49 is derived from a sarA transcript and regulates virulence genes independent of SarA in *Staphylococcus aureus*. *Infect. Immun.* 86:17. doi: 10.1128/IAI.00635-617

Marden, J. N., Diaz, M. R., Walton, W. G., Gode, C. J., Betts, L., Urbanowski, M. L., et al. (2013). An unusual CsrA family member operates in series with RsmA to amplify posttranscriptional responses in *Pseudomonas aeruginosa*. *Proc. Natl. Acad. Sci. U.S.A.* 110, 15055–15060. doi: 10.1073/pnas.1307217110

Marinho, C. M., Dos Santos, P. T., Kallipolitis, B. H., Johansson, J., Ignatov, D., Guerreiro, D. N., et al. (2019). The σB-dependent regulatory sRNA Rli47 represses isoleucine biosynthesis in *Listeria monocytogenes* through a direct interaction with the ilvA transcript. *RNA Biol.* 16, 1424–1437. doi: 10.1080/15476286.2019.1632776

Massé, E., and Gottesman, S. (2002). A small RNA regulates the expression of genes involved in iron metabolism in *Escherichia coli*. *Proc. Natl. Acad. Sci. U.S.A.* 99, 4620–4625. doi: 10.1073/pnas.032066599

Massé, E., Majdalani, N., and Gottesman, S. (2003). Regulatory roles for small RNAs in bacteria. *Curr. Opin. Microbiol.* 6, 120–124. doi: 10.1016/S1369-5274(03)00027-24

McPhearson, R. M., DePaola, A., Zywno, S. R., Motes, M. L., and Guarino, A. M. (1991). Antibiotic resistance in Gram-negative bacteria from cultured catfish and aquaculture ponds. *Aquaculture* 99, 203–211. doi: 10.1016/0044-8486(91)90241-X

Melson, E. M., and Kendall, M. M. (2019). The sRNA DicF integrates oxygen sensing to enhance enterohemorrhagic *Escherichia coli* virulence via distinctive RNA control mechanisms. *Proc. Natl. Acad. Sci. U.S.A.* 116, 14210–14215. doi: 10.1073/pnas.1902725116

Mey, A. R., Butz, H. A., and Payne, S. M. (2015). *Vibrio cholerae* CsrA regulates ToxR levels in response to amino acids and is essential for virulence. *mBio* 6:15. doi: 10.1128/mBio.01064-1015

Milillo, M. A., Trotta, A., Serafino, A., Marin Franco, J. L., Marinho, F. V., Alcain, J., et al. (2019). Bacterial RNA contributes to the down-modulation of MHC-II expression on monocytes/macrophages diminishing CD4+ T cell responses. *Front. Immunol.* 10:2181. doi: 10.3389/fimmu.2019.02181

Miller, C. L., Romero, M., Karna, S. L. R., Chen, T., Heeb, S., and Leung, K. P. (2016). RsmW, *Pseudomonas aeruginosa* small non-coding RsmA-binding RNA upregulated in biofilm versus planktonic growth conditions. *BMC Microbiol.* 16:155. doi: 10.1186/s12866-016-0771-y

Moresco, E. M. Y., LaVine, D., and Beutler, B. (2011). Toll-like receptors. *Curr. Biol.* 21:39. doi: 10.1016/j.cub.2011.05.039

Mustachio, L. M., Aksit, S., Mistry, R. H., Scheffler, R., Yamada, A., and Liu, J. M. (2012). The *Vibrio cholerae* mannitol transporter is regulated posttranscriptionally by the MtlS small regulatory RNA. *J. Bacteriol.* 194, 598–606. doi: 10.1128/JB.06153-6111

Nadal Jimenez, P., Koch, G., Thompson, J. A., Xavier, K. B., Cool, R. H., and Quax, W. J. (2012). The multiple signaling systems regulating virulence in *Pseudomonas aeruginosa*. *Microbiol. Mol. Biol. Rev.* 76, 46–65. doi: 10.1128/mmbr.05007-5011

Nakatsu, Y., Matsui, H., Yamamoto, M., Noutoshi, Y., Toyoda, K., and Ichinose, Y. (2019). Quorum-dependent expression of rsmX and rsmY, small non-coding RNAs, in *Pseudomonas* syringae. *Microbiol. Res.* 22, 72–78. doi: 10.1016/j.micres.2019.04.004

Napoli, C., Lemieux, C., and Jorgensen, R. (1990). Introduction of a chimeric chalcone synthase gene into petunia results in reversible co-suppression of homologous genes in trans. *Plant Cell* 2, 279–289. doi: 10.1105/tpc.2.4.279

Narberhaus, F. (2010). Translational control of bacterial heat shock and virulence genes by temperature-sensing mRNAs. *RNA Biol.* 7:501. doi: 10.4161/rna.7.1.10501

Narberhaus, F., Waldminghaus, T., and Chowdhury, S. (2006). RNA thermometers. *FEMS Microbiol. Rev.* 30, 3–16. doi: 10.1111/j.1574-6976.2005.004.x

Ng, D., Harn, T., Altindal, T., Kolappan, S., Marles, J. M., Lala, R., et al. (2016). The *Vibrio cholerae* minor pilin TcpB initiates assembly and retraction of the toxin-*Coregulated Pilus*. *PLoS Pathog.* 12:e1006109. doi: 10.1371/journal.ppat.1006109

Oh, C. S., and Beer, S. V. (2005). Molecular genetics of *Erwinia amylovora* involved in the development of fire blight. *FEMS Microbiol. Lett.* 253, 185–192. doi: 10.1016/j.femsle.2005.09.051

Okamura, K., and Lai, E. C. (2008). Endogenous small interfering RNAs in animals. *Nat. Rev. Mol. Cell Biol.* 9, 673–678. doi: 10.1038/nrm2479

Olejniczak, M., and Storz, G. (2017). ProQ/FinO-domain proteins: another ubiquitous family of RNA matchmakers? *Mol. Microbiol.* 104, 905–915. doi: 10.1111/mmi.13679

O'Neill, J. (2014). The review on antimicrobial resistance tackling drug-resistant infections globally: final report and recommendations. *U. K. Rev. Antimicrob. Resist.* 80. Available online at: https://wellcomecollection.org/works/thvwsuba

Ong, S. T., Shan, Ho, J. Z., Ho, B., and Ding, J. L. (2006). Iron-withholding strategy in innate immunity. *Immunobiology* 211, 295–314. doi: 10.1016/j.imbio.2006.02.004

Ostberg, J. R., Taylor, S. L., Baumann, H., and Repasky, E. A. (2000). Regulatory effects of fever-range whole-body hyperthermia on the LPS-induced acute inflammatory response. *J. Leukoc. Biol.* 68, 815–820. doi: 10.1189/jlb.68.6.815

Pallen, M. J., Beatson, S. A., and Bailey, C. M. (2005). Bioinformatics analysis of the locus for enterocyte effacement provides novel insights into type-III secretion. *BMC Microbiol.* 5:9. doi: 10.1186/1471-2180-5-9

Papenfort, K., and Vogel, J. (2010). Regulatory RNA in bacterial pathogens. *Cell Host Microb.* 8, 116–127. doi: 10.1016/j.chom.2010.06.008

Pena, R. T., Blasco, L., Ambroa, A., González-Pedrajo, B., Fernández-García, L., López, M., et al. (2019). Relationship between quorum sensing and secretion systems. *Front. Microbiol.* 10:1100. doi: 10.3389/fmicb.2019.01100

Pita, T., Feliciano, J. R., and Leitão, J. H. (2018). Small noncoding regulatory RNAs from *Pseudomonas aeruginosa* and *Burkholderia cepacia* complex. *Int. J. Mol. Sci.* 19:3759. doi: 10.3390/ijms19123759

Poole, K. (2012). Bacterial stress responses as determinants of antimicrobial resistance. *J. Antimicrob. Chemother.* 67, 2069–2089. doi: 10.1093/jac/dks196

Popitsch, N., Bilusic, I., Rescheneder, P., Schroeder, R., and Lybecker, M. (2017). Temperature-dependent sRNA transcriptome of the Lyme disease spirochete. *BMC Genomics* 18:28. doi: 10.1186/s12864-016-3398-3393

Pounds, J. A., Bustamante, M. R., Coloma, L. A., Consuegra, J. A., Fogden, M. P. L., Foster, P. N., et al. (2006). Widespread amphibian extinctions from epidemic disease driven by global warming. *Nature* 439, 161–167. doi: 10.1038/nature04246

Puzari, M., Sharma, M., and Chetia, P. (2018). Emergence of antibiotic resistant *Shigella* species: a matter of concern. *J. Infect. Public Health* 11, 451–454. doi: 10.1016/j.jiph.2017.09.025

Radolf, J. D., Caimano, M. J., Stevenson, B., and Hu, L. T. (2012). Of ticks, mice and men: Understanding the dual-host lifestyle of Lyme disease spirochaetes. *Nat. Rev. Microbiol.* 10, 87–99. doi: 10.1038/nrmicro2714

Ramamoorthi, N., Narasimhan, S., Pal, U., Bao, F., Yang, X. F., Fish, D., et al. (2005). The Lyme disease agent exploits a tick protein to infect the mammalian host. *Nature* 436, 573–577. doi: 10.1038/nature03812

Ratner, H. K., Escalera-Maurer, A., Le Rhun, A., Jaggavarapu, S., Wozniak, J. E., Crispell, E. K., et al. (2019). Catalytically Active Cas9 mediates transcriptional interference to facilitate bacterial virulence. *Mol. Cell* 75, 498–510. doi: 10.1016/j.molcel.2019.05.029

Records, A. R., and Gross, D. C. (2010). Sensor kinases RetS and LadS regulate *Pseudomonas* syringae Type VI secretion and virulence factors. *J. Bacteriol.* 192, 3584–3596. doi: 10.1128/JB.00114-110

Rochat, T., Bohn, C., Morvan, C., Le Lam, T. N., Razvi, F., Pain, A., et al. (2018). The conserved regulatory RNA RsaE down-regulates the arginine degradation pathway in *Staphylococcus aureus*. *Nucleic Acids Res.* 46, 8803–8816. doi: 10.1093/nar/gky584

Rodó, X., Pascual, M., Fuchs, G., and Faruque, A. S. G. (2002). ENSO and cholera: a nonstationary link related to climate change? *Proc. Natl. Acad. Sci. U.S.A.* 99, 12901–12906. doi: 10.1073/pnas.182203999

Rohmer, L., Hocquet, D., and Miller, S. I. (2011). Are pathogenic bacteria just looking for food? metabolism and microbial pathogenesis. *Trends Microbiol.* 19, 341–348. doi: 10.1016/j.tim.2011.04.003

Romeo, T., and Babitzke, P. (2018). Global regulation by CsrA and Its RNA antagonists. *Microbiol. Spectr.* 6, 1321–1330. doi: 10.1128/microbiolspec.rwr-0009-2017

Romero, D., Traxler, M. F., López, D., and Kolter, R. (2011). Antibiotics as signal molecules. *Chem. Rev.* 111, 5492–5505. doi: 10.1021/cr2000509

Romero, M., Silistre, H., Lovelock, L., Wright, V. J., Chan, K.-G., Hong, K.-W., et al. (2018). Genome-wide mapping of the RNA targets of the *Pseudomonas aeruginosa* riboregulatory protein RsmN. *Nucleic Acids Res.* 46, 6823–6840. doi: 10.1093/nar/gky324

Ross, J. A., Thorsing, M., Lillebæk, E. M. S., Teixeira Dos Santos, P., and Kallipolitis, B. H. (2019). The LhrC sRNAs control expression of T cell-stimulating antigen TcsA in *Listeria monocytogenes* by decreasing tcsA mRNA stability. *RNA Biol.* 16, 270–281. doi: 10.1080/15476286.2019.1572423

Roy, B., Ahamed, S. T., Bandyopadhay, B., and Giri, N. (2020). Development of quinolone resistance and prevalence of different virulence genes among *Shigella flexneri* and *Shigella dysenteriae* in environmental water samples. *Lett. Appl. Microbiol.* 13262. doi: 10.1111/lam.13262

Ruano-Gallego, D., Álvarez, B., and Fernández, L. Á (2015). Engineering the controlled assembly of filamentous injectisomes in *E. coli K*-12 for protein translocation into mammalian cells. *ACS Synth. Biol.* 4, 1030–1041. doi: 10.1021/acssynbio.5b00080

Rübsam, H., Kirsch, F., Reimann, V., Erban, A., Kopka, J., Hagemann, M., et al. (2018). The iron-stress activated RNA 1 (IsaR1) coordinates osmotic acclimation and iron starvation responses in the cyanobacterium *Synechocystis* sp. *PCC* 6803. *Environ. Microbiol.* 20, 2757–2768. doi: 10.1111/1462-2920.14079

Sahni, A., Hajjari, M., Raheb, J., Foroughmand, A. M., and Asgari, M. (2019). The non-coding RNA rprA can increase the resistance to ampicillin in *Escherichia coli*. *Microb. Pathog.* 129, 266–270. doi: 10.1016/j.micpath.2019.02.021

Saliba, A. E., Santos, C., and Vogel, J. (2017). New RNA-seq approaches for the study of bacterial pathogens. *Curr. Opin. Microbiol.* 35, 78–87. doi: 10.1016/j.mib.2017.01.001

Sanderson, S., Campbell, D. J., and Shastri, N. (1995). Identification of a CD4+ T cell-stimulating antigen of pathogenic bacteria by expression cloning. *J. Exp. Med.* 182, 1751–1757. doi: 10.1084/jem.182.6.1751

Santiago-Frangos, A., Fröhlich, K. S., Jeliazkov, J. R., Małecka, E. M., Marino, G., Gray, J. J., et al. (2019). Caulobacter crescentus Hfq structure reveals a conserved mechanism of RNA annealing regulation. *Proc. Natl. Acad. Sci. U.S.A.* 166, 10978–10987. doi: 10.1073/pnas.1814428116

Sassi, M., Augagneur, Y., Mauro, T., Ivain, L., Chabelskaya, S., Hallier, M., et al. (2015). SRD: A *Staphylococcus* regulatory RNA database. *RNA* 21, 1005–1017. doi: 10.1261/rna.049346.114

Sauder, A. B., and Kendall, M. M. (2018). After the fact(or): posttranscriptional gene regulation in enterohemorrhagic *Escherichia coli* O157:H7. *J. Bacteriol.* 200:e00228-18. doi: 10.1128/JB.00228-218

Schachterle, J. K., Zeng, Q., and Sundin, G. W. (2019). Three Hfq-dependent small RNAs regulate flagellar motility in the fire blight pathogen Erwinia *amylovora*. *Mol. Microbiol.* 111, 1476–1492. doi: 10.1111/mmi.14232

Schuster, M., Hawkins, A. C., Harwood, C. S., and Greenberg, E. P. (2004). The *Pseudomonas aeruginosa* RpoS regulon and its relationship to quorum sensing. *Mol. Microbiol.* 51, 973–985. doi: 10.1046/j.1365-2958.2003.03886.x

Segovia, C., Arias-Carrasco, R., Yañez, A. J., Maracaja-Coutinho, V., and Santander, J. (2018). Core non-coding RNAs of *Piscirickettsia salmonis*. *PLoS One* 13:e0197206. doi: 10.1371/journal.pone.0197206

Sellge, G., and Kufer, T. A. (2015). PRR-signaling pathways: learning from microbial tactics. *Semin. Immunol.* 27, 75–84. doi: 10.1016/j.smim.2015.03.009

Sheehan, L. M., and Caswell, C. C. (2018). An account of evolutionary specialization: the AbcR small RNAs in the rhizobiales. *Mol. Microbiol.* 107, 24–33. doi: 10.1111/mmi.13869

Shimizu, K. (2013). Regulation systems of bacteria such as *Escherichia coli* in response to nutrient limitation and environmental stresses. *Metabolites* 4, 1–35. doi: 10.3390/metabo4010001

Shin, G. Y., Schachterle, J. K., Shyntum, D. Y., Moleleki, L. N., Coutinho, T. A., and Sundin, G. W. (2019). Functional characterization of a global virulence regulator Hfq and identification of Hfq-dependent sRNAs in the plant pathogen *Pantoea ananatis*. *Front. Microbiol.* 10:2075. doi: 10.3389/fmicb.2019.02075

Shyp, V., Tankov, S., Ermakov, A., Kudrin, P., English, B. P., Ehrenberg, M., et al. (2012). Positive allosteric feedback regulation of the stringent response enzyme RelA by its product. *EMBO Rep.* 13, 835–839. doi: 10.1038/embor.2012.106

Silva, I. J., Barahona, S., Eyraud, A., Lalaouna, D., Figueroa-Bossi, N., Massé, E., et al. (2019). SraL sRNA interaction regulates the terminator by preventing premature transcription termination of rho mRNA. *Proc. Natl. Acad. Sci. U.S.A.* 116, 3042–3051. doi: 10.1073/pnas.1811589116

Sinha, D., Matz, L. M., Cameron, T. A., and de Lay, N. R. (2018). Poly(A) polymerase is required for RyhB sRNA stability and function in *Escherichia coli*. *RNA* 24, 1496–1511. doi: 10.1261/rna.067181.118

Slingenbergh, J., Gilbert, M., De Balogh, K., and Wint, W. (2004). Ecological sources of zoonotic diseases. *OIE Rev. Sci. Tech.* 23, 467–484. doi: 10.20506/rst.23.2.1492

Smirnov, A., Förstner, K. U., Holmqvist, E., Otto, A., Günster, R., Becher, D., et al. (2016). Grad-seq guides the discovery of ProQ as a major small RNA-binding protein. *Proc. Natl. Acad. Sci. U.S.A.* 113, 11591–11596. doi: 10.1073/pnas.1609981113

Sonnleitner, E., Gonzalez, N., Sorger-Domenigg, T., Heeb, S., Richter, A. S., Backofen, R., et al. (2011). The small RNA PhrS stimulates synthesis of the *Pseudomonas aeruginosa* quinolone signal. *Mol. Microbiol.* 80, 868–885. doi: 10.1111/j.1365-2958.2011.07620.x

Sparling, P. F. (1983). Bacterial virulence and pathogenesis: an overview. *Rev. Infect. Dis.* 5, 637–646.

Steere, A. C., Strle, F., Wormser, G. P., Hu, L. T., Branda, J. A., Hovius, J. W. R., et al. (2016). Lyme borreliosis. *Nat. Rev. Dis. Prim.* 2, 1–19. doi: 10.1038/nrdp.2016.90

Streinzer, M., Paulus, H. F., and Spaethe, J. (2009). Floral colour signal increases short-range detectability of a sexually deceptive orchid to its bee pollinator. *J. Exp. Biol.* 212, 1365–1370. doi: 10.1242/jeb.027482

Sudo, N., Soma, A., Iyoda, S., Oshima, T., Ohto, Y., Saito, K., et al. (2018). Small RNA Esr41 inversely regulates expression of LEE and flagellar genes in enterohaemorrhagic *Escherichia coli*. *Microbiology* 164, 821–834. doi: 10.1099/mic.0.000652

Sudo, N., Soma, A., Muto, A., Iyoda, S., Suh, M., Kurihara, N., et al. (2014). A novel small regulatory RNA enhances cell motility in enterohemorrhagic *Escherichia coli*. *J. Gen. Appl. Microbiol.* 60, 44–50. doi: 10.2323/jgam.60.44

Suh, S. J., Silo-Suh, L., Woods, D. E., Hassett, D. J., West, S. E. H., and Ohman, D. E. (1999). Effect of rpoS mutation on the stress response and expression

of virulence factors in *Pseudomonas aeruginosa*. *J. Bacteriol.* 181, 3890–3897. doi: 10.1128/jb.181.13.3890-3897.1999

Sundberg, L. R., Ketola, T., Laanto, E., Kinnula, H., Bamford, J. K. H., Penttinen, R., et al. (2016). Intensive aquaculture selects for increased virulence and interference competition in bacteria. *Proc. R. Soc. B Biol. Sci.* 283:3069. doi: 10.1098/rspb.2015.3069

Swaminathan, B., and Gerner-Smidt, P. (2007). The epidemiology of human listeriosis. *Microb. Infect.* 9, 1236–1243. doi: 10.1016/j.micinf.2007.05.011

Tanji, T., and Ip, Y. T. (2005). Regulators of the toll and Imd pathways in the drosophila innate immune response. *Trends Immunol.* 26, 193–198. doi: 10.1016/j.it.2005.02.006

Taylor, A. F. (2016). Small molecular replicators go organic. *Nature* 537, 627–628. doi: 10.1038/537627a

Thairu, M. W., Cheng, S., and Hansen, A. K. (2018). A sRNA in a reduced *Mutualistic symbiont* genome regulates its own gene expression. *Mol. Ecol.* 27, 1766–1776. doi: 10.1111/mec.14424

Thairu, M. W., and Hansen, A. K. (2019). Changes in aphid host plant diet influence the small-RNA expression profiles of its obligate nutritional symbiont, *Buchnera*. *mBio* 10:e01733-19. doi: 10.1128/mBio.01733-1719

Thi Bach Nguyen, H., Romero, A. D., Amman, F., Sorger-Domenigg, T., and Tata, M. (2018). Negative control of RpoS synthesis by the sRNA ReaL in *Pseudomonas aeruginosa*. *Front. Microbiol.* 9:2488. doi: 10.3389/fmicb.2018.02488

Thomason, M. K., Voichek, M., Dar, D., Addis, V., Fitzgerald, D., Gottesman, S., et al. (2019). A rhlI 5′ UTR-Derived sRNA regulates RhlR-dependent quorum sensing in *Pseudomonas aeruginosa*. *mBio* 10:e02253-19. doi: 10.1128/mBio.02253-2219

Tomasini, A., François, P., Howden, B. P., Fechter, P., Romby, P., and Caldelari, I. (2014). The importance of regulatory RNAs in *Staphylococcus aureus*. *Infect. Genet. Evol.* 21, 616–626. doi: 10.1016/j.meegid.2013.11.016

Toyofuku, M., Nomura, N., and Eberl, L. (2019). Types and origins of bacterial membrane vesicles. *Nat. Rev. Microbiol.* 17, 13–24. doi: 10.1038/s41579-018-0112-112

Trewavas, A. J. (2001). The population/biodiversity paradox. Agricultural efficiency to save wilderness. *Plant Physiol.* 125, 174–179. doi: 10.1104/pp.125.1.174

Trullàs, R. (2019). *El Fracaso De La Ciencia Con Adjetivos, Por Ramon Trullàs. El Periódico*. Available online at: https://www.elperiodico.com/es/opinion/20180201/el-fracaso-de-la-ciencia-con-adjetivos-articulo-ramon-trullas-6594038 (accessed December 23, 2019).

Valentini, M., Gonzalez, D., Mavridou, D. A., and Filloux, A. (2018). Lifestyle transitions and adaptive pathogenesis of *Pseudomonas aeruginosa*. *Curr. Opin. Microbiol.* 41, 15–20. doi: 10.1016/j.mib.2017.11.006

van der Krol, A. R., Mur, L. A., Beld, M., Mol, J. N., and Stuitje, A. R. (1990). Flavonoid genes in petunia: addition of a limited number of gene copies may lead to a suppression of gene expression. *Plant Cell* 2, 291–299. doi: 10.1105/tpc.2.4.291

Van Elsas, J. D., Semenov, A. V., Costa, R., and Trevors, J. T. (2011). Survival of *Escherichia coli* in the environment: fundamental and public health aspects. *ISME J.* 5, 173–183. doi: 10.1038/ismej.2010.80

Wassenaar, T. M., and Gaastra, W. (2001). Bacterial virulence: can we draw the line? *FEMS Microbiol. Lett.* 201, 1–7. doi: 10.1111/j.1574-6968.2001.tb10724.x

Waters, L. S., and Storz, G. (2009). Regulatory RNAs in bacteria. *Cell* 136, 615–628. doi: 10.1016/j.cell.2009.01.043

Wei, B. L., Brun-Zinkernagel, A. M., Simecka, J. W., Prüß, B. M., Babitzke, P., and Romeo, T. (2001). Positive regulation of motility and flhDC expression by the RNA-binding protein CsrA of *Escherichia coli*. *Mol. Microbiol.* 40, 245–256. doi: 10.1046/j.1365-2958.2001.02380.x

Weiberg, A., Wang, M., Lin, F. M., Zhao, H., Zhang, Z., Kaloshian, I., et al. (2013). Fungal small RNAs suppress plant immunity by hijacking host RNA interference pathways. *Science* 342, 118–123. doi: 10.1126/science.1239705

Wernegreen, J. J. (2002). Genome evolution in bacterial endosymbionts of insects. *Nat. Rev. Genet.* 3, 850–861. doi: 10.1038/nrg931

Werren, J. H., Baldo, L., and Clark, M. E. (2008). Wolbachia: master manipulators of invertebrate biology. *Nat. Rev. Microbiol.* 6, 741–751. doi: 10.1038/nrmicro1969

Westermann, A. J., Barquist, L., and Vogel, J. (2017). Resolving host-pathogen interactions by dual RNA-seq. *PLoS Pathog.* 13:e06033. doi: 10.1371/journal.ppat.1006033

Westermann, A. J., Förstner, K. U., Amman, F., Barquist, L., Chao, Y., Schulte, L. N., et al. (2016). Dual RNA-seq unveils noncoding RNA functions in host-pathogen interactions. *Nature* 529, 496–501. doi: 10.1038/nature16547

Westermann, A. J., Gorski, S. A., and Vogel, J. (2012). Dual RNA-seq of pathogen and host. *Nat. Rev. Microbiol.* 10, 618–630. doi: 10.1038/nrmicro2852

Westermann, A. J., Venturini, E., Sellin, M. E., Förstner, K. U., Hardt, W. D., and Vogel, J. (2019). The major RNA-binding protein ProQ impacts virulence gene expression in *Salmonella enterica* serovar *Typhimurium*. *mBio* 10:e002504-18. doi: 10.1128/mBio.02504-2518

Wightman, B., Ha, I., and Ruvkun, G. (1993). Posttranscriptional regulation of the heterochronic gene lin-14 by lin-4 mediates temporal pattern formation in *C. elegans*. *Cell* 75, 855–862. doi: 10.1016/0092-8674(93)90530-4

Wilderman, P. J., Sowa, N. A., FitzGerald, D. J., FitzGerald, P. C., Gottesman, S., Ochsner, U. A., et al. (2004). Identification of tandem duplicate regulatory small RNAs in *Pseudomonas aeruginosa* involved in iron homeostasis. *Proc. Natl. Acad. Sci. U.S.A.* 101, 9792–9797. doi: 10.1073/pnas.0403423101

Wilms, I., Voss, B., Hess, W. R., Leichert, L. I., and Narberhaus, F. (2011). Small RNA-mediated control of the *Agrobacterium tumefaciens* GABA binding protein. *Mol. Microbiol.* 80, 492–506. doi: 10.1111/j.1365-2958.2011.07589.x

Witzany, G. (2010). Biocommunication and natural genome editing. *World J. Biol. Chem.* 1:348. doi: 10.4331/wjbc.v1.i11.348

Woolfit, M., Algama, M., Keith, J. M., McGraw, E. A., and Popovici, J. (2015). Discovery of putative small non-coding RNAs from the obligate intracellular bacterium *Wolbachia pipientis*. *PLoS One* 10:e0118595. doi: 10.1371/journal.pone.0118595

Xi, D., Li, Y., Yan, J., Li, Y., Wang, X., and Cao, B. (2020). Small RNA *coaR* contributes to intestinal colonization in *Vibrio cholerae* via the two-component system EnvZ/OmpR. *Environ. Microbiol.* 1462. doi: 10.1111/1462-2920.14906

Yakhnin, A. V., Baker, C. S., Vakulskas, C. A., Yakhnin, H., Berezin, I., Romeo, T., et al. (2013). CsrA activates flhDC expression by protecting flhDC mRNA from RNase E-mediated cleavage. *Mol. Microbiol.* 87, 851–866. doi: 10.1111/mmi.12136

Yuan, X., Zeng, Q., Khokhani, D., Tian, F., Severin, G. B., Waters, C. M., et al. (2019). A feed-forward signalling circuit controls bacterial virulence through linking cyclic di-GMP and two mechanistically distinct sRNAs, ArcZ and RsmB. *Environ. Microbiol.* 21, 2755–2771. doi: 10.1111/1462-2920.14603

Zapf, R. L., Wiemels, R. E., Keogh, R. A., Holzschu, D. L., Howell, K. M., Trzeciak, E., et al. (2019). The small RNA Teg41 regulates expression of the alpha phenol-soluble modulins and is required for virulence in *Staphylococcus aureus*. *mBio* 10:e02484-18. doi: 10.1128/mBio.02484-2418

Zeng, G., Yang, J., and Zhu, G. (2019). Cross-kingdom small RNAs among animals, plants and microbes. *Cells* 8:371. doi: 10.3390/cells8040371

Zeng, Q., and Sundin, G. W. (2014). Genome-wide identification of Hfq-regulated small RNAs in the fire blight pathogen *Erwinia amylovora* discovered small RNAs with virulence regulatory function. *BMC Genom.* 15:414. doi: 10.1186/1471-2164-15-414

Zhang, M. G., and Liu, J. M. (2019). Transcription of cis antisense small RNA MtlS in *Vibrio cholerae* is regulated by transcription of its target gene, mtlA. *J. Bacteriol.* 201:e00178-19. doi: 10.1128/JB.00178-119

Zhang, Y. J., and Rubin, E. J. (2013). Feast or famine: the host-pathogen battle over amino acids. *Cell. Microbiol.* 15, 1079–1087. doi: 10.1111/cmi.12140

Conflict of Interest: The author declares that the research was conducted in the absence of any commercial or financial relationships that could be construed as a potential conflict of interest.

frontiers in Molecular Biosciences

HYPOTHESIS AND THEORY
published: 10 July 2020
doi: 10.3389/fmolb.2020.00127

Comparative Genomics and Evolutionary Analysis of RNA-Binding Proteins of the CsrA Family in the Genus *Pseudomonas*

*Patricio Martín Sobrero and Claudio Valverde**

Laboratorio de Fisiología y Genética de Bacterias Beneficiosas para Plantas, Centro de Bioquímica y Microbiología del Suelo, Departamento de Ciencia y Tecnología, Universidad Nacional de Quilmes - CONICET, Buenos Aires, Argentina

Gene expression is adjusted according to cellular needs through a combination of mechanisms acting at different layers of the flow of genetic information. At the posttranscriptional level, RNA-binding proteins are key factors controlling the fate of nascent and mature mRNAs. Among them, the members of the CsrA family are small dimeric proteins with heterogeneous distribution across the bacterial tree of life, that act as global regulators of gene expression because they recognize characteristic sequence/structural motifs (short hairpins with GGA triplets in the loop) present in hundreds of mRNAs. The regulatory output of CsrA binding to mRNAs is counteracted in most cases by molecular mimic, non-protein coding RNAs that titrate the CsrA dimers away from the target mRNAs. In γ-proteobacteria, the regulatory modules composed by CsrA homologs and the corresponding antagonistic sRNAs, are mastered by two-component systems of the GacS-GacA type, which control the transcription and the abundance of the sRNAs, thus constituting the rather linear cascade Gac-Rsm that responds to environmental or cellular signals to adjust and coordinate the expression of a set of target genes posttranscriptionally. Within the γ-proteobacteria, the genus *Pseudomonas* has been shown to contain species with different number of active CsrA (RsmA) homologs and of molecular mimic sRNAs. Here, with the help of the increasing availability of genomic data we provide a comprehensive state-of-the-art picture of the remarkable multiplicity of CsrA lineages, including novel yet uncharacterized paralogues, and discuss evolutionary aspects of the CsrA subfamilies of the genus *Pseudomonas*, and implications of the striking presence of *csrA* alleles in natural mobile genetic elements (phages and plasmids).

Keywords: RNA-binding proteins, CsrA, RsmA, *Pseudomonas*, comparative genomics, evolutionary analysis, plasmids, phages

OPEN ACCESS

Edited by:
Olga N. Ozoline, Institute of Cell Biophysics (RAS), Russia

Reviewed by:
Stephan Heeb, University of Nottingham, United Kingdom
Dimitris Georgellis, National Autonomous University of Mexico, Mexico

****Correspondence:***
Claudio Valverde
cvalver@unq.edu.ar; valverdecl@hotmail.com

Specialty section:
This article was submitted to Protein and RNA Networks, a section of the journal Frontiers in Molecular Biosciences

Received: *10 April 2020*
Accepted: *02 June 2020*
Published: *10 July 2020*

Citation:
Sobrero PM and Valverde C (2020) Comparative Genomics and Evolutionary Analysis of RNA-Binding Proteins of the CsrA Family in the Genus Pseudomonas. Front. Mol. Biosci. 7:127. doi: 10.3389/fmolb.2020.00127

INTRODUCTION

Regulation of gene expression is key to the metabolic economy of the prokaryotic cell. The pathway from the gene sequence to the encoded final active polypeptide offers several opportunities for adjusting the flow of gene expression. For decades, the focus of gene regulatory processes in prokaryotes has been the control of transcription initiation by protein regulatory factors

(i.e., transcriptional regulation), and it was deemed a taxonomically widespread and most efficient way to limit the amount of macromolecule synthesis depending on cues perceived from the environment or the inner cell compartment. However, during the last 30 years there has been an enormous input of genetic, biochemical, physiological, and omics data strongly supporting the pervasive and critical role of genetic regulatory mechanisms that operate on top of transcription initiation to modulate the fate of the nascent or mature transcripts (i.e., posttranscriptional control of gene expression). Although in most cases the degree of regulatory effect introduced by these mechanisms is mild and serve to fine-tune the outcome of transcriptional regulatory controls, in some cases, posttranscriptional regulations can introduce a quantitatively significant adjustment to become the master control of the genetic flow of a certain pathway or process. At the molecular level, the posttranscriptional control of gene expression can be executed by sequence portions of the mRNA themselves (e.g., cis-acting motifs like riboswitches and thermosensors), by non-protein coding, small regulatory RNAs (sRNAs) that base-pair with mRNAs, or by RNA-binding proteins that have preference for sequence and/or structural motifs on target mRNAs. For updates on *cis*-acting RNA regulatory elements and sRNAs we refer the reader to recent comprehensive reviews (Quereda and Cossart, 2017; Desgranges et al., 2019; Bedard et al., 2020; Jorgensen et al., 2020; Mandin and Johansson, 2020).

Prokaryotic genomes encode over a hundred of RNA-binding proteins, being the majority of them devoted to scaffold the ribosomal subunits or to catalytically process RNA molecules for maturation or defense (Holmqvist and Vogel, 2018). A third functional class of RNA-binding proteins is involved in posttranscriptional control of gene expression (Quendera et al., 2020), with some outstanding cases acting as global regulators of major influence in the fate of hundreds of mRNAs, as is the case of the broadly studied chaperone Hfq (Vogel and Luisi, 2011; Sobrero and Valverde, 2012; Kavita et al., 2018; Santiago-Frangos and Woodson, 2018), or the members of the CsrA family (Romeo and Babitzke, 2019), which is the subject of this article. Here, we will review the features of the RNA-binding proteins of the CsrA superfamily, with an emphasis on the representatives of the genus *Pseudomonas*, for which our comparative genome analysis revealed a prolific evolutionary spreading of multiple paralogues.

THE CsrA PROTEIN FAMILY

CsrA stands for Carbon storage regulator A and it was discovered almost 30 years ago in a Tn*5* mutagenic screen of *E. coli* as a 61-amino acid polypeptidic regulatory factor of glycogen biosynthesis genes, and soon revealed its role as a global regulator of gene expression (Romeo et al., 1993). The regulatory mechanism underlying CsrA activity was obscure at that time. The first study to explore the phylogenetic distribution relied on the detection of homolog sequences by Southern blot using a PCR probe consisting of the *E. coli csrA* gene, and a sequence homology search in nucleotide sequence databases (White et al., 1996); although a very limited number of bacterial genomes were explored with both techniques, the results suggested a broad distribution of this kind of novel regulatory protein in eubacteria. Currently, the Pfam entry CsrA (PF02599) and the InterPro entry IPR003751, together include over 16.000 polypeptidic sequences from more than 2900 species. Intriguingly, representatives of this large protein superfamily have been detected exclusively in the chromosomes of eubacterial species (**Figure 1**). Nevertheless, the increasing availability of genomes from environmental metagenomic projects may prompt the identification of CsrA remote homologs in archaeal lineages.

Members of the CsrA family are rather well conserved polypeptides of relatively short length (65–75 residues on average) that function as homodimers (**Figure 2**). Heterodimerization in bacteria encoding more than one paralogue has not been demonstrated yet, but it may be plausible. The secondary structure predicted for most representatives indicate that CsrA monomers fold into five consecutive, antiparallel β-strands (β1β2β3β4β5) followed by one short α-helix (H1), and the unstructured C-terminus of variable length (Gutierrez et al., 2005) (**Figure 2B**). The dimeric and biologically active structure (Gutierrez et al., 2005; Rife et al., 2005; Heeb et al., 2006; Schubert et al., 2007) is formed by intertwining of β1 and β5, which results in a sandwich of two, five-stranded, antiparallel β-sheets, with the two α-helixes projected out from the dimer core (**Figure 2D**). The RNA-binding sites lay in the conserved and positively charged regions adjacent to strands β1, β4, β5, and the N-terminal region of helix H1, on each side of the dimer (**Figure 2E**). These two sites have a marked preference for RNA sequence/structural motifs characterized by short stem-loops exposing the trinucleotide GGA in the apical loop (**Figure 2F**). A strongly conserved arginine residue at the interface of β5 and H1 is fundamental for the recognition of the first G of the GGA trinucleotide, and its replacement abolishes the regulatory binding of CsrA proteins to their RNA targets (Heeb et al., 2006; Schubert et al., 2007).

On the basis of the molecular preference of CsrA binding, and the probability of mRNAs to harbor such sequence/structural recognition motif for CsrA, it is expected that a plethora of mRNAs would be targeted by this protein. This has been recently corroborated by RNA sequencing of the transcripts captured *in vivo* upon crosslinking and affinity purification of CsrA (Holmqvist et al., 2016; Potts et al., 2019). Thus, the proteins of the CsrA family are global regulators of gene expression. Depending on the region of the mRNA where CsrA dimers bind to, the consequence of the interaction may be: (a) translational repression of the mRNA by outcompeting the small ribosomal unit; (b) translational activation upon structural rearrangement of the 5′-untranslated region and exposition of the ribosome binding site; (c) translational regulation by refolding the 5′-UTR such that an sRNA can gain access by base-pairing and prevent ribosomal entry; (d) modulation of mRNA decay by controlling the access of ribonucleases to target sites; (e) modulation of transcription termination (**Figure 3**) (Romeo and Babitzke, 2019).

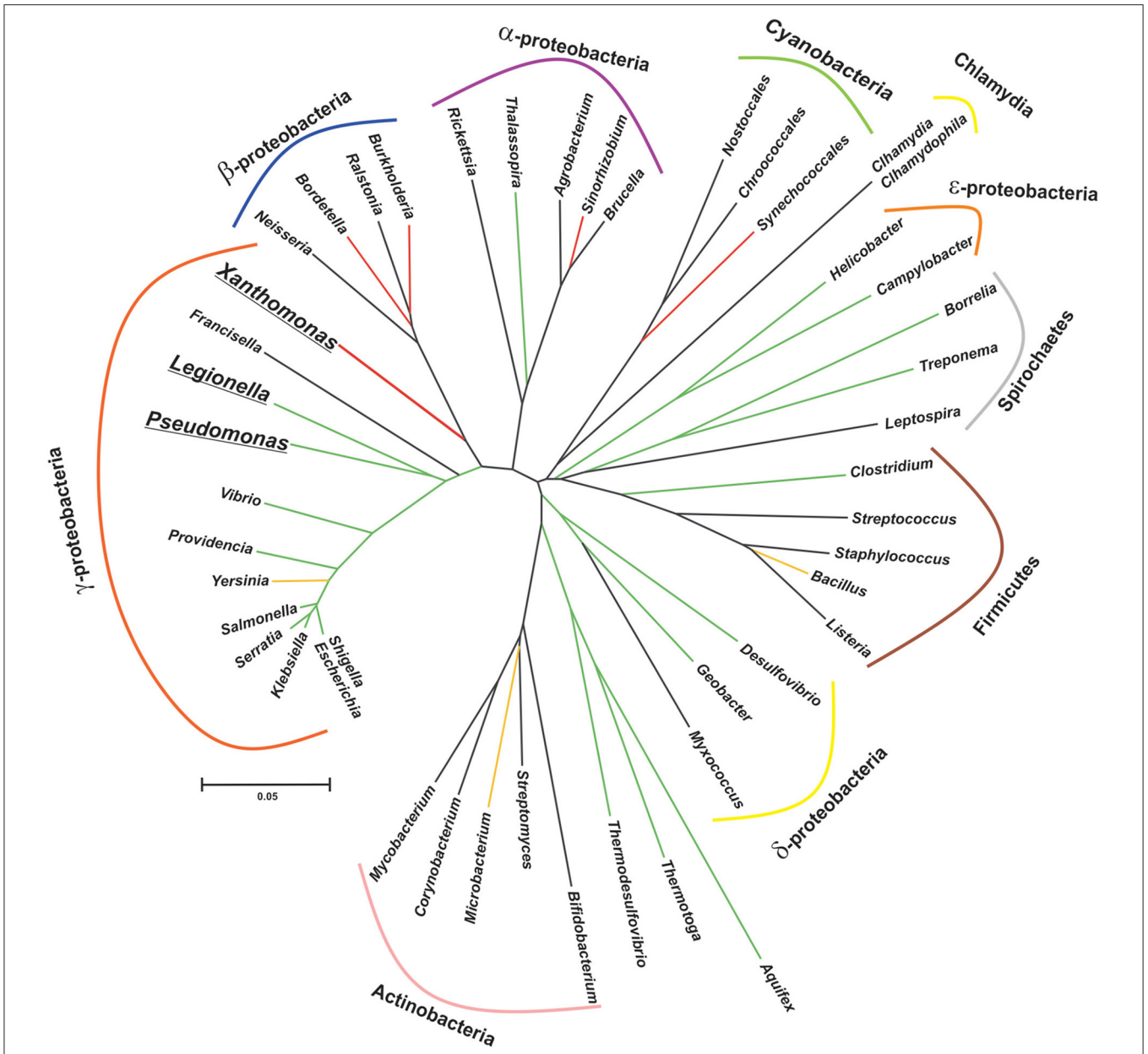

FIGURE 1 | Patched phylogenetic distribution of genes encoding CsrA homologs in major eubacterial taxa. The phylogenetic tree was generated on the basis of the 16S rDNA sequences of one representative species for each eubacterial genus present in the diagram. The evolutionary history was inferred using the Neighbor-Joining method (Saitou and Nei, 1987). The optimal tree with the sum of branch length = 3.385 is shown. The tree is drawn to scale, with branch lengths in the same units as those of the evolutionary distances used to infer the phylogenetic tree. The evolutionary distances were computed using the Kimura 2-parameter method (Kimura, 1980) and are in the units of the number of base substitutions per site. This analysis involved 46 nucleotide sequences. All positions with <95% site coverage were eliminated, i.e., fewer than 5% alignment gaps, missing data, and ambiguous bases were allowed at any position (partial deletion option). There were a total of 1,174 positions in the final dataset. Evolutionary analyses were conducted in MEGA X (Kumar et al., 2018). The reference bar length indicates the number of nucleotide substitution per site. The branch color corresponds to the proportion of species per class that contain at least one *csrA* allele, as follows: black, 0% (no homologs in this class); red, <10%; yellow, >50%; green, 100%. Bolded and underlined taxon names denote those genera which present more than one allele per genome.

PATCHY DISTRIBUTION OF *csrA* GENES ACROSS EUBACTERIA

CsrA-like proteins exhibit a remarkably non-uniform distribution in the eubacterial kingdom (**Figure 1**). This heterogeneous distribution contrasts with the widespread (although non ubiquitous) presence of other bacterial proteins involved in riboregulatory processes, like Hfq or the endoribonuclease E (RNAse E) (**Supplementary Table 1**; Sobrero and Valverde, 2012). As for Hfq, CsrA proteins seem to

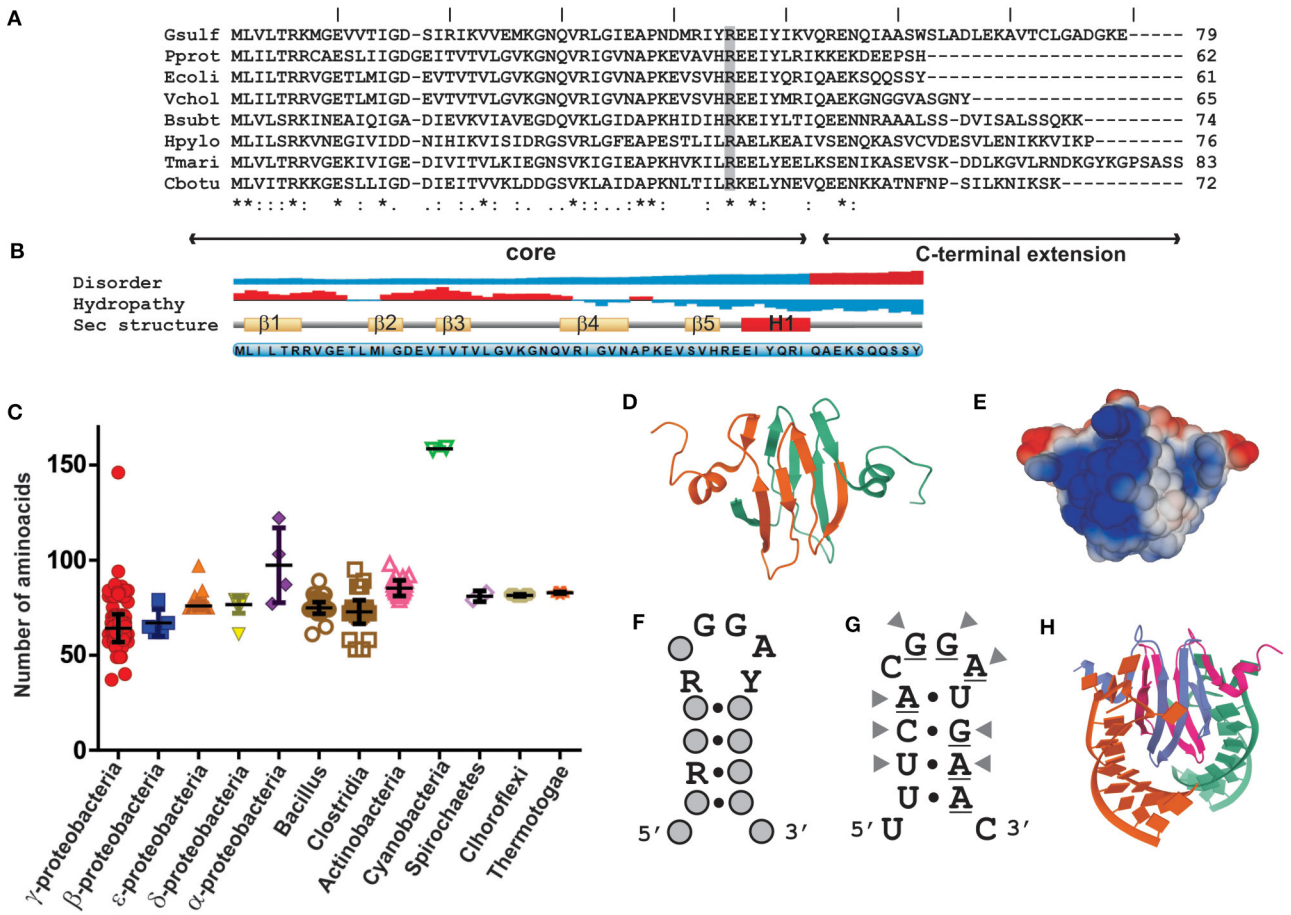

FIGURE 2 | Structural properties of CsrA proteins and their interaction with RNA sequence/structural motifs. **(A)** Primary sequence alignment of CsrA polypeptides from selected eubacterial species: Gsulf, *Geobacter sulfurreducens*; Pprot, *Pseudomonas protegens*; Ecoli, *Escherichia coli*; Vchol, *Vibrio cholerae*; Bsubt, *Bacillus subtilis*; Hpylo, *Helicobacter pylori*; Tmari, *Thermotoga maritima*; Cbotu, *Clostridium botulinum*. The degree of residue conservation is indicated below each position of the alignment, as follows: an (*) indicates positions with a fully conserved residue; a (:) indicates conservation between amino acid groups of strongly similar biochemical properties; a (.) indicates conservation between groups of weakly similar properties. The residue shaded in gray (R) corresponds to the conserved arginine (R44 in *E. coli* CsrA) that is essential for the RNA-binding activity of CsrA proteins (Heeb et al., 2006; Schubert et al., 2007). The core region comprises the prototypical portion of the molecule that defines the CsrA fold, namely the β1β2β3β4β5H1 arrangement; the C-terminal extension is highly variable among different taxa. **(B)** Secondary structure properties the *E. coli* CsrA polypeptide. The data was generated with the Protein feature view tool of the RCSB PDB server www.rcsb.org (Berman et al., 2000). **(C)** The graph shows the length distribution of CsrA homologs within different eubacterial classes. For each group the average length (nr. of residues) ± standard deviation is indicated. **(D)** Ribbon diagram of the solution quaternary structure of the *E. coli* CsrA dimeric protein (PDB 1Y00). **(E)** Predicted charge distribution along the surface of the dimeric *P. protegens* RsmE protein (PDB 2JPP). **(F)** Consensus sequence/structural motif preferentially bound by *E. coli* CsrA *in vivo*, as detected following CLIP-Seq (adapted from Potts et al., 2019). R = G or A, Y = C or U. **(G)** Predicted secondary structure of the 14-mer encompassing the Shine-Dalgarno sequence (underlined nucleotides) of the *hcnA* 5′-UTR from *P. protegens* strain CHA0, an experimentally validated target for the CsrA homolog protein RsmE (Lapouge et al., 2007; Schubert et al., 2007). The arrowheads point to the nucleotides contacted by specific RsmE residues in the complex shown in **(H)** (Schubert et al., 2007). **(H)** Ribbon diagram of the NMR solution structure of the RsmE–*hcnA* 5′-UTR complex (PDB 2JPP). Each RNA binding site of the dimeric RsmE protein is interacting with one of two identical synthetic 20-mers containing the sequence-structural motif shown in **(G)**.

be absent in bacterial species that have adopted an intracellular lifestyle (e.g., *Rickettsia*, *Chlamydia* and the γ-proteobacterium *Francisella*). Even within the proteobacterial branch, some classes lack CsrA homologs, raising the question about the essentially of this regulatory protein. As we can imagine for every protein-coding gene, its evolutionary trajectory is directly related to its biological function. CsrA structure can serve as a scaffold for protein-RNA or protein-protein interactions, both impacting on gene expression. For instance, in certain lineages, CsrA co-occurs with the protein FliW, a regulator of flagellar gene expression (Mukherjee et al., 2011) (**Supplementary Table 1** and **Supplementary Figure 1**). This co-occurrence can explain the evolution of CsrA in *Bacillus* and ε-proteobacteria (Altegoer et al., 2016), and other bacterial genera presenting both genetic elements. Moreover, the co-occurrence of CsrA and FliW is associated with longer CsrA polypeptides with extended C-termini acting as a binding surface for protein-protein interaction with FliW (**Figure 4B**).

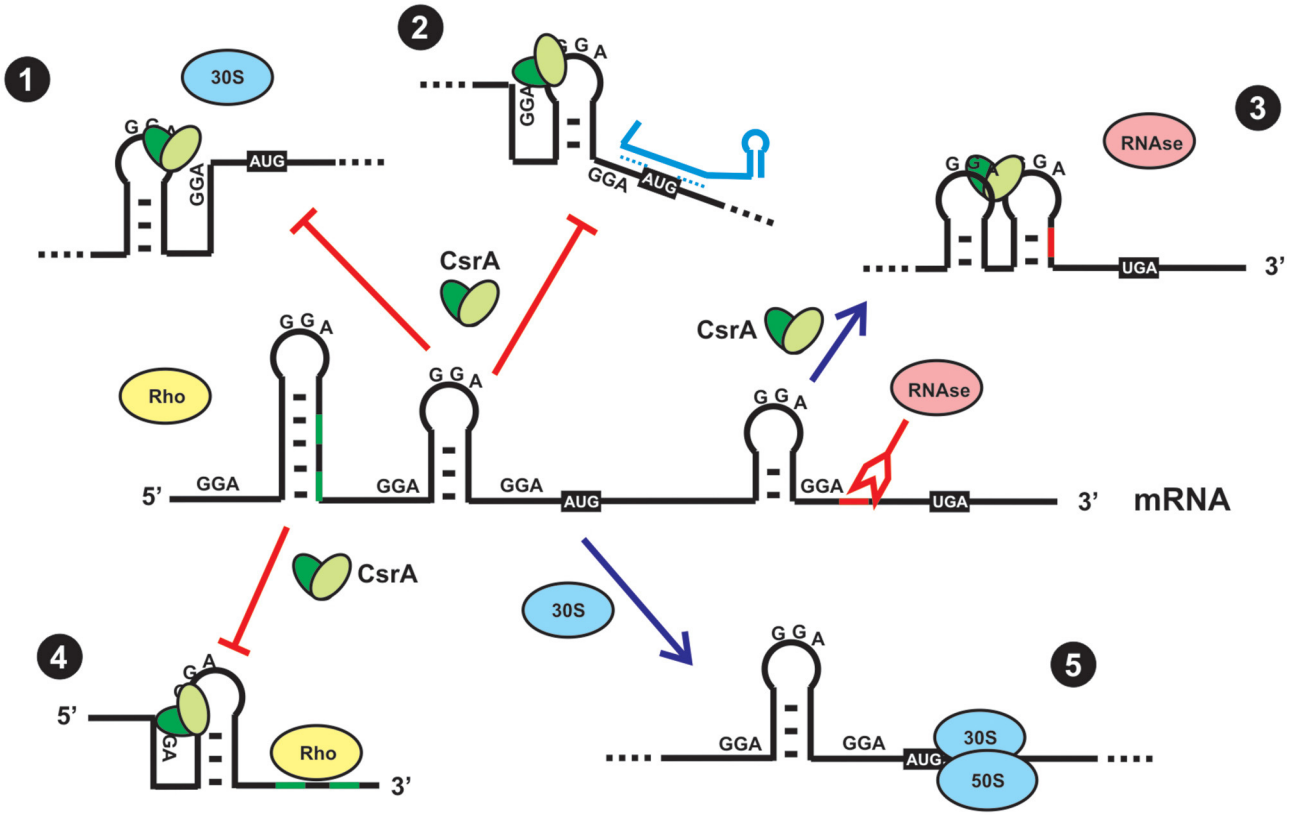

FIGURE 3 | Direct and indirect regulatory effects of CsrA binding to a mRNA. (1) Direct translational repression. In most cases, CsrA binds to target sites around or within the Shine-Dalgarno region, and as a consequence it outcompetes binding of the small ribosomal subunit and its engagement in translation initiation. (2) Indirect translational repression. CsrA binds to target sites in the 5′-UTR and induces a conformational change that exposes the Shine-Dalgarno region to base-pairing by a small regulatory RNA, thus impeding access of the ribosome. (3) Indirect control of mRNA stability. CsrA binds to a target site that upon refolding, impedes access of a ribonuclease. (4) Indirect control of transcriptional termination. CsrA binds to a target site in the mRNA and induces a conformational change that exposes Rho-utilization sequences that can now be exploited by Rho protein to stop transcription elongation of the mRNA. (5) In the absence of CsrA (either due to a mutation that abolishes its function or due to sequestration by CsrA-antagonists, as depicted in **Figure 4**), a ribosome can recognize the Shine-Dalgarno sequence and initiate mRNA translation. Usually, translationally active mRNAs are protected from the action of ribonucleases.

An intriguing observation is the presence of CsrA homologs in a very limited subset of lineages within the β-proteobacterial clade (**Figure 1**). Our genomic survey detected only two β-proteobacterial species bearing CsrA homologs: *Bordetella petrii* and *Burkholderia pseudomallei* TSV202 (**Supplementary Table 1**). *Bordetella petrii* is the only environmental *Bordetella* species hitherto found among the otherwise host-restricted and pathogenic members of the genus *Bordetella* (Von Wintzingerode et al., 2001), and it comprises a group of opportunistic pathogens, mostly associated to lung infections (Mattoo and Cherry, 2005). Interestingly, both *B. petrii* and *Pseudomonas aeruginosa* can share a common niche during the infection of patients suffering of cystic fibrosis (Le Coustumier et al., 2011). In *B. petrii*, we found an annotation (Bpet1351) of 62 amino acids sharing 67% identity with the CsrA counterpart of *P. aeruginosa* strain PAO1 (RsmA). The genomic context of Bpet1351 did not reveal evidences of mobile genetic elements. Thus, Bpet1351 most likely represents a core genetic element of the *B. petrii* genome. As for other β-proteobacteria, we did not detect a homolog of FliW in *B. petrii*. Thus, Bpet1351 is a chromosomally encoded CsrA homolog with a potential role of interaction with RNAs in *B. petrii*. The second β-proteobacterial *csrA* allele is X994_313 in chromosome 1 of *Burkholderia pseudomallei* strain TSV202, which encodes a 79 amino acid polypeptide with a predicted secondary structure consisting in a $\beta_1\beta_2\beta_3\beta_4\alpha_1\alpha_2$ topology. Such a slightly longer than the average chain of this protein suggests a possible evolutionary link to the CsrA representatives of ε-proteobacteria or *Bacillus* (**Supplementary Table 1**); however, the protein encoded by X994_313 is 46% identical to *P. aeruginosa* RsmA (including a clear conservation of the residues involved in protein-RNA interaction) but it is only 25% identical to the CsrA homolog of the ε-proteobacterium *Helicobacter pylori*. Clearly, only an experimental functional approach can give support to the type of regulatory interactions that this CsrA homolog performs in *B. pseudomallei*. Interestingly, a simple inspection of the genomic context of X994_313 reveals the presence of adjacent annotations related to mobile genetic elements.

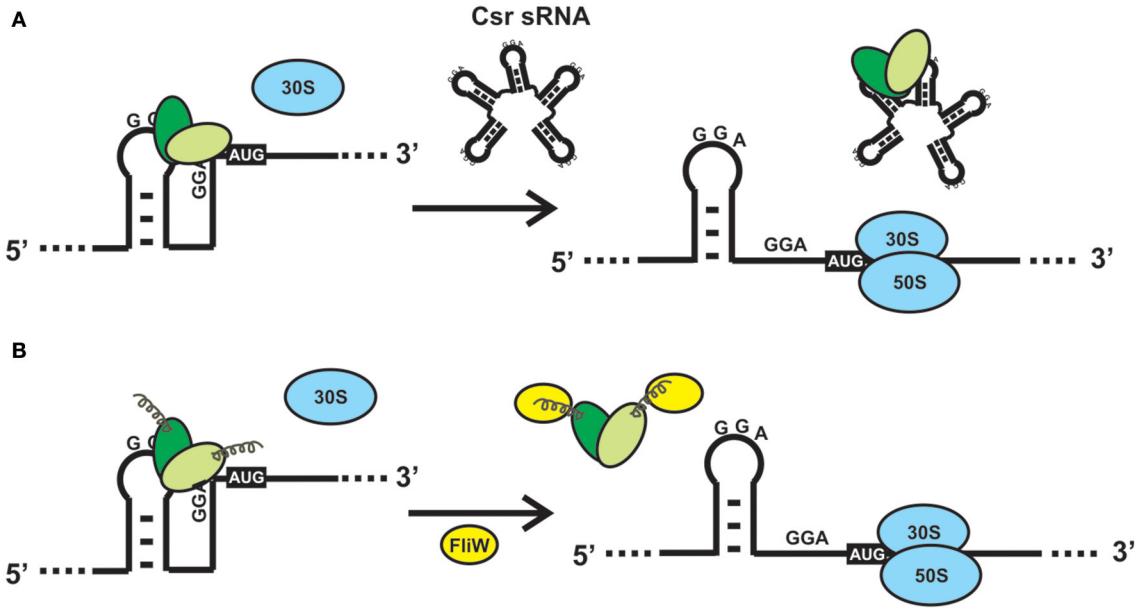

FIGURE 4 | Alternative mechanisms to relieve the direct or indirect effects of CsrA binding to a mRNA. **(A)** Sequestration of CsrA by molecular mimic sRNAs. The sRNAs of the Csr/Rsm family act like protein sponges by offering multiple sequence/structural motifs that fulfill the features shown in **Figure 2F**. The availability of CsrA dimers for binding to multiple mRNAs is modulated by the intracellular concentration of one or more of these molecular mimic sRNAs. **(B)** CsrA can be displaced from its mRNA substrates upon interaction of a protein like FliW of *B. subtilis* with the extended C-terminal region (Altegoer et al., 2016). Such interaction provokes a conformational change in the protein dimer that reduces the affinity for the RNA.

HOW DO BACTERIA RELIEVE THE REGULATORY EFFECTS OF CsrA?

CsrA is a highly abundant molecule in the *E. coli* cytosol, being included within the top 17% of abundant proteins constituted by a group of 179 molecules with more than 2050 copies per cell (Ishihama et al., 2008). The abundance of CsrA is not static, oscillating within 10.000 to 30.000 dimers per cell during the batch growth of *E. coli* (Gudapaty et al., 2001). Similarly, the cellular level of the CsrA ortholog of *Pseudomonas aeruginosa* strain PAO1, RsmA, increases 3-fold in stationary phase (Pessi et al., 2001), whereas the level of the main CsrA ortholog of *P. protegens* strain CHA0 (RsmA) is rather stable along the growth curve (Reimmann et al., 2005). This scenario suggests that there would be a considerable potential for posttranscriptional control by CsrA within the cell, and that it may even increase during growth. Thus, there should be antagonizing mechanisms to relieve the control exerted by CsrA (or its orthologs), when required. Up to date, two mutually exclusive mechanisms for antagonizing the activity of CsrA proteins have been described: 1) molecular mimicry by sRNAs (**Figure 4A**); 2) allosteric interaction with proteins, like FliW (**Figure 4B**). The latter has been described in species for which sRNA antagonists have not been found yet, like *Bacillus subtilis* and *Campylobacter jejuni* (Altegoer et al., 2016; Dugar et al., 2016). During the early stages of flagellum assembly in *B. subtilis*, FliW forms a complex with the filament protein Hag; when Hag is secreted to complete the flagellum, FliW is dissociated and it becomes available for interaction with CsrA. At this stage, FliW binds to the C-terminal extension of CsrA and induces the release of the mRNA bound to the RNA pockets, in a non-competitive way (Mukherjee et al., 2016) (**Figure 4B**). Similar molecular interactions occur between CsrA and CesT in enteropathogenic *E. coli* (Ye et al., 2018). Interestingly, the FliW-CsrA regulatory switch is not only devoted to flagellar gene regulation, because in the absence of FliW, *C. jejuni* experiences differential accumulation of non-flagellar proteins in a CsrA-dependent mechanism (Li et al., 2018).

However, the most pervasive antagonizing strategy to relieve posttranscriptional control by proteins of the CsrA family, is through the expression of molecular mimic sRNAs (Romeo and Babitzke, 2019). This class of non-protein coding regulatory RNA molecules behave as protein sponges that form ribonucleoprotein complexes that temporarily relieve the regulatory effect that CsrA proteins have on their mRNA targets (**Figure 4B**). To achieve this, molecular mimic sRNAs offer multiple sequence-structural motifs formed by short hairpins exposing unpaired ANGGA pentanucleotides, that is, the preferred molecular target of CsrA proteins (**Figures 2F,G**). At physiological conditions in which the cellular level of molecular mimic sRNAs is low, proteins of the CsrA superfamily are bound to equivalent motifs typically present in hundreds of target mRNAs. Upon an increase in the intracellular level of the molecular mimic sRNAs, the CsrA-hostage mRNAs are released, and the regulatory effects are reversed (**Figure 4A**). In essence, the biological function of this class of sRNAs is to modulate the distribution

TABLE 1 | Signal transducing two-component systems and their cognate posttranscriptional modules involving CsrA homologs and CsrA-antagonistic sRNAs in γ-proteobacteria.

Species	TCS	Stimulus	CsrA homolog*	Molecular mimic sRNA(s)*	Controlled phenotypes	References
Acinetobacter baumannii	GacS-GacA	Unkown	[CsrA]	[RsmX, RsmY, RsmZ]	Pili, motility, biofilm, metabolism of aromatic compounds, virulence	Kulkarni et al., 2006; Cerqueira et al., 2014
Azotobacter vinelandii	GacS-GacA	Unknown	RsmA	RsmZ1-7, RsmY1-2	Alginate, PHB and alkyl resorcinol lipid biosynthesis	Lopez-Pliego et al., 2018, 2020
Erwinia amylovora	GrrS-GrrA	Unknown	RsmA	RsmB	Flagella, T3SS, amylovoran biosynthesis	Ancona et al., 2016
Escherichia coli	BarA-UvrY	Acetate, formate	CsrA	CsrB, CsrC	Glycogen synthesis, gluconeogenesis, motility, biofilm	Chavez et al., 2010
Halomonas anticariensis	GacS-GacA	Unknown	[CsrA]	Unknown	Quorum sensing, exopolysaccharide, biofilm.	Tahrioui et al., 2013
Legionella pneumophila	LetS-LetA	Unknown	CsrA	RsmY, RsmZ	>40 effector proteins secreted by T4SS (cytotoxicity), motility	Nevo et al., 2014; Feldheim et al., 2018
Pectobacterium carotovorum	ExpS-ExpA	Unknown	RsmA	RsmB	Extracellular lytic enzymes, T3SS-secreted harpin	Cui et al., 2001
Salmonella enterica serovar Typhimurium	BarA-SirA	Acetate, formate	CsrA	CsrB, CsrC	Stress resistance, virulence (HilD), aerobic and nitrate respiration, motility, fimbriae	Lawhon et al., 2002; Zere et al., 2015
Serratia mascescems	GacS-GacA	Unknown	CsrA	CsrB, CsrC	Motility, biofilm, coral mucus utilization	Krediet et al., 2013; Ito et al., 2014
Vibrio cholerae	VarS-VarA	Unknown	CsrA	CsrB, CsrC, CsrD	Virulence, biofilm, quorum sensing	Lenz et al., 2005; Butz et al., 2019
Vibrio fischeri	GacS-GacA	Citrate?	CsrA	CsrB, CsrC, CsrD	Luminiscence, siderophores, motility	Septer et al., 2015
Vibrio tasmaniensis	VarS-VarA	Unknown	CsrA	CsrB1-4	Metalloproteases	Nguyen et al., 2018

**Proteins or sRNAs between brackets were found by genome inspection and have not been experimentally characterized yet.*

of CsrA dimers into alternative ribonucleoprotein complexes, i.e., CsrA-trapped mRNAs or sRNA-sequestered CsrA dimers (**Figure 4A**).

In Enterobacteriaceae, the molecular mimic sRNAs that titrate CsrA dimers are referred to as Csr RNAs because, together with the CsrA protein, they were originally characterized as carbon storage regulators (Liu et al., 1997; Weilbacher et al., 2003), whereas in *Pseudomonas* species the so-called Rsm sRNAs were first discovered in association with the CsrA-like counterparts known as RsmA and its close paralogues (Heeb et al., 2002; Valverde et al., 2003; Kay et al., 2005). Csr and Rsm sRNAs are functional and structural homologs that are interchangeable between these γ-proteobacterial taxa (Valverde et al., 2004) but display an enormous divergence at the sequence level with sizes ranging 100 to 400 nt. In addition, from a single gene copy to up to seven functional Csr/Rsm homologs have been detected in different bacterial species (**Supplementary Figure 1**) (Moll et al., 2010; Lopez-Pliego et al., 2018). Recently, two novel sRNAs with similar sequestering capabilities, RsmV (Janssen et al., 2018) and RsmW (Miller et al., 2016), were discovered in *Pseudomonas aeruginosa*, although in contrast to RsmX, RsmY and RsmZ, their transcription is independent of the GacS-GacA two-component system, and they seem to represent *P. aeruginosa*-specific representatives and are probably of independent evolutionary origin.

CsrA PROTEINS AND THEIR MOLECULAR MIMIC sRNA PARTNERS ARE SUBSIDIARIES OF SIGNAL TRANSDUCTION SYSTEMS

With the high cellular level of CsrA dimers fluctuating within a relatively narrow range, the role of antagonizing molecules becomes critical to relieve posttranscriptional control of target mRNAs. To achieve this, different bacterial taxa have recruited two-component sensory-transducing systems (TCS) to manipulate the intracellular level of the molecular mimic sRNAs of the Csr type (**Table 1**) (Valverde and Haas, 2008). In these circuits, mainly characterized for members of the γ- proteobacteria, an environmental stimulus is perceived by the membrane-bound sensor protein that modulates the phosphorylation status of the partner transcriptional factor; the latter then controls the expression of the gene(s) encoding the molecular mimic sRNA(s), which in turn will adjust the cellular level of these sRNAs to modulate the balance of CsrA distribution between target mRNAs and sRNAs (**Figure 4A**). The nature of the stimulus and the complexity of the signal transduction cascade (i.e., the number of CsrA protein and Csr sRNA homologs) vary between different species (**Tables 1**, **2**; **Supplementary Figure 1**), but the basic architecture of the

TABLE 2 | Diversity of the posttranscriptional Csr(Rsm) regulatory module of the Gac-Rsm cascade in the genus *Pseudomonas*.

***Pseudomonas* species—strain**	**Additional factors controlling Gac-Rsm cascade**	**CsrA homolog(s)**	**Molecular mimic sRNA(s)**	**Controlled phenotypes**	**References**
P. aeruginosa PAO1	LadS, RetS and PA1611 histidine kinases	RsmA, RsmN (RsmF)	RsmY, RsmZ, RsmW (Gac-independent), RsmV (Gac-independent)	Quorum sensing; virulence factors, sessile-to-biofilm switch	Ventre et al., 2006; Marden et al., 2013; Morris et al., 2013; Chambonnier et al., 2016; Miller et al., 2016; Schulmeyer et al., 2016; Janssen et al., 2018; Romero et al., 2018
P. brassicacearum NFM421	Unknown	RsmA, RsmE	RsmX, RsmY, RsmZ	Antibiotics, indole acetate, extracellular enzymes, quorum sensing, T6SS, alginate, biofilm	Lalaouna et al., 2012
P. chlororaphis 30-84	Unknown	RsmA, RsmE	RsmX, RsmY, RsmZ	Biosynthesis of phenazines, quorum sensing, extracellular enzymes	Chancey et al., 1999; Wang et al., 2013
P. donghuensis HYS/SVBP6/P482	Unknown	RsmA, RsmE, Rsm3	RsmY, RsmZ	Biosynthesis of 7-hydroxytropolone, antifungal activity, production of HCN and other volatile compounds	Yu et al., 2014; Ossowicki et al., 2017; Agaras et al., 2018; Chen et al., 2018; Muzio et al., 2020
P. entomophila Pe	Unknown	RsmA1, RsmA2, RsmA3	RsmY, RsmZ	Insect virulence factors, exopotease, lipopeptide	Vodovar et al., 2006; Vallet-Gely et al., 2010
P. fluorescens SS101	Unknown	RsmA, RsmE	RsmY, RsmZ	Lipopeptide, iron acquisition, motility, chemotaxis T6SS	Song et al., 2015
P. protegens CHA0	Temperature, ppGpp, Krebs cycle intermediates, LadS, RetS	RsmA, RsmE	RsmX, RsmY, RsmZ	Biocontrol properties (antifungal compounds, HCN, extracellular enzymes, lipopeptide)	Heeb et al., 2002; Valverde et al., 2003; Reimmann et al., 2005; Humair et al., 2009; Takeuchi et al., 2009; Workentine et al., 2009; Sobrero et al., 2017
P. putida KT2440	Unknown	RsmA, RsmE, RsmI	RsmY, RsmZ, RsmX?	Motility, biofilm formation (LapA adhesin)	Martinez-Gil et al., 2014; Huertas-Rosales et al., 2016
P. syringae pv *syringae* DC3000	LadS, RetS	CsrA1 (RsmI), CsrA2 (RsmA), CsrA3 (RsmE), CsrA4, CsrA5	RsmX1-5, RsmY, RsmZ	Carbon metabolism, virulence, motility, production of secondary metabolism, quorum sensing	Moll et al., 2010; Records and Gross, 2010; Ferreiro et al., 2018

regulatory cascade is similar: a TCS converts a physicochemical input into a primary transcriptional output (i.e., activation of sRNA gene expression), then it is converted into a subsequent global posttranscriptional reversion of the pre-existing effect of CsrA dimers over multiple mRNAs (**Figure 5**).

The cascades come in different flavors. For instance, in *E. coli*, the TCS BarA-UvrY responds to acetate and formate, as well as to the medium pH (Mondragon et al., 2006; Chavez et al., 2010), to activate the expression of *csrB* and *csrC* encoding the two molecular mimic sRNAs CsrB and CsrC, bearing 18 and 11 CsrA binding sites, respectively (Liu et al., 1997; Weilbacher et al., 2003), which in turn modulate the availability of the single CsrA protein of this species; the outcome of the cascade activation is the regulation of carbon polymer biosynthesis, motility and biofilm formation (Romeo and Babitzke, 2019). In the plant pathogen *Pectobacterium wasabiae* (formerly *Erwinia carotovora*), the BarA-UvrY homolog TCS named ExpS-ExpA controls expression of a single molecular mimic sRNA RsmB (containing 19 recognition motifs) to interact with a single CsrA ortholog (RsmA); the major characterized regulatory targets are a series of extracellular plant cell wall-degrading enzymes (Mukherjee et al., 1996). In *Vibrio cholerae*, the TCS VarS-VarA regulates the activity of a single CsrA protein through the activation of three genes encoding the molecular mimic sRNAs CsrB, CsrC, and CsrD (with 23 to 28 putative recognition motifs); the cascade has a major impact on the expression of the quorum sensing system, thus indirectly controlling biofilm formation and virulence (Lenz et al., 2005). So far, proteins of the two-component system formed by BarA/GacS/VarS and UvrY/GacA/VarA families are a hallmark of γ-proteobacterial taxa (**Supplementary Table 1**).

THE Gac-Rsm CASCADE OF *PSEUDOMONAS* SPECIES

The genus *Pseudomonas* comprises over 250 defined species, with a remarkable distribution across major ecological niches, either as free-living or in close interactions with animals, insects, plants and fungi, at relatively mild or extreme conditions (Palleroni, 2015). An important number of species are opportunistic pathogens of clinical relevance for humans, and of economic

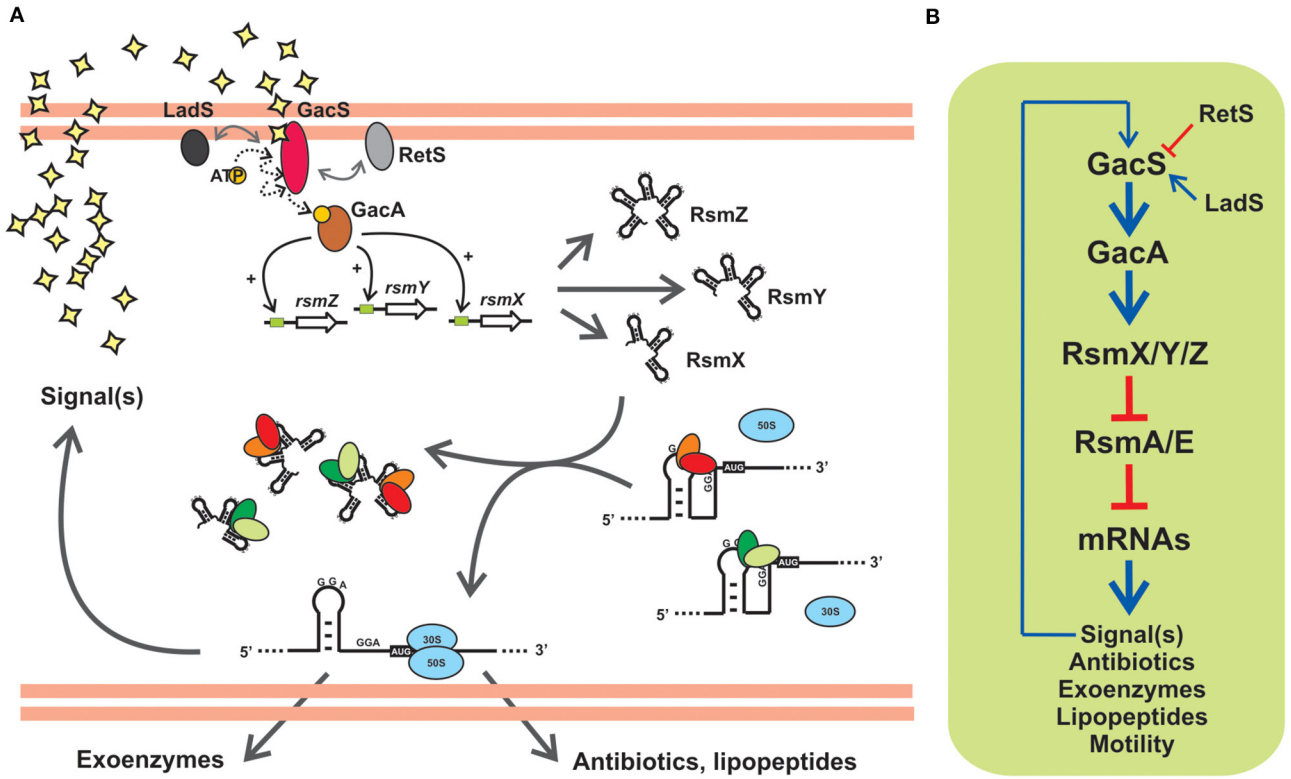

FIGURE 5 | The posttranscriptional Gac-Rsm cascade of *Pseudomonas protegens* strain CHA0: An archetypal signal transduction pathway of γ-proteobacteria controlling the activity of CsrA proteins with molecular mimic sRNAs. **(A)** In strain CHA0, the GacS-GacA TCS responds to uncharacterized autoinducing signals, and promotes translation of various mRNAs involved in exoproduct formation and control of plant root pathogens (antibiotics, lipopeptides, extracellular lytic enzymes), by relieving the translational blockage caused by the two CsrA homologs RsmA and RsmE. This is achieved by activating transcription of *rsmX*, *rsmY* and *rsmZ* genes, thereby increasing the intracellular abundance of the three sponge RNAs RsmX, RsmY and RsmZ, that sequester RsmA and RsmE. Two accessory orphan sensor kinases, RetS and LadS, modulate the activity of GacS. **(B)** Schematic linear representation of the Gac-Rsm regulatory pathway of *P. protegens* strain CHA0. The biosynthesis of a diffusible signal compound is also under the control of the cascade, as a number of other phenotypes contributing to the antifungal ability of this strain, and it represents a positive feedback input for the pathway. This diagram, as well as the scheme in **(A)**, is simplified and omits modulatory aspects like the requirement of RsmA/E proteins for a proper expression of *rsmX/Y/Z* genes (Valverde et al., 2003; Kay et al., 2005). The number of components in the posttranscriptional module formed by Rsm proteins and Rsm sRNAs, as well as the nature of the target mRNAs, vary between different species (see **Tables 1**, **2**).

concern in animal and plant production; however, there are also an important number of species with probiotic traits for animals and plants, and representatives with metabolic capacities for bioremediation purposes (Palleroni, 2015). Their ease to isolate and culture in the lab has resulted in the availability of an important wealth of physiological, biochemical, genetic, and genomic resources. All the accesible *Pseudomonas* genomes reveal the existence of a posttranscriptional regulatory cascade having the general features described in the previous section, which is known as the Gac-Rsm system.

Gac stands for global antibiotic and cyanide control (Laville et al., 1992) and Rsm stands form regulator of secondary metabolism (Blumer et al., 1999). The two regulatory phenomena were discovered in the plant-probiotic isolate *P. protegens* (ex-*fluorescens*) CHA0 and linked to each other upon the identification of the gene *rsmA* encoding the CsrA ortholog RsmA (Blumer et al., 1999). The prototypic backbone of the Gac-Rsm cascade of *Pseudomonas* is illustrated in **Figure 5A** for the case of *P. protegens* CHA0. The sensor kinase GacS responds to a solvent-extractable extracellular compound (of yet unknown chemistry) produced by the cells and that accumulates as a function of cell density in batch cultures, and most likely autophosphorylates and then transfers a phosphoryl moiety to the GacA transcriptional regulator. Phosphorylated GacA, or an intermediary factor, act on DNA sequences upstream the promoters of the *rsmX*, *rsmY* and *rsmZ* genes to activate their transcription, which results in the intracellular accumulation of the corresponding molecular mimic sRNAs. At the end of the pathway, the two RNA-binding proteins of the CsrA family, RsmA and RsmE, are titrated away from their complexes with different target mRNAs to form inactive dead-end ribonucleoprotein assemblages with the sponge sRNAs. As a consequence of this cascade of molecular events, the mRNAs encoding proteins and enzymes required for the synthesis of a variety of secondary metabolites are engaged into translation (**Figure 5A**). At the population level, the activation of the Gac-Rsm cascade in *P. protegens* CHA0 provokes a coordinated behavioral change which is evidenced as a marked increase (and

social sharing) in the biosynthesis of antifungal compounds, extracellular enzymes, cyclic lipopeptides (Lapouge et al., 2008; Sobrero et al., 2017), and interestingly, of the GacS-inducing signal itself (Dubuis et al., 2006), which implies a positive-forward loop (**Figure 5**), As deduced from the linearity of the cascade (**Figure 5B**) and the molecular mechanism of each of the components, deleting the *rsmA* and *rsmE* genes provokes activation of all these biosynthetic pathways ahead of time, an observation that originated the naming of the CsrA homologs of *P. protegens* CHA0 as RsmA first, and RsmE some years later (Heeb et al., 2002; Reimmann et al., 2005). Additionally, deleting either *gacS* or *gacA*, impede the removal of RsmA and RsmE from their target mRNAs, and such single mutations logically result in a global fall in the production of all secondary metabolites, a phenotype that inspired naming of the components of the signal-transducing cascade GacS-GacA (Laville et al., 1992; Zuber et al., 2003). At the ecological level, the cascade is key for the cells to avoid predation by eukaryotic bacterivores that dislike some of the extracellular compounds (Jousset et al., 2006), and, at the same time, it confers protection from fungal pathogens to the roots of plants that are colonized by this strain (Lapouge et al., 2008). Hence, the Gac-Rsm cascade of *P. protegens* CHA0 has deep implications at the individual, collective and ecological levels.

The backbone of the Gac-Rsm cascade -as detailed for strain CHA0- is conserved in the genus *Pseudomonas*, but it presents several species-specific variations: first, the number of components downstream of the TCS GacS-GacA is highly variable in terms of the number of molecular mimic sRNA molecules and of CsrA homologs (the latter will be thoroughly discussed in the next sections) (**Table 2**); second, there are additional factors that modulate the functioning of the cascade (**Table 2** and **Supplementary Table 1**); third, the regulon and/or the main characterized phenotypes that are subject to Gac-Rsm control differ across species and determine the outcome of their interactions with other bacteria or with eukaryotic hosts (**Table 2**).

With regard to the occurrence of additional factors influencing the Gac-Rsm cascade, two additional sensor kinases have been reported to modulate the activity of GacS directly: LadS, that stimulates GacS activity, and RetS, that is a negative regulator (**Figure 5**, **Table 2**) (Ventre et al., 2006; Chambonnier et al., 2016). Whereas, the master components of the cascade GacS and GacA are broadly distributed within the γ-proteobacteria, LadS and RetS show a more sporadic occurrence (**Supplementary Table 1**). Both genes encoding LadS and RetS are present together with *gacS* and *gacA* homologs only in *Pseudomonas*, *Lysobacter,* and *Alcanivorax* species (**Supplementary Table 1**). GacS and GacA are present together with LadS (but not with RetS) in five γ-proteobacterial genera (*Alteromonas*, *Halomonas*, *Idiomarina*, *Marinibacter,* and *Pseudoalteromonas*); conversely, GacS, GacA, and RetS (but not LadS) co-occur only in *Azotobacter* species (**Supplementary Table 1**). Thus, although not exclusively restricted to members of the genus *Pseudomonas*, the genes encoding the accessory sensor histidine kinases LadS and RetS are present together with *gacS* and *gacA* in a few γ-proteobacterial taxa, suggesting that they have emerged recently in the evolutionary history of these closely related genera.

When inspecting the occurrence of homolog genetic elements that constitute the Gac-Rsm cascade in the KEGG database (**Supplementary Table 1**), we found the surprising and unexpected case of the Gram-positive bacterium *Streptococcus dysgalactiae* subsp. *equisimilis* having ortholog genes encoding the BarA/GacS/VarS sensor kinase (locus tag NCTC11565_05684; 62% identical to *P. protegens* GacS), the UvrY/GacA/VarA response regulator (locus tag NCTC11565_03616; 87% identical to *P. protegens* GacA), and two CsrA proteins (locus tags NCTC11565_05400 and NCTC11565_00091; 81% and 30% identical to *P. protegens* GacA, respectively) (**Supplementary Table 1**). Worth mentioning is the fact that the most similar *csrA* allele to that of *P. protegens rsmA*, displays the same local genetic arrangement as in *Pseudomonas* genomes (*alaS-lysA-csrA-tRNA*^{Ser}*-tRNA*^{Arg}), and it is immediately flanked downstream by a large cluster of genes of a Mu-like prophage. No other Gram-positive species contains a set of genes so closely resembling that of the Gac-Rsm cascade of γ-proteobacteria (**Supplementary Table 1**).

HOW MANY DIFFERENT CsrA (Rsm) ORTHOLOGS IN *PSEUDOMONAS*?

Up to date, dozens of articles have reported on the impact of CsrA proteins in bacterial fitness by reverse genetics approaches (**Table 1**). The isolation of *csrA* deletion mutants in many different bacterial species demonstrates that *csrA* is not an essential gene. The essentially of *csrA* has been only argued in *E. coli*, which develops a conditional growth behavior in the presence of a glycolitic carbon source (Timmermans and Van Melderen, 2009). Interestingly, whereas the ample majority of the genomes we have inspected have only one CsrA homolog, there are few lineages in which at least two independent *csrA*-like copies are found. This is the special case of the genera *Pseudomonas* and *Legionella*. The latter holds the highest average number of CsrA paralogues per genome (**Supplementary Table 1**) (Chien et al., 2004; Abbott et al., 2015). From now on, we will focus in the multiplicity of CsrA paralogues in the *Pseudomonas* pangenome.

In contrast to the rest of γ-proteobacterial branches other than *Legionella*, more than 90% of *Pseudomonas* species present at least two *csrA* alleles per genome (**Supplementary Tables 1**, **3**). Historically, the first experimentally characterized representatives in the genus *Pseudomonas* were designated *rsmA* in *P. aeruginosa* strain PAO1 (Blumer et al., 1999) and in *P. protegens* (ex-*fluorescens*) strain CHA0 (Heeb et al., 2002). However, the *Pseudomonas* RsmA proteins are structural and functional homologs of the enterobacterial CsrA protein (see above; **Figure 2**). For historical reasons, in the next paragraphs we will stick to the Rsm naming when discussing the phylogenetic aspects of these proteins in the genus *Pseudomonas*.

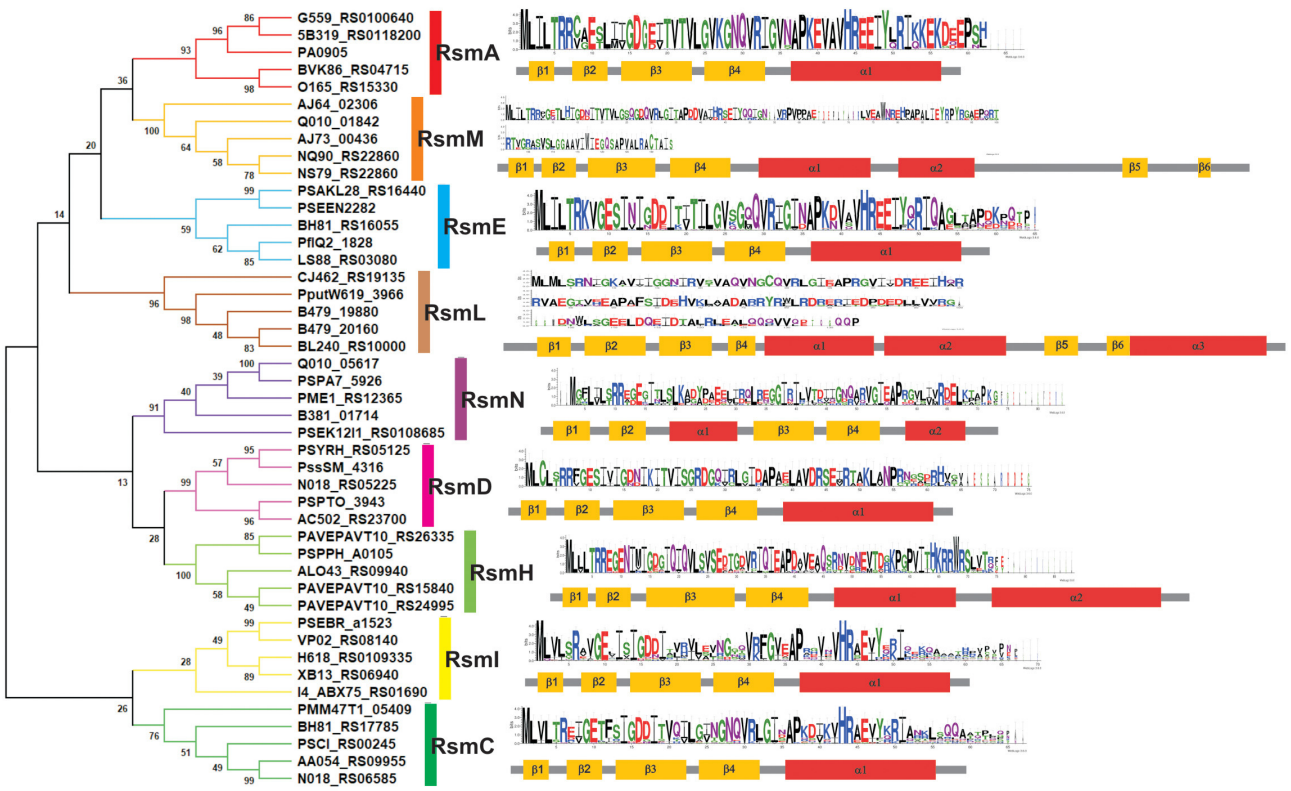

FIGURE 6 | Families of Rsm (CsrA) proteins within the genus *Pseudomonas* as deduced from comparative genomics. Phylogenetic relationships of the 9 subfamilies of *Pseudomonas* Rsm proteins. The evolutionary history was inferred using the Neighbor-Joining method (Saitou and Nei, 1987). The optimal tree with the sum of branch length = 7.34 is shown. The percentage of replicate trees in which the associated taxa clustered together in the bootstrap test (1000 replicates) are shown next to the branches (Felsenstein, 1985). The evolutionary distances were computed using the JTT matrix-based method (Jones et al., 1992) and are in the units of the number of amino acid substitutions per site. This analysis involved 45 amino acid sequences. For each one, the locus tag identification is presented in the figure. All positions containing gaps and missing data were eliminated (complete deletion option). There was a total of 46 positions in the final dataset. Evolutionary analyses were conducted in MEGA X (Kumar et al., 2018). Secondary structure was predicted with JPRED4 server (Drozdetskiy et al., 2015). For each Rsm subfamily, a sequence logo (Crooks et al., 2004) was generated from multiple alignment data by MUSCLE (Edgar, 2004).

The developers of the *Pseudomonas* Genome Database (www.pseudomonas.com) have generated *Pseudomonas*-specific orthologous groups (POGs) based on protein sequence-similarity algorithms (Buchfink et al., 2015). This sensitive and fast tool allowed us to fetch a detailed list of protein homologs from available genomes using a query sequence. As a starting point, we used the amino acid sequence of RsmA from the *P. aeruginosa* PAO1 annotation PA0905, and we retrieved 7 different POGs (**Supplementary Table 2**). In order to obtain a more precise picture of the evolution of these groups, we randomly extracted 10 sequences from each POG and inferred their phylogenetic relationship by Neighbor Joining (NJ) (**Supplementary Figure 2**). A simplified version of this analysis, with only 5 sequences per POG, is presented in **Figure 6**. The NJ inference actually shows the existence of 9 different Rsm protein subfamilies within the genus *Pseudomonas*. If we consider that each POG represents a standalone protein subfamily, our phylogenetic analysis has uncovered two novel subfamilies not previously detected in the *Pseudomonas* Genome Database. Four out of the 9 groups correspond to the well characterized paralogue subfamilies RsmA (Blumer et al., 1999; Pessi et al., 2001), RsmE (Reimmann et al., 2005), RsmI (Huertas-Rosales et al., 2016) and RsmN (also referred to as RsmF in the literature) (Marden et al., 2013; Morris et al., 2013). On the basis of the POG definition in the *Pseudomonas* database and of our NJ clustering, we propose the novel paralogue subfamilies RsmC, RsmD, RsmH, RsmL and RsmM (**Figure 6**). Interestingly, all the paralogue groups present a high degree of conservation of the amino acids involved in the interaction with RNA molecules (at least for nucleotide contacts reported for RsmE Schubert et al., 2007) (**Supplementary Figure 3**). Except for RsmN (Marden et al., 2013; Morris et al., 2013), the rest of *Pseudomonas* Rsm subfamilies present the archetypical topologic fold $\beta_1\beta_2\beta_3\beta_4\alpha_1$ (**Figure 2B**), with some minor variations (**Figure 6**). The first noticeable difference among the subfamilies is the polypeptide size, which occurs particularly at the C-terminal region. As expected, this extension at the C-terminus has an impact on protein topology (**Figure 6**). RsmM and RsmH members present an additional alpha helix, whilst RsmL members have 2 extra helices; RsmM and RsmL also show two additional short β-sheets

(**Figure 6**). The fact that these extended C-terminal regions does not seem to be unstructured in these subfamilies, suggests that it may have an important contribution to protein stability and/or in protein networking. By analogy to the CsrA homologs that interact with FliW (**Figure 4**, **Supplementary Table 1**), the extended C-terminal regions of RsmM, RsmH, and RsmL could function as a scaffold region for protein-protein interactions. In fact, there are no experimental evidences yet of which are the direct or indirect proteins interactors of members of the CsrA superfamily. Because of its major role in posttranscriptional control of mRNAs, most efforts have been directed to reveal the RNA interactome of CsrA proteins, but it may be expected that accessory proteins would be recruited to the CsrA-RNA ribonucleoprotein complex, like Hfq and the degradosome (Sorger-Domenigg et al., 2007; De Lay et al., 2013; Bruce et al., 2018).

PHYLOGENETIC DISTRIBUTION OF THE Rsm SUBFAMILIES WITHIN THE GENUS *PSEUDOMONAS*

Once we defined the number of Rsm paralogue subfamilies of the genus (**Figure 6**), we set out to explore the distribution of each paralogue group among the different *Pseudomonas* species. The genetic diversity and metabolic flexibility of the genus has

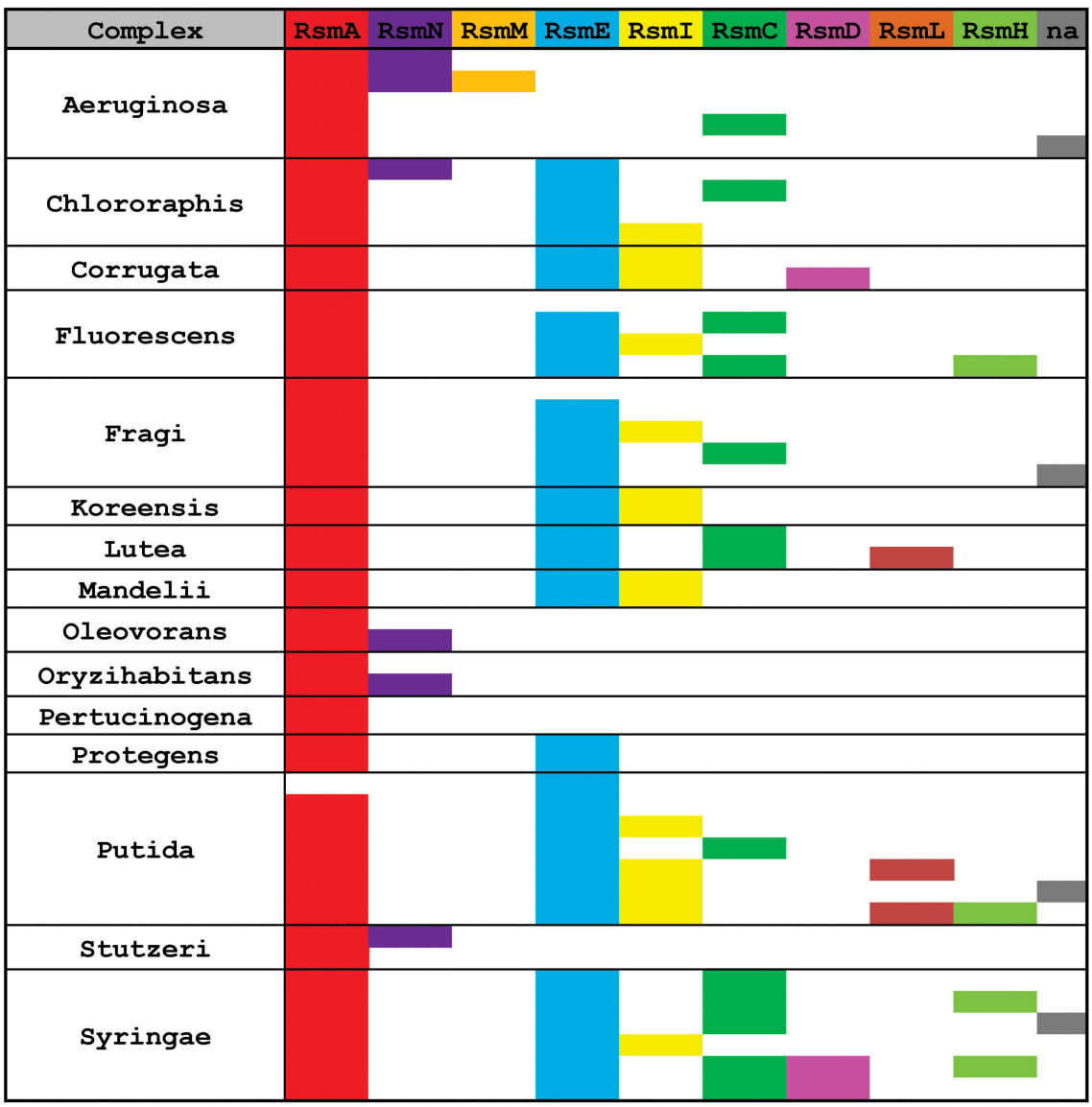

FIGURE 7 | Distribution of Rsm paralogues in the major *Pseudomonas* taxonomic subgroups. Within each subgroup, each row represents different species or strains displaying different combinations of alleles (see extended data in **Supplementary Table 4**). n.a., the sequence of the *rsm* paralogue could not be assigned with enough confidence to any of the 9 subfamilies.

contributed to the successful colonization of a broad variety of ecosystems in our planet (Silby et al., 2011). Besides, an important number of species interact with most eukaryotic taxa (Silby et al., 2011), contributing to their health or their disease (Mercado-Blanco and Bakker, 2007; Loper et al., 2012; Winstanley et al., 2016). Thus, the distribution of Rsm paralogues among different species, each with different niches and lifestyles, might be related to its function. We then inspected 137 *Pseudomonas* genomes (**Supplementary Table 3**), trying to cover all the reported taxonomic groups (Peix et al., 2018). We applied BLASTP under non-restrictive conditions with *P. aeruginosa* RsmA as the bait, in order to retrieve the different paralogues from each genome (**Supplementary Tables 3**, **4**). Next, we added each retrieved paralogue sequence to the dataset used for our NJ phylogenetic analysis so that we could infer which Rsm subfamily it belongs to (**Supplementary Table 5**). We here present the distribution of Rsm paralogues for 8 different taxonomic clades, which roughly represent the diversity of the genus (**Figure 7**; for an extended version, see **Supplementary Figure 4**).

RsmA is the most broadly distributed Rsm subfamily (**Figure 7**). Almost all *Pseudomonas* genomes have one *rsmA* allele. RsmE appears as the second most represented subfamily. Yet, *P. aeruginosa* and its close relatives (like *P. stutzeri* and *P. oryzihabitants*) do not have RsmE paralogues (**Figure 7**). Instead, it appears that RsmN has become the RsmA sidekick within the *P. aeruginosa*, *P. stutzeri*, *P. oleovorans* and *P. oryzihabitants* branches (**Figure 7**). Much to our surprise, we found an *rsmN* homolog in the chromosome of a strain phylogenetically distant from the former 4 species, *P. chlororaphis* HT66 (**Supplementary Table 4**). However, the contig that contains the *rsmN* allele (locus tag M217_RS0107790) does not reveal clear evidences of association to mobile genetic elements that would explain an interspecies lateral transfer. In contrast, the *rsmN* homolog (locus tag PME1_RS12365) of *P. mendocina* NBRC 14162 (belonging to the Oleovorans clade) is found nearby an integrase gene (PME1_RS12365) located just downstream a tRNA gene (PME1_RS12285). This genetic organization is typical of genomic islands (Williams, 2002). As we did not find this genetic arrangement in neither of the other *rsmN* homologs, the case of *P. mendocina* NBRC 14162 is unusual in that *rsmN* lies within a possible genomic island.

Another striking observation of the distribution of Rsm subfamilies, is the fact that there is no single genome containing both RsmI and RsmC; rather, we found either RsmI or RsmC within a genome (**Figure 7**). As both homologs share a common ancestor (**Figure 6**), this is a clear example of a putative gene duplication and speciation event, for which the host or environmental constraints have shaped the pathway and consolidated either one of the two homologs. Nevertheless, RsmI and RsmC have a fairly broad distribution across the genus (**Figure 7**).

In contrast to the rather ample distribution of RsmA, RsmE, RsmC, and RsmI, the rest of the *Pseudomonas*' Rsm subfamilies have a much more restricted distribution (**Figure 7**). RsmL is present only in some members of the *P. putida* and *P. lutea* branches, RsmD in some species within the *P. syringae* and *P. corrugata* clades, and RsmH only in a few species within the *P. syringae*, *P. putida,* and *P. fluorescens* groups (**Figure 7** and **Supplementary Table 5**). Notably, a subset of *P. aeruginosa* genomes bears a third Rsm paralogue, RsmM, in addition to RsmA and RsmN (**Figure 7**). As members of the RsmM paralogue subfamily were not detected out of *P. aeruginosa*, RsmM is a species-specific Rsm paralogue.

Finally, we have detected the presence of multiple copies of alleles from the same subfamily; for instance, two *rsmA* alleles in *P. corrugata* and three *rsmH* genes in *P. tolaasii* (**Supplementary Table 4**). In summary, the distribution pattern of Rsm paralogues in the chromosomes of the genus *Pseudomonas* is another trait that reflects the dynamic plasticity of their genomes and provides evidences of evolutionary genetic processes at different stages of progress.

HEAVY TRAFFIC OF CsrA (Rsm) HOMOLOGS IN *PSEUDOMONAS* PLASMIDS AND PHAGES

To the best of our knowledge, only two scientific reports have revealed the presence of *csrA* alleles in plasmids from environmental bacterial isolates. The first one described a *csrA* allele in the replication region of the cryptic plasmid pMBA19a from a *Sinorhizobium meliloti* environmental isolate (Agaras et al., 2013). The encoded CsrA homolog has a high degree of identity with typical γ-proteobacterial CsrA proteins but presents a C-terminal extension that may fold into an extra α-helix (Agaras et al., 2013). Genetic complementation of Δ*rsm* mutants from *P, aeruginosa* PA01 or *P. protegens* CHA0 suggests that the plasmidic *S. meliloti* homolog is functional and that the extra α-helix is most likely involved in protein stability and that it does not interfere with mRNA binding and riboregulatory functions (Agaras et al., 2013). The second case is a *csrA*-like sequence (PSLF89_RS34715) also found in a cryptic plasmid from the fish pathogen *Piscirickettsia salmonis* (Ortiz-Severin et al., 2019). *P. salmonis* is a γ-proteobacterium related to the intracellularly adapted species of *Coxiella*, *Francisella* and *Wolbachia* genera (Fryer et al., 1992). The authors suggested that the plasmidic *csrA* allele could be involved in the regulation of the expression of other plasmidic genes related to a conjugative-type secretion system, by analogy to the genetic context of a *csrA* allele of two genomic islands of *Legionella pneumophila* Corby (Glockner et al., 2008). Nevertheless, the actual role of these *csrA* elements for the fitness of each plasmid remains obscure.

In contrast to plasmids, there is no single report on the presence of *csrA* alleles in phage genomes. A hint pointing to the possible association of *csrA* genes with phages comes from the inspection of the genomic context of the *csrA* allele X994_313 of *Burkholderia pseudomallei* TSV202, which shows several genes encoding functions related to genetic mobility like type IV secretion system (X994_330), conjugative transfer (X994_308), and a phage-related protein (X994_344). An exhaustive functional analysis of the X994_313 genomic context would be required to reveal if this genetic cluster represent a new class of putative mobile genetic element, such as phage-inducible chromosomal islands (Penades and Christie, 2015).

Although few in number, the findings discussed above suggest a possible contribution of mobile genetic elements and horizontal gene transfer (HGT) mechanisms to the dynamic evolution of CsrA-dependent regulatory pathways. Moreover, the presence of *csrA*-like alleles could be itself linked to the transfer process, as proposed for the CsrA homologs of in *Legionella pneumophila*, denoted as CsrT, which are co-inherited with type IV secretion system genes in all known integrative and conjugative elements (ICEs) of legionellae; it was suggested that CsrT regulate ICE activity to increase their horizontal spread (Abbott et al., 2015). Nevertheless, the sole horizontal movement of a *csrA* allele and its incorporation into the genetic wealth of a receptor bacterium does not guarantee its establishment, and furthermore, to be maintained it requires to be recruited by pre-existing regulatory networks and confer a fitness benefit for the new host cell. Examples of how sRNAs, and their RNA auxiliary proteins like Hfq or RNAse E, contribute to riboregulatory processes in the interplay of core genomic elements and foreign DNA acquired by HGT can be found elsewhere (Frohlich and Papenfort, 2016). Thus, at this point, we asked ourselves whether the presence of *csrA* alleles in plasmids and phages is a rare phenomenon, or if instead, it is a quantifiable property of *crsA* genes.

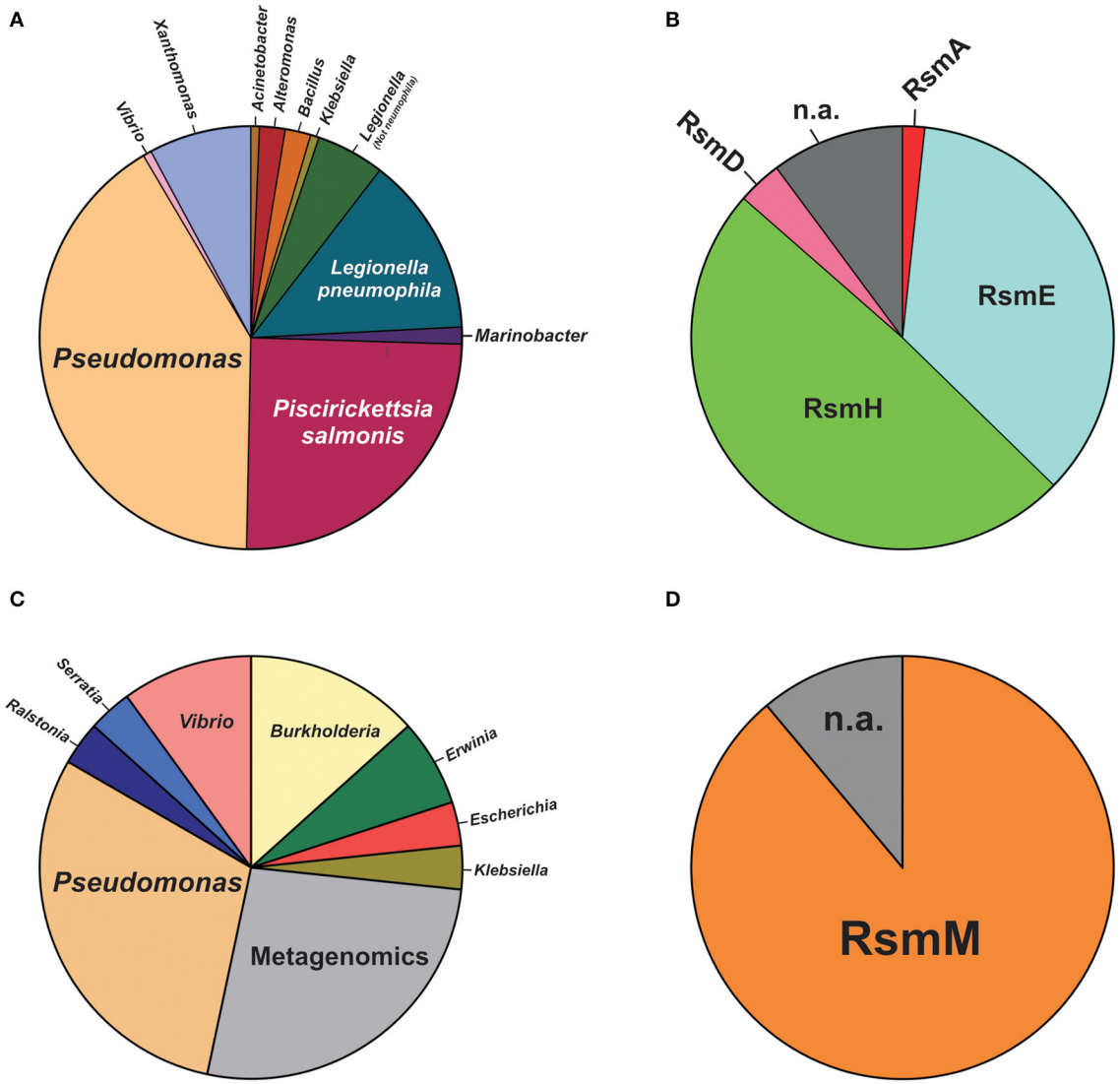

FIGURE 8 | Species distribution of CsrA homologs in natural plasmids and phages of the genus *Pseudomonas*. **(A)** Pie chart illustrating the proportional distribution (%) of plasmids deposited in the PLSDB database (https://ccb-microbe.cs.uni-saarland.de/plsdb/) bearing a *csrA* allele and hosted by different eubacterial host taxa. The total number of plasmids is 161 (for details, see **Supplementary Table 6**). **(B)** Distribution of Rsm paralogues within the 61 plasmids hosted by *Pseudomonas* species. n.a.: not assigned. **(C)** Distribution (%) of phages deposited in the NCBI viral genomes database (https://www.ncbi.nlm.nih.gov/genomes/GenomesGroup.cgi?taxid=10239) bearing a *csrA* allele and hosted by different eubacterial host taxa. The total number of phages is 30 (for details, see **Supplementary Table 7**). **(D)** Distribution of Rsm paralogues within the 9 phage genomes hosted by *Pseudomonas* species. n.a., not assigned.

For plasmids, we carried out a tBLASTn search in the plasmid database PLSDB (Galata et al., 2019), using the *E. coli csrA* gene sequence as query (minimum query coverage of 30%). Among 20668 natural plasmids in the database, we found 161 (0.8%) containing a *csrA* allele (**Supplementary Table 6**). The phylogenetic distribution of $csrA^+$ plasmids is shown in **Figure 8**. The genera with the highest number of $csrA^+$ plasmids were *Pseudomonas* (63; 39%), *Piscirikketsia* (38; 24%), *Legionella* (29; 18%) and *Xanthomonas* (12; 8%) (**Figure 8A**). If we consider the total number of plasmids deposited in the database for each genus, it comes out that the lineages with the highest proportion of $csrA^+$ are *Legionella* (29 $csrA^+$ out of 92 plasmids; 32%) and *Pseudomonas* (63 $csrA^+$ out of 330 plasmids; 19%). Within *Pseudomonas*, by far, the species with the highest number of $csrA^+$ plasmids are *P. syringae* (18/63) and *P. aeruginosa* (15/63); the rest of the $csrA^+$ plasmids of the genus are distributed in another 17 species (**Figure 8B**, **Supplementary Table 6**). Notably, the most frequent paralogues present in *Pseudomonas* natural plasmids were RsmH (49%) and RsmE (36%) (**Figure 8B**), being the RsmE paralogues exclusively associated with plasmids hosted by representatives of the *P. aeruginosa* cluster, whereas the RsmH paralogues were exclusively present in plasmids hosted by representatives of the *P. syringae* cluster (**Supplementary Table 6**). Two interesting observations derive from these findings. First, the paralogues present in plasmids of the *P. aeruginosa* lineage (RsmE-type) have not been detected yet in the *P. aeruginosa* chromosomes, for which the *rsmE* type of paralogues seem to have been evolutionary excluded (**Figure 7**). Second, the paralogues present in plasmids of the *P. syringae* lineage (RsmH-type) have been found in only a fraction of the *P. syringae* chromosomes (**Figure 7**), suggesting that (in contrast to *rsmA* and *rsmE* alleles) *rsmH* is not part of the core genome of *P. syringae*. In support of the latter hypothesis, a micro-genomic context analysis of different *rsmH* alleles let us reveal the presence of genes encoding relaxases and mobilization proteins. One example is *P. caripapayae* ICMP2855, in which the *rsmH* homolog (ALO80_RS00560) is located nearby genes encoding a resolvase (ALO80_RS00585), a relaxase (ALO80_RS00615) and a plasmid mobilization protein (ALO80_RS00610). Another illustrative example is that of the environmental isolate *P. brassicacearum* LZ-4, which belongs to the Corrugata group (Huang et al., 2017) and that represents, according our genome mining analysis, the unique example of a *Pseudomonas* isolate bearing an *rsmH* homolog outside the Syringae clade (**Supplementary Table 5**). The genomic context of this *rsmH* homolog (LZ_RS24290) includes genes for a putative relaxase (LZ_RS24345) and a conjugal transfer protein (LZ_RS24350). Altogether, these observations bring us closer to a plausible link between RsmH paralogues and conjugative mobile elements, due to the neighboring association with genes encoding resolvases and integrases. In summary, it appears that there is an important proportion of *Pseudomonas* natural plasmids that contain genes encoding members of the CsrA (Rsm) family of posttranscriptional regulatory proteins, with RsmH and RsmE being the most frequent types (**Figure 8**).

For phages, we interrogated the NCBI non-redundant protein database with PSI-BLAST using the *E. coli* CsrA sequence as query and narrowing the search to the Viruses taxid:10239. After 10 iterations, the list of hits saturated in 30 phages among a total of 2517 bacteriophage genomes (1.2%). The list of detected $csrA^+$ phages is shown in **Table 3**. Interestingly, the genus with the highest number of $csrA^+$ phages is *Pseudomonas* (9) (**Figure 8C**) and most of them (8) correspond to *P. aeruginosa* isolates (**Table 3**). The proportion of *Pseudomonas* phages deposited in the NCBI database that contain a *csrA* allele is 9 out of 185 (5%). Remarkably, all 8 *P. aeruginosa* phages contain an allele of the *rsmM* type (**Figure 8B**, **Supplementary Table 7**), an Rsm subfamily that we only found in the chromosomes of a subset of *P. aeruginosa* isolates (**Figure 7**), like strain Hex1T that contains an *rsmM* allele (ABI36_RS00125) in a genomic locus flanked by genes reminiscent of phages (ABI36_RS00135 and downstream genes). We hypothesize that a similar scenario would be possible for members of the RsmD and RsmL sub-families; in both cases, we found alleles in genomic contexts flanked by phage-related genes, consistent with prophages or phage remnants. Thus, the evidences presented here for the first time, strongly suggest that members of the genus *Pseudomonas* are active in shuttling *csrA* alleles in mobile genetic elements, including (pro)phages, conjugative elements and plasmids.

Another interesting feature of the search of *csrA* alleles in phage genomes, is the fact that we detected bacterial lineages acting as hosts for $csrA^+$ phages that do not contain chromosomal *csrA* genes; this is the case of *Burkholderia cepacia* and *Burkholderia cenocepacia* (**Table 3**). This situation is similar to that of the *csrA* gene detected in the plasmid pMBA19a hosted in a bacterial species (*S. meliloti*) devoid of chromosomal *csrA* homologs (Agaras et al., 2013).

Circumstantial associations between CsrA proteins and mobile genetic elements other than plasmids and phages, have also been reported. In addition to the case of CsrT and the ICEs of *L. pneumophila* (Abbott et al., 2015), several integrative elements of the Gram-negative anaerobic pathogen *Dichelobacter nodosus* have insertion target sites adjacent to the chromosomal *csrA* gene (Cheetham et al., 2008), whereas in *Serratia* sp. ATCC 39006, CsrA controls prophage activation (Wilf et al., 2013). These findings, and the significant presence of *csrA* alleles in plasmids and phages reported here (**Figure 8**, **Table 3**, **Supplementary Tables 6**, **7**), altogether strongly suggest that members of the CsrA family are important regulatory factors for the success of mobile genetic elements, and that there is a fairly substantial pool of *csrA* genes in the bacterial mobilome.

CONCLUDING REMARKS

Members of the CsrA family are small dimeric RNA binding proteins apparently restricted to Eubacterial species, but with a non-uniform distribution (**Figure 1**). The preferred target RNA motif is a relatively short hairpin with an unpaired GGA triplet in the loop. Each CsrA dimer can bind simultaneously to two of these target RNA motifs (**Figure 2**). Hundreds of cellular mRNAs contain one or more target motifs, which

TABLE 3 | Csr homologs in bacterial phages.

Phage	Host bacteria	Score	Query cover	E value	Identity	Genbank accession	References
AUS531phi	*Pseudomonas aeruginosa*	80.1	90%	1,00E-19	63%	QGF21359.1	
YMC11/07/P54_PAE_BP	*Pseudomonas aeruginosa*	80.1	90%	1,00E-19	63%	YP_009273743.1	
vB_Pae_BR153a]	*Pseudomonas aeruginosa*	79.7	90%	2,00E-19	62%	QBI80752.1	Tariq et al., 2019
phi297	*Pseudomonas aeruginosa*	79.0	90%	3,00E-19	62%	YP_005098048.1	Krylov et al., 2013
vB_Pae_CF24a	*Pseudomonas aeruginosa*	74.0	95%	3,00E-17	57%	QBI82405.1	Tariq et al., 2019
H66	*Pseudomonas aeruginosa*	73.6	95%	4,00E-17	55%	YP_009638943.1	
F116	*Pseudomonas aeruginosa*	72.8	95%	8,00E-17	55%	YP_164288.1	Byrne and Kropinski, 2005
vB_Pae_CF63a	*Pseudomonas aeruginosa*	72.4	95%	1,00E-16	55%	QBI82448.1	Tariq et al., 2019
1.232.O._10N.261.51.E11	*Vibrio tasmaniensis*	68.2	93%	1,00E-15	59%	AUR96800.1	
Prokaryotic dsDNA virus sp.	Marine metagenome	67.8	98%	2,00E-15	53%	QDP60892.1	Roux et al., 2016
Caudovirales phage	Male skin metagenome	64.3	88%	5,00E-14	50%	ASN71505.1	
Prokaryotic dsDNA virus sp.	Marine metagenome	63.2	93%	1,00E-13	42%	QDP52503.1	
Marine virus	Marine metagenome	63.6	96%	9,00E-13	30%	AKH48332.1	Chow et al., 2015
GP4	*Ralstonia solanacearum*	61.2	96%	9,00E-13	25%	AXG67699.1	Wang et al., 2019
DC1	*Burkholderia cepacia* LMG 18821	60.9	98%	1,00E-12	28%	YP_006589976.1	Lynch et al., 2012
VvAW1	*Vibrio vulnificus*	60.5	98%	2,00E-12	52%	YP_007518368.1	Nigro et al., 2012
Bcep22	*Burkholderia cenocepacia*	58.9	96%	6,00E-12	30%	NP_944283.1	Gill et al., 2011
Parlo	*Serratia* sp.	57.4	98%	3,00E-11	31%	QBQ72211.1	Bockoven et al., 2019
Bcepil02	*Burkholderia cenocepacia*	57.0	96%	4,00E-11	32%	YP_002922721.1	Gill et al., 2011
Bcepmigl	*Burkholderia cenocepacia*	56.6	96%	5,00E-11	32%	YP_007236796.1	
PEp14	*Erwinia pyrifoliae*	56.6	95%	6,00E-11	27%	YP_005098413.1	
SopranoGao_25	*Klebsiella pneumoniae* 51503	56.2	93%	9,00E-11	26%	ASV45048.1	Gao et al., 2017
Prokaryotic dsDNA virus sp.	Marine metagenome	55.1	96%	2,00E-10	40%	QDP56147.1	Roux et al., 2016
Pavtok	*Erwinia amylovora*	54.7	90%	3,00E-10	29%	AXF51437.1	
Skulduggery	*Pseudomonas fluorescens* SBW25	53.9	85%	6,00E-10	32%	ARV77111.1	Wojtus et al., 2017
Prokaryotic dsDNA virus sp.	Marine metagenome	53.5	90%	9,00E-10	28%	QDP46120.1	Roux et al., 2016
VH2_2019	*Vibrio natriegens*	55.1	81%	1,00E-09	41%	QHJ74590.1	
vB_EcoP_PTXU04	*Escherichia coli*	53.2	72%	1,00E-09	36%	QBQ76642.1	Korf et al., 2019
uvMED	Mediterranean Sea metagenome	47.4	83%	2,00E-07	29%	BAR35878.1	Mizuno et al., 2013
Prokaryotic dsDNA virus sp.	Marine metagenome	41.6	72%	3,00E-05	36%	QDP60323.1	Roux et al., 2016

CsrA homologs were identified with the NCBI PSI-BLAST tool using the E. coli CsrA sequence as query and narrowing the database search to the Viruses taxid:10239 (database accessed on April 2, 2020). A total of 10 iterations was needed until no further hits were added to the results list.

expose them to CsrA binding and its subsequent regulatory effects. Depending on the position of the RNA motif, CsrA may control translation efficiency, transcript stability of transcription termination (**Figure 3**). The regulation by CsrA may be reversed by antagonizing proteins (like FliW or CesT), or more often by molecular mimic sRNAs that offer multiple target sites so that CsrA dimers become sequestered in large ribonucleoprotein complexes (**Figure 4**). The cellular concentration of the antagonistic sRNAs is typically modulated by signal transducing cascades mastered by TCSs of the BarA/GacS-UvrY/GacA type (**Figure 5**, **Table 1**).

Two intriguing aspects of the biology of the CsrA family are its variegated presence in different phylogenetic lineages and its disparate multiplicity of alleles, the latter occurring particularly in certain γ-proteobacterial lineages like *Xanthomonas*, *Legionella*, and *Pseudomonas* (**Figure 1**). Within the *Pseudomonas* genus, the CsrA protein homologs and their antagonistic sRNAs have been thoroughly characterized for *P. aeruginosa* and *P. protegens*, although exploration of other species revealed an increasing diversity of CsrA (Rsm) proteins (**Table 2**). Here, by exploiting the available genomic resources of the genus, we identified novel subfamilies of Rsm proteins (**Figure 6**). We propose that the *Pseudomonas* pangenome contains 9 subfamilies of Rsm proteins, of which 5 are reported here for the first time: RsmC, RsmD, RsmH, RsmL, and RsmM (**Figure 6**). Despite their sequence variability, they all share conserved residues that are relevant for RNA-binding (**Supplementary Figure 3**) thus suggesting they are all involved in posttranscriptional regulation of gene expression. When inspecting the distribution of paralogues among species, it appears that RsmA and RsmE are the most widespread representatives, followed by RsmC and RsmI (**Figure 7**). On the other hand, one paralogue subfamily seems to be lineage-specific -RsmM for *P. aeruginosa*- whereas two others are restricted to a few lineages: RsmL in *P. putida* and *P. lutea*, and RsmH and RsmD mostly in *P. syringae* (**Figure 7**). Strikingly, the closely related paralogues RsmI and RsmC never coexist in the same lineages, pointing to a possible exclusion phenomenon (**Figure 7**).

An important feature uncovered in this genomic survey is the conspicuous presence of *csrA* alleles in natural plasmids and bacteriophages (**Table 3**, **Figure 8**, **Supplementary Tables 6**, **7**), confirming and extending previous secluded observations (Agaras et al., 2013; Ortiz-Severin et al., 2019). Of interest are our findings that there seems to be a bias toward the presence of certain types of *rsm* alleles in plasmids (encoding RsmH or RsmE) and in phages (RsmM) from *Pseudomonas* strains (**Figure 8**). Overall, these findings strongly suggest that CsrA proteins are instrumental for the fitness of mobile genetic elements, and as a side effect, to increase the rate of dispersal and speciation of these proteins. Loss-of-function experiments are required to test the requirement of CsrA proteins for mobility and establishment of plasmids and phages.

An overall view of the distribution of Rsm subfamilies in the chromosomes and in the extrachromosomal genetic pool of the genus (**Figures 6–8**, **Table 3**, **Supplementary Tables 6**, **7** and **Supplementary Figure 4**) suggests that the RsmA subfamily is the ancestor paralogue of the genus *Pseudomonas* that was inherited from a γ-proteobacterial predecessor. As suggested in a previous report (Morris et al., 2013), a duplication and speciation event gave origin to the RsmE and RsmN paralogue subfamilies, being RsmE subsequently spread into most lineages other than *P. aeruginosa*. We propose that within the *P. aeruginosa* lineage, a more recent duplication and speciation event originated the *rsmM* allele that was co-opted by species-specific phages. Most likely, a second wave of duplications and speciation from *rsmA* gave origin to *rsmC*, *rsmH,* and *rsmI* subfamilies, which have a patchier genomic distribution than RsmA and RsmE. Of these, *rsmE* and *rsmH* succeeded to be incorporated into species-specific plasmids from different lineages. Finally, the more recently evolved chromosomal paralogues would be *rsmD* and *rsmL*, which are restricted to a few lineages and that may have an alien origin from phages. Overall, our *Pseudomonas* dataset shows that this genus possesses a core set of Rsm genes, and a set of accessory Rsm types strongly associated with mobile genetic elements.

The multiplicity of *rsm* alleles per chromosome in *Pseudomonas* species (**Figure 7**, **Supplementary Figure 4**) does not have an obvious explanation. It implies, however, that (if expressed) all alleles are functional and contribute to bacterial fitness, and that the layer of posttranscriptional regulation under Rsm control in *Pseudomonas* lineages is key. Despite the significant contribution of gene duplication to bacterial evolution, the increase of the genome size represents a cost for the organism. So, there must be a balancing evolutionary force to retain the duplicate gene. Instead of performing a new function, the paralogue functions under a different condition (Lynch and Force, 2000). In this context, the multiplicity of paralogues in *Pseudomonas* genomes may offer the possibility of defining subsets of target mRNAs that require differential regulation under distinct environmental or cellular conditions. What clearly follows as a perspective to obtain support to this hypothesis is the need to characterize the function of all Rsm paralogues in a genome, their expression pattern, their interaction with sRNA antagonists, and their corresponding set of target mRNAs.

AUTHOR CONTRIBUTIONS

PS and CV conceived and designed the article, performed the database and bibliographic searches, and prepared tables and figures. All authors shared writing of the manuscript, revised it and approved the submitted version.

FUNDING

This work was supported by grants from Universidad Nacional de Quilmes (PUNQ 1306/19) and from CONICET (PIP 11220150100388CO).

ACKNOWLEDGMENTS

CV and PS are members of CONICET. We dedicate this article to the memory of Prof. Dr. Dieter Haas, an inspiring pioneer in the genetic characterization of the Gac-Rsm regulatory cascade of *Pseudomonas*.

SUPPLEMENTARY MATERIAL

The Supplementary Material for this article can be found online at: https://www.frontiersin.org/articles/10.3389/fmolb.2020.00127/full#supplementary-material

Supplementary Figure 1 | Phylogenetic distribution of genes encoding CsrA, FliW, Hfq, RNAse and UvrY proteins in Eubacteria. The heat map shows the presence of homolog genes for each considered protein in representative species from different classes in the Eubacterial kingdom. At the bottom of the Figure, the heat scale denotes the number of paralogues present per genome.

Supplementary Figure 2 | Phylogenetic inference defining the families of Rsm paralogues within the genus *Pseudomonas*. The evolutionary history was inferred using the Neighbor-Joining method (Saitou and Nei, 1987). The optimal tree with the sum of branch length = 9.08 is shown. This analysis involved 75 amino acid sequences. For each sequence, the locus tag identification is presented in the figure. All positions containing gaps and missing data were eliminated (complete deletion option). There was a total of 42 positions in the final dataset. Evolutionary analyses were conducted in MEGA X (Kumar et al., 2018).

Supplementary Figure 3 | Amino acid conservation across all families of *Pseudomonas* Rsm paralogues. A multiple alignment was generated with MUSCLE (Edgar, 2004) containing all the 45 Rsm paralogues used for the phylogenetical inference (see **Figure 6**). The sequence LOGO is the graphical representation of this multiple alignment.

Supplementary Figure 4 | Phylogenetic distribution of members of the Rsm paralogue subfamilies within the genus *Pseudomonas*. The phylogeny of the genus was built using the sequence of the *gyrB* gene. The evolutionary history was inferred using the Neighbor-Joining method (Saitou and Nei, 1987). The optimal tree with the sum of branch length = 5.65 is shown. The evolutionary distances were computed using the Kimura 2-parameter method (Kimura, 1980) and are in units of number of base substitutions per site. This analysis involved 138 nucleotide sequences. All positions with <95% site coverage were eliminated, i.e., fewer than 5% alignment gaps, missing data, and ambiguous bases were allowed at any position (partial deletion option). There were a total of 2,414 positions in the final dataset. Evolutionary analyses were conducted in MEGA X (Kumar et al., 2018). For each *Pseudomonas* strain, the subfamily of Rsm paralogues present in the corresponding genome is indicated with colored filled circles, following the color scheme shown at the bottom of the figure.

Supplementary Table 1 | Phylogenetic distribution of genes encoding CsrA, FliW, Hfq, RNAse, BarA, LadS, RetS and UvrY proteins in Eubacteria. Data was

obtained from KEGG database (Kanehisa and Goto, 2000). Briefly, we inspected the presence of each gene using the KEGG ontology tool: *csrA* (K03563), *barA* (K07678), *ladS* (K20971), *retS* (K20972), *uvrY* (K07689), *rne* (K08300), *hfq* (K03366) and *fliW* (K13626).

Supplementary Table 2 | Number of proteins of each Rsm subfamily detected in the *Pseudomonas* genome database. The dataset was generated using the *Pseudomonas* orthologous groups (POGs) from the *Pseudomonas* genome database (Winsor et al., 2016). Non annotated Rsm paralogues within the POGs were identified by interrogating all available *Pseudomonas* genomes with BLASTP using the amino acid sequence of RsmA from *Pseudomonas aeruginosa* (PA0905) as query (Expect value cut-off = 1).

Supplementary Table 3 | Number of Rsm paralogues per genome in *Pseudomonas* species. The table lists the number of different Rsm paralogues present in the chromosome of each *Pseudomonas* species studied in this work. For some species (e.g., *P. aeruginosa* or *P. putida*), we included several different strains, some of them bearing different combinations of paralogues.

Supplementary Table 4 | Amino acid sequence of Rsm paralogues in *Pseudomonas* species. For paralogue identification, we used a phylogenetic inference approach based on the analysis presented in **Figure 6**. Each sequence was evaluated under the same phylogenetical analysis to assign it into an Rsm subfamily.

Supplementary Table 5 | Distribution of Rsm paralogues in the major *Pseudomonas* taxonomic subgroups. The table details the presence of an allele of each different Rsm subfamily in the genome of the *Pseudomonas* species and strains listed in **Supplementary Table 4**.

Supplementary Table 6 | CsrA homologs in natural plasmids. The unpublished *csrA* alleles in natural plasmids were identified with the tBLASTn tool of the plasmid database PLSDB v2020_03_04 (Galata et al., 2019), accessed on April 2, 2020, using the *E. coli csrA* gene sequence as query, and setting a minimum query coverage of 30%.

Supplementary Table 7 | CsrA homologs in phages. The unpublished *csrA* alleles in natural phages were identified by querying the NCBI non-redundant protein database with PSI-BLAST using the *E. coli* CsrA sequence as a bait and narrowing the search to the Viruses taxid:10239 (accessed on April 2, 2020). After 10 iterations, the hit list reached a plateau with 30 identified sequences.

REFERENCES

Abbott, Z. D., Yakhnin, H., Babitzke, P., and Swanson, M. S. (2015). csrR, a paralog and direct target of CsrA, promotes legionella pneumophila resilience in water. *MBio.* 6:e00595. doi: 10.1128/mBio.00595-15

Agaras, B., Sobrero, P., and Valverde, C. (2013). A CsrA/RsmA translational regulator gene encoded in the replication region of a sinorhizobium meliloti cryptic plasmid complements *Pseudomonas fluorescens* rsmA/E mutants. *Microbiology* 159, 230–242. doi: 10.1099/mic.0.061614-0

Agaras, B. C., Iriarte, A., and Valverde, C. F. (2018). Genomic insights into the broad antifungal activity, plant-probiotic properties, and their regulation, in *Pseudomonas donghuensis* strain SVBP6. *PLoS ONE* 13:e0194088. doi: 10.1371/journal.pone.0194088

Altegoer, F., Rensing, S. A., and Bange, G. (2016). Structural basis for the CsrA-dependent modulation of translation initiation by an ancient regulatory protein. *Proc. Natl. Acad. Sci. U.S.A.* 113, 10168–10173. doi: 10.1073/pnas.1602425113

Ancona, V., Lee, J. H., and Zhao, Y. (2016). The RNA-binding protein CsrA plays a central role in positively regulating virulence factors in erwinia amylovora. *Sci. Rep.* 6:37195. doi: 10.1038/srep37195

Bedard, A. V., Hien, E. D. M., and Lafontaine, D. A. (2020). Riboswitch regulation mechanisms: RNA, metabolites and regulatory proteins. *Biochim. Biophys. Acta Gene Regul. Mech.* 1863:194501. doi: 10.1016/j.bbagrm.2020.194501

Berman, H. M., Westbrook, J., Feng, Z., Gilliland, G., Bhat, T. N., Weissig, H., et al. (2000). The protein data bank. *Nucleic Acids Res.* 28, 235–242. doi: 10.1093/nar/28.1.235

Blumer, C., Heeb, S., Pessi, G., and Haas, D. (1999). Global GacA-steered control of cyanide and exoprotease production in *Pseudomonas fluorescens* involves specific ribosome binding sites. *Proc. Natl. Acad. Sci. U.S.A.* 96, 14073–14078. doi: 10.1073/pnas.96.24.14073

Bockoven, R., Gutierrez, J., Newkirk, H., Liu, M., Cahill, J., and Ramsey, J. (2019). Complete genome sequence of serratia marcescens podophage parlo. *Microbiol. Resour. Announc.* 8:e00569–19. doi: 10.1128/MRA.00569-19

Bruce, H. A., Du, D., Matak-Vinkovic, D., Bandyra, K. J., Broadhurst, R. W., Martin, E., et al. (2018). Analysis of the natively unstructured RNA/protein-recognition core in the *Escherichia coli* RNA degradosome and its interactions with regulatory RNA/Hfq complexes. *Nucleic Acids Res.* 46, 387–402. doi: 10.1093/nar/gkx1083

Buchfink, B., Xie, C., and Huson, D. H. (2015). Fast and sensitive protein alignment using DIAMOND. *Nat. Methods* 12, 59–60. doi: 10.1038/nmeth.3176

Butz, H. A., Mey, A. R., Ciosek, A. L., and Payne, S. M. (2019). *Vibrio cholerae* CsrA directly regulates varA to increase expression of the three nonredundant Csr small RNAs. *MBio.* 10:e01042-19. doi: 10.1128/mBio.01042-19

Byrne, M., and Kropinski, A. M. (2005). The genome of the *Pseudomonas aeruginosa* generalized transducing bacteriophage F116. *Gene* 346, 187–194. doi: 10.1016/j.gene.2004.11.001

Cerqueira, G. M., Kostoulias, X., Khoo, C., Aibinu, I., Qu, Y., Traven, A., et al. (2014). A global virulence regulator in acinetobacter baumannii and its control of the phenylacetic acid catabolic pathway. *J. Infect. Dis.* 210, 46–55. doi: 10.1093/infdis/jiu024

Chambonnier, G., Roux, L., Redelberger, D., Fadel, F., Filloux, A., Sivaneson, M., et al. (2016). The hybrid histidine kinase lads forms a multicomponent signal transduction system with the GacS/GacA two-component system in *Pseudomonas aeruginosa*. *PLoS Genet* 12:e1006032. doi: 10.1371/journal.pgen.1006032

Chancey, S. T., Wood, D. W., and Pierson, L. S. 3rd (1999). Two-component transcriptional regulation of N-acyl-homoserine lactone production in *Pseudomonas aureofaciens*. *Appl. Environ. Microbiol.* 65, 2294–2299. doi: 10.1128/AEM.65.6.2294-2299.1999

Chavez, R. G., Alvarez, A. F., Romeo, T., and Georgellis, D. (2010). The physiological stimulus for the BarA sensor kinase. *J. Bacteriol.* 192, 2009–2012. doi: 10.1128/JB.01685-09

Cheetham, B. F., Parker, D., Bloomfield, G. A., Shaw, B. E., Sutherland, M., Hyman, J. A., et al. (2008). Isolation of the bacteriophage DinoHI from dichelobacter nodosus and its interactions with other integrated genetic elements. *Open Microbiol. J.* 2, 1–9. doi: 10.2174/1874285800802010001

Chen, M., Wang, P., and Xie, Z. (2018). A complex mechanism involving LysR and TetR/AcrR that regulates iron scavenger biosynthesis in *Pseudomonas donghuensis* HYS. *J. Bacteriol.* 200, e00087–18. doi: 10.1128/JB.00087-18

Chien, M., Morozova, I., Shi, S., Sheng, H., Chen, J., Gomez, S. M., et al. (2004). The genomic sequence of the accidental pathogen *Legionella pneumophila*. *Science* 305, 1966–1968. doi: 10.1126/science.1099776

Chow, C. E., Winget, D. M., White, R. A. III, Hallam, S. J., and Suttle, C. A. (2015). Combining genomic sequencing methods to explore viral diversity and reveal potential virus-host interactions. *Front. Microbiol.* 6:265. doi: 10.3389/fmicb.2015.00265

Crooks, G. E., Hon, G., Chandonia, J. M., and Brenner, S. E. (2004). WebLogo: a sequence logo generator. *Genome Res.* 14, 1188–1190. doi: 10.1101/gr.849004

Cui, Y., Chatterjee, A., and Chatterjee, A. K. (2001). Effects of the two-component system comprising GacA and GacS of *Erwinia carotovora* subsp. carotovora on the production of global regulatory rsmB RNA,

extracellular enzymes, and harpinEcc. *Mol. Plant Microbe Interact.* 14, 516–526. doi: 10.1094/MPMI.2001.14.4.516

De Lay, N., Schu, D. J., and Gottesman, S. (2013). Bacterial small RNA-based negative regulation: hfq and its accomplices. *J. Biol. Chem.* 288, 7996–8003. doi: 10.1074/jbc.R112.441386

Desgranges, E., Marzi, S., Moreau, K., Romby, P., and Caldelari, I. (2019). Noncoding RNA. *Microbiol. Spectr.* 7:GPP3-0038-2018. doi: 10.1128/microbiolspec.GPP3-0038-2018

Drozdetskiy, A., Cole, C., Procter, J., and Barton, G. J. (2015). JPred4: a protein secondary structure prediction server. *Nucleic Acids Res.* 43, W389–W394. doi: 10.1093/nar/gkv332

Dubuis, C., Rolli, J., Lutz, M., Defago, G., and Haas, D. (2006). Thiamine-auxotrophic mutants of *Pseudomonas fluorescens* CHA0 are defective in cell-cell signaling and biocontrol factor expression. *Appl. Environ. Microbiol.* 72, 2606–2613. doi: 10.1128/AEM.72.4.2606-2613.2006

Dugar, G., Svensson, S. L., Bischler, T., Waldchen, S., Reinhardt, R., Sauer, M., et al. (2016). The CsrA-FliW network controls polar localization of the dual-function flagellin mRNA in *Campylobacter jejuni*. *Nat. Commun.* 7:11667. doi: 10.1038/ncomms11667

Edgar, R. C. (2004). MUSCLE: multiple sequence alignment with high accuracy and high throughput. *Nucleic Acids Res.* 32, 1792–1797. doi: 10.1093/nar/gkh340

Feldheim, Y. S., Zusman, T., Kapach, A., and Segal, G. (2018). The single-domain response regulator LerC functions as a connector protein in the *Legionella pneumophila* effectors regulatory network. *Mol. Microbiol.* 110, 741–760. doi: 10.1111/mmi.14101

Felsenstein, J. (1985). Confidence limits on phylogenies: an approach using the bootstrap. *Evolution* 39, 783–791. doi: 10.1111/j.1558-5646.1985.tb00420.x

Ferreiro, M. D., Nogales, J., Farias, G. A., Olmedilla, A., Sanjuan, J., and Gallegos, M. T. (2018). Multiple CsrA proteins control key virulence traits in *Pseudomonas syringae* pv. tomato DC3000. *Mol. Plant. Microbe Interact.* 31, 525–536. doi: 10.1094/MPMI-09-17-0232-R

Frohlich, K. S., and Papenfort, K. (2016). Interplay of regulatory RNAs and mobile genetic elements in enteric pathogens. *Mol. Microbiol.* 101, 701–713. doi: 10.1111/mmi.13428

Fryer, J. L., Lannan, C. N., Giovannoni, S. J., and Wood, N. D. (1992). *Piscirickettsia salmonis* gen. nov., sp. nov., the causative agent of an epizootic disease in salmonid fishes. *Int. J. Syst. Bacteriol.* 42, 120–126. doi: 10.1099/00207713-42-1-120

Galata, V., Fehlmann, T., Backes, C., and Keller, A. (2019). PLSDB: a resource of complete bacterial plasmids. *Nucleic Acids Res.* 47, D195–D202. doi: 10.1093/nar/gky1050

Gao, S., Linden, S. B., and Nelson, D. C. (2017). Complete genome sequence of klebsiella pneumoniae phages sopranogao, mezzogao, and altogao. *Genome Announc.* 5:e01036–19. doi: 10.1128/genomeA.01009-17

Gill, J. J., Summer, E. J., Russell, W. K., Cologna, S. M., Carlile, T. M., Fuller, A. C., et al. (2011). Genomes and characterization of phages Bcep22 and BcepIL02, founders of a novel phage type in *Burkholderia cenocepacia*. *J. Bacteriol.* 193, 5300–5313. doi: 10.1128/JB.05287-11

Glockner, G., Albert-Weissenberger, C., Weinmann, E., Jacobi, S., Schunder, E., Steinert, M., et al. (2008). Identification and characterization of a new conjugation/type IVA secretion system (trb/tra) of *Legionella pneumophila* Corby localized on two mobile genomic islands. *Int. J. Med. Microbiol.* 298, 411–428. doi: 10.1016/j.ijmm.2007.07.012

Gudapaty, S., Suzuki, K., Wang, X., Babitzke, P., and Romeo, T. (2001). Regulatory interactions of Csr components: the RNA binding protein CsrA activates csrB transcription in *Escherichia coli*. *J. Bacteriol.* 183, 6017–6027. doi: 10.1128/JB.183.20.6017-6027.2001

Gutierrez, P., Li, Y., Osborne, M. J., Pomerantseva, E., Liu, Q., and Gehring, K. (2005). Solution structure of the carbon storage regulator protein CsrA from *Escherichia coli*. *J. Bacteriol.* 187, 3496–3501. doi: 10.1128/JB.187.10.3496-3501.2005

Heeb, S., Blumer, C., and Haas, D. (2002). Regulatory RNA as mediator in GacA/RsmA-dependent global control of exoproduct formation in *Pseudomonas fluorescens* CHA0. *J. Bacteriol.* 184, 1046–1056. doi: 10.1128/jb.184.4.1046-1056.2002

Heeb, S., Kuehne, S. A., Bycroft, M., Crivii, S., Allen, M. D., Haas, D., et al. (2006). Functional analysis of the post-transcriptional regulator RsmA reveals a novel RNA-binding site. *J. Mol. Biol.* 355, 1026–1036. doi: 10.1016/j.jmb.2005.11.045

Holmqvist, E., and Vogel, J. (2018). RNA-binding proteins in bacteria. *Nat. Rev. Microbiol.* 16, 601–615. doi: 10.1038/s41579-018-0049-5

Holmqvist, E., Wright, P. R., Li, L., Bischler, T., Barquist, L., Reinhardt, R., et al. (2016). Global RNA recognition patterns of post-transcriptional regulators Hfq and CsrA revealed by UV crosslinking *in vivo*. *EMBO J.* 35, 991–1011. doi: 10.15252/embj.201593360

Huang, H., Tao, X., Jiang, Y., Khan, A., Wu, Q., Yu, X., et al. (2017). The naphthalene catabolic protein NahG plays a key role in hexavalent chromium reduction in *Pseudomonas brassicacearum* LZ-4. *Sci. Rep.* 7:9670. doi: 10.1038/s41598-017-10469-w

Huertas-Rosales, O., Ramos-Gonzalez, M. I., and Espinosa-Urgel, M. (2016). Self-regulation and interplay of rsm family proteins modulate the lifestyle of *Pseudomonas putida*. *Appl. Environ. Microbiol.* 82, 5673–5686. doi: 10.1128/AEM.01724-16

Humair, B., Gonzalez, N., Mossialos, D., Reimmann, C., and Haas, D. (2009). Temperature-responsive sensing regulates biocontrol factor expression in *Pseudomonas fluorescens* CHA0. *ISME J.* 3, 955–965. doi: 10.1038/ismej.2009.42

Ishihama, Y., Schmidt, T., Rappsilber, J., Mann, M., Hartl, F. U., Kerner, M. J., et al. (2008). Protein abundance profiling of the *Escherichia coli* cytosol. *BMC Genomics* 9:102. doi: 10.1186/1471-2164-9-102

Ito, M., Nomura, K., Sugimoto, H., Watanabe, T., and Suzuki, K. (2014). Identification of a Csr system in *Serratia marcescens* 2170. *J. Gen. Appl. Microbiol.* 60, 79–88. doi: 10.2323/jgam.60.79

Janssen, K. H., Diaz, M. R., Gode, C. J., Wolfgang, M. C., and Yahr, T. L. (2018). RsmV, a small noncoding regulatory RNA in *Pseudomonas aeruginosa* that sequesters RsmA and RsmF from target mRNAs. *J. Bacteriol.* 200:e00277-18. doi: 10.1128/JB.00277-18

Jones, D. T., Taylor, W. R., and Thornton, J. M. (1992). The rapid generation of mutation data matrices from protein sequences. *Comput. Appl. Biosci.* 8, 275–282. doi: 10.1093/bioinformatics/8.3.275

Jorgensen, M. G., Pettersen, J. S., and Kallipolitis, B. H. (2020). sRNA-mediated control in bacteria: an increasing diversity of regulatory mechanisms. *Biochim. Biophys. Acta Gene Regul. Mech.* 1863:194504. doi: 10.1016/j.bbagrm.2020.194504

Jousset, A., Lara, E., Wall, L. G., and Valverde, C. (2006). Secondary metabolites help biocontrol strain *Pseudomonas fluorescens* CHA0 to escape protozoan grazing. *Appl. Environ. Microbiol.* 72, 7083–7090. doi: 10.1128/AEM.00557-06

Kanehisa, M., and Goto, S. (2000). KEGG: kyoto encyclopedia of genes and genomes. *Nucleic Acids Res.* 28, 27–30. doi: 10.1093/nar/28.1.27

Kavita, K., De Mets, F., and Gottesman, S. (2018). New aspects of RNA-based regulation by Hfq and its partner sRNAs. *Curr. Opin. Microbiol.* 42, 53–61. doi: 10.1016/j.mib.2017.10.014

Kay, E., Dubuis, C., and Haas, D. (2005). Three small RNAs jointly ensure secondary metabolism and biocontrol in *Pseudomonas fluorescens* CHA0. *Proc. Natl. Acad. Sci. U.S.A.* 102, 17136–17141. doi: 10.1073/pnas.0505673102

Kimura, M. (1980). A simple method for estimating evolutionary rates of base substitutions through comparative studies of nucleotide sequences. *J. Mol. Evol.* 16, 111–120. doi: 10.1007/BF01731581

Korf, I. H. E., Meier-Kolthoff, J. P., Adriaenssens, E. M., Kropinski, A. M., Nimtz, M., Rohde, M., et al. (2019). Still something to discover: novel insights into *Escherichia coli* phage diversity and taxonomy. *Viruses* 11:454. doi: 10.3390/v11050454

Krediet, C. J., Carpinone, E. M., Ritchie, K. B., and Teplitski, M. (2013). Characterization of the gacA-dependent surface and coral mucus colonization by an opportunistic coral pathogen Serratia marcescens PDL100. *FEMS Microbiol. Ecol.* 84, 290–301. doi: 10.1111/1574-6941.12064

Krylov, S. V., Kropinski, A. M., Shaburova, O. V., Miroshnikov, K. A., Chesnokova, E. N., and Krylov, V. N. (2013). [New temperate *Pseudomonas aeruginosa* phage, phi297: specific features of genome structure]. *Genetika* 49, 930–942. doi: 10.7868/S0016675813080079

Kulkarni, P. R., Cui, X., Williams, J. W., Stevens, A. M., and Kulkarni, R. V. (2006). Prediction of CsrA-regulating small RNAs in bacteria and their experimental verification in *Vibrio fischeri*. *Nucleic Acids Res.* 34, 3361–3369. doi: 10.1093/nar/gkl439

Kumar, S., Stecher, G., Li, M., Knyaz, C., and Tamura, K. (2018). MEGA X: molecular evolutionary genetics analysis across computing platforms. *Mol. Biol. Evol.* 35, 1547–1549. doi: 10.1093/molbev/msy096

Lalaouna, D., Fochesato, S., Sanchez, L., Schmitt-Kopplin, P., Haas, D., Heulin, T., et al. (2012). Phenotypic switching in *Pseudomonas brassicacearum* involves GacS- and GacA-dependent Rsm small RNAs. *Appl. Environ. Microbiol.* 78, 1658–1665. doi: 10.1128/AEM.06769-11

Lapouge, K., Schubert, M., Allain, F. H., and Haas, D. (2008). Gac/Rsm signal transduction pathway of gamma-proteobacteria: from RNA recognition to regulation of social behaviour. *Mol. Microbiol.* 67, 241–253. doi: 10.1111/j.1365-2958.2007.06042.x

Lapouge, K., Sineva, E., Lindell, M., Starke, K., Baker, C. S., Babitzke, P., et al. (2007). Mechanism of hcnA mRNA recognition in the Gac/Rsm signal transduction pathway of *Pseudomonas fluorescens*. *Mol. Microbiol.* 66, 341–356. doi: 10.1111/j.1365-2958.2007.05909.x

Laville, J., Voisard, C., Keel, C., Maurhofer, M., Defago, G., and Haas, D. (1992). Global control in *Pseudomonas fluorescens* mediating antibiotic synthesis and suppression of black root rot of tobacco. *Proc. Natl. Acad. Sci. U.S.A.* 89, 1562–1566. doi: 10.1073/pnas.89.5.1562

Lawhon, S. D., Maurer, R., Suyemoto, M., and Altier, C. (2002). Intestinal short-chain fatty acids alter *Salmonella typhimurium* invasion gene expression and virulence through BarA/SirA. *Mol. Microbiol.* 46, 1451–1464. doi: 10.1046/j.1365-2958.2002.03268.x

Le Coustumier, A., Njamkepo, E., Cattoir, V., Guillot, S., and Guiso, N. (2011). *Bordetella petrii* infection with long-lasting persistence in human. *Emerging Infect. Dis.* 17, 612–618. doi: 10.3201/eid1704.101480

Lenz, D. H., Miller, M. B., Zhu, J., Kulkarni, R. V., and Bassler, B. L. (2005). CsrA and three redundant small RNAs regulate quorum sensing in *Vibrio cholerae*. *Mol. Microbiol.* 58, 1186–1202. doi: 10.1111/j.1365-2958.2005.04902.x

Li, J., Gulbronson, C. J., Bogacz, M., Hendrixson, D. R., and Thompson, S. A. (2018). FliW controls growth-phase expression of Campylobacter jejuni flagellar and non-flagellar proteins via the post-transcriptional regulator CsrA. *Microbiology* 164, 1308–1319. doi: 10.1099/mic.0.000704

Liu, M. Y., Gui, G., Wei, B., Preston, J. F. 3rd, Oakford, L., Yuksel, U., Giedroc, D. P., et al. (1997). The RNA molecule CsrB binds to the global regulatory protein CsrA and antagonizes its activity in *Escherichia coli*. *J. Biol. Chem.* 272, 17502–17510. doi: 10.1074/jbc.272.28.17502

Loper, J. E., Hassan, K. A., Mavrodi, D. V., Davis, E. W. 2nd, Lim, C. K., Shaffer, B. T., Elbourne, L. D., et al. (2012). Comparative genomics of plant-associated *Pseudomonas* spp.: insights into diversity and inheritance of traits involved in multitrophic interactions. *PLoS Genet.* 8:e1002784. doi: 10.1371/journal.pgen.1002784

Lopez-Pliego, L., Garcia-Ramirez, L., Cruz-Gomez, E. A., Dominguez-Ojeda, P., Lopez-Pastrana, A., Fuentes-Ramirez, L. E., et al. (2018). Transcriptional Study of the RsmZ-sRNAs and their relationship to the biosynthesis of alginate and alkylresorcinols in *Azotobacter vinelandii*. *Mol. Biotechnol.* 60, 670–680. doi: 10.1007/s12033-018-0102-7

Lopez-Pliego, L., Mena-Munoz, G., Teran-Melo, J. L., Fuentes, L. E., Nunez, C. E., and Castaneda, M. (2020). Study of the sRNA RsmY involved in the genetic regulation of the synthesis of alginate and alkyl resorcinols in *Azotobacter vinelandii*. *Arch. Microbiol.* 202, 579–589. doi: 10.1007/s00203-019-01769-y

Lynch, K. H., Stothard, P., and Dennis, J. J. (2012). Characterization of DC1, a broad-host-range Bcep22-like podovirus. *Appl. Environ. Microbiol.* 78, 889–891. doi: 10.1128/AEM.07097-11

Lynch, M., and Force, A. (2000). The probability of duplicate gene preservation by subfunctionalization. *Genetics* 154, 459–473.

Mandin, P., and Johansson, J. (2020). Feeling the heat at the millennium: thermosensors playing with fire. *Mol. Microbiol.* 113, 588–592. doi: 10.1111/mmi.14468

Marden, J. N., Diaz, M. R., Walton, W. G., Gode, C. J., Betts, L., Urbanowski, M. L., et al. (2013). An unusual CsrA family member operates in series with RsmA to amplify posttranscriptional responses in *Pseudomonas aeruginosa*. *Proc. Natl. Acad. Sci. U.S.A.* 110, 15055–15060. doi: 10.1073/pnas.1307217110

Martinez-Gil, M., Ramos-Gonzalez, M. I., and Espinosa-Urgel, M. (2014). Roles of cyclic Di-GMP and the Gac system in transcriptional control of the genes coding for the *Pseudomonas putida* adhesins LapA and LapF. *J. Bacteriol.* 196, 1484–1495. doi: 10.1128/JB.01287-13

Mattoo, S., and Cherry, J. D. (2005). Molecular pathogenesis, epidemiology, and clinical manifestations of respiratory infections due to bordetella pertussis and other bordetella subspecies. *Clin. Microbiol. Rev.* 18, 326–382. doi: 10.1128/CMR.18.2.326-382.2005

Mercado-Blanco, J., and Bakker, P. A. (2007). Interactions between plants and beneficial *Pseudomonas* spp.: exploiting bacterial traits for crop protection. *Antonie Van Leeuwenhoek* 92, 367–389. doi: 10.1007/s10482-007-9167-1

Miller, C. L., Romero, M., Karna, S. L., Chen, T., Heeb, S., and Leung, K. P. (2016). RsmW, *Pseudomonas aeruginosa* small non-coding RsmA-binding RNA upregulated in biofilm versus planktonic growth conditions. *BMC Microbiol.* 16:155. doi: 10.1186/s12866-016-0771-y

Mizuno, C. M., Rodriguez-Valera, F., Kimes, N. E., and Ghai, R. (2013). Expanding the marine virosphere using metagenomics. *PLoS Genet.* 9:e1003987. doi: 10.1371/journal.pgen.1003987

Moll, S., Schneider, D. J., Stodghill, P., Myers, C. R., Cartinhour, S. W., and Filiatrault, M. J. (2010). Construction of an rsmX co-variance model and identification of five rsmX non-coding RNAs in *Pseudomonas syringae* pv. tomato DC3000. *RNA Biol.* 7, 508–516. doi: 10.4161/rna.7.5.12687

Mondragon, V., Franco, B., Jonas, K., Suzuki, K., Romeo, T., Melefors, O., et al. (2006). pH-dependent activation of the BarA-UvrY two-component system in *Escherichia coli*. *J. Bacteriol.* 188, 8303–8306. doi: 10.1128/JB.01052-06

Morris, E. R., Hall, G., Li, C., Heeb, S., Kulkarni, R. V., Lovelock, L., et al. (2013). Structural rearrangement in an RsmA/CsrA ortholog of *Pseudomonas aeruginosa* creates a dimeric RNA-binding protein, RsmN. *Structure* 21, 1659–1671. doi: 10.1016/j.str.2013.07.007

Mukherjee, A., Cui, Y., Liu, Y., Dumenyo, C. K., and Chatterjee, A. K. (1996). Global regulation in Erwinia species by Erwinia carotovora rsmA, a homologue of *Escherichia coli* csrA: repression of secondary metabolites, pathogenicity and hypersensitive reaction. *Microbiology* 142, 427–434. doi: 10.1099/13500872-142-2-427

Mukherjee, S., Oshiro, R. T., Yakhnin, H., Babitzke, P., and Kearns, D. B. (2016). FliW antagonizes CsrA RNA binding by a noncompetitive allosteric mechanism. *Proc. Natl. Acad. Sci. U.S.A.* 113, 9870–9875. doi: 10.1073/pnas.1602455113

Mukherjee, S., Yakhnin, H., Kysela, D., Sokoloski, J., Babitzke, P., and Kearns, D. B. (2011). CsrA-FliW interaction governs flagellin homeostasis and a checkpoint on flagellar morphogenesis in *Bacillus subtilis*. *Mol. Microbiol.* 82, 447–461. doi: 10.1111/j.1365-2958.2011.07822.x

Muzio, F. M., Agaras, B. C., Masi, M., Tuzi, A., Evidente, A., and Valverde, C. (2020). 7-hydroxytropolone is the main metabolite responsible for the fungal antagonism of Pseudomonas donghuensis strain SVBP6. *Environ. Microbiol.* doi: 10.1111/1462-2920.14925

Nevo, O., Zusman, T., Rasis, M., Lifshitz, Z., and Segal, G. (2014). Identification of *Legionella pneumophila* effectors regulated by the LetAS-RsmYZ-CsrA regulatory cascade, many of which modulate vesicular trafficking. *J. Bacteriol.* 196, 681–692. doi: 10.1128/JB.01175-13

Nguyen, A. N., Disconzi, E., Charriere, G. M., Destoumieux-Garzon, D., Bouloc, P., Le Roux, F., et al. (2018). csrB gene duplication drives the evolution of redundant regulatory pathways controlling expression of the major toxic secreted metalloproteases in *Vibrio tasmaniensis* LGP32. *mSphere* 3:e00582–18. doi: 10.1128/mSphere.00582-18

Nigro, O. D., Culley, A. I., and Steward, G. F. (2012). Complete genome sequence of bacteriophage VvAW1, which infects vibrio vulnificus. *Stand. Genomic Sci.* 6, 415–426. doi: 10.4056/sigs.2846206

Ortiz-Severin, J., Travisany, D., Maass, A., Chavez, F. P., and Cambiazo, V. (2019). *Piscirickettsia salmonis* cryptic plasmids: source of mobile DNA and virulence factors. *Pathogens* 8:269. doi: 10.3390/pathogens8040269

Ossowicki, A., Jafra, S., and Garbeva, P. (2017). The antimicrobial volatile power of the rhizospheric isolate *Pseudomonas donghuensis* P482. *PLoS ONE* 12:e0174362. doi: 10.1371/journal.pone.0174362

Palleroni, N. J. (2015). "Pseudomonas," in *Bergey's Manual of Sytematics of Archaea and Bacteria*," ed W. B. Whitman (New Jersey, NY: ohn Wiley & Sons, Inc.). doi: 10.1002/9781118960608.gbm01210

Peix, A., Ramirez-Bahena, M. H., and Velazquez, E. (2018). The current status on the taxonomy of Pseudomonas revisited: an update. *Infect. Genet. Evol.* 57, 106–116. doi: 10.1016/j.meegid.2017.10.026

Penades, J. R., and Christie, G. E. (2015). The phage-inducible chromosomal islands: a family of highly evolved molecular parasites. *Annu Rev. Virol.* 2, 181–201. doi: 10.1146/annurev-virology-031413-085446

Pessi, G., Williams, F., Hindle, Z., Heurlier, K., Holden, M. T., Camara, M., et al. (2001). The global posttranscriptional regulator RsmA modulates production of virulence determinants and N-acylhomoserine lactones in *Pseudomonas aeruginosa*. *J. Bacteriol.* 183, 6676–6683. doi: 10.1128/JB.183.22.6676-6683.2001

Potts, A. H., Guo, Y., Ahmer, B. M. M., and Romeo, T. (2019). Role of CsrA in stress responses and metabolism important for *Salmonella virulence* revealed by integrated transcriptomics. *PLoS ONE* 14:e0211430. doi: 10.1371/journal.pone.0211430

Quendera, A. P., Seixas, A. F., Dos Santos, R. F., Santos, I., Silva, J. P., Arraiano, C. M., et al. (2020). RNA-binding proteins driving the regulatory activity of small non-coding RNAs in bacteria. *Front. Mol. Biosci.* 7:78. doi: 10.3389/fmolb.2020.00078

Quereda, J. J., and Cossart, P. (2017). Regulating bacterial virulence with RNA. *Annu. Rev. Microbiol.* 71, 263–280. doi: 10.1146/annurev-micro-030117-020335

Records, A. R., and Gross, D. C. (2010). Sensor kinases RetS and LadS regulate *Pseudomonas syringae* type VI secretion and virulence factors. *J. Bacteriol.* 192, 3584–3596. doi: 10.1128/JB.00114-10

Reimmann, C., Valverde, C., Kay, E., and Haas, D. (2005). Posttranscriptional repression of GacS/GacA-controlled genes by the RNA-binding protein RsmE acting together with RsmA in the biocontrol strain *Pseudomonas fluorescens* CHA0. *J. Bacteriol.* 187, 276–285. doi: 10.1128/JB.187.1.276-285.2005

Rife, C., Schwarzenbacher, R., Mcmullan, D., Abdubek, P., Ambing, E., Axelrod, H., et al. (2005). Crystal structure of the global regulatory protein CsrA from *Pseudomonas putida* at 2.05 A resolution reveals a new fold. *Proteins* 61, 449–453. doi: 10.1002/prot.20502

Romeo, T., and Babitzke, P. (2019). "Global regulation by CsrA and its RNA antagonists," in *Regulating with RNA in Bacteria and Archaea,* eds G. Storz and K. Papenfort (Washington, DC: ASM Press), 341–354. doi: 10.1128/microbiolspec.RWR-0009-2017

Romeo, T., Gong, M., Liu, M. Y., and Brun-Zinkernagel, A. M. (1993). Identification and molecular characterization of csrA, a pleiotropic gene from *Escherichia coli* that affects glycogen biosynthesis, gluconeogenesis, cell size, and surface properties. *J. Bacteriol.* 175, 4744–4755. doi: 10.1128/JB.175.15.4744-4755.1993

Romero, M., Silistre, H., Lovelock, L., Wright, V. J., Chan, K. G., Hong, K. W., et al. (2018). Genome-wide mapping of the RNA targets of the *Pseudomonas aeruginosa* riboregulatory protein RsmN. *Nucleic Acids Res.* 46, 6823–6840. doi: 10.1093/nar/gky324

Roux, S., Enault, F., Ravet, V., Colombet, J., Bettarel, Y., Auguet, J. C., et al. (2016). Analysis of metagenomic data reveals common features of halophilic viral communities across continents. *Environ. Microbiol.* 18, 889–903. doi: 10.1111/1462-2920.13084

Saitou, N., and Nei, M. (1987). The neighbor-joining method: a new method for reconstructing phylogenetic trees. *Mol. Biol. Evol.* 4, 406–425.

Santiago-Frangos, A., and Woodson, S. A. (2018). Hfq chaperone brings speed dating to bacterial sRNA. *Wiley Interdiscip. Rev. RNA* 9:e1475. doi: 10.1002/wrna.1475

Schubert, M., Lapouge, K., Duss, O., Oberstrass, F. C., Jelesarov, I., Haas, D., et al. (2007). Molecular basis of messenger RNA recognition by the specific bacterial repressing clamp RsmA/CsrA. *Nat. Struct. Mol. Biol.* 14, 807–813. doi: 10.1038/nsmb1285

Schulmeyer, K. H., Diaz, M. R., Bair, T. B., Sanders, W., Gode, C. J., Laederach, A., et al. (2016). Primary and secondary sequence structure requirements for recognition and discrimination of target RNAs by *Pseudomonas aeruginosa* RsmA and RsmF. *J. Bacteriol.* 198, 2458–2469. doi: 10.1128/JB.00343-16

Septer, A. N., Bose, J. L., Lipzen, A., Martin, J., Whistler, C., and Stabb, E. V. (2015). Bright luminescence of *Vibrio fischeri* aconitase mutants reveals a connection between citrate and the Gac/Csr regulatory system. *Mol. Microbiol.* 95, 283–296. doi: 10.1111/mmi.12864

Silby, M. W., Winstanley, C., Godfrey, S. A., Levy, S. B., and Jackson, R. W. (2011). Pseudomonas genomes: diverse and adaptable. *FEMS Microbiol. Rev.* 35, 652–680. doi: 10.1111/j.1574-6976.2011.00269.x

Sobrero, P., Muzlera, A., Frescura, J., Jofr,é, E., and Valverde, C. (2017). A matter of hierarchy: activation of orfamide production by the posttranscriptional Gac-Rsm cascade of *Pseudomonas protegens* CHA0 through expression upregulation of the two dedicated transcriptional regulators. *Environ. Microbiol. Rep.* 9, 599–611. doi: 10.1111/1758-2229.12566

Sobrero, P., and Valverde, C. (2012). The bacterial protein Hfq: much more than a mere RNA-binding factor. *Crit. Rev. Microbiol.* 38, 276–299. doi: 10.3109/1040841X.2012.664540

Song, C., Van Der Voort, M., Van De Mortel, J., Hassan, K. A., Elbourne, L. D., Paulsen, I. T., et al. (2015). The Rsm regulon of plant growth-promoting *Pseudomonas fluorescens* SS101: role of small RNAs in regulation of lipopeptide biosynthesis. *Microb. Biotechnol.* 8, 296–310. doi: 10.1111/1751-7915.12190

Sorger-Domenigg, T., Sonnleitner, E., Kaberdin, V. R., and Blasi, U. (2007). Distinct and overlapping binding sites of *Pseudomonas aeruginosa* Hfq and RsmA proteins on the non-coding RNA RsmY. *Biochem. Biophys. Res. Commun.* 352, 769–773. doi: 10.1016/j.bbrc.2006.11.084

Tahrioui, A., Quesada, E., and Llamas, I. (2013). Genetic and phenotypic analysis of the GacS/GacA system in the moderate halophile halomonas anticariensis. *Microbiology* 159, 462–474. doi: 10.1099/mic.0.061721-0

Takeuchi, K., Kiefer, P., Reimmann, C., Keel, C., Dubuis, C., Rolli, J., et al. (2009). Small RNA-dependent expression of secondary metabolism is controlled by krebs cycle function in *Pseudomonas fluorescens*. *J. Biol. Chem.* 284, 34976–34985. doi: 10.1074/jbc.M109.052571

Tariq, M. A., Everest, F. L. C., Cowley, L. A., Wright, R., Holt, G. S., Ingram, H., et al. (2019). Temperate bacteriophages from chronic *Pseudomonas aeruginosa* lung infections show disease-specific changes in host range and modulate antimicrobial susceptibility. *mSystems* 4:e00191-18. doi: 10.1128/mSystems.00191-18

Timmermans, J., and Van Melderen, L. (2009). Conditional essentiality of the csrA gene in *Escherichia coli*. *J. Bacteriol.* 191, 1722–1724. doi: 10.1128/JB.01573-08

Vallet-Gely, I., Opota, O., Boniface, A., Novikov, A., and Lemaitre, B. (2010). A secondary metabolite acting as a signalling molecule controls *Pseudomonas entomophila* virulence. *Cell. Microbiol.* 12, 1666–1679. doi: 10.1111/j.1462-5822.2010.01501.x

Valverde, C., and Haas, D. (2008). Small RNAs controlled by two-component systems. *Adv. Exp. Med. Biol.* 631, 54–79. doi: 10.1007/978-0-387-78885-2_5

Valverde, C., Heeb, S., Keel, C., and Haas, D. (2003). RsmY, a small regulatory RNA, is required in concert with RsmZ for GacA-dependent expression of biocontrol traits in *Pseudomonas fluorescens* CHA0. *Mol. Microbiol.* 50, 1361–1379. doi: 10.1046/j.1365-2958.2003.03774.x

Valverde, C., Lindell, M., Wagner, E. G., and Haas, D. (2004). A repeated GGA motif is critical for the activity and stability of the riboregulator RsmY of *Pseudomonas fluorescens*. *J. Biol. Chem.* 279, 25066–25074. doi: 10.1074/jbc.M401870200

Ventre, I., Goodman, A. L., Vallet-Gely, I., Vasseur, P., Soscia, C., Molin, S., et al. (2006). Multiple sensors control reciprocal expression of *Pseudomonas aeruginosa* regulatory RNA and virulence genes. *Proc. Natl. Acad. Sci. U.S.A.* 103, 171–176. doi: 10.1073/pnas.0507407103

Vodovar, N., Vallenet, D., Cruveiller, S., Rouy, Z., Barbe, V., Acosta, C., et al. (2006). Complete genome sequence of the entomopathogenic and metabolically versatile soil bacterium *Pseudomonas entomophila*. *Nat. Biotechnol.* 24, 673–679. doi: 10.1038/nbt1212

Vogel, J., and Luisi, B. F. (2011). Hfq and its constellation of RNA. *Nat. Rev. Microbiol.* 9, 578–589. doi: 10.1038/nrmicro2615

Von Wintzingerode, F., Schattke, A., Siddiqui, R. A., Rosick, U., Gobel, U. B., and Gross, R. (2001). *Bordetella petrii* sp. nov., isolated from an anaerobic bioreactor, and emended description of the genus *Bordetella*. *Int. J. Syst. Evol. Microbiol.* 51, 1257–1265. doi: 10.1099/00207713-51-4-1257

Wang, D., Lee, S. H., Seeve, C., Yu, J. M., Pierson, L. S. III, and Pierson, E. A. (2013). Roles of the Gac-Rsm pathway in the regulation of phenazine biosynthesis in *Pseudomonas chlororaphis* 30-84. *Microbiologyopen* 2, 505–524. doi: 10.1002/mbo3.90

Wang, R., Cong, Y., Mi, Z., Fan, H., Shi, T., Liu, H., et al. (2019). Characterization and complete genome sequence analysis of phage GP4, a novel lytic Bcep22-like podovirus. *Arch. Virol.* 164, 2339–2343. doi: 10.1007/s00705-019-04309-7

Weilbacher, T., Suzuki, K., Dubey, A. K., Wang, X., Gudapaty, S., Morozov, I., et al. (2003). A novel sRNA component of the carbon storage

regulatory system of *Escherichia coli*. *Mol. Microbiol.* 48, 657–670. doi: 10.1046/j.1365-2958.2003.03459.x

White, D., Hart, M. E., and Romeo, T. (1996). Phylogenetic distribution of the global regulatory gene csrA among eubacteria. *Gene* 182, 221–223. doi: 10.1016/S0378-1119(96)00547-1

Wilf, N. M., Reid, A. J., Ramsay, J. P., Williamson, N. R., Croucher, N. J., Gatto, L., et al. (2013). RNA-seq reveals the RNA binding proteins, Hfq and RsmA, play various roles in virulence, antibiotic production and genomic flux in *Serratia* sp. ATCC 39006. *BMC Genomics* 14:822. doi: 10.1186/1471-2164-14-822

Williams, K. P. (2002). Integration sites for genetic elements in prokaryotic tRNA and tmRNA genes: sublocation preference of integrase subfamilies. *Nucleic Acids Res.* 30, 866–875. doi: 10.1093/nar/30.4.866

Winsor, G. L., Griffiths, E. J., Lo, R., Dhillon, B. K., Shay, J. A., and Brinkman, F. S. (2016). Enhanced annotations and features for comparing thousands of pseudomonas genomes in the pseudomonas genome database. *Nucleic Acids Res.* 44, D646–D653. doi: 10.1093/nar/gkv1227

Winstanley, C., O'brien, S., and Brockhurst, M. A. (2016). *Pseudomonas aeruginosa* evolutionary adaptation and diversification in cystic fibrosis chronic lung infections. *Trends Microbiol.* 24, 327–337. doi: 10.1016/j.tim.2016.01.008

Wojtus, J. K., Fitch, J. L., Christian, E., Dalefield, T., Lawes, J. K., Kumar, K., et al. (2017). Complete genome sequences of three novel *Pseudomonas fluorescens* SBW25 bacteriophages, noxifer, phabio, and skulduggery. *Genome Announc.* 5:e00725-17. doi: 10.1128/genomeA.00725-17

Workentine, M. L., Chang, L., Ceri, H., and Turner, R. J. (2009). The GacS-GacA two-component regulatory system of *Pseudomonas fluorescens*: a bacterial two-hybrid analysis. *FEMS Microbiol. Lett.* 292, 50–56. doi: 10.1111/j.1574-6968.2008.01445.x

Ye, F., Yang, F., Yu, R., Lin, X., Qi, J., Chen, Z., et al. (2018). Molecular basis of binding between the global post-transcriptional regulator CsrA and the T3SS chaperone CesT. *Nat. Commun.* 9:1196. doi: 10.1038/s41467-018-03625-x

Yu, X., Chen, M., Jiang, Z., Hu, Y., and Xie, Z. (2014). The two-component regulators GacS and GacA positively regulate a nonfluorescent siderophore through the Gac/Rsm signaling cascade in high-siderophore-yielding *Pseudomonas* sp. strain HYS. *J. Bacteriol.* 196, 3259–3270. doi: 10.1128/JB.01756-14

Zere, T. R., Vakulskas, C. A., Leng, Y., Pannuri, A., Potts, A. H., Dias, R., et al. (2015). Genomic targets and features of BarA-UvrY (-SirA) signal transduction systems. *PLoS ONE* 10:e0145035. doi: 10.1371/journal.pone.0145035

Zuber, S., Carruthers, F., Keel, C., Mattart, A., Blumer, C., Pessi, G., et al. (2003). GacS sensor domains pertinent to the regulation of exoproduct formation and to the biocontrol potential of *Pseudomonas fluorescens* CHA0. *Mol. Plant Microbe Interact.* 16, 634–644. doi: 10.1094/MPMI.2003.16.7.634

Conflict of Interest: The authors declare that the research was conducted in the absence of any commercial or financial relationships that could be construed as a potential conflict of interest.

frontiers in Molecular Biosciences

HYPOTHESIS AND THEORY
published: 14 August 2020
doi: 10.3389/fmolb.2020.00187

Are Antisense Proteins in Prokaryotes Functional?

Zachary Ardern, Klaus Neuhaus and Siegfried Scherer*

Chair for Microbial Ecology, Technical University of Munich, Munich, Germany

Many prokaryotic RNAs are transcribed from loci outside of annotated protein coding genes. Across bacterial species hundreds of short open reading frames antisense to annotated genes show evidence of both transcription and translation, for instance in ribosome profiling data. Determining the functional fraction of these protein products awaits further research, including insights from studies of molecular interactions and detailed evolutionary analysis. There are multiple lines of evidence, however, that many of these newly discovered proteins are of use to the organism. Condition-specific phenotypes have been characterized for a few. These proteins should be added to genome annotations, and the methods for predicting them standardized. Evolutionary analysis of these typically young sequences also may provide important insights into gene evolution. This research should be prioritized for its exciting potential to uncover large numbers of novel proteins with extremely diverse potential practical uses, including applications in synthetic biology and responding to pathogens.

Keywords: overlapping gene, antisense transcription, antisense translation, function, selected effects, gene annotation

OPEN ACCESS

Edited by:
Eleonora Leucci,
KU Leuven, Belgium

Reviewed by:
Konrad Ulrich Förstner,
Leibniz Information Centre for Life Sciences (LG), Germany
Gabriele Fuchs,
University at Albany, United States

****Correspondence:***
Zachary Ardern
zachary.ardern@tum.de

Specialty section:
This article was submitted to Protein and RNA Networks, a section of the journal Frontiers in Molecular Biosciences

Received: *20 February 2020*
Accepted: *16 July 2020*
Published: *14 August 2020*

Citation:
Ardern Z, Neuhaus K and Scherer S (2020) Are Antisense Proteins in Prokaryotes Functional? Front. Mol. Biosci. 7:187. doi: 10.3389/fmolb.2020.00187

INTRODUCTION

The Many Functions of Antisense RNAs

A wide range of non-coding RNAs have been characterized in bacterial genomes. Among these putatively non-coding sequences are many antisense transcripts. Indeed, up to 75% of all prokaryotic genes are associated with antisense RNAs – though the number differs significantly between species and according to the methods used (Georg and Hess, 2018). Their functions, if any, are poorly understood in most cases. The characteristics of antisense RNAs range widely in terms for instance of length, location in relation to the sense gene, and mechanisms of regulation (Lejars et al., 2019). In studies so far they are usually associated with reducing transcription of the sense gene, but they can also increase it, for instance by changing the structure of the sense transcript – various mechanisms are known in each case (Lasa et al., 2012). They can influence single genes, or have global effects for instance through a target involved in general translation. Other known effects relate to functions including virulence, motility, various mechanisms of gene transfer, and biofilm formation (Lejars et al., 2019). The numerous examples of antisense transcription which have been investigated do not just include short antisense RNAs, though these are well-known; the many longer examples include a 1200 nucleotide antisense RNA in *Salmonella enterica*, AmgR (Courtney and Chatterjee, 2014). Antisense transcripts have been shown to be co-expressed within a single cell with the use of an antibody against double-stranded RNA in various studies, including in *Escherichia coli* and *Streptomyces coelicolor*, as reviewed in Georg and Hess (2018). Relatively little attention, however, has been paid to the possibility that RNA in antisense

to protein coding genes may also frequently encode proteins (Georg and Hess, 2018). Rather than short, trivial overlaps, which are well known (Saha et al., 2016), here we focus on cases where an antisense (or "antiparallel") ORF with evidence of translation is fully embedded within a known protein coding gene.

The existence of substantially overlapping gene pairs has been known since the beginning of modern genome sequencing, when the proteins directly detected in the bacteriophage phiX174 were shown to not be able to fit into the sequenced genome without the translation of overlapping open reading frames (ORFs; Barrell et al., 1976). Since then, overlapping genes have typically been assumed to be fairly common only in viruses and extremely rare in other taxa, with the possibility of there being multiple examples in other taxa only sporadically discussed, e.g., Chou et al. (1996). However, their occurrence in bacteriophage in particular should raise the suspicion that they may be common in bacteria as well, given for instance the large amounts of genetic material transferred from temperate phage genomes to bacterial genomes (Harrison and Brockhurst, 2017; Owen et al., 2020). The properties of same-strand overlaps between viral genes have been studied (Pavesi et al., 2018; Willis and Masel, 2018), but even in viruses, relatively little attention has been given to antisense overlaps. There is, however, increasing evidence for functional translated antisense ORFs too, notably the antisense protein Asp in HIV-1 (Cassan et al., 2016; Affram et al., 2019; Nelson et al., 2020). In general it can be said that small ncRNAs are well recognized but their coding potential has been overlooked. Many might be protein-coding (i.e., mRNA), some are indeed ncRNA, and several will be dual-functional (Wadler and Vanderpool, 2007; Gimpel and Brantl, 2017; Neuhaus et al., 2017). The same trichotomy of functional categories applies in the case of antisense RNAs.

In bacteria, a number of individual antisense proteins have been discovered; the lines of evidence for some of these will be discussed below. High throughput analyses of ribosome profiling data, which uncovers the part of the transcriptome associated with ribosomes (Ingolia et al., 2009) thus revealing the "translatome," have begun to suggest that many more may be present. Friedman et al. (2017) found evidence for approximately 17 antisense ORFs, previously thought to be non-coding sRNAs, translated over above the level expected by chance in *E. coli* K12. The 10 sRNAs these belong to are shown in **Figure 1A**. Weaver et al. (2019) found ribosome profiling evidence, including evidence specifically for translation initiation (using retapamulin), for nine antisense overlapping gene candidates in *E. coli* K12, also shown, combined with the data from Weaver et al., in **Figure 1A**. As reported in a recent pre-print, Smith et al. (2019) found many overlapping ORFs in *Mycobacterium tuberculosis* associated with ribosomes using retapamulin. From 355 novel ORFs expressed in two replicates they report 241 overlapping and embedded in annotated genes, including both sense, and antisense overlaps, of which many were very short. Of those encoding at least 20 amino acids, 51 are antisense embedded. These antisense ORFs are shown in **Figure 1B**. From **Figure 1** we see that translated antisense overlapping genes are distributed roughly evenly across the genome, and in both frames, in the best-studied example genomes to-date; *E. coli* K-12 and *M. tuberculosis*. We have good reason to expect many similar overlapping genes across prokaryotic genomes.

It has been claimed that as a class the novel ORFs in *M. tuberculosis* are not under selection, and the association with ribosomes was attributed to non-functional pervasive translation (Smith et al., 2019) – this is discussed further in the section on evolution and constraint below. Whatever their selective status, other claims of translation in antisense to known genes continue to accumulate in prokaryotes. Jeong et al. (2016) reported ribosome profiling in *S. coelicolor* – although this result was not highlighted, examining the supplementary data showed 10 antisense putative sRNAs with ribosome profiling evidence. No doubt many more such discoveries await systematic analysis of published ribosome profiling data. There are also many putative same-strand overlapping genes, as discussed early on by Ellis and Brown (2003) showing that alternate frame translation is likely a general phenomenon – but these have also been claimed to not be under selection (Meydan et al., 2019). This increasing evidence for translation of both sense and antisense alternate frame ORFs, currently only typically acknowledged as ncRNAs, should push the question of "pervasive function" and how to categorize the range of translated ORFs to the forefront of microbiology, but it is yet to receive substantial attention. The evidence of expression in alternate frames is generally ignored, and when acknowledged it is generally presumed to be non-functional –, however, we argue this inference is made too quickly on insufficient grounds. Here we explore how to ascertain function and present a few examples of antisense genes with evidence for functionality.

"Function" and Natural Selection

The question of what counts as "function" in a biological context is not straightforward. An interdisciplinary group of researchers have recently discussed the issue in relation specifically to *de novo* gene origin (Keeling et al., 2019) and proposed five categories of meanings of function, pertaining to expression, capacities, interactions, physiology, and evolution. As they helpfully note, "Separating these meanings from one another enables communicating with increased precision about what the findings are, thereby helping to [avoid] fallacious logical shortcuts such as 'this protein is expressed therefore it is functional therefore it is under selection.'" Interestingly, they had limited success in actually applying their categorisation, with most instances in a test set of article abstracts not uniformly assigned to a category by different team members. This suggests that biologists should write with more precision to clarify the sense of function intended. In this article we will focus on the senses relating to the biochemical "capacity" of the products of genetic elements and their evolutionary history, although the other senses will also come into play. The unifying general concept we use is that an element is functional if it does something useful for the organism in ecologically relevant circumstances.

The important philosophical questions have been reviewed elsewhere (Brandon, 2013). Here we summarize some established methods for determining function in the molecular biosciences and how they have been or could be applied to antisense proteins. It has become popular to adopt an etiological account of function,

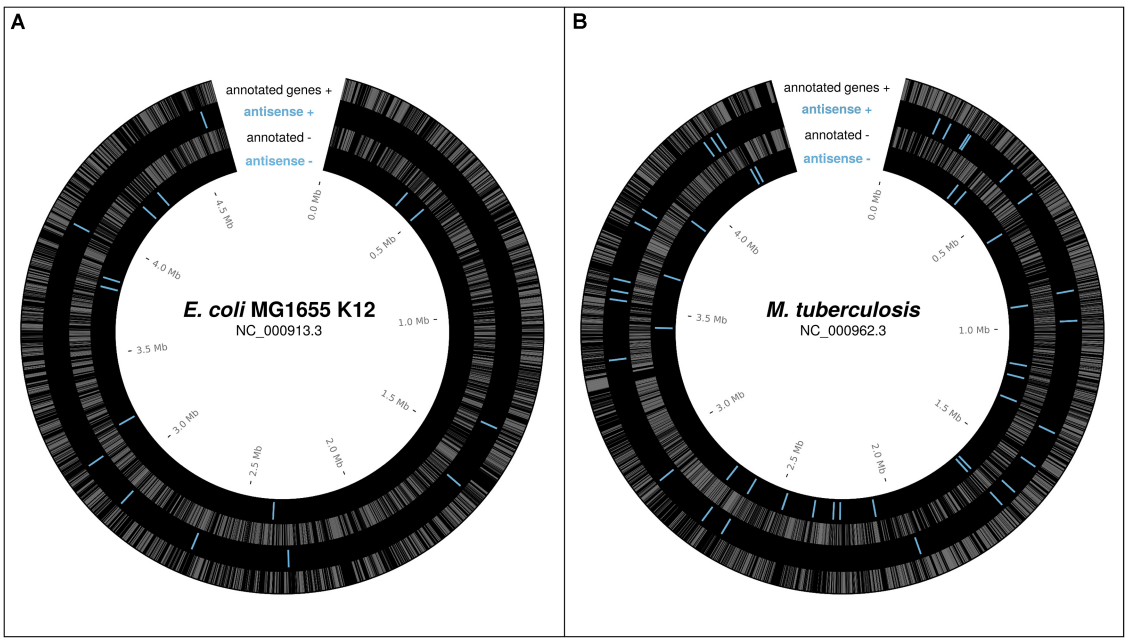

FIGURE 1 | Reported potential protein-coding ORFs overlapping in antisense, based on ribosome profiling experiments. **(A)** Reported antisense OLGs in *E. coli* K12 (NC_000913.3) – Weaver et al. (2019), Friedman et al. (2017; sRNAs with evidence of translation). **(B)** Reported antisense OLGs in *M. tuberculosis* (NC_000962.3) –Smith et al. (2019). Annotated genes gray. Antisense blue.

i.e., that an element's function depends on its selective history, particularly in relation to the dispute over how to assign function to elements in the human genome following the ENCODE project (Graur et al., 2013, 2015; Doolittle et al., 2014; Doolittle, 2018). However, the evolutionary etiology of biological systems is not always fully accessible to us (Ardern, 2018) and sometimes the history of selection in a lineage or for a particular gene may be inaccessible or the accessible parts incomplete in important ways. The genomic influence of different kinds of selection on bacterial genomes, including selective sweeps, background selection, positive selection, and purifying selection, remains a point of contention (Takeuchi et al., 2015; Bendall et al., 2016; Gibson and Eyre-Walker, 2019; Sela et al., 2019). Perhaps the most difficult issue here is how to characterize function in young genes, which may be subject to evolutionary forces lying anywhere along a spectrum between positive selection and purifying selection. Positive selection may be acting to modify a sequence which has only recently evolved or only recently become useful, for instance due to new environmental conditions. At some point, however, modifications are overwhelmingly selected against, i.e., purifying selection dominates. This fascinating transition region to our knowledge has received little study, but it is plausible that most young genes fall within it (Vishnoi et al., 2010). As such, many young genes are likely to be missed by methods seeking clear signatures of either purifying or positive selection. A recent study has shown that embedded overlapping genes in viruses usually evolve faster than the gene they are embedded in (Pavesi, 2019) such cases will tend to be missed by tests of purifying selection.

Additional relevant complexities include recombination, horizontal gene transfer, varying evolutionary rates, and unknown past environmental conditions. Evolutionary analyses certainly can provide strong evidence for function in cases of strong selection, but appropriate lower thresholds for determining that an element is functional while minimizing false negatives are much harder to determine. Arguably of much greater relevance than etiology for molecular biologists is what a genetic element does in the current system, and whether it contributes to the goals or life-conducive activities of that system. That is, as the etiological theorists correctly emphasize, function is not just about "causal role," it concerns a contribution to a wider system which is in some sense goal-directed. However, given complex histories of multiple evolutionary forces this does not necessarily imply anything directly about a particular canonical signature of natural selection being observable in the existing sequence. A good example of these complexities is the prevalence of translation and likely functions in putative "pseudogenes" (Goodhead and Darby, 2015; Cheetham et al., 2019).

EVIDENCE AND OBJECTIONS

High-Throughput Experimental Evidence

The "gold-standard" proof of the active translation of a gene has traditionally been direct evidence from proteomics experiments, a technology which precedes modern genome sequencing by a few years. However, evidence from current proteomics methods is inherently limited even after decades of improvements. For instance, small proteins are notoriously difficult to detect by mass spectrometry, because upon proteolytic digestion they tend to generate no suitable peptides or just a small number.

Another issue for detecting proteins by mass spectrometry is high hydrophobicity (Lescuyer et al., 2004) for example, proteins that contain *trans*-membrane domains are often underrepresented in proteomic data sets. Finally, also factors like a low protein abundance, only context-specific expression, a high turnover rate or protein secretion might all hamper a successful detection of proteins (Elguoshy et al., 2016). Nonetheless, despite these barriers there are a few examples of translated overlapping genes with proteomic evidence. Notably, a large-scale study of 46 bacterial genomes found up to 261 cases of annotation "conflict," i.e., overlaps greater than 40 base pairs with either proteomic evidence for both, or the unevidenced gene being annotated as something other than "hypothetical" (Venter et al., 2011). A more recent study of 11 bacterial transcriptomes (Miravet-Verde et al., 2019) found 185 antisense transcripts previously annotated as non-coding could in fact code for proteins based on a random forest classifier (RanSEPs). A study in *Pseudomonas putida* found proteomic evidence for 44 ORFs embedded in antisense to annotated ORFs (Yang et al., 2016). An improved proteogenomics pipeline reported in a recent pre-print manuscript found numerous gene candidates in *S. enterica* serovar Typhimurium, including a 199 amino acid long protein antisense to the annotated gene CBW18741 (Willems et al., 2019). It is interesting given the previous comment concerning the rate of phage to bacterial gene transfer that a BLAST search shows that this is likely a bacteriophage protein. The same study also found 18 antisense ORFs in *Deinococcus radiodurans* supported by at least two peptides. A search in *Helicobacter pylori* mass spectrometry data from a previously published study designed to find small proteins (Müller et al., 2013) found evidence for a protein encoded by an ORF antisense to a proline/betaine transporter gene (Friedman et al., 2017). A recent discussion paper presented proteomic evidence for many small proteins (sORFs) and overlapping genes ("altORFs"), but did not specifically consider antisense overlaps (Orr et al., 2020).

Aside from proteomics datasets there is extensive publicly available high throughput RNA sequencing data which can be mined for further indicators of specific reproducible regulation of antisense ORFs. There are approximately 1500 relevant RNAseq studies from prokaryotes in the NCBI GEO database (Edgar et al., 2002) each with multiple samples; over 100 ribosome profiling studies, and a number of more bespoke methods which may also provide relevant information. Cappable-seq data, which discovers transcriptional start sites (Ettwiller et al., 2016), helps to delineate the borders of operons and their expression under different conditions. The new method SEnd-seq, through circularisation of transcripts, is able to detect both transcriptional start and termination sites with single nucleotide resolution (Ju et al., 2019). CHiPseq datasets indicate whether known transcription factors are associated with a particular operon of interest (Wade, 2015) other TF-binding assays also have potential for testing hypotheses concerning TF binding, e.g., DNAse footprinting (Haycocks and Grainger, 2016). Each of these methods is yet to be fully utilized in searching for the transcriptional regulation of overlapping genes. At the level of translation, there are a number of variations on ribosome profiling now available, including accurate prediction of translation initiation sites. The first study of ribosome profiling in bacteria used chloramphenicol in one of the two methods presented (Oh et al., 2011), which has since been shown to stall the ribosome at initiation and, thereby, can assist in inferring translation initiation site positions (Mohammad et al., 2019; Glaub et al., 2020). More precise stalling has been achieved with the use of tetracycline (Nakahigashi et al., 2016), retapamulin (Meydan et al., 2019), and the antibacterial peptide Onc112 (Weaver et al., 2019). Properties of ribosomes at different stages of translation, including initiation, have recently been studied in *E. coli* K12 with TCP-seq; translation complex profiling (Sharma and Anand, 2019). Translation stop sites have also been specifically explored (Baggett et al., 2017). Most of these methods, outside the analysis of ribosome profiling discussed above, have not yet been applied to the detection or investigation of protein coding alternate frame ORFs, and any RNAs at these sites are assumed to be non-coding. Perhaps particularly useful will be ribosome profiling experiments conducted for cells grown in different conditions – many relevant contexts may, however, not be able to be surveyed due to technical limitations.

Phenotypes of Antisense Proteins

An important indicator of functionality is specific regulation in response to defined environmental conditions. Some key canonical work in molecular genetics (Jacob and Monod, 1961; Ames and Martin, 1964) has been concerned with the differential induction of genetic elements under varying environmental conditions. Specific differential induction is widely assumed in this kind of literature to be equivalent to function – how precisely to draw a line between functional and non-functional, given the inherent noisiness of biology, is not, however, entirely clear.

In general, what kind of phenotype is a good indicator of functionality? The most obvious case perhaps is an improvement in growth associated with expression of a genetic element. This could be either through improved growth following overexpression, or decreased growth following a deletion in the genomic sequence. Within an evolutionary context, a growth advantage effectively just is what it is to be "useful" or "functional." An example of this for antisense proteins is *citC*, discussed below. However, less intuitively, a decrease in growth associated with expression, as seen in the cases of *asa*, *laoB*, and *ano* is also an indicator of functionality in the right context. Most simply, the gene might literally function as a toxin. More generally though, overexpression of many functional genes is deleterious – in fact in *E. coli* the majority of annotated genes have a deleterious effect on growth in overexpression constructs (Kitagawa et al., 2005). Similarly, a condition-specific positive growth phenotype following knockout of an expressed gene is also indicative of function. Such a phenotype could be simply because the protein is not required in this environment and so losing it decreases the cost of expression. Or it could be because losing a gene with, for instance, a regulatory or inhibitory function is beneficial under certain conditions where regulation of a process is not useful. Indeed, whatever the underlying mechanisms, adaptation in bacteria following loss of function is pervasive (Behe, 2010; Hottes et al., 2013; Albalat and Cañestro, 2016).

Possible reasons for the high tendency toward deleterious over-expression phenotypes in bacteria compared with organisms such as yeast are discussed in Bhattacharyya et al. (2016). This situation should perhaps not be surprising given the extreme optimality of bacterial metabolism (Schuetz et al., 2012) significant disturbance of such a finely tuned system is unlikely to be beneficial under most conditions. This general principle follows from, for instance, Fisher's Geometric Model, in which random changes are less likely to be beneficial when a population is close to a fitness optimum (Tenaillon, 2014). Overexpression of a non-functional "junk" genetic sequence, however, is also likely to be deleterious (Weisman and Eddy, 2017; Knopp and Andersson, 2018) so such a phenotype does not by itself provide evidence for functionality. What is important in the examples discussed above is that the deleterious growth phenotypes are observed as a significant difference between environmental (media) conditions. This implies a specificity of interaction which appears improbable under the "junk" hypothesis, and so constitutes evidence of function.

A number of antisense overlapping genes in *E. coli* have been analyzed regarding expression and phenotypes across different environmental conditions. The gene *nog1* is almost fully embedded in antisense to *citC*. A strand-specific deletion mutant has a growth advantage over the wildtype in LB, and a stronger advantage in medium supplemented with magnesium chloride (Fellner et al., 2015). The gene *asa*, embedded in antisense to a transcriptional regulator in *E. coli* O157:H7 strains, was found to be regulated in response to arginine, sodium, and different growth phases. Overexpression resulted in a negative growth phenotype in both excess sodium chloride and excess arginine, and no phenotype in LB medium (Vanderhaeghen et al., 2018). The gene *laoB* is embedded in antisense to a CadC-like transcriptional regulator (**Figure 2A**). A strand-specific genomic knock-out mutant was shown to provide a growth advantage specific to media supplemented with arginine. Further, the differential phenotype was replicated with the addition of inducible plasmid constructs bearing Δ*laoB* and WT *laoB*, showing that the phenotype is removed through complementation (Hücker et al., 2018b). How to mechanistically interpret such a growth advantage following gene knockout is unclear, but the condition-specific clear phenotype implies a functional role. The gene *ano* is nearly fully embedded antisense to an L,D-transpeptidase (**Figure 2B**). Similarly to *laoB*, a knock-out mutant showed a condition-specific phenotype. In this case it occurs in anaerobic conditions, and could be partially complemented with a plasmid construct (Hücker et al., 2018a). The putative protein-coding gene *aatS* was found in the pathogenic *E. coli* strain ETEC H10407 fully embedded in antisense to the ATP transporter ATB binding protein AatC (Haycocks and Grainger, 2016). It was shown to be transcribed, to have a functional ribosome binding sequence, and to have widespread homologs including a conserved domain of unknown function. **Figure 2** illustrates the expression of three examples of antisense genes, with the gene in *Staphylococcus aureus* (**Figure 2C**) a special case, as discussed below.

Other than the high-level phenotypes (e.g., expression under particular conditions) determined for some candidates, very little is known about the possible roles or mechanisms of action of antisense proteins. Signaling or interactions between cells will be a significant area to investigate regarding possible functions. This suggestion is based on both the evidence gained so far for small proteins (Neuhaus et al., 2016; Hücker et al., 2017a; Sberro et al., 2019) and the particular importance of signaling or interaction proteins, meaning that this hypothesis derived from findings on small proteins more generally, deserves special attention This area is a crucial field of research as infectious disease continues to be a major health burden and the long natural history of interactions between microbes has been a fruitful source of new antimicrobial strategies.

Simultaneous Transcription?

In response to the evidence for overlapping genes, the question is often raised concerning how two genes could be simultaneously expressed from opposite strands. Indeed, the phenomenon of RNA polymerase collision is a real barrier to antisense transcription in at least some instances and is involved in transcriptional silencing or reduction via various mechanisms (Courtney and Chatterjee, 2014). Bypass of sense and antisense RNA polymerases has been shown for bacteriophage RNA polymerases (Ma and McAllister, 2009) but *in vitro* experiments have shown no such bypass in bacterial systems (Crampton et al., 2006). The role of accessory helicases in removing barriers to replication due to the presence of RNA polymerases has recently been highlighted (Hawkins et al., 2019) expanding on knowledge of simultaneous transcription and replication (Helmrich et al., 2013). It is conceivable that transcribing alongside the formation of a replication fork could facilitate antisense transcription, but this would restrict antisense transcription to the replication process. However, even in cases of collision of RNA polymerases operating in antisense, transcriptional stalling is not guaranteed. A recent study argues on the basis of simulations and careful assays with reporter constructs that RNA polymerases trailed by an active ribosome are, remarkably, about 13-times more likely to resume transcription following collision than those without the translation apparatus following (Hoffmann et al., 2019). This finding follows on from a range of similar work in recent years showing multiple mechanisms involved in ensuring that RNA polymerases stall and are subsequently released less in protein coding than non-coding RNAs (Proshkin et al., 2010; Brophy and Voigt, 2016; Ju et al., 2019). We suggest that this phenomenon likely applies to antisense embedded protein-coding genes as much as to convergent antisense transcripts and thereby facilitates antisense protein expression.

Recent detailed elucidation showed the working of an operon in *S. aureus* with a functional gene encoded in antisense to a contiguous set of co-transcribed genes (Sáenz-Lahoya et al., 2019). The authors showed that despite being encoded on opposite strands (although not directly overlapping in this case), these elements comprised a single transcriptional unit (**Figure 2C**). This study highlights a mechanism which may be widespread and may apply to genes which are directly antiparallel as well. Results from Weaver et al. (2019) obtained

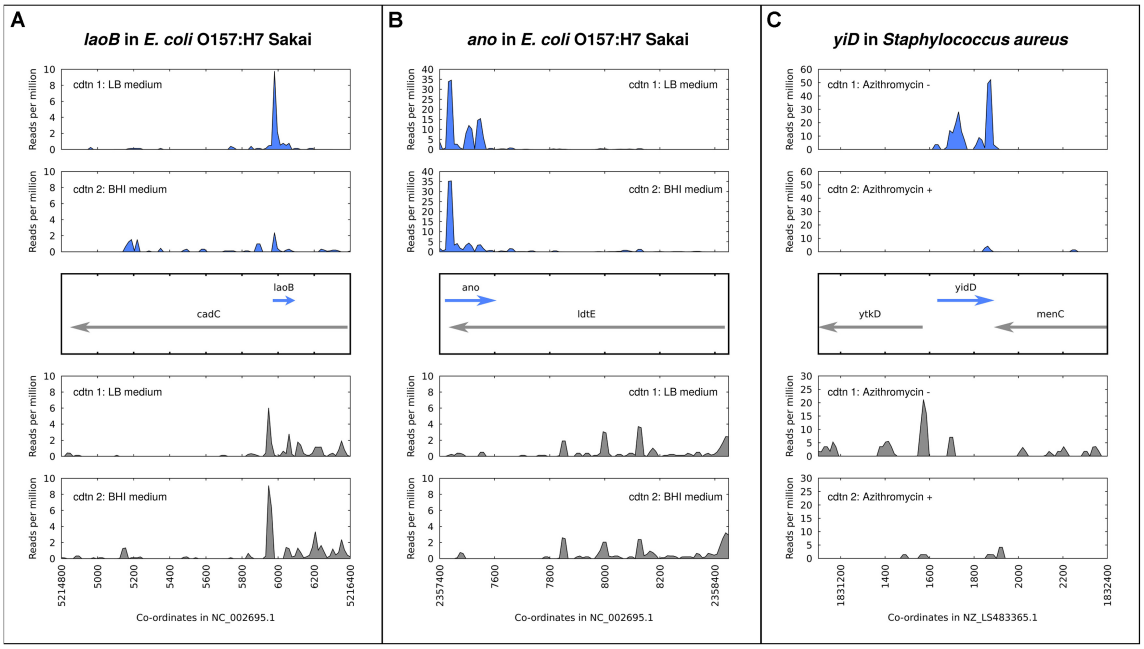

FIGURE 2 | Expression and regulation of antisense genes as demonstrated by ribosome profiling experiments; aligned ribosome protected fragments shown as reads per million at each site after removal of rRNA and tRNA reads. **(A)** *laoB* gene in *E. coli* O157:H7 Sakai; expression in LB medium is higher than in BHI. **(B)** *ano* gene in *E. coli* O157:H7 Sakai; expression in LB medium versus BHI is constant. **(C)** *yidD* (MW1733) gene, part of non-contiguous (antisense) operon, in *Staphylococcus aureus*. Expression in positive and negative strands is positively correlated – high in the absence of the antibiotic azithromycin, low when it is added.

by chromosomal tagging of three antisense proteins show that proteins encoded in antisense can be expressed simultaneously, i.e., under the same growth conditions. All this evidence for simultaneous antiparallel gene expression notwithstanding, it may be that antiparallel overlapping genes are generally translated under different conditions, or separated in time – this is yet to be determined.

Evolution and Constraint in Antisense Proteins

The evolutionary analysis of function at the nucleotide sequence level is a fairly recent development (Robinson-Rechavi, 2019) so we should not be surprised at unexpected results in this rapidly developing field. While the evolutionary analysis of antisense proteins in prokaryotes awaits further investigation of strong overlapping gene candidates, those discovered so far are typically relatively young (Fellner et al., 2014, 2015; Hücker et al., 2018a). This may be seen as a point against their functionality, particularly for candidates limited to just one species. However, a number of genome elements with undisputed functionality are also evolutionarily young. Various functional putatively ncRNA elements are known to have high evolutionary turnover, see Dutcher and Raghavan (2018). For instance, an sRNA found only in *E. coli* was shown to be derived from a pseudogenized bacteriophage gene (Kacharia et al., 2017). Also relevant here is the large literature on the functions of "orphan" or taxonomically restricted genes restricted to a single genome or small clade (Satoshi and Nishikawa, 2004; Tautz and Domazet-Lošo, 2011) and orphan genes may play diverse important roles in bacteria (Hu et al., 2009).

It appears likely that antisense proteins are often less constrained in sequence than most protein-coding genes currently known. For one, antisense proteins are typically quite small and hence unlikely to fold into complex structures. Secondly, given initial evidence from viruses that protein domains in overlapping genes may be situated so as to not overlap (Fernandes et al., 2016), it seems that overlapping gene sequences are unlikely to be comprized of a high proportion of constrained sequence domains. While our previous analyses of individual prokaryotic overlapping genes have shown that they are typically young compared to the genes in which they are embedded (Hücker et al., 2018a) many embedded ORFs are quite well conserved beyond the genus. As a conservative example, we take a subset of the Enterobacteriaceae family, the smallest clade including both *Citrobacter rodentium* and *E. coli* (**Figure 3A**). We find that out of the 3391 antisense embedded ORFs predicted as having single homologs in all 13 representative genomes assessed, 29.5% exceed the conservation level of the lower quartile of annotated genes (**Figures 3B,C**). Here, conservation is judged by median pairwise amino acid similarity between genomes. Given the conservative nature of this analysis and that less than half of even annotated genes met the criterion of having single homologs in all of these genomes, we posit that thousands of embedded antisense ORFs are sufficiently conserved beyond the *Escherichia* genus to be candidates for functional genes in this particular respect. Factors affecting these conservation statistics,

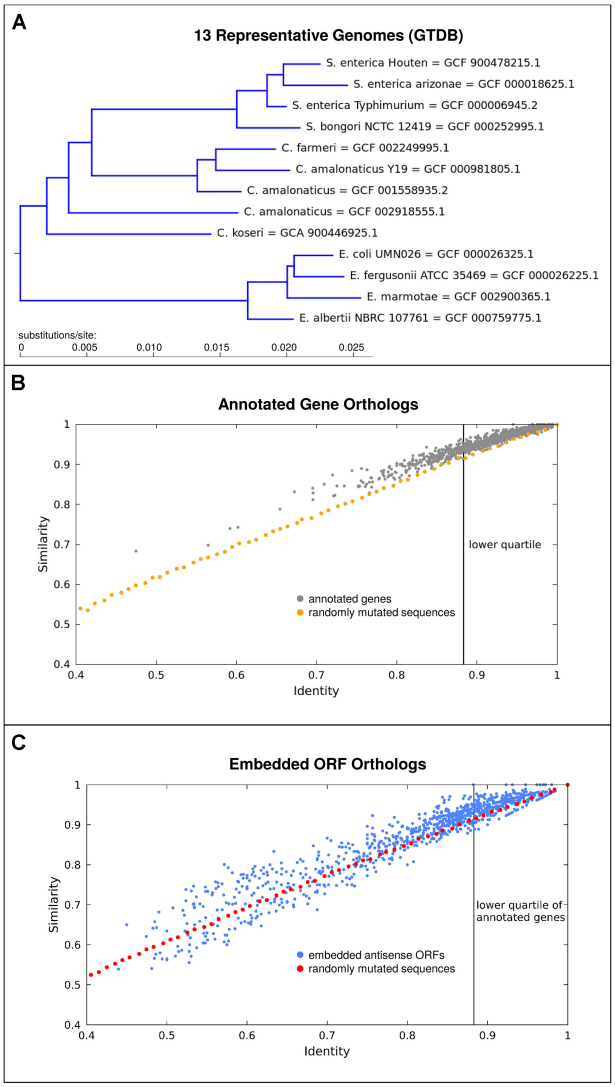

FIGURE 3 | A subset of embedded antisense ORFs are well conserved in the genomes situated taxonomically between *E. coli* and *Citrobacter rodentium*. **(A)** Phylogenetic tree showing 13 representative genomes used, derived from the genome taxonomy database (GTDB). **(B)** Median pairwise amino acid identity and similarity (gray) among orthologs for 1000 annotated genes with single copy orthologs in all of the 13 genomes. As a comparison, the effect on identity and similarity of adding random mutations to simulated sequences is shown (orange). There is a clear bias toward variants which result in higher "similarity." **(C)** Conservation of antisense embedded ORFs (blue), as compared to the identity-similarity relationship observed for control randomly mutated sequences (red) simulated as before but translated in antisense. Many antisense embedded ORFs are highly conserved and a subset also shows a bias toward similarity.

and additional criteria for gene-likeness which distinguish coding from non-coding antisense sequences deserve further study.

The orange and red lines in **Figures 3B,C** show the effect of randomly mutating a sequence created based on the codon usage in the annotated genes in *E. coli* K12. The points plotted represent median identities and similarities in comparison to originally simulated sequences, following successive rounds of random mutation, approximately mimicking the mutational distances observed between the orthologs of annotated genes and embedded ORFs. We suggest that two main results should be taken from **Figure 3**. Firstly, the blue cluster in the top right of **Figure 3C** shows that many embedded antisense ORFs are highly conserved across a significant evolutionary distance – they are not all immediately degraded following mutations in the alternate frame as might be naively assumed. Secondly, the bias above the orange and red lines shows that nearly all annotated genes and many embedded antisense ORFs tend toward fixing more "similar" mutations than might be predicted based on amino acid identity statistics alone. This result may be partly due to the structure of the genetic code, i.e., when a "mother gene" in the reference frame is conserved there is some tendency for conservation in the alternative strand (Wichmann and Ardern, 2019), but it is also suggestive of a kind of purifying selection where mutations to biochemically similar amino acids are preferred in a subset of embedded antisense ORFs. It has previously been shown that long antisense ORFs appear more often in natural genomes than expected based on codon composition of annotated coding genes (Mir et al., 2012), another hint of selective processes preserving some antisense ORFs.

A recent, currently unpublished, study in *M. tuberculosis* (Smith et al., 2019) has claimed that novel ORFs identified by ribosome profiling typically do not illustrate the strong codon bias evident in annotated mycobacterial genes and therefore cannot be expected to be functional. Given that many of these ORFs are situated in antisense to annotated genes, where the genetic code limits the possibilities for achieving optimal codon usage, this result is not surprising, and we suggest provides little evidence for the claim that they are nonfunctional. There is a problematic circularity here as well, as annotation of prokaryotic ORFs is based on models which take into account codon usage, based on usage in long ORFs – so short ORFs with "abnormal" codon usage will likely remain unannotated, reinforcing any bias in codon usage statistics in annotated genes. In general, short and weakly expressed genes should not be expected to match "canonical" highly expressed genes in terms of codon usage (Gupta and Ghosh, 2001), although the relationship between expression and codon usage is not straightforward (Dos Reis et al., 2003). Careful evolutionary sequence analyses are required here. A study of some putative same-strand overlapping genes also suggested that they are not under constraint (Meydan et al., 2019). However, more biologically nuanced analyses of sequence constraint, for instance after partitioning the homologs into phylostrata, would be useful. Further, a fundamental assumption of methods for detecting selection (e.g., Firth, 2014; Wei and Zhang, 2015), is the neutrality of synonymous mutations, but this assumption has been shown to be false, with the rate of synonymous mutations varying widely across sites (Wisotsky et al., 2020). The extent to which this affects conclusions regarding dN/dS as calculated with the various available methods remains unexplored. More generally, to our knowledge, there has been no demonstration of any synthesis of non-functional protein in prokaryotes. The high bioenergetic cost of protein production (Lynch and Marinov, 2015) would seem to militate against such a phenomenon being widespread in bacteria, where

costs are minimized through gene loss (Koskiniemi et al., 2012). As such, we argue that the default assumption following demonstration of a clear signal of translation should be that the product plays a functional role.

DISCUSSION

The Context: Unexpected Complexity

The historical trajectory in bacterial genomics has been toward finding previously unappreciated layers of complexity (Grainger, 2016). In particular, the number of different kinds of functional elements recognized has continued to increase in recent years. Examples of genetic elements previously ignored or written off as background noise which are now known to be functional in some or many cases include antisense transcription, small RNAs, and microRNAs, proteins with alternative start sites, small proteins (Storz et al., 2014), and micropeptides. Antisense transcription has been widely disregarded as noise (Raghavan et al., 2012; Lloréns-Rico et al., 2016). However, despite these generalizations, these elements have recently been found to at least sometimes have physiological roles (Wade and Grainger, 2014; Lejars et al., 2019). Functional RNAs which are not yet well understood include structured noncoding RNAs such as riboswitches (Hücker et al., 2017b; Stav et al., 2019). Proteins with alternative start sites, designated isoforms or "proteoforms," have also been reported in a few bacterial systems (Berry et al., 2016; Nakahigashi et al., 2016; Meydan et al., 2019). These genetic elements are all yet to be incorporated into genome annotation files and gene prediction algorithms. As such, genome annotation is years behind the leading edge of research in bacterial genetics, and various functional elements remain unannotated.

Recommendations for Further Research

Even recent attempts at comprehensive studies of small proteins have tended to ignore antisense proteins or to use methods unintentionally biased against them – perhaps unsurprising given the reigning paradigm in genome annotation, which excludes substantive overlaps as a matter of principle. As an example, the NCBI prokaryotic genome annotation standards include among the minimum standards that there can be "[no] gene completely contained in another gene on the same or opposite strand" (NCBI 2020). For instance, a recent study investigated small proteins in the human microbiome (Sberro et al., 2019) finding hundreds of previously unknown small proteins with evidence from evolutionary sequence constraint, and many also with evidence of transcription and/or translation. Two key steps were the use of MetaProdigal for gene prediction and RNAcode for inference of conservation. Both of these are implicitly biased against overlapping genes, in that Prodigal explicitly excludes long overlaps, and RNAcode looks for patterns of sequence constraint associated with normal non-overlapping genes, which are unlikely to be found in overlapping genes.

The bacteriological research community ought to relinquish the common assumption that unannotated functional elements are only to be found in intergenic regions. We must also be aware that antisense regions often need to be treated differently from intergenic regions, for instance in analyses of sequence constraint. Developing appropriate corrections to take into account the sequence context of antisense overlapping ORFs is an important area for further work. A major emphasis should be on high-throughput functional studies. For in-depth laboratory studies dissecting the details of an overlapping gene's regulation and function, the focus should be on the strongest candidates as determined with sequence and expression data. One key criterion here is evidence of reproducible regulated translation from one of the various ribosome profiling methods now available. Sequence properties determined from such sets should help to find strong candidates which are not expressed under already-assayed conditions. It is also clear that further advances in proteomics for small proteins should result in proteomic evidence for the translation of many more antisense proteins in bacteria and other systems. Following on from this, the discovery of any protein structures would be a major step forward toward understanding the molecular mechanisms of function. Finally, studying the evolutionary history of antisense proteins may provide useful insights on function. In this aspect these genes have a significant advantage over others in that their genomic context is relatively fixed by the gene in which they are embedded. This study has focused on eubacteria, but the same principles conceivably apply in archaea. A recent study, for instance, chose to only consider same-frame overlapping ORFs (proteoforms) on account of an absence of proteomics results and reliable BLAST hits for out-of-frame overlapping ORFs (Ten-Caten et al., 2018). Neither of these negative results are surprising, however, given the limitations of proteomics discussed above and the current bias against annotating out-of-frame overlaps; as such, archaeal datasets ought also be re-examined for functional overlapping genes.

In summary, what is required in order to assign the descriptor 'functional' to a putative gene, such as a gene encoded in antisense to a known gene? Regarding evolutionary evidence, a codon-level pattern of sequence constraint is sufficient to guarantee function, as constraint matching expectations for amino acids is unexpected in coding sequences. Detecting such constraint is a challenge for antisense sequences, however. Regarding evidence from wet-lab experiments, a condition-specific phenotype is also sufficient to establish functionality. The "gold standard" in this area would be a condition-specific negative growth phenotype in a genomic knock-out mutant, which could be complemented in *trans* (e.g., with a plasmid construct). Regarding high-throughput evidence, significant protein expression is evidence of functionality in highly optimized bacterial genomes, particularly if shown to be consistent across species or highly diverged strains. Appropriate thresholds for significant expression and sufficient evolutionary divergence in order to be able to confidently infer function are yet to be established. While each of these three lines of evidence is arguably sufficient to establish function, none is necessary, as there are functional elements which fail to meet at least one of these criteria.

We have collated evidence from diverse bacteria (including the genera *Escherichia*, *Pseudomonas*, and *Mycobacterium*) for

protein coding ORFs embedded in antisense to annotated genes, discussed reasons to believe that they are biologically functional, and responded to common objections, informed by the most recent work in bacterial molecular genetics. We suggest that a pro-function attitude regarding antisense prokaryotic transcripts and the antisense translatome is both more useful for research and justified by multiple lines of evidence. How many of these elements are functional and what they do remain contentious, however, and worthy of significant further investigation.

METHODS

For **Figure 1**, positions of previously discovered putative antiparallel genes in *E. coli* K12 and *M. tuberculosis* were extracted from the supplementary data of previous studies (Friedman et al., 2017; Smith et al., 2019; Weaver et al., 2019); information on those with ribosome profiling reads was provided by Robin Friedman. Positions are shown visualized with Circos (Krzywinski et al., 2009).

For **Figure 2**, ribosome profiling ("RIBO-seq") data was visualized to show examples of antisense overlapping genes. In each case, adapter sequences were predicted using DNApi.py (Tsuji and Weng, 2016), trimmed with cutadapt (Martin, 2011) using a minimum length of 19 and quality score of 10, and aligned (local alignment) with bowtie2 (Langmead and Salzberg, 2012). Fastq data from SRR5874479 (LB) and SRR5874484 (BHI) for *E. coli* O157:H7 Sakai was aligned against the genome GCF_000008865.1_ASM886v1. Fastq data from SRR1265839 (without azithromycin) and SRR1265836 (with azithromycin) for *S. aureus* was aligned against genome GCF_900475245.1_43024_E01. Reads mapping at each site per million total mapped reads (RPM) are calculated from aligned bam files with reads mapping to rRNA and tRNA locations removed, using samtools (Li et al., 2009). Images of RPM in the region around the putative antisense gene are drawn in gnuplot with "smooth csplines."

For **Figure 3**, the relationship between similarity and identity in comparisons of different ORF homologs was compared. Representative genomes from release 89 of the genome taxonomy database (GTDB; Parks et al., 2018) in the smallest clade uniting *E. coli* and *C. rodentium* (**Figure 3A**) were chosen. Of these 23 strains, 13 had a GenBank genome and feature table with the same accession version available. These were downloaded, and annotated ORFs in each compared to each other using OrthoFinder (Emms and Kelly, 2015). Genes with a single copy ortholog present in all 13 genomes were extracted, and members of each ortholog family were aligned against each other using the EMBOSS (Rice et al., 2000) program needleall to determine median similarity and identity at the amino acid level (**Figure 3B**). As a control, 50 sequences of 333 codons length were created based on codon usage in *E. coli* K12, using EMBOSS programs cusp and makenucseq. These were then mutated through 70 rounds of point mutation (10 mutations per round) using the EMBOSS program msbar, and translated in order to determine the relationship between varying levels of amino acid identity and similarity. In each case, the mutated sequences were compared to the original simulated sequence they were derived from, using EMBOSS needle. For each percent decrease in identity observed, results were collated and the median values of identity and similarity reported. The procedure used initially for annotated genes was repeated using all antisense embedded ORFs (using the bacterial genetic code, NCBI code table 11), found using a Perl script "ORFFinder" (available from Christopher Huptas) and Bedtools (Quinlan and Hall, 2010). A negative control for these sequences was also created similarly, to before, but using an antisense reading frame. As the particular antisense frame used had no significant effect on the sequence similarities obtained in the simulation, for the data shown the initial sequences based on codon usage in *E. coli* K12 were directly reverse complemented with no further frame-shift, prior to the 70 rounds of random mutation.

DATA AVAILABILITY STATEMENT

The datasets generated for this study are available on request to the corresponding author.

AUTHOR CONTRIBUTIONS

ZA drafted the manuscript and prepared the figures. KN and SS assisted with drafting the manuscript and conceiving of the project. All authors read and approved the final version of the manuscript.

FUNDING

ZA was supported by the Bavarian State Government and the National Philanthropic Trust.

ACKNOWLEDGMENTS

Thanks to Christina Ludwig for advice on proteomics references, Christopher Huptas for development of an ORF finder Perl script, and Robin Friedman for providing ribosomal profiling information for putative sRNAs.

REFERENCES

Affram, Y., Zapata, J. C., Zhou, W., Pazgier, M., Iglesias-Ussel, M., Ray, K., et al. (2019). PJ-1 The HIV-1 antisense protein ASP is a structural protein of the viral envelope. *J. Acquir. Immune Defic. Syndr.* 81:79. doi: 10.1097/01.qai.0000558040.82718.71

Albalat, R., and Cañestro, C. (2016). Evolution by gene loss. *Nat. Rev. Genet.* 17, 379–391.

Ames, B. N., and Martin, R. G. (1964). Biochemical aspects of genetics: the operon. *Annu. Rev. Biochem.* 33, 235–258. doi: 10.1146/annurev.bi.33.070164.001315

Ardern, Z. (2018). Dysfunction, disease, and the limits of selection. *Biol. Theory* 13, 4–9. doi: 10.1007/s13752-017-0288-0

Baggett, N. E., Zhang, Y., and Gross, C. A. (2017). Global analysis of translation termination in *E. coli*. *PLoS Genet.* 13:e1006676. doi: 10.1371/journal.pgen.1006676

Barrell, B. G., Air, G., and Hutchison, C. (1976). Overlapping genes in bacteriophage φX174. *Nature* 264, 34–41. doi: 10.1038/264034a0

Behe, M. J. (2010). Experimental evolution, loss-of-function mutations, and "the first rule of adaptive evolution". *Q. Rev. Biol.* 85, 419–445. doi: 10.1086/656902

Bendall, M. L., Stevens, S. L., Chan, L.-K., Malfatti, S., Schwientek, P., Tremblay, J., et al. (2016). Genome-wide selective sweeps and gene-specific sweeps in natural bacterial populations. *ISME J.* 10, 1589–1601. doi: 10.1038/ismej.2015.241

Berry, I. J., Steele, J. R., Padula, M. P., and Djordjevic, S. P. (2016). The application of terminomics for the identification of protein start sites and proteoforms in bacteria. *Proteomics* 16, 257–272. doi: 10.1002/pmic.201500319

Bhattacharyya, S., Bershtein, S., Argun, T., Gilson, A. I., Trauger, S. A., and Shakhnovich, E. I. (2016). Transient protein-protein interactions perturb *E. coli* metabolome and cause gene dosage toxicity. *eLife* 5:e20309.

Brandon, R. N. (2013). "A general case for functional pluralism," in *Functions: Selection and Mechanisms*, ed. P. Huneman, (Dordrecht: Springer), 97–104. doi: 10.1007/978-94-007-5304-4_6

Brophy, J. A., and Voigt, C. A. (2016). Antisense transcription as a tool to tune gene expression. *Mol. Syst. Biol.* 12:854. doi: 10.15252/msb.20156540

Cassan, E., Arigon-Chifolleau, A. M., Mesnard, J. M., Gross, A., and Gascuel, O. (2016). Concomitant emergence of the antisense protein gene of HIV-1 and of the pandemic. *Proc. Natl. Acad. Sci. U.S.A.* 113, 11537–11542. doi: 10.1073/pnas.1605739113

Cheetham, S. W., Faulkner, G. J., and Dinger, M. E. (2019). Overcoming challenges and dogmas to understand the functions of pseudogenes. *Nat. Rev. Genet.* 21, 191–201. doi: 10.1038/s41576-019-0196-1

Chou, K.-C., Zhang, C.-T., and Elrod, D. W. (1996). Do "antisense proteins" exist? *J. Protein Chem.* 15, 59–61. doi: 10.1007/bf01886811

Courtney, C., and Chatterjee, A. (2014). cis-Antisense RNA and transcriptional interference: coupled layers of gene regulation. *J. Gene Ther.* 1, 1–9.

Crampton, N., Bonass, W. A., Kirkham, J., Rivetti, C., and Thomson, N. H. (2006). Collision events between RNA polymerases in convergent transcription studied by atomic force microscopy. *Nucleic Acids Res.* 34, 5416–5425. doi: 10.1093/nar/gkl668

Doolittle, W. F. (2018). We simply cannot go on being so vague about 'function'. *Genome Biol.* 19:223.

Doolittle, W. F., Brunet, T. D., Linquist, S., and Gregory, T. R. (2014). Distinguishing between "function" and "effect" in genome biology. *Genome Biol. Evol.* 6, 1234–1237. doi: 10.1093/gbe/evu098

Dos Reis, M., Wernisch, L., and Savva, R. (2003). Unexpected correlations between gene expression and codon usage bias from microarray data for the whole *Escherichia coli* K-12 genome. *Nucleic Acids Res.* 31, 6976–6985. doi: 10.1093/nar/gkg897

Dutcher, H. A., and Raghavan, R. (2018). Origin, evolution, and loss of bacterial small RNAs. *Microbiol. Spectr.* 6:RWR-0004-2017.

Edgar, R., Domrachev, M., and Lash, A. E. (2002). Gene expression omnibus: NCBI gene expression and hybridization array data repository. *Nucleic Acids Res.* 30, 207–210. doi: 10.1093/nar/30.1.207

Elguoshy, A., Magdeldin, S., Xu, B., Hirao, Y., Zhang, Y., Kinoshita, N., et al. (2016). Why are they missing?: Bioinformatics characterization of missing human proteins. *J. Proteomics* 149, 7–14. doi: 10.1016/j.jprot.2016.08.005

Ellis, J. C., and Brown, J. W. (2003). Genes within genes within bacteria. *Trends Biochem. Sci.* 28, 521–523. doi: 10.1016/j.tibs.2003.08.002

Emms, D. M., and Kelly, S. (2015). OrthoFinder: solving fundamental biases in whole genome comparisons dramatically improves orthogroup inference accuracy. *Genome Biol.* 16:157.

Ettwiller, L., Buswell, J., Yigit, E., and Schildkraut, I. (2016). A novel enrichment strategy reveals unprecedented number of novel transcription start sites at single base resolution in a model prokaryote and the gut microbiome. *BMC Genomics* 17:199. doi: 10.1186/s12864-016-2539-z

Fellner, L., Bechtel, N., Witting, M. A., Simon, S., Schmitt-Kopplin, P., Keim, D., et al. (2014). Phenotype of *htgA* (*mbiA*), a recently evolved orphan gene of *Escherichia coli* and *Shigella*, completely overlapping in antisense to *yaaW*. *FEMS Microbiol. Lett.* 350, 57–64.

Fellner, L., Simon, S., Scherling, C., Witting, M., Schober, S., Polte, C., et al. (2015). Evidence for the recent origin of a bacterial protein-coding, overlapping orphan gene by evolutionary overprinting. *BMC Evol. Biol.* 15:283. doi: 10.1186/s12862-015-0558-z

Fernandes, J. D., Faust, T. B., Strauli, N. B., Smith, C., Crosby, D. C., Nakamura, R. L., et al. (2016). Functional segregation of overlapping genes in HIV. *Cell* 167, 1762–1773.e12. doi: 10.1016/j.cell.2016.11.031

Firth, A. E. (2014). Mapping overlapping functional elements embedded within the protein-coding regions of RNA viruses. *Nucleic Acids Res.* 42, 12425–12439. doi: 10.1093/nar/gku981

Friedman, R. C., Kalkhof, S., Doppelt-Azeroual, O., Mueller, S. A., Chovancova, M., Von Bergen, M., et al. (2017). Common and phylogenetically widespread coding for peptides by bacterial small RNAs. *BMC Genomics* 18:553. doi: 10.1186/s12864-017-3932-y

Georg, J., and Hess, W. R. (2018). Widespread antisense transcription in prokaryotes. *Microbiol. Spectr.* 6:RWR-0029-2018.

Gibson, B., and Eyre-Walker, A. (2019). Investigating evolutionary rate variation in bacteria. *J. Mol. Evol.* 87, 317–326. doi: 10.1007/s00239-019-09912-5

Gimpel, M., and Brantl, S. (2017). Dual-function small regulatory RNAs in bacteria. *Mol. Microbiol.* 103, 387–397. doi: 10.1111/mmi.13558

Glaub, A., Huptas, C., Neuhaus, K., and Ardern, Z. (2020). Recommendations for bacterial ribosome profiling experiments based on bioinformatic evaluation of published data. *J. Biol. Chem.* 295, 8999–9011. doi: 10.1074/jbc.ra119.012161

Goodhead, I., and Darby, A. C. (2015). Taking the pseudo out of pseudogenes. *Curr. Opin. Microbiol.* 23, 102–109. doi: 10.1016/j.mib.2014.11.012

Grainger, D. C. (2016). The unexpected complexity of bacterial genomes. *Microbiology* 162, 1167–1172. doi: 10.1099/mic.0.000309

Graur, D., Zheng, Y., and Azevedo, R. B. (2015). An evolutionary classification of genomic function. *Genome Biol. Evol.* 7, 642–645. doi: 10.1093/gbe/evv021

Graur, D., Zheng, Y., Price, N., Azevedo, R. B., Zufall, R. A., and Elhaik, E. (2013). On the immortality of television sets:"function" in the human genome according to the evolution-free gospel of ENCODE. *Genome Biol. Evol.* 5, 578–590. doi: 10.1093/gbe/evt028

Gupta, S., and Ghosh, T. (2001). Gene expressivity is the main factor in dictating the codon usage variation among the genes in *Pseudomonas aeruginosa*. *Gene* 273, 63–70. doi: 10.1016/s0378-1119(01)00576-5

Harrison, E., and Brockhurst, M. A. (2017). Ecological and evolutionary benefits of temperate phage: what does or doesn't kill you makes you stronger. *Bioessays* 39:1700112. doi: 10.1002/bies.201700112

Hawkins, M., Dimude, J. U., Howard, J. A. L., Smith, A. J., Dillingham, M. S., Savery, N. J., et al. (2019). Direct removal of RNA polymerase barriers to replication by accessory replicative helicases. *Nucleic Acids Res.* 47, 5100–5113. doi: 10.1093/nar/gkz170

Haycocks, J. R., and Grainger, D. C. (2016). Unusually situated binding sites for bacterial transcription factors can have hidden functionality. *PLoS One* 11:e0157016. doi: 10.1371/journal.pone.0157016

Helmrich, A., Ballarino, M., Nudler, E., and Tora, L. (2013). Transcription-replication encounters, consequences and genomic instability. *Nat. Struct. Mol. Biol.* 20, 412–418. doi: 10.1038/nsmb.2543

Hoffmann, S. A., Hao, N., Shearwin, K. E., and Arndt, K. M. (2019). Characterizing transcriptional interference between converging genes in bacteria. *ACS Synth. Biol.* 8, 466–473. doi: 10.1021/acssynbio.8b00477

Hottes, A. K., Freddolino, P. L., Khare, A., Donnell, Z. N., Liu, J. C., and Tavazoie, S. (2013). Bacterial adaptation through loss of function. *PLoS Genet.* 9:e1003617. doi: 10.1371/journal.pgen.1003617

Hu, P., Janga, S. C., Babu, M., Díaz-Mejía, J. J., Butland, G., Yang, W., et al. (2009). Global functional atlas of *Escherichia coli* encompassing previously uncharacterized proteins. *PLoS Biol.* 7:e96. doi: 10.1371/journal.pbio.1000096

Hücker, S. M., Ardern, Z., Goldberg, T., Schafferhans, A., Bernhofer, M., Vestergaard, G., et al. (2017a). Discovery of numerous novel small genes in the intergenic regions of the *Escherichia coli* O157:H7 Sakai genome. *PLoS One* 12:e0184119. doi: 10.1371/journal.pone.0184119

Hücker, S. M., Simon, S., Scherer, S., and Neuhaus, K. (2017b). Transcriptional and translational regulation by RNA thermometers, riboswitches and the sRNA DsrA in *Escherichia coli* O157: H7 Sakai under combined cold and osmotic stress adaptation. *FEMS Microbiol. Lett.* 364:fnw262. doi: 10.1093/femsle/fnw262

Hücker, S. M., Vanderhaeghen, S., Abellan-Schneyder, I., Scherer, S., and Neuhaus, K. (2018a). The novel anaerobiosis-responsive overlapping gene *ano* is

overlapping antisense to the annotated gene ECs2385 of *Escherichia coli* O157:H7 Sakai. *Front. Microbiol.* 9:931. doi: 10.3389/fmicb.2018.00931

Hücker, S. M., Vanderhaeghen, S., Abellan-Schneyder, I., Wecko, R., Simon, S., Scherer, S., et al. (2018b). A novel short L-arginine responsive protein-coding gene (*laoB*) antiparallel overlapping to a CadC-like transcriptional regulator in *Escherichia coli* O157:H7 Sakai originated by overprinting. *BMC Evol. Biol.* 18:21. doi: 10.1186/s12862-018-1134-0

Ingolia, N. T., Ghaemmaghami, S., Newman, J. R., and Weissman, J. S. (2009). Genome-wide analysis in vivo of translation with nucleotide resolution using ribosome profiling. *Science* 324, 218–223. doi: 10.1126/science.1168978

Jacob, F., and Monod, J. (1961). Genetic regulatory mechanisms in the synthesis of proteins. *J. Mol. Biol.* 3, 318–356. doi: 10.1016/s0022-2836(61)80072-7

Jeong, Y., Kim, J.-N., Kim, M. W., Bucca, G., Cho, S., Yoon, Y. J., et al. (2016). The dynamic transcriptional and translational landscape of the model antibiotic producer *Streptomyces coelicolor* A3(2). *Nat. Commun.* 7:11605.

Ju, X., Li, D., and Liu, S. (2019). Full-length RNA profiling reveals pervasive bidirectional transcription terminators in bacteria. *Nat. Microbiol.* 4, 1907–1918. doi: 10.1038/s41564-019-0500-z

Kacharia, F. R., Millar, J. A., and Raghavan, R. (2017). Emergence of new sRNAs in enteric bacteria is associated with low expression and rapid evolution. *J. Mol. Evol.* 84, 204–213. doi: 10.1007/s00239-017-9793-9

Keeling, D. M., Garza, P., Nartey, C. M., and Carvunis, A.-R. (2019). The meanings of'function'in biology and the problematic case of de novo gene emergence. *eLife* 8:e47014.

Kitagawa, M., Ara, T., Arifuzzaman, M., Ioka-Nakamichi, T., Inamoto, E., Toyonaga, H., et al. (2005). Complete set of ORF clones of *Escherichia coli* ASKA library (a complete set of *E. coli* K-12 ORF archive): unique resources for biological research. *DNA Res.* 12, 291–299. doi: 10.1093/dnares/dsi012

Knopp, M., and Andersson, D. I. (2018). No beneficial fitness effects of random peptides. *Nat. Ecol. Evol.* 2, 1046–1047. doi: 10.1038/s41559-018-0585-4

Koskiniemi, S., Sun, S., Berg, O. G., and Andersson, D. I. (2012). Selection-driven gene loss in bacteria. *PLoS Genet.* 8:e1002787. doi: 10.1371/journal.pgen.1002787

Krzywinski, M., Schein, J., Birol, I., Connors, J., Gascoyne, R., Horsman, D., et al. (2009). Circos: an information aesthetic for comparative genomics. *Genome Res.* 19, 1639–1645. doi: 10.1101/gr.092759.109

Langmead, B., and Salzberg, S. L. (2012). Fast gapped-read alignment with Bowtie 2. *Nat. Methods* 9, 357–359. doi: 10.1038/nmeth.1923

Lasa, I., Toledo-Arana, A., and Gingeras, T. R. (2012). An effort to make sense of antisense transcription in bacteria. *RNA Biol.* 9, 1039–1044. doi: 10.4161/rna.21167

Lejars, M., Kobayashi, A., and Hajnsdorf, E. (2019). Physiological roles of antisense RNAs in prokaryotes. *Biochimie* 164, 3–16. doi: 10.1016/j.biochi.2019.04.015

Lescuyer, P., Hochstrasser, D. F., and Sanchez, J. C. (2004). Comprehensive proteome analysis by chromatographic protein prefractionation. *Electrophoresis* 25, 1125–1135. doi: 10.1002/elps.200305792

Li, H., Handsaker, B., Wysoker, A., Fennell, T., Ruan, J., Homer, N., et al. (2009). The sequence alignment/map format and SAMtools. *Bioinformatics* 25, 2078–2079. doi: 10.1093/bioinformatics/btp352

Lloréns-Rico, V., Cano, J., Kamminga, T., Gil, R., Latorre, A., Chen, W.-H., et al. (2016). Bacterial antisense RNAs are mainly the product of transcriptional noise. *Sci. Adv.* 2:e1501363. doi: 10.1126/sciadv.1501363

Lynch, M., and Marinov, G. K. (2015). The bioenergetic costs of a gene. *Proc. Natl. Acad. Sci. U.S.A.* 112, 15690–15695. doi: 10.1073/pnas.1514974112

Ma, N., and McAllister, W. T. (2009). In a head-on collision, two RNA polymerases approaching one another on the same DNA may pass by one another. *J. Mol. Biol.* 391, 808–812. doi: 10.1016/j.jmb.2009.06.060

Martin, M. (2011). Cutadapt removes adapter sequences from high-throughput sequencing reads. *EMBnet J.* 17, 10–12.

Meydan, S., Marks, J., Klepacki, D., Sharma, V., Baranov, P. V., Firth, A. E., et al. (2019). Retapamulin-assisted ribosome profiling reveals the alternative bacterial proteome. *Mol. Cell* 74, 481–493.e6. doi: 10.1016/j.molcel.2019.02.017

Mir, K., Neuhaus, K., Scherer, S., Bossert, M., and Schober, S. (2012). Predicting statistical properties of open reading frames in bacterial genomes. *PLoS One* 7:e45103. doi: 10.1371/journal.pone.0045103

Miravet-Verde, S., Ferrar, T., Espadas-García, G., Mazzolini, R., Gharrab, A., Sabido, E., et al. (2019). Unraveling the hidden universe of small proteins in bacterial genomes. *Mol. Syst. Biol.* 15:e8290.

Mohammad, F., Green, R., and Buskirk, A. R. (2019). A systematically-revised ribosome profiling method for bacteria reveals pauses at single-codon resolution. *eLife* 8:e42591.

Müller, S. A., Findeiß, S., Pernitzsch, S. R., Wissenbach, D. K., Stadler, P. F., Hofacker, I. L., et al. (2013). Identification of new protein coding sequences and signal peptidase cleavage sites of *Helicobacter* pylori strain 26695 by proteogenomics. *J. Proteomics* 86, 27–42. doi: 10.1016/j.jprot.2013.04.036

Nakahigashi, K., Takai, Y., Kimura, M., Abe, N., Nakayashiki, T., Shiwa, Y., et al. (2016). Comprehensive identification of translation start sites by tetracycline-inhibited ribosome profiling. *DNA Res.* 23, 193–201. doi: 10.1093/dnares/dsw008

NCBI (2020). *NCBI Prokaryotic Genome Annotation Standards*. Available online at: https://www.ncbi.nlm.nih.gov/genome/annotation_prok/standards/ (accessed 20.02.2020).

Nelson, C. W., Ardern, Z., and Wei, X. (2020). OLGenie: estimating natural selection to predict functional overlapping genes. *Mol. Biol. Evol.* msaa087. doi: 10.1093/molbev/msaa087

Neuhaus, K., Landstorfer, R., Fellner, L., Simon, S., Schafferhans, A., Goldberg, T., et al. (2016). Translatomics combined with transcriptomics and proteomics reveals novel functional, recently evolved orphan genes in *Escherichia coli* O157:H7 (EHEC). *BMC Genomics* 17:133. doi: 10.1186/s12864-016-2456-1

Neuhaus, K., Landstorfer, R., Simon, S., Schober, S., Wright, P. R., Smith, C., et al. (2017). Differentiation of ncRNAs from small mRNAs in *Escherichia coli* O157: H7 EDL933 (EHEC) by combined RNAseq and RIBOseq–*ryhB* encodes the regulatory RNA RyhB and a peptide, RyhP. *BMC Genomics* 18:216. doi: 10.1186/s12864-017-3586-9

Oh, E., Becker, A. H., Sandikci, A., Huber, D., Chaba, R., Gloge, F., et al. (2011). Selective ribosome profiling reveals the cotranslational chaperone action of trigger factor *in vivo*. *Cell* 147, 1295–1308. doi: 10.1016/j.cell.2011.10.044

Orr, M. W., Mao, Y., Storz, G., and Qian, S.-B. (2020). Alternative ORFs and small ORFs: shedding light on the dark proteome. *Nucleic Acids Res.* 48, 1029–1042. doi: 10.1093/nar/gkz734

Owen, S. V., Canals, R., Wenner, N., Hammarlöf, D. L., Kröger, C., and Hinton, J. C. (2020). A window into lysogeny: revealing temperate phage biology with transcriptomics. *Microb. Genomics* 6:e000330.

Parks, D. H., Chuvochina, M., Waite, D. W., Rinke, C., Skarshewski, A., Chaumeil, P.-A., et al. (2018). A standardized bacterial taxonomy based on genome phylogeny substantially revises the tree of life. *Nat. Biotechnol.* 36, 996–1004. doi: 10.1038/nbt.4229

Pavesi, A. (2019). Asymmetric evolution in viral overlapping genes is a source of selective protein adaptation. *Virology* 532, 39–47. doi: 10.1016/j.virol.2019.03.017

Pavesi, A., Vianelli, A., Chirico, N., Bao, Y., Blinkova, O., Belshaw, R., et al. (2018). Overlapping genes and the proteins they encode differ significantly in their sequence composition from non-overlapping genes. *PLoS One* 13:e0202513. doi: 10.1371/journal.pone.0202513

Proshkin, S., Rahmouni, A. R., Mironov, A., and Nudler, E. (2010). Cooperation between translating ribosomes and RNA polymerase in transcription elongation. *Science* 328, 504–508. doi: 10.1126/science.1184939

Quinlan, A. R., and Hall, I. M. (2010). BEDTools: a flexible suite of utilities for comparing genomic features. *Bioinformatics* 26, 841–842. doi: 10.1093/bioinformatics/btq033

Raghavan, R., Sloan, D. B., and Ochman, H. (2012). Antisense transcription is pervasive but rarely conserved in enteric bacteria. *mBio* 3:e00156-12.

Rice, P., Longden, I., and Bleasby, A. (2000). EMBOSS: the European molecular biology open software suite. *Trends Genet.* 16, 276–277. doi: 10.1016/s0168-9525(00)02024-2

Robinson-Rechavi, M. (2019). Molecular evolution and gene function. *arXiv*. Availble at: https://arxiv.org/abs/1910.01940#:~{}:text=Functional%20data%20provides%20information%20on,e.g.%2C%20substitutions%20or%20duplications (accessed July 31, 2020).

Sáenz-Lahoya, S., Bitarte, N., García, B., Burgui, S., Vergara-Irigaray, M., Valle, J., et al. (2019). Noncontiguous operon is a genetic organization for coordinating bacterial gene expression. *Proc. Natl. Acad. Sci. U.S.A.* 116, 1733–1738. doi: 10.1073/pnas.1812746116

Saha, D., Podder, S., Panda, A., and Ghosh, T. C. (2016). Overlapping genes: a significant genomic correlate of prokaryotic growth rates. *Gene* 582, 143–147. doi: 10.1016/j.gene.2016.02.002

Satoshi, F., and Nishikawa, K. (2004). Estimation of the number of authentic orphan genes in bacterial genomes. *DNA Res.* 11, 219–231. doi: 10.1093/dnares/11.4.219

Sberro, H., Fremin, B. J., Zlitni, S., Edfors, F., Greenfield, N., Snyder, M. P., et al. (2019). Large-scale analyses of human microbiomes reveal thousands of small, novel genes. *Cell* 178, 1245–1259.e14. doi: 10.1016/j.cell.2019.07.016

Schuetz, R., Zamboni, N., Zampieri, M., Heinemann, M., and Sauer, U. (2012). Multidimensional optimality of microbial metabolism. *Science* 336, 601–604. doi: 10.1126/science.1216882

Sela, I., Wolf, Y. I., and Koonin, E. V. (2019). Selection and genome plasticity as the key factors in the evolution of bacteria. *Phys. Rev. X* 9:031018.

Sharma, H., and Anand, B. (2019). Ribosome assembly defects subvert initiation Factor3 mediated scrutiny of bona fide start signal. *Nucleic Acids Res.* 47, 11368–11386. doi: 10.1093/nar/gkz825

Smith, C., Canestrari, J., Wang, J., Derbyshire, K., Gray, T., and Wade, J. (2019). Pervasive translation in *Mycobacterium tuberculosis*. *bioRxiv* [Preprint]. doi: 10.1101/665208

Stav, S., Atilho, R. M., Arachchilage, G. M., Nguyen, G., Higgs, G., and Breaker, R. R. (2019). Genome-wide discovery of structured noncoding RNAs in bacteria. *BMC Microbiol.* 19:66. doi: 10.1186/s12866-019-1433-7

Storz, G., Wolf, Y. I., and Ramamurthi, K. S. (2014). Small proteins can no longer be ignored. *Annu. Rev. Biochem.* 83, 753–777. doi: 10.1146/annurev-biochem-070611-102400

Takeuchi, N., Cordero, O. X., Koonin, E. V., and Kaneko, K. (2015). Gene-specific selective sweeps in bacteria and archaea caused by negative frequency-dependent selection. *BMC Biol.* 13:20. doi: 10.1186/s12915-015-0131-7

Tautz, D., and Domazet-Lošo, T. (2011). The evolutionary origin of orphan genes. *Nat. Rev. Genet.* 12, 692–702. doi: 10.1038/nrg3053

Tenaillon, O. (2014). The utility of Fisher's geometric model in evolutionary genetics. *Annu. Rev. Ecol. Evol. Syst.* 45, 179–201. doi: 10.1146/annurev-ecolsys-120213-091846

Ten-Caten, F., Vêncio, R. Z., Lorenzetti, A. P. R., Zaramela, L. S., Santana, A. C., and Koide, T. (2018). Internal RNAs overlapping coding sequences can drive the production of alternative proteins in archaea. *RNA Biol.* 15, 1119–1132.

Tsuji, J., and Weng, Z. (2016). DNApi: a de novo adapter prediction algorithm for small RNA sequencing data. *PLoS One* 11:e0164228. doi: 10.1371/journal.pone.0164228

Vanderhaeghen, S., Zehentner, B., Scherer, S., Neuhaus, K., and Ardern, Z. (2018). The novel EHEC gene *asa* overlaps the TEGT transporter gene in antisense and is regulated by NaCl and growth phase. *Sci. Rep.* 8:17875.

Venter, E., Smith, R. D., and Payne, S. H. (2011). Proteogenomic analysis of bacteria and archaea: a 46 organism case study. *PLoS One* 6:e27587. doi: 10.1371/journal.pone.0027587

Vishnoi, A., Kryazhimskiy, S., Bazykin, G. A., Hannenhalli, S., and Plotkin, J. B. (2010). Young proteins experience more variable selection pressures than old proteins. *Genome Res.* 20, 1574–1581. doi: 10.1101/gr.109595.110

Wade, J. T. (2015). Mapping transcription regulatory networks with ChIP-seq and RNA-seq. *Adv. Exp. Med. Biol.* 883, 119–134. doi: 10.1007/978-3-319-23603-2_7

Wade, J. T., and Grainger, D. C. (2014). Pervasive transcription: illuminating the dark matter of bacterial transcriptomes. *Nat. Rev. Microbiol.* 12, 647–653. doi: 10.1038/nrmicro3316

Wadler, C. S., and Vanderpool, C. K. (2007). A dual function for a bacterial small RNA: SgrS performs base pairing-dependent regulation and encodes a functional polypeptide. *Proc. Natl. Acad. Sci. U.S.A.* 104, 20454–20459. doi: 10.1073/pnas.0708102104

Weaver, J., Mohammad, F., Buskirk, A. R., and Storz, G. (2019). Identifying small proteins by ribosome profiling with stalled initiation complexes. *mBio* 10:e02819-18.

Wei, X., and Zhang, J. (2015). A simple method for estimating the strength of natural selection on overlapping genes. *Genome Biol. Evol.* 7, 381–390. doi: 10.1093/gbe/evu294

Weisman, C. M., and Eddy, S. R. (2017). Gene evolution: getting something from nothing. *Curr. Biol.* 27, R661–R663.

Wichmann, S., and Ardern, Z. (2019). Optimality in the standard genetic code is robust with respect to comparison code sets. *Biosystems* 185:104023. doi: 10.1016/j.biosystems.2019.104023

Willems, P., Fijalkowski, I., and Van Damme, P. (2019). Lost and found: re-searching and re-scoring proteomics data aids the discovery of bacterial proteins and improves proteome coverage. *bioRxiv* [Preprint]. doi: 10.1101/2019.12.18.881375

Willis, S., and Masel, J. (2018). Gene birth contributes to structural disorder encoded by overlapping genes. *Genetics* 210, 303–313. doi: 10.1534/genetics.118.301249

Wisotsky, S. R., Kosakovsky Pond, S. L., Shank, S. D., and Muse, S. V. (2020). Synonymous site-to-site substitution rate variation dramatically inflates false positive rates of selection analyses: ignore at your own peril. *Mol. Biol. Evol.* msaa037.

Yang, X., Jensen, S. I., Wulff, T., Harrison, S. J., and Long, K. S. (2016). Identification and validation of novel small proteins in *Pseudomonas putida*. *Environ. Microbiol. Rep.* 8, 966–974. doi: 10.1111/1758-2229.12473

Conflict of Interest: The authors declare that the research was conducted in the absence of any commercial or financial relationships that could be construed as a potential conflict of interest.

frontiers in Molecular Biosciences

ORIGINAL RESEARCH
published: 25 September 2020
doi: 10.3389/fmolb.2020.580913

Effect of the Extracellular Vesicle RNA Cargo From Uropathogenic *Escherichia coli* on Bladder Cells

Priscila Dauros-Singorenko[1,2], Jiwon Hong[2,3,4], Simon Swift[1], Anthony Phillips[2,3,4] and Cherie Blenkiron[1,5]*

[1] Department of Molecular Medicine and Pathology, Faculty of Medical and Health Sciences, The University of Auckland, Auckland, New Zealand, [2] Department of Surgery, Faculty of Medical and Health Sciences, The University of Auckland, Auckland, New Zealand, [3] School of Biological Sciences, Faculty of Science, The University of Auckland, Auckland, New Zealand, [4] Surgical and Translational Research Centre, The University of Auckland, Auckland, New Zealand, [5] Auckland Cancer Society Research Centre, Faculty of Medical and Health Sciences, The University of Auckland, Auckland, New Zealand

Iron restriction in mammals, part of innate antimicrobial defense, may be sensed as a signal by an infecting pathogen. Iron-dependent regulators not only activate the pathogen's specific iron acquisition and storage mechanisms needed for survival but also influence a number of other processes. Bacterial extracellular vesicles (EVs) are a conserved communication mechanism, which can have roles in host colonization, transfer of antimicrobial resistance, modulation of the host's immune response, and biofilm formation. Here we analyze the iron-responsive effect of RNA cargo from *Escherichia coli* EVs in bladder cells. No differences were found in total RNA quantified from EVs released from representative pathogenic and probiotic strains grown in different iron conditions; nevertheless, lipopolysaccharide (LPS) associated with purified RNA was 10 times greater from EVs derived from the pathogenic strain. The pathogen and probiotic EV-RNA have no substantial toxic effect on the viability of cultured bladder cells, regardless of the iron concentration during bacterial culture. Transcriptomic analysis of bladder cells treated with pathogen EV-RNA delivered in artificial liposomes revealed a gene expression profile with a strong similarity to that of cells treated with liposomes containing LPS alone, with the majority being immune response pathways. EV-RNA from the probiotic strain gave no significant perturbation of gene expression in bladder cells. Cytokine profiling showed that EV-LPS has a role modulating the immune response when internalized by bladder cells, highlighting a key factor that must be considered when evaluating functional studies of bacterial RNA.

Keywords: *Escherichia coli*, extracellular vesicles, RNA, bladder cells, lipopolysaccharide

OPEN ACCESS

Edited by:
Olga N. Ozoline, Institute of Cell Biophysics (RAS), Russia

Reviewed by:
Heon-Jin Lee, Kyungpook National University, South Korea
Juan José González Plaza, Czech University of Life Sciences Prague, Czechia

***Correspondence:**
Simon Swift
s.swift@auckland.ac.nz

Specialty section:
This article was submitted to Protein and RNA Networks, a section of the journal Frontiers in Molecular Biosciences

Received: *07 July 2020*
Accepted: *03 September 2020*
Published: *25 September 2020*

Citation:
Dauros-Singorenko P, Hong J, Swift S, Phillips A and Blenkiron C (2020) Effect of the Extracellular Vesicle RNA Cargo From Uropathogenic Escherichia coli on Bladder Cells. Front. Mol. Biosci. 7:580913. doi: 10.3389/fmolb.2020.580913

INTRODUCTION

It is well established that extracellular vesicles (EVs), also known as membrane vesicles, are a conserved communication vehicle across prokaryotes (Chernov et al., 2014; Brown et al., 2015; Schwechheimer and Kuehn, 2015; Erdmann et al., 2017). Regardless of the phylogenetic group of origin, EVs are spherical nanostructures derived from the membrane(s) of parental cells that are

released into their extracellular milieu (Gill et al., 2019). Bacterial EVs have been described to carry a diverse molecular cargo (proteins, DNA, RNA, glycolipids, organic small molecules) derived from assorted cellular origins (Nagakubo et al., 2020). Evidence has accumulated to show that bacterial EVs are important signaling packages within the microbial community, which quickly react in response to changes in the environment (Caruana and Walper, 2020). A recent overview of all bacterial EV types has suggested that the two main routes of EV biogenesis, namely, membrane blebbing and cell lysis, strongly influence the EV composition (Toyofuku et al., 2019). The mode of EV biogenesis can be favored by environmental conditions. For example, antibiotics known to cause DNA damage such as fluoroquinolones trigger a SOS response and lyse cells to induce the production of EVs with a double bilayer EV morphology and predominantly cytoplasm-derived protein content (Devos et al., 2017).

When the bacterium's environment is a mammalian host, EVs are tailored to secure the cell's survival. In this context, bacterial EVs have been reported with diverse roles in the infection process such as host colonization (Chen et al., 2017), protection against antimicrobials (Chatterjee et al., 2017; Karthikeyan et al., 2020), modulation of the host's immune response (Davis et al., 2006; Vdovikova et al., 2017), and biofilm formation (Yonezawa et al., 2009; Wang et al., 2015; Grande et al., 2017). Thus, there is a growing need to understand how the host's cues may specifically impact bacterial EV production and composition, ultimately affecting their biological roles during infection.

Iron is an essential nutrient for many cellular processes of all microorganisms. In the human body and due to its toxicity, most available iron is sequestered, bound to proteins, and therefore restricted as a resource for bacteria (Andrews et al., 2003; Cassat and Skaar, 2013). This scenario in the host, which is part of the innate antimicrobial defense, may be sensed as a signal for the infecting pathogen. Iron-dependent regulators sense iron restriction and activate expression of genes encoding the pathogen's specific iron acquisition and storage mechanisms needed for survival and at the same time influence a number of other processes, including expression of virulence factors, biofilm formation, acid-shock responses, expression of antigens, and regulation of small RNAs (Dauros-Singorenko and Swift, 2014).

Extracellular Vesicles may also have roles in the process of iron acquisition. For example, in *Mycobacterium tuberculosis*, an iron-restricted environment increases overall EV production along with an EV-mediated iron-scavenging capacity enabling survival of iron-starved cells (Prados-Rosales et al., 2014). In *Pseudomonas aeruginosa*, EVs carrying iron bound to quinolone quorum sensing signals can be scavenged by cells by a Type 6 Secretion System substrate, contributing to survival in iron-depleted environments (Lin et al., 2017). In uropathogenic *Escherichia coli* (UPEC), iron availability in growth conditions can change the biophysical properties of EVs, suggesting modifications in EV composition (Dauros-Singorenko et al., 2017). Moreover, while the quantity of EVs produced by extraintestinal pathogenic *E. coli* is not affected by iron starvation, changes in the EV proteome reflect a stressed cellular state (Chan et al., 2017). Finally, we have seen that iron-replete conditions cause UPEC EVs to be enriched in outer membrane components, while low iron conditions caused no enrichment, suggesting evidence of two different EV biogenesis mechanisms or differential packaging dependent on iron availability (Hong et al., 2019).

Importantly, we identified that UPEC-derived EVs carried proteins enriched in ribosome-related processes, themselves carriers of RNA (Hong et al., 2019). RNA is considered an important and complex communication signal within eukaryotes, prokaryotes, or trans-kingdom (Zeng et al., 2019). Particularly, bacterial small RNAs (sRNA) are reported to modulate gene expression through several mechanisms to control multiple aspects of their life cycle (Storz et al., 2011). Of significant importance to infectious diseases is the utility of RNA-dependent control of virulence factor expression during infection (Quereda and Cossart, 2017). RNA association with EVs has been confirmed in many microorganisms (Sjöström et al., 2015; Blenkiron et al., 2016; Choi et al., 2016). Only a handful of investigations have investigated the functionality of these EV RNAs during the infection on their target host cell with particular roles in subversion of the immune system (Dauros-Singorenko et al., 2018). Examples of such studies include a tRNA fragment identified in *Pseudomonas aeruginosa* EVs demonstrated to reduce EV-induced IL-8 secretion in human bronchial epithelial (HBE) cells (Koeppen et al., 2016) and microRNA-sized RNA fragments identified in periodontal pathogen EVs that reduce IL-5, IL-13, and IL-15 secretion in lymphocytes Jurkat T-cells (Choi et al., 2017). Additionally, periodontal pathogen *Aggregatibacter actinomycetemcomitans* whole EV-RNA cargo induces TNF-α in *in vitro* induced U937 macrophages while also traveling through the blood–brain barrier in mice to induce TNF-α in the brain (Han et al., 2019). Finally, EV-RNA from the foodborne pathogen *Listeria monocytogenes* induces IFN-β in bone marrow-derived macrophages (BMDM), while specific EV-enriched synthesized sRNA species also increase IFN-β in BMDMs and kidney HEK293 cells (Frantz et al., 2019).

Extracellular Vesicles RNA packaging is not however universal. Variations of the RNA composition of EVs in response to different *in vitro* culture conditions have been reported in *Salmonella enterica* Serovar Typhimurium (Malabirade et al., 2018). This study showed that *in vivo* relevant growth conditions to *S. enterica*'s infection life cycle, such as low pH and low phosphate found in the macrophage phagosome or high cell densities that are achieved in the gut extracellular space, induced differential expression of *Salmonella* Pathogenicity Islands in the cell while changing the EV-RNA composition (Malabirade et al., 2018). This highlights the adjustability of the EV-RNA cargo to the growth environment.

Altogether, EV-RNA has potential to be a powerful virulence factor, coupling RNA's intrinsic variability with the protection, targeting, and delivery granted by EVs. Thus, in this study, we investigated if mimicking the human host's protective iron-restriction response could influence *E. coli* EV-RNA and any subsequent effects on bladder cells. We show that RNA preparations from bacterial EVs from pathogenic *E. coli* significantly influence transcription in cultured bladder cells, regardless of their iron availability during growth conditions,

while non-pathogenic EV-RNA does not. However, the pathogen EV-RNA effect is difficult to differentiate from the effects of LPS co-purifying with RNA preparations, as gene expression and cytokine secretion profiles closely overlap. EV-LPS has a role modulating the immune response when internalized by bladder cells, highlighting a key factor that must be considered when evaluating functional studies of bacterial RNA.

MATERIALS AND METHODS

Strains and Culture Conditions

Uropathogenic *E. coli* (UPEC) strain 536 (O6:K15:H31) (Knapp et al., 1986) and probiotic Nissle 1917 (O6:K5:H1) (Nissle, 1918) were grown to exponential phase in iron-restricted RPMI 1640 medium (R) (Thermo Fisher Scientific) or RPMI supplemented with 10 μM $FeCl_3$ (RF), at 37°C with shaking at 200 rpm. The cultures were diluted 1:100 in 2 L of RF or R medium to an optical density (OD) at 600 nm of ∼0.015 and grown to stationary phase for ∼16 h overnight.

EV Purification and Analysis

Extracellular Vesicles methodology is reported as per the Minimal Information for Studies of Extracellular Vesicles (MISEV) 2018 guidelines (Théry et al., 2018). Bacterial cells were depleted from 2 L of culture broth by centrifuging twice at 7,000 × *g* for 10 min at 4°C. Residual cells and large debris were further removed from the supernatant by filtration using a 0.22-μm PES filter (Merck Millipore). Cell-free supernatants were concentrated using a 100 kDa Vivaflow 200 cassette (Sartorius AG) before pelleting EVs by ultracentrifugation at 75,000 × *g* for 2.5 h at 4°C (Avanti J-30I centrifuge with JA-30.50 Ti rotor, Beckman). EV pellets were resuspended in PBS (Sigma-Aldrich) and filtered using a 0.22-μm PES syringe filter and further concentrated using 100 kDa Vivaspin 500 columns (Sartorius AG). The resulting "crude" EV preparation (400–600 μg of EV protein in 500 μL) was loaded into a Size Exclusion Chromatography (SEC) column (qEVoriginal, 70 nm, IZON) following the manufacturer's instructions, with thirteen 0.5-mL eluant fractions collected manually. Reproducibility of this method has been previously described (Dauros-Singorenko et al., 2017).

Extracellular Vesicles fractions were quantified for protein content using bicinchoninic acid (BCA) assay (Thermo Fisher Scientific) according to the manufacturer's instructions. EVs were counted and sized by nanoparticle tracking analysis (NTA) using a NanoSight NS300 system (Malvern Instruments Ltd.). Each sample was diluted 100–10,000 times in PBS, administered at constant flow rate (50 AU) with an automated syringe pump, and recorded in sets of three videos of 30 s each. The data were analyzed using NTA software version 3.0. Camera level varied between 7 and 8, and detection threshold was 5. Each sample was measured in triplicate, and data were combined for analysis.

Each SEC fraction was quantified for protein content and particle counts to determine EV-rich fractions (Fractions 8–10 in Nissle and Fractions 8–11 in UPEC), which were pooled and concentrated with 100-kDa Vivaspin 500 columns. The resulting "pure" EV preparation was stored at −80°C for further use in RNA extraction.

Lipopolysaccharide (LPS) Quantification

Lipopolysaccharide was quantified by EndoZyme recombinant Factor C Endotoxin Detection Assay (Hyglos GmbH, Germany). The procedure was performed as per the manufacturer's instructions. Plates were read on a PerkinElmer EnSpire 2300 plate reader, and the results were expressed in endotoxin units (EU) and transformed to nanograms of LPS by the equation 10 EU/mL = 1.0 ng/mL.

EV-RNA Extraction

Pure bacterial EV preparations were resuspended in TRIzol LS (Thermo Fisher Scientific), 200 μL of chloroform, and 2 μL of 5 mg/mL glycogen (Thermo Fisher Scientific) added. Samples were vortexed for 15 s, incubated for 10 min on ice, and centrifuged at 13,000 × *g* for 10 min at 4°C. The upper aqueous phase was collected and mixed with 1.25 volumes of 100% ethanol, and RNA purified using mirVana RNA isolation kit (Thermo Fisher Scientific), according to the manufacturer's protocol for total RNA isolation. Cultured 5637 human bladder carcinoma cells in TRIzol (Thermo Fisher Scientific) were mixed with 50 μL of miRNA Homogenate Additive (mirVana RNA isolation kit), 100 μL of chloroform, and 2 μL of 5 mg/mL glycogen. Samples were vortexed and incubated for 10 min on ice to continue with protocol as described above for extractions from bacterial EVs. RNA yields were determined by a Qubit 2.0 fluorometer using Qubit RNA HS assay kit (Thermo Fisher Scientific).

Viability Assays

Human bladder carcinoma cells (5637 ATCC HTB-9) were maintained with RPMI 1640 medium supplemented with 10% vol/vol fetal bovine serum (Moregate Biotech). For the assay, bladder cells were seeded in tissue culture-treated 96-well plates and incubated at 37°C and 5% CO_2 to reach a density of 60,000 cells/cm^2. A concentration range of RNA extracted from bacterial EVs (EV-RNA), UltraPure LPS (*E. coli* O111:B4, InvivoGen), Poly I:C at 0.1 μg/mL (polyinosinic–polycytidylic acid sodium salt, Sigma), or R848 at 1 μg/mL (Resiquimod, InvivoGen) was mixed with transfection vehicle Lipofectamine 2000 (LF, Thermo Fisher Scientific), following the manufacturer's instructions. EV-RNA/LF mixtures were added onto bladder cells in triplicate wells along with reduced serum medium Opti-MEM (Thermo Fisher Scientific) with a final volume of 200 μL. Control wells were treated with equivalent amounts of LF. At the 4-h viability assessment, the supernatant (SN) was removed and stored for cytokine assays, and 90 μL of fresh growth medium and 10 μL of PrestoBlue (Thermo Fisher Scientific) were added to each well and incubated for 1 h. Fluorescence (excitation/emission 560 nm/590 nm) was read in a plate reader (EnSpire, PerkinElmer). For the 24-h time point, 4 h SN was discarded from wells and replaced with 200 μL of fresh growth media with growth allowed to continue up to 24 h of incubation, whereupon the viability assessment was repeated.

Transcriptome Analysis

Bladder cells were seeded at a density of 50,000 cells/cm^2 in tissue culture-treated 24-well plates and incubated at 37°C and 5% CO_2. Forty-eight hours later, 2 ng/mL of EV-RNA or 1000 ng/mL of LPS mixed with Lipofectamine was added onto triplicate bladder cell wells along with reduced serum medium Opti-MEM with a final volume of 1 mL. Control/untreated wells contained cells treated with PBS. After incubation for 4 h, SN was removed, and 500 μL of TRIzol was added to adherent cells, resuspended, and stored at −80°C until RNA extraction. Transcriptomic profiling of RNA from treated bladder cells was performed using Affymetrix Clariom S Human GeneChip arrays (Thermo Fisher Scientific) as a contract service by the Auckland Genomics facility. Quality control, normalization, and differential gene expression analysis was performed using Transcriptome Analysis Console (TAC) Software Version 4.0.2.15 (Thermo Fisher Scientific). Analysis of variance across all conditions was performed with ANOVA *F*-test, and false discovery rate (FDR) p-value < 0.0001 was considered significant. Differential gene expression in pairwise comparisons (compared to untreated) were included as significant with fold changes (FC) > 2 or -2, $p < 0.05$ and t-test with FDR $p < 0.05$. Array data has been deposited in the GEO database[1] accession number GSE148711.

Pathway Analysis

Pathway analysis was performed with upregulated genes from pairwise comparisons in PANTHER http://www.pantherdb.org/(Mi and Thomas, 2009; Mi et al., 2019) version 14.1 from the 2018_04 release of the Reference Proteome dataset. The following selections were used in the analysis: PANTHER Overrepresentation Test (Released 20190711); Annotation Version and Release Date: Reactome version 65 Released 2019-12-22; Reference List: Homo sapiens (all genes in database); Test Type: Fisher's Exact with FDR $p < 0.05$.

Cytokine Profiling

Cytokine quantification on cell culture SN from viability assays was performed using a human cytokine/chemokine magnetic bead panel, premixed with 29-plex immunology assay in a 96-well plate (MILLIPLEX MAP). The assay was performed according to the manufacturer's instructions, and the plate was read and analyzed with a Luminex MAGPIX instrument.

RESULTS

Iron Culture Conditions Do Not Determine EV RNA Total Content

Extracellular Vesicles from pathogenic UPEC 536 (UPEC) and probiotic Nissle 1917 (Nissle) *E. coli* strains were purified from 3 independent replicate cultures. Each EV crude preparation was purified by SEC and resulting fractions quantified in protein and particle counts to demonstrate EV enrichment in fractions (Dauros-Singorenko et al., 2017). EV morphological analysis on these types of samples by transmission electron microscopy has been previously described (Hong et al., 2019).

There were no significant differences in the overall particle count or protein content of EVs isolated from either UPEC or Nissle, grown in iron starved (R) or iron replete (RF) conditions (**Figures 1A,B**). Similarly, the RNA concentration of EVs showed no significant differences between strains or iron conditions (**Figure 1C**).

Extracellular Vesicles from Gram-negative bacteria constitutively harbor LPS (Ellis and Kuehn, 2010); thus, we questioned if RNA from EVs could co-isolate with LPS. LPS was indeed found in all EV-RNA preparations. No differences were found in LPS from EV-RNA preparations between cells grown in two iron conditions (**Figure 1D**), although UPEC EV-RNA contained 10 times more LPS than Nissle EV-RNA (UPEC EV-RNA LPS mean of 263 ng of LPS/ng of RNA, Nissle EV-RNA LPS mean of 24 ng of LPS/ng of RNA).

Bacterial EV-RNA Is Not Cytotoxic to Bladder Cells

We next set out to determine the phenotypic effect of bacterial EV-RNA on mammalian cells, by analyzing the viability of cultured bladder cells after treatment. To mimic EV-mediated entry into cells, RNA was mixed with a liposome-forming transfection agent prior to treatment. Previously, we have shown that UPEC EVs are quickly taken up by bladder cells (within 2 h) and 1% of delivered EV-RNA can be detected in the same time frame (Blenkiron et al., 2016). In line with this, two concentrations of EV-RNA were tested (dose of 0.5 ng or 2 ng EV-RNA/mL) in order to determine and confirm a non-toxic dose and time point for further studies. At 4 and 24 h posttreatment, there was no significant difference in the viability of cells treated with either dose of EV-RNA from UPEC or Nissle irrespective of whether the cultures from which the EVs were purified were grown in iron-sufficient (RF) or iron-restricted (R) conditions (**Figures 2A–D**). LPS (1000 ng/mL) showed no cytotoxic effect at 4 h but gave a pronounced effect on cell viability in Nissle at 24 h, averaging 30–40% reduction in viability when compared to control. These results suggest that overall, there is no effect on cell viability from EV-RNA. Consequently, we chose 2 ng/mL as a non-cytotoxic treatment dose and 4 hours as the time point for further early response experiments.

Transcriptomic Response of Bladder Cells to RNA Isolated From Bacterial EVs

To investigate the early effects of EV-RNA on bladder cells, transcriptome analysis was performed on bladder cells treated for 4 h with 2 ng/mL of EV-RNA from UPEC 536 (U) and Nissle 1917 (N) grown in iron-sufficient (RF) and iron-restricted (R) media. For comparison, bladder cells were challenged with LPS at two doses, 1000 ng/mL (HL) and 8 ng/mL (LL). HL and LL treatment doses were chosen based on the highest and lowest LPS contents found in RNA preparations of UPEC EV-RNA and Nissle EV-RNA, respectively.

[1] https://www.ncbi.nlm.nih.gov/geo/

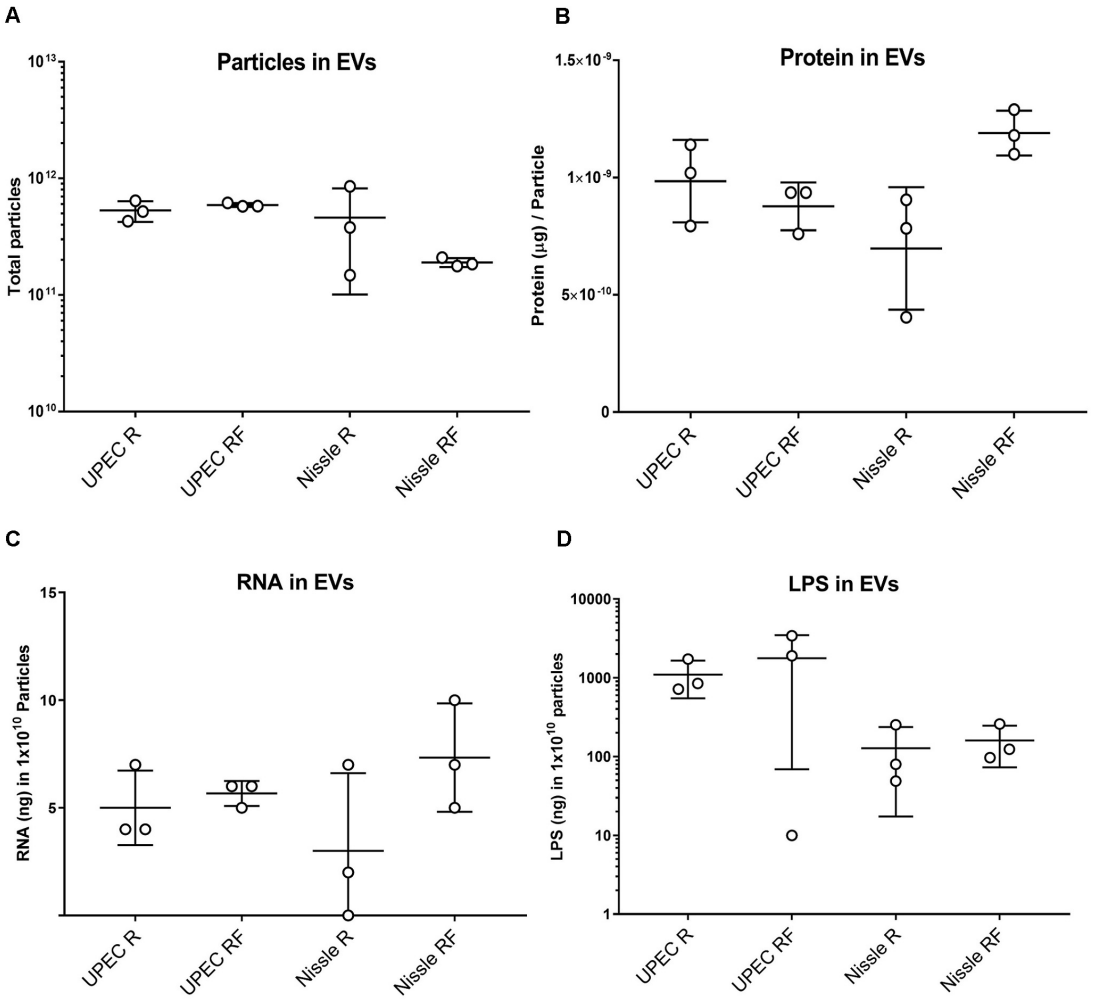

FIGURE 1 | Comparison of molecular content in SEC-purified EVs isolated from UPEC and Nissle grown with different iron availabilities (low iron R and high iron RF). **(A)** Total particles in EV preparations. **(B)** Protein content in EV preparations (µg of protein per particle). **(C)** RNA content in EV preparations (ng of RNA in 10^{10} particles). **(D)** LPS content in EV preparations (ng of LPS in 10^{10} particles). Data showing mean and standard deviation from three biological replicates.

Firstly, unsupervised clustering was performed on all samples using the most significantly differential genes across all conditions (ANOVA *F*-test FDR $p < 0.0001$). Clustering using expression levels of these highly variable genes identified two main groups: Cluster 1, UPEC RF EV-RNA (URF), UPEC R EV-RNA (UR), high-dose LPS (HL) and Cluster 2, Nissle RF EV-RNA (NRF), Nissle R EV-RNA (NR), low-dose LPS (LL), and untreated (UT) (**Figure 3A**). Selected genes with the most significant FDRs are shown in **Figure 3B**, where a high gene expression in treatments with UR and URF EV-RNA is evident and also seen in the High LPS treatment. A low dose of LPS (LL), a treatment selected due to the average LPS amount found in Nissle EV-RNA, consistently showed gene expression similar to Nissle EV-RNA-treated cells. From literature review, it is clear that the most significantly differential genes across conditions are involved in immune response (**Table 1**). Upregulation of common genes such as *EGR1* and *CXCL8* in HL, UR, and URF conditions suggests that this effect may be in part due to the higher levels of LPS contamination in UPEC EV-RNA samples than in Nissle EV-RNA.

Iron-Mediated Effect of Bacterial EV-RNA on Host Cell Transcriptional Pathways

For a detailed exploration of effects of EV-RNA on bladder cell gene expression, we performed pathway analysis on all regulated genes from selected pairwise comparisons (FC > 2 or -2 and *t*-test FDR $p < 0.05$) using PANTHER (Mi and Thomas, 2009; Mi et al., 2019). Comparisons of UPEC EV-RNA treatments UR, URF, or HL individually to the untreated (UT) revealed 25, 25, and 37 upregulated genes, respectively (**Figure 4A**). Only URF had significantly downregulated genes compared to untreated (8 genes). From the diagram in **Figure 4B**, we can see that most upregulated genes (19) are shared between the three treatments, with one gene being unique to URF and 4 to UR. These results corroborate that a large part of the effect of pathogenic UPEC

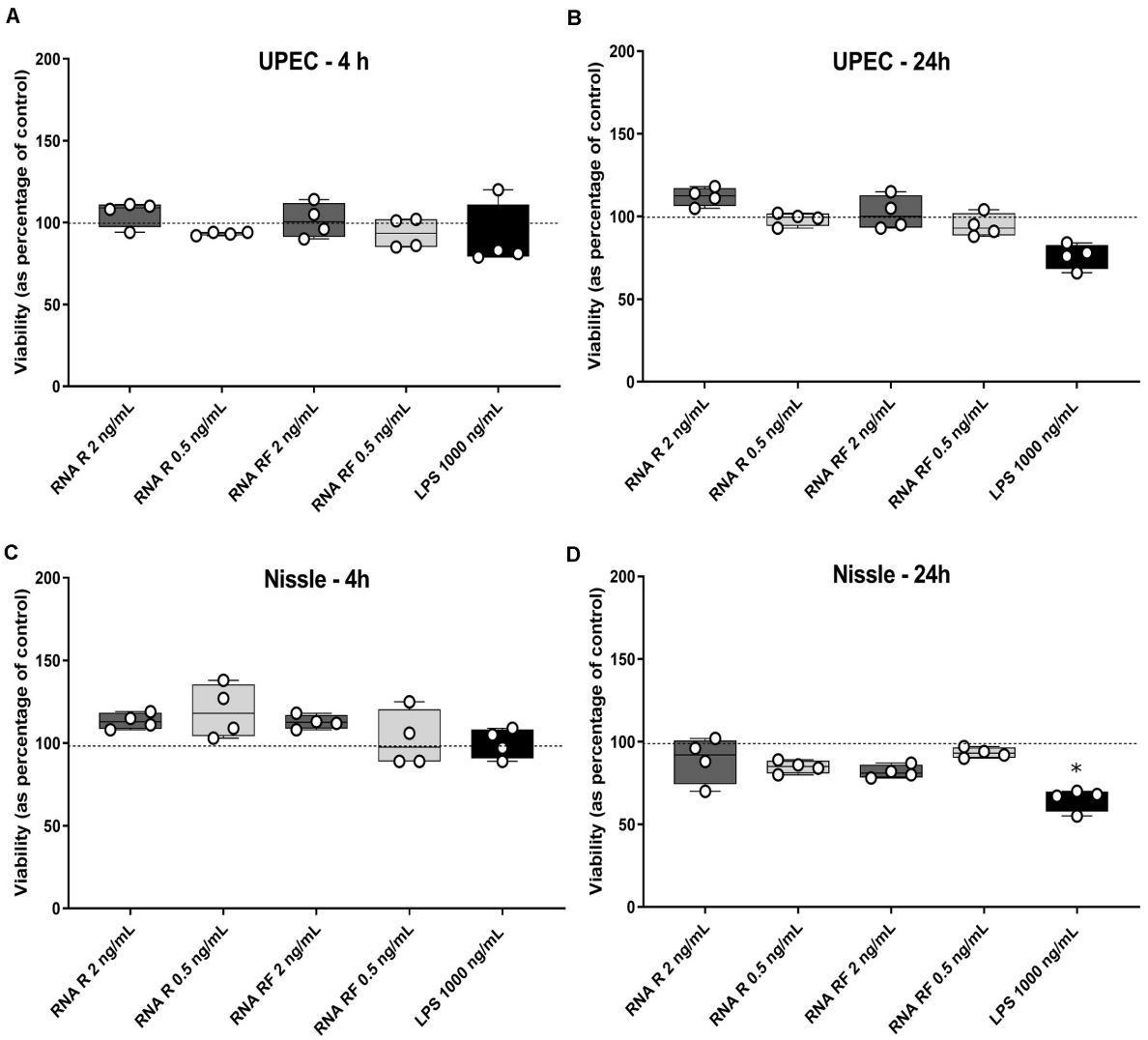

FIGURE 2 | EV-RNA is not cytotoxic to cultured bladder cells. Viability of cultured bladder cells treated with UPEC and Nissle EV-RNA for 4 h **(A,C)** and 24 h **(B,D)**. Viability shown as percentage of control (transfection agent only in dotted line). Data plotted as box and whiskers (box represented by upper and lower quartile, line = median, bars = min and max values) of 4 replicates (circles) and stars denote significant differences compared to control (transfection agent only) determined by one-way ANOVA Kruskal–Wallis and Dunn's posttest ($p < 0.05$).

EV-RNA may be attributed to its LPS content, more than any effect from the bacterial growth conditions and differential EV-RNA packaging.

Pairwise comparisons of Nissle EV-RNA, R, and RF to the UT showed no significantly regulated genes with a FDR $p < 0.05$; therefore, no pathway analysis could be performed. This suggests that the overall RNA cargo from Nissle EVs does not elicit a significant transcriptomic response in bladder cells compared to the normal growth course of these cells.

Reactome pathway analysis in cells treated with UPEC EV-RNA or LPS revealed that there is a significant overlap of pathways induced by these treatments (**Figure 4C**). Pathways such as inactivation of "Interleukin-1 processing," "Interleukin-10 signaling," "Interleukin-4 and Interleukin-13 signaling," "Interleukin-1 signaling," "Chemokine receptors bind chemokines," and "Innate Immune System" are strongly enriched due to shared upregulation of cytokine genes *IL6*, *CXCL8*, *IL1A*, *IL1B*, *CCL20*, *CXCL2*, and *CXCL1*. A second subset of enriched pathways is shared among the three treatments UR, URF, and HL: "RAF-independent MAPK1/3 activation" and "Negative regulation of MAPK pathway." Upregulated genes of dual-specificity phosphatases (*DUSP1*, *DUSP4*, *DUSP5*, and *DUSP6*) are responsible for inactivating the mitogen-activated protein kinase (MAPK) pathway, which communicates extracellular signals to gene expression changes affecting cell-cycle progression and survival (Lang and Raffi, 2019). Another extracellular signal pathway "PIP3 activates AKT signaling" is overrepresented only in HL and URF treatments, mainly due to upregulation

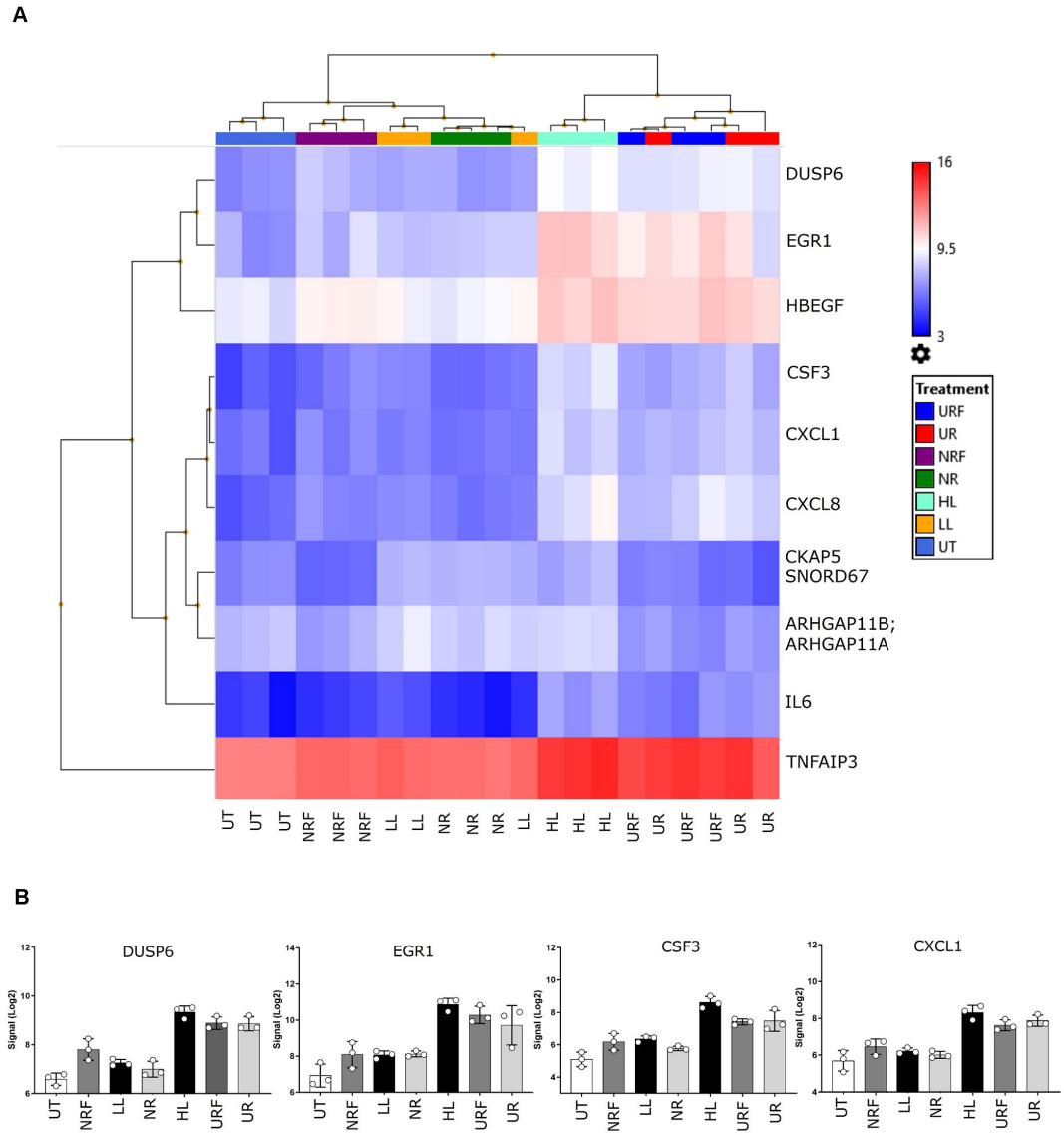

FIGURE 3 | Transcriptional response of bladder cells to bacterial EV-RNA. **(A)** Unsupervised clustered heat map of analysis of variance in expression array data from bacterial EV-RNA or LPS-treated bladder cells selected for the most significantly regulated genes across all conditions (ANOVA $p < 0.05$, FDR $p < 0.0001$) on the *Y*-axis and all treatments on the *X*-axis ($n = 3$). Color scale indicates intensity of signal (Log2) in arbitrary range, blue gradient < 9.5 < red gradient. **(B)** Gene expression of selected genes across all treatments, intensity of signal (Log2) on the *Y*-axis and all treatments on the *X*-axis. Data plotted as mean and SD of 3 replicates. HL, high dose of LPS (1000 ng/mL); LL, low dose of LPS (8 ng/mL); NR, Nissle EV-RNA from iron-starved conditions; NRF, Nissle EV-RNA from iron-replete conditions; UR, UPEC EV-RNA from iron-starved conditions; URF, UPEC EV-RNA from iron-replete conditions; UT, untreated PBS control.

of genes *JUN*, *EGR1*, *CDKN1A*, *IER3*, and *HBEGF*, whereas the enrichment of pathway "Dissolution of Fibrin Clot" is unique to HL treatment.

Effect of EV-RNA on Host Secretome

In order to determine the early EV-RNA effect on cellular immune responses, cytokine secretion assays were performed on conditioned media from EV-RNA-treated bladder cells after 4 h of treatment. Firstly, we investigated whether the effects of EV-RNA on IL-8 are caused solely by the contaminant LPS cargo. Comparison of gene expression and cytokine secretion data from bladder cells treated with UPEC EV-RNA or LPS revealed that at 4 h *CXCL8* transcripts increase, to a similar extent, in response to LPS or EV-RNA, regardless of the iron culture conditions (**Figure 5A**). Conversely, while IL-8 cytokine secretion was induced at 4 h after LPS challenge, there was no substantial response to UPEC EV-RNA (**Figure 5B**).

Next, investigating the dose response of host cells to EV-RNA from different strains, we observed that secretion of IL-8 was inversely proportional to the amount of EV-RNA from UPEC, i.e., 0.5 ng/mL of EV-RNA induced secretion of 1.6 × more IL-8 protein than when cells were treated with 2 ng/mL EV-RNA

TABLE 1 | Differentially expressed genes driving grouping of the two distinctive treatment clusters.

Gene	FDR p-value	Function
DUSP6	1.09E-06	Dual-specificity phosphatase 6; inactivates ERK1/2 in cytoplasm, which mediates cell division, migration, and survival
CSF3	3.53E-06	Granulocyte-colony-stimulating factor (G-CSF); stimulates the survival, proliferation, differentiation, and function of neutrophils.
CXCL8	6.63E-06	Chemokine (C–X–C motif) ligand 8 (interleukin 8), proinflammatory cytokine recruits and activates neutrophils during inflammation
CXCL1	6.63E-06	Chemokine (C–X–C motif) ligand 1 (GROA); induces neutrophil release from the bone marrow and recruits them to inflammation site
IL6	9.41E-06	Interleukin 6, pro-inflammatory cytokine inducing synthesis and secretion of acute-phase proteins by the liver
EGR1	1.90E-05	Early growth response protein 1, transcriptional regulator (activator) of genes involved in differentiation and mitogenesis
HBEGF	4.38E-05	Heparin-binding EGF-like growth factor, involved in cell growth and tumor progression
TNFAIP3	4.38E-05	Tumor necrosis factor alpha-induced protein 3; inhibits NF-kappa B activation, limiting inflammation
CKAP5; SNORD67	5.63E-05	Cytoskeleton-associated protein 5 (CKAP5), roles in spindle formation during mitosis; small nucleolar RNA (SNORD67), modifies other snRNAs which help in processing pre-mRNA
ARHGAP11A; ARHGAP11B	6.81E-05	ARHGAP11A encodes a Rho GTPase-activating-protein; ARHGAP11B (truncated version of ARHGAP11A), does not show RhoGAP activity

(**Figure 5C**). This effect was seen for EV-RNA isolated from UPEC in both iron growth conditions. Treatment with Nissle EV-RNA did not however induce IL-8 secretion (**Figure 5C**).

Next, we characterized secretion of pro-inflammatory cytokines, by treating cells with a known TLR3 dsRNA-response inducer Poly I:C (Alexopoulou et al., 2001), a TLR7/8 ssRNA-response inducer R848 (Jurk et al., 2002), 1000 ng/mL of LPS delivered to culture media (free LPS), or 1000 ng/mL of LPS delivered to the cytoplasm with Lipofectamine (LF-LPS). **Figure 5D** shows that both Poly I:C and LF-LPS induce IL-8 (and GM-CSF, **Supplementary Figure S1A**) secretion to a similar range, unlike R848 which is unaltered from control. Cytokines IL-6 (and TNF-α, **Supplementary Figure S1B**) and IL-1α are strongly induced preferentially by Poly I:C and LPS, respectively (**Figures 5E,F**), when cell viability at the time of cytokine assessment was similar for all treatments (**Supplementary Figures S1C,D**). INF-α2 levels were below the sensitivity of the assay for all treatments (data not shown). It is worth noting that extracellular free LPS and R848 did not trigger any cytokine secretion in bladder cells, suggesting that TLR4 LPS cell surface receptor and TLR7/8 ssRNA receptor are somehow not responsive in these bladder cells.

Since cellular transcriptomic and cytokine analyses revealed no substantial differences between the effect of EV-RNA from R and RF conditions (**Supplementary Figure S1E**), from here on we present the effects of EV-RNA cargo secreted under iron-limiting R conditions, as the most relevant growth scenario in the host (Robinson et al., 2018).

One hypothesis for the role of EV-RNA in pathogenesis would be to dampen the immune response that is triggered by other secreted bacterial components (Koeppen et al., 2016; Choi et al., 2017). To investigate this, we treated cells with EV-RNA (0.5 or 2 ng/mL), LPS (1000 ng/mL), or a combination of EV-RNA and LPS delivered to the cytoplasm using Lipofectamine. We hypothesized that the EV-RNA would reduce cytokine secretion initiated by LPS when treated in concert. A dose of 2 ng/mL of UPEC EV-RNA supplemented with LPS was found to reduce IL-8 and IL-1α secretion, in average by 53 and 54%, respectively, when compared to the same dose of LPS alone, suggesting that internalization of UPEC EV-RNA cargo in bladder cells suppresses a simultaneously induced LPS response (**Figures 5G,I**). In contrast, the dsRNA-induced response is unaltered by cotreatment with LPS and UPEC EV-RNA, characterized by a stable IL-6 and TNF-α secretion throughout all treatments (**Figure 5H**, **Supplementary Figure S1F**).

For Nissle EV-RNA, induction of IL-8, IL-6, and IL-1α secretion was only seen when LPS was added (**Figures 5J–L**, respectively). TNF-α, in turn, remained unchanged regardless of LPS addition (**Supplementary Figure S1G**), becoming apparent that IL-6 and TNF-α are differentially regulated by Nissle EV-RNA. Addition of LPS to 2 ng/mL Nissle EV-RNA caused a smaller reduction (∼24%) of IL-1α secretion compared to LPS alone, suggesting that the dampening of IL-1α LPS-induced response in presence of EV-RNA might be modulated by the concentration of native LPS found in EV-RNA.

DISCUSSION

Extracellular Vesicles structure in Gram-negative bacteria is largely determined by their biogenesis mechanism. EVs generated by blebbing of the outer membrane (OM) are enriched in outer membrane components, including large quantities of LPS. In these OM-derived EV types, LPS can be highly abundant in a 10:1 ratio compared to the protein content (Ellis and Kuehn, 2010). EVs generated by an explosive lysis mechanism will contain outer and inner membrane components, and cytosolic ones, such as RNA (Toyofuku et al., 2019). As significant amounts of LPS were found in RNA extractions from EVs, we highly recommend that LPS in EVs should not be overlooked, especially its persistence in samples when investigating other molecules of interest, such as our RNA extractions. Many LPS extraction methods overlay with RNA extraction methods (Johnson and Perry, 1976), even with the use of ready-made RNA-extracting commercial reagents (Yi and Hackett, 2000). Native EVs in an infection carry both RNA and LPS;

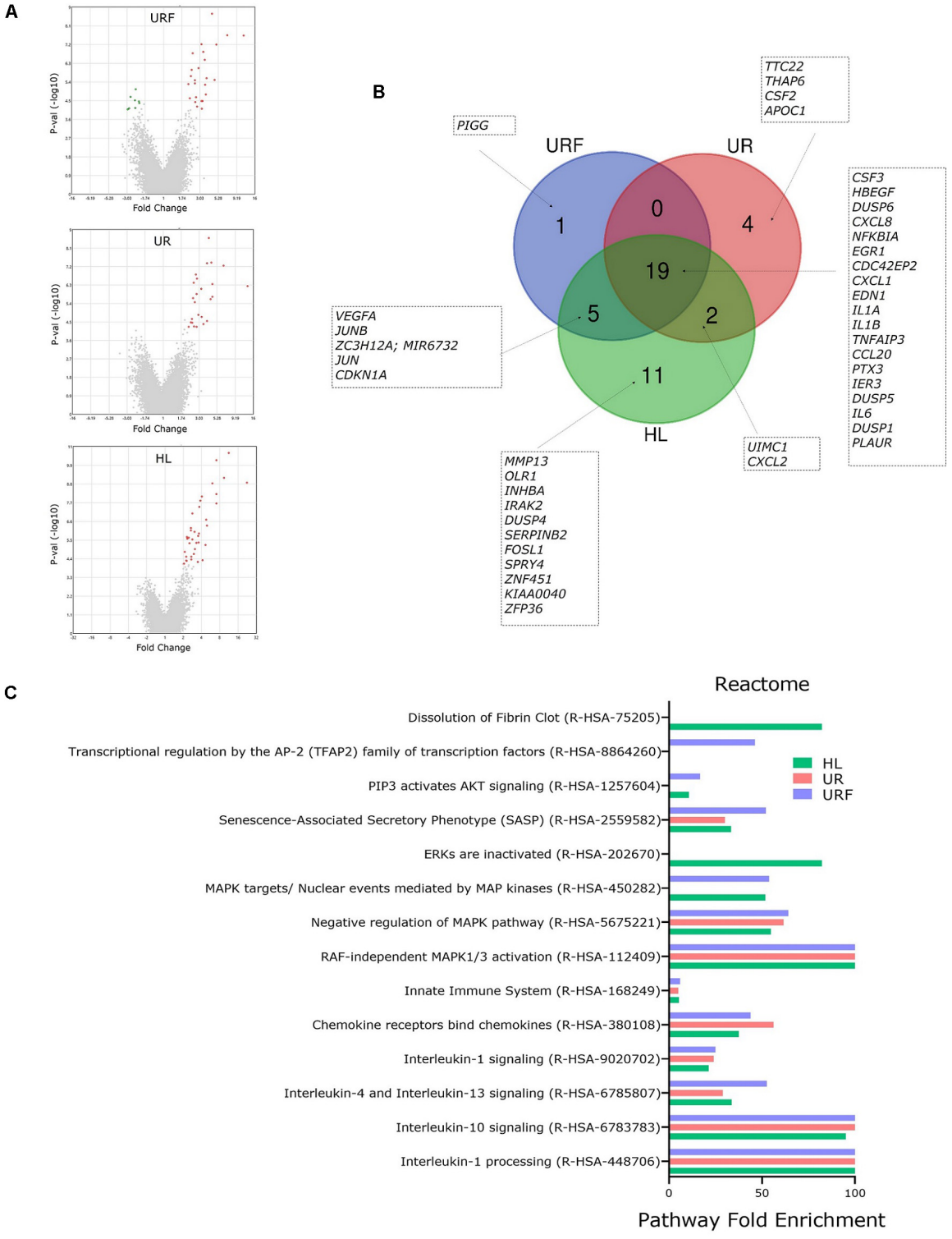

FIGURE 4 | Pathway analysis of regulated genes in bladder cells treated with iron-responsive UPEC EV-RNA. **(A)** Volcano plots of all regulated genes in bladder cells in response to UPEC EV-RNA or LPS treatments (compared to untreated control). **(B)** Venn diagram with details of upregulated genes in bladder cells in response to UPEC EV-RNA or LPS treatments (compared to untreated control). **(C)** Pathway analysis performed by PANTHER Overrepresentation Test, using Reactome annotation dataset in upregulated genes in bladder cells in response to UPEC EV-RNA or LPS treatments (compared to untreated control). Enriched pathways (FDR $p < 0.05$) are shown in *Y*-axis and fold enrichment in *X*-axis. UR, UPEC EV-RNA from iron-starved conditions; URF, UPEC EV-RNA from iron-replete conditions; HL, high dose of LPS (1000 ng/mL).

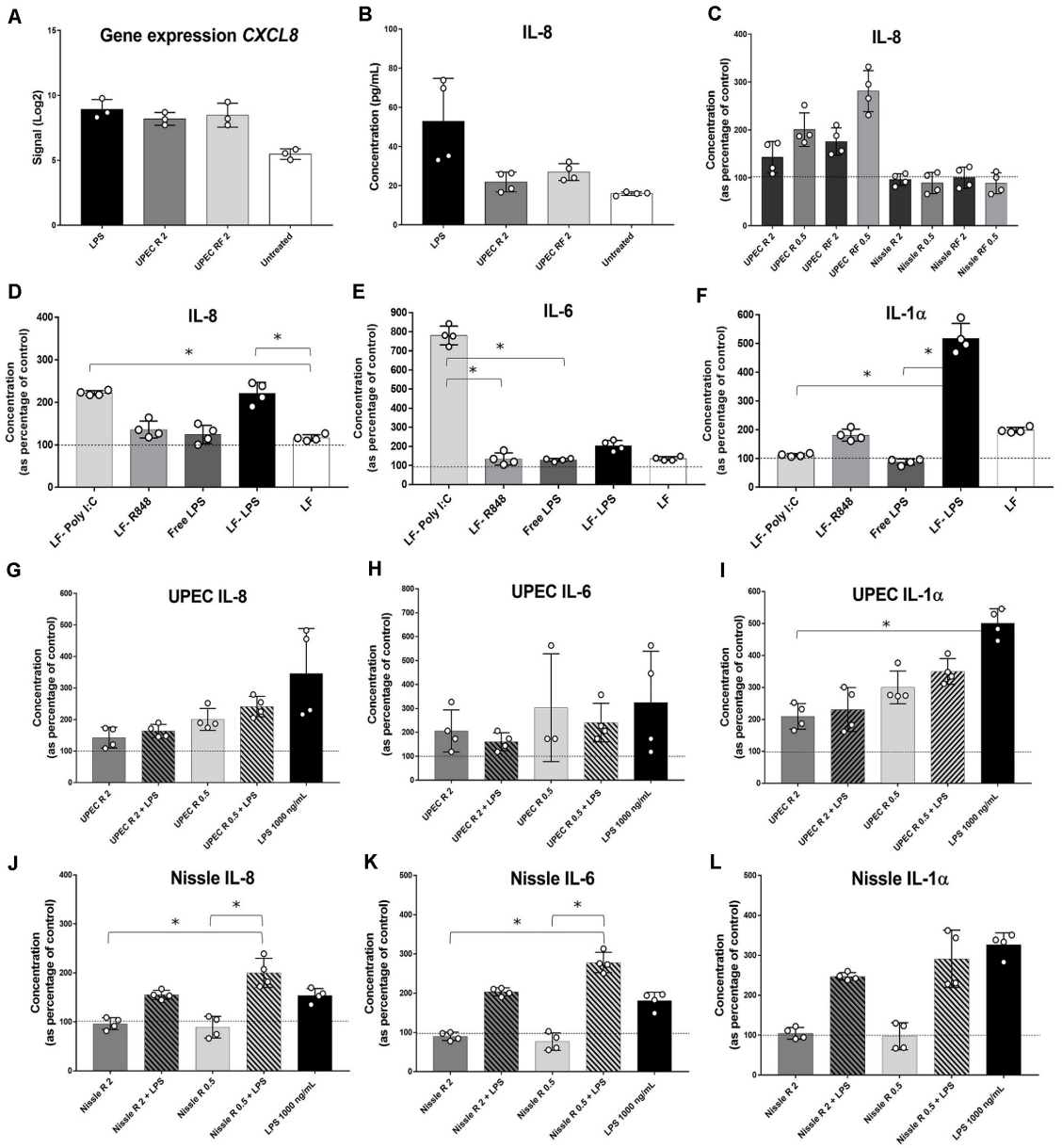

FIGURE 5 | Cytokine profiling in bladder cells in response to EV-RNA. **(A)** Gene expression of *CXCL8* assessed by microarray. **(B–F,H–L)** bladder cells treated with different treatments for 4 h, after which supernatants were assessed by Luminex assays. UPEC, EV-RNA from UPEC strain; Nissle, EV-RNA from Nissle strain; R, EV-RNA obtained from iron-limiting culture conditions; RF, EV-RNA obtained from iron-sufficient culture conditions; 2, EV-RNA at 2 ng/mL; 0.5, EV-RNA at 0.5 ng/mL; LPS, LPS at 1000 ng/mL delivered with transfection agent unless stated, Free-LPS; LF-Poly I:C, Poly I:C delivered with transfection agent; LF-R848, Resiquimod R848 delivered with transfection agent. Data is plotted as mean and SD of 4 replicates, concentration in *Y*-axis as percentage of control (transfection agent only in dotted line in **C**,**G–L**; PBS only in dotted lines in **D–F**). Stars denote significant differences between treatments determined by one-way ANOVA Kruskal–Wallis and Dunn's posttest ($p < 0.05$).

therefore, their contribution to an effect in the host should be analyzed conjointly.

Differences in the amount of EV-associated LPS were identified here between *E. coli* strains, regardless of pathogenic UPEC 536 and non-pathogenic Nissle 1917 belonging to the same O6 serotype. This effect has been previously reported between pathogenic and non-pathogenic *E. coli* EVs (Behrouzi et al., 2018). Pathogens, such as UPEC, have evolved to succeed in infection, with mechanisms of LPS modification that work toward immune system evasion (Maldonado et al., 2016), ultimately affecting the LPS load in EVs. Although strain differences were seen, we did not find differences in total quantification of LPS content in EVs secreted under iron restriction compared to iron sufficient conditions in both

strains. It is interesting to note, however, that differences in the LPS composition, with shorter O-chains, has been reported in *Helicobacter pylori* EVs released under iron restriction (Keenan et al., 2008), as well as other culture conditions being able to remodel the LPS structure and stability (Needham and Trent, 2013; Sharp et al., 2019). It is unclear to us the mechanistic nature of differences of LPS quantity in EVs between strains used in this study; nevertheless, these differences may have a great impact on the EV uptake by the host cell (O'Donoghue et al., 2017).

From analysis of transcriptomic data in the host cell when exposed to EV-RNA from different strains or two doses of LPS, we could see that probiotic Nissle strain EV-RNA had a minimal effect on cultured bladder cells, and this was similar to the low dose of LPS and untreated cells. It has been reported that Nissle 1917 EVs are taken up; induce secretion of IL-6, IL-8, and TNF-α; and prevent enteropathogenic *E. coli* (EPEC)-mediated barrier disruption in Caco-2 intestinal epithelial cells (Fábrega et al., 2016; Alvarez et al., 2019). It is clear in our study that Nissle 1917 EV-associated RNA cargo is not however involved in any significant transcriptional or cytokine secretion by bladder cells. The most significant changes in gene expression were elicited by pathogen UPEC 536 EV-RNA and a high dose of LPS (1000 ng/mL), clustering together in the heat map from the microarray data. In this study, treatment of 5637 bladder cells with pathogen EV-RNA or high-dose LPS lead to a unique early response cytokine profile characterized by increased gene expression of *IL6*, *CXCL8*, *IL1A*, *IL1B*, *CCL20*, *CXCL2*, and *CXCL1*. All these genes have many layers of transcriptional regulation reflected in part in their promoter regions containing binding sites for numerous transcription factors, such as AP-1, NF-IL6, SP1, and CREB. More importantly, all the aforementioned genes are subject to control of NF-κB, one of the most important transcription factors, central to the pro-inflammatory response in cells (Liu et al., 2017).

Pathway analysis of regulated genes in pairwise comparisons with untreated controls revealed, again, that treatments of high dose of LPS or UPEC 536 EV-RNA induce predominantly the same pathways, falling into two categories: regulation of extracellular signal transduction and secretion of effector cytokines. The regulation of an immune response is complex, where the duration and intensity are tightly regulated and may be substantially dissimilar in different cell types. Dual-specificity phosphatases (DUSPs) are involved in aspects of balancing the response of extracellular signal kinase-mediated pathways, mainly ERK, JNK, and p38 pathways (Ahmad et al., 2018). While specific ligands can induce specific DUSPs, also the same stimulus can generate different DUSP expression responses depending on cell type (Lang and Raffi, 2019). Here, we found that 5637 bladder cells increase expression of *DUSP1*, *DUSP4*, *DUSP5*, and *DUSP6* when challenged with UPEC EV-RNA or LPS. It has been previously reported that DUSP1, DUSP4, and DUSP5 are induced by LPS, and DUSP1, DUSP5, and DUSP6 negatively regulate their corresponding kinase-substrates (Lang and Raffi, 2019). Other DUSPs (e.g., DUSP11) have an affinity for triphosphorylated RNA substrates (bacterial and viral RNA) (Lang and Raffi, 2019); however, we did not find these upregulated.

The immune response to LPS has been extensively investigated; however, it is still far from a complete understanding. Toll-like receptor 4 (TLR4) is the most important cell-surface LPS-sensing mechanism, but it involves many accessory molecules that vary in presence or abundance between species (mouse or human) and among cell types (immune or non-immune cells). Lipid A-binding protein (LBP), CD14, MD-2, and TLR4 have distinctive roles in recognizing extracellular LPS, with the signal activating two main pathways: MYD88 or TRIF (Steimle et al., 2016). The MYD88 pathway recruits several kinases (e.g., MAPK, IKK), which then cascades into activation of transcription factors AP-1 and NF-κB, leading to upregulation of pro-inflammatory cytokines such as IL-6, IL-18, IL-1β, and tumor necrosis factor (TNF) (Lu et al., 2008). Endocytosis of TLR4 triggers the TRIF pathway activating transcription factor IRF3 and late-phase activation of NF-κB, resulting in upregulation of type-I interferon (IFN) (Rosadini and Kagan, 2017). Intracellular LPS-sensing occurs through the cytosolic multiprotein complex NLRP3 inflammasome, requiring two independent events (Steimle et al., 2016; Rathinam et al., 2019). Firstly, a TLR-mediated signal must induce the expression of inflammasome members and translation of inactive pro-IL-1β and pro-IL-18 pro-inflammatory cytokines. Secondly, caspase 4 or 5 binds directly to LPS in the cytosol, with the subsequent activation of the NLRP3 inflammasome and pro-IL-1β and pro-IL-18 cleavage by caspase 1, leading to pyroptosis death (Diamond et al., 2015; Barker and Weiss, 2019). In this study, transcription of *IL1B* was increased in bladder cells exposed to UPEC 536 EV-RNA or LPS; however, *NLRP3* transcripts were unaffected by these treatments.

RNA-sensing occurs through intracellular endosome receptors. TLR3 detects dsRNA and signals via the TRIF pathway, whereas TLR7/8 detects dsRNA and activates the MYD88 pathway (Heil et al., 2004; Biondo et al., 2012). There is also accumulating evidence of activation of NLRP3 inflammasome by bacterial RNA in immune cells (Sander et al., 2012; Sha et al., 2014; Vierbuchen et al., 2017); however, there is no defined cytosolic RNA-binding receptor directly linked with the inflammasome. In this study, there were no genes exclusively induced by EV-RNA, suggesting that the LPS content in our EV-RNA samples is fundamental in overall responses seen in bladder cells to UPEC 536 EV-RNA.

The majority of receptor-induction, signaling pathways and effector outcomes have been deciphered in immune cells and show that the choice and intensity of the immune response depends on the specific cell type, making many reports not directly translatable to the scenario seen in, for example, epithelial cells. Here, characterization of the response of cultured bladder cells to known RNA inducers showed us a differential response to RNA mimics or LPS. We saw that dsRNA (Poly I:C, TLR3) strongly induces IL-6 and TNF-α, while ssRNA (R848, TLR7/8) and LPS do not. This is in contrast to reports of other similar cell lines, intestinal Caco2 or kidney 293T, which are not responsive to Poly I:C (Alexopoulou et al., 2001). In macrophages, transfected dsRNA binds to TLR3, with subsequent NF-κB activation and secretion of IL-6, IL-12, TNF, and type 1 IFN (Alexopoulou et al., 2001). We found negligible amounts of IFN-α2, a type I IFN,

released from treated bladder cells, suggesting no activation of transcription factor IRF3. These characterizations suggest that 5637 cells are inherently responsive to TLR3-dsRNA-NF-κB-IL-6/TNFa but not to TLR7/8-ssRNA-IRF3-IFN signaling.

When we sought to analyze the dynamic of LPS sensing by the TLR4 surface receptor, we saw that 1000 ng/mL of LPS delivered to extracellular space did not induce any cytokine secretion in 5637 bladder cells at 4 h of treatment. This outcome is in contrast with other studies where 5637 bladder cells express TLR4 accessory molecule CD14, their transcription factor NF-κB is active, and 6-h treatments with 1000 ng/mL of LPS or 3-h treatments with 5000 ng/mL of extracellular LPS increased IL-6 secretion significantly (Schilling et al., 2003; Shimizu et al., 2004; Hunstad et al., 2005). Discrepancies between this and the published studies may be due to different LPS used in the assays, *E. coli* 0111:B4 and *E. coli* O55:B5, respectively.

We observed that cytosolic Lipofectamine delivered LPS strongly induced IL-1α in cultured 5637 bladder cells (more than 400% of control) and mildly induced IL-8 but had no effect on IL-1β, IL-6, and TNF-α secretion. Increased *IL1A* gene expression was seen in cells treated with LPS or UPEC 536 EV-RNA; however, IL-1α secretion into supernatant was only increased by transfected LPS, suggesting posttranscriptional control. TLR4-mediated extracellular LPS stimulation leads to increased secreted IL-1α only when accompanied by NLRP3 inflammasome activation (Fettelschoss et al., 2011); thus, it is unknown to us fully how cytosolic LPS-sensing can induce significant amounts of secreted IL-1α in 5637 cells.

Secreted IL-1β is a strong signature cytokine for NLRP3 inflammasome activation by cytosolic LPS sensing, with a critical role for the development of acute cystitis (Ambite et al., 2016). LPS inflammasome activation has been mainly investigated in immune cells (Vanaja et al., 2016; Santos et al., 2018); however, some non-immune cells may also have this machinery, mostly depending whether caspase 4 is expressed or not (Shi et al., 2014). Specifically, 5637 bladder cells are known to have a responsive NLRP3 inflammasome, as they significantly increase IL-1β secretion when challenged with live *E. coli* UPEC, not commensal strain *E. coli* K-12 (Demirel et al., 2018). Thus, the lack of IL-1β secretion upon treatment with LPS or EV-RNA suggests that neither is able to induce early inflammasome activation in 5637 bladder cells. Guanylate-binding proteins (GBP), important in leaking phagosome content into cytosol, are induced by type 1 IFN (Santos et al., 2018), a cytokine which is absent in SNs from our LPS-treated bladder cells. This information is in accordance with our transcriptomic data, where *IL1B* was induced by LPS alone, possibly due to activation of NF-κB (Di Paolo and Shayakhmetov, 2016), but lacked secretion of the active protein IL-1β, which requires NLRP3 inflammasome-mediated cleavage (Steimle et al., 2016).

Our previous investigations into proteome of EVs showed that UPEC 536 EVs are enriched in rRNA-binding proteins in contrast to Nissle EVs, which are enriched in proteins involved in glycolytic process and ligase activity, leading us to believe that differential packaging of RNA may be causing some of the differences seen between UPEC and Nissle EV-RNA (Hong et al., 2019). A key investigation of this study was to delineate the effects of *E. coli* EV-RNA on host cell responses. UPEC EV-RNA is enriched for rRNA but carries all forms of RNA types (Blenkiron et al., 2016), likely in both ss and dsRNA forms. Bacterial rRNA has been shown to induce IFN in a TLR7-dependent way (Eberle et al., 2009); however, 5637 bladder cells have been found in this study to not be responsive to TLR7/8-ssRNA, and therefore, the use of this cell line may not be fully representative of all cell types.

We hypothesized that culturing bacteria in iron-replete and iron-starved conditions may influence the EV-RNA cargo in a way that would impact transcriptional responses when delivered to cultured bladder cells. Our results did not support this hypothesis, showing no difference in the immune responses of bladder cells when challenged with bacterial total EV-RNA produced under different iron culture conditions. These findings do not invalidate the notion that there might be substantial differences in the RNA composition of EVs isolated from cultures grown in iron-starved and iron-replete conditions. However, in order to investigate this, qualitative assays of greater depth are necessary, such as RNA sequencing.

There are limited publications about the effect of probiotic bacterial RNA on host cells. Transfected mRNA, tRNA, and rRNA from *E. coli* strain ATCC25922 (non-pathogenic) were shown to activate NLRP3 inflammasome and induce IL-1β secretion in human macrophages, an effect independent of double-strand and secondary RNA structure or the presence of 5′-end triphosphate moieties (Sha et al., 2014). Moreover, transfected non-pathogenic *E. coli* total RNA into hepatic stellate cells also induces the NLRP3 inflammasome (Wang et al., 2016).

Combination of treatments of LPS and EV-RNA allowed us to unveil some particular responses in bladder cells. EV-RNA cargo suppresses an LPS-induced IL-1α response, suppression which is proportional to the amount of native LPS in EV-RNA preparations. Since UPEC releases more LPS in their EVs than Nissle, this trait might be an additional virulence advantage.

Although the transcriptome data suggested that much of the early transcriptional response may be confounded by LPS in the EV-RNA, the finding that cotreatment of bladder cells with LPS and UPEC EV-RNA depressed IL-1α secretion is of interest. This suppression response could be explained by development of LPS tolerance in 5637 bladder cells. This is supported by findings of live pathogenic UPEC strains UT189 and NU14 suppressing IL-6 secretion to non-pathogenic *E. coli* K-12 in 5637 bladder cells, an effect which depends on UPEC LPS structure (Hunstad et al., 2005). However, LPS tolerance, shown *in vitro* in immune cells and 5637 bladder cells, leading to subsequent suppression of cytokine TNF-α or IL-6, so far has required prolonged LPS pretreatments and a TLR4-dependent route, as LPS is delivered in extracellular space (Seeley and Ghosh, 2017; Schilling et al., 2003). There is no information about LPS tolerance induced by cytosolic LPS sensing mechanisms nor IL-1α involvement. However, it appears that the ultimate goal of LPS tolerance is to help host cells resist following infections (Seeley and Ghosh, 2017); thus, the EV-LPS-induced response may have important biological consequences in the infection outcome.

Moreover, both dsRNA-induced IL-6 and TNF-α responses were unchanged for UPEC EV-RNA/LPS treatments and dissimilar for Nissle EV-RNA/LPS. These results corroborate that

IL-6 and TNF-α have different regulatory networks under low levels of transfected LPS in 5637 bladder cells. Other authors have previously reported a possible defect in the MYD88/IRAK pathway in 5637 bladder cells, since tolerance to extracellular LPS affects IL-6 and not TNF-α secretion, both transcriptionally regulated by NF-κB (Schilling et al., 2003).

Beyond the challenges with appropriate selection of an active recipient cell line, our study might have limitations regarding a relatively low amount of EV-RNA used throughout all the experiments (2 ng/mL). Our purified EV preparations yielded a mean of 350 ng RNA from 2 L of bacterial cultures, meaning a 0.4-ng EV-RNA treatment dose for bladder cells in 200 μl represents 7×10^8 bacterial EVs purified from ≈2.3 mL of bacterial culture. We can only speculate that this is an EV-RNA dose that could be deliverable *in vivo*. Other studies have used significantly higher amounts, i.e., 1–10 μg/mL of bacterial RNA in immune cells (Eberle et al., 2009; Sander et al., 2012; Sha et al., 2014). Furthermore, our study has focused initially upon the acute effects of a single challenge with EV-RNA, and we acknowledge that the evaluation of a chronic effect, perhaps from experiments providing a continuous and longer exposure to EV-RNA, could offer valuable insights.

It is well established that many UPEC virulence factors are responsible for its pathogenicity, including hemolysins, cytotoxins, fimbriae for attachment, flagella for motility, and siderophores, in addition to the ability to form intracellular bacterial communities (IBC) and biofilms (Subashchandrabose and Mobley, 2015). Many *E. coli* virulence factors can be secreted via EVs (Bielaszewska et al., 2017), which provides the opportunity to elicit their effects at distance, in a targeted manner and prior to contact of bacteria live cells with host cells. In this study, we aimed to expand the knowledge of virulence factors involved in the pathogenesis of urinary tract infection, by deciphering the role of the RNA cargo of UPEC EVs. One of the challenges noted were the substantial levels of LPS found in UPEC EVs, which was likely to explain the early transcriptomic response and suppression of IL-1α secretion in bladder cells. This data highlights the importance of understanding the role of EVs as a complex cocktail of factors, which can have unknown interrelations among one another and certainly pleiotropic effects on the host.

DATA AVAILABILITY STATEMENT

The datasets presented in this study can be found in online repositories. The names of the repository/repositories and accession number(s) can be found below: https://www.ncbi.nlm.nih.gov/geo/, GSE148711.

AUTHOR CONTRIBUTIONS

PD-S, JH, SS, AP, and CB designed the experiments and wrote and edited the manuscript. PD-S, JH, and CB performed the experiments and analyzed the results. All authors contributed to the article and approved the submitted version.

FUNDING

This study was funded by a Smart Ideas award [UOAX1507] from the Ministry of Business, Innovation and Employment (MBIE), New Zealand. JH was funded by the Hugo Charitable Trust.

SUPPLEMENTARY MATERIAL

The Supplementary Material for this article can be found online at: https://www.frontiersin.org/articles/10.3389/fmolb.2020.580913/full#supplementary-material

FIGURE S1 | (A,B,E–G) Cytokine profiling in bladder cells in response to EV-RNA. Bladder cells were treated with different treatments for 4 h, after which supernatants were assessed by Luminex assays. UPEC, EV-RNA from UPEC strain; Nissle, EV-RNA from Nissle strain; R, EV-RNA obtained from iron limiting culture conditions; RF, EV-RNA obtained from iron sufficient culture conditions; 2, EV-RNA at 2 ng/mL; 0.5, EV-RNA at 0.5 ng/mL; LPS, LPS at 1000 ng/mL delivered with transfection agent unless stated, Free-LPS; LF-Poly I:C, Poly I:C delivered with transfection agent; LF-R848, Resiquimod R848 delivered with transfection agent. Data is plotted as mean and SD of 4 replicates, concentration in *Y*- axis as percentage of control (transfection agent in dotted line). **(C,D)** Viability of cultured bladder cells. Data plotted as Box and whiskers (box represented by upper and lower quartile, line = median, bars = min and max values) of 4 replicates (circles). Stars denote significant differences compared to control (transfection agent only) determined by One-way ANOVA Kruskal–Wallis and Dunn's posttest ($p < 0.05$).

REFERENCES

Ahmad, M., Abdollah, N., Shafie, N., Yusof, N., and Razak, S. (2018). Dual-specificity phosphatase 6 (DUSP6): a review of its molecular characteristics and clinical relevance in cancer. *Cancer Biol. Med.* 15, 14–28. doi: 10.20892/j.issn.2095-3941.2017.0107

Alexopoulou, L., Holt, A., Medzhitov, R., and Flavell, R. (2001). Recognition of double-stranded RNA and activation of NF-kB by Toll-like receptor 3. *Nature* 413, 732–738. doi: 10.1038/35099560

Alvarez, C., Giménez, R., Cañas, M., Vera, R., Díaz-Garrido, N., Badia, J., et al. (2019). Extracellular vesicles and soluble factors secreted by *Escherichia coli* Nissle 1917 and ECOR63 protect against enteropathogenic *E. coli*-induced intestinal epithelial barrier dysfunction. *BMC Microbiol.* 19:166. doi: 10.1186/s12866-019-1534-3

Ambite, I., Puthia, M., Nagy, K., Cafaro, C., Nadeem, A., Butler, D., et al. (2016). Molecular basis of acute cystitis reveals susceptibility genes and immunotherapeutic targets. *PLoS Pathog.* 12:e1005848. doi: 10.1371/journal.ppat.1005848

Andrews, S., Robinson, A., and Rodríguez-Quiñones, F. (2003). Bacterial iron homeostasis. *FEMS Microbiol. Rev.* 27, 215–237. doi: 10.1016/S0168-6445(03)00055-X

Barker, J., and Weiss, J. (2019). Detecting lipopolysaccharide in the cytosol of mammalian cells: lessons from MD-2/TLR4. *J. Leukoc. Biol.* 106, 127–132. doi: 10.1002/JLB.3MIR1118-434R

Behrouzi, A., Vaziri, F., Rad, F., Amanzadeh, A., Fateh, A., Moshiri, A., et al. (2018). Comparative study of pathogenic and non-pathogenic *Escherichia coli* outer membrane vesicles and prediction of host-interactions with TLR signaling pathways. *BMC Res. Notes* 11:539. doi: 10.1186/s13104-018-3648-3

Bielaszewska, M., Ruèter, C., Bauwens, A., Greune, L., Jarosch, K., Steil, D., et al. (2017). Host cell interactions of outer membrane vesicle-associated virulence factors of enterohemorrhagic *Escherichia coli* O157: intracellular delivery,

trafficking and mechanisms of cell injury. *PLoS Pathog.* 13:e1006159. doi: 10.1371/journal.ppat.1006159

Biondo, C., Mancuso, G., Beninati, C., Iaria, C., Romeo, O., Cascio, A., et al. (2012). The role of endosomal toll-like receptors in bacterial recognition. *Eur. Rev. Med. Pharmacol. Sci.* 16, 1506–1512.

Blenkiron, C., Simonov, D., Muthukaruppan, A., Tsai, P., Dauros, P., Green, S., et al. (2016). Uropathogenic *Escherichia coli* releases extracellular vesicles that are associated with RNA. *PLoS One* 11:e0160440. doi: 10.1371/journal.pone.0160440

Brown, L., Wolf, J., Prados-Rosales, R., and Casadevall, A. (2015). Through the wall: extracellular vesicles in Gram-positive bacteria, mycobacteria and fungi. *Nat. Rev. Microbiol.* 13, 621–630. doi: 10.1038/nrmicro3480

Caruana, J., and Walper, S. (2020). bacterial membrane vesicles as mediators of microbe – microbe and microbe – host community interactions. *Front. Microbiol.* 11:432. doi: 10.3389/fmicb.2020.00432

Cassat, J., and Skaar, E. (2013). Iron in infection and immunity. *Cell. Host Microbe* 13, 509–519. doi: 10.1016/j.chom.2013.04.010

Chan, K., Shone, C., and Hesp, J. (2017). Antibiotics and iron-limiting conditions and their effect on the production and composition of outer membrane vesicles secreted from clinical isolates of extraintestinal pathogenic *E. coli*. *Proteomics Clin. Appl.* 11:1600091. doi: 10.1002/prca.201600091

Chatterjee, S., Mondal, A., Mitra, S., and Basu, S. (2017). *Acinetobacter baumannii* transfers the blaNDM-1 gene via outer membrane vesicles. *J. Antimicrob. Chemother.* 72, 2201–2207. doi: 10.1093/jac/dkx131

Chen, F., Cui, G., Wang, S., Nair, M., He, L., Qi, X., et al. (2017). Outer membrane vesicle associated lipase FtlA enhances cellular invasion and virulence in *Francisella tularensis* LVS. *Emerg. Microbes Infect.* 6:e66. doi: 10.1038/emi.2017.53

Chernov, V., Mouzykantova, A., Baranovaa, N., Medvedevaa, E., Grygorievaa, T., Trushin, M., et al. (2014). Extracellular membrane vesicles secreted by mycoplasma *Acholeplasma laidlawii* PG8 are enriched in virulence proteins. *J. Proteomics* 110, 117–128. doi: 10.1016/j.jprot.2014.07.020

Choi, J., Kim, S., Hong, S., and Lee, H. (2017). Secretable small RNAs via outer membrane vesicles in periodontal pathogens. *J. Dent. Res.* 96, 458–466. doi: 10.1177/0022034516685071

Choi, J., Kwon, T., Hong, S., and Lee, H. (2016). Isolation and characterization of a microRNA-size secretable small RNA in *Streptococcus sanguinis*. *Cell Biochem. Biophys.* 76, 293–301. doi: 10.1007/s12013-016-0770-5

Dauros-Singorenko, P., Blenkiron, C., Phillips, A., and Swift, S. (2018). The functional RNA cargo of bacterial membrane vesicles. *FEMS Microbiol. Lett.* 365:fny023. doi: 10.1093/femsle/fny023

Dauros-Singorenko, P., Chang, V., Whitcombe, A., Simonov, D., Hong, J., Phillips, A., et al. (2017). Isolation of membrane vesicles from prokaryotes: a technical and biological comparison reveals heterogeneity. *J. Extracell. Vesicles* 6:1324731. doi: 10.1080/20013078.2017.1324731

Dauros-Singorenko, P., and Swift, S. (2014). The transition from iron starvation to iron sufficiency as an important step in the progression of infection. *Sci. Prog.* 97, 371–382. doi: 10.3184/003685014X14151846374739

Davis, K., Carvalho, H., Rasmussen, S., and O'Brien, A. (2006). Cytotoxic necrotizing factor type 1 delivered by outer membrane vesicles of Uropathogenic *Escherichia coli* attenuates polymorphonuclear leukocyte antimicrobial activity and chemotaxis. *Infect. Immun.* 74, 4401–4408. doi: 10.1128/IAI.00637-06

Demirel, I., Persson, A., Brauner, A., Särndahl, E., Kruse, R., and Persson, K. (2018). Activation of the NLRP3 inflammasome pathway by uropathogenic *escherichia coli* is virulence factor-dependent and influences colonization of bladder epithelial cells. *Front. Cell. Infect. Microbiol.* 8:81. doi: 10.3389/fcimb.2018.00081

Devos, S., Van Putte, W., Vitse, J., Van Driessche, G., Stremersch, S., Van Den Broek, W., et al. (2017). Membrane vesicle secretion and prophage induction in multidrug-resistant *Stenotrophomonas maltophilia* in response to ciprofloxacin stress. *Environ. Microbiol.* 19, 3930–3937. doi: 10.1111/1462-2920.13793

Di Paolo, N., and Shayakhmetov, D. (2016). Interleukin 1α and the inflammatory process. *Nat. Immunol.* 17, 906–913. doi: 10.1038/ni.3503

Diamond, C., Khameneh, H., Brough, D., and Mortellaro, A. (2015). Novel perspectives on non-canonical inflammasome activation. *Immuno Targets Ther.* 4, 131–141. doi: 10.2147/ITT.S57976

Eberle, F., Sirin, M., Binder, M., and Dalpke, A. (2009). Bacterial RNA is recognized by different sets of immunoreceptors. *Eur. J. Immunol.* 39, 2537–2547. doi: 10.1002/eji.200838978

Ellis, T., and Kuehn, M. (2010). Virulence and immunomodulatory roles of bacterial outer membrane vesicles. *Microbiol. Mol. Biol. Rev.* 74, 81–94. doi: 10.1128/MMBR.00031-09

Erdmann, S., Tschitschko, B., Zhong, L., Raftery, M., and Cavicchioli, R. (2017). A plasmid from an Antarctic haloarchaeon uses specialized membrane vesicles to disseminate and infect plasmid-free cells. *Nat. Microbiol.* 2, 1446–1455. doi: 10.1038/s41564-017-0009-2

Fábrega, M., Aguilera, L., Giménez, R., Varela, E., Cañas, M., Antolín, M., et al. (2016). Activation of immune and defense responses in the intestinal mucosa by outer membrane vesicles of commensal and probiotic *Escherichia coli* strains. *Front. Microbiol.* 7:705. doi: 10.3389/fmicb.2016.00705

Fettelschoss, A., Kistowska, M., LeibundGut-Landmann, S., Beer, H., Johansen, P., Senti, G., et al. (2011). Inflammasome activation and IL-1β target IL-1α for secretion as opposed to surface expression. *Proc. Natl. Acad. Sci. U.S.A.* 108, 18055–18060. doi: 10.1073/pnas.1109176108

Frantz, R., Teubner, L., Schultze, T., La Pietra, L., Müller, C., Gwozdzinski, K., et al. (2019). The secRNome of *Listeria monocytogenes* harbors small noncoding RNAs that are potent inducers of beta interferon. *mBio* 10:e01223-19. doi: 10.1128/mBio.01223-19

Gill, S., Catchpole, R., and Forterre, P. (2019). Extracellular membrane vesicles in the three domains of life and beyond. *FEMS Microbiol. Rev.* 43, 273–303. doi: 10.1093/femsre/fuy042

Grande, R., Celia, C., Mincione, G., Stringaro, A., Di Marzio, L., Colone, M., et al. (2017). Detection and physicochemical characterization of membrane vesicles (MVs) of *Lactobacillus reuteri* DSM 17938. *Front. Microbiol.* 8:1040. doi: 10.3389/fmicb.2017.01040

Han, E., Choi, S., Lee, Y., Park, J., Hong, S., and Lee, H. (2019). Extracellular RNAs in periodontopathogenic outer membrane vesicles promote TNF-a production in human macrophages and cross the blood–brain barrier in mice. *FASEB J.* 33, 13412–13422. doi: 10.1096/fj.201901575R

Heil, F., Hemmi, H., Hochrein, H., Ampenberger, F., Kirschning, C., Akira, S., et al. (2004). Species-specific recognition of single-stranded RNA via Toll-like Receptor 7 and 8. *Science* 303, 1526–1529. doi: 10.1126/science.1093620

Hong, J., Dauros-Singorenko, P., Whitcombe, A., Payne, L., Blenkiron, C., Phillips, A., et al. (2019). Analysis of the *Escherichia coli* extracellular vesicle proteome identifies markers of purity and culture conditions. *J. Extracell. Vesicles* 8:1632099. doi: 10.1080/20013078.2019.1632099

Hunstad, D., Justice, S., Hung, C., Lauer, S., and Hultgren, S. (2005). Suppression of Bladder Epithelial Cytokine Responses by Uropathogenic *Escherichia coli*. *Infect. Immun.* 73, 3999–4006. doi: 10.1128/IAI.73.7.3999-4006.2005

Johnson, K., and Perry, M. (1976). Improved techniques for the preparation of bacterial lipopolysaccharides. *Can. J. Microbiol.* 22, 29–34. doi: 10.1139/m76-004

Jurk, M., Heil, F., Vollmer, J., Schetter, C., Krieg, A., Wagner, H., et al. (2002). Human TLR7 or TLR8 independently confer responsiveness to the antiviral compound R-848. *Nat. Immunol.* 3:499. doi: 10.1038/ni0602-499

Karthikeyan, R., Gayathri, P., Gunasekaran, P., Jagannadham, M., and Rajendhrana, J. (2020). Functional analysis of membrane vesicles of *Listeria monocytogenes* suggests a possible role in virulence and physiological stress response. *Microb. Pathog.* 142:104076. doi: 10.1016/j.micpath.2020.104076

Keenan, J., Davis, K., Beaugie, C., McGovern, J., and Moran, A. (2008). Alterations in *Helicobacter pylori* outer membrane and outer membrane vesicle-associated lipopolysaccharides under iron-limiting growth conditions. *Innate Immun.* 14, 279–290. doi: 10.1177/1753425908096857

Knapp, S., Hacker, J., Jarchau, T., and Goebel, W. (1986). Large, unstable inserts in the chromosome affect virulence properties of Uropathogenic *Escherichia coli* 06 strain 536. *J. Bacteriol.* 168, 22–30. doi: 10.1128/jb.168.1.22-30.1986

Koeppen, K., Hampton, T., Jarek, M., Scharfe, M., Gerber, S., Mielcarz, D., et al. (2016). A novel mechanism of host-pathogen interaction through srna in bacterial outer membrane vesicles. *PLoS Pathog.* 12:e1005672. doi: 10.1371/journal.ppat.1005672

Lang, R., and Raffi, F. (2019). Dual-specificity phosphatases in immunity and infection: an update. *Int. J. Mol. Sci.* 20:2710. doi: 10.3390/ijms20112710

Lin, J., Zhang, W., Cheng, J., Yang, X., Zhu, K., Wang, Y., et al. (2017). A *Pseudomonas* T6SS effector recruits PQS-containing outer membrane vesicles for iron acquisition. *Nat. Commun.* 8:14888. doi: 10.1038/ncomms14888

Liu, T., Zhang, L., Joo, D., and Sun, S. (2017). NF-κB signaling in inflammation. *Signal. Transduct. Target Ther.* 2:17023. doi: 10.1038/sigtrans.2017.23

Lu, Y., Yeh, W., and Ohashi, P. (2008). LPS/TLR4 signal transduction pathway. *Cytokine* 42, 145–151. doi: 10.1016/j.cyto.2008.01.006

Malabirade, A., Habier, J., Heintz-Buschart, A., May, P., Godet, J., Halder, R., et al. (2018). The RNA complement of outer membrane vesicles from *Salmonella enterica* Serovar Typhimurium under distinct culture conditions. *Front. Microbiol.* 9:2015. doi: 10.3389/fmicb.2018.02015

Maldonado, R., Sá-Correia, I., and Valvano, M. (2016). Lipopolysaccharide modification in Gram-negative bacteria during chronic infection. *FEMS Microbiol. Rev.* 40, 480–493. doi: 10.1093/femsre/fuw007

Mi, H., Muruganujan, A., Ebert, D., Huang, X., and Thomas, P. (2019). PANTHER version 14: more genomes, a new PANTHER GO-slim and improvements in enrichment analysis tools. *Nucl. Acids Res.* 47, D419–D426. doi: 10.1093/nar/gky1038

Mi, H., and Thomas, P. (2009). Protein networks and pathway analysis. *Methods Mol. Biol.* 563, 123–140. doi: 10.1007/978-1-60761-175-2_7

Nagakubo, T., Nomura, N., and Toyofuku, M. (2020). Cracking open bacterial membrane vesicles. *Front. Microbiol.* 10:3026. doi: 10.3389/fmicb.2019.03026

Needham, B., and Trent, S. (2013). Fortifying the barrier: the impact of lipid A remodelling on bacterial pathogenesis. *Nat. Rev. Microbiol.* 11, 467–481. doi: 10.1038/nrmicro3047

Nissle, A. (1918). Die antagonistische *Behandlung chronischer* darmstörungen mit colibakterien. *Med. Klin.* 2, 29–33.

O'Donoghue, E., Sirisaengtaksin, N., Browning, D., Bielska, E., Hadis, M., Fernandez-Trillo, F., et al. (2017). Lipopolysaccharide structure impacts the entry kinetics of bacterial outer membrane vesicles into host cells. *PLoS Pathog.* 13:e1006760. doi: 10.1371/journal.ppat.1006760

Prados-Rosales, R., Weinrick, B., Piqué, D., Jacobs, W., Casadevall, A., and Rodriguez, M. (2014). Role for *Mycobacterium tuberculosis* membrane vesicles in iron acquisition. *J. Bacteriol.* 196, 1250–1256. doi: 10.1128/JB.01090-13

Quereda, J., and Cossart, P. (2017). Regulating bacterial virulence with RNA. *Annu. Rev. Microbiol.* 71, 263–280. doi: 10.1146/annurev-micro-030117-020335

Rathinam, V., Zhao, Y., and Shao, F. (2019). Innate immunity to intracellular LPS. *Nat. Immunol.* 20, 527–533. doi: 10.1038/s41590-019-0368-3

Robinson, A., Heffernan, J., and Henderson, J. (2018). The iron hand of uropathogenic *Escherichia coli*: the role of transition metal control in virulence. *Future Microbiol.* 13, 813–829. doi: 10.2217/fmb-2017-0295

Rosadini, C., and Kagan, J. (2017). Early innate immune responses to bacterial LPS. *Curr. Opin. Immunol.* 44, 14–19. doi: 10.1016/j.coi.2016.10.005

Sander, L., Davis, M., Boekschoten, M., Amsen, D., Dascher, C., Ryffel, B., et al. (2012). Sensing prokaryotic mRNA signifies microbial viability and promotes immunity. *Nature* 474, 385–389. doi: 10.1038/nature10072

Santos, J., Dick, M., Lagrange, B., Degrandi, D., Pfeffer, K., Yamamoto, M., et al. (2018). LPS targets host guanylate-binding proteins to the bacterial outer membrane for non-canonical inflammasome activation. *EMBO J.* 37:e98089. doi: 10.15252/embj.201798089

Schilling, J., Martin, S., Hunstad, D., Patel, K., Mulvey, M., Justice, S., et al. (2003). CD14- and Toll-like receptor-dependent activation of bladder epithelial cells by lipopolysaccharide and Type 1 piliated *Escherichia coli*. *Infect. Immun.* 71, 1470–1480. doi: 10.1128/iai.71.3.1470-1480.2003

Schwechheimer, C., and Kuehn, M. (2015). Outer-membrane vesicles from Gram-negative bacteria: biogenesis and functions. *Nat. Rev. Microbiol.* 13, 605–619. doi: 10.1038/nrmicro3525

Seeley, J., and Ghosh, S. (2017). Molecular mechanisms of innate memory and tolerance to LPS. *J. Leukoc. Biol.* 101, 107–119. doi: 10.1189/jlb.3MR0316-118RR

Sha, W., Mitoma, H., Hanabuchi, S., Bao, M., Weng, L., Sugimoto, N., et al. (2014). Human NLRP3 inflammasome senses multiple types of bacterial RNAs. *Proc. Natl. Acad. Sci. U.S.A.* 111, 16059–16064. doi: 10.1073/pnas.1412487111

Sharp, C., Boinett, C., Cain, A., Housden, N., Kumar, S., Turner, K., et al. (2019). O-antigen-dependent colicin insensitivity of uropathogenic *Escherichia coli*. *J. Bacteriol.* 201:e00545-18. doi: 10.1128/JB.00545-18

Shi, J., Zhao, Y., Wang, Y., Gao, W., Ding, J., Li, P., et al. (2014). Inflammatory caspases are innate immune receptors for intracellular LPS. *Nature* 514, 187–192. doi: 10.1038/nature13683

Shimizu, T., Yokota, S., Takahashi, S., Kunishima, Y., Takeyama, K., Masumori, N., et al. (2004). Membrane-anchored CD14 is important for induction of interleukin-8 by lipopolysaccharide and peptidoglycan in uroepithelial cells. *Clin. Diagn. Lab. Immunol.* 11, 969–976. doi: 10.1128/CDLI.11.5.969-976.2004

Sjöström, A., Sandblad, L., Uhlin, B., and Wai, S. (2015). Membrane vesicle-mediated release of bacterial RNA. *Sci Rep.* 5:15329. doi: 10.1038/srep15329

Steimle, A., Autenrieth, I., and Frick, J. (2016). Structure and function: lipid A modifications in commensals and pathogens. *Int. J. Med. Microbiol.* 306, 290–301. doi: 10.1016/j.ijmm.2016.03.001

Storz, G., Vogel, J., and Wassarman, K. (2011). Regulation by small RNAs in bacteria: expanding frontiers. *Mol. Cell.* 43, 880–891. doi: 10.1016/j.molcel.2011.08.022

Subashchandrabose, S., and Mobley, H. (2015). Virulence and fitness determinants of uropathogenic *Escherichia coli*. *Microbiol. Spectr.* 3, 235–261. doi: 10.1128/microbiolspec.UTI-0015-2012

Théry, C., Witwer, K., Aikawa, E., Alcaraz, M., Anderson, J., Andriantsitohaina, R., et al. (2018). Minimal information for studies of extracellular vesicles 2018 (MISEV2018): a position statement of the international society for extracellular vesicles and update of the MISEV2014 guidelines. *J. Extracell. Vesicles* 7:1535750. doi: 10.1080/20013078.2018.1535750

Toyofuku, M., Nomura, N., and Eberl, L. (2019). Types and origins of bacterial membrane vesicles. *Nat. Rev. Microbiol.* 17, 13–24. doi: 10.1038/s41579-018-0112-2

Vanaja, S., Russo, A., Behl, B., Banerjee, I., Yankova, M., Deshmukh, S., et al. (2016). Bacterial outer membrane vesicles mediate cytosolic localization of LPS and caspase-11 activation. *Cell* 165, 1106–1119. doi: 10.1016/j.cell.2016.04.015

Vdovikova, S., Luhr, M., Szalai, P., Skalman, L., Francis, M., Lundmark, R., et al. (2017). A novel role of *Listeria monocytogenes* membrane vesicles in inhibition of autophagy and cell death. *Front. Cell. Infect. Microbiol.* 7:154. doi: 10.3389/fcimb.2017.00154

Vierbuchen, T., Bang, C., Rosigkeit, H., Schmitz, R., and Heine, H. (2017). The human-associated archaeon *Methanosphaera stadtmanae* is recognized through its RNA and induces TLR8-dependent NLRP3 inflammasome activation. *Front. Immunol.* 8:1535. doi: 10.3389/fimmu.2017.01535

Wang, H., Liu, S., Wang, Y., Chang, B., and Wang, B. (2016). Nod-like receptor protein 3 inflammasome activation by *Escherichia coli* RNA induces transforming growth factor beta 1 secretion in hepatic stellate cells. *Bosn J. Basic Med. Sci.* 16, 126–131. doi: 10.17305/bjbms.2016.699

Wang, W., Chanda, W., and Zhong, M. (2015). The relationship between biofilm and outer membrane vesicles: a novel therapy overview. *FEMS Microbiol. Lett.* 362:fnv117. doi: 10.1093/femsle/fnv117

Yi, E., and Hackett, M. (2000). Rapid isolation method for lipopolysaccharide and lipid A from Gram-negative bacteria. *Analyst* 125, 651–656. doi: 10.1039/b000368i

Yonezawa, H., Osaki, T., Kurata, S., Fukuda, M., Kawakami, H., Ochiai, K., et al. (2009). Outer membrane vesicles of *Helicobacter pylori* TK1402 are involved in biofilm formation. *BMC Microbiol.* 9:197. doi: 10.1186/1471-2180-9-197

Zeng, J., Gupta, V., Jiang, Y., Yang, B., Gong, L., and Zhu, H. (2019). Cross-kingdom small RNAs among animals, plants and microbes. *Cells* 8:371. doi: 10.3390/cells8040371

Conflict of Interest: The authors declare that the research was conducted in the absence of any commercial or financial relationships that could be construed as a potential conflict of interest.

frontiers in Molecular Biosciences

ORIGINAL RESEARCH
published: 24 November 2020
doi: 10.3389/fmolb.2020.596366

Delivery of Periodontopathogenic Extracellular Vesicles to Brain Monocytes and Microglial IL-6 Promotion by RNA Cargo

*Jae Yeong Ha[1], Song-Yi Choi[1], Ji Hye Lee[2], Su-Hyung Hong[1] and Heon-Jin Lee[1,3]**

[1] Department of Microbiology and Immunology, School of Dentistry, Kyungpook National University, Daegu, South Korea, [2] Department of Oral Pathology, Dental and Life Science Institute, School of Dentistry, Pusan National University, Yangsan, South Korea, [3] Brain Science and Engineering Institute, Kyungpook National University, Daegu, South Korea

Gram-negative bacterial extracellular vesicles (EVs), also known as outer membrane vesicles (OMVs), are secreted from bacterial cells and have attracted research attention due to their role in cell-to-cell communication. During OMV secretion, a variety of cargo such as extracellular RNA (exRNA) is loaded into the OMV. The involvement of exRNAs from a range of bacteria has been identified in several diseases, however, their mechanism of action has not been elucidated. We have recently demonstrated that OMVs secreted by the periodontopathogen *Aggregatibacter actinomycetemcomitans* can cross the blood–brain barrier (BBB) and that its exRNA cargo could promote the secretion of proinflammatory cytokines in the brain. However, it was unclear whether the brain immune cells could actually take up bacterial OMVs, which originate outside of the brain, in an appropriate immune response. In the present study, using monocyte-specific live CX3CR1-GFP mice, we visualized OMV-colocalized meningeal macrophages and microglial cells into which bacterial OMVs had been loaded and intravenously injected through tail veins. Our results suggested that meningeal macrophages uptake BBB-crossed OMVs earlier than do cortex microglia. BV2 cells (a murine microglia cell line) and exRNAs were also visualized after OMV treatment and their proinflammatory cytokine levels were observed. Interleukin (IL)-6 and NF-κB of BV2 cells were activated by *A. actinomycetemcomitans* exRNAs but not by OMV DNA cargo. Altogether, these findings indicate that OMVs can successfully deliver exRNAs into brain monocyte/microglial cells and cause neuroinflammation, implicating a novel pathogenic mechanism in neuroinflammatory diseases.

Keywords: periodontitis, small RNA, extracellular vesicle, *Aggregatibacter actinomycetemcomitans*, outer membrane vesicle

OPEN ACCESS

Edited by:
Olga N. Ozoline, Institute of Cell Biophysics (RAS), Russia

Reviewed by:
Simon Swift, The University of Auckland, New Zealand
Yosuke Tashiro, Shizuoka University, Japan

***Correspondence:**
Heon-Jin Lee
heonlee@knu.ac.kr

Specialty section:
This article was submitted to Protein and RNA Networks, a section of the journal Frontiers in Molecular Biosciences

Received: *19 August 2020*
Accepted: *02 November 2020*
Published: *24 November 2020*

Citation:
Ha JY, Choi S-Y, Lee JH, Hong S-H and Lee H-J (2020) Delivery of Periodontopathogenic Extracellular Vesicles to Brain Monocytes and Microglial IL-6 Promotion by RNA Cargo. Front. Mol. Biosci. 7:596366. doi: 10.3389/fmolb.2020.596366

INTRODUCTION

Bacterial extracellular vesicles (EVs), also known as outer membrane vesicles (OMVs) in gram-negative bacteria, are around 10–300 nm sized particles released during all growth stages (Bonnington and Kuehn, 2014). Extracellular RNAs (exRNAs) are RNAs that are incorporated in EVs, which can transport them to other cells. Moreover, as bacterial exRNAs are well protected

by EV membranes from the harsh milieu outside of cells, they have been suggested to function as intercellular communication molecules (Choi et al., 2017a; Das et al., 2019). Not only RNAs but also various types of cargo such as proteins, DNA, and lipids are transported by EVs, however, RNAs have gained more research attention due to their sustained biological activities in recipient cells (Lee, 2019). In addition, a recent study suggested the potential involvement of bacterial exRNAs in systemic diseases and their use as biomarkers (Lee, 2020). The majority of exRNAs in OMVs are small RNAs in the size range of 15 and 40 nucleotides (nts) (Ghosal et al., 2015), similar in size to eukaryotic microRNAs (miRNAs) or miRNA-sized small RNAs (msRNAs) in bacteria, implying their regulatory role in host cells (Lee and Hong, 2012; Kang et al., 2013; Blenkiron et al., 2016; Koeppen et al., 2016). Although their precise mechanism of action has not been clearly elucidated, microbial exRNAs are known to have certain roles in host gene regulation, immune response, and diseases (see the review Lee, 2020). For these reasons, the degree of penetration of bacterial EVs to tissues and organs from circulation in the blood from their originated bacterial residency remains an important question to uncover the function of bacterial exRNAs and their relationship with systemic diseases.

A previous short report asserted that intracisternally inoculated *Haemophilus influenzae* type b OMVs could increase the permeability of BBB in rat, which was tested by using radioisotope-labeled albumin (Wispelwey et al., 1989), but it was not clear whether OMVs themselves could actually cross the BBB until our recent demonstration of the evidence (Han et al., 2019). We reported that OMVs from the periodontopathogen *Aggregatibacter actinomycetemcomitans* (*Aa*) could cross the BBB after intracardiac injection, being detectable in the cortex of mice by using brain clearance technique. Furthermore, we observed that exRNAs contained in the *Aa* OMVs activate TNF-α in the mouse brain cortex (Han et al., 2019). However, it was not clear what type of brain cells were responsible for promoting the production of TNF-α by *Aa* exRNAs even though the exRNAs of *Aa* increased the expression of TNF-α in the activated human-macrophage-like cells.

Mononuclear phagocytes, i.e., monocytes and macrophages, are key players in protective immunity and homeostasis (Ginhoux and Jung, 2014). Microglial cells are resident monocytes/macrophages in the central nervous system (CNS) whose primary role as immune defense against infection is critical in modulating neuroinflammation as well as the development of several neurodegenerative disorders such as Alzheimer's disease (AD) (Block et al., 2007; Ginhoux et al., 2013; Li and Barres, 2018).

In the present study, to explore the neuroinflammatory effect of pathogenic OMVs, we characterize how intravenously injected *Aa* OMVs can be taken up by monocyte-derived cells using intravital imaging analysis of monocyte marker-expressing CX3CR1-GFP knock-in mice. Tail-vein-injected OMVs and exRNA cargo were delivered into meningeal macrophages and cortex microglial cells in a time-sequential manner. Moreover, analysis of the effect of *Aa* exRNAs on the murine microglial BV2 cell line showed that a proinflammatory cytokine other than TNF-α, Interleukin (IL)-6, is promoted in microglia cells by *Aa* exRNAs. We anticipate that our results will shed light on the novel mechanisms underlying immune signals to the brain in response to systemic pathogenic infection.

MATERIALS AND METHODS

Culture

A. actinomycetemcomitans (*Aa*, ATCC 33384) was inoculated on brain heart infusion (BHI; Difco, Sparks, MD, United States) agar plates in an anaerobic incubator. After 24 h, the colonies were picked and cultured in BHI media for 48 h. Picked colonies were also checked for ribosomal DNA to avoid any contamination. The anaerobic incubator was maintained at 37°C in 5% CO_2, 5% H_2, and 90% N_2. *Aa* were grown anaerobically in BHI until the desired optical density (OD) was reached (around 0.7 of OD_{600}).

Supernatants were collected for OMV purification and bacterial pellets were collected for RNA isolation and purity evaluation.

The BV2 cells, mouse macrophage-like microglial brain cells, were maintained on 6-well plates with 5×10^5 cells per well in DMEM medium supplemented with 10% FBS and 100 IU/ml penicillin G. The complete medium was changed three times a week.

Animals

The G-protein-coupled receptor CX3CR1 is expressed in human monocytes, and CX3CR1-GFP transgenic mice are widely used in studies on microglial cells (Jung et al., 2000). The CX3CR1-GFP mice (B6.Cg-Ptprca Cx3cr1tm1Litt/LittJ, The Jackson Laboratory, Bar Harbor, ME, United States) were housed in accordance with the standard guidelines for the care and use of laboratory animals, the animal protocols having been approved by the Institutional Animal Care and Use Committee (IACUC) of the Korean Advanced Institute of Science and Technology (KAIST, Daejeon, South Korea) for the company IVIM Technology (Daejeon, South Korea). All mice underwent surgery under anesthesia, and all efforts were made to minimize their suffering. Mice were individually housed in ventilated, temperature- and humidity-controlled cages (22.5°C, 52.5%) under a 12:12 h light:dark cycle and provided with standard diet and water ad libitum.

OMV Sample Preparation

Aa OMV samples were prepared as previously described (Han et al., 2019). Briefly, OMVs were obtained from the filtered and concentrated supernatant using ExoBacteria OMV Isolation Kits (SBI, Mountain View, CA, United States) according to the manufacturer's protocol. The isolated OMVs were treated with 1 μl of RNase A (1 U/μl, Thermo Fisher Scientific, Wilmington, DE, United States) and DNase I (2 U/μl, Thermo Fisher Scientific) to make a 1.5 ml volume of the OMVs, which was then incubated at 37°C for 25 min. This was done to remove any residual nucleic acids in the OMV preparation. The OMVs were purified again using the ExoBacteria OMV Isolation Kits to get rid of unnecessary remained enzymes. Transmission electron

micrographs (TEM) of *Aa* OMVs (pre-purification and purified) were compared in **Supplementary Figure S1**.

For physical lysis, the OMVs were frozen and thawed five times followed by sonication using a sonicator (100 W and 20 KHz; KSC-100 portable ultrasonicator, Korea Process Technology, Seoul, South Korea) for 30 s and then placed on ice for 30 s. Subsequently, 1 μl of RNase A and/or DNase I was added to 1 ml of the lysed OMVs and incubated at 37°C for 25 min. The purified OMVs were checked for sterility by spreading 10 μl of the purified OMVs on BHI agar plates for 3–4 days and stored at −80°C until use.

For staining, the OMVs (resuspended in 100 μl in PBS, without calcium and magnesium; GE Healthcare Bio-Sciences, Pittsburgh, PA, United States) were incubated with 2 μM SYTO RNASelect Green Fluorescent Cell Stain Kit (Thermo Fisher Scientific) and/or 10 μM red fluorescent Lipophilic Tracer DiD (1,1'-dioctadecyl-3, 3, 39, 39-tetramethylindodicarbocyanine, 4-chlorobenzenesulfonate salt; Thermo Fisher Scientific) for 1 h at 37°C. The samples were washed once with PBS followed by ultracentrifugation at 150,000 × *g* for 1 h at 4°C.

Both intact OMVs and lysed OMVs were analyzed for lipopolysaccharide (LPS) concentrations, for which the Pierce LAL Chromogenic Endotoxin Quantitation Kit (Thermo Fisher Scientific) was used according to the manufacturer's instructions.

OMV Analysis

The OMVs underwent nanoparticle tracking analysis using the NanoSight system (NanoSight NS300; Malvern Panalytical, Malvern, United Kingdom) according to the manufacturer's protocols. Samples were diluted 100 times in a total volume of 1 ml of PBS. PBS was introduced into the chamber using a 1 ml syringe and assessed whether it was free from particles and whether the chamber was clean (i.e., no light scattering). Particle size was measured based on Brownian movement and particle concentration was quantified in each sample. Protein quantification of OMVs and OMV lysates were done using Bradford reagent (Bio-Rad, Hercules, CA, United States) and the NanoSight system as previously described (Han et al., 2019).

Intravital Imaging

Three weeks before intravital imaging, cranial window surgery of CX3CR1-GFP mice was accomplished according to a previously published protocol (Holtmaat et al., 2009). Briefly, the skin and skull were removed followed by drilling to remove the cranial bone. The exposed brain was covered by glass, and dental cement was applied on the top of the skull and part of the cover glass, sealing off the exterior. All the exposed skull and wound edges were covered with dental cement. The strategy used for the intravital image acquisition of *Aa* OMV-injected mice is depicted in **Figure 1A**. Mice were housed for 3 weeks for stabilization before conducting intravital imaging.

After performing mouse tail vein (intravenous, i.v.) injections of DiD-stained OMVs (100 μl; approximately 3.0×10^8 particles) and anti-CD31 monoclonal antibody (60 μl; 553708, BD Bioscience) conjugated with Alexa Fluor 555 (A- 20009, Invitrogen), a laser scanning intravital confocal microscope (IVM-C, IVIM Technology) with an objective lens (Nikon, Japan; magnifications: × 25; numerical aperture: 1.1) was used to visualize the brain cellular uptake of OMVs. During the intravital imaging, the body temperature of the mouse was maintained at 37°C using a homeothermic controller. Mice were anesthetized using intramuscular injections of a cocktail mixture of zoletil (30 mg/kg) and xylazine (10 mg/kg). The imaging analysis was conducted as previously described (Ahn et al., 2017). All experiments were performed in duplicate using two independent OMV sample preparations and at least two mice for each experiments.

All the intravital imaging experiments conducted using mice were performed by IVIM Technology according to institutional and national guidelines.

Confocal Microscopic Imaging

The OMVs and RNAs inside were stained as described earlier in the OMV sample preparation section of "Materials and Methods." Stained OMVs were added to BV2 cells cultured on chamber slides and incubated for 24 h at 37°C, then washed four times with 500 μl of PBS, followed by incubation with DAPI (Vector Laboratories, Burlingame, CA, United States). The stained OMVs with the added cells were visualized on a laser scanning confocal microscope (LSM Zeiss 800; Carl Zeiss Microscopy, Jena, Germany) equipped with an objective lens (magnifications: × 40 with water immersion; numerical aperture: 1.2; resolution: 0. 28 μ m).

Total RNA Extraction

Total RNA was extracted using both TRIzol (Invitrogen, Carlsbad, CA, United States) and the miRNeasy Mini Kit (QIAGEN, Valencia, CA, United States) according to the manufacturers' protocols, with some modifications. Each sample was resuspended in 300 μl TRIzol reagent (Invitrogen). Resuspension was homogenized for 30 s using a Kontes Pellet Pestle Cordless Motor (Sigma-Aldrich, St. Louis, MO, United States) and placed on ice for 30 s, the steps being repeated 5 times for full homogenization. Then, an additional 700 μl TRIzol was added to the samples and incubated at room temperature for 5 min. 1-bromo-3-chloropropane (200 μl, Sigma-Aldrich) was then added to each sample, followed by incubation for 3 min. Next, the samples were centrifuged at 13,499 × g for 15 min at 4°C using a centrifuge (Smart R17 plus, Hanil Science, Incheon, South Korea). The supernatant (approximately 750 μl) of each sample was mixed with 750 μl of 100% isopropanol. The mixed samples were incubated at -20°C for 2 h. The columns of miRNeasy Mini Kit (QIAGEN) were additionally used to purify the small RNA-enriched RNA and clean RNA according to the manufacturer's protocol.

qRT-PCR

Total RNA (1 μg) was reverse-transcribed using OmniScript (QIAGEN). The qRT-PCR was performed with diluted cDNA using primer sets for TNF-α, IL-1β, IL-6, and β-actin (**Supplementary Table S1**). The PCR was performed in 96-well plates using the 7,500 Real-Time PCR System (Applied Biosystems, Foster City, CA, United States). The expression

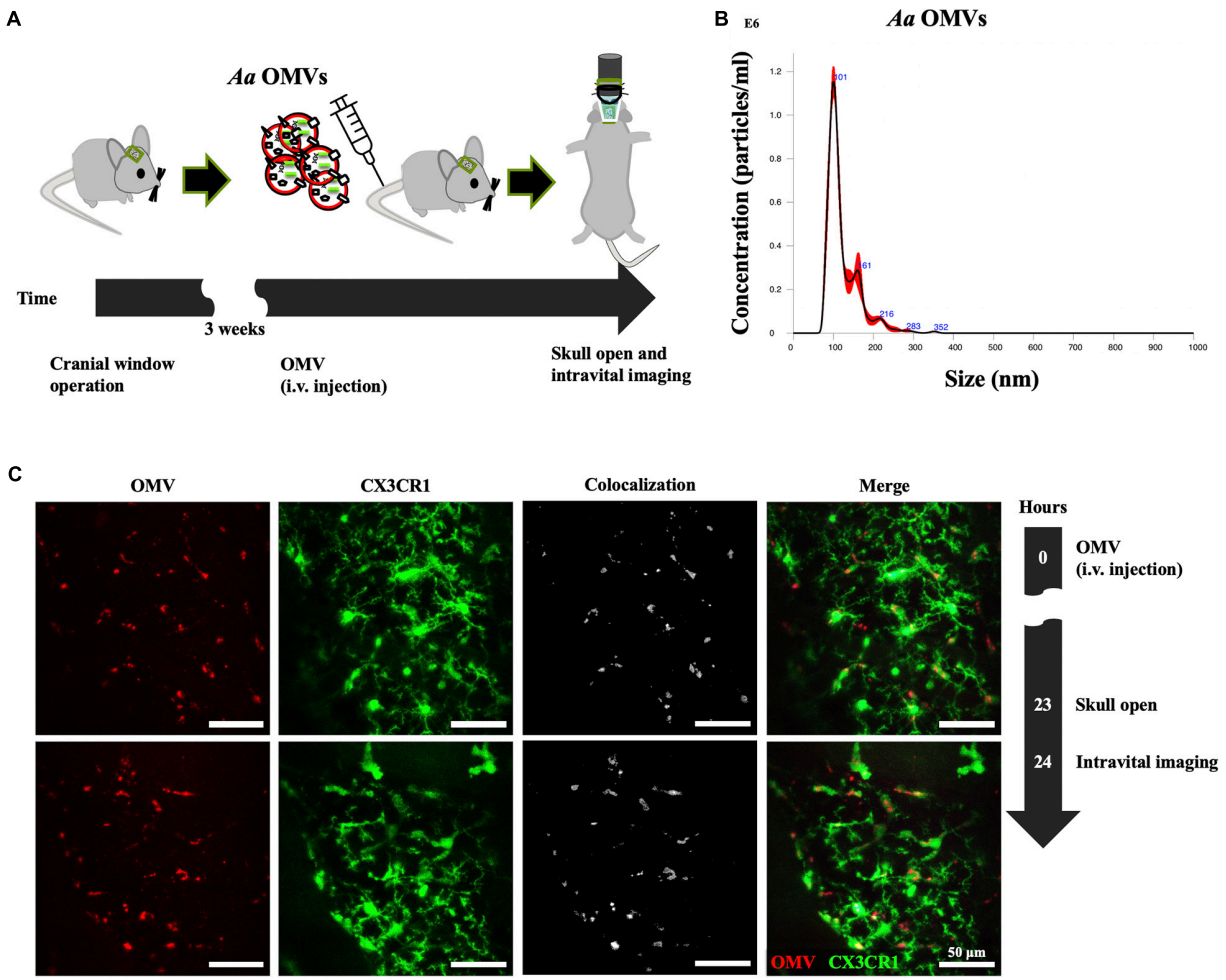

FIGURE 1 | Delivery of *Aa* OMVs into microglial cells. **(A)** Schematic diagram of intravital imaging process performed in this study. **(B)** Nanoparticle tracking analysis (NTA) of *Aa* OMVs used in this study. OMVs from *Aa* were analyzed using the NanoSight system to visualize the size distribution (*X*-axis) and particle numbers (*Y*-axis). **(C)** Intravital image was captured 24 h after *Aa* OMV i.v. injection. OMVs were colocalized with GFP-positive microglial cells. Scale bar: 50 μm. Additional Figures can be found in **Supplementary Figure S3**.

of each gene was determined from three replicates in a single qRT-PCR experiment.

Immunoassays of Cytokines

BV2 cells were incubated with purified OMVs for 24 h, after which the filtered supernatants using 0.22 μm pore filter (Sigma-Aldrich) were analyzed for four cytokines (IL-1β, IL-6, TNF-α, and IFN-γ) using a quantitative multiplex ELISA (Mouse Cytokine Panel 2 (4-plex); QUANSYS Biosciences, Logan, UT, United States) according to the manufacturer's instruction. Data were analyzed using the Q-View Software (Quansys Biosciences). All experiments were conducted in triplicate.

Western Blotting

For the western blotting of NF-κB p65 and phospho-p65, 20 μg of whole cell lysates was used for SDS polyacrylamide gel-running, followed by transfer to a polyvinylidene difluoride (PVDF) membrane using Pierce Power Blotter (Thermo Fisher Scientific) at 110 V (80 mA) for 80 min. The membrane was incubated in 5% skim milk/0.1% TBS-Tween 20 at room temperature for 1 h, followed by incubation with a 1:1,000 final diluted NF-κB p65 (#8242, Cell Signaling Technology) and phospho-p65 antibody (Ser536, #3033, Cell Signaling Technology) and then an anti-rabbit secondary antibody conjugated with horseradish peroxidase (#7074, Cell Signaling Technology). The control for loading was assessed using a β-actin antibody (at a dilution of 1:1,000, SC-47778, Santa Cruz Biotechnology Inc., Santa Cruz, CA, United States).

Statistical Analysis

All data are presented as mean ± SD. Differences among sample group values were analyzed using a one-way ANOVA and *post hoc* analyses were performed using the Tukey Test. All analyses were conducted using Origin 8.0 software (OriginLab, Northampton,

MA, United States), and $p < 0.05$ were considered to be statistically significant.

RESULTS

Intravital Imaging Reveals That Tail-Vein-Injected *Aa* OMVs Can Enter Mouse Brain Monocytes

Unlike eukaryotic EV (exosomes), which have been shown to deliver cargo to the brain after crossing BBB (Matsumoto et al., 2017; Yuan et al., 2017), little is known about the ability of peripheral bacterial EVs to reach the brain; we recently suggested that *Aa* exRNAs are the primary causative agents promoting the secretion of proinflammatory cytokines in macrophages and the mouse brain (Han et al., 2019). We therefore intended to confirm, using intravital imaging technique, whether brain monocytes or microglial cells can take up bacterial OMVs and their cargo when injected through the tail vein.

To investigate whether *Aa* OMVs can be taken up by mouse microglial cells, we first investigated the *Aa* OMVs injected (tail i.v. injection) into monocyte-specific CX3CR1-GFP mice using the intravital imaging system (**Figure 1A**). The number and size distribution of *Aa* OMVs used in this study were analyzed using a nanoparticle tracking analysis system. The majority of OMVs were in the size range of 100–280 nm (**Figure 1B**). As the NTA system could not precisely detect particle sizes < 60 nm (Bachurski et al., 2019), some smaller OMVs of *Aa* might have been missed. Therefore, the actual particle numbers might be greater than the measurement results we present here. Our previous study found that *Aa* OMVs apparently crossed the mouse BBB after 24 h of intracardiac injection (Han et al., 2019). To reduce the risk of cardiac damage, we switched to i.v. tail injections to administer stained *Aa* OMVs. Membrane-stained (red) OMVs were colocalized with GFP+ microglial cells 24 h after the injection of *Aa* OMVs into the cortex (**Figure 1C** and **Supplementary Figure S3**).

To ensure detection of localized of OMVs, brain blood vessels were also fluorescently labeled by i.v. injection of anti-CD31 antibody 1 h before imaging. At an imaging depth of around 80 μm (from surface of the brain), where mouse meninges are located, the GFP-positive meningeal monocytes/macrophages were first identified using intravital imaging analysis. As shown in **Figure 2A**, the majority of OMVs in the meningeal blood vessel lumen are observed at 4 h, suggesting that tail-injected OMVs can disseminate into several organs through blood vessels. OMVs were taken up by GFP-positive "patrolling" monocytes/macrophages in the lumen of vessel (yellow arrow), whereas some OMVs began to cross the blood vessel wall and colocalize with meningeal macrophages at 8 h (white arrowhead in **Figure 2A**). The magnified and stack images of monocytes/macrophages shown in **Figure 2A** at 8 h clearly demonstrate the OMVs and GFP-positive cell colocalization (**Figure 2B**). Another region of colocalized monocytes/macrophages (the dotted area in the magnified images) inside and outside of the meningeal blood vessel was also observed at 4–8 h, as seen in the magnified images in the region marked with yellow squares (**Figure 2C**). Colocalized monocytes (marked in yellow in the merged images) in the dotted area are clearly observed in both the exterior and lumen of the meningeal blood vessel.

To observe whether the injected OMVs can reach microglial cells, intravital images of cortex were captured at 24 and 48 h as more time was required for observation. Three random field images (**Figure 3A**) revealed that the OMVs (red) taken up by GFP-positive microglial cells (**Figure 3A**, arrowheads). Moreover, in the magnified stack images acquired during confocal imaging shown in **Figure 3A**, the OMV-colocalized microglial cells are clearly visualized in the exterior region of the vessel at 48 h (**Figure 3B**, arrowheads of S1 and S2 random fields). Although we could not observe whether the OMVs had crossed the BBB and colocalized with cortex microglial cells at 8 h of OMV injection, it was assumed that OMVs that were i.v. injected into the tail crossed the BBB and reached the cortex sometime after 8 h (**Figure 3C**). These data demonstrate that OMVs can pass through the BBB and internalize into meningeal macrophages, thus allowing cargo into microglial cells of the brain.

Aa OMVs Are Delivered Into the BV2 Microglial Cells

We previously reported that *Aa* OMVs can penetrate macrophage cells along with their RNA cargo (Han et al., 2019). Due to differences between macrophages and microglial cells, we repeated the confocal microscopy analysis of OMVs with the RNA cargo. As the SYTO RNA-Select reagent is membrane-permeable, we could detect RNA colocalization with the OMV membrane inside BV2 cells (**Figure 4**). The stained OMVs along with the RNA cargo were incubated with BV2 cells for 24 h, followed by counterstaining with DAPI to visualize the nuclei. Observation indicated OMVs and RNA cargo can internalize microglial cells, consistent with previous studies conducted using other cell types (Ho et al., 2015; Blenkiron et al., 2016; Koeppen et al., 2016; Choi et al., 2017a; Han et al., 2019).

Aa exRNAs in OMVs Activate IL-6 in BV2 Microglial Cells Through NF-κB Activation

To explore the effect of *Aa* OMVs and the RNAs in OMVs on BV2 cells, we treated BV2 cells with *Aa* OMVs and OMV lysate for 16 h (the LPS levels being approximately 50 ng/ml in both OMV and OMV lysates). We infected around 4.5×10^8 particles of *Aa* OMVs to the cells (5×10^5 cells), the higher number of OMVs resulting in cell death under our experimental condition (cell viability results are shown in **Supplementary Figure S2**).

We performed 4-flex cytokine (IL-1β, IL-6, TNF-α, and IFN-γ) arrays from the BV2 cells treated with *Aa* OMVs and OMV

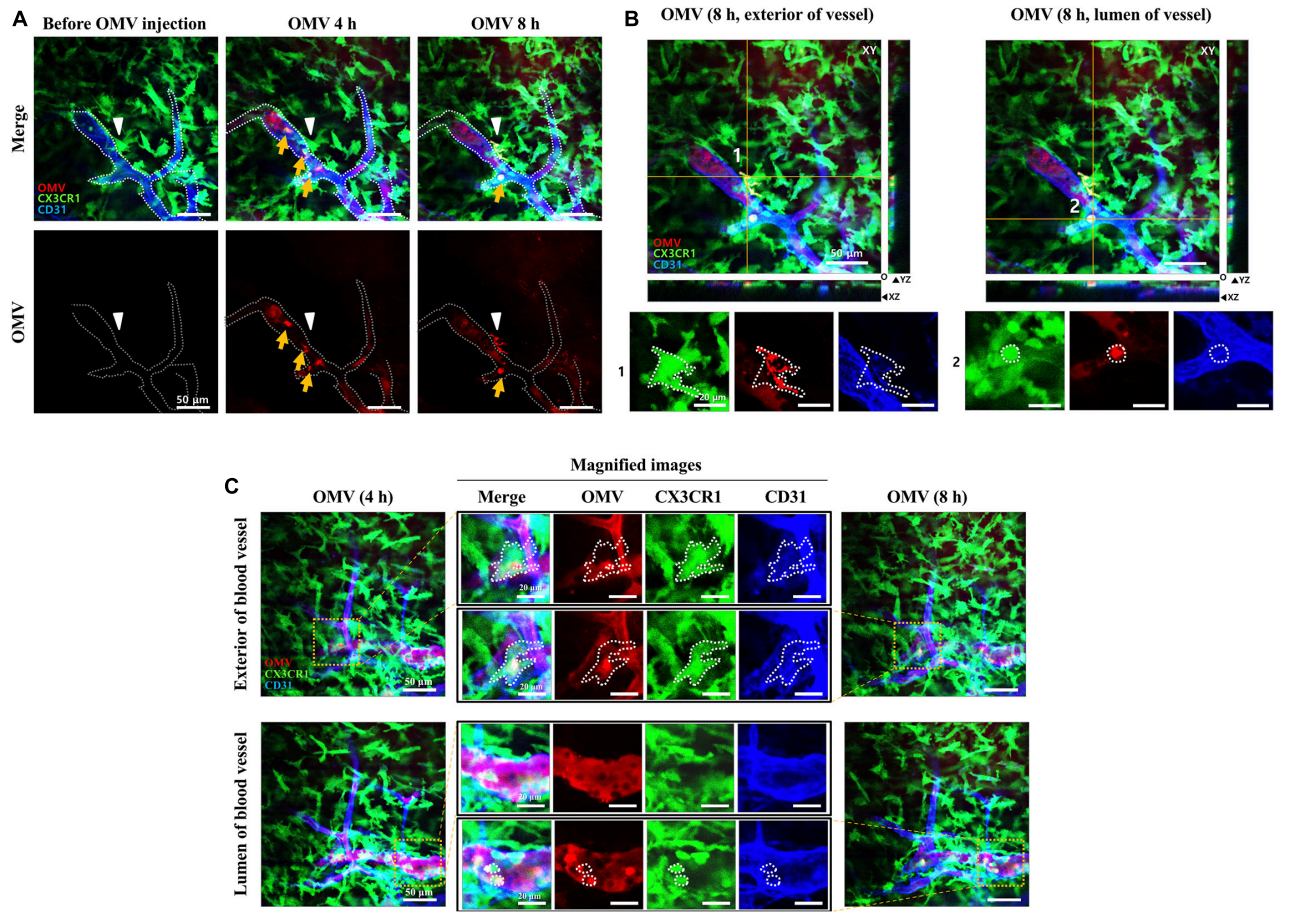

FIGURE 2 | Visualization of tail-vein-injected OMVs and meningeal macrophages of live CX3CR1-GFP mice. **(A,B)** OMVs taken up by monocytes were compared between 4 and 8 h after OMV injection. Confocal microscopic acquisition results show the OMV distribution before and 4 and 8 h after OMV i.v. injection of mice. **(A)** The white dotted line delineates the lumen of blood vessels. White arrowheads indicate *Aa* OMV-colocalized meningeal macrophages, and yellow arrows indicate OMV-colocalized monocytes/macrophages in the lumen of vessel. Scale bar: 50 μm. **(B)** Representative image stacks (5 μm intervals) acquired during confocal imaging of mice with GFP-positive microglial cells for OMVs injected (8 h) shown in **(A)**. The white dotted area refers to the colocalization of OMVs (red) and CX3CR1-GFP-positive monocytes (green). Scale bar: 50 μm; magnified scale: 20 μm. **(C)** Colocalized monocytes/macrophages (dotted areas in the magnified images) in the exterior and lumen of the meningeal blood vessel were compared. Magnified images (scale bar: 20 μm) of colocalized monocytes (shown in yellow in the merged images) in the dotted area are clearly seen in both the exterior and lumen of the meningeal blood vessel.

lysate to investigate the effect of *Aa* OMVs and exRNAs on microglial cells. The levels of IL-1β and IFN-γ were too low to detect, whereas IL-6 and TNF-α levels were detectable. However, unlike macrophage-like U937 cells (Han et al., 2019), TNF-α was not detectable in the BV2 cells treated OMVs and OMV lysates (**Supplementary Table S2**). The level of IL-6 protein measured from accumulated culture media of BV2 cells was upregulated by intact OMVs but not in OMV lysates treated with nucleases (DNase and RNase). This result indicated that the nucleic acid cargo of *Aa* OMVs is responsible for the activation of IL-6. Moreover, OMV lysates were treated with DNase or RNase to examine whether DNA or RNA is further responsible for the elevated IL-6 secretion. The result indicated that RNA rather than DNA cargo is the pivotal factor for IL-6 promotion because the OMV lysate treated with only RNase demonstrated less IL-6 secretion than that treated with only DNase (**Figure 5A**). Similar results were obtained at the RNA transcript level of IL-6, which was measured by qRT-PCR (**Figure 5B**).

The human IL-6 gene promoter possesses a binding site for NF-κB, which activates the expression of IL-6 [known to be induced by various stimuli such as LPS, TNF-α, and Poly (I:C) (Tanaka et al., 2014; Kumar, 2019)]. Our previous investigation demonstrated that OMV RNA of *Aa* promoted the activation of NF-κB via TLR8 in macrophage U937 cells (Han et al., 2019). Therefore, to explore the effect of *Aa* exRNAs on NF-κB activation, we performed western blotting using anti-phospho-p65 antibody to detect phosphorylated p65, which is the active subunit of NF-κB. We found that removal of RNA cargo of OMVs by treatment with RNase reduced phosphorylation activity, whereas total p65 expression showed no apparent differences (**Figure 5C**). The overall findings indicated that *Aa* exRNAs promote

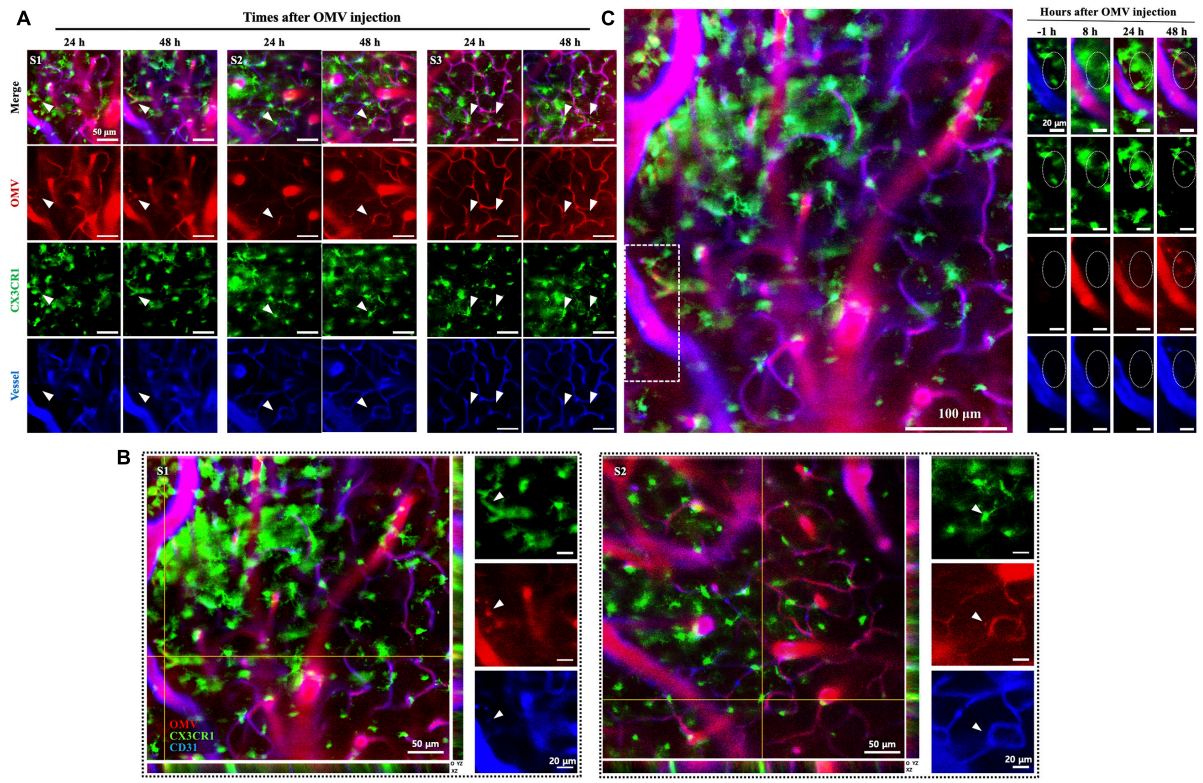

FIGURE 3 | Visualization of tail-vein-injected OMVs and microglial cells in the cortex of live CX3CR1-GFP mice. **(A)** OMVs taken up by microglial cells were imaged at 24 and 48 h after OMV injection. White arrowheads indicate OMVs taken up by microglial cells. Fluorescence-dye-conjugated anti-CD31 antibody was injected 1 h before imaging. Three different regions were captured. Scale bar: 50 μm. **(B)** Representative image stacks (5 μm intervals) acquired during confocal imaging of experimental mice with GFP-positive microglial cells for OMVs injected (48 h). The arrowheads refer to the colocalization of BBB-crossed OMVs (red) and CX3CR1-positive microglial cells (green) localized in the exterior of vessels. Scale bar: 50 μm; magnified scale: 20 μm. **(C)** Confocal microscopic acquisition results showing the OMV distribution before OMV injection (–1 h) and 8, 24, and 48 h after OMV i.v. injection of mice. The white dotted rectangle in the left panel was magnified. Right panel: magnified images of OMVs taken up by microglial cells (dotted circles). Scale bar: 100 μm; magnified scale: 20 μm.

the production of IL-6 in microglial BV2 cells through NF-κ B activation.

DISCUSSION

Among the numerous bacteria involved in periodontitis, *Aa* is a small gram-negative bacterium previously well-known for causing localized aggressive periodontitis (Henderson et al., 2010). *Aa* is also implicated in various systemic diseases such as non-alcoholic fatty liver disease (Komazaki et al., 2017), diabetes (Demmer et al., 2015), and rheumatoid arthritis (Konig et al., 2016). Furthermore, recent evidence suggests that *Aa* and other oral microorganisms are associated with neuroinflammatory diseases such as AD (Laugisch et al., 2018; Dominy et al., 2019; Díaz-Zúñiga et al., 2019; Han et al., 2019; Wu et al., 2019). However, whether bacteria themselves directly or their derivatives are involved in diseases remains debatable (Lee, 2020).

Microglial cells are activated by various stimuli such as LPS, IFN-γ, and β-amyloid and also release proinflammatory cytokines such as IL-6, IL-1β, and TNF-α, which have been investigated with regard to AD (Wang et al., 2015). However, there is limited information regarding the effect of pathogenic exRNAs in microglial cells on proinflammatory cytokine secretion.

The meninges consist of three layers, the dura mater, the arachnoid mater, and the pia mater. The arachnoid mater is a membrane barrier that separates the dura mater from the remaining portion of the brain and has well-regulated junctions, similar to the BBB (Rua and McGavern, 2018). Studies conducted using CX3CR1-GFP transgenic mice reported a high density of meningeal macrophages in the dura mater and pia mater (Chinnery et al., 2010). Along with other CNS macrophages (perivascular and choroid plexus), meningeal macrophages are non-parenchymal immune modulators at brain boundaries (Goldmann et al., 2016; Rua and McGavern, 2018). Therefore, their immune response against infection could have pivotal consequences for CNS homeostasis and diseases. However, these macrophages have received little research attention with respect to oral pathogens and commensal bacteria in the context of brain pathogenesis due to the tight defenses of the CNS. Recently, considerable effort has been devoted to understanding tiny

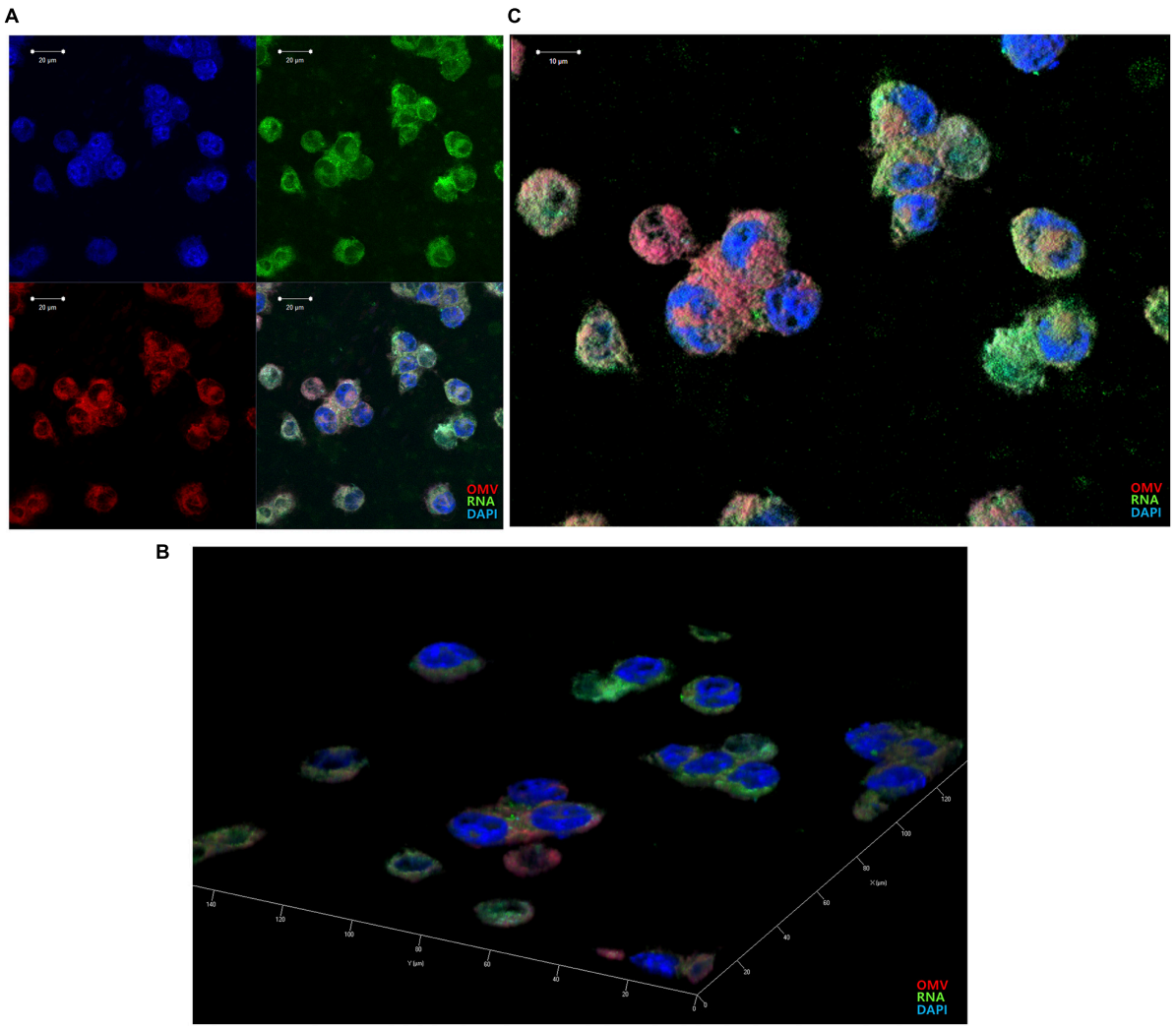

FIGURE 4 | Delivery of *Aa* OMVs and RNA into BV2 cells. *Aa* OMVs were prestained with the lipid tracer dye DiD (red) and RNA-specific dye SYTO RNASelect (green). Stained OMVs (approximately 4.5×10^8 particles) were incubated with BV2 cells on a chamber slide for 24 h at 37°C. DAPI was also counterstained with DAPI (blue) to visualize the nuclei. **(A)** Confocal microscopy analysis of *Aa* OMVs revealed colocalized OMVs and the RNA cargo inside (overlay). Bar = 20 μm. **(B,C)** 3D rendering of confocal fluorescence images. Bar = 10 μm.

particles originated from bacteria (i.e., bacterial EVs) and their roles as messengers in human diseases given their ability to travel freely from cell to cell in the body (Choi et al., 2017b; Lee, 2019).

In the present study, we demonstrated for the first time, using intravital imaging analysis, the transport of OMVs from peripheral introduction to brain microglial cells through the meninges. The delivery of bacterial EVs into the brain after crossing the BBB suggests that infection at any place in the body can cause a fatal immune response in the brain. Since the number of human commensal bacteria has been estimated to be the same as the total number of human cells (Sender et al., 2016), bacterial EVs would be continually produced and the effect of chronic brain stimulation by bacterial EVs from commensal bacteria may be attributed bacterial OMVs crossing the BBB.

OMVs are taken up by host cells through various methods, and it is known that *Aa* OMVs are internalized into cells by membrane fusion or clathrin-mediated endocytosis (Rompikuntal et al., 2012; Thay et al., 2014). Our results clearly demonstrated that *Aa* OMVs and RNA cargo (i.e., exRNA) can enter into microglial cells (**Figure 4**).

It is known that LPS isolated from *Aa* has the ability to stimulate the production of TNF-α, IL-1β, and IL-6 in human whole blood (Schytte Blix et al., 1999) and microglial cells (Díaz-Zúñiga et al., 2019), however, little is known about the effect of other pathogenic factors of *Aa* on microglial cells. Because intact LPS of OMVs might have less effect than purified or released forms of OMVs, internalized OMVs and their cargo may activate various immune signals as cytosolic LPS activates caspase-11 and exRNAs enhance the TLR8 pathway (Vanaja et al., 2016; Han et al., 2019).

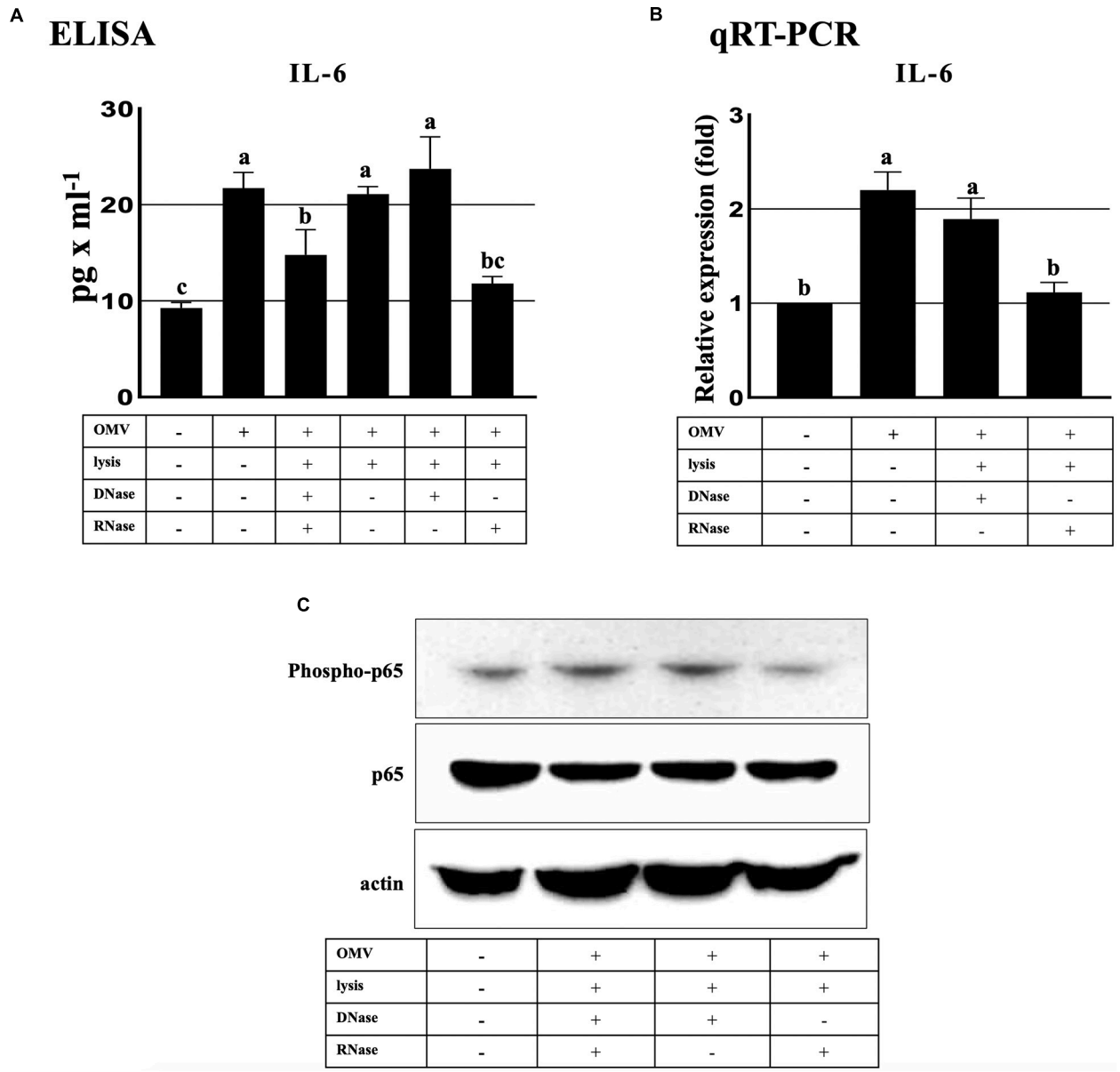

FIGURE 5 | ExRNAs of *Aa* activate IL-6 in BV2 cells through the NF-κB signaling pathway. **(A)** Secreted IL-6 protein levels were upregulated at 16 h after treatment with intact OMVs. IL-6 secretion by OMV lysate was decreased by RNase-only treated OMV lysates in BV2 cells at 16 h. **(B)** qRT-PCR analysis revealed that the transcript levels of IL-6 activation by *Aa* OMV lysates were decreased by RNase-only pretreatment at 16 h. **(C)** NF-κB activation (phospho-p65, upper panel) was significantly decreased by RNase-only-treated OMV lysates compared with DNase-treated OMV lysates at 16 h. Total NF-κB p65 (middle panel) and actin (bottom panel) levels were assessed for controls. BV2 cells were seeded onto 6-well plates (5×10^5 cells/well) and treated with *Aa* OMVs (approximately 4.5×10^8 particles/well in 2 ml of media) and OMV lysates (the same amount of proteins as in 4.5×10^8 OMV particles). Data are presented as mean ± SD from three independent experiments. The letters (a–c) indicate significant differences at $p < 0.05$.

Interestingly, murine BV2 microglial cells reacted in a manner unlike human U937 macrophage cells upon treatment with *Aa* OMVs and exRNAs. Because we used a relatively low number (4.5×10^8 particles) of OMVs compared to that in a previous study (4.5×10^{10} particles) to infect macrophage cells while avoiding BV2 cell damage, the lower dose of OMVs may be similar to the actual immune response that occurs *in vivo*. Among the various proinflammatory cytokines, IL-6 is the main player as it elevates the activity of proinflammatory signaling pathways and is associated with a large number of immune diseases (Luo and Zheng, 2016). Therefore, the increased IL-6 production in BV2 microglial cells by *Aa* exRNAs might be a novel causative agent of neuroinflammatory diseases.

Furthermore, our previous data showing that increased production of TNF-α by *Aa* OMVs in the mouse brain (Han et al., 2019) might be modulated by other cell types such as

astrocytes suggests that activated microglial cells induce the secretion of TNF-α by astrocytes (Liddelow et al., 2017). As TNF-α stimulates the induction of IL-6 production as observed in brain pericytes and astrocytes and pericyte-originated IL-6 activated BV2 microglial cells (Matsumoto et al., 2018), various types of brain cells interact with each other via cytokines they produce in response to exogenous bacterial EVs and their cargo.

Taken together, our findings reveal a previously unrecognized mechanism of RNA transport in bacterial EV-based induction of brain immune response to peripheral bacterial infections. Further studies are necessary to investigate the range of bacterial EVs and exRNAs that are constantly produced and affect entire organs. It is also necessary to further explore strategies for preventing the chronic stress caused by bacterial EVs and exRNAs in relevant immune diseases.

DATA AVAILABILITY STATEMENT

The original contributions presented in the study are included in the article/**Supplementary Material**, further inquiries can be directed to the corresponding author.

ETHICS STATEMENT

The animal study was reviewed and approved by the Institutional Animal Care and Use Committee (IACUC) of the Korean Advanced Institute of Science and Technology (KAIST, Daejeon, South Korea).

AUTHOR CONTRIBUTIONS

JH, S-YC, and JL contributed to the data collection and analysis. S-HH contributed to the data analysis and critically revised the manuscript. H-JL drafted the manuscript and contributed to the data collection and analysis as well as conception and design. All authors gave their final approval and agreed to be held accountable for all aspects of the work.

FUNDING

This research was supported by the Basic Science Research Program through the National Research Foundation of Korea (NRF), funded by the Korean Government (MSIT 2017R1A5A2015391 and 2018R1D1A3B07043539).

SUPPLEMENTARY MATERIAL

The Supplementary Material for this article can be found online at: https://www.frontiersin.org/articles/10.3389/fmolb.2020.596366/full#supplementary-material

REFERENCES

Ahn, S., Choe, K., Lee, S., Kim, K., Song, E., Seo, H., et al. (2017). Intravital longitudinal wide-area imaging of dynamic bone marrow engraftment and multilineage differentiation through nuclear-cytoplasmic labeling. *PLoS One* 12:e0187660. doi: 10.1371/journal.pone.0187660

Bachurski, D., Schuldner, M., Nguyen, P.-H., Malz, A., Reiners, K. S., Grenzi, P. C., et al. (2019). Extracellular vesicle measurements with nanoparticle tracking analysis - An accuracy and repeatability comparison between NanoSight NS300 and ZetaView. *J. Extracell. Vesicles* 8:1596016. doi: 10.1080/20013078.2019.1596016

Blenkiron, C., Simonov, D., Muthukaruppan, A., Tsai, P., Dauros, P., Green, S., et al. (2016). Uropathogenic *Escherichia coli* releases extracellular vesicles that are associated with RNA. *PLoS One* 11:e0160440. doi: 10.1371/journal.pone.0160440

Block, M. L., Zecca, L., and Hong, J.-S. (2007). Microglia-mediated neurotoxicity: uncovering the molecular mechanisms. *Nat. Rev. Neurosci.* 8, 57–69. doi: 10.1038/nrn2038

Bonnington, K. E., and Kuehn, M. J. (2014). Protein selection and export via outer membrane vesicles. *Biochim. Biophys. Acta* 1843, 1612–1619. doi: 10.1016/j.bbamcr.2013.12.011

Chinnery, H. R., Ruitenberg, M. J., and McMenamin, P. G. (2010). Novel characterization of monocyte-derived cell populations in the meninges and choroid plexus and their rates of replenishment in bone marrow chimeric mice. *J. Neuropathol. Exp. Neurol.* 69, 896–909. doi: 10.1097/NEN.0b013e3181edbc1a

Choi, J.-W., Kim, S. C., Hong, S.-H., and Lee, H.-J. (2017a). Secretable small RNAs via outer membrane vesicles in periodontal pathogens. *J. Dent. Res.* 96, 458–466. doi: 10.1177/0022034516685071

Choi, J.-W., Um, J.-H., Cho, J.-H., and Lee, H.-J. (2017b). Tiny RNAs and their voyage via extracellular vesicles: secretion of bacterial small RNA and eukaryotic microRNA. *Exp. Biol. Med.* 242, 1475–1481. doi: 10.1177/1535370217723166

Das, S., Extracellular RNA Communication Consortium, Ansel, K. M., Bitzer, M., Breakefield, X. O., Charest, A., et al. (2019). The Extracellular RNA communication consortium: establishing foundational knowledge and technologies for extracellular RNA research. *Cell* 177, 231–242. doi: 10.1016/j.cell.2019.03.023

Demmer, R. T., Jacobs, D. R., Singh, R., Zuk, A., Rosenbaum, M., Papapanou, P. N., et al. (2015). Periodontal bacteria and prediabetes prevalence in ORIGINS: the oral infections, glucose intolerance, and insulin resistance study. *J. Dent. Res.* 94, 201S–211S. doi: 10.1177/0022034515590369

Díaz-Zúñiga, J., Muñoz, Y., Melgar-Rodríguez, S., More, J., Bruna, B., Lobos, P., et al. (2019). Serotype b of *Aggregatibacter actinomycetemcomitans* triggers pro-inflammatory responses and amyloid beta secretion in hippocampal cells: a novel link between periodontitis and Alzheimer's disease? *J. Oral Microbiol.* 11:1586423. doi: 10.1080/20002297.2019.1586423

Dominy, S. S., Lynch, C., Ermini, F., Benedyk, M., Marczyk, A., Konradi, A., et al. (2019). Porphyromonas gingivalis in Alzheimer's disease brains: evidence for disease causation and treatment with small-molecule inhibitors. *Sci. Adv.* 5:eaau3333. doi: 10.1126/sciadv.aau3333

Ghosal, A., Upadhyaya, B. B., Fritz, J. V., Heintz-Buschart, A., Desai, M. S., Yusuf, D., et al. (2015). The extracellular RNA complement of *Escherichia coli*. *Microbiologyopen* 4, 252–266. doi: 10.1002/mbo3.235

Ginhoux, F., and Jung, S. (2014). Monocytes and macrophages: developmental pathways and tissue homeostasis. *Nat. Rev. Immunol.* 14, 392–404. doi: 10.1038/nri3671

Ginhoux, F., Lim, S., Hoeffel, G., Low, D., and Huber, T. (2013). Origin and differentiation of microglia. *Front. Cell. Neurosci.* 7:45. doi: 10.3389/fncel.2013.00045

Goldmann, T., Wieghofer, P., Jordão, M. J. C., Prutek, F., Hagemeyer, N., Frenzel, K., et al. (2016). Origin, fate and dynamics of macrophages at central nervous system interfaces. *Nat. Immunol.* 17, 797–805. doi: 10.1038/ni.3423

Han, E.-C., Choi, S.-Y., Lee, Y., Park, J.-W., Hong, S.-H., and Lee, H.-J. (2019). Extracellular RNAs in periodontopathogenic outer membrane vesicles promote TNF-α production in human macrophages and cross the blood-brain barrier in mice. *FASEB J.* 33, 13412–13422. doi: 10.1096/fj.201901575R

Henderson, B., Ward, J. M., and Ready, D. (2010). Aggregatibacter (Actinobacillus) actinomycetemcomitans: a triple A* periodontopathogen? *Periodontol. 2000*, 54, 78–105. doi: 10.1111/j.1600-0757.2009.00331.x

Ho, M.-H., Chen, C.-H., Goodwin, J. S., Wang, B.-Y., and Xie, H. (2015). Functional advantages of *Porphyromonas gingivalis* Vesicles. *PLoS One* 10:e0123448. doi: 10.1371/journal.pone.0123448

Holtmaat, A., Bonhoeffer, T., Chow, D. K., Chuckowree, J., De Paola, V., Hofer, S. B., et al. (2009). Long-term, high-resolution imaging in the mouse neocortex through a chronic cranial window. *Nat. Protoc.* 4, 1128–1144. doi: 10.1038/nprot.2009.89

Jung, S., Aliberti, J., Graemmel, P., Sunshine, M. J., Kreutzberg, G. W., Sher, A., et al. (2000). Analysis of fractalkine receptor CX(3)CR1 function by targeted deletion and green fluorescent protein reporter gene insertion. *Mol. Cell. Biol.* 20, 4106–4114. doi: 10.1128/mcb.20.11.4106-4114.2000

Kang, S.-M., Choi, J.-W., Lee, Y., Hong, S.-H., and Lee, H.-J. (2013). Identification of microRNA-Size, small RNAs in *Escherichia coli*. *Curr. Microbiol.* 67, 609–613. doi: 10.1007/s00284-013-0411-9

Koeppen, K., Hampton, T. H., Jarek, M., Scharfe, M., Gerber, S. A., Mielcarz, D. W., et al. (2016). A Novel mechanism of host-pathogen interaction through sRNA in bacterial outer membrane vesicles. *PLoS Pathog.* 12:e1005672. doi: 10.1371/journal.ppat.1005672

Komazaki, R., Katagiri, S., Takahashi, H., Maekawa, S., Shiba, T., Takeuchi, Y., et al. (2017). Periodontal pathogenic bacteria, *Aggregatibacter actinomycetemcomitans* affect non-alcoholic fatty liver disease by altering gut microbiota and glucose metabolism. *Sci. Rep.* 7:13950. doi: 10.1038/s41598-017-14260-9

Konig, M. F., Abusleme, L., Reinholdt, J., Palmer, R. J., Teles, R. P., Sampson, K., et al. (2016). *Aggregatibacter actinomycetemcomitans*-induced hypercitrullination links periodontal infection to autoimmunity in rheumatoid arthritis. *Sci. Transl. Med.* 8:369ra176. doi: 10.1126/scitranslmed.aaj1921

Kumar, V. (2019). Toll-like receptors in the pathogenesis of neuroinflammation. *J. Neuroimmunol.* 332, 16–30. doi: 10.1016/j.jneuroim.2019.03.012

Laugisch, O., Johnen, A., Maldonado, A., Ehmke, B., Bürgin, W., Olsen, I., et al. (2018). Periodontal pathogens and associated intrathecal antibodies in early stages of Alzheimer's disease. *J. Alzheimers Dis.* 66, 105–114. doi: 10.3233/JAD-180620

Lee, H.-J. (2019). Microbe-host communication by small RNAs in extracellular vesicles: vehicles for transkingdom RNA transportation. *Int. J. Mol. Sci.* 20:1487. doi: 10.3390/ijms20061487

Lee, H.-J. (2020). Microbial extracellular RNAs and their roles in human diseases. *Exp. Biol. Med.* 245, 845–850. doi: 10.1177/1535370220923585

Lee, H.-J., and Hong, S.-H. (2012). Analysis of microRNA-size, small RNAs in Streptococcus mutans by deep sequencing. *FEMS Microbiol. Lett.* 326, 131–136. doi: 10.1111/j.1574-6968.2011.02441.x

Li, Q., and Barres, B. A. (2018). Microglia and macrophages in brain homeostasis and disease. *Nat. Rev. Immunol.* 18, 225–242.

Liddelow, S. A., Guttenplan, K. A., Clarke, L. E., Bennett, F. C., Bohlen, C. J., Schirmer, L., et al. (2017). Neurotoxic reactive astrocytes are induced by activated microglia. *Nature* 541, 481–487. doi: 10.1038/nature21029

Luo, Y., and Zheng, S. G. (2016). Hall of fame among pro-inflammatory cytokines: interleukin-6 gene and its transcriptional regulation mechanisms. *Front. Immunol.* 7:604. doi: 10.3389/fimmu.2016.00604

Matsumoto, J., Dohgu, S., Takata, F., Machida, T., Bölükbaşi Hatip, F. F., Hatip-Al-Khatib, I., et al. (2018). TNF-α-sensitive brain pericytes activate microglia by releasing IL-6 through cooperation between IκB-NFκB and JAK-STAT3 pathways. *Brain Res.* 1692, 34–44. doi: 10.1016/j.brainres.2018.04.023

Matsumoto, J., Stewart, T., Banks, W. A., and Zhang, J. (2017). The transport mechanism of extracellular vesicles at the blood-brain barrier. *Curr. Pharm. Des.* 23, 6206–6214. doi: 10.2174/1381612823666170913164738

Rompikuntal, P. K., Thay, B., Khan, M. K., Alanko, J., Penttinen, A.-M., Asikainen, S., et al. (2012). Perinuclear localization of internalized outer membrane vesicles carrying active cytolethal distending toxin from *Aggregatibacter actinomycetemcomitans*. *Infect. Immun.* 80, 31–42. doi: 10.1128/IAI.06069-11

Rua, R., and McGavern, D. B. (2018). Advances in meningeal immunity. *Trends Mol. Med.* 24, 542–559. doi: 10.1016/j.molmed.2018.04.003

Schytte Blix, I. J., Helgeland, K., Hvattum, E., and Lyberg, T. (1999). Lipopolysaccharide from Actinobacillus actinomycetemcomitans stimulates production of interleukin-1beta, tumor necrosis factor-alpha, interleukin-6 and interleukin-1 receptor antagonist in human whole blood. *J. Periodont. Res.* 34, 34–40. doi: 10.1111/j.1600-0765.1999.tb02219.x

Sender, R., Fuchs, S., and Milo, R. (2016). Revised Estimates for the number of human and bacteria cells in the body. *PLoS Biol.* 14:e1002533. doi: 10.1371/journal.pbio.1002533

Tanaka, T., Narazaki, M., and Kishimoto, T. (2014). IL-6 in inflammation, immunity, and disease. *Cold Spring Harb. Perspect. Biol.* 6:a016295. doi: 10.1101/cshperspect.a016295

Thay, B., Damm, A., Kufer, T. A., Wai, S. N., and Oscarsson, J. (2014). *Aggregatibacter actinomycetemcomitans* outer membrane vesicles are internalized in human host cells and trigger NOD1- and NOD2-dependent NF-κB activation. *Infect. Immun.* 82, 4034–4046. doi: 10.1128/IAI.01980-14

Vanaja, S. K., Russo, A. J., Behl, B., Banerjee, I., Yankova, M., Deshmukh, S. D., et al. (2016). Bacterial outer membrane vesicles mediate ytosolic localization of LPS and Caspase-11 activation. *Cell* 165, 1106–1119. doi: 10.1016/j.cell.2016.04.015

Wang, W.-Y., Tan, M.-S., Yu, J.-T., and Tan, L. (2015). Role of pro-inflammatory cytokines released from microglia in Alzheimer's disease. *Ann. Transl. Med.* 3:136. doi: 10.3978/j.issn.2305-5839.2015.03.49

Wispelwey, B., Hansen, E. J., and Scheld, W. M. (1989). *Haemophilus influenzae* outer membrane vesicle-induced blood-brain barrier permeability during experimental meningitis. *Infect. Immun.* 57, 2559–2562. doi: 10.1128/IAI.57.8.2559-2562.1989

Wu, Y., Du, S., Johnson, J. L., Tung, H.-Y., Landers, C. T., Liu, Y., et al. (2019). Microglia and amyloid precursor protein coordinate control of transient Candida cerebritis with memory deficits. *Nat. Commun.* 10:58. doi: 10.1038/s41467-018-07991-4

Yuan, D., Zhao, Y., Banks, W. A., Bullock, K. M., Haney, M., Batrakova, E., et al. (2017). Macrophage exosomes as natural nanocarriers for protein delivery to inflamed brain. *Biomaterials* 142, 1–12. doi: 10.1016/j.biomaterials.2017.07.011

Conflict of Interest: The authors declare that the research was conducted in the absence of any commercial or financial relationships that could be construed as a potential conflict of interest.

frontiers in Molecular Biosciences

ORIGINAL RESEARCH
published: 13 January 2021
doi: 10.3389/fmolb.2020.566207

Transcriptome Profiling of *Staphylococcus aureus* Associated Extracellular Vesicles Reveals Presence of Small RNA-Cargo

Bishnu Joshi[1], *Bhupender Singh*[1], *Aftab Nadeem*[2,3], *Fatemeh Askarian*[1,4], *Sun Nyunt Wai*[2,3], *Mona Johannessen*[1*†] *and Kristin Hegstad*[1,5*†]

[1] Department of Medical Biology, Research Group for Host-Microbe Interactions, UiT The Arctic University of Norway, Tromsø, Norway, [2] Umeå Centre for Microbial Research (UCMR), Umeå University, Umeå, Sweden, [3] Department of Molecular Biology, Umeå University, Umeå, Sweden, [4] Faculty of Chemistry, Biotechnology and Food Science, The Norwegian University of Life Sciences (NMBU), Ås, Norway, [5] Norwegian National Advisory Unit on Detection of Antimicrobial Resistance, Department of Microbiology and Infection Control, University Hospital of North-Norway, Tromsø, Norway

OPEN ACCESS

Edited by:
Olga N. Ozoline,
Institute of Cell Biophysics (RAS), Russia

Reviewed by:
Simon Swift,
The University of Auckland, New Zealand
Irina Masulis,
Institute of Cell Biophysics (RAS), Russia

***Correspondence:**
Mona Johannessen
Mona.johannessen@uit.no
Kristin Hegstad
Kristin.hegstad@uit.no

[†]These authors have contributed equally to this work

Specialty section:
This article was submitted to Protein and RNA Networks, a section of the journal Frontiers in Molecular Biosciences

Received: 27 May 2020
Accepted: 14 December 2020
Published: 13 January 2021

Citation:
Joshi B, Singh B, Nadeem A, Askarian F, Wai SN, Johannessen M and Hegstad K (2021) Transcriptome Profiling of Staphylococcus aureus Associated Extracellular Vesicles Reveals Presence of Small RNA-Cargo. Front. Mol. Biosci. 7:566207. doi: 10.3389/fmolb.2020.566207

Bacterial extracellular vesicles (EVs) have a vital role in bacterial pathogenesis. However, to date, the small RNA-cargo of EVs released by the opportunistic pathogen *Staphylococcus aureus* has not been characterized. Here, we shed light on the association of small RNAs with EVs secreted by *S. aureus* MSSA476 cultured in iron-depleted bacteriologic media supplemented with a subinhibitory dosage of vancomycin to mimic infection condition. Confocal microscopy analysis on intact RNase-treated EVs indicated that RNA is associated with EV particles. Transcriptomic followed by bioinformatics analysis of EV-associated RNA revealed the presence of potential gene regulatory small RNAs and high levels of tRNAs. Among the EV-associated enriched small RNAs were SsrA, RsaC and RNAIII. Our finding invites new insights into the potential role of EV-associated RNA as a modulator of host-pathogen interaction.

Keywords: *Staphylococcus aureus*, transcriptomic analysis, small RNAs, tRNA, extracellular vesicle

INTRODUCTION

Staphylococcus aureus (*S. aureus*), a Gram-positive bacterium, is a frequent colonizer of anterior nares of the healthy human population. This bacterium can cause various infections ranging from minor superficial skin infections to severe life-threatening infections such as osteomyelitis, pneumonia, endocarditis, bacteremia and sepsis (Wertheim et al., 2005; Mccaig et al., 2006; Foster et al., 2014). The adaptation of diverse lifestyles and the ability to cause diseases is due to the fact that *S. aureus* harbors arsenals of virulence factors involved in adhesion, invasion and dissemination (Novick, 2003).

Small RNA (sRNA) are heterogeneous small-sized transcripts (50–500 nucleotides) expressed under stressful environmental conditions which play important roles in growth processes, metabolism, stress adaptation and virulence (Tomasini et al., 2014; Westermann, 2018). Prokaryotic sRNAs are often non-coding and mainly originate from intergenic regions (Wagner and Vogel, 2003). They generally form secondary structures such as hairpins and stem-loops (Wagner and Romby, 2015). There are varieties of techniques to identify and characterize sRNAs (Lagos-Quintana et al., 2001; Wang et al., 2009; Li et al., 2012). Mizuno et al. first reported sRNAs with regulatory functions in *Escherichia coli* in 1980's, and a decade later Novick et al. reported

regulatory sRNAs in *S. aureus* (Mizuno et al., 1984; Novick et al., 1989). Currently, there are about 250 sRNAs discovered in various strains of *S. aureus* grown under different experimental conditions, and the biological functions of most of them are yet to be determined (Guillet et al., 2013; Hermansen et al., 2018). Still, novel sRNA transcripts are reported from *S. aureus* strains, and the number is increasing with the advancement of high-throughput sequencing technology as well as robust computational methods (Liu W. et al., 2018; Westermann, 2018).

Extracellular Vesicles (EVs) are nanosized-proteolipids, with a spherical shape that are heterogeneous in size ranging from 50 to 500 nm (Askarian et al., 2018). Sometimes fusion of vesicles have resulted in formation of filamentous structures, also known as nanopods or nanotubes (Dongre et al., 2011; Dubey and Ben-Yehuda, 2011; Gill et al., 2018). EVs may contain virulence factors (Devos et al., 2015; Askarian et al., 2018; Wagner et al., 2018; Nadeem et al., 2020), such as toxins (Rivera et al., 2010; Coelho et al., 2019) as well as other enzymes (Smalley and Birss, 1987; Elhenawy et al., 2014), quorum sensing molecules (Mashburn and Whiteley, 2005; Brameyer et al., 2018; Morinaga et al., 2018) and nucleic acids such as DNA (Hagemann et al., 2014; Bitto et al., 2017; Langlete et al., 2019) and RNA (Sjöström et al., 2015; Koeppen et al., 2016; Choi J.-W. et al., 2017). Their content may vary depending on species and growth conditions (Bager et al., 2013; Ghosal et al., 2015; Koeppen et al., 2016). EVs might act as a decoy against antimicrobial peptides and phages (Manning and Kuehn, 2011), and are also involved in co-operation and/or competition with other pathogens (Lynch and Alegado, 2017; Choi et al., 2020). EVs can also influence biofilm formation and modulate host-immune responses (Manning and Kuehn, 2013; Schwechheimer and Kuehn, 2015; Liu Y. et al., 2018).

EVs from Gram-negative bacteria harbor sRNA involved in intra-species (microbe-microbe) (Whitworth, 2018) and inter-kingdom (microbe-host) interactions (Koeppen et al., 2016; Frantz et al., 2019) as well as pathogenicity (Song and Wai, 2009). However, scant functional and analytical data exist to support these claims in Gram-positive bacteria (Ghosal et al., 2015; Sjöström et al., 2015; Koeppen et al., 2016; Choi et al., 2018; Malabirade et al., 2018).

During infection, the availability of iron is strictly controlled by the host, and in order to survive pathogens must adapt their transcriptomic and metabolic pathways accordingly (Wilderman et al., 2004; Oglesby-Sherrouse and Murphy, 2013; Mäder et al., 2016). Nutrient limitation and antibiotics is furthermore known to increase vesiculation (Toyofuku et al., 2019). Subinhibitory concentrations of the last resort anti-staphylococcal antibiotic, vancomycin, has been shown to influence physiology, growth and toxin production by *S. aureus* (Hsu et al., 2011; Cafiso et al., 2012; He et al., 2017), and has been found to increase EV production in another Gram-positive species, *Enterococcus faecium* (Kim et al., 2019). Hence, in this study, we used iron-chelated media supplemented with vancomycin to evaluate whether the EVs produced by *S. aureus* MSSA476 are associated with sRNAs when grown in conditions that mimic an infection that is being treated with an antibiotic.

Abbreviations: ATCC, American type culture collection; AFM, Atomic Force Microscopy; KEGG, Kyoto Encyclopedia of Genes and Genomes; IGV, Integrative Genomics Viewer; EVs, Extracellular vesicles; NTA, Nanoparticle Tracking Analysis; EVs, Extracellular Vesicles; rRNA, Ribosomal RNA; RNA-Seq, RNA Sequencing; sRNA, Small RNA; TEM, Transmission Electron Microscopy; tRNA, transfer RNA; UTRs, Untranslated regions.

MATERIALS AND METHODS

Strain and Growth Conditions

S. aureus subsp. *aureus* Rosenbach MSSA476 was purchased from LGC standard AB (ATCC- BAA-1721) (Sweden). The bacteria were grown at 37°C on BHI agar plate, BHI broth, or in trace metal-depleted BHI broth containing 0.5 μg/mL of vancomycin. The trace metals including divalent cations such as iron were lowered by treating the BHI broth with 2 g/L of chelex-100 resin (Bio-Rad, Californa, USA). The medium was subsequently filtered according to the manufacturer's instructions.

Isolation of Bacterial Extracellular Vesicles

The bacterial EVs were isolated by a procedure described earlier (Askarian et al., 2018; Wagner et al., 2018), with slight modifications. A fresh overnight culture of the methicillin-susceptible *S. aureus* MSSA476 (1:100 dilution) was inoculated into 500 mL BHI (normal conditions) or Chelex-treated BHI broth containing 0.5 μg/mL of vancomycin (stressed conditions) at least two to five different days. The cultures were grown with shaking at 37°C for 16 h. The cultures were then centrifuged at 6,000 × g for 30 min. Bacterial pellets were discarded, and the supernatants was filtered through 0.2 μm filters (Millipore Express™ Plus, USA) and ultra-centrifuged at 100,000 × g for 3 h at 4°C in a 45 Ti rotor (Beckman, USA). EV pellets from each isolation were re-suspended in 500 μL RNAlater (Thermo Fisher Scientific, Massachusetts, USA) or in Phosphate-buffered saline (PBS) if EVs were to be used for microscopy or Nanoparticle Tracking Analysis, and kept at −80°C until further use. Prior to RNA isolation for RNA-seq, EVs from several isolations were thawed, pooled and concentrated using ultrafiltration (10 kDa Vivaspin 20, Sartorius, Germany). An overview of EV isolations from bacteria grown under stressed conditions and its downstream applications is provided in **Supplementary Table 1**.

Transmission Electron Microscopy (TEM)

TEM was performed as described previously (Cavanagh et al., 2018; Wagner et al., 2018). Briefly, 5 μL of purified EVs were applied to Formvar coated 75 mesh hexagonal copper grids (Electron Microscopy Science, Pennsylvania, USA) and incubated for 5 min. Grids were washed with MQ water, and negatively stained with 2% methylcellulose and 3% uranyl acetate in a ratio of 9:1. The excess of stain was blotted away, and grids were then left to dry at room temperature. The samples were then visualized with a JEOL JEM 1010 transmission electron microscope (JEOL, Tokyo, Japan) operated at 80 kV.

Atomic Force Microscopy (AFM)

The EVs were imaged by AFM, as described previously (Lindmark et al., 2009; Ahmad et al., 2019). Briefly, EVs were deposited onto a freshly cleaved mica surface (Goodfellow

Cambridge Ltd., Cambridge, UK). Prior to imaging, EVs on mica were dried in a desiccator for about 2 h. Images were recorded on a Multimode 8 Nanoscope AFM equipment (Bruker AXS GmbH, Karlsruhe, Germany) using TappingMode. Images were gathered by NanoScope software using ScanAsyst in air with ScanAsyst cantilevers, at a scan rate of ∼0.8–1.5 Hz. The final images were plane fitted in both axes and presented in a surface plot of the height mode.

Nanoparticle Tracking Analysis (NTA)

The size distribution of EVs were determined using NanoSight NS300 (Malvern Instruments Ltd., Worcestershire, UK) equipped with CMOS camera and a blue laser module (488 nm, LM12 version C) (Jamaly et al., 2018). Briefly, EV samples were thawed and diluted (500×) in PBS to obtain a concentration within the recommended measurement range (1–10 × 10^8 particles/mL). Using a 1 mL syringe, the sample was injected into the instrument and videos were captured in triplicate for 30 s. The mean values for size and concentration were analyzed using the NanoSight (NTA software, version 3.0).

Labeling of Extracellular Vesicles

The EVs were stained using a previously described protocol with slight modifications (Nicola et al., 2009; Vdovikova et al., 2017). The vesicles were either untreated or treated with RNase (Roche diagnostics, Basel, Switzerland) to remove extracellular RNA then stained with lipid-specific dye, PKH2 or DiD (Sigma Aldrich) and subsequently with RNA specific dye SYTO RNASelect Green (Thermo Fisher Scientific, Massachusetts, USA). The stained vesicles were then ultra-centrifuged at a speed of 100,000 × g for 1 h at 4°C. The stained EVs were resuspended in PBS. Samples were mounted on a glass slide and examined by Leica SP8 inverted confocal system (Leica Microsystems) equipped with a HC PL APO 63 ×/1.40 oil immersion lens. Images were captured and processed using LasX (Leica Microsystems). Fluorescence intensity profiles were generated using the plot profile command in ImageJ-FIJI distribution (Schindelin et al., 2012) For quantification, EVs from 8 randomly selected fields (180 μm^2) were counted. Results were pooled from two independent experiments and data are expressed as percentage.

Bacterial Growth Curve and Viability Assay

A single colony of MSSA476 was inoculated into two 5 mL of BHI broth and grown overnight with shaking at 37°C. The 5 mL cultures were used to inoculate 500 mL BHI (normal) and 500 mL iron depleted BHI containing antibiotics (stressed). The cultures were incubated with shaking at 37°C, and optical density was measured every 30 min for 16 h. For the viability assay, 500 μL of each culture of bacteria grown under normal and stressed conditions for 16 h, were harvested. Viable plate count was carried out by plating 20 μL of 10-fold serial dilutions (from 10^{-5} to 10^{-10}) on blood agar plates, which were incubated for 24 h at 37°C. Dilutions containing 10–100 colonies were counted, and the concentration was calculated as CFU/mL.

Live and Dead Count

Bacterial cultures grown for 16 h in BHI (normal) and iron depleted BHI containing antibiotics (stressed) were analyzed for live and dead cells using LIVE/DEAD BacLight bacterial Viability and Counting Kit (Thermo Fisher Scientific, Waltham, USA) and BD LSRFortessa flow cytometer. Each bacterial culture was diluted 1,000-fold in 1 mL 0.85% filtered NaCl, which contain 0.5 μL SYTO 9, 2.5 μL Propidium iodide (PI), and 10 μL beads of size 6 μm. Beads had a concentration of 1 × 10^8/mL and were diluted 100-fold. Cells were stained for 10–15 min at room temperature. Stained bacteria were analyzed using BD LSRFortessa flow cytometer using a voltage of 600, 250, 400, and 800 for forward scatter (FSC), side scatter (SCC), AF488 and PI, respectively. All scales were set to logarithmic amplification with gain voltages of 300, 250 and 200 for FSC, SSC, and AF488, respectively. Data were recorded for 1,000 bead events. Total events were recorded and density of bacterial culture in terms of bacteria/mL was calculated as (numbers of events in bacterial region) × (dilution factor)/(numbers of events in the bead region × 10^{-6}).

Extraction of RNAs

The crude collection EVs was stored in RNAlater; which is a preservative compatible with RNA isolation and downstream applications such as RNA sequencing and Reverse transcription. The EVs were centrifuged using Vivaspin® ultrafiltration spin columns (cutoff 10000MWCO) at 5,000 RPM for 15 min. The concentrated EVs were treated with RNaseA (50 μg/mL) for 30 min at room temperature to degrade all forms of extracellular RNA. Thereafter, to stop the RNase activity, EVs were treated with 5 μL of RNase inhibitor (Applied Biosystems, Massachusetts, USA) for 15 min at 37°C. Then the small RNA from *S. aureus* EVs were isolated by miRNeasy kit (Qiagen, Hilden, Germany), according to the manufacturer's instruction. Trizol and Chloroform used during RNA isolation are sufficient to remove traces of RNAlater. The concentration of RNA was measured by Qubit HS kit, which quantify sample concentration ranging from 250 pg/μL to 100 ng/μL (Thermo Fisher Scientific, Waltham, USA), and the quality of RNA was assessed by Nanodrop (Thermo Fisher Scientific, Waltham, USA, USA). A 260/280 ratio of 1.8 or higher was considered optimal. In our RNA prep it was found to be 1.85. In order to evaluate whether the isolated RNA was extravesicular or associated with EVs, RNA concentration was measured on crude EVs, RNase treated EVs and finally in RNA isolated from the RNase-treated EVs.

rRNA Depletion, Library Preparation, and Sequencing

The isolated EV-associated RNA was treated with Ribo-zero rRNA removal kit (Illumina, Munich, Germany) according to the manufacturer's instructions to reduce ribosomal RNA (rRNA). Thereafter, the concentration of RNA was measured using Experion RNA HighSense Chips (Bio-Rad Laboratories, Inc, USA). The depleted RNA was cleaned and concentrated using RNeasy MinElute Cleanup kit (Qiagen, Hilden, Germany) and RNA clean & concentrator-5 kit (Zymo Research, California, USA). The rRNA-depleted RNA was fragmented, and reverse

transcribed into cDNA using high capacity cDNA reverse transcription kit (Applied Biosystems, California, USA), and sequenced on an Illumina NextSeq550 platform.

RNA Preparation, cDNA Synthesis, and qPCR

qPCR was used to confirm the presence of the three enriched sRNAs (SsrA, RSaC, and RNAIII). The EV-associated RNA was isolated as described above and treated with DNase (ArcticZymes, Tromsø, Norway) before RNA integrity and quantity were measured both by NanoDrop and Qubit. cDNA was prepared by reverse transcription kit (Applied Biosystems) using 100 ng RNA. qPCR reactions were performed in technical duplicates for pooled EV samples using SYBR Green master mix (Applied Biosystem) with the following primer pairs: SsrA-F/R: CACTCTGCATCGCCTAACAG/ GCGTCCAG AGGTCCTGATAC, RsaC-F/R: CAAAGGAAAGGGGCATAC AA/ ACGCCATTCCCTACACACTC, RNAIII-F/R: AGTTTC CTTGGACTCAGTGCT/ GGGGCTCACGACCATACTTA. To perform qPCR, briefly, 2 μL of cDNA was used as a template for each 20 μL reaction, which was carried out with 100 nM of primers. Cycling conditions were as follows: initial denaturation 10 min at 95°C, 40 cycles of 15 s at 95°C and 60°C for 1 min as annealing and elongation temperature. The data were treated and analyzed with the Applied Biosystems (7300 Real-Time PCR System) to determine the Ct.

PCR and Sanger Sequencing

RT-PCR was carried out in a Thermal Cycler (Applied Biosystems, Foster City, CA) in order to verify the three PCR amplicons (SsrA, RsaC and RNAIII) by agarose gel and DNA sequencing. The PCR was performed in a 20 μL reaction, containing gene-specific primers mentioned above and DreamTaq Green PCR Master Mix (Thermo Fischer Scientific, USA) according to the manufacturer's instruction. One μL of cDNA was used as the template. The cycling conditions were performed as follows: after an initial denaturation step of 2 min at 95 °C, 40 cycles were performed for 30 s at 95 °C, 60 s at 60 °C, and 1 min at 72 °C. A final extension step for 10 min at 72 °C was used. PCR products were further separated on a 1% agarose gel, stained with GelRed and visualized using Syngen Gel Imaging (Bio-Rad Laboratories Inc, USA). The PCR product was cleaned using PCR Clean-Up Kit (Promega, Norway). Sequencing reactions were performed in using a BigDye Terminator version 3.1 kit (Applied Biosystems) according to the manufacturer's instructions with the same primers as for the real-time PCR assay. Sequencing was performed on an Applied Biosystems 3,130 × l genetic analyzer.

Bioinformatics Analysis

The fastQ files obtained after paired-end sequencing was checked for quality using the Galaxy webserver (https://galaxy-uit.bioinfo.no). Bcl2fastq program supplied by Illumina was used to convert bcl files to fastQ files, which automatically trims the adapters and generates clean reads. The clean reads were aligned with the reference genome (MSSA476; GenBank accession no. NC_002953.3) using Bowtie 2 (Langmead and Salzberg, 2012). Mapping of the EV reads to the reference genome resulted in a Sequence Alignment Map file that was converted to a Binary Alignment Map (BAM) file. The BAM and its associated annotation files of the reference genome were loaded into Artemis where manual searches for sRNAs were performed. Visualization and manual inspection of reading coverage were conducted using Artemis version 1.0 (Rutherford et al., 2000). All the sRNAs are listed based on genomic coordinates provided from the bacterial small regulatory RNA repository BSRD (http://kwanlab.bio.cuhk.edu.hk/BSRD). The sRNAs identified from Artemis were run separately for Rfam search in Artemis to gather information about RNA families and RNA elements, including accession numbers. In addition, the Rockhopper tool (Tjaden, 2019) was used to identify transcripts and operons and to elucidate bacterial transcriptomes. Transcripts from Rockhopper were visualized (.wig files) in the Integrative Genomics Viewer (IGV) (Robinson et al., 2011).

RESULTS

RNA Is Associated With *S. aureus*-Derived EVs

The MSSA476 bacterial growth in BHI (normal condition) or trace metal-depleted BHI supplemented with a subinhibitory concentration of vancomycin mimicking infection (stress condition) were compared and found to be similar at 16 h (**Supplementary Figure 1**). The viability of bacteria was evaluated by flow cytometry and colony-forming units (CFU) enumeration and showed similar viability which was above 99.6% (**Table 1**, **Supplementary Figure 2**).

Then, EVs were isolated from *S. aureus* grown for 16 h under normal or stressed conditions. EVs were obtained from bacteria grown under both conditions. However, the number of particles, as well as protein concentration, was increased when bacteria were stressed (**Supplementary Figure 3**). Unfortunately, the yield of sRNA obtained from EVs isolated bacteria grown under normal condition was too low for RNA-seq. Therefore, we focused the study on EVs isolated from stressed bacteria. The morphology of EVs was evaluated by AFM and TEM. Aligned with other studies on MSSA476 (Gurung et al., 2011; Askarian et al., 2018), EVs were spherical in shape, though minor fusions were observed (**Figures 1A,B**, **Supplementary Figure 4**). In addition, the size distribution of vesicles was measured using NTA which revealed that the sizes ranged from 20 nm to 200 nm, although the majority of vesicles are between 100 and 150 nm. The analysis also showed some particles with sizes above 200 nm (**Figure 1C**), which might be due to aggregation or fusion of EVs.

Next, we wanted to evaluate whether RNA is associated with the EVs. The EVs were left untreated or treated with RNase to remove extravesicular RNA, and thereafter stained with RNA specific dye (green). EVs are known to contain lipids (Ghosal et al., 2015), and were therefore stained with a lipid-specific dye (red). The RNA and lipid-stained particles, which we assumed to be aggregated EVs (Ter-Ovanesyan et al., 2017), were then analyzed by confocal microscopy. As seen in **Figures 2A,B** and

TABLE 1 | Summary of bacterial counts using flow cytometry and total plate count method.

Sample	Flow cytometry data			Plate count (CFU)
	Bacterial count (bacteria/mL)	Live bacteria (%)	Dead bacteria (%)	
S. aureus grown under normal condition	1.8×10^{10}	99.9	0.1	3.0×10^{10}
S. aureus grown under stress condition	8.8×10^{9}	99.6	0.4	2.3×10^{10}

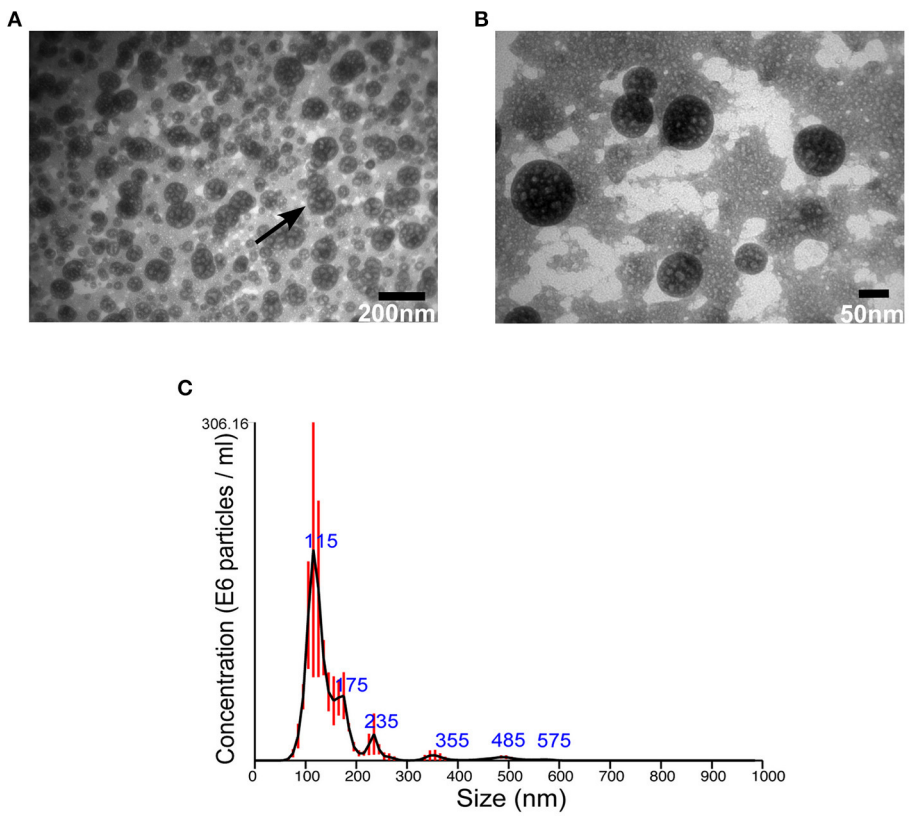

FIGURE 1 | *S. aureus* MSSA 476 grown under infection mimicking condition produces spherical EVs of various sizes. **(A)** Low and **(B)** high magnification TEM images of crude EVs isolated from bacteria grown in iron-depleted BHI supplemented with subinhibitory concentration of vancomycin (black arrow indicates vesicles) **(C)** NTA showing total number and size distribution of EVs (mean in nm ± SD) isolated from *S. aureus* MSSA476. E6 particles/ml is the standard NTA output, and means 10^6 particles/ml.

Supplementary Figures 5, **6**, RNA and lipid stain co-localized in the majority of EVs. To confirm the sensitivity of the method, the fluorescence intensity (**Figure 2C**) was determined in co-stained and only lipid stained EVs indicated with dotted line (**Figure 2B**). Finally, we quantified co-localization of RNA and lipid particles by counting 8 random microscopic fields in both untreated and RNase-treated EVs. In RNase- treated EVs, we observed ∼70% co-localization of RNA and lipid stained particles, while ∼20% percent of the lipid stained particles were without any RNA stain (**Figure 2D**, **Supplementary Figure 6B**). Approximately 20% of the particles were only RNA-stained in untreated EVs, while only 6% of the RNase-treated EV particles were stained by RNA-specific stain only, supporting the efficacy of RNase treatment (**Figure 2D**, **Supplementary Figure 6B**). This low level of RNA stained particles in RNase-treated EVs might represent either non-specific aggregations of RNA dye, or a leakage of RNA from broken EVs during sample preparation, or the presence of small amounts of extra-vesicular RNA even after RNase treatment (**Figure 2D**).

Having found that RNA was associated with RNase-treated EVs, we isolated sRNA which was analyzed further by bioanalyser. A smear of RNA in size range 50–200 bp was seen

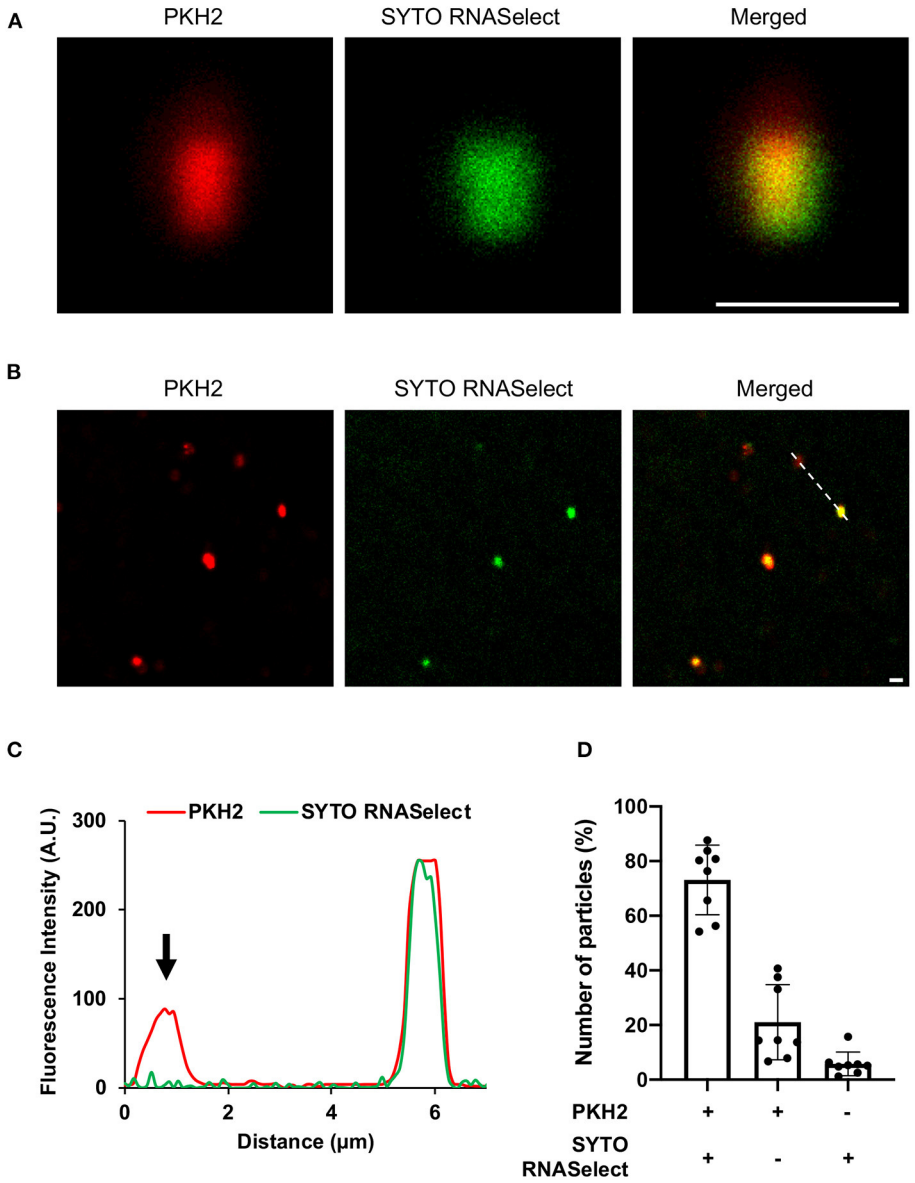

FIGURE 2 | Confocal microscopy of **(A)** enlarged extracellular vesicle particles/aggregates and **(B)** multiple EV particles/aggregates from the field of view. The vesicles were stained with lipid specific dye, PKH2 (red) and RNA-specific dye, SYTO RNASelect (green). Scale bar, 1 μm [zoom 1 μm of **(A)**]. **(C)** Line graph showing fluorescence intensity profile of the dotted line across the extracellular vesicles in panel **(B)**. Arrowhead indicates absence of SYTO RNASelect fluorescence in the PKH2 stained extracellular vesicle. **(D)** Quantification of RNA and lipid positive particles. Data points from two different experiments and 8 fields of view.

(**Figure 3A**). The obtained RNA was treated using the rRNA depletion kit, which reduced the average concentration of RNA from 77 to 40 ng/μL. Further analysis of the rRNA-depleted samples using bioanalyser revealed appearance of four peaks (**Figure 3B**, black arrows) at 24–28 s, known to be typical peak for < 200 bp sRNA. Of note, no strong peaks appeared for ribosomal RNA (16S and 23S), indicating efficiency of sRNA enrichment by the miRNA kit and subsequent depletion of rRNAs. Hence, our data demonstrated that sRNA are associated with *S. aureus* EVs.

tRNAs and sRNAs Were Enriched in *S. aureus* Derived EVs

The transcriptome profiling of the sRNA content in EVs was performed using RNA-seq analysis. Paired-end sequencing resulted in ∼458,000 reads with lengths varied from 35 to 151 nucleotides. Eighty-seven percentage of the reads were aligned and found to be well-distributed over the reference genome of *S. aureus* strain MSSA476 (GenBank accession no. NC_002953.3) (**Supplementary Table 2** - mapping statistics) (**Supplementary Figure 7**). The majority of reads corresponded

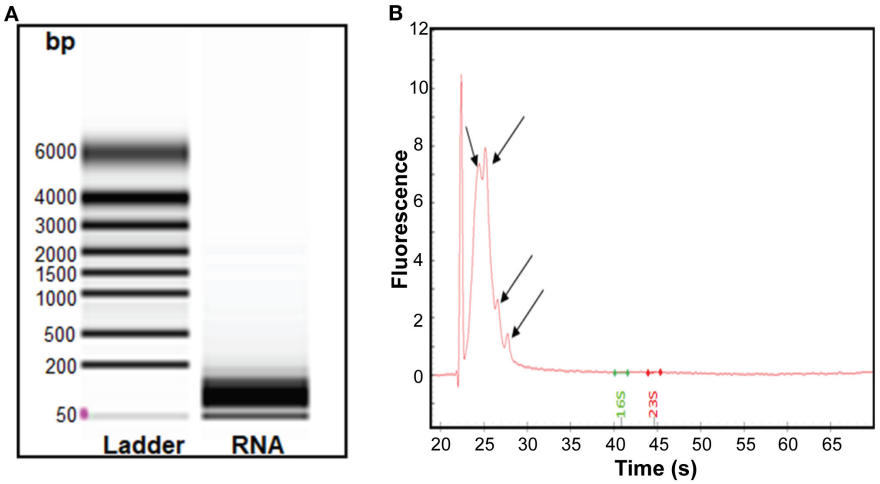

FIGURE 3 | Analysis of the sRNA isolated from *S. aureus* EVs. **(A)** Virtual gel like image from bioanalyser. L, Ladder and lane 2 shows the RNA of the EVs. **(B)** Electropherogram displaying sRNA. The first peak in the electropherogram represent lower marker that is used as an alignment to RNA ladder. Other four small peaks appearing at the interval of migration time 24–28 s represent sRNA.

to protein encoding RNAs, while 4 and 3.5% corresponded to rRNAs and tRNAs, respectively, 0.5% of the reads obtained by RNA-seq corresponded to sRNAs (**Supplementary Figure 8**). The sRNA reads corresponded to sRNAs with size distribution from 20 to 500 nt (**Supplementary Figure 9**).

A total of 62 RNAs, 276 5′ untranslated regions (5′ UTRs) and 276 3′ untranslated regions (3′ UTRs) were detected. Similarly, further aligning of the reads against *S. aureus* MSSA476 plasmid pSAS resulted in detection of five RNAs, seven 5′ UTRs, and 11 3′ UTRs (**Supplementary Table 2** - Summary Rockhopper output). Next, operons in the *S. aureus* genome were defined as regions with continuous coverage of whole transcript reads by RNA-seq. This resulted in identification of 486 multi-gene operons consisting of 2–18 genes (for a total of 1,415 genes) (**Supplementary Table 2** - operon Rockhopper output). Phage RNAs, e. g, transcripts encoding terminase subunits, tail proteins and portal protein, were detected among the protein encoding RNAs (**Supplementary Table 2** - Rockhopper transcript output). Since our focus is on sRNAs, we chose to further describe only the tRNA and sRNA content.

Coverage of tRNA upstream of a regulatory region is shown in **Supplementary Figure 10.** The read counts of tRNAs in EVs varied from 4 to 984, with cove scores from 36.67 to 101.60 (**Supplementary Table 2** - tRNAs in EVs). The most enriched tRNAs includes tRNA for Met, Asp, Leu, Tyr, Ser, Thr, Gly, and Phe (**Table 2**).

The 67 sRNAs identified by Rockhopper software were manually checked with Artemis and 49 sRNAs were validated using the Rfam database. The MSSA476-derived EVs carried several sRNAs with read counts varying from 1 to 80 (**Supplementary Table 2** - small RNA in EVs). 6S RNA and SsrA showed the highest read counts of 80 and 65, respectively (**Table 3**, read density of SsrA, 6S RNA, RNAIII, and RsaC are shown in **Supplementary Figure 11).**

Validation of *S. aureus* SrrA, RsaC, and RNAIII RNA Associated With EVs

Among the enriched sRNA were SsrA, RsaC, and RNAIII (**Table 3**). SsrA and RsaC RNAs are involved in antibiotic resistance through their modulation of RNA fate and protein activity (Lalaouna et al., 2014), while RNAIII, not only have regulatory function but also encode 26 amino acid long δ-toxin (Novick et al., 1993; Caldelari et al., 2013). To validate our results obtained from transcriptomic analyses, we performed qPCR on RNA obtained from EVs using primers targeting SsrA, RsaC and RNAIII. The results presented in boxplot (**Figure 4A**) are based on three biological repeats (**Supplementary Table 3)** which confirmed presence of these three transcripts associated with EVs. The presence was finally confirmed by PCR of cDNA yielding DNA fragments of expected sizes (**Figure 4B**), and by Sanger sequencing which confirmed the identity of *ssrA, RsaC,* and *RNAIII* (**Supplementary Figure 12**).

DISCUSSION

S. aureus harbors a multitude of virulence factors that are tightly regulated during infection. Several studies have shown that exposure to sub-MIC antibiotic concentrations enhances *S. aureus* ability to adapt to physiological changes, survive and persist in human hosts (Kaplan et al., 2012; Howden et al., 2013). One of the mechanisms modulating virulence and pathogenicity of *S. aureus* is via the release of EVs (Gurung et al., 2011; Thay et al., 2013; Askarian et al., 2018; Schlatterer et al., 2018; Andreoni et al., 2019). Virulence factors such as hemolysin, loaded as vesicular cargo, are delivered to host cells via fusion of vesicles with the host cholesterol-rich membrane. In addition, *S. aureus*-derived EVs also release lipoproteins, which play a significant role in modulating TLR2 activation and are involved in pathogenesis. In general, various pathophysiological functions ranging from

TABLE 2 | The most enriched MSSA476 EV-associated tRNAs based on read counts.

Element	Genomic coordinates	Full name (anticodon)	Cove score	Read count	GC content	Bases of selection
tRNA	1937102..1937175	tRNA Met (CAT)	75.92	984	62.16	CGCGGGATGGAGCAGTTCGGTAGCTCGTCGGGCTCATAA CCCGAAGGTCGGTGGTTCAAATCCGCCTCCCGCAA
tRNA	1937017..1937092	tRNA Asp (GTC)	83.32	859	61.84	GGTCTCGTAGTGTAGCGGTTAACACGCCTGCCTGTC ACGCAGGAGATCGCGGGTTCGATTCCCGTCGAGACCGCCA
tRNA	533919..534007	tRNA Leu (TAA)	75.33	607	61.80	GCCGGGGTGGCGGAACTGGCAGACGCACAGGACTTAAA ATCCTGCGGTGAGAGATCACCGTACCGGTTCGATTCC GGTCCTCGGCACCA
tRNA	1937971..1938059	tRNA Leu (TAA)	76.44	590	61.80	GCCGGGGTGGCGGAACTGGCAGACGCACAGGACTTAAAAT CCTGCGGTGAGTGATCACCGTACCGGTTCGATTCCGGT CCTCGGCACCA
tRNA	1936757..1936837	tRNA Tyr (GTA)	69.29	525	61.73	GGAGGGGTAGCGAAGTGGCTAAACGCGGCGGACT GTAAATCCGCTCCTTCGGGTTCGGCAGTTCGAATCTGC CCCCCTCCA
tRNA	1937190..1937282	tRNA Ser (TGA)	74.09	829	61.29	GGAGGAATACCCAAGTCCGGCTGAAGGGATCGGT CTTGAAAACCGACAGGGCCTTAACGGGCCGCGGGGGT TCGAATCCCTCTTCCTCCGCCA
tRNA	1937407..1937496	tRNA Ser (TGA)	61.04	657	60.00	GGAGGAATACCCAAGTCCGGCTGAAGGGATCGGTCTT GAAAACCGACAGGGGCTTAACGGCTCGCGGGGGTTCG AATCCCTCTTCCTCCG
tRNA	1936843..1936918	tRNA Thr (TGT)	92.93	560	55.26	GCCGGCCTAGCTCAATTGGTAGAGCAACTGACTTGTAAT CAGTAGGTTGGGGGTTCAAGTCCTCTGGCCGGCACCA
tRNA	533837..533911	tRNA Gly (GCC)	86.82	518	54.67	GCAGAAGTAGTTCAGCGGTAGAATACAACCTTGCCAAG GTTGGGGTCGCGGGTTCGAATCCCGTCTTCTGCTCCA
tRNA	1936926..1936998	tRNA Phe (GAA)	76.42	635	50.68	GGTTCAGTAGCTCAGTTGGTAGAGCAATGGATTGAA GCTCCATGTGTCGGCAGTTCGACTCTGTCCTGAACCA

*See **Supplementary Table 2** for the full list of tRNAs.*

cellular inflammation to host cell death could be mediated by *S. aureus* EVs (Hong et al., 2011; Kim et al., 2012).

The first report of RNA associated with EVs was published in 1989 in Neisseria gonorrhoeae (Dorward and Garon, 1989). Henceforth, many intensive studies have been conducted to characterize RNAs and their functions (Scanlan, 2014; Sjöström et al., 2015; Blenkiron et al., 2016; Koeppen et al., 2016; Choi et al., 2018; Malabirade et al., 2018).

A crude EV pellet was used as the source material to enable isolation of sufficient sRNA for sequencing. The crude EV pellet was further concentrated using ultrafiltration columns with cutoff of 10 kDa, which remove lipoprotein aggregates (Ramirez et al., 2018). The crude EVs were RNase treated to remove any RNA that is not associated with EVs, before sRNA was isolated for high-throughput RNA sequencing. Adequately replicated RNA quantification isolated from EVs and RNase-treated EVs confirmed a reduction in RNA from RNase treatment (**Supplementary Table 1**). Since staining of RNase-treated EVs with RNA and lipid dyes showed RNase-mediated reduction in particles that were only RNA stained, the ∼70% co-localization of RNA and lipid particles were assumed to be EVs (**Figure 2**, **Supplementary Figures 5**, **6**). We could isolate sRNA from RNase-treated EVs, and thus we concluded that sRNA is associated with EVs. RNA-seq data revealed that SsrA, RsaC, and RNAIII were among the most enriched sRNAs associated with the EVs. To validate our findings, we repeated isolation of sRNA in triplicates from RNase treated EVs and confirmed presence SsrA, RsaC, and RNAIII by qPCR, conventional PCR and Sanger sequencing of the PCR products (**Figure 4**, **Supplementary Table 1**).

We also identified phage-like sequences in EVs by RNA-seq (**Supplementary Table 2**). The presence of these might be due to vancomycin-induced activation of one or two of the prophages harbored by *S. aureus* MSSA476 (Holden et al., 2004), which then pelleted with the vesicles. This agrees with others, who also obtained phage or phage tail particles in EVs when bacteria were exposed to antibiotics (Kharina et al., 2015; Devos et al., 2017; Andreoni et al., 2019). One of the limitations of using the crude pellet as the source of EVs for isolation of RNA is that it not only contains EVs, but also other nanoscale contaminants (e.g., the filaments and bacteriophages). We assumed that the source of RNA, in our study, is predominantly from RNase-treated EVs, but it is conceivable that some sequences are from other nanoscale contaminants pelleted along with the EVs, in a form that is protected from RNase, and at a concentration or of a size that is not visible by the fluorescence microscopy.

In bacteria, 16S and 23S rRNA are the most abundant RNAs that accounts for more than 90% of the total RNA biotype (Petrova et al., 2017). The abundance of rRNA reduces the sequencing depth for other RNA classes, thus an rRNA depletion strategy was implemented to ensure sufficient coverage of the transcriptome from bacterial RNA-seq data. Although in our study, fragments of mRNA were most abundant, we focused on characterizing sRNA, given they play important roles in EV

TABLE 3 | The most enriched MSSA476 EVs- associated small RNAs ranked based on read counts[a].

Element	RFAM accession	Description	Functions	Genomic coordinates	Gene length (nt)	Strand[b] (F/R)	Read count[c]	Bit score	GC content (%)
6S RNA	RF00013	Protein-binding small RNA	Involved in antibiotic resistance (Lalaouna et al., 2014)	1685656..1685846	197	R	80	97.5	42.41
SsrA RNA	RF00023	Protein-binding small RNA	Rescues stalled ribosomes during translation of defective mRNAs and biosynthesis of pigment (Liu et al., 2010; Guillet et al., 2013)	837496..837857	362	F	65	162.6	43.92
RsaC	RF0188	Trans-encoded antisense RNA	Oxidative stress and metal-dependent nutritional immunity (Lalaouna et al., 2019)	673626..674066	441	R	33	555.6	35.37
T-box	RF00230	Regulatory elements	Involved in amino acid metabolism (Schoenfelder et al., 2013)	1674489..1674687 385924..386088 386093..386293 1199542..1199714 12486..12696	178 165 201 173 211	R F R F F	32 24 22 16 13	90.55 96.6 114.2 80.94 93.3	34.27 31.52 39.8 34.10 33.65
4.5S RNA	RF00169	Trans-encoded antisense RNA	Processing of tRNAs (Szafranska et al., 2014)	485461..485730	270	F	24	69.1	48.52
FMN riboswitch	RF00050	Regulatory element	Controls expression of de novo riboflavin	1551305..1551439	135	R	23	121.7	46.67
SAM riboswitch	RF00162	Regulatory element	Involved in amino acid (methionine) metabolism	2372869..2372964	96	R	21	78.2	47.92
fstAT	RF01797	Trans-encoded antisense RNA	Type I toxin-antitoxin system that interfere with bacterial membrane (Schuster and Bertram, 2016)	1873399..1873493	95	R	19	90.2	42.11
rli28	RF01492	Trans-encoded antisense RNA	Role in virulence (Romby and Charpentier, 2010)	2205592..2205772	181	R	19	123.8	34.25
L19_leader	RF00556	Regulatory element	NA	1254259..1254301	43	F	18	50.0	41.86
yjdF	RF01764	Regulatory element	Regulate gene expression upon binding with heterocyclic aromatic compounds (Li et al., 2016).	423980..424080	101	F	17	92.9	38.61
rli28	RF01492	Trans-encoded antisense RNA	Role in virulence (Romby and Charpentier, 2010)	2030445..2030623	179	R	17	85.6	37.43
TPP riboswitch	RF00059	Regulatory element	Involved in biosynthesis and transport of thiamine (Sudarsan et al., 2005)	2155664..2155766	103	F	16	70.9	40.78
T-box leader	RF00230	Regulatory element	Involved in amino acid metabolism	1791148..1791366	203	R	15	80.52	31.53
RNAIII	RF00503	Trans-encoded antisense RNA	Involved in virulence (hemolysins) (Boisset et al., 2007)	2086458..2086973	516	R	14	472.2	28.68
RsaJ	RF01822	Trans-encoded antisense RNA	NA	2479454..2479740	287	F	13	332.1	30.66
Lysine riboswitch	RF00168	Regulatory element	Regulate expression of lysine biosynthesis and transport genes (Blount et al., 2007)	1732415..1732590	176	F	12	104.6	31.82
fstAT	RF01797	Trans-encoded antisense RNA	Type-I toxin-antitoxin systems (Blenkiron et al., 2016)	2483979..2484075	97	F	12	78.12	40.21
L10_Leader	RF00557	Regulatory element	NA	566720..566866	127	F	10	86.8	31.21

*See **Supplementary Table 2** for the full list of sRNAs.*

[a]The cutoff value was assigned as >10, [b]Direction of strand alignment, F, Forward; R, Reverse; [c]The total number of sRNA sequence reads. NA, Not available.

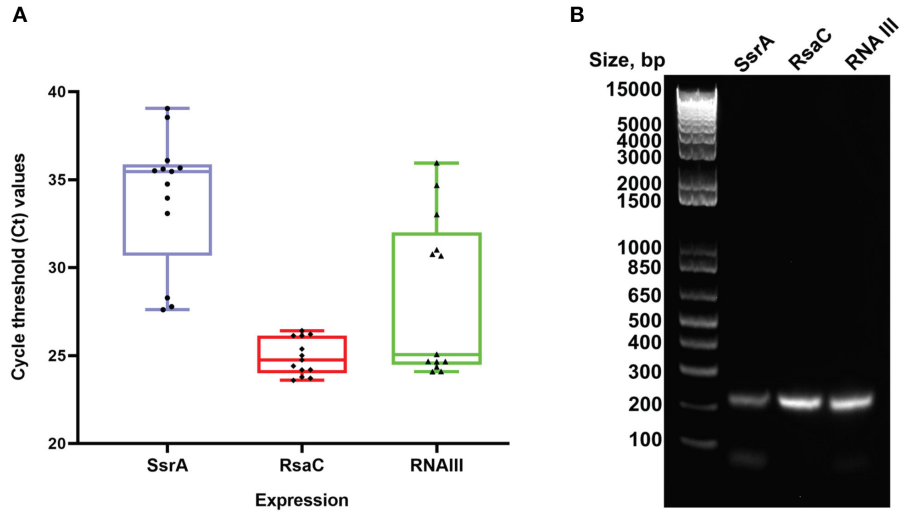

FIGURE 4 | Real Time PCR validation analysis. **(A)** Boxplot representation of Ct values for SsrA, RsaC and RNAIII isolated from *S. aureus* EVs. Boxes represent interquartile range, central line is median, Whiskers are upper and lower adjacent values and Dots represent number of data points. **(B)** Agarose gel electrophoresis of the RT-PCR products obtained from RNA isolated from RNase-treated EVs. The expected amplicon sizes for SsrA, RsaC, and RNAIII are 204, 204, and 202 bp, respectively. The left lane shows molecular weight markers.

biogenesis and virulence (Diallo and Provost, 2020; Lécrivain and Beckmann, 2020).

The observed EV sizes agreed with other studies from *S. aureus* (Gurung et al., 2011; Askarian et al., 2018; Wang et al., 2018; He et al., 2019). Antibiotics and other stressful conditions are considered as trigger factors for EV formation (Maredia et al., 2012; Prados-Rosales et al., 2014; Andreoni et al., 2019). In agreement with this, we observed a higher yield of EVs when the bacteria were grown in iron-limited media supplemented with vancomycin compared to typical bacteriologic media (**Supplementary Figure 3**).

Since we inoculated iron-chelated BHI media with an overnight grown inoculum in 1:100 dilutions, there is the possibility of transfer of trace amounts of iron. However, it has been shown that *S. aureus* utilizes a large proportion of iron within 6 h of aerobic growth in tryptic soy broth media (Ledala et al., 2014). Iron utilization by *S. aureus* in BHI might be similar. In addition, the traces of iron transferred through the inoculum would have been utilized by growing *S. aureus*, leaving media chelated for iron after a 16 h incubation (Ledala et al., 2010 and Ledala et al., 2014). It will, however, be interesting in the future to explore other culture media, such as RPMI 1640, which may better reflect infection conditions (Dauros-Singorenko et al., 2017).

Although there are multiple studies in Gram-positive bacteria showing altered sRNA expression due to antibiotic treatment (Felden and Cattoir, 2018; Gao et al., 2020), few studies have evaluated RNA content associated with EVs upon antibiotics exposure. Exposure to antimicrobials such as ciprofloxacin, tetracycline and melittin treatment of *Acholeplasma laidlawii* resulted in very variable numbers of sequence reads of predominantly 14–60 nt RNAs associated with EVs. In addition, tRNA fragments (mainly tRNA-Leu, tRNA-Arg, tRNA-Asn, and tRNA-Met) were predominant (Chernov et al., 2018) which is in line with our study. There are also few reports in eukaryotic exosomes and protozoal EVs confirming that exosome RNA levels altered by cellular stress (Bayer-Santos et al., 2014).

In general, RNAs are unstable and prone to degradation by RNase present in the extracellular milieu. However, recent reports indicate that RNAs encapsulated in EVs are protected from degradation by the exogenous RNase (Weber et al., 2010; Dauros-Singorenko et al., 2018), which support our results where we could isolate RNA from the RNase-treated EVs. Our RNase treatment of EVs would also facilitate degradation of eventual contaminating RNA that might passively have been released from the 0.4% dead cells in the culture used for vesicle isolation. Nevertheless, some of the RNA-protein complex sticking to the EVs might still have been protected from RNase treatment (Ramirez et al., 2018).

Transcriptome analysis of the EVs revealed the presence of tRNAs and sRNAs (**Tables 2**, **3** and **Supplementary Table 2**). Based on the read counts, the tRNA fragments were found to be most abundant. Abundant reads of tRNA fragments have previously been found in EVs released by bacteria (Ghosal et al., 2015; Koeppen et al., 2016), fungi (*Paracoccidiodes brasiliensis*, *Histoplasma capsulatum*) (Da Silva et al., 2015; Alves et al., 2019) and protists (*Trypanosoma cruzi*, *Leishmania* species) (Garcia-Silva et al., 2014; Lambertz et al., 2015). Interestingly, EVs of *Pseudomonas aeruginosa* also contained tRNA-Met fragments which entered the host cell and inhibited IL-8 secretion, which are considered as a chemoattractant of neutrophils (Koeppen et al., 2016).

There has been discussed whether RNAs associated with EVs are "intact," fragmented or specifically processed products. EVs

have been found to be associated with various fragments derived from mRNAs, rRNA and tRNA (Mateescu et al., 2017), which is in agreement with our study. Due to the small size of vesicles (20–200 nm), we might speculate that inside EVs, mostly smaller fragmented RNAs should be enriched. However, we cannot exclude the possibility of having full length RNA, given Buck and colleagues reported full length YRNAs exclusively inside Nematode-derived EVs (Buck et al., 2014). In our case, we see fragment lengths of 35–150 nt.

It has been reported that sRNA present in Vibrio and other Gram-negative bacteria play a role in vesicle biogenesis (Song et al., 2008; Choi H.-I. et al., 2017). MicA from *E. coli* induce EV biogenesis. Likewise, Song and collaborators also identified VrrA, a homolog of *E. coli* MicA in *Vibrio cholera* that controls EV formation and contributes to bacterial fitness in certain stressful environments (Song et al., 2008). Besides sRNAs, Sle1, an autolysin, has been shown to facilitate vesicle biogenesis (Wang et al., 2018).

The presence of EV-associated sRNA (SsrA, RsaC, and RNAIII) was confirmed by RNA-seq, qPCR, RT-PCR, and sequencing of obtained replicons. Among these, SsrA is involved in defective mRNAs decay, rescue of stalled ribosomes, support of phage growth, and modulation of the activity of DNA binding proteins (Karzai et al., 2000; Janssen and Hayes, 2012). Earlier reports have shown an increase of SsrA RNA in *Streptococcus pyogenes* and *Helicobacter pylori* in the presence of antibiotics (Steiner and Malke, 2001; Thibonnier et al., 2008). In our study, the high coverage of SsrA RNA associated with *S. aureus* EVs might be due to the use of vancomycin stress prior to vesicle isolation. 6S RNA plays an important role in cell survival and persistence during the stationary phase (Wassarman and Storz, 2000; Trotochaud and Wassarman, 2004) and was also found associated with the EVs. Interestingly, RNAIII (**Table 3**), which has major roles in virulence and pathogenicity (Boisset et al., 2007; Toledo-Arana et al., 2007), was also associated with EVs of *S. aureus.* The validation of RNAIII associated with EVs of *S. aureus* opens further study on the possibility of sRNA-mediated interspecies communication, as RNAIII has already been proved to be involved in the regulation of quorum sensing communication systems to coordinate the expression of virulence factors (Diallo and Provost, 2020; Lécrivain and Beckmann, 2020). Indeed, EVs could be used as communication vehicles only if they could transfer associated RNA into host cells and have a functional effect. Another possibility is that bacteria utilize EVs to eliminate unwanted RNAs, including sRNA and tRNA fragments (Groot and Lee, 2020).

Importantly, EVs influence *S. aureus* virulence over the course of systemic infection (Askarian et al., 2018). Recently, RNAs (circulatory/and or EV-associated) were considered as virulence factors due to their role in the infection process via multifaceted signaling pathways. The signaling pathways involved depend upon the delivery of bacterial RNA into the host cells. It has been shown that bacterial RNA can be delivered to human cytosol (Vanaja et al., 2014) and the phagosomal compartment (Cervantes et al., 2013) and EV-associated RNA has been localized in the human cell nucleus of human bladder carcinoma cells (Blenkiron et al., 2016). The sRNAs associated with EVs found in this study has been shown to be involved in quorum sensing (Novick and Geisinger, 2008), oxidative stress (Lalaouna et al., 2019), antibiotic resistance and metabolism (Lalaouna et al., 2014). All these processes are important for virulence and modulation of bacterial pathogenicity. EVs have some striking similarities with exosomes that are secreted from most mammalian cell types. Exosomes are involved in transport of mRNAs and miRNAs from donor to recipient cells to modulate gene expression (Zhang et al., 2015; Lu et al., 2019). They have similar size (around 50–200 nm in diameter) and carry payloads of proteins, lipids, and genetic materials such as the bacterial membrane vesicles. Both types can deliver functional molecules to distant extracellular compartments and tissues.

Recently, it was described that eukaryotic sRNA profiles of serum exosomes derived from individuals with tuberculosis can facilitate the development of potential molecular targets for detection/diagnosis of latent and active tuberculosis (Lvu et al., 2019). In addition to eukaryotic sRNA in exosomes, circulating sRNA (ASdes) from *Mycobacterium tuberculosis* was found in patients suffering from active tuberculosis, implicating their role as diagnostic biomarkers (Fu et al., 2018). This makes us hypothesize that some of the sRNAs we have validated in EVs (RNAIII and SsrA) have a potential to be used as biomarkers for bloodstream infections (Bordeau et al., 2016), joint infections (osteomyelitis) (Deng et al., 2020), tissues infections (e.g., chronic biofilm infections) and/or bacterial persistence (Romilly et al., 2014; Schoenfelder et al., 2019). Identifying sRNAs as biomarkers should not be limited to pathogenic strains but also to nasal and other commensal strains.

A previous study compared RNA contents of group A streptococcal cells vs. their EVs, and found that some RNA species were differentially abundant (Resch et al., 2016). For future studies, it would be interesting to do similar studies in *S. aureus*, and also to compare whether media or antibiotics influence the EV cargo. Further investigation is also needed to address whether RNAs found inside the vesicles are entrapped during vesicle biogenesis or if there are some sorting of RNA into the vesicles.

In conclusion, to our knowledge, this is the first study describing sRNAs associated with *S. aureus* extracellular vesicles. Various tRNA and sRNA associated fragments with several biological or regulatory functions have been identified associated with the EVs. This study opens further questions concerning sorting mechanisms by which RNA can be packed inside EVs and their roles in host-microbe as well as microbe-microbe interactions. Targeting those sRNA may open avenues toward a novel anti-virulence strategy to treat intractable bacterial infections.

DATA AVAILABILITY STATEMENT

The datasets presented in this study can be found in online repositories. The names of the repository/repositories and accession number(s) can be found in the article/**Supplementary Material**.

AUTHOR CONTRIBUTIONS

BJ, MJ, and KH designed the experiments and prepared the manuscript. BJ performed the majority of the lab experiment. AN assisted in confocal microscopy and image analysis. KH assisted in bioinformatics analysis, while BS did flow cytometry, and assisted in qPCR experiments. FA and BS contributed to writing of the results-section. BJ, BS, FA, AN, SW, MJ, and KH gave intellectual input. All authors read and approved the final manuscript.

FUNDING

This work was supported by grants from joint Miljøstøtte financed by Strategisk-HN05–14 (Helse Nord RFH) and Faculty of Health Sciences A20389 (2014–2017), and by travel grants from the National Graduate School in Infection Biology and Antimicrobials (grant number 249062). The publication charges for this article have been funded by a grant from the publication fund of UiT The Arctic University of Norway. The funders had no role in study design, data collection and analysis, decision to publish, or preparation of the manuscript.

ACKNOWLEDGMENTS

We are grateful for excellent technical assistance from Ahmed Mekhlif, Kjersti Julin, and Hagar Taman. We thank Christopher G. Fenton, Endre Anderssen, and Jessin Janice for technical support in bioinformatics work. We are grateful to Kyaw Min Aung and Si Lhyam Myint at Umeå University for technical support with atomic force microscopy and Augusta Hlin Aspar with electron microscopy. We acknowledge the Biochemical Imaging Center (BICU) at Umeå University and the National Microscopy Infrastructure (NMI) for providing assistance in confocal microscopy. We are thankful to Deanna Lynn Wolfson, Department of Physics and Technology at UiT the Arctic University of Norway, for co-localization analysis and image processing of confocal data. We are grateful to Line Wilsgård for NTA particle analysis.

SUPPLEMENTARY MATERIAL

The Supplementary Material for this article can be found online at: https://www.frontiersin.org/articles/10.3389/fmolb.2020.566207/full#supplementary-material

Supplementary Figure 1 | Growth curves of *S. aureus* grown under BHI (normal condition) and iron-depleted BHI media with subinhibitory concentration of vancomycin (stressed condition).

Supplementary Figure 2 | Flow cytometry analysis of S. *aureus* grown in **(A)** BHI (normal condition) **(B)** iron-depleted BHI media with subinhibitory concentration of vancomycin (stressed condition) for 16 h. Side scatter is represented on X-axis and AF488 on Y-axis. Gates P1, P3, and P6 were set for beads, live cells and dead cells, respectively.

Supplementary Figure 3 | Measurement of EV yield obtained from bacteria grown in BHI (normal condition) and iron-depleted BHI with subinhibitory concentration of vancomycin (stressed condition). **(A)** EV number quantified by NTA. **(B)** Protein concentration in EVs measured by Qubit (protein assay kit). The mean ± SD is shown. The results represent three biological repeats (individual EV isolations) (NTA and protein concentration measurements). $*P < 0.05$, unpaired *t*-test.

Supplementary Figure 4 | AFM image of EVs isolated from bacteria grown in iron-depleted BHI supplemented with subinhibitory concentration of vancomycin (White arrow indicates vesicles).

Supplementary Figure 5 | Confocal microscopy on intact RNase-treated EV particles/aggregates stained with **(A)** lipid specific dye, DiD (red), and **(B)** RNA-specific dye, SYTO RNAselect (green). **(C)** The image shows the overlay observed under the microscope. The overall percentage of co-localization in one microscopic field was found to be 78.3% which is in line with the results using another lipid specific dye in **Figure 2**. The white rectangular box and lower panel highlights the magnified region in the inset. The scale bar is drawn to 7.5 μm.

Supplementary Figure 6 | (A) Confocal microscopy of extracellular vesicles without RNase treatment stained with lipid specific dye, PKH2 (red) and RNA-specific dye, SYTO RNASelect (green). Arrowhead (white) indicates absence of PKH2 fluorescence for the particle, while arrowhead (blue) shows co-localization of PKH2 stained extracellular vesicle with SYTO RNASelect dye. Scale bar, 1 μm. **(B)** Arrowhead indicates absence of PKH2 fluorescence in the SYTO RNASelect stained particle. **(C)** Quantification of RNA and lipid positive particles. Data points from two different experiments and 8 fields of view.

Supplementary Figure 7 | Transcriptome landscape of *S. aureus* EVs. RNA sequencing reads were mapped to reference genome (NC_002953) using Rockhopper v 2.0.3. The mapped RNAs, UTRs and, multi-gene operons were visualized in the IGV genome browser. The first red track corresponds to RNA transcripts. The blue track corresponds to UTRs of protein coding genes. The pink track corresponds to multi-gene operons. The final purple track at the bottom of the image corresponds to protein coding genes and RNA genes annotated in RefSeq.

Supplementary Figure 8 | Distribution of EV RNAs showing percent of reads mapped to each RNA biotype in *S. aureus* chromosomes **(A)** and plasmid **(B)**, respectively.

Supplementary Figure 9 | (A) Schematic representation of sRNA identification. **(B)** Size length distribution of sRNAs associated with EVs of *S. aureus*.

Supplementary Figure 10 | Read density profiles of tRNAs (pink highlighted region) downstream of the PerR regulatory region visualized by Artemis genome browser. The abundant loci close to tRNAs are ribosomal RNA. The X-axis represent the position in the genome and the Y-axis represent the numbers of reads mapped (coverage) at that location.

Supplementary Figure 11 | Artemis genome viewer windows showing read density profiles of **(A)** SsrA, **(B)** 6S RNA, **(C)** RNAIII, and **(D)** RsaC RNA (pink highlighted regions). X-axis represent the position in the genome and the Y-axis represent the numbers of reads mapped (coverage) at the specific location.

Supplementary Figure 12 | Sanger sequencing alignment of SsrA, RsaC and RNAIII RNAs. Sequences were aligned using BioEdit alignment tool.

REFERENCES

Ahmad, I., Karah, N., Nadeem, A., Wai, S. N., and Uhlin, B. E. (2019). Analysis of colony phase variation switch in *Acinetobacter baumannii* clinical isolates. *PLoS ONE* 14:e0210082. doi: 10.1371/journal.pone.0210082

Alves, L. R., Da Silva, R. P., Sanchez, D. A., Zamith-Miranda, D., Rodrigues, M. L., Goldenberg, S., et al. (2019). Extracellular vesicle-mediated RNA release in *Histoplasma capsulatum*. *mSphere* 4:e00176–19. doi: 10.1128/mSphere.00176-19

Andreoni, F., Toyofuku, M., Menzi, C., Kalawong, R., Shambat, S. M., François, P., et al. (2019). Antibiotics stimulate formation of vesicles in

Staphylococcus aureus in both phage-dependent and-independent fashions and via different routes. *Antimicrob. Agents Chemother*. 63:e01439–18. doi: 10.1128/AAC.01439-18

Askarian, F., Lapek J. D. Jr, Dongre, M., Tsai, C.-M., Kumaraswamy, M., Kousha, A., et al. (2018). *Staphylococcus aureus* membrane-derived vesicles promote bacterial virulence and confer protective immunity in murine infection models. *Front. Microbiol*. 9:262. doi: 10.3389/fmicb.2018.00262

Bager, R. J., Persson, G., Nesta, B., Soriani, M., Serino, L., Jeppsson, M., et al. (2013). Outer membrane vesicles reflect environmental cues in *Gallibacterium anatis*. *Vet. Microbiol*. 167, 565–572. doi: 10.1016/j.vetmic.2013.09.005

Bayer-Santos, E., Lima, F. M., Ruiz, J. C., Almeida, I. C., and Da Silveira, J. F. (2014). Characterization of the small RNA content of *Trypanosoma cruzi* extracellular vesicles. *Mol. Biochem. Parasitol*. 193, 71–74. doi: 10.1016/j.molbiopara.2014.02.004

Bitto, N. J., Chapman, R., Pidot, S., Costin, A., Lo, C., Choi, J., et al. (2017). Bacterial membrane vesicles transport their DNA cargo into host cells. *Sci. Rep*. 7:7072. doi: 10.1038/s41598-017-07288-4

Blenkiron, C., Simonov, D., Muthukaruppan, A., Tsai, P., Dauros, P., Green, S., et al. (2016). Uropathogenic *Escherichia coli* releases extracellular vesicles that are associated with RNA. *PLoS ONE* 11:e0160440. doi: 10.1371/journal.pone.0160440

Blount, K. F., Wang, J. X., Lim, J., Sudarsan, N., and Breaker, R. R. (2007). Antibacterial lysine analogs that target lysine riboswitches. *Nat. Chem. Biol*. 3, 44–49. doi: 10.1038/nchembio842

Boisset, S., Geissmann, T., Huntzinger, E., Fechter, P., Bendridi, N., Possedko, M., et al. (2007). *Staphylococcus aureus* RNAIII coordinately represses the synthesis of virulence factors and the transcription regulator Rot by an antisense mechanism. *Genes Dev*. 21, 1353–1366. doi: 10.1101/gad.423507

Bordeau, V., Cady, A., Revest, M., Rostan, O., Sassi, M., Tattevin, P., et al. (2016). *Staphylococcus aureus* regulatory RNAs as potential biomarkers for bloodstream infections. *Emerging Infect. Dis*. 22, 1570–1578. doi: 10.3201/eid2209.151801

Brameyer, S., Plener, L., Müller, A., Klingl, A., Wanner, G., and Jung, K. (2018). Outer membrane vesicles facilitate trafficking of the hydrophobic signaling molecule CAI-1 between *Vibrio harveyi* cells. *J. Bacteriol*. 200:e00740-17. doi: 10.1128/JB.00740-17

Buck, A. H., Coakley, G., Simbari, F., Mcsorley, H. J., Quintana, J. F., Le Bihan, T., et al. (2014). Exosomes secreted by nematode parasites transfer small RNAs to mammalian cells and modulate innate immunity. *Nat. Commun*. 5:5488. doi: 10.1038/ncomms6488

Cafiso, V., Bertuccio, T., Spina, D., Purrello, S., Campanile, F., Di Pietro, C., et al. (2012). Modulating activity of vancomycin and daptomycin on the expression of autolysis cell-wall turnover and membrane charge genes in hVISA and VISA strains. *PLoS ONE* 7:e29573. doi: 10.1371/journal.pone.0029573

Caldelari, I., Chao, Y., Romby, P., and Vogel, J. (2013). RNA-mediated regulation in pathogenic bacteria. *Cold Spring Harb. Perspect. Med*. 3:a010298. doi: 10.1101/cshperspect.a010298

Cavanagh, J. P., Pain, M., Askarian, F., Bruun, J.-A., Urbarova, I., Wai, S. N., et al. (2018). Comparative exoproteome profiling of an invasive and a commensal *Staphylococcus haemolyticus* isolate. *J. Proteomics* 197, 106–114. doi: 10.1016/j.jprot.2018.11.013

Cervantes, J. L., La Vake, C. J., Weinerman, B., Luu, S., O'Connell, C., Verardi, P. H., et al. (2013). Human TLR8 is activated upon recognition of *Borrelia burgdorferi* RNA in the phagosome of human monocytes. *J. Leukoc. Biol*. 94, 1231–1241. doi: 10.1189/jlb.0413206

Chernov, V. M., Chernova, O. A., Mouzykantov, A. A., Medvedeva, E. S., Baranova, N. B., Malygina, T. Y., et al., (2018). Antimicrobial resistance in mollicutes: known and newly emerging mechanisms. *FEMS Microbiol. Lett*. 365. doi: 10.1093/femsle/fny185

Choi, H.-I., Kim, M., Jeon, J., Han, J. K., and Kim, K.-S. (2017). Overexpression of MicA induces production of OmpC-enriched outer membrane vesicles that protect against Salmonella challenge. *Biochem. Biophys. Res. Commun*. 490, 991–996. doi: 10.1016/j.bbrc.2017.06.152

Choi, J.-W., Kim, S.-C., Hong, S.-H., and Lee, H.-J. (2017). Secretable small RNAs via outer membrane vesicles in periodontal pathogens. *J. Dent. Res*. 96, 458–466. doi: 10.1177/0022034516685071

Choi, J.-W., Kwon, T.-Y., Hong, S.-H., and Lee, H.-J. (2018). Isolation and Characterization of a microRNA-size secretable Small RNA in *Streptococcus sanguinis*. *Cell Biochem. Biophys*. 76, 293–301. doi: 10.1007/s12013-016-0770-5

Choi, S. Y., Lim, S., Cho, G., Kwon, J., Mun, W., Im, H., et al. (2020). Chromobacterium violaceum delivers violacein, a hydrophobic antibiotic, to other microbes in membrane vesicles. *Environ. Microbiol*. 22, 705–713. doi: 10.1111/1462-2920.14888

Coelho, C., Brown, L., Maryam, M., Vij, R., Smith, D. F., Burnet, M. C., et al. (2019). Listeria monocytogenes virulence factors, including listeriolysin O, are secreted in biologically active extracellular vesicles. *J. Biol. Chem*. 294, 1202–1217. doi: 10.1074/jbc.RA118.006472

Da Silva, R. P., Puccia, R., Rodrigues, M. L., Oliveira, D. L., Joffe, L. S., César, G. V., et al. (2015). Extracellular vesicle-mediated export of fungal RNA. *Sci. Rep*. 5:7763. doi: 10.1038/srep07763

Dauros-Singorenko, P., Chang, V., Whitcombe, A., Simonov, D., Hong, J., Phillips, A., et al. (2017). Isolation of membrane vesicles from prokaryotes: a technical and biological comparison reveals heterogeneity. *J. Extracell Vesicles* 6:1324731. doi: 10.1080/20013078.2017.1324731

Dauros-Singorenko, P., Blenkiron, C., Phillips, A., and Swift, S. (2018). The functional RNA cargo of bacterial membrane vesicles. *FEMS Microbiol. Lett*. 365. doi: 10.1093/femsle/fny023

Deng, S., Wang, Y., Liu, S., Chen, T., Hu, Y., Zhang, G., et al. (2020). Extracellular vesicles: a potential biomarker for quick identification of infectious osteomyelitis. *Front. Cell. Infect. Microbiol*. 10:323. doi: 10.3389/fcimb.2020.00323

Devos, S., Van Oudenhove, L., Stremersch, S., Van Putte, W., De Rycke, R., Van Driessche, G., et al. (2015). The effect of imipenem and diffusible signaling factors on the secretion of outer membrane vesicles and associated Ax21 proteins in *Stenotrophomonas maltophilia*. *Front. Microbiol*. 6:298. doi: 10.3389/fmicb.2015.00298

Devos, S., Van Putte, W., Vitse, J., Van Driessche, G., Stremersch, S., Van Den Broek, W., et al. (2017). Membrane vesicle secretion and prophage induction in multidrug-resistant *Stenotrophomonas maltophilia* in response to ciprofloxacin stress. *Environ. Microbiol*. 19, 3930–3937. doi: 10.1111/1462-2920.13793

Diallo, I., and Provost, P. (2020). RNA-sequencing analyses of small bacterial rnas and their emergence as virulence factors in host-pathogen interactions. *Int. J. Mol. Sci*. 21:1627. doi: 10.3390/ijms21051627

Dongre, M., Uhlin, B. E., and Wai, S. N. (2011). Bacterial nanotubes for intimate sharing. *Front. Microbiol*. 2:108. doi: 10.3389/fmicb.2011.00108

Dorward, D. W., and Garon, C. (1989). DNA-binding proteins in cells and membrane blebs of *Neisseria gonorrhoeae*. *J. Bacteriol*. 171, 4196–4201. doi: 10.1128/JB.171.8.4196-4201.1989

Dubey, G. P., and Ben-Yehuda, S. (2011). Intercellular nanotubes mediate bacterial communication. *Cell* 144, 590–600. doi: 10.1016/j.cell.2011.01.015

Elhenawy, W., Debelyy, M. O., and Feldman, M. F. (2014). Preferential packing of acidic glycosidases and proteases into bacteroides outer membrane vesicles. *MBio* 5:e00909-14. doi: 10.1128/mBio.00909-14

Felden, B., and Cattoir, V. (2018). Bacterial adaptation to antibiotics through regulatory RNAs. *Antimicrob. Agents Chemother*. 62:e02503-17. doi: 10.1128/AAC.02503-17

Foster, T. J., Geoghegan, J. A., Ganesh, V. K., and Höök, M. (2014). Adhesion, invasion and evasion: the many functions of the surface proteins of *Staphylococcus aureus*. *Nat. Rev. Microbiol*. 12, 49–62. doi: 10.1038/nrmicro3161

Frantz, R., Teubner, L., Schultze, T., La Pietra, L., Müller, C., Gwozdzinski, K., et al. (2019). The secRNome of Listeria monocytogenes harbors small non-coding RNAs that are potent inducers of beta interferon. *MBio* 10:e01223–19. doi: 10.1128/mBio.01223-19

Fu, Y., Li, W., Wu, Z., Tao, Y., Wang, X., Wei, J., et al. (2018). Detection of mycobacterial small RNA in the bacterial culture supernatant and plasma of patients with active tuberculosis. *Biochem. Biophys. Res. Commun*. 503, 490–494. doi: 10.1016/j.bbrc.2018.04.165

Gao, W., Guérillot, R., Lin, Y. H., Tree, J., Beaume, M., François, P., et al. (2020). Comparative transcriptomic and functional assessments of linezolid-responsive small RNA genes in *Staphylococcus aureus*. *mSystems* 5:e00665–19. doi: 10.1128/mSystems.00665-19

Garcia-Silva, M. R., Das Neves, R. F. C., Cabrera-Cabrera, F., Sanguinetti, J., Medeiros, L. C., Robello, C., et al. (2014). Extracellular vesicles shed by

Trypanosoma cruzi are linked to small RNA pathways, life cycle regulation, and susceptibility to infection of mammalian cells. *Parasitol. Res.* 113, 285–304. doi: 10.1007/s00436-013-3655-1

Ghosal, A., Upadhyaya, B. B., Fritz, J. V., Heintz-Buschart, A., Desai, M. S., Yusuf, D., et al. (2015). The extracellular RNA complement of *Escherichia coli*. *Microbiologyopen* 4, 252–266. doi: 10.1002/mbo3.235

Gill, S., Catchpole, R., and Forterre, P. (2018). Extracellular membrane vesicles (EVs) in the three domains of life and beyond. *FEMS Microbiol. Rev*. 43, 273–303. doi: 10.1093/femsre/fuy042

Groot, M., and Lee, H. (2020). Sorting mechanisms for MicroRNAs into extracellular vesicles and their associated diseases. *Cells* 9:1044. doi: 10.3390/cells9041044

Guillet, J., Hallier, M., and Felden, B. (2013). Emerging functions for the *Staphylococcus aureus* RNome. *PLoS Pathog.* 9:e1003767. doi: 10.1371/journal.ppat.1003767

Gurung, M., Moon, D. C., Choi, C. W., Lee, J. H., Bae, Y. C., Kim, J., et al. (2011). *Staphylococcus aureus* produces membrane-derived vesicles that induce host cell death. *PLoS ONE* 6:e27958. doi: 10.1371/journal.pone.0027958

Hagemann, S., Stöger, L., Kappelmann, M., Hassl, I., Ellinger, A., and Velimirov, B. (2014). DNA-bearing membrane vesicles produced by Ahrensia kielensis and *Pseudoalteromonas marina*. *J. Basic Microbiol.* 54, 1062–1072. doi: 10.1002/jobm.201300376

He, X., Li, S., Yin, Y., Xu, J., Gong, W., Li, G., et al. (2019). Membrane vesicles are the dominant structural components of ceftazidime-induced biofilm formation in an oxacillin-sensitive MRSA. *Front. Microbiol.* 10:571. doi: 10.3389/fmicb.2019.00571

He, X., Yuan, F., Lu, F., Yin, Y., and Cao, J. (2017). Vancomycin-induced biofilm formation by methicillin-resistant *Staphylococcus aureus* is associated with the secretion of membrane vesicles. *Microb. Pathog.* 110, 225–231. doi: 10.1016/j.micpath.2017.07.004

Hermansen, G. M., Sazinas, P., Kofod, D., Millard, A., Andersen, P. S., and Jelsbak, L. (2018). Transcriptomic profiling of interacting nasal staphylococci species reveals global changes in gene and non-coding RNA expression. *FEMS Microbiol. Lett.* 365. doi: 10.1093/femsle/fny004

Holden, M. T., Feil, E. J., Lindsay, J. A., Peacock, S. J., Day, N. P., Enright, M. C., et al. (2004). Complete genomes of two clinical *Staphylococcus aureus* strains: evidence for the rapid evolution of virulence and drug resistance. *Proc. Natl. Acad. Sci. U.S.A.* 101, 9786–9791. doi: 10.1073/pnas.0402521101

Hong, S. W., Kim, M. R., Lee, E. Y., Kim, J., Kim, Y. S., Jeon, S., et al. (2011). Extracellular vesicles derived from *Staphylococcus aureus* induce atopic dermatitis-like skin inflammation. *Allergy* 66, 351–359. doi: 10.1111/j.1398-9995.2010.02483.x

Howden, B. P., Beaume, M., Harrison, P. F., Hernandez, D., Schrenzel, J., Seemann, T., et al. (2013). Analysis of the small RNA transcriptional response in multidrug resistant *Staphylococcus aureus* after antimicrobial exposure. *Antimicrob. Agents Chemother.* 57, 3864–3874. doi: 10.1128/AAC.00263-13

Hsu, C. Y., Lin, M. H., Chen, C. C., Chien, S. C., Cheng, Y. H., Su, I. N., et al. (2011). Vancomycin promotes the bacterial autolysis, release of extracellular DNA, and biofilm formation in vancomycin-non-susceptible *Staphylococcus aureus*. *FEMS Immunol. Med. Microbiol.* 63, 236–247. doi: 10.1111/j.1574-695X.2011.00846.x

Jamaly, S., Ramberg, C., Olsen, R., Latysheva, N., Webster, P., Sovershaev, T., et al. (2018). Impact of preanalytical conditions on plasma concentration and size distribution of extracellular vesicles using nanoparticle tracking analysis. *Sci. Rep.* 8:17216. doi: 10.1038/s41598-018-35401-8

Janssen, B. D., and Hayes, C. S. (2012). The tmRNA ribosome-rescue system. *Adv. Protein Chem. Struct. Biol.* 86, 151–191. doi: 10.1016/B978-0-12-386497-0.00005-0

Kaplan, J. B., Izano, E. A., Gopal, P., Karwacki, M. T., Kim, S., Bose, J. L., et al. (2012). Low levels of β-lactam antibiotics induce extracellular DNA release and biofilm formation in *Staphylococcus aureus*. *MBio* 3:e00198-12. doi: 10.1128/mBio.00198-12

Karzai, A. W., Roche, E. D., and Sauer, R. T. (2000). The SsrA–SmpB system for protein tagging, directed degradation and ribosome rescue. *Nat. Struct. Biol.* 7, 449–455. doi: 10.1038/75843

Kharina, A., Podolich, O., Faidiuk, I., Zaika, S., Haidak, A., Kukharenko, O., et al. (2015). Temperate bacteriophages collected by outer membrane vesicles in Komagataeibacter intermedius. *J. Basic Microbiol.* 55, 509–513. doi: 10.1002/jobm.201400711

Kim, M. H., Kim, S. Y., Son, J. H., Kim, S. I., Lee, H., Kim, S., et al. (2019). Production of membrane vesicles by *Enterococcus faecium* cultured with or without subinhibitory concentrations of antibiotics and their pathological effects on epithelial cells. *Front. Cell. Infect. Microbiol.* 9:295. doi: 10.3389/fcimb.2019.00295

Kim, M. R., Hong, S. W., Choi, E. B., Lee, W. H., Kim, Y. S., Jeon, S., et al. (2012). *Staphylococcus aureus*-derived extracellular vesicles induce neutrophilic pulmonary inflammation via both T h1 and T h17 cell responses. *Allergy* 67, 1271–1281. doi: 10.1111/all.12001

Koeppen, K., Hampton, T. H., Jarek, M., Scharfe, M., Gerber, S. A., Mielcarz, D. W., et al. (2016). A novel mechanism of host-pathogen interaction through sRNA in bacterial outer membrane vesicles. *PLoS Pathog.* 12:e1005672. doi: 10.1371/journal.ppat.1005672

Lagos-Quintana, M., Rauhut, R., Lendeckel, W., and Tuschl, T. (2001). Identification of novel genes coding for small expressed RNAs. *Science* 294, 853–858. doi: 10.1126/science.1064921

Lalaouna, D., Baude, J., Wu, Z., Tomasini, A., Chicher, J., Marzi, S., et al. (2019). RsaC sRNA modulates the oxidative stress response of *Staphylococcus aureus* during manganese starvation. *Nucleic Acids Res.* 47, 9871–9887. doi: 10.1093/nar/gkz728

Lalaouna, D., Eyraud, A., Chabelskaya, S., Felden, B., and Masse, E. (2014). Regulatory RNAs involved in bacterial antibiotic resistance. *PLoS Pathog.* 210:e1004299. doi: 10.1371/journal.ppat.1004299

Lambertz, U., Ovando, M. E. O., Vasconcelos, E. J., Unrau, P. J., Myler, P. J., and Reiner, N. E. (2015). Small RNAs derived from tRNAs and rRNAs are highly enriched in exosomes from both old and new world Leishmania providing evidence for conserved exosomal RNA packaging. *BMC Genomics* 16:151. doi: 10.1186/s12864-015-1260-7

Langlete, P., Krabberød, A. K., and Winther-Larsen, H. C. (2019). Vesicles from Vibrio cholerae contain AT-rich DNA and shorter mRNAs that do not correlate with their protein products. *Front. Microbiol.* 10:2708. doi: 10.3389/fmicb.2019.02708

Langmead, B., and Salzberg, S. L. (2012). Fast gapped-read alignment with Bowtie 2. *Nat. Methods* 9, 357–359. doi: 10.1038/nmeth.1923

Lécrivain, A. L., and Beckmann, B. M. (2020). Bacterial RNA in extracellular vesicles: a new regulator of host-pathogen interactions? *Biochim. Biophys. Acta Gene Regul. Mech.* 1863:194519. doi: 10.1016/j.bbagrm.2020.194519

Ledala, N., Sengupta, M., Muthaiyan, A., Wilkinson, B. J., and Jayaswal, R. K. (2010). Transcriptomic response of Listeria monocytogenes to iron limitation and Fur mutation. *Appl. Environ. Microbiol.* 76, 406–416. doi: 10.1128/AEM.01389-09

Ledala, N., Zhang, B., Seravalli, J., Powers, R., and Somerville, G. A. (2014). Influence of iron and aeration on *Staphylococcus aureus* growth, metabolism, and transcription. *J. Bacteriol.* 196, 2178–2189. doi: 10.1128/JB.01475-14

Li, S., Hwang, X. Y., Stav, S., and Breaker, R. R. (2016). The yjdF riboswitch candidate regulates gene expression by binding diverse azaaromatic compounds. *RNA* 22, 530–541. doi: 10.1261/rna.054890.115

Li, W., Ying, X., Lu, Q., and Chen, L. (2012). Predicting sRNAs and their targets in bacteria. *Genomics Proteomics Bioinformatics* 10, 276–284. doi: 10.1016/j.gpb.2012.09.004

Lindmark, B., Rompikuntal, P. K., Vaitkevicius, K., Song, T., Mizunoe, Y., Uhlin, B. E., et al. (2009). Outer membrane vesicle-mediated release of cytolethal distending toxin (CDT) from *Campylobacter jejuni*. *BMC Microbiol.* 9:220. doi: 10.1186/1471-2180-9-220

Liu, W., Rochat, T., Toffano-Nioche, C., Lam, L., Nguyen, T., Bouloc, P., et al. (2018). Assessment of Bona Fide sRNAs in *Staphylococcus aureus*. *Front. Microbiol.* 9:228. doi: 10.3389/fmicb.2018.00228

Liu, Y., Defourny, K. A., Smid, E. J., and Abee, T. (2018). Gram-positive bacterial extracellular vesicles and their impact on health and disease. *Front. Microbiol.* 9:1502. doi: 10.3389/fmicb.2018.01502

Liu, Y., Wu, N., Dong, J., Gao, Y., Zhang, X., Shao, N., et al. (2010). SsrA (tmRNA) acts as an antisense RNA to regulate *Staphylococcus aureus* pigment synthesis by base pairing with crtMN mRNA. *FEBS Lett.* 584, 4325–4329. doi: 10.1016/j.febslet.2010.09.024

Lu, K.-C., Zhang, Y., and Song, E. (2019). Extracellular RNA: mechanisms of it's transporting into target cells. *ExRNA* 1:22. doi: 10.1186/s41544-019-0020-2

Lvu, L., Zhang, X., Li, C., Yang, T., Wang, J., Pan, L., et al. (2019). Small RNA profiles of serum exosomes derived from individuals with latent and active tuberculosis. *Front. Microbiol.* 10:1174. doi: 10.3389/fmicb.2019.01174

Lynch, J. B., and Alegado, R. A. (2017). Spheres of hope, packets of doom: the good and bad of outer membrane vesicles in interspecies and ecological dynamics. *J. Bacteriol.* 199:e00012-17. doi: 10.1128/JB.00012-17

Mäder, U., Nicolas, P., Depke, M., Pané-Farré, J., Debarbouille, M., van Der Kooi-Pol, M. M., et al. (2016). *Staphylococcus aureus* transcriptome architecture: from laboratory to infection-mimicking conditions. *PLoS Genet*. 12:e1005962. doi: 10.1371/journal.pgen.1005962

Malabirade, A., Habier, J., Heintz-Buschart, A., May, P., Godet, J., Halder, R., et al. (2018). The RNA complement of outer membrane vesicles from *Salmonella enterica* serovar Typhimurium under distinct culture conditions. *Front. Microbiol.* 9:2015. doi: 10.3389/fmicb.2018.02015

Manning, A. J., and Kuehn, M. J. (2011). Contribution of bacterial outer membrane vesicles to innate bacterial defense. *BMC Microbiol.* 11:258. doi: 10.1186/1471-2180-11-258

Manning, A. J., and Kuehn, M. J. (2013). Functional advantages conferred by extracellular prokaryotic membrane vesicles. *J. Mol. Microbiol. Biotechnol.* 23, 131–141. doi: 10.1159/000346548

Maredia, R., Devineni, N., Lentz, P., Dallo, S. F., Yu, J., Guentzel, N., et al. (2012). Vesiculation from Pseudomonas aeruginosa under SOS. *ScientificWorldJournal.* 2012:402919. doi: 10.1100/2012/402919

Mashburn, L. M., and Whiteley, M. (2005). Membrane vesicles traffic signals and facilitate group activities in a prokaryote. *Nature* 437, 422–425. doi: 10.1038/nature03925

Mateescu, B., Kowal, E. J., Van Balkom, B. W., Bartel, S., Bhattacharyya, S. N., Buzás, E. I., et al. (2017). Obstacles and opportunities in the functional analysis of extracellular vesicle RNA–an ISEV position paper. *J. Extracell Vesicles* 6:1286095. doi: 10.1080/20013078.2017.1286095

Mccaig, L. F., Mcdonald, L. C., Mandal, S., and Jernigan, D. B. (2006). *Staphylococcus aureus*–associated skin and soft tissue infections in ambulatory care. *Emerg. Infect Dis.* 12, 1715–1723. doi: 10.3201/eid1211.060190

Mizuno, T., Chou, M.-Y., and Inouye, M. (1984). A unique mechanism regulating gene expression: translational inhibition by a complementary RNA transcript (micRNA). *Proc. Natl. Acad. Sci. U.S.A.* 81, 1966–1970. doi: 10.1073/pnas.81.7.1966

Morinaga, K., Yamamoto, T., Nomura, N., and Toyofuku, M. (2018). Paracoccus denitrificans can utilize various long-chain N-acyl homoserine lactones and sequester them in membrane vesicles. *Environ. Microbiol. Rep.* 10, 651–654. doi: 10.1111/1758-2229.12674

Nadeem, A., Oscarsson, J., and Wai, S. N. (2020). "Delivery of virulence factors by bacterial membrane vesicles to mammalian host cells," in *Bacterial Membrane Vesicles*, eds M. Kaparakis-Liaskos and T. Kufer (Cham: Springer), 131–158.

Nicola, A. M., Frases, S., and Casadevall, A. (2009). Lipophilic dye staining of *Cryptococcus neoformans* extracellular vesicles and capsule. *Eukaryotic Cell* 8, 1373–1380. doi: 10.1128/EC.00044-09

Novick, R. P. (2003). Autoinduction and signal transduction in the regulation of staphylococcal virulence. *Mol. Microbiol.* 48, 1429–1449. doi: 10.1046/j.1365-2958.2003.03526.x

Novick, R. P., and Geisinger, E. (2008). Quorum sensing in staphylococci. *Annu. Rev. Genet.* 42, 541–564. doi: 10.1146/annurev.genet.42.110807.091640

Novick, R. P., Iordanescu, S., Projan, S. J., Kornblum, J., and Edelman, I. (1989). pT181 plasmid replication is regulated by a countertranscript-driven transcriptional attenuator. *Cell* 59, 395–404. doi: 10.1016/0092-8674(89)90300-0

Novick, R. P., Ross, H., Projan, S., Kornblum, J., Kreiswirth, B., and Moghazeh, S. (1993). Synthesis of staphylococcal virulence factors is controlled by a regulatory RNA molecule. *EMBO J.* 12, 3967–3975. doi: 10.1002/j.1460-2075.1993.tb06074.x

Oglesby-Sherrouse, A. G., and Murphy, E. R. (2013). Iron-responsive bacterial small RNAs: variations on a theme. *Metallomics* 5, 276–286. doi: 10.1039/c3mt20224k

Petrova, O. E., Garcia-Alcalde, F., Zampaloni, C., and Sauer, K. (2017). Comparative evaluation of rRNA depletion procedures for the improved analysis of bacterial biofilm and mixed pathogen culture transcriptomes. *Sci. Rep.* 7:41114. doi: 10.1038/srep41114

Prados-Rosales, R., Weinrick, B. C., Piqué, D. G., Jacobs, W. R., Casadevall, A., and Rodriguez, G. M. (2014). Role for *Mycobacterium tuberculosis* membrane vesicles in iron acquisition. *J. Bacteriol.* 196, 1250–1256. doi: 10.1128/JB.01090-13

Ramirez, M. I., Amorim, M. G., Gadelha, C., Milic, I., Welsh, J. A., Freitas, V. M., et al. (2018). Technical challenges of working with extracellular vesicles. *Nanoscale* 10, 881–906. doi: 10.1039/C7NR08360B

Resch, U., Tsatsaronis, J. A., Le Rhun, A., Stübiger, G., Rohde, M., Kasvandik, S., et al. (2016). A two-component regulatory system impacts extracellular membrane-derived vesicle production in group A *Streptococcus*. *MBio* 7:e00207–16. doi: 10.1128/mBio.00207-16

Rivera, J., Cordero, R. J., Nakouzi, A. S., Frases, S., Nicola, A., and Casadevall, A. (2010). Bacillus anthracis produces membrane-derived vesicles containing biologically active toxins. *Proc. Natl. Acad. Sci. U.S.A.* 107, 19002–19007. doi: 10.1073/pnas.1008843107

Robinson, J. T., Thorvaldsdóttir, H., Winckler, W., Guttman, M., Lander, E. S., Getz, G., et al. (2011). Integrative genomics viewer. *Nat. Biotechnol.* 29, 24–26. doi: 10.1038/nbt.1754

Romby, P., and Charpentier, E. (2010). An overview of RNAs with regulatory functions in gram-positive bacteria. *Cell. Mol. Life Sci.* 67, 217–237. doi: 10.1007/s00018-009-0162-8

Romilly, C., Lays, C., Tomasini, A., Caldelari, I., Benito, Y., Hammann, P., et al. (2014). A non-coding RNA promotes bacterial persistence and decreases virulence by regulating a regulator in *Staphylococcus aureus*. *PLoS Pathog.* 10:e1003979. doi: 10.1371/journal.ppat.1003979

Rutherford, K., Parkhill, J., Crook, J., Horsnell, T., Rice, P., Rajandream, M.-A., et al. (2000). Artemis: sequence visualization and annotation. *Bioinformatics* 16, 944–945. doi: 10.1093/bioinformatics/16.10.944

Scanlan, D. (2014). Bacterial vesicles in the ocean. *Science* 343, 143–144. doi: 10.1126/science.1248566

Schindelin, J., Arganda-Carreras, I., Frise, E., Kaynig, V., Longair, M., Pietzsch, T., et al. (2012). Fiji: an open-source platform for biological-image analysis. *Nat. Methods* 9, 676–682. doi: 10.1038/nmeth.2019

Schlatterer, K., Beck, C., Hanzelmann, D., Lebtig, M., Fehrenbacher, B., Schaller, M., et al. (2018). The mechanism behind bacterial lipoprotein release: phenol-soluble modulins mediate toll-like receptor 2 activation via extracellular vesicle release from *Staphylococcus aureus*. *MBio* 9:e01851–18. doi: 10.1128/mBio.01851-18

Schoenfelder, S. M., Lange, C., Prakash, S. A., Marincola, G., Lerch, M. F., Wencker, F. D., et al. (2019). The small non-coding RNA RsaE influences extracellular matrix composition in Staphylococcus epidermidis biofilm communities. *PLoS Pathog.* 15:e1007618. doi: 10.1371/journal.ppat.1007618

Schoenfelder, S. M., Marincola, G., Geiger, T., Goerke, C., Wolz, C., and Ziebuhr, W. (2013). Methionine biosynthesis in *Staphylococcus aureus* is tightly controlled by a hierarchical network involving an initiator tRNA-specific T-box riboswitch. *PLoS Pathog.* 9:e1003606. doi: 10.1371/journal.ppat.1003606

Schuster, C. F., and Bertram, R. (2016). Toxin-antitoxin systems of *Staphylococcus aureus*. *Toxins* 8:140. doi: 10.3390/toxins8050140

Schwechheimer, C., and Kuehn, M. J. (2015). Outer-membrane vesicles from Gram-negative bacteria: biogenesis and functions. *Nat. Rev. Microbiol.* 13, 605–619. doi: 10.1038/nrmicro3525

Sjöström, A. E., Sandblad, L., Uhlin, B. E., and Wai, S. N. (2015). Membrane vesicle-mediated release of bacterial RNA. *Sci. Rep.* 5:15329. doi: 10.1038/srep15329

Smalley, J., and Birss, A. (1987). Trypsin-like enzyme activity of the extracellular membrane vesicles of Bacteroides gingivalis W50. *Microbiology* 133, 2883–2894. doi: 10.1099/00221287-133-10-2883

Song, T., Mika, F., Lindmark, B., Liu, Z., Schild, S., Bishop, A., et al. (2008). A new Vibrio cholerae sRNA modulates colonization and affects release of outer membrane vesicles. *Mol. Microbiol.* 70, 100–111. doi: 10.1111/j.1365-2958.2008.06392.x

Song, T., and Wai, S. N. (2009). A novel sRNA that modulates virulence and environmental fitness of *Vibrio cholerae*. *RNA Biol.* 6, 254–258. doi: 10.4161/rna.6.3.8371

Steiner, K., and Malke, H. (2001). relA-independent amino acid starvation response network of *Streptococcus pyogenes*. *J. Bacteriol.* 183, 7354–7364. doi: 10.1128/JB.183.24.7354-7364.2001

Sudarsan, N., Cohen-Chalamish, S., Nakamura, S., Emilsson, G. M., and Breaker, R. R. (2005). Thiamine pyrophosphate riboswitches are targets for the antimicrobial compound pyrithiamine. *Chem. Biol.* 12, 1325–1335. doi: 10.1016/j.chembiol.2005.10.007

Szafranska, A. K., Oxley, A. P., Chaves-Moreno, D., Horst, S. A., Roßlenbroich, S., Peters, G., et al. (2014). High-resolution transcriptomic analysis of the adaptive response of *Staphylococcus aureus* during acute and chronic phases of osteomyelitis. *MBio* 5:e01775-14. doi: 10.1128/mBio.01775-14

Ter-Ovanesyan, D., Kowal, E. J., Regev, A., Church, G. M., and Cocucci, E. (2017). Imaging of isolated extracellular vesicles using fluorescence microscopy. *Methods Mol. Biol.* 1660, 233–241. doi: 10.1007/978-1-4939-7253-1_19

Thay, B., Wai, S. N., and Oscarsson, J. (2013). *Staphylococcus aureus* α-toxin-dependent induction of host cell death by membrane-derived vesicles. *PLoS ONE* 8:e54661. doi: 10.1371/journal.pone.0054661

Thibonnier, M., Thiberge, J.-M., and De Reuse, H. (2008). Trans-translation in *Helicobacter pylori*: essentiality of ribosome rescue and requirement of protein tagging for stress resistance and competence. *PLoS ONE* 3:e3810. doi: 10.1371/journal.pone.0003810

Tjaden, B. (2019). A computational system for identifying operons based on RNA-Seq data. *Methods* 176, 62–70. doi: 10.1016/j.ymeth.2019.03.026

Toledo-Arana, A., Repoila, F., and Cossart, P. (2007). Small noncoding RNAs controlling pathogenesis. *Curr. Opin. Microbiol.* 10, 182–188. doi: 10.1016/j.mib.2007.03.004

Tomasini, A., François, P., Howden, B. P., Fechter, P., Romby, P., and Caldelari, I. (2014). The importance of regulatory RNAs in *Staphylococcus aureus*. *Infect. Genet. Evol.* 21, 616–626. doi: 10.1016/j.meegid.2013.11.016

Toyofuku, M., Nomura, N., and Eberl, L. (2019). Types and origins of bacterial membrane vesicles. *Nat. Rev. Microbiol.* 17, 13–24. doi: 10.1038/s41579-018-0112-2

Trotochaud, A. E., and Wassarman, K. M. (2004). 6S RNA function enhances long-term cell survival. *J. Bacteriol.* 186, 4978–4985. doi: 10.1128/JB.186.15.4978-4985.2004

Vanaja, S. K., Rathinam, V. A., Atianand, M. K., Kalantari, P., Skehan, B., Fitzgerald, K. A., et al. (2014). Bacterial RNA: DNA hybrids are activators of the NLRP3 inflammasome. *Proc. Natl. Acad. Sci. U.S.A.* 111, 7765–7770. doi: 10.1073/pnas.1400075111

Vdovikova, S., Luhr, M., Szalai, P., Nygård Skalman, L., Francis, M. K., Lundmark, R., et al. (2017). A novel role of Listeria monocytogenes membrane vesicles in inhibition of autophagy and cell death. *Front. Cell. Infect. Microbiol.* 7:154. doi: 10.3389/fcimb.2017.00154

Wagner, E. G. H., and Romby, P. (2015). "Small RNAs in bacteria and archaea: who they are, what they do, and how they do it. *Adv. Genet.* 90, 133–208. doi: 10.1016/bs.adgen.2015.05.001

Wagner, E. G. H., and Vogel, J. (2003). *Noncoding RNAs Encoded by Bacterial Chromosomes. Noncoding RNAs: Molecular Biology and Molecular Medicine*. New York, NY: Kluwer Academic/Plenum Publishers.

Wagner, T., Joshi, B., Janice, J., Askarian, F., Škalko-Basnet, N., Hagestad, O., et al. (2018). *Enterococcus faecium* produces membrane vesicles containing virulence factors and antimicrobial resistance related proteins. *J. Proteomics* 187, 28–38. doi: 10.1016/j.jprot.2018.05.017

Wang, X., Thompson, C. D., Weidenmaier, C., and Lee, J. C. (2018). Release of *Staphylococcus aureus* extracellular vesicles and their application as a vaccine platform. *Nat. Commun.* 9:1379. doi: 10.1038/s41467-018-03847-z

Wang, Z., Gerstein, M., and Snyder, M. (2009). RNA-Seq: a revolutionary tool for transcriptomics. *Nat. Rev. Genet.* 10, 57–63. doi: 10.1038/nrg2484

Wassarman, K. M., and Storz, G. (2000). 6S RNA regulates *E. coli* RNA polymerase activity. *Cell* 101, 613–623. doi: 10.1016/S0092-8674(00)80873-9

Weber, J. A., Baxter, D. H., Zhang, S., Huang, D. Y., Huang, K. H., Lee, M. J., et al. (2010). The microRNA spectrum in 12 body fluids. *Clin. Chem.* 56, 1733–1741. doi: 10.1373/clinchem.2010.147405

Wertheim, H. F., Melles, D. C., Vos, M. C., Van Leeuwen, W., Van Belkum, A., Verbrugh, H. A., et al. (2005). The role of nasal carriage in *Staphylococcus aureus* infections. *Lancet Infect. Dis.* 5, 751–762. doi: 10.1016/S1473-3099(05)70295-4

Westermann, A. J. (2018). Regulatory RNAs in virulence and host-microbe interactions. *Microbiol Spectr.* 6. doi: 10.1128/9781683670247.ch18

Whitworth, D. E. (2018). Interspecies conflict affects RNA expression. *FEMS Microbiol. Lett.* 365. doi: 10.1093/femsle/fny096

Wilderman, P. J., Sowa, N. A., Fitzgerald, D. J., Fitzgerald, P. C., Gottesman, S., Ochsner, U. A., et al. (2004). Identification of tandem duplicate regulatory small RNAs in Pseudomonas aeruginosa involved in iron homeostasis. *Proc. Natl. Acad. Sci. U.S.A.* 101, 9792–9797. doi: 10.1073/pnas.0403423101

Zhang, J., Li, S., Li, L., Li, M., Guo, C., Yao, J., et al. (2015). Exosome and exosomal microRNA: trafficking, sorting, and function. *Genomics Proteomics Bioinform.* 13, 17–24. doi: 10.1016/j.gpb.2015.02.001

Conflict of Interest: The authors declare that the research was conducted in the absence of any commercial or financial relationships that could be construed as a potential conflict of interest.

frontiers in Molecular Biosciences

HYPOTHESIS AND THEORY
published: 03 March 2021
doi: 10.3389/fmolb.2021.610453

Divergently Transcribed ncRNAs in *Escherichia coli*: Refinement of the Transcription Starts Assumes Functional Diversification

*Sergey Kiselev, Natalia Markelova and Irina Masulis**

Department of Functional Genomics and Cellular Stress, Institute of Cell Biophysics Russian Academy of Sciences, Pushchino, Russia

Non-coding regulatory RNAs (ncRNAs) comprise specialized group of essential genetically encoded biological molecules involved in the wide variety of cellular metabolic processes. The progressive increase in the number of newly identified ncRNAs and the defining of their genome location indicate their predominant nesting in intergenic regions and expression under the control of their own regulatory elements. At the same time, the regulation of ncRNA's transcription cannot be considered in isolation from the processes occurring in the immediate genetic environment. A number of experimental data indicate the notable impact of positional regulation of gene expression mediated by dynamic temporal DNA rearrangements accompanying transcription events in the vicinity of neighboring genes. This issue can be perceived as particularly significant for divergently transcribed ncRNAs being actually subjected to double regulatory pressure. Based on available results of RNAseq experiments for *Escherichia coli*, we screened out divergent ncRNAs and the adjacent genes for the exact positions of transcription start sites (TSSs) and relative efficiency of RNA production. This analysis revealed extension or shortening of some previously annotated ncRNAs resulting in modified secondary structure, confirmed stable expression of four ncRNAs annotated earlier as putative, and approved the possibility of expression of divergently transcribed ncRNAs containing repetitive extragenic palindromic (REP) elements. The biogenesis of secreted ncRNAs from divergently transcribed *ffs*, *chi*X, *ral*A, and *ryh*B is discussed taking into account positions of TSSs. Refinement of TSSs for the neighboring genes renders some ncRNAs as true antisense overlapping with 5′UTR of divergently transcribed mRNAs.

Keywords: divergent transcription, non-coding RNAs, genome annotation, REP elements, secreted RNAs

OPEN ACCESS

Edited by:
Klaus Neuhaus, Technical University of Munich, Germany

Reviewed by:
Konrad Ulrich Förstner, Leibniz Information Centre for Life Sciences, Germany
Barbara Zehentner, Technical University of Munich, Germany

****Correspondence:***
Irina Masulis
masulis@icb.psn.ru

Specialty section:
This article was submitted to Protein and RNA Networks, a section of the journal Frontiers in Molecular Biosciences.

Received: *25 September 2020*
Accepted: *07 January 2021*
Published: *03 March 2021*

Citation:
Kiselev S, Markelova N and Masulis I (2021) Divergently Transcribed ncRNAs in Escherichia coli*: Refinement of the Transcription Starts Assumes Functional Diversification. Front. Mol. Biosci. 8:610453. doi: 10.3389/fmolb.2021.610453*

INTRODUCTION

The generally accepted classification of non-coding regulatory RNAs (ncRNAs) is primarily based on their genomic positioning relatively to the target gene subjected to regulation. Thus *cis*- and *trans*-acting subtypes are described (reviewed in Waters and Storz, 2009), implying that the first control the expression of closely located gene (primarily via antisense mechanism and base pairing protruding over 43 to 650 bp) (Brantl, 2007) while *trans*-encoded sRNAs are confirmed to have from one to dozens remote targets detected by means of biochemical and bioinformatics approaches (Vogel and

Wagner, 2007; Hör et al., 2020). Assignment of ncRNAs as powerful and numerous class of metabolic regulators stimulated a flow of works aimed to discover and comprehensively characterize physiologically relevant products. For a long time, the dominated strategies exploited 1) the search of conservative intergenic regions (IGRs), 2) the presence of transcription initiation and termination signals, and 3) the ability of potential ncRNA to adopt stable secondary structure (Altuvia, 2007; Backofen and Hess, 2010). Predicted candidates were experimentally verified using hybridization and reverse transcription approaches. This allowed revealing major ncRNAs as master regulators with defined biological function (Argaman et al., 2001; Dutta and Srivastava, 2018). Selective cloning strategy aimed to hound down small ncRNAs (sRNAs) (Kawano et al., 2005) and high throughput sequence facilities significantly enriching ncRNAs community (Shinhara et al., 2011; Barquist and Vogel, 2015) including independently encoded genes and ncRNAs, originated by cutting-out from mRNAs. In *E. coli*, the observation of non-uniformity in decay rate of entire mRNAs and their internal fragments led to the finding of 58 novel putative ncRNAs partially or completely embedded into the coding regions (Dar and Sorek, 2018). Although recently described ways to produce ncRNAs from 5′ and 3′ untranslated regions of coding sequences contribute to the whole spectrum of riboregulators (Carrier et al., 2018), their transcription from intergenic regions remains one of the primary sources (Adams and Storz, 2020). The mode of ncRNA's biogenesis—from IGRs by means of transcription from specified promoter or from coding genomic region and adjacent loci mediated by RNAse E—implies the involvement of different molecular mechanisms in the regulation of their abundance. ncRNA excised from mRNA precursor follows the pathways implicated in the control of parental RNA synthesis, although additional level of regulation may be imposed by accessibility of distinct structural motifs to RNAses. IGR-derived ncRNA possesses individual control elements including promoter, terminator, and transcription factor binding sites. ncRNAs encoded within IGRs undergo more strict purifying selection if compared to non-coding regions containing promoters or terminators only (Thorpe et al., 2017). Genome-wide analyses encompassing near 900 sRNAs from 13 bacterial species revealed meaningful enrichment of long conserved IGRs by non-coding sRNAs (Tsai et al., 2015). Since these sRNAs may be considered as "self-sufficient" genetic elements, one might expect their conservation between different species and evolutionary distant taxonomic bacterial groups. Nevertheless, comparative analysis highlighted substantial deviation in phylogenetic distances calculated for sRNAs and for protein-coding sequences (Lindgreen et al., 2014). Thus, ncRNAs undergo their own way of emergency and evolution still remaining one of the most obscure matters. It was proposed that promoters for ncRNAs could arise from transcriptional noise in terms of new promoter spontaneously erupting in IGR and conferring beneficial properties (Jose et al., 2019). Such RNAs must go "trial and error" path for the adaptation to the regulatory networks of the cell being probed for the compatibility with different targets among mRNAs and RNA-binding proteins. ncRNA's implementation in metabolic circuits may occur as coevolution with RNA-binding proteins (ChiX, CyaR, FnrS, MicA, SgrS, DsrA, and MicC) or like prevenient gain of novel ncRNAs searching for a target (ArcZ, MicF, OmrA, OxyS, and RprA) (Peer and Margalit, 2014). The lack of the initial destination for the interaction with a specific partner may partially explain the phenomenon of "multi-target" action of many *trans*-encoded ncRNAs. Other possible mechanisms giving rise to the novel ncRNAs may be horizontal gene transfer and duplication of preexisting ncRNAs followed by the acquisition of new functions (Dutcher and Raghavan 2018). Preferential location of ncRNAs in IGRs assumes that, apart from involvement of their own regulatory elements, transcription of neighboring genes may contribute to the maintenance of their expression at appropriate level. Using *lac* promoter-based reporter system (Bryant et al., 2014) or barcoded construct (Scholz et al., 2019), it was demonstrated that transcriptional output varies in the range of 300- or 20-fold, respectively, depending on the local genetic environment. This positional regulation via mechanistic properties of given DNA segment also may affect the "decision" for certain RNA to be expressed from the certain chromosomal region. The influence of genomic context is expected to be quite different for RNAs having collinear or divergent orientation, respectively, to the adjacent gene accounting concomitant conformational effects induced by transcription (**Figure 1**). The model of twine-supercoiling domains postulates the formation of partially unwound DNA regions behind transcription complexes and accumulation of positive supercoils on the front line (Wu et al., 1988). Since initiation of transcription was shown to be sensitive to DNA superhelical state (Lim et al., 2003; Peter et al., 2004; Zhi et al., 2017; Dorman, 2019), the expression of closely located transcription units in fact may be considered as context-encoded regulatory level implicated in the control of ncRNAs synthesis. Gene expression profiling revealed altered response of divergent genes to the global changes in superhelical density induced by DNA gyrase inhibitor norfloxacin indicating the combined effect of local and global DNA conformational changes on transcription (Masulis et al., 2015). In this respect for the case of divergently transcribed ncRNAs, the relative positions of promoter regions and the rate of their utilization by RNAP appear to be critical for the final transcriptional output. As for any pair of divergent transcriptional units, transcript level for each counterpart is expected to be a result of mutual effects mediated by competition for enzyme binding or by means of non-contact structural DNA deformation or by both mechanisms concurrently. Here, we addressed if codirected or divergent positioning of known ncRNAs has any preference and if there is any bias—antagonistic, synergistic, or neutral—between the expression of ncRNAs and their divergent partners.

Totally, 125 genes with established or proposed assignment to non-coding small RNAs are annotated in RegulonDB to date (Santos-Zavaleta et al., 2019). 12 of them overlap with 5′ or 3′ terminal parts of protein-coding sequences assuming that transcription of these RNAs *a priori* is superimposed with read-through of parental mRNA. Based on annotation, 61

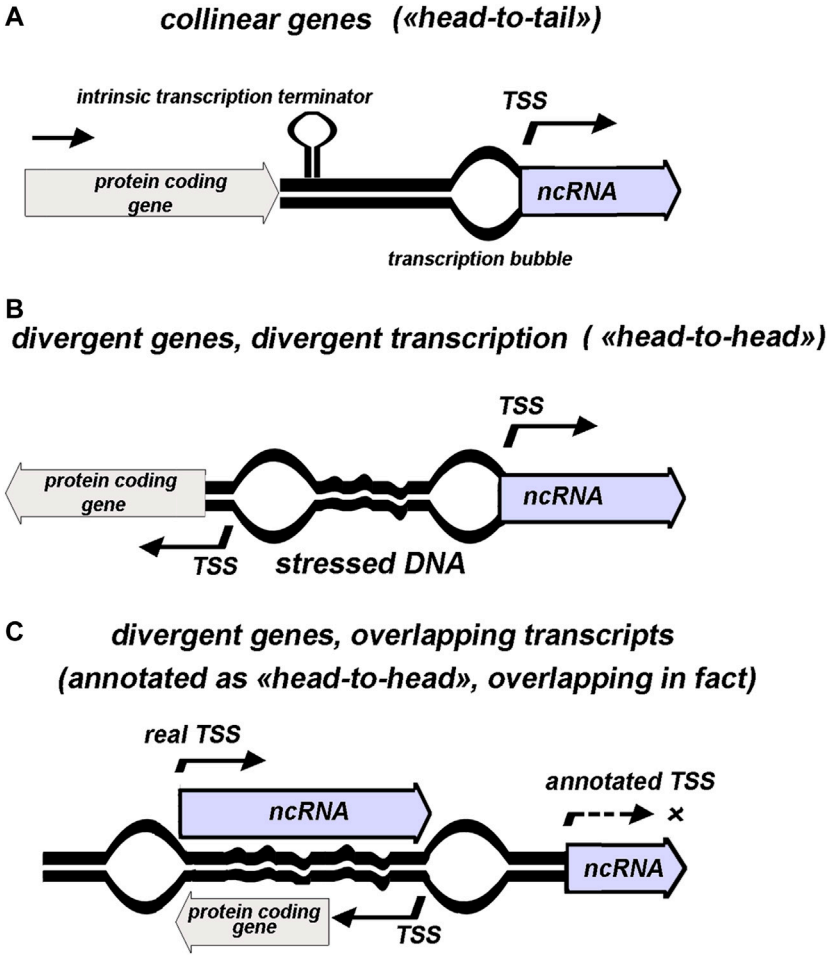

FIGURE 1 | Schematic presentation of various genomic contexts for ncRNAs annotated as separate transcription units. 5′ end of ncRNA assumed to coincide with transcription start site (TSS). "Stressed DNA" and positions of "transcription bubbles" illustrate topology-mediated effects.

codirected and 64 divergently transcribed ncRNAs are revealed in *E. coli* genome demonstrating the lack of predominant orientation of ncRNAs relatively to the adjacent genes—"head-to-tail", "head-to-head", or overlapping over 5′ termini (**Figure 1**). Unambiguous attribution of ncRNA as an independent transcriptional unit and its assignment to one of the three types of relative arrangement with respect to the neighboring gene are fraught with some deceptions arising from incompleteness of our knowledge regarding the exact positions of promoters and terminators (**Figure 1C**). Thus, meta-analysis of data obtained using high-throughput RNAseq and tiling arrays allowed defining true *bona fide* small RNA as a product of gene not overlapping any other genes from the opposite strand (Liu et al., 2018). According to these requirements, antisense RNAs, UTR-processed products, and transcripts derived from premature termination (riboswitch) were sifted out from almost 500 previously proposed staphylococcal ncRNAs resulting in only 46 *bona fide* representatives with high degree of conservation within *Staphylococcaceae* family. Thus, the displacement of TSS into the coding region of the neighboring gene compels to reconsider categorization of ncRNA as *cis*-acting or *trans*-acting. Some cases of this type revealed for *E. coli* ncRNAs are discussed below.

We juxtaposed the location of TSSs predicted by promoter-search algorithm PlatProm (Shavkunov et al., 2009) and experimentally found 5′ termini of ncRNAs and divergently transcribed neighboring genes of *E. coli* using data sets available from Thomason et al. (2015) and Ettwiller et al. (2016). PlatProm was developed to search for potential TSSs accounting sequence features of experimentally characterized *E. coli* promoters. It evaluates each position in the genome for the ability to serve as transcription start assuming essential promoter textual elements formalized in weight matrixes. The score value reflecting similarity with "ideal" promoter is considered as the quantitative measure of transcriptional capacity for given position in the genome (Shavkunov et al., 2009). The data of Thomason et al. (2015) also allow estimating the expression level of ncRNAs under various conditions. The positions of primary TSSs in superimposed transcriptional profiles are in general in good agreement with each other

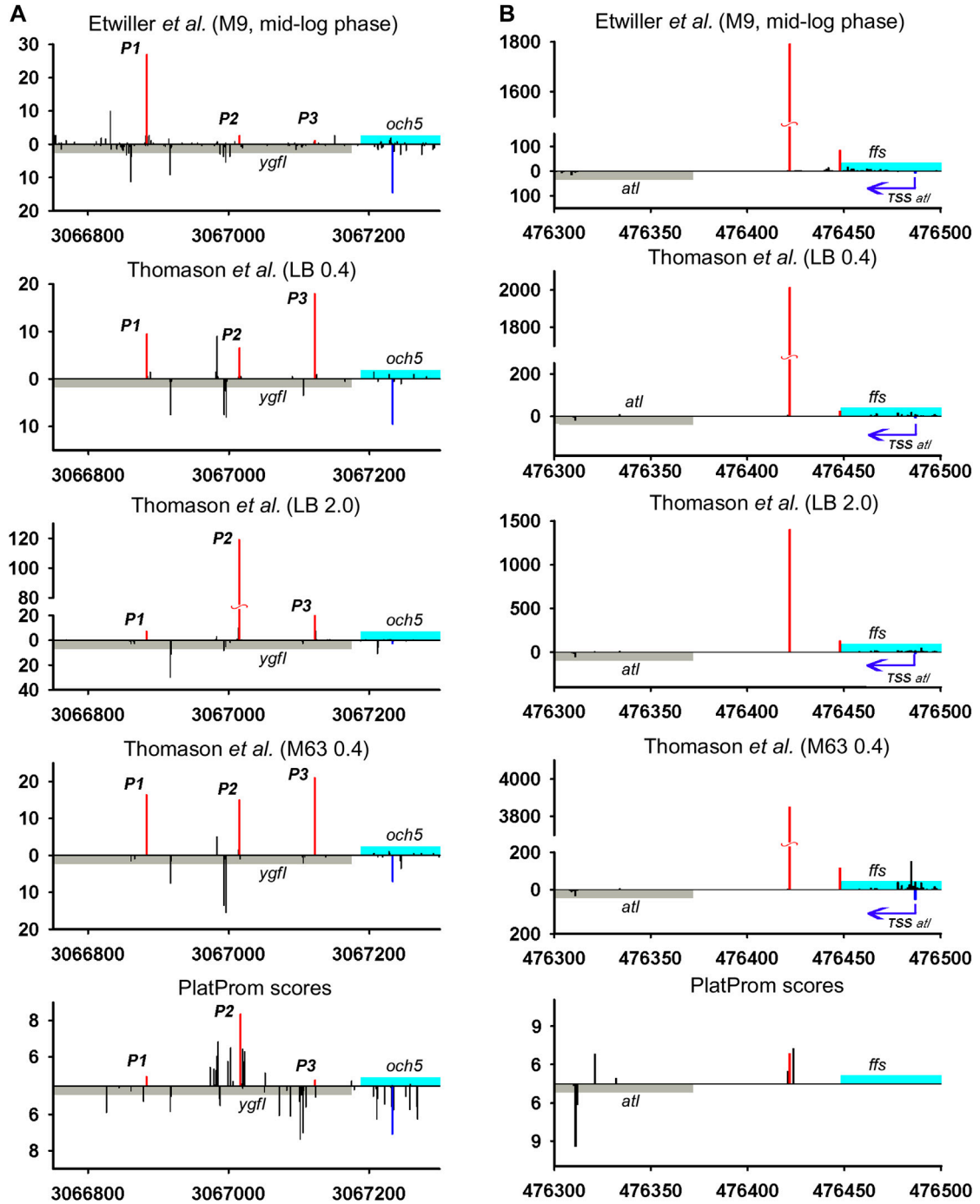

FIGURE 2 | Mapping of TSSs for divergently transcribed ncRNAs according to RNAseq data (Thomason et al., 2015; Ettwiller et al., 2016) and computational prediction (Shavkunov et al., 2009). X axis: coordinates in *E. coli* genome; Y axis: average number of normalized counts with perfect matching for given growth condition. For PlatProm predictions absolute score values are indicated on Y axis. RNA denoted according to the annotation in RegulonDB is shown in cyan; adjacent divergent gene is indicated in gray. Bars above and below X axis correspond to the upper and low DNA strands, respectively. Exactly matching TSSs for ncRNAs are presented in red and for divergently transcribed gene are indicated in blue. Transcriptional landscapes upstream and downstream relatively to the genomic regions depicted in **Figure 2** are shown in **Supplementary Figure S2**.

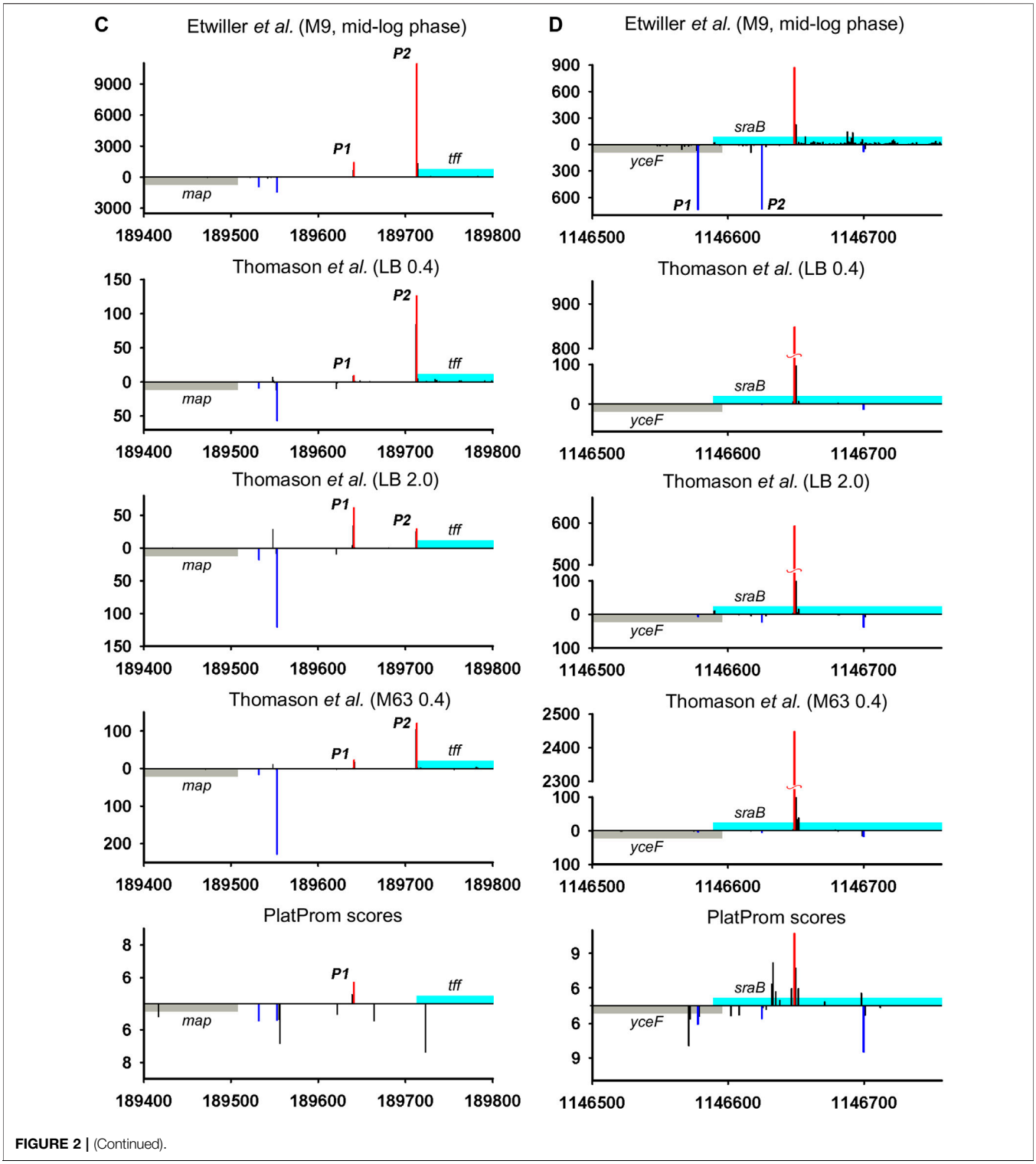

FIGURE 2 | (Continued).

(**Figure 2**) confirming the highest value and objectivity of such data for the reconstruction of the genome-wide transcriptional profile as an integral fingerprint of bacterial physiological status in given growth conditions.

Evidence and Objections

Upshift or Downshift of sRNA 5′ End

RNAseq data allowed verifying the exact positions of transcription starts for divergently transcribed ncRNAs

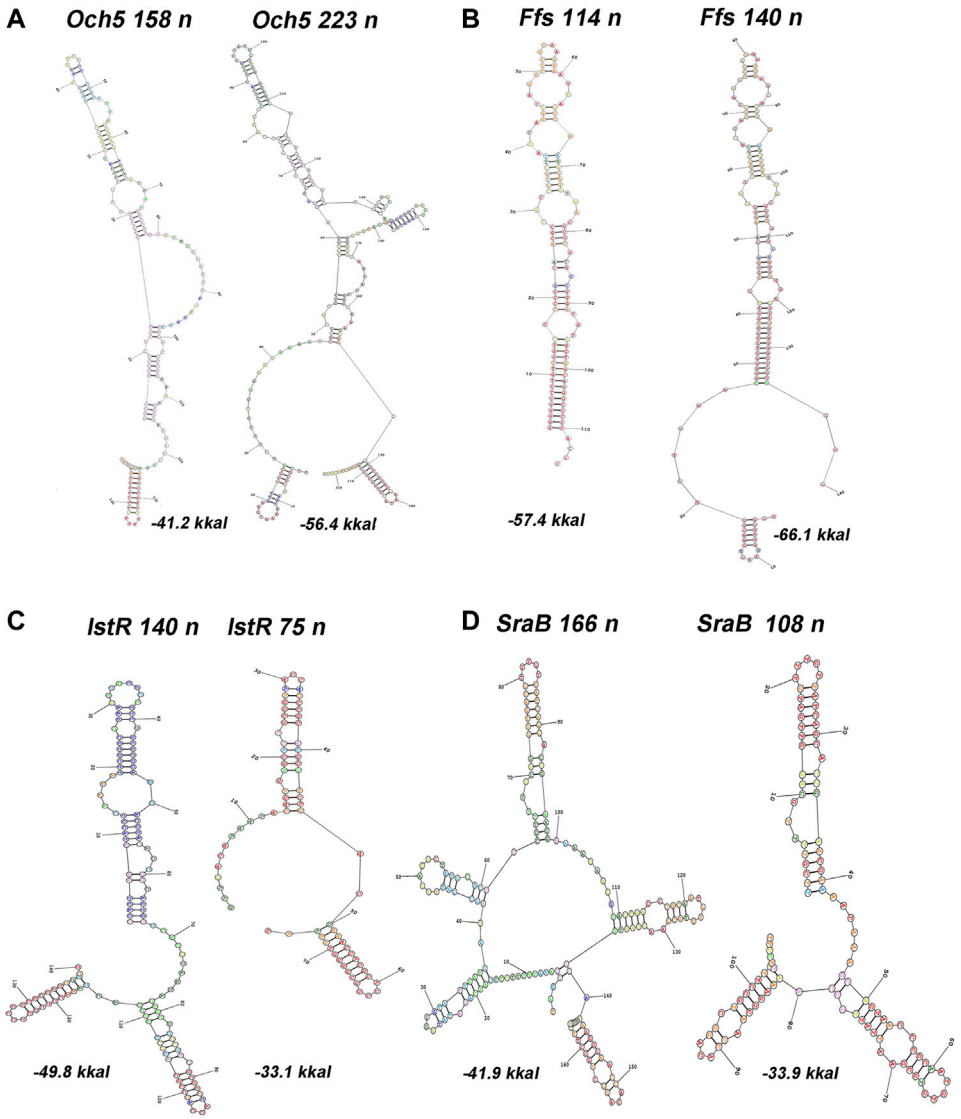

FIGURE 3 | Predictions of secondary structures for 5′-extended or shortened ncRNAs. RNA structure was modeled using server http://rna.urmc.rochester.edu/RNAstructureWeb/Servers (Reuter and Mathews, 2010). Transcripts originating from two TSSs, one corresponding to annotated start (RegulonDB) and the other inferred from RNAseq data (Thomason et al., 2015), were subjected as a query using default parameters. Annotated position of 3′-end was assumed for both variants. Energy of folding is indicated below the structures.

(**Supplementary Table S1**). Although the coordinates of primary TSSs for the majority of ncRNAs are in good agreement with their 5′ ends mapped in RegulonDB, the overall transcriptional landscape of near 30 genomic loci needs some corrections. The most notable examples are considered here. Thus, for G0-8898 putative ncRNA annotated as "phantom gene" TSS seems to be located 27 bp upstream from 5′ end indicated in RegulonDB, (**Supplementary Table S1**) for *och*5 this shift is 65 bp, and for *ffs* it is 26 bp (**Figure 2A,B**; **Supplementary Figures S2A,B**). The opposite deviation toward 3′ end was observed for *rse*X, *ytf*L5′ (**Supplementary Table S1**), *sra*B (**Figure 2D**; **Supplementary Figure S2D**) genes—TSSs were moved downstream by 29, 43, 60, and 65 bp, respectively, resulting in shortening of corresponding ncRNAs. Additional TSS exactly matching computational predictions by PlatProm and prevailing in stationary phase was found for *tff* (**Figure 2C**; **Supplementary Figure S2C**). Thus, *map-tff* genomic loci may produce two divergently transcribed growth-phase dependent ncRNAs differing in length by 71 nt. Nor synergistic or cooperative effect in the expression of *map* and *tff* was observed assuming their autonomous regulation. For *crp*T, double-side deviation was revealed—weak promoter with start point was pushed 164 bp upstream to the annotated start and primary TSS shifted 6 bp downstream (**Supplementary Figure S1B**). Second-order 5′-extended CrpT RNA with considerable expression level only at stationary phase may serve as antisense for yheU mRNA forming

the duplex with 5′UTR (promoter P2). RydC, one of the most abundant and early described sRNAs implicated in the wide spectrum of regulatory networks (Antal et al., 2005) possesses upstream TSS remote from the primary start by 96 bp which enlarges the secondary putative sRNA by a factor 3.

The upshift as well as downshift of ncRNA's 5′ ends if compared to previously accepted positions may account for changing of folding properties and thus selectivity to RNA binding proteins and mRNA targets. Extension or shortening of ncRNA may result in 1) considerable rearrangements of folding pattern (Och5, **Figure 3A**), 2) addition of a new structural motif like when it happens in the case of Ffs and IstR while the "core" ncRNA's structure remains the same (**Figures 3B,C**), or 3) elimination of intramolecular stem-loop structures if TSS appears to be pushed downstream (SraB, **Figure 3D**). Newly attached or removed structural details in ncRNA's architecture may serve as anchors for the interaction with partner molecules, thus determining the spectrum of ncRNA's targets. Noteworthy enlargement or trimming of ncRNAs deduced from refined TSS position does not noticeably change energy of folding and specific impact of nucleotides in RNA stability. SraB and IstR are the exceptions showing increased nucleotide impact in free energy of folding by 26% and 23.8% correspondently when shortened from 5′ end, respectively, to the annotated length. SraB belongs to the classic type of divergently transcribed overlapping ncRNAs, firstly discovered by Argaman et al., 2001, confirmed by Northern blot and *in vitro* transcription assay, and conserved in *Salmonella typhimurium*, *Klebsiella pneumoniae*, and *Yersinia pestis*. Although in early experiments the expression of *sra*B was proposed to be growth phase dependent and was detected in late stationary phase in LB but not in the mineral medium, RNAseq data pointed out stable production of this RNA in 5′-truncated form in exponential phase in LB as well as in M63 with threefold increase in minimal medium. Surprisingly, in virulent *S. typhimurium* strain, SL1344 *sra*B TSS corresponds to TSS revealed for *E. coli* in Thomason et al. (2015) and Ettwiller et al. (2016), and the length of homologous RNA is expected to be 99 nucleotides, close to that of "shortened" *E. coli* derivative (data from **Supplementary Table S8** in Ramachandran et al., 2014). *S. typhimurium* SraB is shown to be significantly suppressed by ppGpp (Ramachandran et al., 2014) and is proposed to confer resistance to egg albumin (Jiang et al., 2010). The discrepancy in the positioning of SraB 5′-end was probably caused by the presence of deceptively "attractive" canonical sigma70 promoter related to the previously annotated TSS. Downshifted transcription start highlighted by RNAseq on the contrary corresponds to poorly defined promoter although it was indicated as "predicted" in RegulonDB (Santos-Zavaleta et al., 2019). It remains questionable why of the two promoters only one possessing less similarity to consensus is engaged in RNA synthesis. One of the possible explanations may assume collision effects due to transcription initiated at *yce*F P1 promoter (**Figure 2D**, data set of Ettwiller et al. (2016)). At the same time, *sra*B transcription is insensitive to the activity of divergent overlapping promoter *yce*F P2. Another data set used in

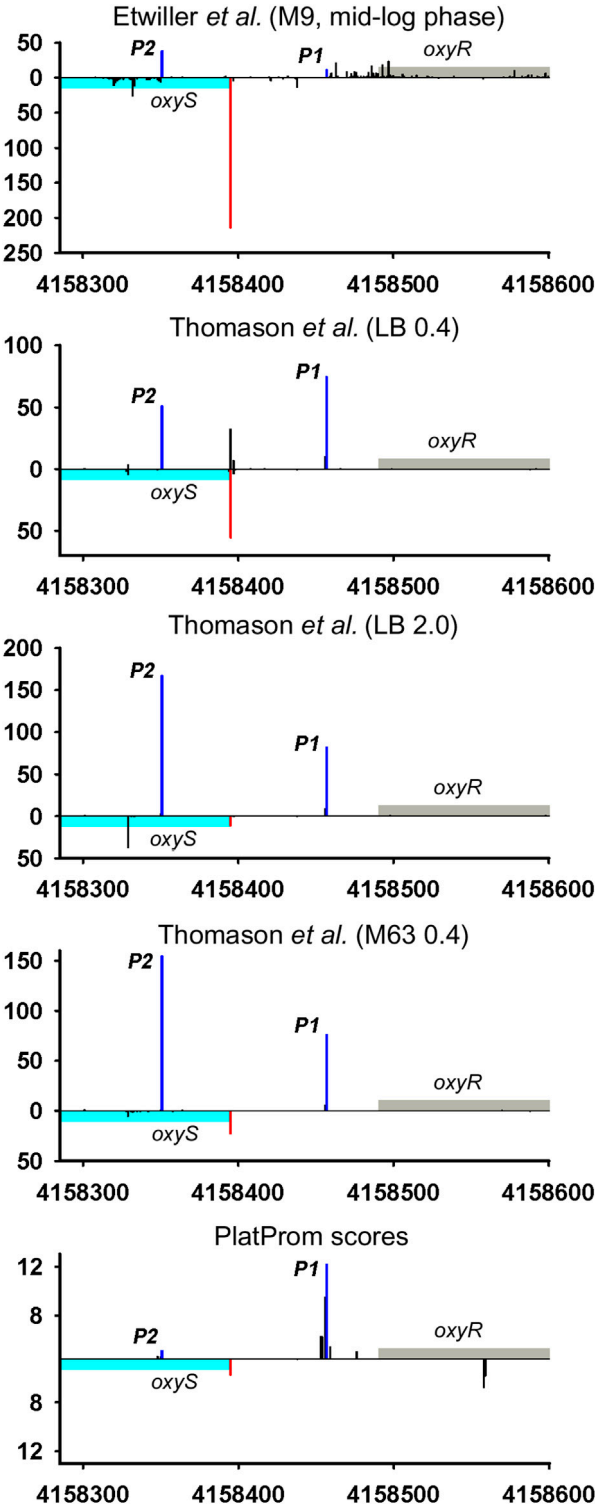

FIGURE 4 | Mapping of TSSs for *oxy*S-*oxy*R genomic region according to RNAseq data (Thomason et al., 2015; Ettwiller et al., 2016). All designations are the same as in **Figure 2**. Transcriptional landscape upstream and downstream relatively to the genomic region depicted in **Figure 4** is shown in **Supplementary Figure S4**.

this study (Thomason et al., 2015) has not confirmed transcriptional activity of *yce*F while the position of SraB TSS perfectly coincides for all RNAseq experiments and computational scanning by PlatProm (**Figure 2D**; **Supplementary Figure S2D**).

Ffs ncRNA overlaps with divergent *atl* transcript by 65 bp although the level of *atl* transcript appeared to be negligible (**Figure 2B**; **Supplementary Figure S2B**). Ffs named also 4.5S is one of the most "deserved" among ncRNAs in the historical aspect due to its function as an essential component of signal recognition particles (SRP). Motif 5′ACCAGGTCAGGTCCG GAAGGAAGCAGC responsible for the formation of apical helix structure was shown to be critical for the interaction with Ffh protein and conserved in bacteria and even high organisms (Peterson and Philips, 2008). Extension by 26 bases from 5′ end does not interfere with the overall folding pattern although additional stem-loop structure appears at the terminus (**Figure 3B**). This appendage as a consequence of TSS upshift is conserved among *Enterobacteriaceae* including *Escherichia*, *Shigella*, *Salmonella*, *Enterobacter*, *Citrobacter*, *Klebsiella*, *Kluyvera*, *Kosakonia*, and *Trabulsiella* as confirmed by Microbial Nucleotide BLAST when extended *ffs* gene was submitted as a query. It is noticeable that in spite of location on plus or minus strand *ffs* retains opposite orientation to the neighboring gene. The relative efficiency of transcription in the pair *ffs*P1 /*atl* P1 for the three experimental conditions used in Thomason et al. (2015) implies antagonistic rather than supporting effect of atlP1 on ffsP1 activity consistent with collision model (Callen et al., 2004).

Duplicated promoters are likely to regulate the expression of *rye*G having two TSSs separated by 26 bp. The amount of corresponding ncRNAs depends on the growth conditions. Both short and long RNAs are consistently activated in stationary phase along with the transcription of the adjacent *tfa*S gene demonstrating cooperative behavior (**Supplementary Figure S1A**, data set of Thomason et al., 2015). Indeed, the distances between TSSs related to promoters P1 and P2 and the start point of TfaS mRNA (57 and 83 bp correspondently) allow alternate or simultaneous binding of RNA polymerase to transiently unwound DNA and transcription initiation in opposite directions. Two variants of RyeG RNA of 194 and 220 nt in length having identical folding in the core part of the molecule differ in the structure of 3′terminus (**Supplementary Figure S3**) that may result in altered recognition of their targets.

Thus, the same genomic region may be the source of two or more specious ncRNAs differing in length, shape, and stability, thereby assuming to expand the whole spectrum of related functions.

Potential Antisense Transcripts Inferred From TSSs Mapping

Divergently encoded ncRNAs may be added to the family of antisense ncRNAs accounting for newly discovered or corrected positions of TSSs for adjacent divergent genes. Thus, OxyS may overlap 5′UTR of its *vis*-à-*vis oxy*R by 41bp. Described in 1997 (Altuvia et al., 1997), this RNA for more than 20 years has never ceased to amaze researchers with the variety of its functions. Annotated TSS was concurrently detected in all RNAseq experiments and exactly predicted by PlatProm algorithm (**Figure 4**; **Supplementary Figure S4**). Assuming the activity of sole P1 *oxy*R promoter OxyS may be defined as typical *bona fide* ncRNA although obvious activity of P2 promoter coming to be major in stationary phase and in mineral medium allows to ascribe to OxyS potential role of antisense RNA.

Similarly, MicC over its entire length may serve as antisense for *omp*N mRNA having long 5′UTR with TSS remote from initiation codon by 408 bp (**Supplementary Table S1**). In the pair, *mic*A/*lux*S highly expressed *mic*A sRNA is overlapped with 5′UTRs of one of two *lux*S-related mRNAs. MicA is involved in a number of RNA-RNA interactions in *trans* presumably with mRNAs related to cell-envelop stress (PhoP, LamB, OmpA, OmpW, Tsx, OmpX, FimB) (Mihailovic et al., 2018). For example, MicA is capable of forming stable duplex with OmpA mRNA as confirmed *in vitro* using SPR technique (Vincent et al., 2013). Overlapping of ncRNAs with 5′UTRs of divergent mRNAs allowing ascribing to the non-coding transcripts potential antisense functions may be proposed for the pairs G0-10702/YhcC (15 bp duplex), G0-10703/yhcG (128 bp), RdlD/ldrD (136 bp), G0-10705/GlnA (63 bp, significant for stationary phase), SymR/SymE (76 bp, entire length), G0-10703/YhcG, ArrS/GadE (68 bp, entire length) (**Supplementary Table S1**).

Therefore, two types of corrections based on RNAseq data make it possible to consider ncRNA as antisense, identifying a previously unknown TSS for the divergent gene and/or discovering additional TSSs for ncRNA. Transcriptional regulation via multiple promoters is widely exploited in prokaryotes and it seems to be a general principle of promoters evolving in intergenic loci. Thus, from 28 to 40% of experimentally found promoters for mRNA are accompanied by the "second-order" regulatory sites within 250 bp long region upstream to the ORFs (Huerta and Collado-Vides, 2003). The classical example of paired promoters for the transcription of rRNA separated by 120 bp ensures flexible growth rate-dependent regulation of ribosome synthesis (Gourse et al., 1996). *dad*A encoding D-amino acid dehydrogenase is transcribed from three consecutive promoters differing in their activity and selective response to cAMP-CRP (Zhi et al., 1998). In some cases, tandemly arranged promoters may be recognized by RNA polymerase holoenzyme containing alternative sigma-factors and adopted to respond to changing environmental conditions, thus providing reserve facilities for transcriptional regulation. For example, AppY mRNA may be initiated at two promoters separated by 76 bp and recognized by sigma70 or sigma38 RNAP (Rangarajan and Schnetz, 2018). Sigma70 and sigma38 dependent TSSs of *nha*A are separated by 141 bp demonstrating differential sensitivity to HNS and elevated sodium concentrations (Dover and Padan, 2001). Promoter duplication may obviously be exploited in bacteria for the fine turning of ncRNA's expression and the extension of accessibility of divergent mRNAs for regulation via antisense mechanism.

Divergent ncRNAs as Purveyors of Extracellular exRNAs

Besides indubitable universality of ncRNAs in coordination of intracellular regulatory processes, their role as messenger molecules in cell communications is coming to be more and more appreciable. RNA is exported as small fragments (less than 60 nt in length) in a controlled manner exploiting outer membrane vesicles (OMV) or yet unrevealed secretion machinery (Ghosal, 2018). Among the total pool of extracellular RNAs, ncRNA's derivatives comprise a substantial fraction along with rRNA's and tRNA's generated fragments. Divergently transcribed Ffs RNA contributes to this set being preferentially exported in OMV-free manner in *E. coli* (Ghosal et al., 2015). Its function as external signal molecule in bacterial population is likely to be conserved since homologous ncRNA of *Salmonella enterica* serovar Typhimurium LT2 was detected in OMV-enriched samples (Malabirade et al., 2018). Nevertheless, pathways of processing and secretion of Ffs ncRNA differ in two Enterobacteria—in *E. coli* only short fragment of 29 nt was shown to be exported while in *S. Typhimurium* LT2 full-length transcript enclosed in or bound to OMV was revealed. The involvement of Ffs in intercellular communication is confirmed by the observation of considerable increase (up to 13-fold) in its amount in cultivation medium for mixed bacterial population (*E. coli—Paenibacillus bisonicum*) if compared to pure *E. coli* culture (Alikina et al., 2018). Another three extracellular exRNAs originated from divergently transcribed precursors (ChiX, RalA, and RyhB) demonstrated opposite reaction on the presence of competing bacterium resulting in 2- to 20-fold decrease in their secretion. It should be noted that 5′ ends of short fragments of ChiX (5′ ACACCGTCGCTTAAAG) and RalA (5′ GAGGACTGAAGT) revealed in cultural fluid (Alikina et al., 2018) exactly correspond to primary TSSs of parental ncRNAs indicating possible endonuclease cutting out or release of aborted transcripts generated upon initiation of RNA synthesis. RyhB-related exRNA (5′CCGGGTGCTGGCTTTTTTT), and vice versa, may be ascribed to 3′ terminus of full-length ncRNA. 5′-end of Ffs-born intracellular fragment (Alikina et al., 2018; **Supplementary Table S1**) is shifted down by 11 nt relatively to TSS refined according to the data of Thomason et al. (2015). It means that additional stem-loop structure expected to form in 5′extended transcript (**Figure 3B**) may exert functional role for nibbling out short RNA. Ffs, ChiX, and RyhB belong to the group of the most abundant ncRNAs with enhanced expression in stationary phase (Thomason et al., 2015) raising the possibility of their involvement in the control of cell density in bacterial population. Otherwise, RalA is accumulated at very low level which makes the presence of its fragment among secreted RNAs rather intriguing, indicating selectivity of export.

Putative Divergent ncRNAs Containing REP Elements

Intergenic regions, along with the fact that they serve as reservoir of ncRNAs, may contain repeating sequences with mirror-symmetry, so called REP (repetitive extragenic palindromic) elements. The transcription of these sequences yielding RNAs with potential regulatory functions is still questionable. REP elements represent conservative universal structural modules of bacterial genomes. Deduced on the base of the alignment of 35 *E. coli* and *S. typhimurium* intergenic regions, REP sequence was proposed to be 35 bp long symmetrical motif GC (g/t) GATGGCG (g/a)GC (g/t)…(g/a)CG (c/t)CTTATC (c/a) GGCCTAC (Stern et al., 1984). Similar stretches homologous to 5′TGCCGGATGCGGCGTAAACGCCTTATCCGGCCTAC (Tobes and Ramos, 2005) and 5′GCCGGATGCGGCGTGAAC GCCTTATCCGGCCTACGA (Markelova et al., 2016) were found in *E. coli* genome in 290 and 224 copies correspondently without any preferential location between convergent or codirectional genes. Self-complementarity assuming the ability to form hairpin structures in RNA or in negatively supercoiled DNA propelled to discuss the involvement of REP elements in regulation of gene expression (Higgins et al., 1988). In spite of efforts to confirm their role in transcription activation, attenuation, or maintenance of mRNA stability (Higgins et al., 1988), the only function related to premature termination of translation can be considered as experimentally approved (Liang et al., 2015). Thus, REP motif located at a distance no longer than 15 bp from translation termination codon in 3′UTR of mRNA affects the abundance of corresponding protein. At the same time, near 80% of REP elements are pushed down from the 3′ terminus of adjacent gene at a longer distance (Markelova et al., 2016) implying another biological function. It was suggested that REP sequences may be read-through as autonomous transcription units contributing to the family of novel non-coding RNAs (Qian and Adhya, 2017). ncRNA CbsR16 originated from REP-containing repeat-reach region of *Coxiella burnetii* chromosome was described recently (Wachter et al., 2018). Here, we analyzed 79 REP-containing genomic loci separating collinear protein-coding genes for the presence of TSSs providing divergently transcribed RNAs encompassing REP elements. Indeed in 35 cases TSSs were found indicating transcription in opposite direction relatively to the juxtaposed gene (**Supplementary Material**, List of REP-containing genomic regions). Two representative examples are shown in **Figure 5**. In the case of *ppc-arg*E intergenic region *bona fide* divergent transcription expected to capture 3 and 2 consecutive REP elements was registered (**Figure 5A**; Thomason et al., 2015). For *yid*B-*gyr*B loci, divergent RNA initiated between two codirected genes seems to be true antisense product complementary to *yid*B 5′UTR (**Figure 5B**). Weak expression of *bona fide* ncRNA trimmed from 5′ end was detected only for stationary phase and mineral medium. Does the presence of REP elements as a structure-forming motifs impact in the functional properties of corresponding RNAs remains unclear. Obviously, REPs may be included in novel divergently transcribed RNAs if there is no intrinsic terminator between TSS and the 5′-end of REP. Only 16 of 35 REP-containing intergenic regions have T_n tracks indicating potential intrinsic terminator between TSS and 5′-end of REP, though not all T-rich blocks are preceded by self-complementary sequence essential for transcription termination. It increases the probability of transcription passing through REP motifs. The distance from TSSs to REP 5′ end varies from 16 to 298 bp allowing also to assume their function in rho-dependent transcription termination proposed in Espeli et al. (2001).

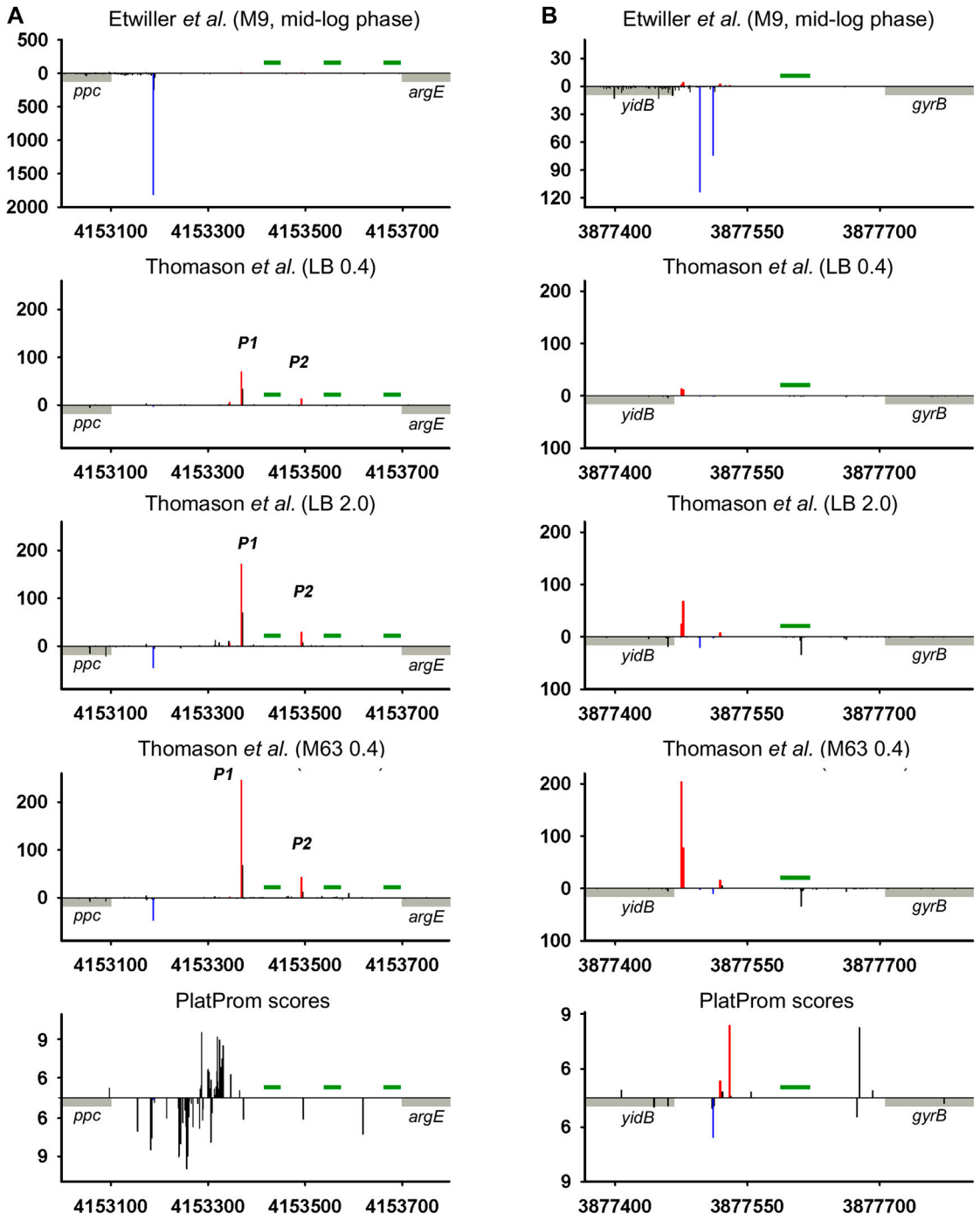

FIGURE 5 | Mapping of TSSs for divergently transcribed REP elements according to RNAseq data (Thomason et al., 2015; Ettwiller et al., 2016) and computational prediction (Shavkunov et al., 2009). X axis: coordinates in *E. coli* genome; Y axis: average number of normalized counts with perfect matching for given growth condition. For PlatProm predictions absolute score values are indicated on Y axis. REP element is denoted in green; adjacent genes are indicated in gray. Bars above and below X axis correspond to the upper and low DNA strands, respectively. Exactly matching TSSs related to divergently transcribed REP sequence are presented in red and for protein-coding genes are shown in blue.

The relative positions of TSSs and the borders of REPs admit the possibility of their inclusion in ncRNAs as well as return us to the early hypothesis regarding the role of REPs as transcription punctuation signals. In the last case, REPs may serve to block transcription of divergent ncRNAs, thus determining their length.

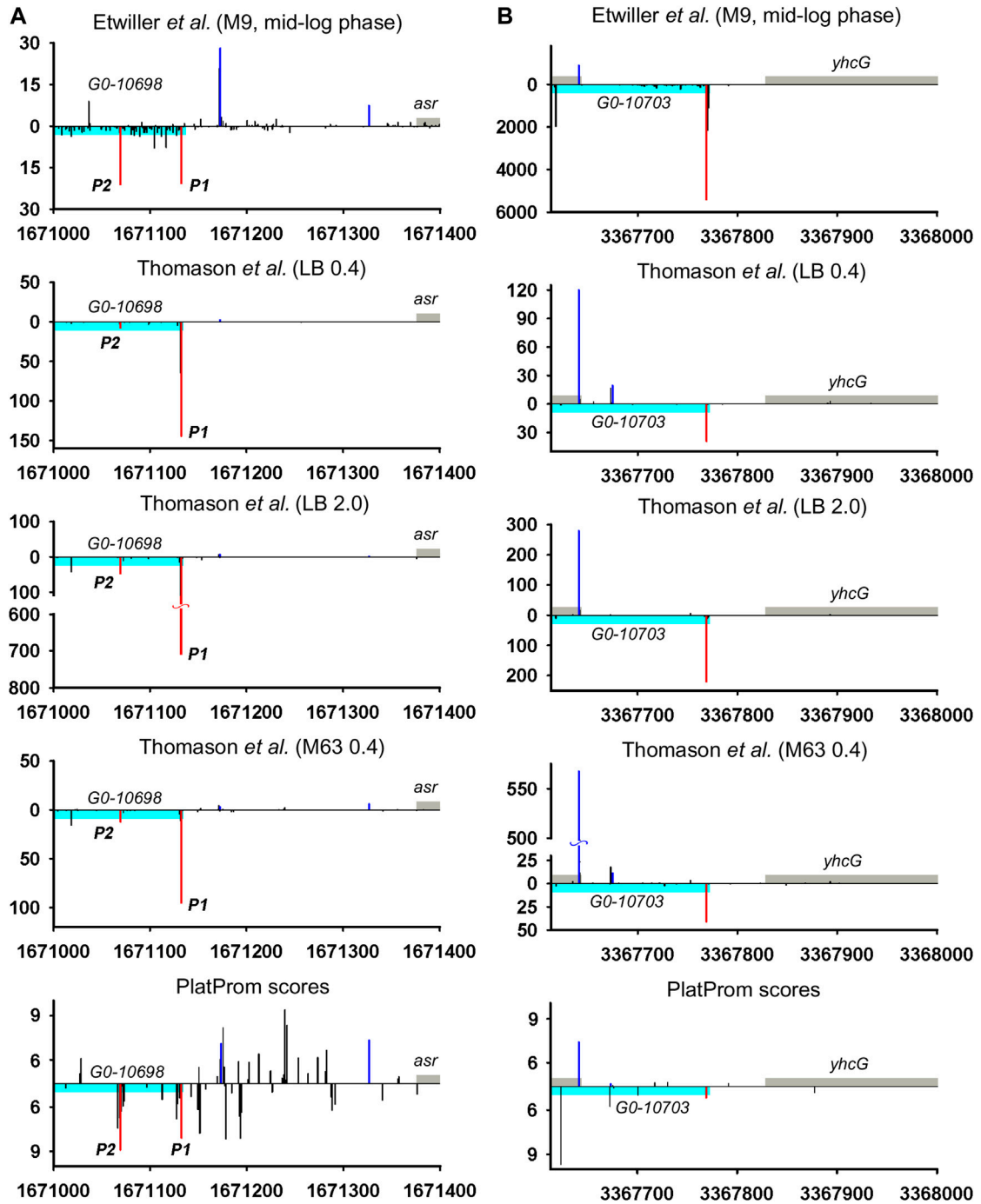

FIGURE 6 | Mapping of TSSs for divergent potential ncRNAs—G0-10698, G0-10703, G0-10702, and G0-10705 according to RNAseq data (Thomason et al., 2015; Ettwiller et al., 2016) and computational prediction (Shavkunov et al., 2009). X axis: coordinates in *E. coli* genome; Y axis: average number of normalized counts with perfect matching for given growth condition. For PlatProm predictions absolute score values are indicated on Y axis. RNA denoted according to the annotation in RegulonDB is shown in cyan; adjacent divergent gene is indicated in gray. Bars above and below X axis correspond to the upper and low DNA strands, respectively. Exactly matching TSSs for ncRNAs are presented in red and for divergently transcribed gene are shown in blue. Transcriptional landscapes upstream and downstream relatively to the genomic regions corresponding to G0-10698-*asr* and G0-10703- *yhc*G are shown in **Supplementary Figure S5**.

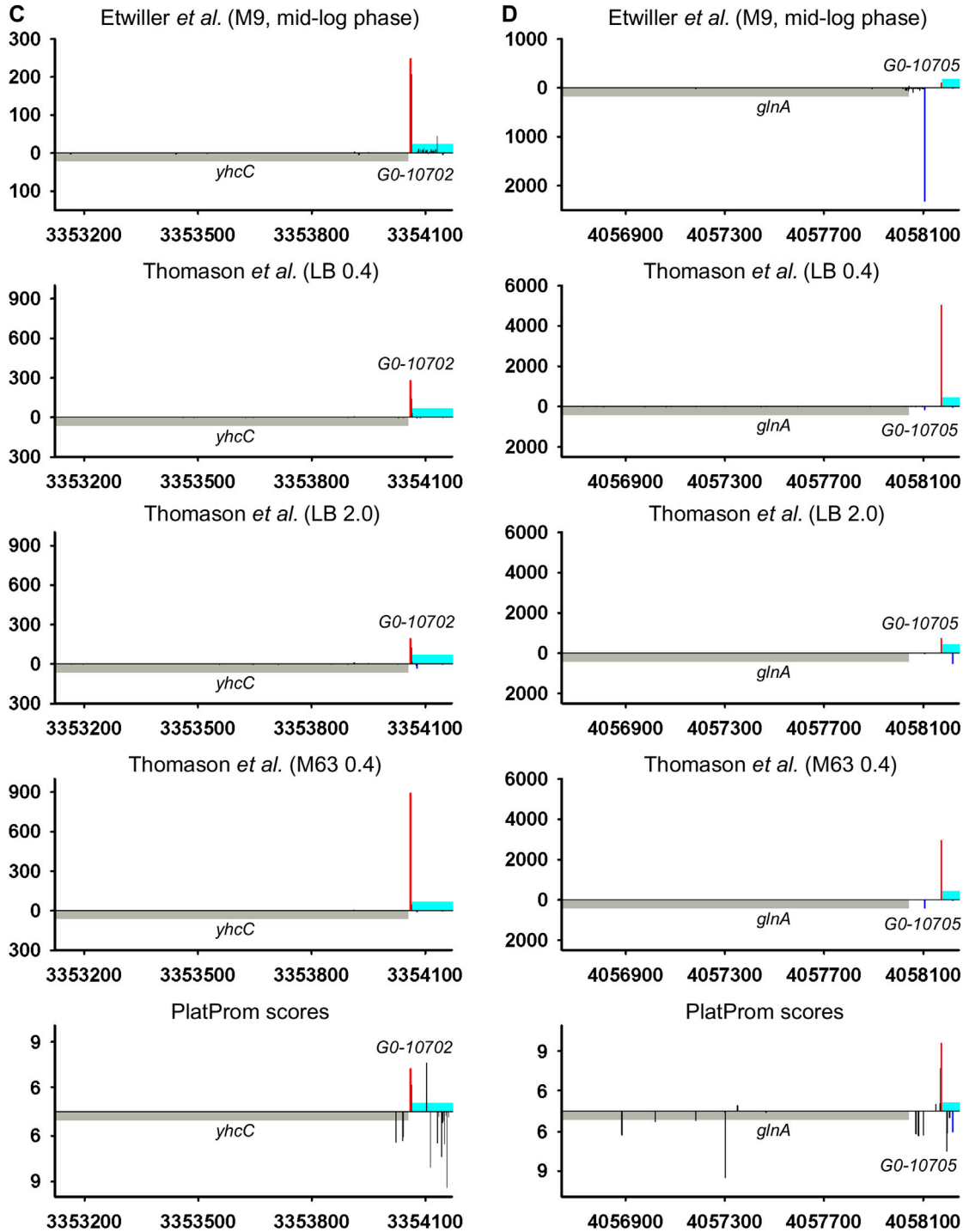

FIGURE 6 | (Continued).

ncRNAs Under the Question—Are They Really Transcribed or Not?

Hypothetical ncRNAs inferred from the data of Raghavan et al. (2011) so far remained as the candidates for the experimental validation and in 2019 were even excluded from EcoCyc database (Keseler et al., 2017) as lacking of sufficient experimental evidences of their expression. 5′-specific RNAseq (Thomason et al., 2015; Ettwiller et al., 2016) unambiguously confirmed the

TABLE 1 | Data used for TSSs mapping.

Accession numbers	Total number of reads after adapter trimming and sifting out of reads less than 16 bp in length	Number of reads perfectly matching the genome	Normalizing coefficient (N_{av}/N_i)
Ettwiller et al., 2016 (M9, mid-log phase)			
ERR930221	14.063,469	11,015,459	0.7322
ERR930222	9,184,197	5,116,134	1.5765
Thomason et al., 2015 (LB 0.4)			
SRR1173969	6,145,538	4886330	0.9927
SRR1173970	5,834,605	4,814,550	1.0075
Thomason et al., 2015 (LB 2.0)			
SRR1173974	5,627,281	3,341,088	1.3391
SRR1173978	6,967,456	5,072,554	0.8821
SRR1173979	7,691,759	5,861,466	0.7633
SRR1173980	6,214,631	3,621,841	1.2353
Thomason et al., 2015 (M63 0.4)			
SRR1173985	8,368,755	5,128,824	1.0292
SRR1173986	8,445,228	5,428,622	0.9724

transcription of four divergent potential ncRNAs—G0-10698, G0-10703, G0-10702, and G0-10705 (**Figure 6**; **Supplementary Figure S5**). Detected TSS in generals correspond to 5′ ends annotated in RegulonDB and are in perfect agreement with PlatProm predictions. Expression of these RNAs demonstrates clear dependence on growth phase, especially for G0-10698 and G0-10703 activated in stationary phase. G0-10703 RNA may be attributed as antisense transcript for *yhc*G gene with yet uncertain function whose expression follows from all sets of experimental data as well as from computational predictions (**Figure 6B**; **Supplementary Figure S5B**). G0-10698 and G0-10702 are conserved among *Enterobacteriaceae* (*E. coli, Shigella*, *Salmonella* sp. HNK130, *Salmonella* sp. S13, and *Enterobacter hormaechei* str. RHBSTW-00218). G0-10703 is found in some strains of *E. coli* and in *Salmonella* sp. HNK130, whereas G0-10705 is more widely spread among *E. coli, Shigella, Salmonella enterica*, *Salmonella* sp. HNK130, *Salmonella* sp. S13, *Enterobacter hormaechei* str. RHBSTW-00218, *Citrobacter rodentium* ICC168, and *Citrobacter* sp. RHB25-C09. Thus, undeservedly rejected divergently transcribed ncRNAs may regain their place in *E. coli* genome annotation.

DISCUSSION

High-throughput sequencing data provide a truly inexhaustible source for the deduction of new molecular relationships in microbial physiology. Mapping of additional TSSs in upstream regions of annotated ncRNAs not only contributes to our knowledge regarding the diversity of specious RNA produced from the same intergenic region, but also enforces us to reconsider functional attribution of certain ncRNAs. More than a half of divergently transcribed ncRNAs are present as a pair or triplet of collinear products transcribed from different TSSs what is consistent with the phenomenon of promoter duplication or multiplication well known for protein-coding genes (Huerta and Collado-Vides, 2003). Despite the role of RNAP "concentrator" additional promoters may provide optimal transcription processivity for ncRNAs according to the cooperation model proposed in Kim et al., 2019. The promoters of known ncRNAs often occur as a sequential array with separate TSSs providing the accumulation of ncRNAs of different lengths and potentially different specificities. The ratio of the activity of alternative promoters for ncRNA is not a stable characteristic and depends on growth conditions. In the case of *och*5 in mineral medium, all three promoters (P1, P2, and P3) demonstrate comparable activity, whereas in LB stationary phase P2 becomes the most active (**Figure 2A**; **Supplementary Figure S2A**). For REP-associated potential ncRNA in *ppc-arg*E intergenic region, synergistic effect of individual promoters seems to be rather probable (**Figure 5**; **Supplementary Figure S5**) although for *och*5 and *tff* (**Figure 2A,C**; **Supplementary Figures S2A,C**) cooperation between promoters for ncRNAs may interfere with transcription in opposite direction. It also cannot be excluded that less active promoters represent residual traces or, on the contrary, novel signs on the way of ncRNA selection. It is consistent with the observation that young ncRNAs usually are expressed with low efficiency if compared to evolutionary fixed ones (Kacharia et al., 2017).

Only 30 ncRNAs of 61 chosen as divergently transcribed examples accounting for their genomic context may be attributed as *bona fide* non-overlapped RNAs. The remaining 31 ncRNAs appeared to have TSS within coding part or 5′UTR of the adjacent gene rendering them as potential antisense regulators. Their expression may be subjected to the collision effects (Callen et al., 2004) resulting in substantial decrease in the level of ncRNA caused by convergent transcription. It is illustrated by the case of *oxy*R-*oxy*S pair when engagement of oxyR P2 promoter reduces the level of OxyS (**Figure 4**). We intended to outline correlation between transcriptional rate of true divergent ncRNAs and their counter-partners. However, the level of transcription of the opposite genes was often hardly detectable whereas ncRNA was rather abundant (*atl-ffs*, *yce*F-*sra*B, **Figure 2B,D**, *yhc*C-G0-10702, **Figure 6C**). The number of examples available from RNA-seq data and used here did not allow us to conclude that the proximity of highly expressed divergent ncRNAs with transcriptionally "sluggish" genes is

more a rule than an exception. Antagonistic rather than supporting effect of divergent transcription on the activity of model promoter mediated by excessive superhelical tension in intervening region was recently reported (Kim et al., 2019). One cannot exclude that this mechanism is implemented in the pairs "ncRNA/adjacent protein-coding gene" when active transcription of ncRNA suppresses the production of mRNA. The extent of mutual promoter interference should obviously depend on the distance between TSSs located on opposite DNA strands, which in the case of true divergent ncRNAs varies in the range from 7 to 290 bp with a median value of 84 bp.

One of the noteworthy observations is that two essential ncRNAs expressed from strong single promoters, Ffs and SraB, appeared to be longer and shorter correspondently than it was previously assumed. The exact nucleotide sequence of RNA, accounting for the position of TSS, is important for the formation of its secondary structure, which is recognized by target molecules. For Ffs, addition of stem-loop structure at 5′end may serve a hallmark for enzymatic degradation. It is confirmed by the finding that Ffs-derivative protruding upstream from the annotated TSP was detected in intracellular RNA fraction indicating the presence of the extended precursor (Alikina et al., 2018). SraB presumed to start from the position 1,146,589 on plus strand (NC_000913.3) that overlaps with early translated region of *yce*F and is likely to be initiated 60 bp downstream. The refined position of TSS was reproduced for all data sets used in our analysis and was also supported by computational prediction (**Figure 2D**). The exact length of SraB was discussed when it was detected for the first time and the presence of shortened 105 bp product was also mentioned (Argaman et al., 2001). At least seven ncRNAs are likely to wait for rescaling of their size and re-drawing folding pattern. Focusing here on divergently encoded *E. coli* ncRNAs, we did not focus on collinear regulatory RNAs, for which new boundaries can also be established and, accordingly, new functions and ways for the regulation of their expression can be proposed.

METHODS

Raw data available from Thomason et al. (2015) and Ettwiller et al. (2016) (**Table 1**) were used for the mapping of 5′ ends of transcripts on the genome *E. coli* K-12 str. MG1655 (NC_000913.3). Data processing was carried out in the following stages: 1) 3′-terminal adapter sequence (AAAAAAAAAA–in Thomason et al., 2015; AGATCGGAAGA–in Ettwiller et al., 2016) was cut off; 2) sequences less than 16 bp in length were removed from the whole massive of reads, and residual reads were mapped using bowtie2, generating sam-file1 (Langmead and Salzberg, 2012), with parameter L 16; 3) resulting sam-file1 was used for the extraction of reads perfectly matching the genome (only those containing both labels XM:i:0 and NM:i:0 were selected) generating sam-file2; 4) sam-file2 was converted into bam-format using SAMtools (Li et al., 2009), and the same program was used for the sorting of bam-files; 5) distribution of 5′ ends along both DNA strands was obtained using BEDtools (Quinlan and Hall, 2010). The number of 5′ ends for given position in the genome was normalized using coefficient calculated as ratio of the average number of perfectly matching reads in a series of experiments (N_{av}) to the number of perfectly matching reads in given experiment (N_i). The data shown in **Figure 2** (2 S), **Figure 4** (4 S), **Figure 5**, **Figure 6** (5 S), and **Supplementary Figure S1** represent an average number of normalized counts corresponding to two biological replicates of Ettwiller et al. (2016), two biological replicates for LB OD_{600} = 0.4 (Thomason et al., 2015), 4 biological replicates for LB OD_{600} = 2.0 (Thomason et al., 2015), and two biological replicates for M63 OD_{600} = 0.4 (Thomason et al., 2015). Accession numbers of data used in this study are given in **Table 1**.

DATA AVAILABILITY STATEMENT

Publicly available datasets (from Thomason et al., 2015; Etwiller et al., 2016) were analyzed in this study. This data can be found in European Nucleotide Archive (ERR930221, ERR930222) and NCBI Sequence Read Archive (SRR1173969, SRR1173970, SRR1173974, SRR1173978, SRR1173979, SRR1173980, SRR1173985, SRR1173986).

AUTHOR CONTRIBUTIONS

IM was responsible for writing the manuscript; SK for transcriptome data processing and writing the manuscript; NM for transcriptome data processing.

FUNDING

This work was supported by the Russian Science Foundation under grant number 18-14-00348.

SUPPLEMENTARY MATERIAL

The Supplementary Material for this article can be found online at: https://www.frontiersin.org/articles/10.3389/fmolb.2021.610453/full#supplementary-material.

REFERENCES

Adams, P. P., and Storz, G. (2020). Prevalence of small base-pairing RNAs derived from diverse genomic loci. *Biochim. Biophys. Acta Gene Regul. Mech.* 1863, 194524. doi:10.1016/j.bbagrm.2020.194524

Alikina, O. V., Glazunova, O. A., Bykov, A. A., Kiselev, S. S., Tutukina, M. N., Shavkunov, K. S., et al. (2018). A cohabiting bacterium alters the spectrum of short RNAs secreted by *Escherichia coli*. *FEMS Microbiol. Lett.* 365 (24). doi:10.1093/femsle/fny262

Altuvia, S. (2007). Identification of bacterial small non-coding RNAs: experimental approaches. *Curr. Opin. Microbiol.* 10, 257–261. doi:10.1016/j.mib.2007.05.003

Altuvia, S., Weinstein-Fischer, D., Zhang, A., Postow, L., and Storz, G. (1997). A small, stable RNA induced by oxidative stress: role as a pleiotropic regulator and antimutator. *Cell* 90, 43–53. doi:10.1016/s0092-8674(00)80312-8

Antal, M., Bordeau, V., Douchin, V., and Felden, B. (2005). A small bacterial RNA regulates a putative ABC transporter. *J. Biol. Chem.* 280, 7901–7908. doi:10.1074/jbc.M413071200

Argaman, L., Hershberg, R., Vogel, J., Bejerano, G., Wagner, E. G. H., Margalit, H., et al. (2001). Novel small RNA-encoding genes in the intergenic regions of *Escherichia coli*. *Curr. Biol.* 11, 941–950. doi:10.1016/s0960-9822(01)00270-6

Backofen, R., and Hess, W. R. (2010). Computational prediction of sRNAs and their targets in bacteria. *RNA Biol.* 7, 33–42. doi:10.4161/rna.7.1.10655

Barquist, L., and Vogel, J. (2015). Accelerating discovery and functional analysis of small RNAs with new technologies. *Annu. Rev. Genet.* 49, 367–394. doi:10.1146/annurev-genet-112414-054804

Brantl, S. (2007). Regulatory mechanisms employed by cis-encoded antisense RNAs. *Curr. Opin. Microbiol.* 10, 102–109. doi:10.1016/j.mib.2007.03.012

Bryant, J. A., Sellars, L. E., Busby, S. J., and Lee, D. J. (2014). Chromosome position effects on gene expression in *Escherichia coli* K-12. *Nucleic Acids Res.* 42, 11383–11392. doi:10.1093/nar/gku828

Callen, B. P., Shearwin, K. E., and Egan, J. B. (2004). Transcriptional interference between convergent promoters caused by elongation over the promoter. *Mol. Cell* 14, 647–656. doi:10.1016/j.molcel.2004.05.010

Carrier, M. C., Lalaouna, D., and Massé, E. (2018). Broadening the definition of bacterial small RNAs: characteristics and mechanisms of action. *Annu. Rev. Microbiol.* 72, 141–161. doi:10.1146/annurev-micro-090817-062607

Dar, D., and Sorek, R. (2018). Bacterial noncoding RNAs excised from within protein-coding transcripts. *mBio*, 9, e01730–18. doi:10.1128/mBio.01730-18

Dorman, C. J. (2019). DNA supercoiling and transcription in bacteria: a two-way street. *BMC Mol. Cell Biol.* 20, 26. doi:10.1186/s12860-019-0211-6

Dover, N., and Padan, E. (2001). Transcription of *nha*A, the main Na^+/H^+ antiporter of *Escherichia coli*, is regulated by Na(+) and growth phase. *J. Bacteriol.* 183, 644–653. doi:10.1128/JB.183.2.644-653.2001

Dutcher, H. A., and Raghavan, R. (2018). Origin, evolution, and loss of bacterial small RNAs. *Microbiol. Spectrum* 6 (2), 10. doi:10.1128/microbiolspec.RWR-0004-2017

Dutta, T., and Srivastava, S. (2018). Small RNA-mediated regulation in bacteria: a growing palette of diverse mechanisms. *Gene* 656, 60–72. doi:10.1016/j.gene.2018.02.068

Espéli, O., Moulin, L., and Boccard, F. (2001). Transcription attenuation associated with bacterial repetitive extragenic BIME elements. *J. Mol. Biol.* 314, 375–386. doi:10.1006/jmbi.2001.5150

Ettwiller, L., Buswell, J., Yigit, E., and Schildkraut, I. (2016). A novel enrichment strategy reveals unprecedented number of novel transcription start sites at single base resolution in a model prokaryote and the gut microbiome. *BMC Genom.* 17, 199–210. doi:10.1186/s12864-016-2539-z

Ghosal, A. (2018). Secreted bacterial RNA: an unexplored avenue. *FEMS Microbiol. Lett.* 365. doi:10.1093/femsle/fny036

Ghosal, A., Upadhyaya, B. B., Fritz, J. V., Heintz-Buschart, A., Desai, M. S., Yusuf, D., et al. (2015). The extracellular RNA complement of *Escherichia coli*. *MicrobiologyOpen* 4, 252–266. doi:10.1002/mbo3.235

Gourse, R. L., Gaal, T., Bartlett, M. S., Appleman, J. A., and Ross, W. (1996). rRNA transcription and growth rate-dependent regulation of ribosome synthesis in *Escherichia coli*. *Annu. Rev. Microbiol.* 50, 645–677. doi:10.1146/annurev.micro.50.1.645

Higgins, C. F., McLaren, R. S., and Newbury, S. F. (1988). Repetitive extragenic palindromic sequences, mRNA stability and gene expression: evolution by gene conversion? a review. *Gene* 72, 3–14. doi:10.1016/0378-1119(88)90122-9

Hör, J., Matera, G., Vogel, J., Gottesman, S., and Storz, G. (2020). Trans-acting small RNAs and their effects on gene expression in *Escherichia coli* and *Salmonella enterica*. *EcoSal Plus*. doi:10.1128/ecosalplus.ESP-0030-2019

Huerta, A. M., and Collado-Vides, J. (2003). Sigma70 Promoters in *Escherichia coli*: specific transcription in dense regions of overlapping promoter-like signals. *J. Mol. Biol.* 333, 261–278. doi:10.1016/j.jmb.2003.07.017

Jiang, H., Cao, M., Cao, X., Gu, H., and Zeng, K. (2010). [sRNA (sraB) regulate the resistant ability of *Salmonella enterica* serovar enteritidis to egg albumen]. *Wei Sheng Wu Xue Bao* 50, 1537–1544. doi:10.13343/j.cnki.wsxb.2010.11.017

Jose, B. R., Gardner, P. P., and Barquist, L. (2019). Transcriptional noise and exaptation as sources for bacterial sRNAs. *Biochem. Soc. Trans.* 47, 527–539. doi:10.1042/BST20180171

Kacharia, F. R., Millar, J. A., and Raghavan, R. (2017). Emergence of new sRNAs in enteric bacteria is associated with low expression and rapid evolution. *J. Mol. Evol.* 84, 204–213. doi:10.1007/s00239-017-9793-9

Kawano, M., Reynolds, A. A., Miranda-Rios, J., and Storz, G. (2005). Detection of 5'- and 3'-UTR-derived small RNAs and cis-encoded antisense RNAs in *Escherichia coli*. *Nucleic Acids Res.* 33, 1040–1050. doi:10.1093/nar/gki256

Keseler, I. M., Mackie, A., Santos-Zavaleta, A., Billington, R., Bonavides-Martínez, C., Caspi, R., et al. (2017). The EcoCyc database: reflecting new knowledge about *Escherichia coli* K-12. *Nucleic Acids Res.* 45, D543–D550. doi:10.1093/nar/gkw1003

Kim, S., Beltran, B., Irnov, I., and Jacobs-Wagner, C. (2019). Long-distance cooperative and antagonistic RNA polymerase dynamics via DNA supercoiling. *Cell* 179, 106–119.e16. doi:10.1016/j.cell.2019.08.033

Langmead, B., and Salzberg, S. (2012). Fast gapped-read alignment with bowtie 2. *Nat. Methods* 9, 357–359. doi:10.1038/nmeth.1923

Li, H., Handsaker, B., Wysoker, A., Fennell, T., Ruan, J., Homer, N., et al. (2009). The sequence alignment/map format and SAMtools. *Bioinformatics* 25, 2078–2079. doi:10.1093/bioinformatics/btp352

Liang, W., Rudd, K. E., and Deutscher, M. P. (2015). A role for REP sequences in regulating translation. *Mol. Cell* 58, 431–439. doi:10.1016/j.molcel.2015.03.019

Lim, H. M., Lewis, D. E., Lee, H. J., Liu, M., and Adhya, S. (2003). Effect of varying the supercoiling of DNA on transcription and its regulation. *Biochemistry* 42, 10718–10725. doi:10.1021/bi030110t

Lindgreen, S., Umu, S. U., Lai, A. S., Eldai, H., Liu, W., McGimpsey, S., et al. (2014). Robust identification of noncoding RNA from transcriptomes requires phylogenetically-informed sampling. *PLoS Comput. Biol.* 10, e1003907. doi:10.1371/journal.pcbi.1003907

Liu, W., Rochat, T., Toffano-Nioche, C., Le Lam, T. N., Bouloc, P., and Morvan, C. (2018). Assessment of *bona fide* sRNAs in *Staphylococcus aureus*. *Front. Microbiol.* 9, 228. doi:10.3389/fmicb.2018.00228

Malabirade, A., Habier, J., Heintz-Buschart, A., May, P., Godet, J., Halder, R., et al. (2018). The RNA complement of outer membrane vesicles from *Salmonella enterica* serovar Typhimurium under distinct culture conditions. *Front. Microbiol.* 9 (9), 2015. doi:10.3389/fmicb.2018.02015

Markelova, N. Yu., Masulis, I. S., and Ozoline, O. N. (2016). REP-elements of the *Escherichia coli* genome and transcription signals: positional and functional analysis. *Mat. Biolog. Bioinform.* 11 (Issue Suppl), 1–14. doi:10.17537/2016.11.t1

Masulis, I. S., Babaeva, Z. Sh., Chernyshov, S. V., and Ozoline, O. N. (2015). Visualizing the activity of *Escherichia coli* divergent promoters and probing their dependence on superhelical density using dual-colour fluorescent reporter vector. *Sci. Rep.* 5, 11449. doi:10.1038/srep11449

Mihailovic, M. K., Vazquez-Anderson, J., Li, Y., Fry, V., Vimalathas, P., Herrera, D., et al. (2018). High-throughput *in vivo* mapping of RNA accessible interfaces to identify functional sRNA binding sites. *Nat. Commun.* 9, 4084. doi:10.1038/s41467-018-06207-z

Peer, A., and Margalit, H. (2014). Evolutionary patterns of *Escherichia coli* small RNAs and their regulatory interactions. *RNA* 20, 994–1003. doi:10.1261/rna.043133.113

Peter, B. J., Arsuaga, J., Breier, A. M., Khodursky, A. B., Brown, P. O., and Cozzarelli, N. R. (2004). Genomic transcriptional response to loss of chromosomal supercoiling in *Escherichia coli*. *Genome Biol.* 5, R87. doi:10.1186/gb-2004-5-11-r87

Peterson, J. M., and Phillips, G. J. (2008). Characterization of conserved bases in 4.5S RNA of *Escherichia coli* by construction of new F' factors. *J. Bacteriol.* 190, 7709–7718. doi:10.1128/JB.00995-08

Qian, Z., and Adhya, S. (2017). DNA repeat sequences: diversity and versatility of functions. *Curr. Genet.* 63, 411–416. doi:10.1007/s00294-016-0654-7

Quinlan, A. R., and Hall, I. M. (2010). BEDTools: a flexible suite of utilities for comparing genomic features. *Bioinformatics* 26, 841–842. doi:10.1093/bioinformatics/btq033

Raghavan, R., Groisman, E. A., and Ochman, H. (2011). Genome-wide detection of novel regulatory RNAs in *E. coli*. *Genome Res.* 21, 1487–1497. doi:10.1101/gr.119370.110

Ramachandran, V. K., Shearer, N., and Thompson, A. (2014). The primary transcriptome of *Salmonella enterica* Serovar Typhimurium and its dependence on ppGpp during late stationary phase. *PloS One* 9 (3), e92690. doi:10.1371/journal.pone.0092690/

Rangarajan, A. A., and Schnetz, K. (2018). Interference of transcription across H-NS binding sites and repression by H-NS. *Mol. Microbiol.* 108, 226–239. doi:10.1111/mmi.13926

Reuter, J. S., and Mathews, D. H. (2010). RNAstructure: software for RNA secondary structure prediction and analysis. *BMC Bioinformatics* 11, 129. doi:10.1186/1471-2105-11-129

Santos-Zavaleta, A., Salgado, H., Gama-Castro, S., Sánchez-Pérez, M., Gómez-Romero, L., Ledezma-Tejeida, D., et al. (2019). RegulonDB v 10.5: tackling challenges to unify classic and high throughput knowledge of gene regulation in *E. coli* K-12. *Nucleic Acids Res.* 47 (D1), D212–D220. doi:10.1093/nar/gky1077

Scholz, S. A., Diao, R., Wolfe, M. B., Fivenson, E. M., Lin, X. N., and Freddolino, P. L. (2019). High-resolution mapping of the *Escherichia coli* chromosome reveals positions of high and low transcription. *Cell Syst.* 8, 212–225.e9. doi:10.1016/j.cels.2019.02.004

Shavkunov, K. S., Masulis, I. S., Tutukina, M. N., Deev, A. A., and Ozoline, O. N. (2009). Gains and unexpected lessons from genome-scale promoter mapping. *Nucleic Acids Res.* 37, 4919–4931. doi:10.1093/nar/gkp490

Shinhara, A., Matsui, M., Hiraoka, K., Nomura, W., Hirano, R., Nakahigashi, K., et al. (2011). Deep sequencing reveals as-yet-undiscovered small RNAs in *Escherichia coli*. *BMC Genom.* 12, 428. doi:10.1186/1471-2164-12-428

Stern, M. J., Ames, G. F., Smith, N. H., Robinson, E. C., and Higgins, C. F. (1984). Repetitive extragenic palindromic sequences: a major component of the bacterial genome. *Cell* 37, 1015–1026. doi:10.1016/0092-8674(84)90436-7

Thomason, M. K., Bischler, T., Eisenbart, S. K., Förstner, K. U., Zhang, A., Herbig, A., et al. (2015). Global transcriptional start site mapping using differential RNA sequencing reveals novel antisense RNAs in *Escherichia coli*. *J. Bacteriol.* 197, 18–28. doi:10.1128/JB.02096-14

Thorpe, H. A., Bayliss, S. C., Hurst, L. D., and Feil, E. J. (2017). Comparative analyses of selection operating on nontranslated intergenic regions of diverse bacterial species. Genetics. 206, 363–376. doi:10.1534/genetics.116.195784

Tobes, R., and Ramos, J. L. (2005). REP code: defining bacterial identity in extragenic space. *Environ. Microbiol.* 7, 225–228. doi:10.1111/j.1462-2920.2004.00704.x

Tsai, C. H., Liao, R., Chou, B., Palumbo, M., and Contreras, L. M. (2015). Genome-wide analyses in bacteria show small-RNA enrichment for long and conserved intergenic regions. *J. Bacteriol.* 197, 40–50. doi:10.1128/JB.02359-14

Vincent, H. A., Phillips, J. O., Henderson, C. A., Roberts, A. J., Stone, C. M., Mardle, C. E., et al. (2013). An improved method for surface immobilisation of RNA: application to small non-coding RNA-mRNA pairing. *PLoS One* 8 (11), e79142. doi:10.1371/journal.pone.0079142

Vogel, J., and Wagner, E. G. (2007). Target identification of small noncoding RNAs in bacteria. *Curr. Opin. Microbiol.* 10, 262–270. doi:10.1016/j.mib.2007.06.001

Wachter, S., Raghavan, R., Wachter, J., and Minnick, M. F. (2018). Identification of novel MITEs (miniature inverted-repeat transposable elements) in *Coxiella burnetii*: implications for protein and small RNA evolution. *BMC Genomics* 19, 247. doi:10.1186/s12864-018-4608-y

Waters, L. S., and Storz, G. (2009). Regulatory RNAs in bacteria. *Cell* 136, 615–628. doi:10.1016/j.cell.2009.01.043

Wu, H. Y., Shyy, S. H., Wang, J. C., and Liu, L. F. (1988). Transcription generates positively and negatively supercoiled domains in the template. *Cell* 53, 433–440. doi:10.1016/0092-8674(88)90163-8

Zhi, J., Mathew, E., and Freundlich, M. (1998). *In vitro* and *in vivo* characterization of three major *dad*AX promoters in *Escherichia coli* that are regulated by cyclic AMP-CRP and Lrp. *Mol. Gen. Genet.* 258, 442–447. doi:10.1007/s004380050754

Zhi, X., Dages, S., Dages, K., Liu, Y., Hua, Z. C., Makemson, J., et al. (2017). Transient and dynamic DNA supercoiling potently stimulates the leu-500 promoter in *Escherichia coli*. *J. Biol. Chem.* 292, 14566–14575. doi:10.1074/jbc.M117.794628

Conflict of Interest: The authors declare that the research was conducted in the absence of any commercial or financial relationships that could be construed as a potential conflict of interest.

frontiers in Molecular Biosciences

ORIGINAL RESEARCH
published: 15 April 2021
doi: 10.3389/fmolb.2021.609979

Suppression of *Escherichia coli* Growth Dynamics via RNAs Secreted by Competing Bacteria

Natalia Markelova[1], *Olga Glazunova*[1], *Olga Alikina*[1], *Valeriy Panyukov*[2,3], *Konstantin Shavkunov*[1,2] *and Olga Ozoline*[1,2]*

[1] *Laboratory of Functional Genomics and Cellular Stress, Institute of Cell Biophysics of the Russian Academy of Sciences, Pushchino Scientific Center for Biological Research of the Russian Academy of Sciences, Pushchino, Russia,* [2] *Department of Structural and Functional Genomics, Pushchino Scientific Center for Biological Research of the Russian Academy of Sciences, Pushchino, Russia,* [3] *Laboratory of Bioinformatics, Institute of Mathematical Problems of Biology, Pushchino, Russia*

With the discovery of secreted RNAs, it has become apparent that the biological role of regulatory oligonucleotides likely goes beyond the borders of individual cells. However, the mechanisms of their action are still comprehended only in general terms and mainly for eukaryotic microRNAs, which can interfere with mRNAs even in distant recipient cells. It has recently become clear that bacterial cells lacking interference systems can also respond to eukaryotic microRNAs that have targets in their genomes. However, the question of whether bacteria can perceive information transmitted by oligonucleotides secreted by other prokaryotes remained open. Here we evaluated the fraction of short RNAs secreted by *Escherichia coli* during individual and mixed growth with *Rhodospirillum rubrum or Prevotella copri*, and found that in the presence of other bacteria *E. coli* tends to excrete oligonucleotides homologous to alien genomes. Based on this observation, we selected four RNAs secreted by either *R. rubrum* or *P. copri*, together with one *E. coli*-specific oligonucleotide. Both fragments of *R. rubrum* 23S-RNA suppressed the growth of *E. coli*. Of the two fragments secreted by *P. copri*, one abolished the stimulatory effect of *E. coli* RNA derived from the 3′-UTR of ProA mRNA, while the other inhibited bacterial growth only in the double-stranded state with complementary RNA. The ability of two RNAs secreted by cohabiting bacteria to enter *E. coli* cells was demonstrated using confocal microscopy. Since selected *E. coli*-specific RNA also affected the growth of this bacterium, we conclude that bacterial RNAs can participate in inter- and intraspecies signaling.

Keywords: secreted RNAs, RNA-mediated bacterial communications, transcription, *Prevotella copri*, *Rhodospirillum rubrum*, 5′/3′-specific RNA-Seq

OPEN ACCESS

Edited by:
Elsa Zacco,
Italian Institute of Technology (IIT), Italy

Reviewed by:
Natalia Sanchez De Groot,
Universitat Autònoma de Barcelona, Spain
Akira Ishihama,
Hosei University, Japan
Dipankar Chatterji,
Indian Institute of Science (IISc), India

***Correspondence:**
Olga Ozoline
ozoline@rambler.ru

Specialty section:
This article was submitted to Protein and RNA Networks, a section of the journal Frontiers in Molecular Biosciences

Received: *24 September 2020*
Accepted: *11 March 2021*
Published: *15 April 2021*

Citation:
Markelova N, Glazunova O, Alikina O, Panyukov V, Shavkunov K and Ozoline O (2021) Suppression of Escherichia coli Growth Dynamics via RNAs Secreted by Competing Bacteria. Front. Mol. Biosci. 8:609979. doi: 10.3389/fmolb.2021.609979

INTRODUCTION

High-throughput sequencing techniques have provided a favorable environment for cellular transcriptome characterization and a much deeper investigation of the RNA world (Forde and O'Toole, 2013; Kukurba and Montgomery, 2015). A great many of transcripts with poorly studied or unobvious functions have been identified in all types of organisms, and the diversity of their roles raises numerous questions in terms of structure and function to be addressed (Chen and Conn, 2017; Leighton and Bredy, 2018; Rosace et al., 2020). For instance, in eukaryotes particular

non-coding RNAs (ncRNAs) are known to mediate epigenetic modifications (Castel and Martienssen, 2013), are involved in chromatin remodeling (Nozawa et al., 2017) and participate in the DNA damage response (d'Adda di Fagagna, 2014). Yet, it is not clear how crucial RNA molecules are in these processes. Comprehensively studied systems of higher organisms employing microRNAs (21−25 nt in length) for mRNAs degradation (Miyoshi et al., 2016; Nakanishi, 2016) have not been registered in prokaryotes so far, though bacteria possess single-stranded RNAs sized 15-26 nt (Lee and Hong, 2012; Kang et al., 2013; Bloch et al., 2017). The unique CRISPR-Cas systems of prokaryotes can be considered as functional analogs of eukaryotic small interfering RNAs (siRNAs), mediating protection of the cells against viruses and mobile genetic elements (Obbard et al., 2009; Levanova and Poranen, 2018). Using different mechanisms, both of them rely on RNA sequence specificity.

Many cellular oligonucleotides are products of endonuclease cleavage (Davis and Waldor, 2007; Papenfort et al., 2009; Chao et al., 2017), and some short fragments of tRNAs are proven to be functional (Lalaouna et al., 2015a,b; Diebel et al., 2016; Swiatowy and Jagodziński, 2018). In recent years it has been also witnessed for both bacteria and higher organisms that 3′-terminal regions of mRNAs can also be sources of short regulatory RNAs specifically processed by RNAse E (Eisenhardt et al., 2018; Miyakoshi et al., 2019; Hoyos et al., 2020; Wang et al., 2020). Thus, it is likely that the processing of many RNAs with well-established function plays a specific role in living cells by providing short oligonucleotides for diverse regulatory networks.

It is well-known that eukaryotic microRNAs are abundant in the blood, urine and other specimens (Beatty et al., 2014; Fritz et al., 2016; Wiegand et al., 2018; Yau et al., 2019), where they exhibit high stability (Mall et al., 2013; Glinge et al., 2017), in particular because of the protective effect of exosomes (Cheng et al., 2014). Similarly, prokaryotic small RNAs (exRNAs) have been identified in extracellular media (Ghosal et al., 2015; Blenkiron et al., 2016; Alikina et al., 2018), being protected from cleavage due to incorporation into outer membrane vesicles (Kulp et al., 2015; O'Donoghue and Krachler, 2016; Malabirade et al., 2018), or through complex formation with proteins. If excreted from the cells via vesicular transport, bacterial RNAs can be internalized into the cells of a host, leading to either upregulation (Mills, 2011; Abdullah et al., 2012) or suppression (Koeppen et al., 2016; Ahmadi Badi et al., 2020) of its innate immune system. The main mechanism ensuring discrimination of incoming alien tRNAs and rRNAs from domestic molecules resides on the activity of intracellular type 7 and 8 Toll-like receptors (TLRs) of eukaryotic cells, which recognize single-stranded oligonucleotides with typical for bacteria poly-U- and GU-tracks (Heil et al., 2004; Eigenbrod et al., 2015). TLR7 can be activated by different RNAs, while TLR8 senses fragments of 23S rRNA with UGG, UAA and UGA motifs (Krüger et al., 2015), as well as ultra-short oligonucleotides UG and UUG (Geyer et al., 2015). Unlike type 8 receptors, TLR7 are sensitive to ribose methylation in particular positions of tRNAs, which prevents the development of immune reaction to the host tRNAs (Kaiser et al., 2014; Jung et al., 2015). This exemplifies that existing under conditions of constant close interaction with microbes, eukaryotes have developed an elaborate system for fine and specific sensing of bacterial transcripts.

Microbes inhabiting the intestine are able to affect the spectrum of the host intracellular microRNAs, which in turn influence the expression of the host genes (Dalmasso et al., 2011). Vice versa, it has been demonstrated that synthetic copies of particular mouse/human microRNAs from epithelial cells added *in vitro* to the cultures of *Fusobacterium nucleatum* and *Escherichia coli* shape the expression of certain genes through formation of complementary duplexes, promoting bacterial growth (Liu et al., 2016). Moreover, the population of various microRNAs, produced by the gut epithelial cells has been proven to be critical in shaping the composition of the microbiome. Considering the discovery of Ago protein homologs (Willkomm et al., 2015) and the presence of RNase III family enzymes required for processing in bacteria (Bechhofer and Deutscher, 2019), it is reasonable to expect that prokaryotes are also able to "perceive" the RNA-encoded information from other bacteria. However, so far only the circumstantial evidence discussed above supports this possibility, and there are no model exRNAs that could be used for detailed studies. The main complication in conducting such studies is related to the short length of exRNAs, which requires special efforts to distinguish between RNAs secreted by each type of biological objects in mixed populations. Here we applied differential analysis to visualize changes in the RNA secretomes of *E. coli* in response to the presence of *P. copri* and *R. rubrum*. We also used sets of short oligonucleotides (*k*-mers, $k = 16$, 18, 20, or 22), either unique or common, in the genomes of *E. coli* and two model bacteria, to deduce which of them are predominantly secreted by *E. coli* in response to the presence of another bacterium. This allowed us to identify potentially active exRNAs and for the first time demonstrate the ability of their synthetic analogs to penetrate into *E. coli* cells and influence their growth.

MATERIALS AND METHODS

Bacterial Strains and Growth Conditions

RNA secretion was studied for a laboratory strain of *Escherichia coli* K12 MG1655 (*E. coli*). *Rhodospirillum rubrum* ATCC 11170 (*R. rubrum*) and *Prevotella copri* (*P. copri*) obtained from the DSMZ collection (DSM 467 and DSM 18205, respectively, https://www.dsmz.de/catalogs/parts/culture), were used only as representatives of intestinal microflora, capable of provoking an adaptive response of *E. coli*. Since *P. copri* is an obligate anaerobe, bacteria were grown at a low oxygen concentration (1−1.5%) in all experiments. To control the oxygen level before inoculation, resazurin (1 mg/l) was added to all media.

Oxygen was removed from culture media by gentle heating and rapid cooling in a flow of CO_2. Before cultivation, empty Hungate tubes were treated with a stream of N_2 gas for several minutes, after which they were filled with required volumes of media, again kept under N_2 flow for several minutes, immediately sealed and sterilized (121°C, 20 min). The pH of the medium was controlled before and after autoclaving. To prevent exRNAs

from degradation and favor conditions of rhodospirilla growth (Kaiser and Oelze, 1980), bacteria were cultured at 30°C. Cells were cultured for 8.5 h after inoculation, when the optical density of all individually grown cultures was approximately the same (**Supplementary Figure 2**). Bacterial cells were precipitated by centrifugation at 3,000 rpm (4°C), after which the required volume of supernatant was withdrawn with a syringe. In case when complete removal of cells was required, the medium was filtered twice using Millipore filters with a pore diameter of 0.22 μm and then used for RNA isolation.

Conditions for co-culturing were selected based on preliminary data obtained using a Synergy H1 Hybrid Multi-Mode Reader (BioTek Instruments, USA) with plastic 96-well suspension plates (TC Plate Well, Suspension, F; Sarstedt). Bacterial growth was initiated by inoculation according to the Hungate technique (Hungate, 1969; Wolfe, 1971) with stationary phase cultures (overnight growth for *E. coli* and 48-h cultivation for *P. copri* and *R. rubrum*). The cultures were inoculated anaerobically in 10 ml medium. *E. coli* inoculum was serially diluted and added in 250 μl volume so as to obtain the final dilution ratio of stationary phase cultures 1:2000 or 1:4000 (**Supplementary Figures 1**, **2**). The final ratios for *P. copri* and *R. rubrum* were 1:20 and 1:10, respectively, as chosen empirically between 1:10, 1:20, and 1:50 to obtain approximately the same optical density in individual cultures at the time point of harvesting (OD_{600} = 0.4). Inoculum volumes in these cases varied from 1 ml to 200 μl. Following inoculation, 0.2 ml of prepared cultures were pipetted in the plate wells for incubation in the reader. Examples of dynamic curves for individual and mixed cultures grown in parallel at 30°C are shown in **Supplementary Figure 2**.

Since *R. rubrum* cannot grow on M9 mineral medium [KH_2PO_4-3 g/l, Na_2HPO_4−6 g/l, NaCl−0.5 g/l, NH_4Cl−1 g/l, L-cysteine 0.04 g/l, D-glucose−0.5%, 2 mM $MgSO_4$, $CaCl_2$−0.1 mM (pH = 7.0)], three other media were tested to obtain a comparable growth rate for model bacteria (**Supplementary Figure 1**). Schaedler Anaerobe Broth (Oxoid CM0497) provided a highly efficient growth of all strains (**Supplementary Figure 1A**). However, in addition to mineral components [glucose−5 g/l, cysteine HCl−0.4 g/l, hemin−0.01 g/l, 0.75 g/l Tris buffer (pH 7.6 at 25°C)], and commonly used nutrients (peptone−5 g/l, yeast extract−5 g/l), this broth also contains 10 g/l of Tryptone Soya Broth (Oxoid CM129), which adds plant nucleic acids to the set of contaminating molecules.

Supplement of 0.01 g/l hemin required for prevotella and 0.3% glucose to a very complex medium optimized for rhodospirilla (yeast extract−0.3 g/l; Na_2-succinate−1 g/l; NH_4-acetate−0.5 g/l; 0.1% solution of Fe(III) citrate−5 ml/l; KH_2PO_4-0.5 g/l; $MgSO_4$ x 7 H_2O−0.4 g/l; NaCl−0.4 g/l; NH_4Cl−0.4 g/l; $CaCl_2$ x 2 H_2O−0.05 g/l; 0.01% solution of vitamin B12–0.4 ml/l; L-cysteine chloride−0.3 g/l; 0.1% resazurin−0.5 ml/l; Trace element solution SL-6–1 ml/l. Composition of SL-6: $ZnSO_4$ x 7 H_2O−0.1 g/l; $MnCl_2$ x 4 H_2O−0.03g/l; H_3BO_3-0.3 g/l; $CoCl_2$ x 6 H_2O−0.2 g/l; $CuCl_2$ x 2 H_2O−0.01g/l; $NiCl_2$ x 6 H_2O−0.02 g/l; Na_2MoO_4 x 2 H_2O−0.03 g/l, pH = 6.8) allowed to obtain a comparable growth rate for all the three strains (**Supplementary Figure 1B**). However, the dynamics of growth was very slow, which increased the risk of accumulation of RNA degradation products. Therefore, we used modified Luria-Bertani broth (LB), containing peptone (10 g/l); yeast extract (0.5 g/l); NaCl (10 g/l); L-cysteine HCl (1 g/l); and resazurin (1 mg/l), as a reasonable compromise between a high growth yield and a low level of impurities in the sample (**Supplementary Figure 1C**).

RNA Purification and Sequencing

Bacteria for RNA purification were grown in tightly closed Hungate tubes in 10 ml LB medium (pH=7.0) or LB medium pretreated with 5 M NaOH (**Table 1**). To control anaerobic state, all cultures were grown with 1 mg/l resazurin. To account for extraneous transcripts, fraction of short RNAs was extracted from LB medium using Qiagen miRNeasy Serum/Plasma kit (Qiagen, Germany) (sample LB_1_medium in **Table 1**). For sample LB_2_medium (**Table 1**), fraction of short RNAs was extracted from LB medium reversibly treated with 5M NaOH, as proposed by Pavankumar et al. (2012) using Qiagen miRNeasy Serum/Plasma kit (Qiagen, Germany). Intracellular RNAs were isolated from 0.5 ml cultures as described previously (Bykov et al., 2016; Alikina et al., 2018) with TRIzol RNA extraction reagent (Invitrogen, USA) and the sample was enriched for short RNAs using mirVana miRNA Isolation Kit (Ambion, USA). The concentration of RNA samples was estimated using Nanopore ND-1000 and Qubit 3 (Thermo Fisher Scientific, USA). For extraction of extracellular (secreted) RNAs, 1 ml of cultures were centrifuged for 15 min at 3,000 RCF, followed by supernatant filtration using a sterile syringe and two simultaneously mounted 0.22 mkm filters, followed by purification of short RNA fraction using Qiagen miRNeasy Serum/Plasma kit (Qiagen, Germany). A set of RNAs composed of those detected in either treated or untreated media was used to remove environment-attributed sequences from the resulting ensembles of sequence reads.

Libraries for sequencing were prepared using Ion Total RNA-Seq Kit v2 (Thermo Fisher Scientific, USA) according to the protocol of the manufacturer with modifications. MicroRNA samples were subjected to adapter ligation and reverse transcription according to the protocol, then cleaned using Monarch PCR & DNA Cleanup Kit (New England Biolabs, USA) and fractionated in 6% polyacrylamide gel with subsequent staining with ethidium bromide. Pieces of gel containing DNA fragments of required length (90-123 bp) were cut out, minced and eluted overnight in Elution Buffer from NEBNext Multiplex Small RNA Library Prep Set for Illumina (Set 1) (New England Biolabs). Then ammonium acetate (final concentration of 0.3 M) and linear acrylamide solutions were added to DNA-containing supernatant, followed by 2-h precipitation with absolute ethanol at −80°C and centrifugation at 15,000 RCF (−4°C). The pellet was washed with 80% ethanol, dried at RT for 5–10 min, dissolved in TE buffer from NEBNext Multiplex Small RNA Library Prep Set for Illumina (Set 1) and amplified according to the protocol for Ion Total RNA-Seq Kit v2. The sample was then purified using Nucleic Acid Binding Beads from Ion Total RNA-Seq Kit v2, dissolved in pre-warmed (37°C) nuclease-free water, assessed for concentration using Qubit 3, diluted to 100 pM and used for emulsion PCR on Ion OneTouch^{TM} 2 System with Ion PGM

TABLE 1 | Sequencing statistics of RNA samples.

Sample*	Number of reads		Notes
	Before QC	After QC	
First set (LB-medium without NaOH treatment)			
LB_1_medium	99,347	75,354	
Eco_out_1	1,677,610	1,484,046	RNAs secreted by *E. coli* in monoculture
Eco_Prevot_1	1,532,963	1,290,466	RNAs secreted by *E. coli* and *P. copri* in mixed population
Eco_Rhod_1	1,625,146	1,429,628	RNAs secreted by *E. coli* and *R. rubrum* in mixed population
Second set (LB-medium without NaOH treatment)			
Eco_out_2	1,168,144	846,669	RNAs secreted by *E. coli* in monoculture
Eco_Prevot_2	937,975	662,605	RNAs secreted by *E. coli* and *P. copri* in mixed population
Eco_Rhod_2	807,732	644,415	RNAs secreted by *E. coli* and *R. rubrum* in mixed population
Third set (NaOH treated LB)			
LB_2_medium	2,728,221	2,034,497	
Eco_in	1,320,485	299,167	Intracellular RNAs isolated from *E.coli* monoculture
Eco_Prevot_3	2,377,939	2,097,966	RNAs secreted by *E. coli* and *P. copri* in mixed population
Eco_Prevot_4	711,408	447,987	RNAs secreted by *E. coli* and *P. copri* in mixed population
Eco_Rhod_3	2,123,797	998,024	RNAs secreted by *E. coli* and *R. rubrum* in mixed population

**All sequence reads libraries are available at https://www.ncbi.nlm.nih.gov/bioproject/PRJNA687658).*

Hi-Q View OT2 Kit (Thermo Fisher Scientific). Sequence reads libraries obtained with Ion Torrent PGM analyzer (Thermo Fisher Scientific) are available in https://www.ncbi.nlm.nih.gov/bioproject/PRJNA687658.

Bioinformatic Analysis

The genomes of *E. coli* K12 MG1655 (Blattner et al., 1997) and *R. rubrum* ATCC 11170 (Munk et al., 2011) were taken from the NCBI RefSeq database (accession numbers NC_000913.3 and NC_007641, respectively). The genome of *Prevotella copri* DSM 18205 was obtained from NCBI GenBank (project NZ_ACBX00000000.2, direct submission). Sequence reads were quality filtered (QC) with Filter by Quality tool on Galaxy server (Afgan et al., 2016) using Q15 as the threshold level for nucleotides ($p < 0.036$) and requiring at least 90% presence of such nucleotides in reads. The obtained nucleotide sequences were sorted by size [12–50 nucleotides (n)] and fragments with sequences found in the LB medium were removed from the data sets. Filtered libraries were mapped onto the *E. coli* genome using Matcher algorithm (http://www.mathcell.ru/DnaRnaTools/Matcher.zip) as described previously (Panyukov et al., 2013; Antipov et al., 2017; Alikina et al., 2018). In brief: fragments of each size were evaluated separately, requiring precise matching to the genome. The sequences were assigned to the positions corresponding to the 5′-ends of reads mapped to the top strand of the genome and to the positions corresponding to the 3′-ends if reads were mapped to the bottom strand. Reads with multiple entries in the genome were assigned to all such sites in equal proportion.

The proportion of species-specific RNAs and oligonucleotides common to co-habiting bacteria in the fraction of secreted RNAs was estimated using *k*-mers present in the genome of *E. coli* and either absent or present in the genomes of the competing bacteria. Sets of *E. coli*-specific *k*-mers ($k = 16, 18, 20, 22$) were obtained with UniSeq software (Panyukov et al., 2017, 2020). Sets of common *k*-mers of the same length were collected using a simpler program that sorted all *k*-mers in lexicographic order and searched for those that have copies in the genome of comparison.

Functional Analysis of Selected Oligonucleotides

The candidate oligonucleotides were synthesized and purified by chromatography at Syntol (Russia). They were dissolved in sterile nuclease-free water to a concentration of 100 nmol (stock solution). Their effect was assessed in plastic 96-well suspension plates (TC Plate Well, Suspension, F; Sarstedt) using Synergy H1 Hybrid Multi-Mode Reader (BioTek Instruments, USA). Oligonucleotides were added to bacterial cultures inoculated at a ratio of 1:500 immediately before cultivation in M9 medium. This minimal medium, which supports sufficient growth rate of *E. coli*, was chosen for these functional tests so that to avoid possible interaction between the oligoribonucleotides studied and the inevitable transcripts from the components of rich media, such as yeast extract or peptone. In a pilot experiment carried out with rrs_{-115}, $_{C}$tRNA and ProA-ter, 1 and 2 nmol concentration of oligonucleotides was used. Having found a small dose dependence, we carried out all subsequent experiments with a concentration of 2 nmol, but all samples were used to assess the mean of the observed effects and SEM, because the dose dependence was smaller than the variation between different experiments. Growth dynamics were analyzed using GraphPad Prizm 5 software (Appling, 2008). The area under the growth curves was calculated and the ratio of the values obtained for the experimental and control samples was used as a characteristic for comparison.

Complementary Duplexes Annealing

Three complementary duplexes were prepared to compare the effects from single-stranded oligonucleotides and their double-stranded forms. They included duplexes of tRNA with $_{C}$tRNA, rrs_{-115} with $_{C}rrs_{-115}$ and ProA-ter with *rrl_Pr*. Oligonucleotides from stock solutions were mixed in equimolar concentrations (20 μl), melted and annealed in DTlite 4 Real-Time PCR System (DNA Technology, Russia) according to the following program: heating from RT at a rate of 1°C/0.8 min; melting for 5 min at 75.2°C in the case of tRNA/$_{C}$tRNA duplex and for 5 min at 56°C in the case of $rrs_{-115}/_{C}rrs_{-115}$ and ProA-ter/*rrl_Pr* duplexes; cooling to storage temperature (4°C) at a rate of 1°C/10 min. Single stranded oligonucleotides and their duplex were electrophoretically analyzed in 15% PAGE at 150V using 50+ bp DNA Ladder (Evrogen, Russia) as markers. Freshly

TABLE 2 | Numbers of unique and common *k*-mers in the genome of *E. coli* assessed pairwise with the genomes of *P. copri* and *R. rubrum*.

Type of sequences	$k = 16$	$k = 18$	$k = 20$	$k = 22$
	Number of *E. coli* unique *k*-mers			
Absent in *P. copri*	8,960,945	9,023,619	9,032,272	9,035,542
Absent in *R. rubrum*	8,931,481	9,018,843	9,030,542	9,034,516
	Number of *k*-mers present in the genomes of *E. coli* and competing bacteria			
Overlap with *P. copri*	28,748	2,854	676	376
Overlap with *R. rubrum*	53,512	6,942	2,298	1,360
	Number of *k*-mers present in all the three genomes			
Present in *E. coli*, *P. copri*, *R. rubrum*	778	366	286	222

prepared duplexes were added to the bacterial cultures to a final duplex concentration of 2 nmol.

Confocal Microscopy

E. coli K12 MG1655 cells were tested for the ability to uptake extraneous RNA molecules. Selected RNA molecules (*rrl*_2585 and *rrl*_Pr) were synthesized and labeled with Cy5 on the 3′-ends (Syntol, Russia). Cells were cultured in 0.5 ml of LB medium at 30°C, 32°C or 37°C for 4 h, 8.5 h or 17 h with shaking in the presence of individual Cy5-labeled oligoribonucleotides added to a final concentration of 10 μM at the moment of inoculation. Thirty minutes before the end of culturing, MitoTracker™ Green FM (Thermo Fisher Scientific, USA) was added (2 μM) to provide for cell membrane staining. Following incubation, cells were harvested by centrifugation at room temperature (2,500 RPM) and twice washed with sterile phosphate buffered saline (PBS) to reduce the background fluorescence. After that, pelleted cells were resuspended in 20–50 μl of melted 0.8% agarose; 10 μl of suspension was placed on glass slides and pressed by coverslips. Fluorescent confocal microscopy imaging was obtained on a Leica DMI 6000 CS microscope (Leica, Germany) with a TCS SP5 scanner (Leica, Germany) and LAS X Software (Leica, Germany) with excitation/emission at 640/690 nm and 500/550 nm for Cy5 and MitoTracker™ Green FM, respectively.

Statistics

SigmaStat one-sample *t*-test of SigmaPlot 6 software package was used to calculate SEM values for variables of single groups and the option "compare two groups" was applied to estimate *p*-values of differences (http://www.sigmaplot.co.uk/products/sigmaplot/statistics.php). The percentages of *E. coli*–specific *k*-mers and oligonucleotides with similar sequences in the genomes of *E. coli* and two competing bacteria were estimated for 16−, 18−, 20−, and 22−mers in 2−4 sequencing libraries listed in **Table 2** with subsequent averaging of 8−16 values. The functionality of the selected oligonucleotides was evaluated based on 3−9 growth experiments with three technical replicates in each. Deviations from control cultures that grew in M9 medium without model oligonucleotides were averaged for similar samples in the experiment and the average value between all experiments was used for comparison. The number of biological repeats is indicated in **Figure 3**.

RESULTS

P. copri and *R. rubrum* Affect the Profile of RNAs Secreted by *E. coli*

The main goal of the study was to find oligonucleotides that can affect population homeostasis of *E. coli*. Therefore, we used two bacteria from the human intestinal microbiome, *P. copri* and *R. rubrum* as natural partners of *E. coli* with presumably established RNA-mediated communication systems. According to the ENCODE project, *E. coli* is in antagonistic relationships with both bacteria, which, on the contrary, exhibit mutual symbiosis (Arumugam et al., 2011). The data of our growth experiments are consistent with both these conclusions, since the optical density in the mixed populations of *E. coli* + *P. copri* and *E. coli* + *R. rubrum* increased slower (**Supplementary Figures 2A,B**), while in the pair *P. copri* + *R. rubrum* faster (**Supplementary Figure 2C**) than expected, in the absence of mutual influence of bacterial cultures.

Nine experiments were carried out to collect RNAs secreted by *E. coli* in conditions of individual and mixed growth with each of the two model bacteria (**Table 1**). Only reads 12-50 nucleotides (n) long, precisely matching to the genome of *E. coli*, were taken into account (**Figure 1**). To avoid the contribution of oligonucleotides contaminating the LB environment, independently prepared samples LB_1_medium and LB_2_medium (**Table 1**) were sequenced. Reads from either of these two experiments were subtracted from all experimental libraries, including the set of intracellular RNAs. This procedure reduced the set of internal RNAs by only 10.1%, while the same filtration made for reads from extracellular samples excluded 78.1% of sequences from further analysis (statistical parameters indicated in **Figures 1A,B**). This difference in the degree of extraneous oligonucleotides in the extracellular and intracellular samples means that not every RNA molecule appeared in the medium from peptone or yeast extract can penetrate into bacterial cells.

Approximately 75% of intracellular RNAs were precisely mapped to the genome of *E. coli*, while in the case of external RNAs, this fraction was only 6.2% (statistical parameters in **Figures 1A,B**, respectively). Similar, albeit smaller in scale, losses were observed in extracellular samples obtained from cultures grown on M9 medium (Alikina et al., 2018). Therefore, the residual presence of environmental RNAs, which occasionally

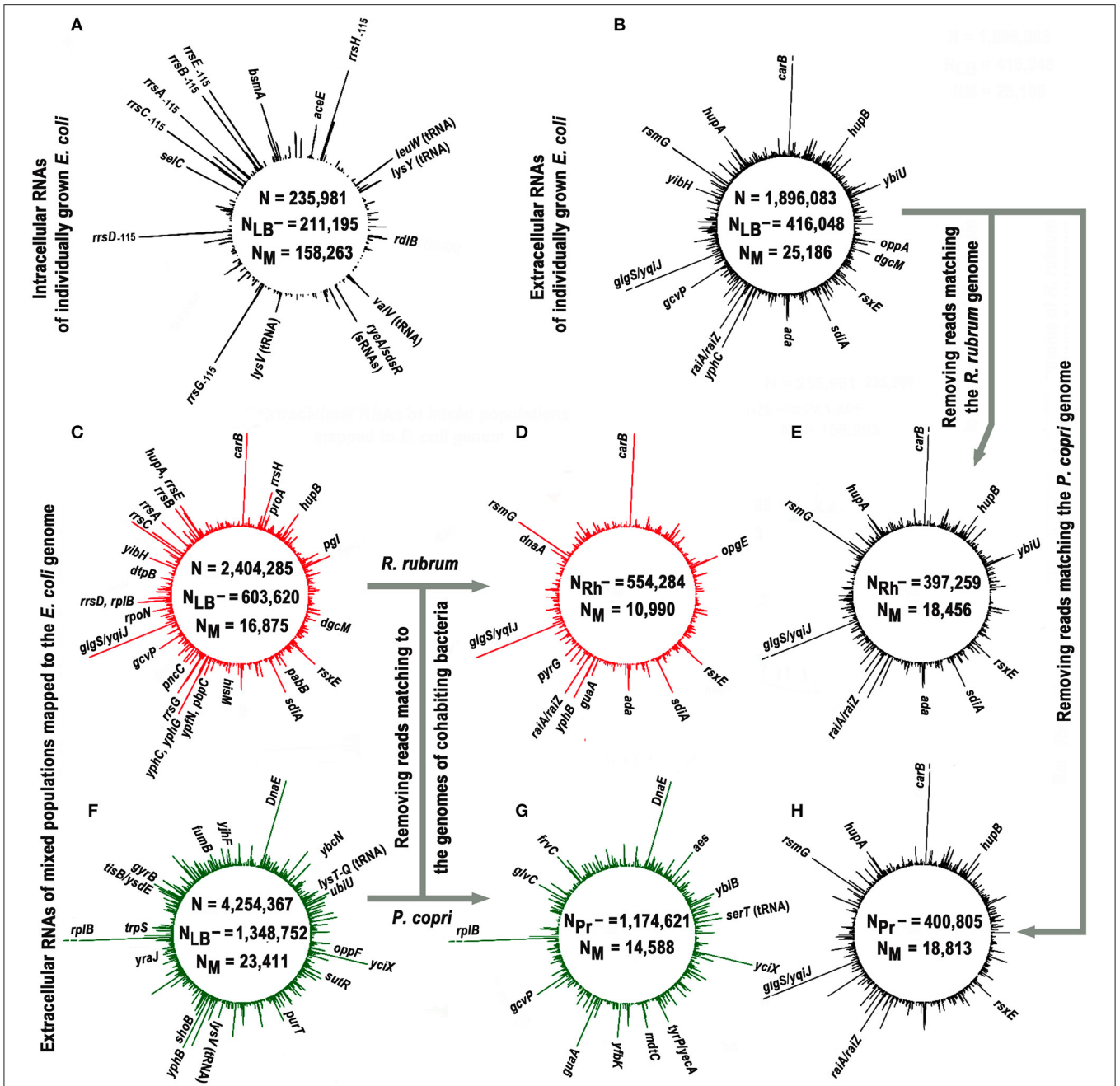

FIGURE 1 | Profiles of short intracellular and secreted (12–50 n) RNAs obtained in monoculture of *E. coli* (black plots) and in its mixed populations with *R. rubrum* (red plots) or *P. copri* (green plots) and mapped to the genome of *E. coli*. The profiles **(A,B)** show the genomic distribution of intracellular (experiment Eco_in) and external RNAs obtained in *E. coli* monocultures (pooled experiments Eco_out_1 and Eco_out_2), respectively. Values N, N_{LB-}, and N_M in all panels indicate the total number of 12–50 nucleotide reads that passed quality control; number of reads passed the filtering against LB-derived sequences and number of sequences mapped to the *E. coli* genome, respectively. The profiles **(C,F)** show distribution of exRNAs obtained from mixed populations (pooled libraries from three experiments Eco_Rhod_1–3 and four experiments Eco_Prevot_1–4). Profiles **(D,G)** show putative contribution of *E. coli* to the population of RNA molecules detected in mixed populations. They were obtained from the same sequence libraries as profiles **(C,F)** after all reads mapped to the genomes of *R. rubrum* and *P. copri* were removed, and highly represented RNA products that remained unchanged are indicated in these panels. The profiles **(E,H)** were plotted in the same way using the set of oligonucleotides profiled in **(B)**. The values N_{Rh-} and N_{Pr-} indicate the number of reads in combined libraries that do not match to the genomes of *R. rubrum* and *P. copri*, respectively. All profiles were drawn with DNAPlotter v. 1.3 (Carver et al., 2009) using a running window of 10 bp and a step size of 1 bp. The scale of such plots is automatically determined by the amplitude of the maximum peak. In profiles with exoRNAs they were equal to 239 **(B,E,H)**, 219 **(C,D),** and 264 **(F,G)** reads. Therefore, to obtain an equal resolution for other peaks in the profiles, the breaks were made at the level of 219 reads [indicated in **(B,E,H)** for similar products from the coding sequence of the *carB* gene and an intergenic space *glgS/yqiJ*, as well as for fragments of *rplB* aRNA in **(F,G)**].

escaped sequencing in our control samples, cannot fully explain the observed mapping deficit. Some of the losses are due to various modifications already found in exRNA, including polyadenylation or the addition of other non-template nucleotides to the 3′-ends (Alikina et al., 2018), but most of them are likely due to accidental ligation, since many of non-mapping oligonucleotides are chimeric. In any case, only 25,186 reads from the secreted fraction precisely matching to the *E. coli* genome were collected in two experiments with individually grown *E. coli* (Eco_out_1 and Eco_out_2 samples in **Table 1**) and were pooled for profiling (**Figure 1B**).

The profile turned out to be clearly different from the one shown in **Figure 1A**, which exemplifies the distribution of intracellular oligonucleotides over the genome (Eco_in sample in **Table 1**). Being consistent with our previously published data for *E. coli* MG1655 grown aerobically in M9 medium (Alikina et al., 2018) and the data obtained by other authors (Ghosal et al., 2015, Blenkiron et al., 2016), this difference is considered as an evidence of the nonrandom selection of RNAs for secretion. The largest contribution to the set of dominant intracellular oligonucleotides (**Figure 1A**; **Supplementary Table 1**) is given by RNA fragments originated from genes of tRNAs, 5S RNAs, and large ribosomal RNAs encoded by seven operons (65.8%), while 48.1% of dominant exRNAs were derived from mRNAs and 36.5% from antisense RNAs (**Figure 1B**; **Supplementary Table 2**). For instance, oligonucleotides from genes *carB*, *ybiU*, *oppA*, *sdiA*, *ada*, *yphC,* and *gcvP* are fragments of mRNAs; products from *yibH* corresponds to its 3′-UTR, while products marked as *hupB*, *dgcM*, *rsxE,* and *hupA* match the antisense strand of protein coding genes. As in the previous study (Alikina et al., 2018), most of the registered mRNA fragments can be products of RNase processing. Others can be transcribed as independent transcriptional units from intragenic/intergenic promoters predicted *in silico*, including multiple transcriptional start points (TSP) of promoter islands (PI) (indicated in **Supplementary Table 2**). Multiplicity of oligonucleotides corresponding to the antisense transcripts (aRNAs) among exRNAs is also in line with the previous data (Alikina et al., 2018). Approximately 42% of them have predicted promoters for transcription. Since in the intracellular fraction we found less than half of the aRNAs that are dominant outside, and only in single or several copies, it is likely that some of them are specifically produced for secretion. Based on this analysis, we chose an oligonucleotide from the leader sequence of 16S rRNAs (rrs_{-115} in **Figure 2A**) for experimental assessment. RNA products from this region of ribosomal operons formed seven peaks with a maximal amplitude in the profile of intracellular short RNAs (**Figure 1A**; **Supplementary Table 1**), but had more than 175-fold lower relative abundance in the fractions of exRNAs (**Figure 2A**). This dramatic decrease made the involvement of rrs_{-115} in cell-to-cell communications unlikely, but not excluded, and we checked this in growth experiments.

The search for RNAs involved in interspecies communication assumes the detection of specific changes in the spectrum of oligonucleotides secreted in the presence and absence of competing bacteria. **Figures 1C,F** show the profiles of exRNAs obtained from mixed populations with *R. rubrum* or *P. copri* and mapped to the genome of *E. coli*. Both obviously differ from the profile of *E. coli* extracellular RNAs shown in **Figure 1B**. For instance, many fragments of 16S rRNA, different from rrs_{-115}, which were detected only at the background level inside and outside of individually grown *E. coli* cells, became abundant in the presence of *R. rubrum* (**Figure 1C**; **Supplementary Table 3**). Likewise, the fragments of *yfbK* mRNA, *yciX* aRNA and transcripts from *tyrP*/*yecA* intergenic region, undetected at all in experiments with a pure culture of *E. coli,* were detected in a large amount in the presence of *P. copri* (**Figures 1F,G**, as well as **Supplementary Table 4**). Since secreted RNAs are short, with a preferable length in the range of about 16-25 nucleotides (Ghosal et al., 2015, Blenkiron et al., 2016; Alikina et al., 2018), many of them map to both genomes in mixed populations. Thus, some of new peaks that appeared in the dominant group in the presence of *R. rubrum* or *P. copri*, may be originated from the transcriptomes of cohabiting bacteria. In order to visualize the individual response of *E. coli* to the presence of competing bacteria, all reads mapped to the genomes of *R. rubrum* or *P. copri* were removed from the libraries obtained from the jointly grown cultures before alignment to the genome of *E. coli* (**Figures 1D,G**). For direct comparison, a similar procedure was performed for reads obtained from an individually grown population of *E. coli* (**Figures 1E,H**). The fourth column in **Supplementary Table 2**, containing a list of 104 genomic regions producing most abundant exRNAs, shows corresponding changes in their number, which in 46 regions remained unchanged, while the contribution given by 15 regions was affected by the removal of reads matching to both *R. rubrum* or *P. copri*. All of them belong to coding sequences that are homologous in different bacterial species.

The dominant peaks obtained in the pooled experiments Eco_Rhod_1, Eco_Rhod_2 and Eco_Rhod_3 (**Figure 1C**; **Supplementary Table 3**) coincide with 69 peaks of the RNA profile, secreted by *E. coli* only (**Figure 1B**; **Supplementary Table 2**). **Figure 1D** shows the profile obtained after all reads mapped to the *R. rubrum* genome had been removed from these sequence libraries. As a result, we did not observe a significant difference between the profiles of *E. coli*-specific RNAs secreted in the presence (**Figure 1D**) and absence (**Figure 1E**) of *R. rubrum*. The dependence on the presence of *P. copri* was more pronounced (**Figures 1G,H**). In this case, the dominant peaks obtained in the four pooled experiments Eco_Prev_1–4 (**Figure 1F**; **Supplementary Table 4**), coincide with only 35 peaks of the RNA profile in **Figure 1B**. However, the products of all but one of the remaining 69 genomic loci, at least at a low level, were found in the secretome of a pure *E. coli* population. Their large number, therefore, may be caused by induced synthesis in *E. coli* cells or enhanced secretion from them. For instance, the percentage of *dnaE* mRNA fragments, which were not dominant in pure culture and did not match to the genome of *P. copri*, increased by 17.5 times. The contribution of RNAs that are presumably synthesized from the promoter region of *yqiJ*, as well as the percentage of oligonucleotides produced from *atpI*/*rsmG* intergenic space, on the contrary, decreased by 27.0 and 2.3 times, respectively.

Since oligonucleotides from both these regions do not match the *P. copri* genome, this decrease is hardly explained by RNA interference. Among 26 oligonucleotides with an abundance of at least 0.2% in Eco_out samples, which can only be produced by *E. coli*, twenty were also abundant in the mixed population with *R. rubrum* but only eight retained a high level during co-cultivation with *P. copri*. Therefore, it is likely that *E. coli* established more RNA-mediated links with bacteria belonging to the dominant genera in the human gut, than with taxa less represented in this ecological niche.

In Mixed Populations Bacteria Tend to Secrete Oligonucleotides With Sequences Present in Both Genomes

The data in **Figure 1** show that the percentage of exRNAs mapped to the *E. coli* genome (N_M) in samples obtained from monocultures decreased from 6.1% (**Figure 1B**) to 4.6-4.7% (**Figures 1D,F**) after exclusion of reads corresponding to the genomes of *R. rubrum* or *P. copri*. However, in the sets obtained from mixed populations, the percentages of RNAs mapped to the genome of *E. coli* in the libraries filtered from *R. rubrum* (N_{Rh-}) and *P. copri* (N_{Pr-}) reads were only 1.98% (**Figure 1C**) and 1.24% (**Figure 1E**). In both cases this is lower than the expected two-fold decrease in mapping due to the presence of two bacteria in the sample. This indirectly indicated an increase in the percentage of identical sequences in the secretomes of co-cultured bacteria. Therefore, we collected all sequences with length k ($k = 16$, 18, 20 and 22 n), which at least once can be found in the genomes of cohabiting bacteria (*E. coli* and *P. copri* or *E. coli* and *R. rubrum*) and also used UniSeq algorithm to identify *k*-mers unique for *E. coli* in each pair. Their numbers with deleted copies from all 16 sets are indicated in **Table 2**.

It turned out that *E. coli* grown as a monoculture secretes mostly RNAs with sequences absent in the genomes of two other bacteria (**Figure 2B**, group 1). In the presence of *R. rubrum* the percentage of RNAs mapped to the genome of *E. coli* and absent in the genome of *P. copri* (cross-talk test) was nearly the same as in the monoculture (cyan bar in group 3). However, in the presence of *P. copri* the percentage of such RNAs was significantly lower (cyan bar in group 2). This is what to be expected, if in mixed populations bacteria tend to secrete *k*-mers with sequences present in both genomes. By contributing to the set of identical *k*-mers secreted by *E. coli* in monoculture, *P. copri* automatically reduces the percentage of *E. coli*-specific RNAs in the common secretome. Thus, it was not surprising that in the presence of *R. rubrum* the percentage of RNAs absent in its genome was also lower than in the monoculture of *E. coli* (magenta bar in group 3), although it was not essentially higher in the common secretome of *E. coli* + *P. copri* (magenta bar in group 2).

To characterize the changes in the presence of common *k*-mers in the fractions of exRNAs, we assessed their diversity, rather than multiplicity (**Figure 2C**) using eight sets of *k*-mers common for the genome pairs *E. coli*-*P. copri* and *E. coli*-*R. rubrum*. Their number is much lower than that of *E. coli*-specific *k*-mers (**Table 2**). Copies were removed from all the sets of 16, 18, 20, and 22 n long sequence reads found in the secreted fractions in each experiment and the percentage of common *k*-mers with the corresponding lengths in the resulting sets was estimated (**Figure 2C**). As a direct consequence of the greater number of identical *k*-mers in the *E. coli*-*R. rubrum* pair, as compared to the *E. coli*-*P. copri* pair (**Table 2**), the percentage of *k*-mers similar with *R. rubrum* was also higher in the *E. coli* monoculture (magenta bar in group 1, **Figure 2C**). It was the same in the mixed population of *E. coli* with *P. copri* (cross-talk test, group 2) but significantly ($p = 0.039$) greater in the mixed culture with *R. rubrum* (magenta bars in group 3). The same relative changes were observed for the identical *k*-mers in the genomes of *E. coli* and *P. copri*: their proportion remained at the monoculture level in the presence of *R. rubrum* (cross-talk test), but was more than twice increased in the presence of *P. copri* (cyan bars in **Figure 2C**). *K*-mers representation in all the three genomes (gray bars) was high and roughly corresponded to the percentage of identical *k*-mers with the lowest abundance. Their high number in the mixed population with *P. copri* explains the low percentage of *E. coli*-specific *k*-mers that are absent in *R. rubrum* (magenta bar in group 2 of **Figure 2B**).

By definition, this type of analysis is completely independent from the copy number of particular *k*-mers. Due to very low percentage of *k*-mers mapped to bacterial genomes from the total fraction of secreted RNAs (**Figures 1B–F**), it is also virtually independent from the contribution of *E. coli*-specific *k*-mers. Therefore, the data obtained indicate that in mixed populations bacteria tend to secrete oligonucleotides with sequences present in the genome of co-grown bacterium. Based on this observation, we selected additional samples for experimental assessment among such exRNAs.

Selection of Oligonucleotides for Experimental Verification

Only common 16, 18, 20 and 22 n long *k*-mers found in all experiments with mixed populations of a certain type and absent in any reads of the medium samples were taken for analysis. As a result, we had 11 oligonucleotides found in the *E. coli*-*R. rubrum* medium and 17 potential candidates revealed in the mixed *E. coli*-*P. copri* populations. Two exRNAs from the first set turned out to be 16S rRNA fragments, while all the others were derived from 23S rRNAs. Two of them, located 2,488 and 2,585 bp from the 5′-end of 23S rRNA molecules (samples *rrl*2488 and *rrl*2585 in **Figures 2A,E**) were selected for experimental testing. Only *rrl*2585 was detected in the secretome and intracellular transcriptome of *E. coli* and exhibited an increase in number in the presence of *R. rubrum* (**Figure 2A**). Located at a distance of 97 bp from each other in both genomes, the selected exRNAs belonged to the regions differing in seven base pairs. In mixed populations, all fragments containing those discriminatory nucleotides belonged to *R. rubrum* and are not among the dominant peaks listed in **Supplementary Table 3**.

Thirteen oligonucleotides from the second set were also processed from structured regions of ribosomal RNAs. Seven of them belong to 23S rRNA and six to 16S rRNA. Two oligonucleotides from 23S rRNA were found in both the common secretomes with *P. copri* and *R. rubrum*. According to

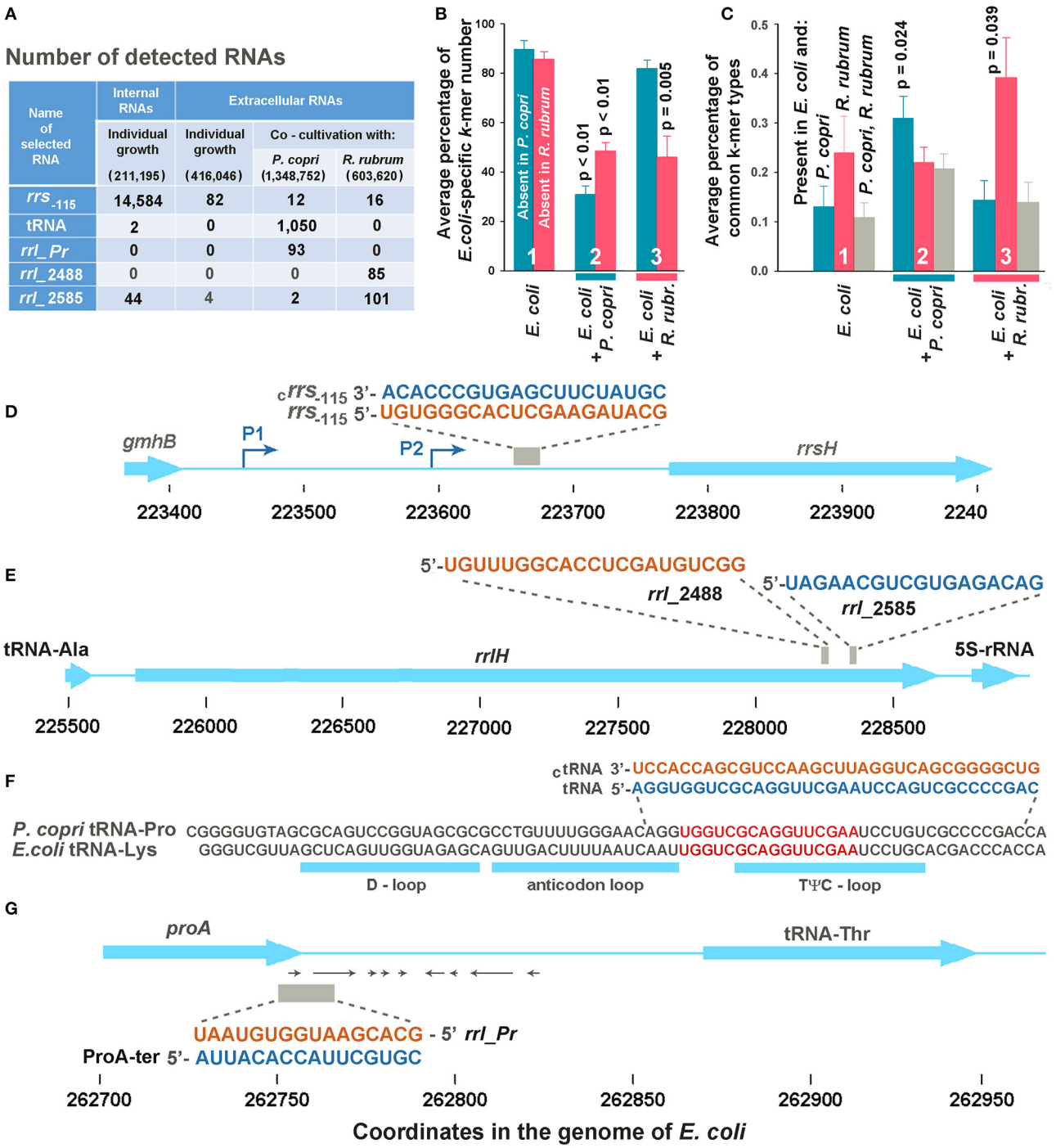

FIGURE 2 | Selection of potentially functional extracellular RNAs. **(A)** Total number of selected *k*-mers found in different RNA fractions in one (Eco_in sample in **Supplementary Table 1**), two (Eco_out samples 1 and 2), three (Eco_Rhod samples 1-3), and four (Eco_Prevot samples 1-4) experiments. Only reads with a length equal to or longer than the selected *k*-mers were taken into account, but reads with flanking sequences belonging to jointly grown bacteria were not ignored. The total number of reads after quality filtration is indicated in parenthesis. **(B)** Average percentage of *E. coli*-specific *k*-mers in reads mapped to the *E. coli* genome and absent in the genomes of *P. copri* (cyan bars) or *R. rubrum* (magenta bars). **(C)** Diversity of common *k*-mers found in different RNA fractions estimated as the percentage from the total number of *k*-mer types found in the secretomes. Statistical parameters in plots **(B,C)** were calculated for all the sets of *k*-mers obtained in mixed populations, compared with the sets of extracellular *k*-mers secreted by individually grown *E. coli*; however, *p*-values are indicated only for statistically significant changes. **(D,E)** Sequences of samples rrs_{-115}, *rrl*_2488 and *rrl*_2585 are identical in all seven ribosomal operons of *E. coli*. **(D,E)** Show them in the environment of the H operon. **(F)** Aligned sequences of *E. coli* tRNA-Lys (genes *lysT*, *lysW*, *lysY*, *lysZ*, *lysQ*, *lysV*) and *P. copri* tRNA-Pro with the indicated locations of tRNA loops. The selection of two 34-mer oligonucleotides, with flanking sequences from the *P. copri* genome, for experimental evaluation, was based on the presence of 16-mers printed in red. **(G)** Sequence and genomic location of ProA-ter sample transcribed in *E. coli* and its complementary fragment *rrl_pr* from 23S rRNA of *P. copri*. All oligonucleotide sequences are printed in colors corresponding to the color code used in **Figure 3**.

Name of selected RNA	Internal RNAs	Extracellular RNAs		
	Individual growth (211,195)	Individual growth (416,046)	Co - cultivation with:	
			P. copri (1,348,752)	*R. rubrum* (603,620)
rrs_{-115}	14,584	82	12	16
tRNA	2	0	1,050	0
rrl_Pr	0	0	93	0
rrl_2488	0	0	0	85
rrl_2585	44	4	2	101

discriminatory base pairs, both were predominantly produced by *P. copri*. Three of the other four exRNAs found almost exclusively in the mixed culture with *P. copri* were associated with tRNA genes. One of them corresponding to the TΨC-loop of the *E. coli* tRNA-Lys was selected for further experiments (**Figures 1F**, **2A,F**; **Supplementary Table 4**). According to Microbial Nucleotide BLAST, this sequence belongs to tRNA-Pro in the *P. copri* genome. Although the sample was selected based on the presence of 16-20-mers (red sequence in **Figure 2F**), many registered exRNAs were longer, and we used a *P. copri*-specific 34-mer molecule to test its possible functionality (tRNA sample).

Oligonucleotides *rrl_Pr* (**Figure 2G**) were found only in *E. coli-P. copri* secretomes (**Figure 2A**) and belong to the end of the prevotella 23S rRNA gene. In the *E. coli* genome, this sequence corresponds to the antisense strand of the *proA* gene in the region of the transcription terminator. We did not register *rrl_Pr* fragments either in the internal transcriptome of *E. coli* or in its secretome (**Figure 2A**), but inside the cells we found complementary fragments that could be cut from the 3′-UTR of ProA mRNA, where several secondary structures can be formed (shown by arrows in **Figure 2G**). Taking into account the regulatory potential of some 3′-UTR fragments, we selected both complementary oligonucleotides (*rrl_Pr* and ProA-ter) for experimental assessment.

A total of six samples were selected for further analysis. Fragments *rrl*_2488, *rrl*_2585, and tRNA have sequences present in the genomes of *E. coli* and the competing bacteria, and could appear in joint secretomes from different populations, but almost all RNAs containing discriminator nucleotides belonged to *R. rubrum* or *P. copri*, respectively. The ProA-ter sequence is present in the genomes of *E. coli* and *P. copri*, but can be produced only in *E. coli*, while their complementary sequences–only in *P. copri*. The last sample (rrs_{-115}) was selected mainly due to its intracellular abundance (**Figures 1A**, **2A**) and also as a potential agent for intraspecific signaling. It is transcribed from an intergenic space and has no sequence homology with the genomes of other model bacteria. Thus, we did not have an opportunity to test the physiological effects of analogs from other genomes.

Extracellular RNAs Can Alter the Dynamics of *Escherichia coli* Growth

To assess the dependence of the bacterial population on the presence of the selected oligonucleotides, only growth curves were analyzed in this study (**Figure 3**). Since in many cases the difference between the optical density of the experimental and control samples was time-dependent, we compared the areas under the recorded 24-h growth curves after subtracting the background level. The addition of *rrl*_2488 and *rrl*_2585 to the culturing medium significantly suppressed the growth of *E. coli* (**Figure 3A**). To our knowledge, this is the first experimental evidence indicating the dependence of *E. coli* growth on the presence of RNAs secreted by a competing bacterium.

No effect was observed for tRNA sample originated from the TΨC-loop of *P. copri* tRNA-Pro (beige bar in **Figure 3B**). However, complementary oligonucleotide $_{C}$tRNA demonstrated a well-pronounced inhibitory effect. Upon entering *E. coli* cells, this RNA can base pair with tRNA-Lys promoting its cleavage by double-stranded RNA-specific nucleases. Therefore, we tried to eliminate the inhibitory effect of $_{C}$tRNA by preparing its duplex with tRNA (**Figure 3C**). Electrophoretic fractionation of single-stranded oligonucleotides revealed a certain portion of duplexes even in their individual samples. This is most likely due to the presence of an inverted repeat in the central part of oligonucleotides. In tRNA, it can form a continuous 10 bp long double-stranded track (5′-GGUUCGAAUC-3′/5′-GGUUCGAAUC-3), and a 12 bp track with two gaps in $_{C}$tRNA (5′-GGaUUCGAAcCU-3′/5′-GGaUUCGAAcCU-3′). In the molten and annealed duplex, single-stranded oligonucleotides were virtually absent (**Figure 3C**), but the physiological effect was on average stronger compared to single-stranded $_{C}$tRNA, indicating that the tRNA/$_{C}$tRNA duplex may be involved in processes similar to RNA interference. The effect of double-stranded RNA on bacterial growth was previously documented only for microRNAs hsa-miR-515-5p and hsa-miR-1226-5p, but they promoted the cultures of *Fusobacterium nucleatum* and *E. coli*, respectively, rather than suppressed them (Liu et al., 2016). Therefore, the duplex tRNA/$_{C}$tRNA can be used as a model for a detailed study of the suppressor mechanism mediated by secreted RNAs.

The addition of *rrl_Pr* originated from the end of 23S RNA and secreted by *P. copri* also did not change the dynamics of *E. coli* growth (beige bar in **Figure 3D**), but ProA-ter, which can only be produced by *E. coli*, stimulated the growth of this bacterium (**Figure 3D**). Thus, it became clear, that *E. coli* endogenous exRNAs can affect the homeostasis of its population exhibiting an opposite effect compared to that registered for *rrl*_2488 and *rrl*_2585. Complementary duplex *rrl_Pr*/ProA-ter, on the contrary, reduced the growth of bacterium to 83.9 ± 10.1%, which statistically significantly differed from the effect rendered by ProA-ter. This can be interpreted as a suppression mediated by RNA secreted by *P. copri*. Considering the faint effect of ProA-ter, we tried to increase it by rising the cultivation temperature from 30°C, previously adjusted to *R. rubrum* growth, to 32°C. However, no significant difference was observed for *rrl_Pr* and ProA-ter, as well as *rrl*_2488, *rrl*_2585, tRNA and $_{C}$tRNA. Thus, the histograms in **Figures 3A,B,D** represent data averaged over all experiments.

The effect of rrs_{-115} sample, selected as a potential agent for intraspecies signaling, on the contrary, turned out to be temperature dependent. We observed a statistically significant decrease in the growth rate at 32°C (**Figure 3E**), which indicates that endogenous oligonucleotides can exert not only stimulating (**Figure 3D**), but also inhibitory effects. However, at 30°C the same affect was statistically insignificant. The influence of the complementary oligonucleotide $_{C}rrs_{-115}$, on the contrary, was well expressed only at 30°C (bar plot in **Figure 3E**), leading to a 26.1±6.6% increase in growth dynamics. Nearly the same effect from well-formed complementary $rrs_{-115}/_{C}rrs_{-115}$ duplex (**Figure 3F**) and a single stranded rrs_{-115}, may be even more important, since it indicates that the double-stranded state does not guarantee the highest effect.

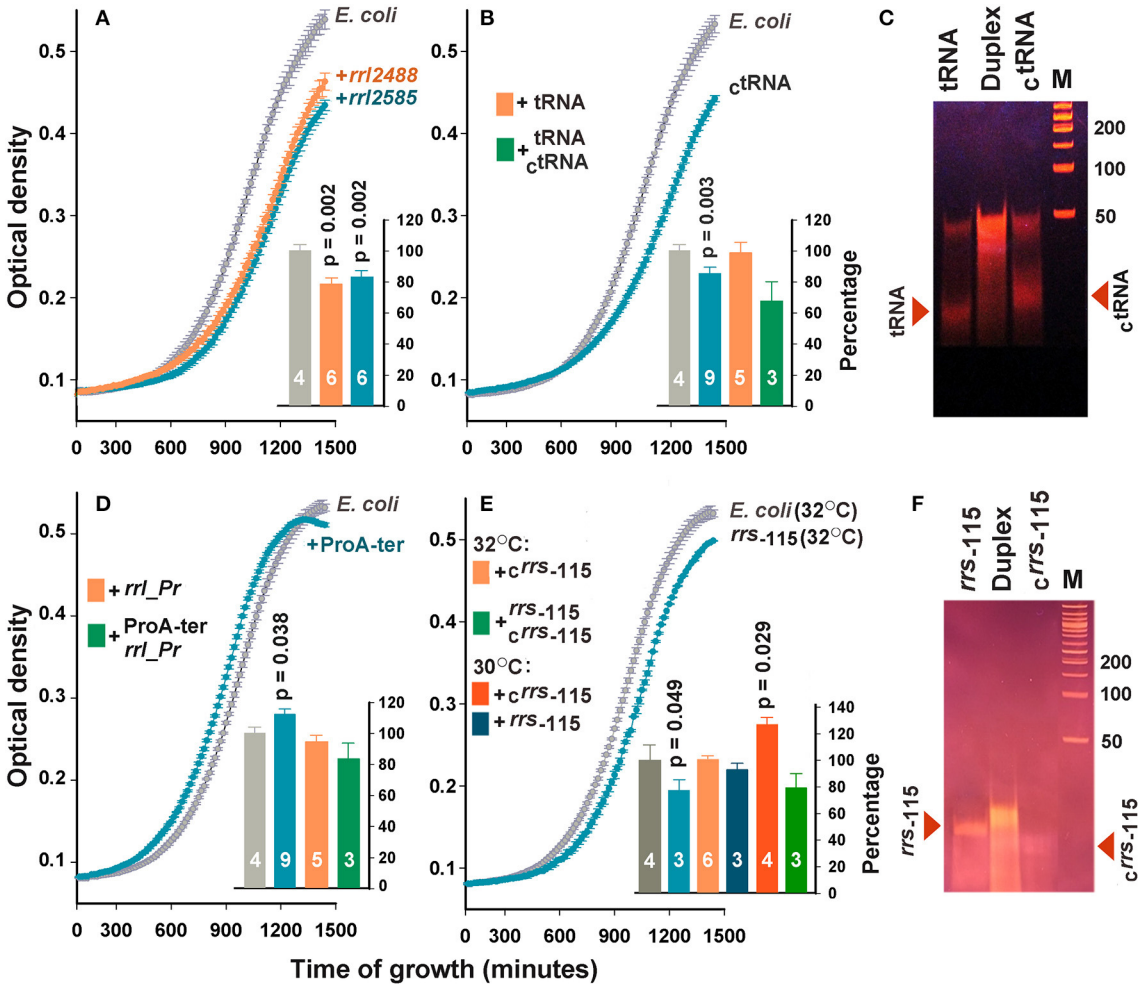

FIGURE 3 | Extracellular RNAs alter the growth dynamics of *E. coli*. Curves in the main plots of **(A,B,D,E)** illustrate the growth rate of *E. coli* in M9 medium at 32°C in the absence (gray plots) and presence (colored plots) of the selected oligonucleotides. The curves obtained in each experiment were averaged over three technical repeats. The number of biological replicates is indicated by white numbers on the columns. Examples of growth curves are shown only for samples with statistically significant effects. Bar plots summarize the results obtained in all experiments of the indicated type. For the samples in plots **(A,B,D)**, the data obtained at 30 and 32°C were pooled and averaged. For the samples rrs_{-115} and $_{c}rrs_{-115}$ **(E)**, the data obtained at different temperatures are shown independently. Error bars represent SEMs calculated for all biological replicates, *p*-values are indicated only in the cases of statistically significant differences from the control samples. Error bars for control samples (light and dark gray bars) show the variability in the growth rate of *E. coli*, estimated from all experiments carried out at 30 **(F)** and 32°C **(A,B,D)**. **(C,F)** illustrate the electrophoretic fractionation profiles of single-stranded oligonucleotides and their complementary duplexes, prepared as described in the section Materials and Methods.

RNAs Secreted by Co-Growing Bacteria Can Enter *E. coli* Cells

Though the observed physiological effects of extracellularly added synthetic oligonucleotides can theoretically be realized both inside and outside the cells, it is much easier to understand and to investigate the mechanisms of action of RNAs capable of penetrating into *E. coli* cells. Therefore, as a final step in this study, we evaluated the ability of two alien oligonucleotides to cross the membrane of *E. coli* cells.

The experiments were conducted using Cy5-labeled synthetic fragments of 23S rRNAs *rrl_2585*, produced by *E. coli* and *R. rubrum* (**Figures 2A,E**), and *rrl_Pr* transcribed only in *P. copri* (**Figures 2A,G**), since an identical sequence is found on an antisense strand in the terminator region of the *proA* gene (**Figures 2A,G**). In order to increase this species specificity of *rrl*_Pr, we extended its sequence by three bases at the 3′-end differing from the sequence in *E. coli* genome. The resulting sequence was 5′-GCACGAATGGTGTAATGAT-Cy5-3′ (5′-GCACGAATGGTGTAATCAC-3′in *E. coli* MG1655). The sequence of *rrl*_2585 was the same as indicated in **Figure 2**.

Bacterial culturing carried out in the presence of modified RNA probes at 37°C, 32°C, or 30°C testified that both molecules can penetrate into the cells, as registered by fluorescence confocal microscopy (**Figure 4**). The efficiency of MitoTracker™ Green staining done at the end of incubation period was approximately the same in all experiments. Yet, as expected,

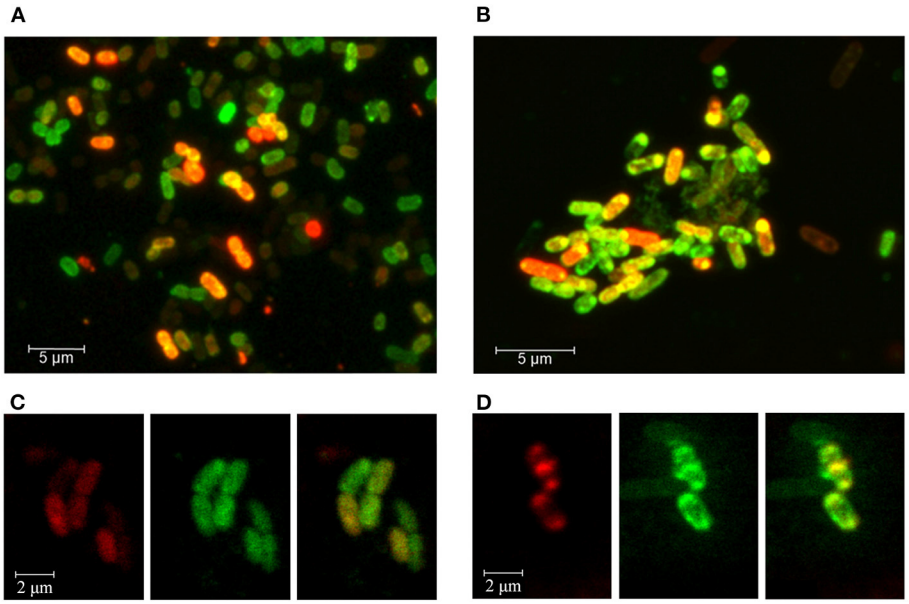

FIGURE 4 | Fluorescence confocal microscopy imaging of *E. coli* cells grown in the presence of Cy5-labeled oligoribonucleotides *rrl*_Pr of *P. copri* **(A,C)** and *rrl*_2585 of *R. rubrum* **(B,D)**. Bacterial cells were cultured for 17 h at 37°C **(A,B)** or 8.5 h at 32°C **(C,D)**. Cell membranes were stained with MitoTracker™ Green FM for 30 min prior to washing-off and microscopy. **(C,D)** are provided as individual fluorescence channels (left and middle blocks) and their superimposition (right blocks).

only part of the cells contained the oligonucleotides tested after 4, 8.5, or 17 h of incubation. Culturing at 37°C provided the highest intensity of Cy5 fluorescence (**Figures 4A,B**), possibly reflecting the more active physiological state of bacteria at this temperature. However, RNA probes also entered the cells at 32°C (**Figures 4C,D**), confirming the ability of *rrl*_2585 to affect the growth of *E. coli* (**Figure 3A**). Although the physiological effect from *rrl_Pr* was much less pronounced (**Figure 3D**), its intracellular accumulation was registered at approximately the same level, probably indicating a difference in the intracellular functioning of two model oligonucleotides. In any case, it became clear that *E. coli* cells can uptake single-stranded RNA molecules originating from other species and react on their presence in environment even if they are available in a free state. Although the potential mechanisms of their delivery and intracellular functioning remain a topic for further research, it is likely that the observed changes in growth dynamics cannot be explained by simple nutritional effects, since at least four of the eight single-stranded RNAs suppressed the growth of *E. coli*, and only two (ProA-ter and ${}_{c}rrs_{-115}$) exhibited notable stimulatory effects.

DISCUSSION

Although bacteria actively use small regulatory and antisense RNAs for adaptive managing of their transcriptomes, the regulatory potential of secreted oligonucleotides in establishing population homeostasis is still questionable. This is only partly due to the rather short history of research on exRNAs of bacteria and to the many problems associated with their short length and specific processing (Alikina et al., 2018). The main reason seems to reside in the absence of a model approach in formulating an idea of how an RNA-mediated signaling system can work in densely populated and highly heterogeneous natural communities of microorganisms. Based on the knowledge accumulated for eukaryotic microRNAs that massively circulate in the blood and can be delivered to target tissues, it is intuitively expected that RNA interference, involving certain bacterial analogs of Ago proteins and other components of RNA-induced silencing complexes, can function in bacterial communities. In this case, the presence of other bacteria should lead not only to the appearance of new RNAs in the common growth medium, but also to a decrease in the number of some exRNAs. This was indeed the case in our previous study, when the joint secretome of symbiotically grown *E. coli* and *P. bisonicum* was analyzed (Alikina et al., 2018) as well as in the present work, as testified by rigorous differential analysis performed for exRNAs of *E. coli* secreted in the presence of competing bacteria (**Figure 1**). Thus, the participation of extracellular RNAs in interference is expected, although a decrease in their abundance may occur due to a variety of other regulatory events taking place inside the bacterial cells or in the growth environment.

The main goal of our study was the search for oligonucleotides that can affect the homeostasis of the bacterial population if added extracellularly. Thus, at the first stage we tried to understand which category of secreted RNAs is more promising for identifying functional molecules. Since previously (Alikina et al., 2018) we noticed that the percentage of RNAs mapped to the genome of the co-habiting bacterium *P. bisonicum* is higher in the extracellular fraction compared to the intracellular content,

here we evaluated the distribution of *k*-mers, both unique and shared by different genomes, in secretomes depending on the co-grown bacteria. As expected, the percentage of unique *E. coli* exRNAs in the medium of both mixed populations decreased. Strongly opposing the possible assumption that the competing microbes provoke massive secretion of oligonucleotides intended for intraspecific signaling, this also provided indirect evidence in favor of the assumption that in response to the presence of other bacteria *E. coli* secretes oligonucleotides with sequences homologous to their genomes. The species-specific increase in the diversity of homologous RNAs secreted by *E. coli* in mixed population confirms this assumption and is probably one of the most important results of the work.

Based on this view, we considered 28 potential candidates and selected four samples from mixed secretomes for experimental verification. Having discovered a well-pronounced suppression of *E. coli* growth in the presence of *rrl*_2488 and *rrl*_2585 secreted by *R. rubrum*, we for the first time obtained two bacterial sequences, with poorly predictable mode of action due to the collinearity of functional molecules and their potential targets. The suppression mediated by artificial oligonucleotide $_{C}$tRNA, on the contrary, is easier understandable. Being complementary to tRNA-Pro of *P. copri*, $_{C}$tRNA can also base pair with tRNA-Lys of *E. coli*, promoting its cleavage by double-stranded RNA-specific nucleases. In this case, this complementary duplex with weakened base pairing is expected to be less efficient, which was not confirmed, possibly due to dependence of the result from some other molecular or cellular processes. For example, easier penetration of duplex RNAs into bacteria compared to single-stranded oligonucleotides can significantly contribute to the overall biological outcome.

The use of complementary oligonucleotides *rrl_Pr* and ProA-ter provide a chance to evaluate the biological effect of double stranded RNAs, which can be formed by natural molecules produced by two different bacteria. *E. coli* cells actually grew slower in the presence of *rrl_Pr*/ProA-ter duplex (**Figure 3D**), exemplifying the situation when oligonucleotide secreted by a competing bacterium (*rrl_Pr*) can inhibit the stimulatory effect given by an *E. coli*-specific RNA product (ProA-ter). Given the negative impact of all three duplexes tested (**Figures 3B,D,E**) it may be prudent to pay attention to secreted oligonucleotides that can form double-stranded RNAs due to their transcription from convergent promoters or processing from stem-loop structures.

Such situation is exemplified by the rrs_{-115} sample, which is derived from the leader sequences of all seven 16S rRNAs of *E. coli*, transcribed from two well-characterized promoters located 286 and 178 bp upstream of the 5′-end of rRNA genes. The 5′-end of the rrs_{-115} fragment is designated in RegulonDB as a potential transcription start site (TSS) due to its identification in 5′-specific RNA-seq libraries (Santos-Zavaleta et al., 2019; http://regulondb.ccg.unam.mx/index.jsp). However, since there are no promoter-like sequences for this TSS (see, for example PlatProm promoter finder web site http://mathcell.ru/model6.php?l=en, Shavkunov et al., 2009), it is likely that this fragment is a product of RNase processing. Moreover, four potential TSSs were predicted on the opposite strand 16, 34, 48 and 74 bp downstream of the 5′-end of rrs_{-115}, and transcripts from P_{34} and P_{74} were found in bacterial cells. Therefore, $_{C}rrs_{-115}$, is also a natural component of the bacterial transcriptome and can be involved in intraspecies signaling.

Thus, using a simple strategy, we identified at least five RNAs (*rrl*_2488, *rrl*_2585, proA-ter, rrs_{-115} and $_{C}rrs_{-115}$) that are produced by bacterial cells and can affect their growth if added extracellularly. Using confocal microscopy, we confirmed the ability of two single-stranded oligonucleotides to penetrate into bacterial cells and anticipate that they retain functionality as it has been demonstrated for eukaryotic microRNAs uptaken by bacterial cells. We also received a large amount of *a priori* unexpected information, such as the low level of intracellular transcriptome contamination from the environment, the functionality of double-stranded RNAs, and the possibility of narrow range temperature dependence for the registered effects. They will definitely come in handy for further research in this area.

DATA AVAILABILITY STATEMENT

All sequence reads libraries are available at: https://www.ncbi.nlm.nih.gov/bioproject/PRJNA687658.

AUTHOR CONTRIBUTIONS

Bacteria were grown and growth curves were obtained by NM and OA. RNAs were isolated and sequenced by OG, KS and OA. Bioinformatic analysis was done by VP and OO, manuscript preparation for publishing was mostly done by OO with a contribution of co-authors. All authors contributed to the article and approved the submitted version.

FUNDING

The study was supported by the Russian Science Foundation (Grant No. 18-14-00348).

ACKNOWLEDGMENTS

The authors are grateful to Sergei Kiselev for preparing the sets of unique for *E. coli* *k*-mers and the sets of *k*-mers of the common use with *R. rubrum* and *P. copri*.

SUPPLEMENTARY MATERIAL

The Supplementary Material for this article can be found online at: https://www.frontiersin.org/articles/10.3389/fmolb.2021.609979/full#supplementary-material

Supplementary Figure 1 | Examples of dynamic curves obtained for *E. coli* (gray plots), *P. copri* (green plots) and *R. rubrum* (red plots) grown in parallel on different media (indicated) at 30°C, in the presence of 1% oxygen, under constant ventilation with CO_2 (20%) and N_2 (79%) and with stirring at a speed of 130 RPM. The cultures were inoculated with different dilutions of overnight cultures (1:2000 for *E. coli* and 1:10 for two other bacteria).

Supplementary Figure 2 | Examples of growth curves obtained for individually cultivated *E. coli* (gray plots, inoculation ratio 1:4000), *P. copri* (green plots, ratio 1:20) and *R. rubrum* (red plots, ratio 1:10). Dynamic curves for mixed populations

E. coli (1:4000) + *P. copri* (1:20), *E. coli* (1:4000) + *R. rubrum* (1:10) and *P. copri* (1:20) + *R. rubrum* (1:10) are shown by cyan plots. Magenta filled circles show the expected OD_{600} values for mixed populations if they grow independently during the logarithmic phase when nutrition is not a limiting factor. Vertical dashed lines mark the 8.5-h time point of RNA extraction.

Supplementary Table 1 | Genomic distribution of dominant oligonucleotides in the intracellular transcriptome of *E. coli* MG1655.

Supplementary Table 2 | Genomic distribution of dominant oligonucleotides in the extracellular RNA fraction of *E. coli* MG1655.

Supplementary Table 3 | Genomic distribution of oligonucleotides dominant in the extracellular RNA fraction of mixed population *E. coli* MG1655–*R. rubrum*.

Supplementary Table 4 | Genomic distribution of oligonucleotides dominant in the extracellular RNA fraction of mixed population *E. coli* MG1655–*P. copri*.

REFERENCES

Abdullah, Z., Schlee, M., Roth, S., Mraheil, M. A., Barchet, W., Böttcher, J., et al. (2012). RIG-I detects infection with live Listeria by sensing secreted bacterial nucleic acids. *EMBO J.* 31, 4153–464. doi: 10.1038/emboj.2012.274

Afgan, E., Baker, D., van den Beek, M., Blankenberg, D., and Bouvier, D., Cech, M., et al. (2016). The Galaxy platform for accessible, reproducible and collaborative biomedical analyses: 2016 update. *Nucleic Acids Res.* 44, W3–W10. doi: 10.1093/nar/gkw343

Ahmadi Badi, S., Bruno, S. P., Moshiri, A., Tarashi, S., Siadat, S. D., and Masotti, A. (2020). Small RNAs in outer membrane vesicles and their function in host-microbe interactions. *Front. Microbiol.* 11:1209. doi: 10.3389/fmicb.2020.01209

Alikina, O. V., Glazunova, O. A., Bykov, A. A., Kiselev, S. S., Tutukina, M. N., Shavkunov, K. S., et al. (2018). A cohabiting bacterium alters the spectrum of short RNAs secreted by Escherichia coli. *FEMS Microbiol. Lett.* 365:fny262. doi: 10.1093/femsle/fny262

Antipov, S. S., Tutukina, M. N., Preobrazhenskaya, E. V., Kondrashov, F. A., Patrushev, M. V., Toshchakov, S. V., et al. (2017). The nucleoid protein Dps binds genomic DNA of Escherichia coli in a non-random manner. *PLoS ONE* 12:e0182800. doi: 10.1371/journal.pone.0182800

Appling, D. R. (2008). Software Review of Prism 5. *J. Am. Chem. Soc.* 130:6056. doi: 10.1021/ja801998j

Arumugam, M., Raes, J., Pelletier, E., Paslier, D., Yamada, T., Mende, D. R., et al. (2011). Enterotypes of the human gut microbiome. *Nature* 473, 174–80. doi: 10.1038/nature09944

Beatty, M., Guduric-Fuchs, J., Brown, E., Bridgett, S., Chakravarthy, U., Hogg, R., et al. (2014). Small RNAs from plants, bacteria and fungi within the order Hypocreales are ubiquitous in human plasma. *BMC Genomics* 15:933. doi: 10.1186/1471-2164-15-933

Bechhofer, D. H., and Deutscher, M. P. (2019). Bacterial ribonucleases and their roles in RNA metabolism. *Crit. Rev. Biochem. Mol. Biol.* 54, 242–300. doi: 10.1080/10409238.2019.1651816

Blattner, F. R., Plunkett, G. 3rd., Bloch, C. A., Perna, N. T., and Burland, V., Riley, M., et al. (1997). The complete genome sequence of *Escherichia coli* K-12. *Science* 277, 1453–1462. doi: 10.1126/science.277.5331.1453

Blenkiron, C., Simonov, D., Muthukaruppan, A., Tsai, P., Dauros, P., Green, S., et al. (2016). Uropathogenic Escherichia coli releases extracellular vesicles that are associated with RNA. *PLoS ONE* 11:e0160440. doi: 10.1371/journal.pone.0160440

Bloch, S., Wegrzyn, A., Wegrzyn, G., and Nejman-Faleńczyk, B. (2017). Small and smaller-sRNAs and MicroRNAs in the regulation of toxin gene expression in prokaryotic cells: a mini-review. *Toxins* 9:181. doi: 10.3390/toxins9060181

Bykov, A. A., Shavkunov, K. S., Panyukov, V. V., and Ozoline, O. N. (2016). Bacterial nucleoid protein Dps binds structured RNA molecules. *Mat. Biolog. Bioinform.* 11, 311–322. doi: 10.17537/2016.11.311

Carver, T., Thomson, N., Bleasby, A., Berriman, M., and Parkhill, J. (2009). DNAPlotter: circular and linear interactive genome visualization. *Bioinformatics* 25, 119–20. doi: 10.1093/bioinformatics/btn578

Castel, S. E., and Martienssen, R. A. (2013). RNA interference in the nucleus: roles for small RNAs in transcription, epigenetics and beyond. *Nat. Rev. Genet.* 14, 100–12. doi: 10.1038/nrg3355

Chao, Y., Li, L., Girodat, D., Förstner, K. U., Said, N., Corcoran, C., et al. (2017). *In vivo* cleavage map illuminates the central role of RNase E in coding and non-coding RNA pathways. *Mol. Cell.* 65, 39–51. doi: 10.1016/j.molcel.2016.11.002

Chen, J., and Conn, S. (2017). Canonical mRNA is the exception, rather than the rule. *Genome Biol.* 18:133. doi: 10.1186/s13059-017-1268-1

Cheng, L., Sharples, R. A., Scicluna, B. J., and Hill, A. F. (2014). Exosomes provide a protective and enriched source of miRNA for biomarker profiling compared to intracellular and cell-free blood. *J. Extracell. Vesicles* 3:23743. doi: 10.3402/jev.v3.23743

d'Adda di Fagagna, F. (2014). A direct role for small non-coding RNAs in DNA damage response. *Trends Cell Biol.* 24, 171–18. doi: 10.1016/j.tcb.2013.09.008

Dalmasso, G., Nguyen, H. T., Yan, Y., Laroui, H., Charania, M. A., Ayyadurai, S., et al. (2011). Microbiota modulate host gene expression via microRNAs. *PLoS ONE* 6:e19293. doi: 10.1371/journal.pone.0019293

Davis, B. M., and Waldor, M. K. (2007). RNase E-dependent processing stabilizes MicX, a Vibrio cholerae sRNA. *Mol. Microbiol.* 65, 373–85. doi: 10.1111/j.1365-2958.2007.05796.x

Diebel, K. W., Zhou, K., Clarke, A. B., and Bemis, L. T. (2016). Beyond the ribosome: extra-translational functions of tRNA fragments. *Biomark. Insights* 11, 1–8. doi: 10.4137/BMI.S35904

Eigenbrod, T., Pelka, K., Latz, E., Kreikemeyer, B., and Dalpke, A. H. (2015). TLR8 senses bacterial RNA in human monocytes and plays a nonredundant role for recognition of *Streptococcus pyogenes*. *J. Immunol.* 195, 1092–1099. doi: 10.4049/jimmunol.1403173

Eisenhardt, K. M. H., Reuscher, C. M., and Klug, G. (2018). PcrX, an sRNA derived from the 3′- UTR of the Rhodobacter sphaeroides puf operon modulates expression of puf genes encoding proteins of the bacterial photosynthetic apparatus. *Mol. Microbiol.* 110, 325–334. doi: 10.1111/mmi.14076

Forde, B. M., and O'Toole, P. W. (2013). Next-generation sequencing technologies and their impact on microbial genomics. *Brief. Funct. Genomics* 12, 440–53. doi: 10.1093/bfgp/els062

Fritz, J. V., Heintz-Buschart, A., Ghosal, A., Wampach, L., Etheridge, A., Galas, D., et al. (2016). Sources and functions of extracellular small RNAs in human circulation. *Annu. Rev. Nutr.* 36, 301–36. doi: 10.1146/annurev-nutr-071715-050711

Geyer, M., Pelka, K., and Latz, E. (2015). Synergistic activation of Toll-like receptor 8 by two RNA degradation products. *Nat. Struct. Mol. Biol.* 22, 99–101. doi: 10.1038/nsmb.2967

Ghosal, A., Upadhyaya, B. B., Fritz, J. V., Heintz-Buschart, A., Desai, M. S., Yusuf, D., et al. (2015). The extracellular RNA complement of *Escherichia coli*. *MicrobiologyOpen* 4, 252–66. doi: 10.1002/mbo3.235

Glinge, C., Clauss, S., Boddum, K., Jabbari, R., Jabbari, J., Risgaard, B., et al. (2017). Stability of circulating blood-based MicroRNAs - pre-analytic methodological considerations. *PLoS ONE* 12:e0167969. doi: 10.1371/journal.pone.0167969

Heil, F., Hemmi, H., Hochrein, H., Ampenberger, F., Kirschning, C., Akira, S., et al. (2004). Species-specific recognition of single-stranded RNA via toll-like receptor 7 and 8. *Science* 303, 1526–159. doi: 10.1126/science.1093620

Hoyos, M., Huber, M., Förstner, K. U., and Papenfort, K. (2020). Gene autoregulation by 3′ UTR-derived bacterial small RNAs. *eLife* 9:e58836. doi: 10.7554/eLife.58836

Hungate, R. E. (1969). A roll tube method for cultivation of strict anaerobes. *Methods Microbiol.* 3, 117–132. doi: 10.1016/S0580-9517(08)70503-8

Jung, S., von Thülen, T., Laukemper, V., Pigisch, S., Hangel, D., Wagner, H., et al. (2015). A single naturally occurring 2'-O-methylation converts a TLR7- and TLR8-activating RNA into a TLR8-specific ligand. *PLoS ONE* 10:e0120498. doi: 10.1371/journal.pone.0120498

Kaiser, I., and Oelze, J. (1980). Grow and adaptation to phototrophic conditions of Rhodospirillum rubrum and Rhodopseudomonas sphaeroides at different temperatures. *Arch. Microbiol.* 126, 187–194. doi: 10.1007/BF00511226

Kaiser, S., Rimbach, K., Eigenbrod, T., Dalpke, A. H., and Helm, M. (2014). A modified dinucleotide motif specifies tRNA recognition by TLR7. *RNA* 20, 1351–135. doi: 10.1261/rna.044024.113

Kang, S. M., Choi, J. W., Lee, Y., Hong, S. H., and Lee, H. J. (2013). Identification of microRNA-size, small RNAs in Escherichia coli. *Curr. Microbiol.* 67, 609–13. doi: 10.1007/s00284-013-0411-9

Koeppen, K., Hampton, T. H., Jarek, M., Scharfe, M., Gerber, S. A., Mielcarz, D. W., et al. (2016). A novel mechanism of host-pathogen interaction through sRNA in bacterial outer membrane vesicles. *PLoS Pathog.* 12:e1005672. doi: 10.1371/journal.ppat.1005672

Krüger, A., Oldenburg, M., Chebrolu, C., Beisser, D., Kolter, J., Sigmund, A. M., et al. (2015). Human TLR8 senses UR/URR motifs in bacterial and mitochondrial RNA. *EMBO Rep.* 16, 1656–1663. doi: 10.15252/embr.201540861

Kukurba, K. R., and Montgomery, S. B. (2015). RNA sequencing and analysis. *Cold Spring Harb. Protoc.* 2015, 951–969. doi: 10.1101/pdb.top084970

Kulp, A. J., Sun, B., Ai, T., Manning, A. J., Orench-Rivera, N., Schmid, A. K., et al. (2015). Genome-wide assessment of outer membrane vesicle production in *Escherichia coli*. *PLoS ONE* 10:e0139200. doi: 10.1371/journal.pone.0139200

Lalaouna, D., Carrier, M. C., and Massé, E. (2015a). Every little piece counts: the many faces of tRNA transcripts. *Transcription* 6, 74–7. doi: 10.1080/21541264.2015.1093064

Lalaouna, D., Carrier, M. C., Semsey, S., Brouard, J. S., Wang, J., Wade, J. T., et al. (2015b). A 3′ external transcribed spacer in a tRNA transcript acts as a sponge for small RNAs to prevent transcriptional noise. *Mol. Cell.* 58, 393–405. doi: 10.1016/j.molcel.2015.03.013

Lee, H. J., and Hong, S. H. (2012). Analysis of microRNA-size, small RNAs in Streptococcus mutans by deep sequencing. *FEMS Microbiol. Lett.* 326, 131–16. doi: 10.1111/j.1574-6968.2011.02441.x

Leighton, L. J., and Bredy, T. W. (2018). Functional interplay between small non-coding RNAs and RNA modification in the brain. *Non-coding RNA* 4:15. doi: 10.3390/ncrna4020015

Levanova, A., and Poranen, M. M. (2018). RNA interference as a prospective tool for the control of human viral infections. *Front. Microbiol.* 9:2151. doi: 10.3389/fmicb.2018.02151

Liu, S., da Cunha, A. P., Rezende, R. M., Cialic, R., Wei, Z., Bry, L., et al. (2016). The host shapes the gut microbiota via fecal MicroRNA. *Cell Host Microbe.* 19, 32–43. doi: 10.1016/j.chom.2015.12.005

Malabirade, A., Habier, J., Heintz-Buschart, A., May, P., Godet, J., Halder, R., et al. (2018). The RNA complement of outer membrane vesicles from salmonella enterica serovar typhimurium under distinct culture conditions. *Front. Microbiol.* 9:2015. doi: 10.3389/fmicb.2018.02015

Mall, C., Rocke, D. M., Durbin-Johnson, B., and Weiss, R. H. (2013). Stability of miRNA in human urine supports its biomarker potential. *Biomark. Med.* 7, 623–31. doi: 10.2217/bmm.13.44

Mills, K. H. (2011). TLR-dependent T cell activation in autoimmunity. *Nat. Rev. Immunol.* 11, 807–22. doi: 10.1038/nri3095

Miyakoshi, M., Matera, G., Maki, K., Sone, Y., and Vogel, J. (2019). Functional expansion of a TCA cycle operon mRNA by a 3′ end-derived small RNA. *Nucleic Acids Res.* 47, 2075–2088. doi: 10.1093/nar/gky1243

Miyoshi, T., Ito, K., Murakami, R., and Uchiumi, T. (2016). Structural basis for the recognition of guide RNA and target DNA heteroduplex by Argonaute. *Nat. Commun.* 7:11846. doi: 10.1038/ncomms11846

Munk, A. C., Copeland, A., Lucas, S., Lapidus, A., del Rio, T. D., Barry, K., et al. (2011). Complete genome sequence of *Rhodospirillum rubrum* type strain (S1). *Stand. Genomic Sci.* 4, 293–302. doi: 10.4056/sigs.1804360

Nakanishi, K. (2016). Anatomy of RISC: how do small RNAs and chaperones activate Argonaute proteins? *Wiley Interdiscip. Rev. RNA.* 7, 637–60. doi: 10.1002/wrna.1356

Nozawa, R. S., Boteva, L., Soares, D. C., Naughton, C., Dun, A. R., Buckle, A., et al. (2017). SAF-A regulates interphase chromosome structure through oligomerization with chromatin-associated RNAs. *Cell* 169, 1214–1227.e18. doi: 10.1016/j.cell.2017.05.029

Obbard, D. J., Gordon, K. H., Buck, A. H., and Jiggins, F. M. (2009). The evolution of RNAi as a defence against viruses and transposable elements. *Philos. Trans. R. Soc. Lond. B. Biol. Sci.* 364, 99–115. doi: 10.1098/rstb.2008.0168

O'Donoghue, E. J., and Krachler, A. M. (2016). Mechanisms of outer membrane vesicle entry into host cells. *Cell. Microbiol.* 18, 1508–1517. doi: 10.1111/cmi.12655

Panyukov, V. V., Kiselev, S. S., Alikina, O. V., Nazipova, N. N., and Ozoline, O. N. (2017). Short unique sequences in bacterial genomes as strain- and species-specific signatures. *Math. Biol. Bioinf.* 12, 547–58. doi: 10.17537/2017.12.547

Panyukov, V. V., Kiselev, S. S., and Ozoline, O. N. (2020). Unique k-mers as strain-specific barcodes for phylogenetic analysis and natural microbiome profiling. *Int. J. Mol. Sci.* 21:944. doi: 10.3390/ijms21030944

Panyukov, V. V., Kiselev, S. S., Shavkunov, K. S., Masulis, I. S., and Ozoline, O. N. (2013). Mixed promoter islands as genomic regions with specific structural and functional properties. *Math. Biol. Bioinf.* 8, 432–448. doi: 10.17537/2013.8.432

Papenfort, K., Said, N., Welsink, T., Lucchini, S., Hinton, J. C. D., and Vogel, J. (2009). Specific and pleiotropic patterns of mRNA regulation by ArcZ, a conserved, Hfq-dependent small RNA. *Mol. Microbiol.* 74, 139–158. doi: 10.1111/j.1365-2958.2009.06857.x

Pavankumar, A. R., Ayyappasamy, S. P., and Sankaran, K. (2012). Small RNA fragments in complex culture media cause alterations in protein profiles of three species of bacteria. *BioTechniques* 52, 167–72. doi: 10.2144/000113819

Rosace, D., López, J., and Blanco, S. (2020). Emerging roles of novel small non-coding regulatory RNAs in immunity and cancer. *RNA Biol.* 17, 1196–1213. doi: 10.1080/15476286.2020.1737442

Santos-Zavaleta, A., Salgado, H., Gama-Castro, S., Sánchez-Pérez, M., Gómez-Romero, L., Ledezma-Tejeida, D., et al. (2019). RegulonDB v 10.5: tackling challenges to unify classic and high throughput knowledge of gene regulation in *E. coli* K-12. *Nucleic Acids Res.* 47, D212–D220. doi: 10.1093/nar/gky1077

Shavkunov, K. S., Masulis, I. S., Tutukina, M. N., Deev, A. A., and Ozoline, O. N. (2009). Gains and unexpected lessons from genome-scale promoter mapping. *Nucleic Acids Res.* 37, 4919–4931. doi: 10.1093/nar/gkp490

Swiatowy, W., and Jagodziński, P. P. (2018). Molecules derived from tRNA and snoRNA: entering the degradome pool. *Biomed. Pharmacother.* 108, 36–42. doi: 10.1016/j.biopha.2018.09.017

Wang, C., Chao, Y., Matera, G., Gao, Q., and Vogel, J. (2020). The conserved 3′ UTR-derived small RNA NarS mediates mRNA crossregulation during nitrate respiration. *Nucleic Acids Res.* 48, 2126–2143. doi: 10.1093/nar/gkz1168

Wiegand, C., Heusser, P., Klinger, C., Cysarz, D., Büssing, A., Ostermann, T., et al. (2018). Stress-associated changes in salivary microRNAs can be detected in response to the Trier Social Stress Test: an exploratory study. *Sci. Rep.* 8:7112. doi: 10.1038/s41598-018-25554-x

Willkomm, S., Zander, A., Gust, A., and Grohmann, D. (2015). A prokaryotic twist on argonaute function. *Life (Basel).* 5, 538–53. doi: 10.3390/life5010538

Wolfe, R. S. (1971). Microbial formation of methane. *Adv. Microb. Physiol.* 6, 107–46. doi: 10.1016/S0065-2911(08)60068-5

Yau, T. O., Tang, C. M., Harriss, E. K., Dickins, B., and Polytarchou, C. (2019). Faecal microRNAs as a non-invasive tool in the diagnosis of colonic adenomas and colorectal cancer: a meta-analysis. *Sci. Rep.* 9:9491. doi: 10.1038/s41598-019-45570-9

Conflict of Interest: The authors declare that the research was conducted in the absence of any commercial or financial relationships that could be construed as a potential conflict of interest.

frontiers in Molecular Biosciences

ORIGINAL RESEARCH
published: 03 November 2021
doi: 10.3389/fmolb.2021.668613

Post-Transcriptional Regulation of RseA by Small RNAs RyhB and FnrS in *Escherichia coli*

Laricca Y. London[1], *Joseph I Aubee*[2], *Jalisa Nurse*[2,3] *and Karl M Thompson*[2]*

[1]Department of Biological and Environmental Sciences, Alabama A&M University, Huntsville, AL, United States, [2]Department of Microbiology, College of Medicine, Howard University, Washington, DC, United States, [3]Department of Biology, Howard University, Washington, DC, United States

RseA is the critical central regulator of the σ^E-dependent stress response in *E. coli* and other related bacteria. The synthesis of RseA is controlled at the transcriptional level by several promoters and transcriptional regulators, including σ^E itself at two σ^E-dependent promoters: $rpoE_P$ and $rseA_{P3}$. The presence of these two independent polycistrons encoding *rseA* is potentially redundant. We hypothesized that post-transcriptional control of the $rseA_{P3}$ transcript was necessary to overcome this redundancy. However, to date, nothing is known about the post-transcriptional control of the $rseA_{P3}$ transcript. We executed a targeted genetic screen to identify small RNA regulators of the $rseA_{P3}$ transcript and identified RyhB and FnrS as small RNA activators of the RseA P3 transcript. Through genetic analysis, we confirmed that a direct interaction occurs between RyhB and RseA. We also identified sequences within the 5′ untranslated region (UTR) of RseA that were inhibitory for RseA expression. Point mutations predicted to prevent an interaction between RyhB and RseA resulted in increased RseA expression. Taken together, this suggests that the 5' UTR of the RseAP3 transcript prevents optimal expression of RseA, preventing redundancy due to RseA expression from the σ^E-dependent $rpoE_P$, and this is overcome by the stimulatory activity of RyhB and FnrS.

Keywords: small RNA, RyhB, FnrS, *Escherichia coli*, envelope stress response

OPEN ACCESS

Edited by:
Olga N. Ozoline, Institute of Cell Biophysics (RAS), Russia

Reviewed by:
Satish Raina, Gdansk University of Technology, Poland
Tracy Raivio, University of Alberta, Canada
Andrey Shadrin, Institute of Biochemistry and Physiology of Microorganisms (RAS), Russia

***Correspondence:**
Karl M Thompson
karl.thompson@howard.edu

Specialty section:
This article was submitted to Protein and RNA Networks, a section of the journal Frontiers in Molecular Biosciences

Received: *16 February 2021*
Accepted: *03 September 2021*
Published: *03 November 2021*

Citation:
London LY, Aubee JI, Nurse J and Thompson KM (2021) Post-Transcriptional Regulation of RseA by Small RNAs RyhB and FnrS in Escherichia coli. *Front. Mol. Biosci. 8:668613. doi: 10.3389/fmolb.2021.668613*

INTRODUCTION

The cell envelope promotes structural integrity of bacteria under dynamic conditions. The cell envelope can be perturbed *via* internal or external cues. Envelope stress occurs as a result of excess or mis-folded outer membrane proteins (OMPs), subsequently resulting in the activation of the extracytoplasmic function (ECF) sigma factor, σ^E (Erickson et al., 1987; Mecsas et al., 1993; Walsh et al., 2003). Over-expression or mis-folding of OMPs can compromise the integrity of the bacterial cell envelope and therefore bacterial cell survival (Walsh et al., 2003).

E. coli and other bacterial species have developed an envelope stress response (ESR) that restores homeostasis following the onset of envelope stress. The ESR can be mediated by several key regulators in *E. coli*, most notably CpxR and σ^E (Ravio, 1999; Ravio et al., 1999). In this work, we focused on the σ^E-dependent ESR. Activation of σ^E-dependent promoters results in the transcriptional initiation of at least 60 genes, many of which encode proteins necessary for the resolution of the ESR (Dartigalongue et al., 2001; Johansen et al., 2006; Rhodius et al., 2006; Thompson et al., 2007). Effectors of the ESR include small RNAs and periplasmic proteases that act to repress OMP levels (Douchin et al., 2006; Johansen et al., 2006; Rhodius et al., 2006; Thompson et al., 2007; Vogt et al., 2014). The stabilization of OMP levels

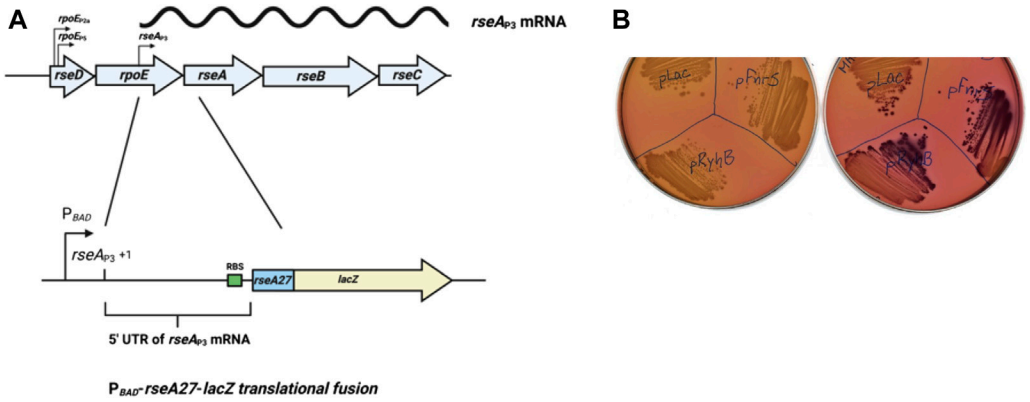

FIGURE 1 | Genetic screen for small RNA regulators **(A)**. Schematic of the *rpoE* operon with selected promoters, including the $rseA_{P3}$ promoter, and the P_{BAD}-*rseA27-lacZ* translational fusion utilized for the small RNA library screen. The *rseA* fusion consists of the *rseA* P3 transcript, and the first nine codons of the *rseA* gene fused in the frame to the ninth codon of *lacZ*, downstream and controlled by the *araBAD* promoter (P_{BAD}-*rseA27-lacZ* translational fusion) **(B)**. P_{BAD}-*rseA27-lacZ* translational fusion strains transformed with an empty vector control (pBR-pLac), pBR-*ryhB*, or pBR-*fnrS* grown overnight at 37°C on MacConkey-Lactose agar plates. One plate was supplemented with 0.0002% arabinose to stimulate basal transcription of the P_{BAD}-*rseA27-lacZ* translational fusion.

restores cell envelope homeostasis. This also results in decreased σ^E activity. It is critically important to ensure that the steady-state levels of σ^E do not increase indefinitely as σ^E over-expression results in cell lysis and death (Nitta et al., 2000; Kabir et al., 2005). The small RNAs that act as σ^E-dependent ESR effectors include MicA, RybB, and MicL; all of which have σ^E-dependent promoters, repress expression of outer membrane proteins, and regulate LPS composition (Johansen et al., 2006; Thompson et al., 2007; Udekwu and Wagner, 2007; Klein et al., 2011; Klein and Raina, 2017).

The σ^E-dependent ESR is tightly controlled *via* regulation of the *rpoE* operon (*rseD-rpoE-rseA-rseB-rseC*) at transcriptional and post-transcriptional levels (Klein et al., 2016; Yakhnin et al., 2017). There are several promoters driving expression of this operon in concert with multiple transcription and sigma factors (Klein et al., 2016; Klein and Raina, 2017; Yakhnin et al., 2017). Transcriptional control of the σ^E-dependent promoters is also controlled by guanosine 3′,5′-bispyrophosphate (ppGpp) and promoter architecture (Costanzo and Ades, 2006; Thompson et al., 2007; Costanzo et al., 2008; Balbontin et al., 2010). Only two of the promoters driving expression of the *rpoE* operon are σ^E-dependent, while the others are cognate partners to σ^{54}, σ^s, σ^{70}, or other transcriptional regulators (Klein et al., 2016). All promoters driving expression of the *rpoE* operon are localized upstream of, or within, the *rpoE* leader peptide (RseD) (**Figure 1A**). The remaining σ^E-dependent promoter ($rseA_{P3}$) is located within the *rpoE* coding region, over 230 nucleotides upstream of the *rseA* start codon (Rhodius et al., 2006). The σ^E-dependent $rseA_{P3}$ promoter drives the synthesis of an *rseA-rseB-rseC* transcript, while the σ^E-dependent promoter $rpoE_P$ drives the synthesis of the entire *rseD-rpoE-rseA-rseB-rseC* transcript (Rhodius et al., 2006). The activity of the σ^E-dependent stress response is also regulated at the transcriptional level by the activity of RseA.

RseA is the anti-sigma factor for σ^E and plays a central role in envelope stress signal transduction (De Las Penans et al., 1997; Missiakas et al., 1997; Ades et al., 1999). RseA spans the inner membrane of the cell envelope and utilizes its cytoplasmic domain to interact with σ^E (Campbell et al., 2003). RseA sequesters σ^E to the inner member under vegetative growth conditions and thereby prevents access of σ^E to its cognate promoters (Campbell et al., 2003). Envelope stress stimulates a signal transduction cascade culminating in regulated intramembrane proteolysis (RIP) of RseA by periplasmic proteases DegS and RseP (De Las Penans et al., 1997; Missiakas et al., 1997; Alba et al., 2002; Kanehara et al., 2002). Following this, the N-terminus of RseA enters the cytoplasm in complex with σ^E, whereby the RseA N-terminus is then cleaved by the adenosine 5′-triphosphate-dependent protease ClpXP (Flynn et al., 2004).

The synthesis of RseA from σ^E-dependent $rseA_{P3}$ and $rpoE_P$ promoters has the potential to be physiologically redundant. It is likely that post-transcriptional regulation of *rpoE* and *rseABC* operons removes any physiological redundancy. While post-transcriptional regulatory mechanisms have been identified for the *rpoE* operon, little is known about post-transcriptional regulation of the *rseABC* operon. The *rseABC* operon has a 228 nucleotide 5′ untranslated region (UTR) (Rhodius et al., 2006). Due to the presence of the relatively long 5′ UTR for the *rseABC* operon, we hypothesized that *cis*-acting RNA structures and *trans*-acting small RNAs regulate the expression of *rseABC* operon. To test this hypothesis, we constructed an arabinose-inducible *rseA-lacZ* translational fusion and screened it with a small RNA library. We identified RyhB and FnrS as factors that stimulate post-transcriptional expression of RseA.

MATERIALS AND METHODS

Media and Growth Conditions

All strains were grown in Luria Bertani (Lennox) liquid media (LB) at 37°C, with the exception of λ–Red-based recombineering strains using mini-λ:tet lysogens. These strains were grown in LB at

TABLE 1 | Strain list.

Strain	Genotype	Source
KMT1	*Escherichia coli* MG1655	
KMT432	MG1655 *lacI*::P_{BAD}:*cat-sacB*:*lacZ*, Δ*araBAD*, *araC*$^+$, *mal*::*lacI*^{q}, minil::*tet* f80$^+$	Pierre Mandin, Ph.D. (PM1205); Mandin and Gottesman (2009)
KMT465	MG1655 Δ*ryhB*::*zeo*	Nicolas DeLay, Ph.D
KMT467	MG1655 *lacI*^{q} Δ*fnrS*::*kan*	Gisela Storz, Ph.D.; Durand and Storz (2010)
KMT519	NM525 pBR-pLac-*fnrS*-I	Giselia Storz, Ph.D.; Durand and Storz (2010)
KMT520	NM525 pBR-pLac-*fnrS*-II	Giselia Storz, Ph.D.; Durand and Storz (2010)
KMT521	NM525 pBR-pLac-*fnrS*-III	Giselia Storz, Ph.D.; Durand and Storz (2010)
KMT590	MG1655 *lacI*::P_{BAD}:*cat-sacB*:*lacZ*, Δ*araBAD*, *araC*+, *mal*::*lacI*^{q}, minil::*tet* ϕ80$^-$	Nadim Majdalani - PM1805
KMT20005	MG1655 Δ*araBAD*, *araC*$^+$, *mal*::*lacI*^{q} *lacI*::P_{BAD}-*rseA27*-*lacZ* translational fusion	This work, KMT432 x P_{BAD} *rseA27*-*lacZ* PCR 42°C induction and selection on M63-Glycerol-XG
KMT20060	MG1655 Δ*araBAD*, *araC*$^+$, *mal*::*lacI*^{q} *lacI*::P_{BAD}-*rseA27*-*lacZ* translational fusion Δ*ryhB*::*zeo*	This work, KMT20005 x P1 (KMT465 - Δ*ryhB*::*zeo* source)
KMT20082	MG1655 Δ*araBAD*, *araC*$^+$, *mal*::*lacI*^{q} *lacI*::P_{BAD}-*rseA27*-*lacZ* translational fusion *(2)* Δ*ryhB*::*zeo* Δ*fnrS*::*kan*	This work, KMT20060 x P1 (KMT467 - Δ*fnrS*::*kan* source)
KMT20088	MG1655 Δ*araBAD*, *araC*$^+$, *mal*::*lacI*^{q} *lacI*::P_{BAD}-*rseA27*-*lacZ* translational fusion Δ*ryhB*::*zeo* Δ*fnrS*::*kan* pBR-pLac	This work, KMT20082 + pBR-pLac (TSS Transformation)
KMT20089	MG1655 Δ*araBAD*, *araC*$^+$, *mal*::*lacI*^{q} *lacI*::P_{BAD}-*rseA27*-*lacZ* translational fusion Δ*ryhB*::*zeo* Δ*fnrS*::*kan* pBR-pLac-*fnrS*	This work, KMT20082 + pBR-pLac-*fnrS* (TSS Transformation)
KMT20090	MG1655 Δ*araBAD*, *araC*$^+$, *mal*::*lacI*^{q} *lacI*::P_{BAD}-*rseA27*-*lacZ* translational fusion Δ*ryhB*::*zeo* Δ*fnrS*::*kan* pBR-pLac-*ryhB*	This work, KMT20082 + pBR-pLac-*ryhB* (TSS Transformation)
KMT20109	MG1655 Δ*araBAD*, *araC*$^+$, *mal*::*lacI*^{q} *lacI*::P_{BAD}-*rseA27*-*lacZ* translational fusion Δ*ryhB*::*zeo* Δ*fnrS*::*kan* pBR-pLac-*ryhBm*1	This work, KMT20082 + pBR-pLac-*ryhBm*1 (TSS Transformation)
KMT20110	MG1655 Δ*araBAD*, *araC*$^+$, *mal*::*lacI*^{q} *lacI*::P_{BAD}-*rseA27*-*lacZ* translational fusion Δ*ryhB*::*zeo* Δ*fnrS*::*kan* pBR-pLac-*ryhBm*2	This work, KMT20082 + pBR-pLac-*ryhBm*2 (TSS Transformation)
KMT20111	MG1655 Δ*araBAD*, *araC*$^+$, *mal*::*lacI*^{q} *lacI*::P_{BAD}-*rseA27*-*lacZ* translational fusion Δ*ryhB*::*zeo* Δ*fnrS*::*kan* pBR-pLac-*ryhBm*3	This work, KMT20082 + pBR-pLac-*ryhBm*3 (TSS Transformation)
KMT20112	MG1655 Δ*araBAD*, *araC*$^+$, *mal*::*lacI*^{q} *lacI*::P_{BAD}-*rseA27*-*lacZ* translational fusion Δ*ryhB*::*zeo* Δ*fnrS*::*kan* pBR-pLac-*ryhBm*4	This work, KMT20082 + pBR-pLac-*ryhBm*4 (TSS Transformation)
KMT20113	MG1655 Δ*araBAD*, *araC*$^+$, *mal*::*lacI*^{q} *lacI*::P_{BAD}-*rseA27*-*lacZ* translational fusion Δ*ryhB*::*zeo* Δ*fnrS*::*kan* pBR-pLac-*fnrS*-I	This work, KMT20082 + pBR-pLac-*fnrS*-I (TSS Transformation)
KMT20114	MG1655 Δ*araBAD*, *araC*$^+$, *mal*::*lacI*^{q} *lacI*::P_{BAD}-*rseA27*-*lacZ* translational fusion Δ*ryhB*::*zeo* Δ*fnrS*::*kan* pBR-pLac-*fnrS*-II	This work, KMT20082 + pBR-pLac-*fnrS*-II (TSS Transformation)
KMT20115	MG1655 Δ*araBAD*, *araC*$^+$, *mal*::lacI^q lacI::P_{BAD}-*rseA27*-*lacZ* translational fusion Δ*ryhB*::*zeo* Δ*fnrS*::*kan* pBR-pLac-*fnrS*-III	This work, KMT20082 + pBR-pLac-*fnrS*-III (TSS Transformation)
KMT20144	MG1655 Δ*araBAD*, *araC*$^+$, *mal*::*lacI*^{q} *lacI*::P_{BAD}-*rseA27*-*lacZ* translational fusion	This work, KMT590 x P_{BAD}-*rseA27*-*lacZ* gBlock amplified with KT902 + KT1137
KMT20146	MG1655 Δ*araBAD*, *araC*$^+$, *mal*::*lacI*^{q} *lacI*::P_{BAD}-*rseA27*cm1-*lacZ* translational fusion	This work, KMT590 x P_{BAD}-*rseA27*cm1-*lacZ* gBlock amplified with KT902 + KT1137
KMT20148	MG1655 Δ*araBAD*, *araC*$^+$, *mal*::*lacI*^{q} *lacI*::P_{BAD}-*rseA27*cm3-*lacZ* translational fusion	This work, KMT590 x P_{BAD}-*rseA27*cm3-*lacZ* gBlock amplified with KT902 + KT1137
KMT20156	MG1655 Δ*araBAD*, *araC*$^+$, *mal*::lacI^q *lacI*::P_{BAD}-*rseA27*-*lacZ* cm1 Δ*fnrS*::*kan*	KMT20146 x P1 (Δ*fnrS*::*kan*)
KMT20160	MG1655 Δ*araBAD*, *araC*$^+$, *mal*::*lacI*^{q} *lacI*::P_{BAD}-*rseA27*-*lacZ* cm3 Δ*fnrS*::*kan*	This work, KMT20148 x P1 (Δ*fnrS*::*kan*)
KMT20172	MG1655 Δ*araBAD*, *araC*$^+$, *mal*::*lacI*^{q} *lacI*::P_{BAD}-*rseA27*cm1-*lacZ* cm1 Δ*fnrS*::*kan* Δ*ryhB*::*zeo*	This work, KMT20156 x P1 (Δ*ryhB*::*zeo*)
KMT20174	MG1655 Δ*araBAD*, *araC*$^+$, *mal*::*lacI*^{q} *lacI*::P_{BAD}-*rseA27*-*lacZ* cm3 Δ*fnrS*::*kan* Δ*ryhB*::*zeo*	This work, KMT20160 x P1 (Δ*ryhB*::*zeo*)
KMT20178	MG1655 Δ*araBAD*, *araC*$^+$, *mal*::*lacI*^{q} *lacI*::P_{BAD}-*rseA27*cm1-*lacZ* Δ*fnrS*::*kan* Δ*ryhB*::*zeo* pBR-pLac	This work, KMT20172 + pBR-pLac (TSS Transformation)
KMT20179	MG1655 Δ*araBAD*, *araC*$^+$, *mal*::*lacI*^{q} *lacI*::P_{BAD}-*rseA27*cm1-*lacZ* Δ*fnrS*::*kan* Δ*ryhB*::*zeo* pBR-pLac-*ryhB*	This work, KMT20172 + pBR-pLac-*ryhB* (TSS Transformation)
KMT20180	MG1655 Δ*araBAD*, *araC*$^+$, *mal*::*lacI*^{q} *lacI*::P_{BAD}-*rseA27*cm1-*lacZ* Δ*fnrS*::*kan* Δ*ryhB*::*zeo* pBR-pLac-*ryhBm*1	This work, KMT20172 + pBR-pLac-*ryhBm*1 (TSS Transformation)
KMT20184	MG1655 Δ*araBAD*, *araC*$^+$, *mal*::*lacI*^{q} *lacI*::P_{BAD}-*rseA27*cm3-*lacZ* Δ*fnrS*::*kan* Δ*ryhB*::*zeo* pBR-pLac	This work, KMT20174 + pBR-pLac (TSS Transformation)
KMT20185	MG1655 Δ*araBAD*, *araC*$^+$, *mal*::*lacI*^{q} *lacI*::P_{BAD}-*rseA27*cm3-*lacZ* Δ*fnrS*::*kan* Δ*ryhB*::*zeo* pBR-pLac-*ryhB*	This work, KMT20174 + pBR-pLac-ryhB (TSS Transformation)
KMT20186	MG1655 Δ*araBAD*, *araC*$^+$, *mal*::*lacI*^{q} *lacI*::P_{BAD}-*rseA27*cm3-*lacZ* Δ*fnrS*::*kan* Δ*ryhB*::*zeo* pBR-pLac-*ryhB*-m3	This work, KMT20174 + pBR-pLac-*ryhBm*3 (TSS Transformation)
KMT20196	MG1655 Δ*araBAD*, *araC*$^+$, *mal*::*lacI*^{q} *lacI*::P_{BAD}-*rseA*-3XFLAG w.t. #1	PM1800 x P_{BAD}-*rseA*-3XFLAG w.t. amplified gBlock KT902 + KT1138
KMT20234	MG1655 Δ*araBAD*, *araC*$^+$, *mal*::*lacI*^{q} *lacI*::P_{BAD}-*rseA*-3XFLAG w.t. #1 Δ*ryhB*::*zeo*	KMT20196 x P1 (Δ*ryhB*::*zeo*)

TABLE 2 | Plasmid list.

Plasmid	Characteristics	References or source
pBR-pLac	pBR322 ori (pMB1), P_{LlacO} promoter-based expression vector, *bla* (Amp^R)	Guillier and Gottesman, 2006
pBR-pLac-*ryhB*	*ryhB* gene cloned into the AatII/EcoRI site of pBR-pLac	Mandin and Gottesman (2009)
pBR-pLac-*ryhBm*1	*ryhB* C14G, C15G, C16G site-directed mutations in pBR-pLac-*ryhB*	This work
pBR-pLac-*ryhBm*2	*ryhB* C18G, G19C, C20G, and G21C site-directed mutations in pBR-pLac-*ryhB*	This work
pBR-pLac-*ryhBm*3	*ryhB* G21C, G22C, A23C, G24A, A25C, and A26C site-directed mutations in pBR-pLac-*ryhB*	This work
pBR-pLac-*fnrS*	*fnrS* gene cloned into the AatII/EcoRI site of pBR-pLac	Mandin and Gottesman (2009)
pBR-pLac-*fnrS*-I	*fnrS* U57A, U58G, U59A site-directed mutations in pBR-pLac-*fnrS*	Gisela Storz, Durand and Storz (2010)
pBR-pLac-*fnrS*-II	*fnrS* C47A U48A U49G site-directed mutations in pBR-pLac-*fnrS*	Gisela Storz, Durand and Storz, (2010)
pBR-pLac-*fnrS*-III	*fnrS* G4C, G5U site-directed mutation in pBR-pLac-*fnrS*	Gisela Storz, Durand and Storz (2010)

TABLE 3 | Oligonucleotide list.

Oligonucleotides	Sequence (5' - 3')	Purpose
KT902	ACCTGACGCTTTTTATCGCAACTCTCTACTGTTTCTCCATGAGACAGATAGTTTTCCGAA	forward primer for amplification of the P_{BAD}-*rseA27-lacZ* fusion recombination substrate
KT903	TAACGCCAGGGTTTTCCCAGTCACGACGTTGTAAAACGACTAAAGCGGAAAGTTGTTCTTTCTGCAT	reverse primer for amplification of the P_{BAD}-*rseA27-lacZ* fusion recombination substrate
KT940	CGAAGCGGCATGCATTTACGTTG	Forward Screening primer for PM1205 fusions
KT950	CGTCGCGATCAGGAAGAGGGTCGCGGAGAACCTGAAA	forward primer for creation of *ryhBm*1 (C14G C15G C16G) by Quickchange mutagenesis
KT950c	TTTCAGGTTCTCCGCGACCCTCTTCCTGATCGCGACG	reverse primer for creation of *ryhBm*1 (C14G C15G C16G) by Quickchange mutagenesis
KT951	GCGATCAGGAAGACCCTGCGCGAGAACCTGAAAGCACG	forward primer for creation of *ryhBm*2 (C18G G19C C20G G21C) for Quickchange mutagenesis
KT951c	CGTGCTTTCAGGTTCTCGCGCAGGGTCTTCCTGATCGC	reverse primer for creation of *ryhBm*2 (C18G G19C C20G G21C) for Quickchange mutagenesis
KT952	GATCAGGAAGACCCTCGCCCCACCCCTGAAAGCACGACATTGGCACGACATTGCTCACCACACTTCCAGTATT	forward primer for creation of *ryhBm*3 (G22C G23C A24C G25A A26C A27C) for Quickchange mutagenesis
KT952c	AATACTGGAAGTGTGGTGAGCAATGTCGTGCCAATGTCGTGCTTTCAGGGGTGGGGCGAGGGTCTTCCTGATC	reverse primer for creation of *ryhBm*3 (G22C G23C A24C G25A A26C A27C) for Quickchange mutagenesis
KT953	GCACGACATTGCTCACCACACTTCCAGTATTACTTA	forward primer for creation of *ryhBm*4 (A51C T52A T53C G54A) for Quickchange mutagenesis
KT953c	TAAGTAATACTGGAAGTGTGGTGAGCAATGTCGTGC	reverse primer for creation of *ryhBm*4 (A51C T52A T53C G54A) for Quickchange mutagenesis
KT1115	CATTGACATTGTGAGCGGATAACAAGATACT	pBR-pLac forward screening and sequencing primer
KT1116	CCGCATTAAAGCTTATCGATGATAAGCTG	pBR-pLac reverse screening and sequencing primer
KT1137	CGCCAGGGTTTTCCCAGTCACGACGTTGTAAAACGACGGCTAAAGCGGAAAGTTGTTCTTTCTGCAT	reverse primer for amplification of the P_{BAD}-*rseA27-lacZ* (wild-type and mutant) fusion recombination substrate

TABLE 4 | List of synthetic DNA used in genetic engineering.

Sequence name	Sequence	Purpose
P_{BAD}-*rseA27-lacZ* gBlock	AcctgacgctttttatcgcaactctctactgtttctccaTGAGACAGATAGTTTTCCGAACTATTGAGTCCCTCCCGGAAGATTTACGCA TGGCAATAACCTTGCGGGAGCTGGATGGCCTGAGCTATGAAGAGATAGCCGCTATCATGGATTGTCCGGTAGGTA CGGTGCGTTCACGTATCTTCCGAGCGAGGGAAGCTATTGATAACAAAGTTCAACCGCTTATCAGGCGTTGACGATAGC GGGATACTGGATAAGGGTATTAGGCatgCAGAAAGAACAACTTTCCGCTTTAGCCGTCGTTTTACAACGTCGTGACTG GGAAAACCCTGGCG	used as a template for amplification of the recombination substrate for creation of P_{BAD}-*rseA27-lacZ* translational fusion
P_{BAD}-*rseA27cm1-lacZ* gBlock	AcctgacgctttttatcgcaactctctactgtttctccaTGAGACAGATAGTTTTCCGAACTATTGAGTCCCTCCCGGAAGATTTACGCA TGGCAATAACCTTGCGGGAGCTGGATGGCCTGAGCTATGAAGAGATAGCCGCTATCATGGATTGTCCGGTAGGTA CGGTGCGTTCACGTATCTTCCGAGCGACCCAAGCTATTGATAACAAAGTTCAACCGCTTATCAGGCGTTGACGATAGC GGGATACTGGATAAGGGTATTAGGCatgCAGAAAGAACAACTTTCCGCTTTAGCCGTCGTTTTACAACGTCGTGACTG GGAAAACCCTGGCG	used as a template for amplification of the recombination substrate for creation of P_{BAD}-*rseA27(cm1)-lacZ* translational fusion
P_{BAD}-*rseA27cm3-lacZ* gBlock	AcctgacgctttttatcgcaactctctactgtttctccaTGAGACAGATAGTTTTCCGAACTATTGAGTCCCTCCCGGAAGATTTACGCA TGGCAATAACCTTGCGGGAGCTGGATGGCCTGAGCTATGAAGAGATAGCCGCTATCATGGATTGTCCGGTAGGTA CGGTGCGTTCACGGAGTGGGCGAGCGAGGGAAGCTATTGATAACAAAGTTCAACCGCTTATCAGGCGTTGACGAT AGCGGGATACTGGATAAGGGTATTAGGCatgCAGAAAGAACAACTTTCCGCTTTAGCCGTCGTTTTACAACGTCGTGA CTGGGAAAACCCTGGCG	used as a template for amplification of the recombination substrate for creation of P_{BAD}-*rseA27(cm3)-lacZ* translational fusion
P_{BAD}-*rseA-3XFLAG* gBlock	AcctgacgctttttatcgcaactctctactgtttctccaTGAGACAGATAGTTTTCCGAACTATTGAGTCCCTCCCGGAAGATTT ACGCATGGCAATAACCTTGCGGGAGCTGGATGGCCTGAGCTATGAAGAGATAGCCGCTATCATGGATTGTCCGGTAG GTACGGTGCGTTCACGTATCTTCCGAGCGAGGGAAGCTATTGATAACAAAGTTCAACCGCTTATCAGGCGTTGACGA TAGCGGGATACTGGATAAGGGTATTAGGCatgCAGAAAGAACAACTTTCCGCTTTAATGGATGGCGAAACGCTGGATA GTGAGCTGCTTAACGAACTGGCTCATAACCCAGAAATGCAGAAAACCTGGGAAAGCTATCACTTAATCCG TGACTCAATGCGGGGTGATACTCCCGAGGTGCTCCATTTCGATATCTCTTCACGCGTGATGGCCGC CATTGAAGAAGAGCCAGTACGTCAACCGGCGACATTGATCCCGGAAGCCCAGCCTGCGCC GCATCAATGGCAGAAAATGCCATTCTGGCAGAAAGTACGTCCGTGGGCGGCACAGCTTACCCAAATGGGCGTAGC CGCATGCGTATCGCTTGCAGTTATCGTTGGCGTCCAGCACTATAATGGACAATCTGAAACGTCCCAGCAGCC CGAAACGCCGGTATTTAATACACTGCCGATGATGGGTAAAGCCAGCCCGGTAAGCCTGGGAGTACCTTCTGAAGCG ACCGCAAACAATGGTCAACAGCAGCAGGTACAGGAGCAGCGTCGTCGCATTAATGCAATGTTGCAGGATTACG AACTGCAACGCCGACTCCACTCTGAACAGCTTCAGTTTGAGCAGGCGCAAACCCAGCAAGCCGCTGTACAG GTGCCAGGAATTCAAACTTTAGGAACGCAATCGCAGGATTACAAAGATCATGACGGGGACTACAAAGA TCACGATATAGATTATAAAGATGACGATGACAAAtaaATTATAAAAATTGCCTGATACGCTGCGCTTATCAGGCCTA	used as a template for amplification of recombination substrate for creation of P_{BAD}-*rseA-3XFLAG*
P_{BAD}-*rseAcm1-3XFLAG* gBlock	AcctgacgctttttatcgcaactctctactgtttctccaTGAGACAGATAGTTTTCCGAACTATTGAGTCCCT CCCGGAAGATTTACGCATGGCAATAACCTTGCGGGAGCTGGATGGCCTGAGCTATGAAGA GATAGCCGCTATCATGGATTGTCCGGTAGGTACGGTGCGTTCACGTATCTTCCGAGCG ACCCAAGCTATTGATAACAAAGTTCAACCGCTTATCAGGCGTTGACGATAGCGGG ATACTGGATAAGGGTATTAGGCatgCAGAAAGAACAACTTTCCGCTTTAATGGATGGCGA AACGCTGGATAGTGAGCTGCTTAACGAACTGGCTCATAACCCAGAAATGCAGAAAACCTG GGAAAGCTATCACTTAATCCGTGACTCAATGCGGGGTGATACTCCCGAGGTGCTCCATTT CGATATCTCTTCACGCGTGATGGCCGCCATTGAAGAAGAGCCAGTACGTCAACCGGCGACAT TGATCCCGGAAGCCCAGCCTGCGCCGCATCAATGGCAGAAAATGCCATTCTGGCAGAA AGTACGTCCGTGGGCGGCACAGCTTACCCAAATGGGCGTAGCCGCATGCGTATCGCTTGCAGTTATCGTTGGCGTCC AGCACTATAATGGACAATCTGAAACGTCCCAGCAGCCCGAAACGCCGGTATTTAATACACTGCCGATGATGGGTAA AGCCAGCCCGGTAAGCCTGGGAGTACCTTCTGAAGCGACCGCAAACAATGGTCAACAGCAGCAGGTACAGGAG CAGCGTCGTCGCATTAATGCAATGTTGCAGGATTACGAACTGCAACGCCGACTCCACTCTGAACAGCTTCAGTT TGAGCAGGCGCAAACCCAGCAAGCCGCTGTACAGGTGCCAGGAATTCAAACTTTAGGAACGCAATCGCAGGA TTACAAAGATCATGACGGGGACTACAAAGATCACGATATAGATTATAAAGATGACGATGACAAAtaaATTATAA AAATTGCCTGATACGCTGCGCTTATCAGGCCTA	used as a template for amplification of recombination substrate for creation of P_{BAD}-*rseAcm1-3XFLAG*

30°C and then shifted 43.5°C to induce expression of λ-Red proteins. Transformants were grown on LB agar plates supplemented with ampicillin, to a final concentration of 100 μg/ml. Zeomycin-resistant recombinants or transductants were selected on LB agar plates supplemented with Zeocin™ (or zeomycin) to a final concentration of 25 μg/ml. Small RNA screens were executed on MacConkey-Lactose (Mac-Lac) agar plates supplemented with ampicillin, to a final concentration of 100 μg/ml, and arabinose to a final concentration of 0.02% or 0.00002%. All gene fusions were created as previously described using recombineering and selecting for recombinant fusions on M63 minimal salt agar plates supplemented with glycerol, 6% sucrose, and 80 μg/ml of X-gal at 30°C (Mandin and Gottesman, 2009). For iron starvation experiments, cultures were grown in LB media in a shaking water bath at 37°C to an OD_{600} of 0.3 and then treated with 2′2-dipyridyl (Sigma Aldrich) to a final concentration of 250 μM for 30 min. For RNA stability assays, rifampicin was added to bacterial cultures to a final concentration of 250 μg/ml.

Bacterial Strains, Plasmids, and Genetic Constructs

All strains used for experiments conducted in this study were derivatives of *Escherichia coli* K-12 MG1655. Cloning reactions were executed in MC1061 or NEB5α (New England Biolabs). All strains are listed in **Table 1**. All plasmids used in this study are listed in **Table 2**. All oligonucleotides used for polymerase chain reaction (PCR)-mediated genetic engineering, PCR screening, or Northern blot analysis are listed in **Table 3**. λ-Red recombineering reactions to gene fusions were executed in strain PM1800. PM1800 has a *cat-sacB* cassette inserted in the *lac* locus and encodes the λ-Red proteins (*gam*, *exo*, and *beta*) on a partial lambda vector marked with tetracycline resistance (mini-λ:*tet*). Plasmids from the small RNA library or their respective mutants were transformed into the P_{BAD}-*rseA27-lacZ* translational fusion strain using TSS transformation (Chung et al., 1989). Mutations were transduced into reporter fusion strains using Bacteriophage P1 transduction.

Construction of P_{BAD}-*rseA27-lacZ* and Translational Fusion and P_{BAD}-*rseA*-3XFLAG Strains

In order to execute our screen for small RNA regulation of the *rseABC* operon, we first created an arabinose-inducible in-frame translational fusion of the first nine codons of the *rseA* gene (*rseA27*) to the ninth codon of *lacZ via* recombineering into strain PM1800 as previously described (Mandin and Gottesman, 2009). We also created a 3XFLAG-tagged allele of the entire *rseA* gene at the lac locus using the same recombineering method (Mandin and Gottesman, 2009). All the fusions contained the entire 5′ UTR of the *rseABC* transcript (**Figure 1A**) immediately downstream from the arabinose-inducible *araBAD* promoter (P_{BAD}). To create the allelic exchange substrates for either the P_{BAD}-*rseA27-lacZ*, P_{BAD}-*rseA27cm1-lacZ*, P_{BAD}-*rseA27cm3-lacZ*, or P_{BAD}-*rseA*-3XFLAG, or P_{BAD}-*rseAcm1*-3XFLAG fusions, we amplified synthetic DNA gBlocks (IDT DNA) corresponding to each fusion using oligonucleotide primers KT902 and KT903. All synthetic DNA sequences used for genetic engineering of gene fusions are listed in **Table 4**. All oligonucleotide primers used for PCR reactions are listed in **Table 3**. We confirmed the presence of the *lacZ* translational fusion inserts by PCR using oligonucleotide primers KT940 and KT903 and DNA sequencing. We confirmed the presence of the 3XFLAG tagged alleles by PCR using oligonucleotide primers KT902 and KT1136 and DNA sequencing.

Site-Directed Mutagenesis of pBR-pLac-*ryhB*

We used the QuikChange® Site-Directed Mutagenesis Kit (Stratagene), according to the manufacturer's recommendations to create ryhB point mutants. Mutagenic primers used for the PCR reaction are listed in **Table 3**. Point mutants were verified by DNA sequencing.

β-Galactosidase Assays

Overnight cultures were grown in Lennox Broth (LB) supplemented with ampicillin and glucose to a final concentration of 100 μg/ml and 0.2%, respectively, at 37°C. The cultures were diluted 1:1000 in fresh Lennox Broth (LB) supplemented with ampicillin and arabinose to a final concentration of 100 μg/ml and 0.02%, respectively. Once the culture reached an OD_{600} of 0.4–0.5, a 100 μL aliquot was taken for the β-galactosidase assay as previously described (Miller, 1992). Alternatively, β-galactosidase assays were executed in 96-well plates as previously described (Zhou and Gottesman, 1998).

Western Blot Analysis

Cell lysates were created as previous described (Ezemaduka et al., 2014). Briefly, cells were harvested and resuspended in 300 ul of 20 mM Tris-HCl, pH 8.0, and lysed by sonication. The resulting cell lysates were centrifuged at 800 × *g* for 5-min to remove cell debris and unbroken cells. The supernatants for the respective samples were then transferred to new 1.5 ml tubes and subjected to centrifugation at 1,000 × *g* for 30 min. The resulting supernatant (soluble proteins) and precipitate (aggregated proteins) from the second centrifugation were then quantified using a Lowry assay and placed on ice. Equivalent amounts of total protein were prepared and subjected to electrophoresis using a Bolt™ 12%, Bis-Tris Protein Gel (Invitrogen), according to the manufacturer's instructions. The total proteins were then transferred to a 0.45 μm pore-size nitrocellulose membrane using a Trans-Blot® Turbo™ System (BIO-RAD) for 10 min at 2.5 A and 25 V. After the successful transfer, the membrane was washed briefly in a phosphate-buffered saline and Tween 20 (PBST) solution and then blocked at room temperature for 30 min in 0.5% Blotting-Grade nonfat milk dissolved in PBST. The membrane was incubated overnight with gentle shaking at 4°C in a 1: 50,000 dilution of a primary antibody and 0.5% Blotting-Grade nonfat milk blocking solution. The membrane was washed with PBST three times for 5 min each and incubated with gentle shaking in a 1:50,000 dilution of a secondary antibody and 0.5% Blotting-Grade nonfat milk blocking solution for 2 h. The signal was developed using a Novex AP Chemiluminescent Kit according to the manufacturer's recommendations (Thermofisher Scientific). The protein signals were visualized using the FluorChem R imager (Protein Simple).

Northern Blot Analysis

Total RNA was isolated using the hot acid phenol method as previously described (Aiba et al., 1981). RNA stability assays were performed as previously described using hot phenol following culture treatment with rifampicin to a final concentration of 250 μg/ml (Masse et al., 2003). Total RNA from each sample was mixed with the 10X RNA gel loading dye (National Diagnostics), 10X MOPS buffer, 100% formaldehyde, and 100% formamide and heated at 65°C for 15 min. The samples were loaded onto a 1% agarose gel and subjected to electrophoresis at 100 V for 40 min. The agarose gel was subjected to a nylon membrane capillary transfer. Following UV cross-linking, the membrane was pre-hybridized for 2 h using PerfectHyb™ Plus Hybridization Buffer (Sigma Aldrich). The membrane was then hybridized with a biotinylated DNA probe against RseA or 16S rRNA transcripts. (IDT DNA) for 4 h (**Table 3**). The membrane was washed with high, medium, and low stringency buffers and processed using a Chemiluminescent Detection Kit (Lifetechnologies) according to the manufacturer's recommendation. The chemiluminescent signal was detected using Fluorochem E (Protein Simple).

Statistical Analysis

All statistical analyses were executed using GraphPad Prism version 9 (GraphPad).

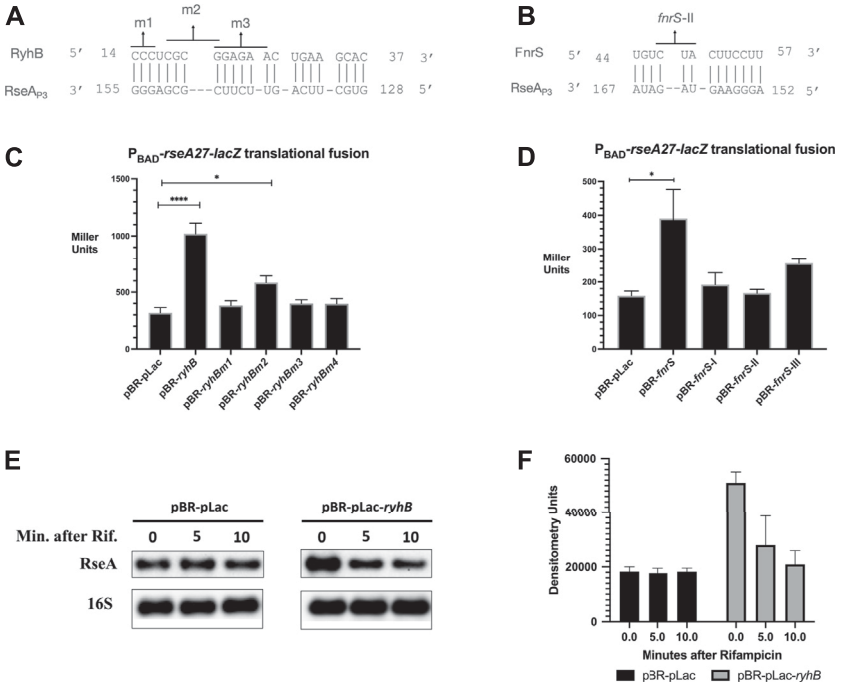

FIGURE 2 | RyhB/FnrS pairing with RseA and β-galactosidase assays **(A)**. Regions of predicted base pairing between the RyhB and RseA sequences were determined using the online computational tool IntaRNA 2.0. Point mutants in the small RNA used for interaction analysis were denoted as m1 (C14G, C15G, C16G), m2 (C18G, G19C, C20G, and G21C), or m3 (G21C, G22C, A23C, G24A, A25C, and A26C) **(B)**. Δ*ryhB* Δ*fnrS* P$_{BAD}$-*rseA27-lacZ* translational fusions containing pBR-pLac, pBR-*ryhB*, pBR-pLac-*ryhBm1*, pBR-pLac-*ryhBm2*, or pBR-pLac-*ryhBm3* were grown in rich media to an OD$_{600}$ of 0.5, and aliquots were isolated for the β-galactosidase assay **(C)**. Regions of predicted base pairing between FnrS small RNA and the 5′ UTR of RseA were determined using the online computational tool IntaRNA 2.0. One of the *fnrS* point mutants tested occurs in the region of pairing shown **(B)**. Δ*ryhB* Δ*fnrS* P$_{BAD}$-*rseA27-lacZ* translational fusions containing pBR-pLac, pBR-*ryhB*, pBR-pLac-*ryhBm1*, pBR-pLac-*ryhBm2*, or pBR-pLac-*ryhBm3* were grown in rich media to an OD$_{600}$ of 0.5, and aliquots were isolated for the β-galactosidase assay **(D)**. Δ*ryhB* Δ*fnrS* P$_{BAD}$-*rseA27-lacZ* translational fusions containing pBR-pLac, pBR-*fnrS*, pBR-pLac-*fnrS*-I, pBR-pLac-*fnrS*-II, or pBR-pLac-*fnrS*-III were grown in rich media to an OD$_{600}$ of 0.5, and aliquots were isolated for the β-galactosidase assay **(E)**. P$_{BAD}$-*rseA*27-lacZ translational fusions were grown to the mid-exponential phase and induced with arabinose and IPTG to a final concentration of 0.2% and 1 mM, respectively. Cultures were then treated with rifampicin, and total RNA was isolated at 5 and 10 min following rifampicin treatment. RNA was subjected to northern blot analysis using a biotinylated RseA probe **(F)**. Densitometric analysis of northern blot is shown in **Panel E**. All β-galactosidase assays and densitometry assays were executed in triplicate and are represented as averages ± the standard error of the mean (SEM). Statistical significance was assessed by one-way ANOVA with Dunnett's post hoc test (*$p < 0.05$, ****$p < 0.0001$).

RESULTS

RyhB and FnrS were Picked up in a Genetic Screen for Small RNA Regulators of RseA Expression

The start site of the *rseA*$_{P3}$ promoter is 228 nucleotides upstream from the *rseA* start codon. The 228 nucleotide 5′ UTR likely forms a secondary structure that influences translational initiation in concert with small RNAs. We therefore hypothesized that the *rseABC* operon, driven by the *rseA*$_{P3}$ promoter, was regulated at the post-transcriptional level by a small RNA. In order to determine if the *rseA*$_{P3}$ transcript was regulated by a small RNA, we constructed an arabinose-inducible *rseA-lacZ* translational gene fusion (**Figure 1A**). We then transformed the P$_{BAD}$-*rseA27-lacZ* translational fusion strain with a plasmid based small RNA library as previously described (Mandin and Gottesman, 2009). This small RNA library contains 30 of the most extensively characterized *E. coli* small RNAs cloned downstream of an isopropyl β-d-1-thiogalactopyranoside (IPTG)-inducible promoter (Mandin and Gottesman, 2009). We executed the small RNA library screen on MacConkey-Lactose (Mac-Lac) agar plates supplemented with ampicillin to a final concentration of 100 μg/ml and arabinose to a final concentration of 0.0002%. This arabinose concentration was sufficient to induce basal transcription from the P$_{BAD}$ promoter without producing a strong Lac$^+$ phenotype. The concentration of lactose in the Mac-Lac plates was sufficient to induce small RNA expression from the IPTG-inducible promoter. We hypothesized that this screening condition was ideal for the possible identification of stimulatory small RNAs. Two of the 30 plasmids, carrying RyhB or FnrS, resulted in an increased Lac phenotype (**Figure 1B**), suggesting that RyhB and FnrS promote post-transcriptional expression of RseA.

RyhB and FnrS Point Mutants are Defective in Stimulating RseA Expression

To validate the results of our genetic screen, we executed computational analysis to identify regions of potential complementary base pairing between RyhB or FnrS and the

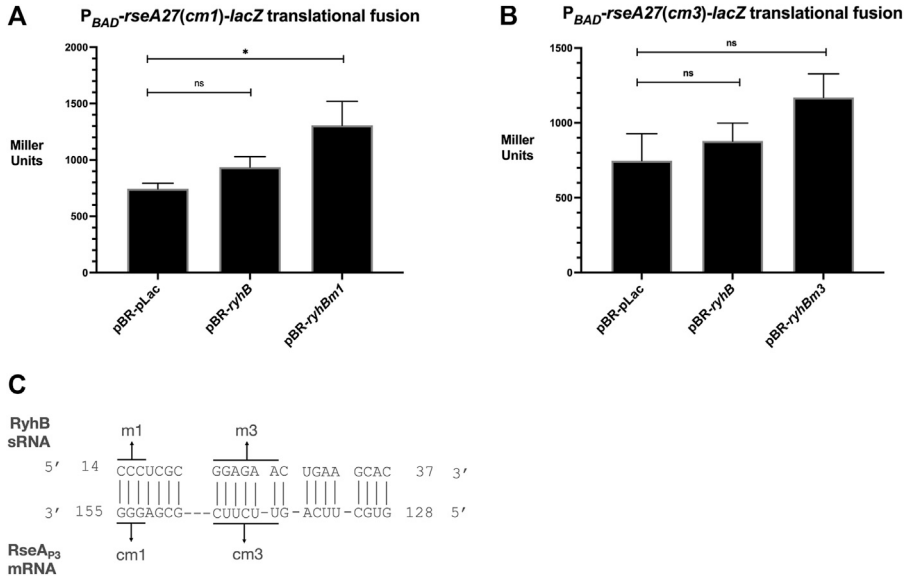

FIGURE 3 | RyhB-RseA compensatory mutational analysis **(A)**. The P$_{BAD}$-*rseA27*cm1-*lacZ* translational fusion strain transformed with pBR-pLac, pBR-pLac-*ryhB*, or pBR-pLac-*ryhBm1* was grown to the mid-log phase (OD$_{600}$ of 0.5) in LB supplemented with ampicillin and arabinose to final concentrations of 100 μg/ml and 0.02%, respectively, and 100 μL aliquots were isolated for the β-galactosidase assay **(B)**. The P$_{BAD}$-*rseA27*cm3-*lacZ* translational fusion strain transformed with pBR-pLac, pBR-pLac-*ryhB*, or pBR-pLac-*ryhBm3* was grown to the mid-log phase (OD$_{600}$ of 0.5) in LB supplemented with ampicillin and arabinose to final concentrations of 100 μg/ml and 0.02%, respectively, and 100 μL aliquots were isolated for the β-galactosidase assay **(C)**. Putative nucleotide interactions between RyhB and RseA tested with RyhB mutants and RseA compensatory mutants. All β-galactosidase assays were executed in triplicate and are represented as averages ± SEM. Statistical significance was assessed by one-way ANOVA with Dunnett's post hoc test (*$p < 0.05$).

RseA leader region (**Figures 2A,B**). Specifically, we screened the RyhB and FnrS sequences against the RseA$_{P3}$ 5′ UTR sequence using IntaRNA 2.0. For RyhB, we identified a semi-continuous stretch of nucleotides between C14 and C37 with complementarity to RseA$_{P3}$ G128 to G155 (**Figure 2A**). The longest stretch of complementarity was seven base pairs between RyhB C14 to RyhB C20 and RseA G148 to G155. For FnrS, we identified a semi-continuous stretch of nucleotides between U44 and U57 with complementarity to RseA$_{P3}$ A152 and A167 (**Figure 2B**). The longest stretch of which was a seven base pair region of complementarity between FnrS C51 to U57 and RseA A152 to G158 (**Figure 2B**). We then created nucleotide point mutants in the plasmid-based RyhB construct that would disrupt the predicted complimentary base pairing between RyhB and RseA (**Figure 2A**). The RyhB point mutants consist of the following changes: m1 (C14G, C15G, C16G), m2 (C18G, G19C, C20G, and G21C), and m3 (G21C, G22C, A23C, G24A, A25C, and A26C) (**Figure 2A**). The FnrS point mutants were previously described and consist of the following changes: *fnrS*-I (U57A, U58G, U59A), *fnrS*-II (C47A U48A U49G), and *fnrS*-III (G4C, G5U) (Durand and Storz, 2010).

In order to determine if the RyhB nucleotides predicted to pair with RseA are necessary for RseA stimulation, we determined the activity of the P$_{BAD}$-*rseA27-lacZ* translational fusion upon over-expression of wild type and mutant alleles of RyhB. We executed these assays in a *ryhB*$^{-}$ *fnrS*$^{-}$ genetic background to ensure that the plasmids were the only source of RyhB or FnrS expression. We grew all strains in LB (Lennox) supplemented with ampicillin and arabinose to final concentrations of 100 μg/ml and 0.02%, respectively. We then obtained 100 μL aliquots of each culture in the mid-log phase of growth (OD$_{600}$ of 0.5) and measured β-galactosidase activity. As expected, plasmid-based RyhB induced P$_{BAD}$-*rseA27-lacZ* activity by approximately 3-fold in comparison to the vector control (**Figure 2C**), while all RyhB point mutants were defective for stimulation of P$_{BAD}$-*rseA27-lacZ* (**Figure 2C**). This confirms the results of our genetic screen and suggests that RyhB stimulates post-transcriptional expression of RseA. Further, it suggests that RyhB nucleotides predicted to pair with nucleotides in the RseA leader region are necessary for RyhB post-transcriptional stimulation of RseA expression (**Figure 2C**). We executed a similar experiment using FnrS and a series of FnrS point mutants to determine if FnrS may stimulate the post-transcriptional expression of RseA. FnrS expression results in a 2-fold increase in P$_{BAD}$-*rseA27-lacZ*. Each of the FnrS point mutants were also defective for stimulation of P$_{BAD}$-*rseA27-lacZ*. To determine if the RyhB stimulatory effect on RseA$_{P3}$ expression was due to an increase in RseA mRNA stability, we tested the stability of the RseA-LacZ following over-expression of RyhB (**Figures 2E,F**). We observed a 2-fold increase in RseA-LacZ mRNA levels prior to the initiation of mRNA stability measures. The change in RseA-LacZ mRNA levels is similar to the change in P$_{BAD}$-*rseA27-lacZ* activity in the presence of RyhB. This suggests that RyhB stimulation of RseA post-transcriptional expression could occur at the level of transcription termination as previously described (Chen et al., 2019).

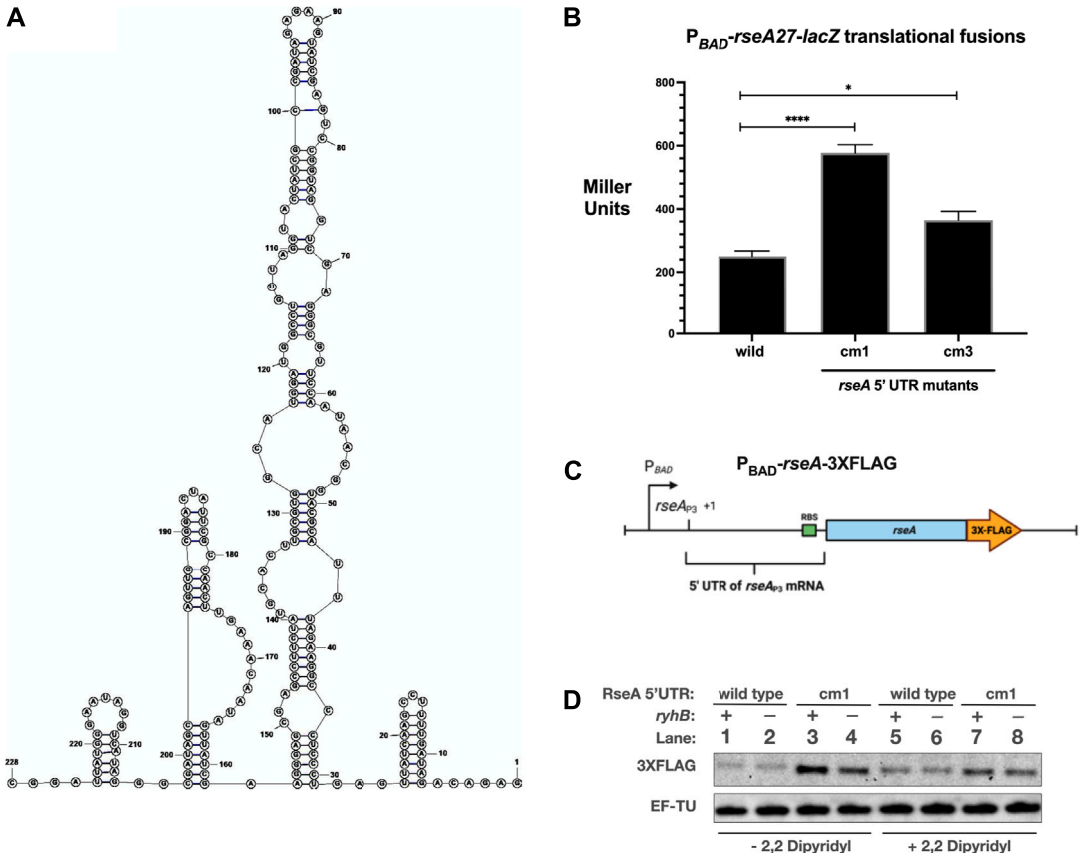

FIGURE 4 | 5′ UTR mutations stimulate RseA translation **(A)**. Predicted structure of RseA$_{P3}$ 5′ UTR using RNAStructure **(B)**. The wild-type, cm1, and cm3 alleles of the P$_{BAD}$-*rseA27-lacZ* translational fusion strains were grown in rich media to the mid-log phase (OD$_{600}$ of 0.5), and aliquots were isolated for β-galactosidase activity **(C)**. Schematic of the P$_{BAD}$-*rseA*-3XFLAG allele utilized for the subsequent RseA-FLAG western blot **(D)**. RseA-FLAG western blot. The wild-type and cm1 P$_{BAD}$-*rseA*-3XFLAG strains were grown in LB supplemented with arabinose to a final concentration of 0.002% to the mid-log phase and then treated with 2,2-dipyridyl to a final concentration of 250 μM. Total proteins were isolated and subjected to western blot analysis using α-FLAG. All β-galactosidase assays were executed in triplicate and are represented as averages ± SEM. Statistical significance was assessed by one-way ANOVA with Dunnett's post hoc test (*$p < 0.05$, ****$p < 0.0001$).

Compensatory Mutations in RseA Suggest that RyhB Interacts with the RseA Leader Region

In order to test the hypothesis that RyhB stimulates RseA through the direct interaction between complementary nucleotides, we designed putative compensatory nucleotide point mutations in the 5′UTR of P$_{BAD}$-*rseA27-lacZ* translational fusions that were predicted to restore the ability of RyhB m1 or RyhB m3 mutants to stimulate P$_{BAD}$-*rseA27-lacZ* activity (**Figure 3C**). The P$_{BAD}$-*rseA27*(*cm1*)-*lacZ* translational fusion contains G153C G154C G155C nucleotide point mutants within the RseA 5′ UTR regions of the fusion, which were predicted to interact with the RyhB m1 allele (**Figure 3C**). The P$_{BAD}$-*rseA27* (*cm3*)-*lacZ* allele contains U139G U141G C142U U143G U144G C145G nucleotide point mutants within the RseA 5′ UTR regions of the fusion, which were predicted to interact with the RyhBm3 allele (**Figure 3C**). RyhB over-expression does not result in the stimulation of cm1 or cm3 mutants of the P$_{BAD}$-*rseA27-lacZ* fusion (**Figures 3A,B**). However, the expression of the RyhBm1 mutant was able to stimulate the P$_{BAD}$-*rseA27*(*cm1*)-*lacZ* fusion, approximately 2-fold in comparison to the vector control (**Figure 3A**). In addition, the RyhBm3 allele was able to stimulate the P$_{BAD}$-*rseA27*(*cm3*)-*lacZ* fusion, approximately 2-fold in comparison to the vector control (**Figure 3B**). These results suggest that RyhB activates post-transcriptional expression of RseA because of a direct interaction between RyhB and the RseA 5′ UTR. Furthermore, this interaction requires RyhB C14 C15 C16 nucleotides and the RseA 5′ UTR G153 G154 G155 nucleotides, as well as RyhB nucleotides G21, G22, A23, G24, A25, A26 and RseA nucleotides U139, U141, C142, U143, U144, C145 (**Figure 3A**).

Optimal Post-Transcriptional Expression of RseA$_{P3}$ is Inhibited by 5′ UTR Sequences

Since the RseA$_{P3}$ transcript is stimulated by RyhB and FnrS and RseA mRNA stability is not affected by RyhB over-expression, it is logical to assume that translation is repressed in the absence of the stimulatory small RNAs. Since the compensatory mutants in the RseA 5′ UTR subdued the ability of RyhB to stimulate RseA

translation, we hypothesized that the cm1 and cm3 mutations would result in increased post-transcriptional expression of RseA in the absence of stimulatory RNAs RyhB and FnrS (**Figures 2**, **3A**,**B**). The 5′ UTR sequence of the $RseA_{P3}$ transcript was analyzed using the RNAStructure program. The predicted secondary structure contains several hairpins that may affect translation efficiency and accessibility of the RseA Shine Delgado sequence (**Figure 4A**). To test the hypothesis that the RseA compensatory mutant alleles have higher expression than wild-type alleles, we measured the activity of wild-type, cm1, and cm3 alleles of the P_{BAD}-*rseA27-lacZ* translational fusion in the mid-log phase in rich media (**Figure 4B**). Both cm1 and cm3 alleles had higher β-galactosidase activity than the wild-type fusion (**Figure 4B**). The activity of the P_{BAD}-*rseA27*(*cm3*)-*lacZ* translational fusion was approximately 3-fold higher than the activity of the wild-type P_{BAD}-*rseA27-lacZ* translational fusion (**Figure 4B**). The activity of the P_{BAD}-*rseA27* (*cm3*)-*lacZ* translational fusion was approximately 1.5–2-fold higher than the activity of the wild-type P_{BAD}-*rseA27-lacZ* translational fusion (**Figure 4B**). We also created a chromosomal 3XFLAG epitope-tagged allele of *rseA*, driven by an arabinose inducible promoter, to measure post-transcriptional expression of the $RseA_{P3}$ transcript in a manner that uncouples its synthesis from envelope stress (P_{BAD}-*rseA*-3XFLAG at the *lac* locus–**Figure 4C**). We also created a cm1 allele of the P_{BAD}-*rseA*-3XFLAG allele. This would allow us to determine if the RseA 5′ UTR mutations that increase P_{BAD}-*rseA27-lacZ* activity correspond to increased RseA protein levels. We then grew (*ryhB*$^+$ and *ryhB*$^-$) wild-type and cm1 5′ UTR alleles of P_{BAD}-*rseA*-3XFLAG in rich media supplemented with 0.002% arabinose to induce RseA-3XFLAG expression. At the mid-logarithmic phase, cultures were treated with 2,2-dipyridyl for 30 min to deplete iron and induce RyhB expression. We then isolated total protein and measured RseA-FLAG expression. RseA-FLAG levels were increased by at least 3-fold in the cm1 5′ UTR genetic background compared to the wild-type 5′ UTR genetic background (**Figure 4D**, lane 3 vs lane 1), consistent with our β-galactosidase assay results in **Figure 4B**. This further supports the idea that the wild-type sequence of the $RseA_{P3}$ 5′ UTR contains secondary structures that prevent optimal translation. Also, the absence of *ryhB* in the cm1 5′ UTR genetic background resulted in a 3-fold decrease in RseA-FLAG protein levels from cells grown in rich media without 2,2-dipyridyl supplementation (**Figure 4D**, lane 4 vs lane 3). This suggests that the cm1 mutation is not sufficient for complete inhibition of RyhB stimulation of RseA expression. Unexpectedly, we did not see this difference in RseA-FLAG protein levels isolated from cells grown in rich media supplemented with 2,2-dipyridyl. In addition, the absence of *ryhB* did not change RseA-FLAG protein levels in the wild-type 5' UTR genetic background for cells grown in rich media without 2,2-dipyridyl, whereby RyhB levels are not expected to be repressed by Fur. (**Figure 4D**, lanes 1 and 2). Unexpectedly, for reasons that are not clear, the absence of *ryhB* had no noticeable effect on the stimulation of RseA-FLAG protein levels under iron starvation conditions (**Figure 4D**, lanes 5 and 6).

DISCUSSION

Optimal levels of σ^E are critically important for a functional ESR. The absence of σ^E precludes the initiation of the ESR. Excess σ^E results in aberrant cell physiology and ultimately cell death (Nitta et al., 2000; Kabir et al., 2005). Fine tuning the synthesis and activity of σ^E is the major tool that the cell uses in order to achieve this goal. The *rpoE* operon includes several negative regulators of σ^E activity: *rseA*, *rseB*, and *rseC*, in addition to the *rpoE* leader peptide *rseD* (Klein et al., 2016). This particular operon has several promoters controlled by several transcriptional regulators and sigma factors, responding to a multitude of conditions (Klein et al., 2016). Since the negative regulators of σ^E are cistronic to *rpoE*, a negative feedback loop for σ^E activity is built into the synthesis of *rpoE*. The $rseA_{P3}$ promoter drives the transcription of the *rseA-rseB-rseC* operon (Rhodius et al., 2006). Since this operon differs from the *rpoE* operon only in the absence of the *rseD* and *rpoE* genes, it suggests that secondary synthesis of the negative regulators of σ^E activity are necessary under conditions that are unique and separate from conditions driving the synthesis of the *rpoE* operon. The $rseA_{P3}$ promoter and one of the several promoters of the *rpoE* operon are σ^E-dependent. This highlights the regulatory redundancy in the σ^E-dependent synthesis of RseA at the level of transcriptional initiation (Rhodius et al., 2006; Klein et al., 2016). This redundancy is likely reconciled through post-transcriptional regulation of $rpoE_P$ and $rseA_{P3}$ transcripts *via* mechanisms described in this work and additional regulatory switches that are undiscovered (Yakhnin et al., 2017). Genetic analysis of the P_{BAD}-*rseA27-lacZ* translational fusion, RseA-FLAG protein levels from a P_{BAD}-*rseA*-3XFLAG epitope-tagged allele, suggests that the wild-type sequence of the $RseA_{P3}$ 5′ UTR prevents optimal RseA expression (**Figure 3**), presumably through RNA secondary structures that prevent efficient translation or promoting degradation of the $RseA_{P3}$ transcript. This likely promotes tight control of RseA levels, specifically preventing excess of RseA levels in response to σ^E activity. However, the existence of the $rseA_{P3}$ transcript driven by σ^E-dependent promoters suggests that under specific conditions in concern with the σ^E-dependent ESR, the cell requires the synthesis of additional RseA to prevent excess activity of σ^E, which is deleterious in nature. The presence of a relatively long 5′ UTR, with a secondary structure suboptimal for the promotion of post-transcriptional expression, is an ideal cognate partner for one or more small regulatory RNAs. While a direct interaction with RseA is necessary for the post-transcriptional regulatory effect of RyhB, its precise molecular mechanism is not clear but a part of an ongoing investigations in our lab. The difference in RyhB-dependent RseA-LacZ mRNA decay rates suggests that a complicated mechanism of action may occur. Possible pathways for the RyhB regulatory effect on RseA include modulation of translation initiation or transcription termination.

We identified RyhB and FnrS as small RNAs with positive regulatory effects on RseA synthesis using a targeted genetic screen of a small RNA library. FnrS expression is induced in response to

oxygen limitation (Durand and Storz, 2010). RyhB is expressed under iron-limiting conditions upon de-activation of the Fur repressesor (Masse and Gottesman, 2002). RyhB was also previously identified as a binding partner for RseA using the RNA interaction by ligation and sequencing (RIL-seq) (Melamed et al., 2016). RyhB is known to repress post-transcriptional expression of a host of genes, including iron sulfur cluster proteins involved in the tricarboxylic acid cycles, in response to iron limitation (Masse and Gottesman, 2002; Masse et al., 2003; Semsey et al., 2006; Desnoyers and Masse, 2012; Wright et al., 2013). There is at least one positive regulatory target for RyhB, the shikimate permease gene ShiA (Prevost et al., 2007). FnrS has several regulatory targets, all of which are negative regulatory targets (Boysen et al., 2010; Durand and Storz, 2010; Wright et al., 2013). The observations in this work expand the RyhB regulon by adding a second positive regulatory target. This work also expands the FnrS regulon by uncovering the first positive regulatory target of FnrS. RyhB and FnrS share three unique targets, SodA, SodB, and MarA (Masse and Gottesman, 2002; Afonyushkin et al., 2005; Boysen et al., 2010; Durand and Storz, 2010; Argaman et al., 2012; Wright et al., 2013). In addition, both RyhB and FnrS have post-transcriptional regulatory targets in the *iscR-iscS-iscU-iscA* operon (Desnoyers et al., 2009; Wright et al., 2013). Our observation of both RyhB and FnrS regulating RseA is consistent with previously reported overlapping targets for RyhB and FnrS. RyhB and RseA are highly conserved in Gram-negative bacteria. It is possible that RyhB homologues or other small RNAs in these bacterial species regulate the post-transcriptional synthesis of RseA homologues.

For reasons that are not clear, there may be an increased requirement for RseA synthesis when iron, or oxygen, limitation occurs simultaneously with envelope stress. In our studies, we observed an increase in RseA-FLAG protein levels under iron-limiting conditions, implicating iron starvation in the post-transcriptional expression of the $RseA_{P3}$ transcript. In the cm1 genetic background, RseA-FLAG protein levels decrease in the absence of RyhB (**Figure 4D**, lanes 3 vs 4). This supports our over-expression studies and implicate RyhB in the post-transcriptional stimulation of the $RseA_{P3}$ expression. However, it is puzzling that the *ryhB* mutant did not prevent an increase in RseA levels under iron-limiting conditions (**Figure 4D**, Lanes 1/2 vs Lanes 5/6). It is possible that the change in RseA protein levels is transient in nature. Further investigated is needed to fully ascertain the physiological link between iron limitation, RyhB, and RseA expression. However, it is clear that both iron limitation and chromosomal RyhB levels affect post-transcriptional expression of the $RseA_{P3}$ transcript. This also further suggests that excess σ^E activity may be especially deleterious to the cell under iron limitation. There have been some studies executed in *E. coli* and *Vibrio sp*. that support a link between envelope stress and iron limitation. Under iron-limiting conditions, suboptimal secretion of the siderophore enterobacterin results in the induction of the Cpx-dependent ESR (Guest et al., 2019). The Cpx-dependent ESR links iron sensing and adaptation in *Vibrio cholerae* (Acosta et al., 2015). The treatment of *Vibrio vulnificus* with the broad-spectrum antibiotic tropodithietic acid (TDA) simultaneously induced the expression of genes involved in cell envelope biogenesis, oxidative stress, and iron limitation (Dittman et al., 2019). Treatment of *V. cholerae* with polymyxin B results in induction of the σ^E-dependent stress response and iron metabolism changes (Sikora et al., 2009). From studies in these systems, there appears to be a link between the iron metabolism and envelope stress. The precise mechanisms linking the iron metabolism and envelope stress are the subject of ongoing investigations in our lab.

DATA AVAILABILITY STATEMENT

The raw data supporting the conclusion of this article will be made available by the authors, without undue reservation.

AUTHOR CONTRIBUTIONS

LL, JA, and JN executed experiments associated with data in the article and also contributed to the writing and editing of the article. KT created the hypotheses driving the experiments in the study, designed the experiments associated with the data in the article, and contributed to the writing and editing of the article.

FUNDING

This work was supported by a grant (SC2GM105419) from the National Institute of General Medical Sciences (NIGMS) of the National Institutes of Health (United States), Howard University College of Medicine Bridge Fund and Pilot Study Award, Howard University Medical Alumni Association Basic Science Chair Award, and the Small Equipment and Research Resource Award from the Howard University Office of the Provost to KT. In addition, this work was also supported by a grant (1011634) from the National Institute of Food and Agriculture (NIFA) of the United States Department of Agriculture (USDA) to LL.

ACKNOWLEDGMENTS

We would like to thank members of the Thompson Lab for their comments and critique of this article. We would also like to thank Gisela Storz for generously donating plasmids pBR-*fnrS*-I, pBR-*fnrS*-II, and pBR-*fnrS*-III for this study.

REFERENCES

Acosta, N., Pukatzki, S., and Raivio, T. L. (2015). The *Vibrio cholerae* Cpx Envelope Stress Response Senses and Mediates Adaptation to Low Iron. *J. Bacteriol.* 197, 262–276. doi:10.1128/jb.01957-14

Ades, S. E., Connolly, L. E., Alba, B. M., and Gross, C. A. (1999). The *Escherichia coli* Sigma E-Dependent Extracytoplasmic Stress Response Is Controlled by the Regulated Proteolysis of an Anti-Sigma Factor. *Genes Develop.* 13, 2449–2461. doi:10.1101/gad.13.18.2449

Afonyushkin, T., Vecerek, B., Moll, I., Blasi, U., and Kaberdin, V. R. (2005). Both RNase E and RNase III Control the Stability of *sodB* mRNA upon Translational Inhibition by the Small Regulatory RNA RyhB. *Nucleic Acids Res.* 33, 1678–1689. doi:10.1093/nar/gki313

Aiba, H., Adhya, S., and De Crombrugghe, B. (1981). Evidence for Two Functional Gal Promoters in Intact *Escherichia coli* Cells. *J. Biol. Chem.* 256, 11905–11910. doi:10.1016/s0021-9258(19)68491-7

Alba, B. M., Leeds, J. A., Onufryk, C., Lu, C. Z., and Gross, C. A. (2002). DegS and YaeL Participate Sequentially in the Cleavage of RseA to Activate the Sigma E-Dependent Extracytoplasmic Stress Response. *Genes Dev.* 16, 2156–2168. doi:10.1101/gad.1008902

Argaman, L., Elgrably-Weiss, M., Hershko, T., Vogel, J., and Altuvia, S. (2012). RelA Protein Stimulates the Activity of RyhB Small RNA by Acting on RNA-Binding Protein Hfq. *Proc. Natl. Acad. Sci.* 109, 4621–4626. doi:10.1073/pnas.1113113109

Balbontín, R., Fiorini, F., Figueroa-Bossi, N., Casadesús, J., and Bossi, L. (2010). Recognition of Heptameric Seed Sequence Underlies Multi-Target Regulation by RybB Small RNA in *Salmonella enterica*. *Mol. Microbiol.* 78, 380–394. doi:10.1111/j.1365-2958.2010.07342.x

Boysen, A., Møller-Jensen, J., Kallipolitis, B., Valentin-Hansen, P., and Overgaard, M. (2010). Translational Regulation of Gene Expression by an Anaerobically Induced Small Non-Coding RNA in *Escherichia coli*. *J. Biol. Chem.* 285, 10690–10702. doi:10.1074/jbc.m109.089755

Campbell, E. A., Tupy, J. L., Gruber, T. M., Wang, S., Sharp, M. M., Gross, C. A., et al. (2003). Crystal Structure of *Escherichia coli* σE with the Cytoplasmic Domain of its Anti-σ RseA. *Mol. Cel* 11, 1067–1078. doi:10.1016/s1097-2765(03)00148-5

Chen, J., Morita, T., and Gottesman, S. (2019). Regulation of Transcription Termination of Small RNAs and by Small RNAs: Molecular Mechanisms and Biological Functions. *Front Cel Infect Microbiol* 9, 201. doi:10.3389/fcimb.2019.00201

Chung, C. T., Niemela, S. L., and Miller, R. H. (1989). One-step Preparation of Competent *Escherichia coli*: Transformation and Storage of Bacterial Cells in the Same Solution. *Proc. Natl. Acad. Sci.* 86, 2172–2175. doi:10.1073/pnas.86.7.2172

Costanzo, A., and Ades, S. E. (2006). Growth Phase-Dependent Regulation of the Extracytoplasmic Stress Factor, σ E , by Guanosine 3′,5′-Bispyrophosphate (ppGpp). *J. Bacteriol.* 188, 4627–4634. doi:10.1128/jb.01981-05

Costanzo, A., Nicoloff, H., Barchinger, S. E., Banta, A. B., Gourse, R. L., and Ades, S. E. (2008). ppGpp and DksA Likely Regulate the Activity of the Extracytoplasmic Stress Factor σEinEscherichia Coliby Both Direct and Indirect Mechanisms. *Mol. Microbiol.* 67, 619–632. doi:10.1111/j.1365-2958.2007.06072.x

Dartigalongue, C., Missiakas, D., and Raina, S. (2001). Characterization of the Escherichia colıçE Regulon. *J. Biol. Chem.* 276, 20866–20875. doi:10.1074/jbc.m100464200

De Las Penans, A., Connolly, L., and Gross, C. A. (1997). The sE-Mediated Response to Extracytoplasmic Stress in *Escherichia coli* Is Transduced by RseA and RseB, Two Negative Regulators of sE. *Mol. Microbiol.* 24, 373–385.

Desnoyers, G., and Masse, E. (2012). Noncanonical Repression of Translation Initiation through Small RNA Recruitment of the RNA Chaperone Hfq. *Genes Develop.* 26, 726–739. doi:10.1101/gad.182493.111

Desnoyers, G., Morissette, A., Prévost, K., and Massé, E. (2009). Small RNA-Induced Differential Degradation of the Polycistronic mRNA iscRSUA. *EMBO J.* 28, 1551–1561. doi:10.1038/emboj.2009.116

Dittmann, K. K., Porsby, C. H., Goncalves, P., Mateiu, R. V., Sonnenschein, E. C., Bentzon-Tilia, M., et al. (2019). Tropodithietic Acid Induces Oxidative Stress Response, Cell Envelope Biogenesis and Iron Uptake in *Vibrio Vulnificus*. *Environ. Microbiol. Rep.* 11, 581–588. doi:10.1111/1758-2229.12771

Douchin, V., Bohn, C., and Bouloc, P. (2006). Down-Regulation of Porins by a Small RNA Bypasses the Essentiality of the Regulated Intramembrane Proteolysis Protease RseP in *Escherichia coli*. *J. Biol. Chem.* 281, 12253–12259. doi:10.1074/jbc.m600819200

Durand, S., and Storz, G. (2010). Reprogramming of Anaerobic Metabolism by the FnrS Small RNA. *Mol. Microbiol.* 75, 1215–1231. doi:10.1111/j.1365-2958.2010.07044.x

Erickson, J. W., Vaughn, V., Walter, W. A., Neidhardt, F. C., and Gross, C. A. (1987). Regulation of the Promoters and Transcripts of rpoH, the *Escherichia coli* Heat Shock Regulatory Gene. *Genes Develop.* 1, 419–432. doi:10.1101/gad.1.5.419

Ezemaduka, A. N., Yu, J., Shi, X., Zhang, K., Yin, C.-C., Fu, X., et al. (2014). A Small Heat Shock Protein Enables *Escherichia coli* to Grow at a Lethal Temperature of 50 C Conceivably by Maintaining Cell Envelope Integrity. *J. Bacteriol.* 196, 2004–2011. doi:10.1128/jb.01473-14

Flynn, J. M., Levchenko, I., Sauer, R. T., and Baker, T. A. (2004). Modulating Substrate Choice: The SspB Adaptor Delivers a Regulator of the Extracytoplasmic-Stress Response to the AAA+ Protease ClpXP for Degradation. *Genes Develop.* 18, 2292–2301. doi:10.1101/gad.1240104

Guest, R. L., Court, E. A., Waldon, J. L., Schock, K. A., and Raivio, T. L. (2019). Impaired Efflux of the Siderophore Enterobactin Induces Envelope Stress in *Escherichia coli*. *Front. Microbiol.* 10, 2776. doi:10.3389/fmicb.2019.02776

Johansen, J., Rasmussen, A. A., Overgaard, M., and Valentin-Hansen, P. (2006). Conserved Small Non-Coding RNAs that Belong to the σE Regulon: Role in Down-Regulation of Outer Membrane Proteins. *J. Mol. Biol.* 364, 1–8. doi:10.1016/j.jmb.2006.09.004

Kabir, M. S., Yamashita, D., Koyama, S., Oshima, T., Kurokawa, K., Maeda, M., et al. (2005). Cell Lysis Directed by σ E in Early Stationary Phase and Effect of Induction of the rpoE Gene on Global Gene Expression in *Escherichia coli*. *Microbiology* 151, 2721–2735. doi:10.1099/mic.0.28004-0

Kanehara, K., Ito, K., and Akiyama, Y. (2002). YaeL (EcfE) Activates the Sigma E Pathway of Stress Response through a Site-2 Cleavage of Anti-Sigma E, RseA. *Genes Dev.* 16, 2147–2155. doi:10.1101/gad.1002302

Klein, G., Lindner, B., Brade, H., and Raina, S. (2011). Molecular Basis of Lipopolysaccharide Heterogeneity in *Escherichia coli*. *J. Biol. Chem.* 286, 42787–42807. doi:10.1074/jbc.m111.291799

Klein, G., and Raina, S. (2017). Small Regulatory Bacterial RNAs Regulating the Envelope Stress Response. *Biochem. Soc. Trans.* 45, 417–425. doi:10.1042/bst20160367

Klein, G., Stupak, A., Biernacka, D., Wojtkiewicz, P., Lindner, B., and Raina, S. (2016). Multiple Transcriptional Factors Regulate Transcription of the rpoE Gene in *Escherichia coli* under Different Growth Conditions and when the Lipopolysaccharide Biosynthesis Is Defective. *J. Biol. Chem.* 291, 22999–23019. doi:10.1074/jbc.m116.748954

Mandin, P., and Gottesman, S. (2009). A Genetic Approach for Finding Small RNAs Regulators of Genes of Interest Identifies RybC as Regulating the DpiA/DpiB Two-Component System. *Mol. Microbiol.* 72, 551–565. doi:10.1111/j.1365-2958.2009.06665.x

Masse, E., Escorcia, F. E., and Gottesman, S. (2003). Coupled Degradation of a Small Regulatory RNA and its mRNA Targets in *Escherichia coli*. *Genes Develop.* 17, 2374–2383. doi:10.1101/gad.1127103

Masse, E., and Gottesman, S. (2002). A Small RNA Regulates the Expression of Genes Involved in Iron Metabolism in *Escherichia coli*. *Proc. Natl. Acad. Sci.* 99, 4620–4625. doi:10.1073/pnas.032066599

Mecsas, J., Rouviere, P. E., Erickson, J. W., Donohue, T. J., and Gross, C. A. (1993). The Activity of Sigma E, an *Escherichia coli* Heat-Inducible Sigma-Factor, Is Modulated by Expression of Outer Membrane Proteins. *Genes Dev.* 7, 2618–2628. doi:10.1101/gad.7.12b.2618

Melamed, S., Peer, A., Faigenbaum-Romm, R., Gatt, Y. E., Reiss, N., Bar, A., et al. (2016). Global Mapping of Small RNA-Target Interactions in Bacteria. *Mol. Cel* 63, 884–897. doi:10.1016/j.molcel.2016.07.026

Miller, J. H. (1992). *A Short Course in Bacterial Genetics*. Plainview, N. Y.: Cold Spring Harbor Laboratory Press.

Missiakas, D., Mayer, M. P., Lemaire, M., Georgopoulos, C., and Raina, S. (1997). Modulation of the *Escherichia coli* σ E (RpoE) Heat-Shock Transcription-Factor Activity by the RseA, RseB and RseC Proteins. *Mol. Microbiol.* 24, 355–371. doi:10.1046/j.1365-2958.1997.3601713.x

Nitta, T., Nagamitsu, H., Murata, M., Izu, H., and Yamada, M. (2000). Function of the ς E Regulon in Dead-Cell Lysis in Stationary-Phase *Escherichia coli*. *J. Bacteriol.* 182, 5231–5237. doi:10.1128/jb.182.18.5231-5237.2000

Prévost, K., Salvail, H., Desnoyers, G., Jacques, J.-F., Phaneuf, É., and Massé, E. (2007). The Small RNA RyhB Activates the Translation of *shiA* mRNA Encoding a Permease of Shikimate, a Compound Involved in Siderophore Synthesis. *Mol. Microbiol.* 64, 1260–1273. doi:10.1111/j.1365-2958.2007.05733.x

Ravio, T. L., Popkin, D. L., and Silhavy, T. J. (1999). The Cpx Envelope Stress Response Is Controlled by Amplification and Feedback Inhibition. *J. Bacteriol.* 18, 5263–5272.

Ravio, T. L. (1999). The sE and Cpx Regulatory Pathways: Overlapping but Distinct Envelope Stress Responses. *Curr. Opin. Microbiol.* 2, 159–165.

Rhodius, V. A., Suh, W. C., Nonaka, G., West, J., and Gross, C. A. (2006). Conserved and Variable Functions of the SigmaE Stress Response in Related Genomes. *Plos Biol.* 4, e2. doi:10.1371/journal.pbio.0040002

Semsey, S., Andersson, A. M. C., Krishna, S., Jensen, M. H., Massé, E., and Sneppen, K. (2006). Genetic Regulation of Fluxes: Iron Homeostasis of *Escherichia coli*. *Nucleic Acids Res.* 34, 4960–4967. doi:10.1093/nar/gkl627

Sikora, A. E., Beyhan, S., Bagdasarian, M., Yildiz, F. H., and Sandkvist, M. (2009). Cell Envelope Perturbation Induces Oxidative Stress and Changes in Iron Homeostasis in *Vibrio cholerae*. *J. Bacteriol.* 191, 5398–5408. doi:10.1128/jb.00092-09

Thompson, K. M., Rhodius, V. A., and Gottesman, S. (2007). σ E Regulates and Is Regulated by a Small RNA in *Escherichia coli*. *J. Bacteriol.* 189, 4243–4256. doi:10.1128/jb.00020-07

Udekwu, K. I., and Wagner, E. G. (2007). Sigma E Controls Biogenesis of the Antisense RNA MicA. *Nucleic Acids Res.* 35, 1279–1288. doi:10.1093/nar/gkl1154

Vogt, S. L., Evans, A. D., Guest, R. L., and Raivio, T. L. (2014). The Cpx Envelope Stress Response Regulates and Is Regulated by Small Noncoding RNAs. *J. Bacteriol.* 196, 4229–4238. doi:10.1128/jb.02138-14

Walsh, N. P., Alba, B. M., Bose, B., Gross, C. A., and Sauer, R. T. (2003). OMP Peptide Signals Initiate the Envelope-Stress Response by Activating DegS Protease via Relief of Inhibition Mediated by its PDZ Domain. *Cell* 113, 61–71. doi:10.1016/s0092-8674(03)00203-4

Wright, P. R., Richter, A. S., Papenfort, K., Mann, M., Vogel, J., Hess, W. R., et al. (2013). Comparative Genomics Boosts Target Prediction for Bacterial Small RNAs. *Proc. Natl. Acad. Sci.* 110, E3487–E3496. doi:10.1073/pnas.1303248110

Yakhnin, H., Aichele, R., Ades, S. E., Romeo, T., and Babitzke, P. (2017). Circuitry Linking the Global Csr- and σE-Dependent Cell Envelope Stress Response Systems. *J. Bacteriol.* 199, e00484–00417. doi:10.1128/JB.00484-17

Zhou, Y., and Gottesman, S. (1998). Regulation of Proteolysis of the Stationary-Phase Sigma Factor RpoS. *J. Bacteriol.* 180, 1154–1158. doi:10.1128/jb.180.5.1154-1158.1998

Conflict of Interest: The authors declare that the research was conducted in the absence of any commercial or financial relationships that could be construed as a potential conflict of interest.

Publisher's Note: All claims expressed in this article are solely those of the authors and do not necessarily represent those of their affiliated organizations, or those of the publisher, the editors, and the reviewers. Any product that may be evaluated in this article, or claim that may be made by its manufacturer, is not guaranteed or endorsed by the publisher.

Advantages of publishing in Frontiers

OPEN ACCESS
Articles are free to read for greatest visibility and readership

FAST PUBLICATION
Around 90 days from submission to decision

HIGH QUALITY PEER-REVIEW
Rigorous, collaborative, and constructive peer-review

TRANSPARENT PEER-REVIEW
Editors and reviewers acknowledged by name on published articles

Frontiers
Avenue du Tribunal-Fédéral 34
1005 Lausanne | Switzerland

Visit us: www.frontiersin.org
Contact us: frontiersin.org/about/contact

REPRODUCIBILITY OF RESEARCH
Support open data and methods to enhance research reproducibility

DIGITAL PUBLISHING
Articles designed for optimal readership across devices

FOLLOW US
@frontiersin

IMPACT METRICS
Advanced article metrics track visibility across digital media

EXTENSIVE PROMOTION
Marketing and promotion of impactful research

LOOP RESEARCH NETWORK
Our network increases your article's readership